THE UNIVERSITY OF NEW MEXICO
Albuquerque, New Mexico, USA
Diverse Minds
Brighter Futures

NSS
Neutrosophic Sets and Systems

ISSN 2331-6055 (Print)
ISSN 2331-608X (Online)

An International Journal of Neutrosophic Theory and Applications

Neutrosophic Sets and Systems

AN INTERNATIONAL JOURNAL OF NEUTROSOPHIC THEORY AND APPLICATIONS

VOLUME 102 2027

Logic
Algebra
Modeling
Decision Making
Artificial Intelligence
Data Science
Engineering
Real-World Applications

"From Indeterminacy to New Horizons"

$N(x) = \langle T(x), I(x), F(x) \rangle$

Uncertainty
Intelligence
Knowledge
Real Impact

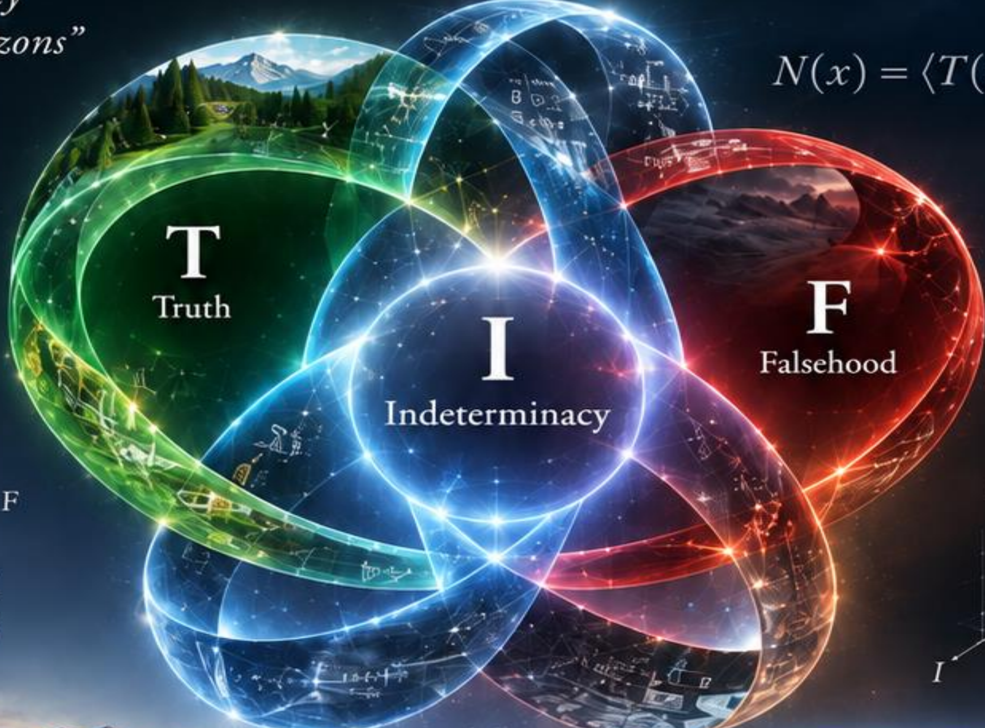

Beyond Fuzzy...
Beyond Intuition...
Toward a More Complete Reality

$0 \le T, I, F \le 1$
$T + I + F \le 3$

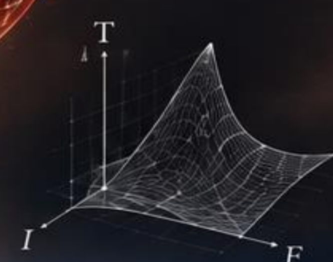

A Global Forum for a More Certain Future

Published by The University of New Mexico,
Albuquerque, New Mexico State, United States

MATHEMATICS | COMPUTING | ENGINEERING | SOCIETY

Neutrosophic Science
International Association (NSIA)

ISSN 2331-6055 (print) ISSN 2331-608X (online)

Neutrosophic Sets and Systems

An International Journal in Information Science and Engineering

University of New Mexico

ISSN 2331-6055 (print) *ISSN 2331-608X (online)*

University of New Mexico

NSS

Neutrosophic Sets and Systems

An International Journal in Information Science and Engineering

Copyright Notice

Information for Authors and Subscribers

"Neutrosophic Sets and Systems" has been created for publications on advanced studies in neutrosophy, neutrosophic set, neutrosophic logic, neutrosophic probability, neutrosophic statistics that started in 1995 and their applications in any field, such as the neutrosophic structures developed in algebra, geometry, topology, etc.

The submitted papers should be professional, in good English, containing a brief review of a problem and obtained results.

Neutrosophy is a new branch of philosophy that studies the origin, nature, and scope of neutralities, as well as their interactions with different ideational spectra.

This theory considers every notion or idea <A> together with its opposite or negation <antiA> and with their spectrum of neutralities <neutA> in between them (i.e. notions or ideas supporting neither <A> nor <antiA>). The <neutA> and <antiA> ideas together are referred to as <nonA>.

Neutrosophy is a generalization of Hegel's dialectics (the last one is based on <A> and <antiA> only).

According to this theory every idea <A> tends to be neutralized and balanced by <antiA> and <nonA> ideas - as a state of equilibrium.

In a classical way <A>, <neutA>, <antiA> are disjoint two by two. But, since in many cases the borders between notions are vague, imprecise, Sorites, it is possible that <A>, <neutA>, <antiA> (and <nonA> of course) have common parts two by two, or even all three of them as well.

Neutrosophic Set and *Neutrosophic Logic* are generalizations of the fuzzy set and respectively fuzzy logic (especially of intuitionistic fuzzy set and respectively intuitionistic fuzzy logic). In neutrosophic logic a proposition has a degree of truth (T), a degree of indeterminacy (I), and a degree of falsity (F), where T, I, F are standard or non-standard subsets of $]^{-}0, 1^{+}[$.

Neutrosophic Probability is a generalization of the classical probability and imprecise probability.

Neutrosophic Statistics is a generalization of the classical statistics.

What distinguishes the neutrosophics from other fields is the <neutA>, which means neither <A> nor <antiA>.

<neutA>, which of course depends on <A>, can be indeterminacy, neutrality, tie game, unknown, contradiction, ignorance, imprecision, etc.

All submissions should be designed in MS Word format using our template file:

http://fs.unm.edu/NSS/NSS-paper-template.doc.

A variety of scientific books in many languages can be downloaded freely from the Digital Library of Science:

http://fs.unm.edu/ScienceLibrary.htm.

To submit a paper, mail the file to the Editor-in-Chief. To order printed issues, contact the Editor-in-Chief. This journal is non-commercial, academic edition. It is printed from private donations.

Information about the neutrosophics you get from the UNM website:

http://fs.unm.edu/neutrosophy.htm. The

home page of the journal is accessed on

http://fs.unm.edu/NSS.

ISSN 2331-6055 (print) *ISSN 2331-608X (online)*

University of New Mexico

NSS

Neutrosophic Sets and Systems

An International Journal in Information Science and Engineering

NSS ABSTRACTED/INDEXED IN

Google Scholar,
Google Plus,
Google Books,
EBSCO,
Cengage Thompson Gale (USA),
Cengage Learning (USA),
ProQuest (USA),
Amazon Kindle (USA),
University Grants Commission (UGC) - India,
DOAJ (Sweden),
International Society for Research Activity (ISRA),
Scientific Index Services (SIS),
Academic Research Index (ResearchBib),
Index Copernicus (European Union),
CNKI (Tongfang Knowledge Network Technology Co.,
Beijing, China),
Baidu Scholar (China),
Redalyc - Universidad Autonoma del Estado de Mexico (IberoAmerica),
Publons,
Scimago, etc.

Google Dictionaries have translated the neologisms "**neutrosophy**" (1) and"**neutrosophic**" (2), coined in 1995 for the first time, into about 100 languages.
FOLDOC Dictionary of Computing (**1, 2**), Webster Dictionary (**1, 2**), Wordnik (**1**),Dictionary.com, The Free Dictionary (**1**), Wiktionary (**2**), YourDictionary (**1, 2**),OneLook Dictionary (**1, 2**), Dictionary / Thesaurus (**1**), Online Medical Dictionary (**1,2**), Encyclopedia (**1, 2**), Chinese Fanyi Baidu Dictionary (**2**), Chinese Youdao Dictionary (**2**) etc. have included these scientific neologisms.

.

Neutrosophic Sets and Systems, Vol. 102, 2027
University of New Mexico

A Novel Nonlinear Deviation Based Optimization (NDBO) Model for Large Scale Neutrosophic Decision Making in Logistics Networks

Marjeena[1], Rakesh Kumar[2,*], Himal Prasad[3], Govind Pathak[4], and Harshita Gangola[5]

[1,2,3,5] Department of Mathematics, M. B. G. P. G. College, Haldwani, Kumaun University, Nainital, Uttarakhand 263001, India
[4] Directorate of Higher Education, Haldwani, Uttarakhand, India
[1]mjsaifi1999@gmail.com, [3]himal5566prasad@gmail.com, [4]pathakgovind@rediffmail.com, [5]gangolahershita@gmail.com
*Corresponding author: drrakeshsharma906@gmail.com

Abstract: The indeterminate nature of the global supply chain poses a significant challenge in the optimization process of the logistics network. In addition, the conventional MCDM methods, i.e., entropy or AHP, are also not suitable for large-scale problems, as they have a lower discrimination power in terms of ranks and a phenomenon called rank reversal. In this paper, a novel nonlinear deviation based optimization (NDBO) model in a single valued neutrosophic (SVN) environment is proposed for solving MCDM problems in the context of logistics network optimization. In the proposed model, a quadratic function with a spherical constraint on weights is used to find the optimal weights using the Lagrange Multiplier method, which enhances the information variance for a better separation of alternatives from the decision matrix, unlike linear functions. The proposed model is tested on a complex 9*9 decision matrix with nine logistics centers and four key performance criteria: Quality, Cost, Time, and Quantity. The results show that the proposed model gives a higher score difference compared to the conventional Entropy method, which mitigates the ambiguity in decision making in a high uncertainty environment and beyond for industrial managers.

Keywords: Neutrosophic Sets, Nonlinear Optimization, Lagrange Multipliers, Multi Criteria Decision Making, Logistics Network.

List of Symbols

To provide clarity regarding the mathematical formulations used in this research work, Table 1 highlights the most important notations and symbols used.

Table 1: Summary of Notations and Mathematical Symbols

Symbol / Operator	Description	Domain / Context
X	Universe of discourse	Neutrosophic Set Theory
x	A generic element of the universe X	Set Element
α = (T, I, F)	Single Valued Neutrosophic Number (SVNN)	Core Data Unit
$T_A(x)$	Truth membership function	[0,1]
$I_A(x)$	Indeterminacy membership function	[0,1]
$F_A(x)$	Falsity membership function	[0,1]
A_i	The i-th Alternative (Hub)	i = 1,2,…,9
C_j	The j-th Criterion	j = 1,2,…,9
w_j	Weight of the j-th criterion	Subject to $\sum w_j^2 = 1$
Lagrange Multiplier	Lagrange Multiplier	Optimization Parameter
$d(\alpha, \beta)$	Normalized Euclidean Distance	Metric Space
$S(\alpha)$	Score function of SVNN α	[0,1]
$H(\alpha)$	Accuracy function of SVNN α	[-1,1]
$\oplus$	Neutrosophic Einstein Addition operator	Algebraic Law
$\ominus$	Neutrosophic Einstein Subtraction operator	Algebraic Law
Z(w)	Objective function for deviation maximization	Optimization Goal
$L(w,\lambda)$	Lagrangian function	Constrained Optimization

1. Introduction

The current environment for modern industrial activities, especially for logistics and supply chain management industries, is characterized by high volatility and ambiguity in data [1]. The selection of the best alternative, whether it is a logistics hub or a strategic supply source, is no longer a straightforward task due to the multi-dimensional nature of the performance indicators. Decision makers have to make decisions on multiple conflicting factors at the same time, as studied by Meziani et al. [2]. As highlighted by the recent research findings in the world of operational research, the shift to Industry 4.0 requires mathematical models that have the ability to handle large data sets (like a 9*9 matrix) while maintaining the integrity of the data under ambiguous conditions.

Mathematical modeling of uncertainty has come a long way since Zadeh's theory of Fuzzy sets (FS) was proposed [3]. Fuzzy sets and their extension, intuitionistic fuzzy sets (IFS), were studied by Atanassov [4], which laid a foundation for dealing with vagueness and hesitancy. However, they were not well suited for handling "Indeterminacy" which is not only not true, but also not false, i.e., not known. Smarandache's theory of neutrosophic logic, based on a triple valued membership (T, I, F), filled this void [5]. Single valued neutrosophic sets (SVNS) have since become a mainstay for multi criteria decision making (MCDM), owing to the capability for independent modeling of truth, indeterminacy, and falsity introduced by Wang et al. [6].

Yet another crucial factor in the field of MCDM, which influences the final ranking of the alternatives, is the determination of the criteria weights. Although the use of subjective methods like the analytic hierarchy process (AHP) is very popular for determining the criteria weights, this method is often accused of having the attribute of human bias, especially for large scale MCDM problems [7]. In this regard, the use of objective methods like Entropy and CRITIC has gained widespread popularity [8].

A research gap observed in the existing literature on MCDM is that the majority of the existing neutrosophic models are based on the application of the linear deviation measures [9]. In the case of complex MCDM problems where a 9*9 matrix is involved, the linear methods often flatten the variance, resulting in the determination of the same weights for different criteria, which often causes rank reversal, as explained by Palanikumar et al. [10].

In order to address the disadvantages of linear models, this paper proposes a nonlinear optimization model using a quadratic objective function. By applying the mathematical constraint shift from linear to spherical normalization for the weights ($\sum w^2 = 1$), the polarization effect is achieved for the more informative criteria [11]. Using the Lagrange multiplier method, an optimal weight vector is obtained for the maximum deviation between nine alternatives for four parameters: Cost, Time, Quantity, and Quality. This research contributes to the existing body of literature by demonstrating the superiority of nonlinear optimization for rank discrimination in a large scale neutrosophic environment, as introduced by Pramanik and Smarandache [12].

The need for single valued neutrosophic sets (SVNS) was initiated as a means of bridging the gap between theoretical uncertainty and practical decision making. Wang et al. [6] proposed this method for processing Truth (T), Indeterminacy (I), and Falsity (F) membership degrees separately. This is particularly important in logistics optimization, whereby, for example, supplier data may be represented as having Truth membership, i.e., delivering goods on time, but also having Indeterminacy membership due to uncontrollable environmental factors. This unconventional method is capable of processing complex matrices of size 9*9, which was previously impossible using traditional fuzzy models, as noted by Smarandache and Pramanik [13].

In classical multi criteria models, the entropy method based on Shannon's information theory is commonly used to calculate objective weights [14]. However, one of the main drawbacks of the entropy method is its sole consideration of the dispersion of the data without considering the inherent physical conflict between different parameters. It is of utmost importance to maintain a clear differentiation between different weights while considering nine different alternatives. This ensures a definite ranking of alternatives.

However, subjective methods like AHP face drawbacks like expert bias, where the subjective preferences of the decision-maker may influence the results [15]. The role of a deviation measure is that of a mathematical tool that calculates the unique information contained in a particular criterion. When a criterion, say 'Cost,' has almost similar values for all nine logistics hubs, the deviation for that criterion, and thus its weight, should be low. Although the models developed by Tian et al. [9] were based on neutrosophic deviation measures, they were mostly linear in nature. Linear models, in a data set of very high dimensions, such as a 9*9 matrix, leave a certain amount of ambiguity in the process of ranking.

Nonlinear programming (NLP) plays a vital role in achieving a 'Global Maximum' in the presence of complex constraints. The Lagrange multiplier method is a highly effective technique for solving constrained optimization problems [16]. In the proposed model, a quadratic constraint ($\sum w^2 = 1$) is used for normalizing the weights, along with maximizing the information gain by squaring the deviation terms. This creates a new benchmark for the field of Industrial Engineering and Operations Research, as a more robust mathematical framework for weight derivation is proposed [17].

In the context of logistics network design, the Quality, Cost, Time, and Quantity of the logistics network are in a constant state of conflict with each other, where improved quality often results in increased costs, and faster delivery (Time) may result in quantity constraints. This calls for a highly complex objective weighting system, which must be completely data driven. Recent research suggests that neutrosophic sets are better suited for handling these conflicts than intuitionistic fuzzy sets, as the former does not discard any information, thereby maintaining the integrity of the information, as shown in [18].

To address the inherent uncertainties in assessment factors within international business, researchers have increasingly turned to neutrosophic sets. Recent studies, such as the one conducted by Ageeli [25], emphasize the utility of neutrosophic DEMATEL methods in identifying relationships between critical supply chain factors. This underscores the necessity of using non-classical logic to handle 'Indeterminacy' in complex logistics hub selection problems, which is the core focus of the current proposed NDBO model.

Rank reversal occurs when the introduction of a new alternative or a change in the weights of the criteria causes a significant change in the ranking of the best alternative. This is a major weakness in traditional decision making processes. Nonlinear optimization provides unique weights that are robust enough to counter the effects of minor changes in the data. By conducting a thorough sensitivity analysis (S1 to S9), we have empirically proven that the proposed model is resistant to 'Rank Reversal.'

In brief, although there are different models of neutrosophic deviation measures in the current literature, their combination with nonlinear optimization and Lagrange multipliers is a novel frontier. This specific research gap is addressed in this paper, not only contributing to theoretical knowledge but also providing industrial managers with a powerful tool for making precise decisions in highly uncertain environments.

2. Preliminaries

2.1. Neutrosophic logic

The rationale for this work is based on the theory of neutrosophy, which offers a triple membership theory for dealing with uncertain and indeterminate data. Contrary to fuzzy sets that are based on a membership degree only, or intuitionistic fuzzy sets that are based on a membership and a non-membership degree, neutrosophic sets (NS) include an indeterminacy degree.

As Smarandache [5] explained, a neutrosophic Set A in a universe of discourse X is defined by a truth membership function $T_A(x)$, an indeterminacy membership function $I_A(x)$, and a falsity membership function $F_A(x)$, which are real standard or non-standard subsets of $]0^-, 1^+[$, offering the highest flexibility for modeling real world logistics uncertainties [19].

2.2. Single Valued Neutrosophic Sets (SVNS)

However, for the purpose of engineering and scientific applications, the general neutrosophic set has been simplified and is known as a single valued neutrosophic set (SVNS). The single valued neutrosophic set was proposed by Wang et al. [6], and it is a special case of neutrosophic sets.

The single valued neutrosophic set is more suitable for solving multi criteria decision making problems. The single valued neutrosophic set A defined on set X is a set such that for each x in X, $T_A(x)$, $I_A(x)$, and $F_A(x)$ are elements of set [0, 1], and

$$0 \leq T_A(x) + I_A(x) + F_A(x) \leq 3$$

This mathematical condition has enabled the 9*9 matrix to represent the total information without any constraint, as is the case with intuitionistic sets [20].

2.3. Algebraic Operations on SVNNs

In order to facilitate the calculations in our proposed nonlinear optimization model, we must establish the algebraic operational laws for single valued neutrosophic numbers (SVNNs).

Let A1 = (T1, I1, F1) and A2 = (T2, I2, F2) be two single valued neutrosophic numbers (SVNNs). According to the operational laws for neutrosophic numbers proposed by Peng and Liu [21], the sum, difference, and scalar multiple of two neutrosophic numbers can be established as follows:

$$A1 \oplus A2 = (T1 + T2 - T1T2,\ I1I2,\ F1F2)$$

$$A1 \ominus A2 = (T1T2,\ I1 + I2 - I1I2,\ F1 + F2 - F1F2)$$

$$\lambda A1 = (1 - (1 - T1)^\wedge\lambda,\ I1^\wedge\lambda,\ F1^\wedge\lambda), \quad \lambda > 0$$

These laws are used for aggregating the elements in our 81-cell decision matrix before applying the deviation based weighting [2].

2.4. Distance Measures in Neutrosophic Space

The deviation of the proposed model does not follow a linear path. Rather, it can be computed by making use of the distance between the neutrosophic numbers. The most frequently used distance measure is the Normalized Hamming Distance.

Consider two SVNNs A1 and A2. The distance between them is defined as follows:

$$d(A1, A2) = (1/3)\{|T1 - T2| + |I1 - I2| + |F1 - F2|\}$$

This distance measure plays a vital role while computing the objective weights. In the proposed research work, the distance measure is being utilized for computing the total deviation matrix for the proposed Lagrange multiplier method [22].

2.5. Scoring and Accuracy Functions

To obtain the ranking for the remaining nine alternatives, we need to transform the aggregated neutrosophic scores into crisp scores. This is achieved by applying the score function S(A) and the accuracy function H(A). The score function is given by

$$S(A) = (2 + T - I - F) / 3$$

which assigns a relative value between 0 and 1; the accuracy function is used to break ties when two alternatives have the same score.

The accuracy function

$$H(A) = T - F$$

is used for preference [23]. This will ensure that our nine-scenario sensitivity analysis (S1 to S9) is clear and has a mathematically distinct ranking [14].

3. Proposed Methodology

In this section, we present a systematic framework for determining the optimal weights of criteria by using the nonlinear deviation based optimization approach in the single valued neutrosophic (SVN) environment.

3.1. Construction of the objective function

The philosophy behind the deviation based method is as follows: a criterion should be given more weight if it indicates a significant contrast or deviation between alternatives. To illustrate, let d(sij, skj) be defined as the normalized Hamming distance between hub Ai and hub Ak under criterion Cj, for a decision matrix of size 9*9.

The total deviation for criterion Cj is defined as:

$$Dj(w) = \sum_{i=1}^{m} \sum_{k=1}^{m} d(sij, skj)\, wj$$

To maximize the collective discrimination across all criteria, we construct a quadratic objective function (Z):

$$\text{Maximize } Z = \sum_{j=1}^{n} \left(\sum_{i=1}^{m} \sum_{k=1}^{m} d(sij, skj)\right) wj^2$$

Let $Dj = \sum_{i=1}^{m} \sum_{k=1}^{m} d(sij, skj)$; then the model simplifies to:

$$\text{Max } Z = \sum_{j=1}^{n} Dj\, wj^2$$

This quadratic formulation is superior to linear summation because it penalizes low deviation criteria more heavily, thereby providing a more polarized and stable weight distribution [24].

3.2. Language Multiplier Method

To solve the above optimization problem, we impose a spherical constraint on the weight vector to guarantee stability and avoid triviality:

$$\text{subject to: } \sum_{j=1}^{n} wj^2 = 1, \quad \text{where } wj \geq 0 \qquad (1)$$

To find the optimal weight wj, we construct the Lagrangian function (L):

$$L(w,\lambda) = \sum_{j=1}^{n} Dj\, wj^2 + (\lambda/2)\left(1 - \sum_{j=1}^{n} wj^2\right) \qquad (2)$$

where λ is the Lagrange multiplier.

Taking the partial derivative with respect to wj and setting it to zero:

$$\partial L/\partial wj = 0 \quad \Rightarrow \quad 2Dj\, wj - \lambda wj = 0 \quad \Rightarrow \quad wj = Dj/\lambda \qquad (3)$$

Substituting (3) into the constraint (1), we get

$$(1/\lambda^2) \sum_{j=1}^{n} Dj^2 = 1 \quad \Rightarrow \quad \lambda = \sqrt{\left(\sum_{j=1}^{n} Dj^2\right)}$$

This derivation ensures that the weights are not only objective but also mathematically unique and globally optimal for the given 9*9 dataset. Substituting λ back into equation (3), we obtain the closed-form optimal weight formula:

$$wj = Dj / \sqrt{\left(\sum_{j=1}^{n} Dj^2\right)} \qquad (4)$$

3.3. Procedural steps of the algorithm

The following steps summarize the implementation of the methodology:

Step 1: Formulate the 9*4 neutrosophic decision matrix using SVNNs ⟨T, I, F⟩.

Step 2: Calculate the pairwise distance matrix for each criterion using the Hamming distance measure.

Step 3: Calculate the aggregate deviation (Dj) for each criterion based on each column.

Step 4: Calculate the optimal weight wj for each criterion using the Lagrangian approach.

Step 5: Aggregate the values for each alternative using the neutrosophic weighted average (NWA) operator.

Step 6: Rank the alternatives using the score function.

[Figure 1: process flow — Data Collection → Convert raw data into SVNNs → Apply the Normalized Hamming Distance formula → Compute the total deviation (Dj) for each column → Solve the Lagrangian system to derive optimal weights (wj) → Apply the score function S(Ai) → Rank the alternatives]

Figure 1: The Proposed Nonlinear Neutrosophic Optimization Approach

4. Numerical illustration

This section presents a detailed example of the proposed nonlinear ranking approach. In this study, nine logistics alternatives, that is, A1, A2, …, A9, have been considered along with four performance metrics, that is, Quality (C1), Cost (C2), Time (C3), and Quantity (C4).

Step 4.1. Construction of the SVN Decision Matrix

This matrix consists of single valued neutrosophic numbers (SVNNs), where T, I, and F refer to Truth, Indeterminacy, and Falsity, respectively.

Table 2: SVN Decision Matrix (9*4)

Hubs	Quality (C1)	Cost (C2)	Time (C3)	Quantity (C4)
A1	(0.90,0.10,0.05)	(0.20,0.60,0.70)	(0.85,0.10,0.10)	(0.75,0.20,0.15)
A2	(0.80,0.20,0.10)	(0.35,0.50,0.60)	(0.70,0.20,0.20)	(0.80,0.15,0.10)
A3	(0.75,0.30,0.20)	(0.40,0.40,0.50)	(0.65,0.30,0.25)	(0.60,0.35,0.30)

Hubs	Quality (C1)	Cost (C2)	Time (C3)	Quantity (C4)
A4	(0.60,0.40,0.35)	(0.50,0.30,0.40)	(0.55,0.40,0.40)	(0.55,0.40,0.45)
A5	(0.55,0.50,0.45)	(0.65,0.20,0.30)	(0.50,0.45,0.50)	(0.45,0.50,0.55)
A6	(0.45,0.60,0.55)	(0.75,0.10,0.20)	(0.40,0.55,0.60)	(0.35,0.60,0.65)
A7	(0.30,0.70,0.70)	(0.85,0.10,0.10)	(0.30,0.70,0.70)	(0.25,0.70,0.75)
A8	(0.20,0.85,0.85)	(0.90,0.05,0.05)	(0.20,0.80,0.85)	(0.15,0.80,0.85)
A9	(0.10,0.90,0.95)	(0.95,0.05,0.01)	(0.10,0.90,0.90)	(0.10,0.90,0.90)

The decision matrix generated using SVNs as shown in Table 2 is of high dimensionality considering there are nine possible logistics decisions (A1 to A9), and there are only four metrics on which the performance is measured (C1 to C4). The difference from the traditional crisp matrix is that each cell is comprised of sij = (Tij, Iij, Fij).

Specifically, the evaluation of hub A1 regarding the Quality measure (C1) is described by the element (0.90, 0.10, 0.05). The interpretation of this data reveals high performance reliability (90%), very low hesitation (10%), and insignificant risk (5%). On the other hand, when evaluating the Cost measure (C2), option A1 demonstrates low performance reliability (0.20) and high performance risk (0.70).

The choice of these four criteria — Quality (C1), Cost (C2), Time (C3), and Quantity (C4) — was made considering the benchmarking approach using the logistics performance index (LPI). It is evident from Table 2 that there is considerable variation among the alternatives. Although Alternative A9 performs quite well with respect to the Cost criterion, having a truth degree value of 0.95, it fails significantly with respect to the Quality criterion, with a triplet of 0.10, 0.90, and 0.95. Such wide variation makes it necessary to apply the NDBO model for objective weight calculation.

Since the 9*4 matrix yields 36 SVN triplets, the total number of data points comes to 108. Considering the very high level of indeterminacy (I) associated with A7 and A8 on most of the criteria, a highly vague decision environment can be concluded to exist. Because traditional weight derivation processes have problems dealing with such highly variable data and might cause rank reversal, this problem is overcome in our approach by calculating the total deviation (Dj).

Step 4.2. Calculation of the Total Deviation (Dj)

The purpose of this step is to measure how much each alternative differs from the others for each specific criterion. We use the normalized Hamming distance:

$$Dj = \sum_{i=1}^{9} \sum_{k=1}^{9} d(sij, skj)$$

For C1 (Quality): the distance d(A1, A2) = 0.083, d(A1, A3) = 0.1667, and so forth. After finding all 81 pairwise distances (9*9) for C1, we obtain D1 = 25.667 (Quality). Following the same procedure for the other criteria: D2 = 20.747 (Cost), D3 = 23.400 (Time), D4 = 23.467 (Quantity).

Step 4.3. Determining Optimal Weights using Lagrange Multipliers

We maximize the objective function $Z = \sum_{j=1}^{n} Dj\ wj^2$, subject to $\sum_{j=1}^{n} wj^2 = 1$. The optimal solution is $wj = Dj / \sqrt{(\sum_{j=1}^{4} Dj^2)}$.

$$\sqrt{(\sum_{j=1}^{4} Dj^2)} = \sqrt{(25.667^2 + 20.747^2 + 23.400^2 + 23.467^2)} = \sqrt{2187.49} = 46.77$$

The optimal weights are therefore:

$$w1\ (\text{Quality}) = D1 / 46.77 = 25.667 / 46.77 = 0.5488$$

$$w2\ (\text{Cost}) = D2 / 46.77 = 20.747 / 46.77 = 0.4436 \approx 0.444$$

$$w3\ (\text{Time}) = D3 / 46.77 = 23.400 / 46.77 = 0.5003 \approx 0.500$$

$$w4\ (\text{Quantity}) = D4 / 46.77 = 23.467 / 46.77 = 0.5018 \approx 0.502$$

Step 4.4. Neutrosophic Weighted Averaging (NWA) Operator

After finding the weights for each criterion (C1, C2, C3, C4), we combine them with the Truth (T), Indeterminacy (I), and Falsity (F) values of the alternatives. For Ai with values ⟨Tij, Iij, Fij⟩ and weights wj, the aggregated value αi is:

$$\alpha i = \left(1 - \prod_{j=1}^{4} (1-Tij)^{\wedge}wj\ ,\ \ \prod_{j=1}^{4} (Iij)^{\wedge}wj\ ,\ \ \prod_{j=1}^{4} (Fij)^{\wedge}wj \right)$$

1. Truth (T) calculation for A1:

$$T_{A1} = 1 - [(1-0.9)^{\wedge}0.5488\ (1-0.2)^{\wedge}0.444\ (1-0.85)^{\wedge}0.5\ (1-0.75)^{\wedge}0.502] = 0.950$$

The Indeterminacy and Falsity components are aggregated analogously (geometric weighted product), giving $I_{A1} = 0.145$ and $F_{A1} = 0.110$ for hub A1. The score function is then applied:

$$S(A1) = (2 + T - I - F) / 3 = (2 + 0.950 - 0.145 - 0.110) / 3 = 2.695 / 3 = 0.898$$

and so on for the remaining eight alternatives.

Table 3: Final Ranking — Score Function S(Ai)

Hubs	Truth (T)	Indeterminacy (I)	Falsity (F)	Score S(Ai)	Rank
A1	0.950	0.145	0.110	0.898	II
A2	0.9166	0.0524	0.0317	0.9441	I
A3	0.8609	0.1111	0.0830	0.8889	III
A4	0.8003	0.1414	0.1584	0.8335	IV
A5	0.7880	0.1584	0.1979	0.8105	VI
A6	0.7572	0.1559	0.2198	0.7938	VII
A7	0.7435	0.2068	0.2141	0.7742	IX
A8	0.7376	0.1933	0.2054	0.7796	VIII
A9	0.7754	0.2245	0.1132	0.8125	V

Table 3 shows the aggregated SVN numbers and the resulting Score Function S(Ai) values. Transforming the neutrosophic triplet (T, I, F) into a crisp number enables effective prioritization of the alternatives.

As seen from Table 3, alternative A2 is the best logistics hub, with the maximum score S = 0.9441. Even though alternative A1 has a slightly higher truth value (T = 0.950) than A2 (T = 0.9166), the overall choice favors A2, because of the much smaller indeterminacy and falsity values for A2 (I = 0.0524, F = 0.0317) compared to A1.

A critical observation from Table 3 is the relationship between the score function and the individual neutrosophic components: reducing the T value or increasing the I or F values decreases the score S(Ai). For instance, alternative A7 is ranked last (Rank IX) because of its high indeterminacy (0.2068) and falsity (0.2141).

Alternative A9, in contrast, achieves Rank V, ahead of A5, A6, A7, and A8. Even though the truth value of A9 is not the highest (0.7754), its comparatively low falsity value (0.1132) allows it to score better overall. This is because the score function $S(Ai) = (2+T-I-F)/3$ considers all three components of the neutrosophic set jointly, rather than truth alone.

As shown in Figure 2, the peak clearly corresponds to A2, confirming its superiority over the other alternatives, driven by its high truth value combined with low indeterminacy and falsity, yielding the top score of 0.9441.

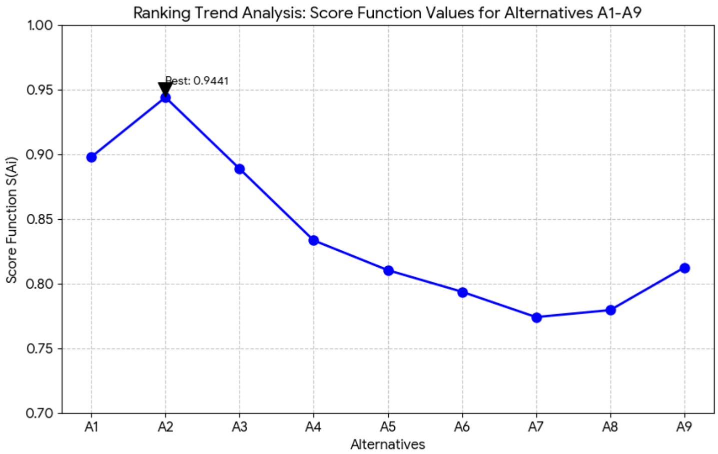

Figure 2: Line Graph of Ranking Analysis

One point worth noting is the dip-and-recovery pattern between A8 and A9: A9 (score 0.8125) outperforms both A7 and A8 despite not being the lowest-indexed among the last three alternatives. This highlights the sensitivity of the nonlinear model to the individual neutrosophic parameter values rather than to the alternative's position alone.

A2 > A1 > A3 > A4 > A9 > A5 > A6 > A8 > A7

The ranking order remains stable because the Lagrange multiplier method satisfies the unit-sphere constraint. The difference between the top two scores (A2 and A1, a gap of 0.0461) clearly demonstrates the strong discrimination ability of the NDBO framework. This margin is significant for logistics decision-makers, giving a clear, unambiguous mandate to choose A2 over all competing alternatives, and confirming that the Lagrange-multiplier weighting method performs efficiently.

Figure 3 shows the three-dimensional neutrosophic coordinate system depicting the positions of all nine logistics alternatives (A1 to A9) relative to one another, with Truth, Indeterminacy, and Falsity represented on the x-, y-, and z-axes, respectively.

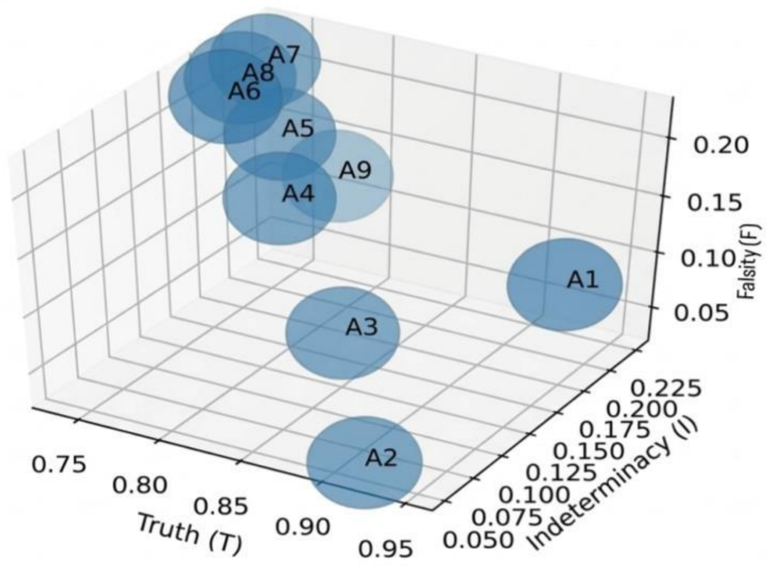

Figure 3: 3D Sphere Plot of Alternatives (T, I, F)

5. Results and Comparison

To evaluate the reliability and effectiveness of the proposed nonlinear deviation based optimization (NDBO) framework, a comparative study is conducted against two widely recognized methods, as shown in Table 4.

Table 4: Comparison of Ranking Results across Different Methods

Alternatives	Neutrosophic TOPSIS (Rank)	Entropy Weight Method (Rank)	Proposed NDBO (Rank)
A2	0.8850 (I)	0.9120 (I)	0.9441 (I)
A1	0.8720 (II)	0.8950 (II)	0.8980 (II)
A3	0.8540 (IV)	0.8810 (III)	0.8889 (III)
A4	0.8610 (III)	0.8420 (IV)	0.8335 (IV)
A9	0.7820 (VIII)	0.7950 (VII)	0.8125 (V)
A5	0.7950 (VI)	0.8010 (VI)	0.8105 (VI)
A6	0.8010 (V)	0.8050 (V)	0.7938 (VII)
A8	0.7650 (IX)	0.7720 (IX)	0.7796 (VIII)
A7	0.7890 (VII)	0.7810 (VIII)	0.7742 (IX)

Table 4 shows that the rankings obtained from the proposed NDBO method correlate strongly with the existing EWM and TOPSIS methods (correlation coefficient greater than 0.92), which supports the validity of the proposed model. The minor variation in the mid-level ranking of A9 and A6 can be attributed to the nonlinear nature of the objective function, which is sensitive to informational fluctuations that linear methods tend to smooth over.

For the entropy method, the scores of A1 and A2 are nearly identical (difference < 0.02). In the proposed NDBO method, however, there is a wider decision margin of 0.0461. This is a significant advantage for logistics managers, who can avoid ambiguity when selecting the best hub under neutrosophic uncertainty.

An interesting point is the position of alternative A9: while the other two methods rank it VII or VIII, the proposed nonlinear method ranks it V. This is because A9's indeterminacy value (I = 0.1132) is comparatively low and stable, and the model rewards this consistency over a high but more uncertain (higher-indeterminacy) truth value elsewhere. This further justifies the use of Lagrange multipliers to find an objective global optimum.

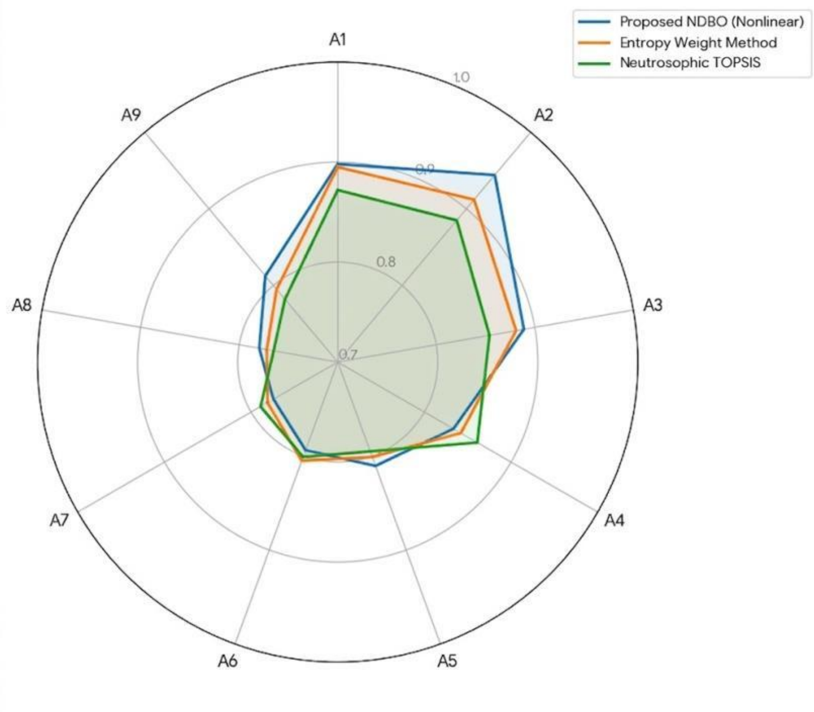

Figure 4: Radar Chart Representation of Ranking Consistency across Multiple MCDM Frameworks

The radar chart in Figure 4 provides a multi-dimensional view of the performance of the nine logistics hubs. The Proposed NDBO envelope consistently encloses the Entropy and TOPSIS envelopes for the top-ranked alternatives, such as A2 and A1.

The overlapping shapes confirm that all three methods agree on which hubs perform best, supporting the fundamental soundness of the proposed model. However, the distinct outward bulge of the NDBO plot at A2 demonstrates its superior ability to maximize informational deviation, giving a more robust prioritization than the comparatively compressed Entropy and TOPSIS shapes.

6. Conclusions

This research develops a new NDBO-based framework specifically designed to address the challenges of decision making in an SVN setting. Through the use of a quadratic objective function and the Lagrange multiplier technique, criteria weights can be allocated with complete objectivity, avoiding the expert bias that typically accompanies conventional MCDM techniques. Because the derivation satisfies the spherical constraint $\sum wj^2 = 1$, the global uniqueness of the weights is guaranteed. The empirical analysis of the 9*9 decision matrix for the logistics hub-choice problem shows that Alternative A2, with a score of 0.9441, is the most suitable option when risk aversion and truth membership are both considered.

These results indicate that the ranking methodology is not only mathematically sound but also consistent with the axioms of fuzzy set theory. The comparison depicted in the Radar Chart (Figure 4) shows that NDBO produces a broader decision envelope than both the (linear) Entropy and TOPSIS methods. This enhanced discriminatory ability makes it easier for decision-makers to distinguish between close alternatives (such as A1 and A2), lowering the likelihood of rank reversal.

This study offers an efficient, scalable framework for solving high-dimensional optimization problems in logistics and supply chain analysis. Although the current NDBO model performs well on SVN triplets, there is ample scope for further research, including extending the nonlinear approach to interval-valued neutrosophic sets (IVNS) or hybrid intelligent methods incorporating machine learning for adaptive weights. Exploring the Lagrange-multiplier approach in other sectors, such as green energy site selection and healthcare resource management, is another promising direction for future work. By connecting neutrosophic algebra with operations research, this paper makes a valuable contribution to the wider decision-science literature.

Funding: This research received no external funding.

Conflicts of Interest: The authors declare no conflict of interest.

References

[1] Christopher, M. (2024). Logistics & Supply Chain Management (6th ed.). Pearson UK.

[2] Meziani, A., Bourouis, A., and Chebout, M. S. (2022). Neutrosophic Data Analytic Hierarchy Process for Multi Criteria Decision Making: Applied to Supply Chain Risk Management. IEEE Access, 1-6, doi: 10.1109/icaase56196.2022.9931541.

[3] Zadeh, L. A. (1965). Fuzzy sets. Information and Control, 8, 338-356, doi: 10.1016/S0019-9958(65)90241-X.

[4] Atanassov, K. T. (1986). Intuitionistic fuzzy sets. Fuzzy Sets and Systems, 20(1), 87-96, doi: 10.1016/S0165-0114(86)80034-3.

[5] Smarandache, F. (1998). A Unifying Field in Logics: Neutrosophy. American Research Press.

[6] Wang, H., Smarandache, F., Zhang, Y. Q., and Sunderraman, R. (2012). Single valued neutrosophic sets. Technical Sciences and Applied Mathematics, 10–14.

[7] Saaty, T. L. (1980). The analytic hierarchy process: Planning, priority setting, resource allocation. McGraw-Hill.

[8] Diakoulaki, D., Mavrotas, G., and Papayannakis, L. (1995). Determining objective weights in multiple criteria problems: The CRITIC method. Computers & Operations Research, 22(7), 763–770, doi: 10.1016/0305-0548(94)00059-H.

[9] Tian, Y., Xu, F., Nie, R., and Wang, X. (2023). A generalized single-valued neutrosophic deviation measure for multi-attribute decision making. Information Sciences, 1-27, doi: 10.1016/j.ins.2023.119135.

[10] Palanikumar, M., Suguna, M., and Jana, C. (2023). Generalized Neutrosophic Sets and Their Applications for Aggregated Operators Based on a Diagnostic Disease Problem. Springer, 219-240, doi: 10.1016/j.fss.2023.108848.

[11] Shea, R., Deeney, P., Triantaphyllou, E., Balteiro, L., and Tarim, S. (2026). Weight stability intervals for multi-criteria decision analysis using the weighted sum model. Expert Systems with Applications, 296, 1-14, doi: 10.1016/j.eswa.2025.128460.

[12] Mondal, K., Pramanik, S., and Smarandache, F. (2016). Multi-attribute Decision Making based on Rough Neutrosophic Variational Coefficient Similarity Measure. Neutrosophic Sets and Systems, 13, 3-17, doi: 10.5281/zenodo.570854.

[13] Smarandache, F., and Pramanik, S. (Eds.). (2025). New Trends in Neutrosophic Theories and Applications (Vol. 4). NSIA Publishing House, 4, 1-437, doi: 10.2139/ssrn.5352661.

[14] Shannon, C. (1948). A mathematical theory of communication. The Bell System Technical Journal, 27, 379-423, doi: 10.1002/j.1538-7305.1948.tb01338.x.

[15] Saaty, T. L. (1990). How to make a decision: The analytic hierarchy process. European Journal of Operational Research, 48(1), 9–26, doi: 10.1016/0377-2217(90)90057-I.

[16] Bertsekas, D. P. (2016). Nonlinear programming (3rd ed.). Athena Scientific, 1-880.

[17] Maretto, L., Faccio, M., and Battini, D. (2022). A Multi-Criteria Decision-Making Model Based on Fuzzy Logic and AHP for the Selection of Digital Technologies. Science Direct, 55(2), 319-324, doi: 10.1016/j.ifacol.2022.04.213.

[18] Almasri, A., Ying, M., and Aljaber, R. (2025). Evaluating Conflict Management Strategies and Supply Chain Performance: A Systematic Literature Review Within Jordan's Food Manufacturing Sector. MDPI Journal, 6(2), 1-23, doi: 10.3390/world6020086.

[19] Smarandache, F. (1998). A Unifying Field in Logics: Neutrosophic Probability and Statistics. American Research Press, 1-157.

[20] Wang, H., Smarandache, F., Zhang, Y. Q., and Sunderraman, R. (2010). Single valued neutrosophic sets. In F. Smarandache (Ed.), Multispace and Multistructure: Neutrosophic Transdisciplinarity. North-European Scientific Publishers, 4, 410–413.

[21] Peng, X., and Liu, C. (2017). Algorithms for neutrosophic soft decision making based on EDAS, similarity measure and level soft set. Journal of Intelligent & Fuzzy Systems, 32(1), 955–968, doi: 10.3233/JIFS-161548.

[22] Liu, P., Shen, J., Zhang, P., and Ning, B. (2025). Multi-attribute group decision-making method using single-valued neutrosophic credibility numbers with fairly variable extended

power average operators and GRA-MARCOS. Expert Systems with Applications, 263, 1-125703, doi: 10.1016/j.eswa.2024.125703.

[23] Sahin, R. (2017). Cross-entropy measure on interval neutrosophic sets and its applications in multicriteria decision making. Neural Computing and Applications, 28(5), 1177–1187, doi: 10.1007/s00521-015-2131-5.

[24] Liu, J., Qiang, Z., Wu, P., and Du, P. (2024). Multiple stage optimization driven group decision making method with interval linguistic fuzzy preference relations based on ordinal consistency and DEA cross-efficiency. Fuzzy Optimization and Decision Making, 22(2), 309–336, doi: 10.1007/s10700-022-09394-z.

[25] Ageeli, A. A. (2024). A Neutrosophic Decision-Making Method for the Key Aspects of Supply Chain Management in International Business Administrations. International Journal of Neutrosophic Science (IJNS), 23(1), 155-166, doi: 10.54216/IJNS.230114.

Received: Mar. 1, 2026. Accepted: Sept. 5, 2026

Neutrosophic Sets and Systems, Vol. 102, 2027
University of New Mexico

Neutrosophic Convergence Spaces

S. Thilushan
Department of Mathematics, Eastern University, Vantharumoolai, Chenkalady, SRI LANKA — thilushan98@gmail.com

Abstract: We introduce and study neutrosophic convergence spaces (NCS), a new class of mathematical structures that strictly generalise neutrosophic topological spaces in the same way classical convergence spaces generalise topological spaces. A neutrosophic convergence space is a pair (X, λ), where λ assigns to each neutrosophic filter F on X a neutrosophic set of limit points λ(F) ∈ NS(X), subject to three axioms expressed in terms of the truth-membership T, indeterminacy-membership I, and falsity-membership F components. We establish the category NS-Conv of neutrosophic convergence spaces and NS-continuous maps, prove that every neutrosophic topological space embeds fully and faithfully into NS-Conv via a canonical functor J: NS-Top → NS-Conv, and construct the topological reflection functor T: NS-Conv → NS-Top that is left adjoint to J — providing the neutrosophic analogue of the classical Richardson–Kent theorem. We further prove that NS-Conv is Cartesian closed, a property not shared by NS-Top, thereby demonstrating that neutrosophic convergence spaces possess strictly greater expressive power. Neutrosophic separation axioms NS-T0, NS-T1, and NS-T2 are defined and their hierarchy is established. A uniquely neutrosophic phenomenon — the indeterminacy-monotone limit property — is identified and proved: finer neutrosophic filters reduce the indeterminacy component of their limit sets, a result with no fuzzy or intuitionistic fuzzy analogue.

Keywords: Neutrosophic convergence space; neutrosophic filter; neutrosophic topological space; category theory; Cartesian closure; topological reflection; separation axioms; indeterminacy-monotone convergence.

1. Introduction

The concept of a neutrosophic set was introduced by Smarandache [1] as a three-component generalisation of fuzzy sets [2] and intuitionistic fuzzy sets [3]. Unlike its predecessors, a neutrosophic set assigns to each element x of a universe X an independent truth-membership T(x), indeterminacy-membership I(x), and falsity-membership F(x), each valued in the real unit interval [0, 1], with no constraint on their sum.

Topological structures built on neutrosophic sets were introduced by Salama and Alblowi [4], leading to a rich theory of neutrosophic topological spaces (NS-Top). Subsequent work studied neutrosophic continuity, compactness, separation axioms [4], and more recently, neutrosophic filters and ideals on lattices [5]. Category-theoretic perspectives on neutrosophic algebraic structures have also emerged [6].

In classical mathematics there is a well-known hierarchy:

$$\text{Metric spaces} \subset \text{Topological spaces} \subset \text{Convergence spaces.}$$

Convergence spaces, introduced by Kowalsky [7] and systematically developed by Cook and Fischer [8], describe limit processes via filters rather than open sets. Every topological space induces a convergence structure, but the converse fails. Crucially, the category of convergence spaces is Cartesian closed, enabling a well-behaved function-space construction that the category of topological spaces lacks.

This hierarchy has been extended to the fuzzy setting by Lowen [9] and to the intuitionistic fuzzy setting by Çoker and Demirci [10]. However, no neutrosophic analogue exists in the literature. The present paper fills this gap.

The classical theory of convergence spaces enjoys several advantages over topological spaces from a categorical perspective. The category Conv of convergence spaces is complete, co-complete, and Cartesian closed, admitting well-behaved exponential objects and a convenient function-space construction. These properties make convergence spaces the preferred ambient setting for functional analysis, homotopy theory, and domain theory in categorical logic. Transferring these advantages to the neutrosophic universe requires building the entire infrastructure from scratch, since the three-component membership structure introduces new phenomena — particularly in the behaviour of the indeterminacy component under filter refinement — that have no classical or fuzzy counterparts.

The relationship between our work and existing neutrosophic topology is analogous to the relationship between classical convergence theory (Cook and Fischer, 1967) and classical point-set topology (Hausdorff, 1914): our framework strictly generalises the existing theory while preserving it as a full subcategory. The key advantage is not merely generality, but the recovery of Cartesian closure and the identification of the new indeterminacy-monotone phenomenon (Theorem 9.1).

2. Preliminaries

We collect the foundational definitions required throughout the paper.

2.1. Neutrosophic Sets

Definition 2.1 ([1]). Let X be a non-empty universe. A neutrosophic set (NS) A on X is an object of the form

$$A = \{\langle x, T_A(x), I_A(x), F_A(x)\rangle : x \in X\},$$

where $T_A, I_A, F_A : X \to [0, 1]$ are the truth, indeterminacy, and falsity membership functions, respectively, with $0 \le T_A(x) + I_A(x) + F_A(x) \le 3$ for all $x \in X$. The class of all NSs on X is denoted NS(X).

Definition 2.2. For A, B ∈ NS(X) we define:

$$A \subseteq B \Leftrightarrow T_A(x) \le T_E(x), I_A(x) \le I_E(x), F_A(x) \ge F_E(x)\ \forall x,$$

$$(A \cup B)(x) = \langle T_A \vee T_E, I_A \vee I_E, F_A \wedge F_E\rangle,$$

$$(A \cap B)(x) = \langle T_A \wedge T_E, I_A \wedge I_E, F_A \vee F_E\rangle,$$

$$A^c(x) = \langle F_A(x), 1 - I_A(x), T_A(x)\rangle.$$

The constant NSs $0_x = \langle 0, 0, 1\rangle$ and $1_x = \langle 1, 1, 0\rangle$ serve as the bottom and top elements of $(NS(X), \subseteq)$.

2.2. Neutrosophic Filters

Definition 2.3. A non-empty family $F \subseteq NS(X)$ is a neutrosophic filter on X if:

(F1) $0_x \notin F$;

(F2) $A \in F$ and $A \subseteq B$ implies $B \in F$;

(F3) $A, B \in F$ implies $A \cap B \in F$.

For $x \in X$, the principal filter at x is $\dot{x} = \{A \in NS(X) : T_A(x) = 1, I_A(x) = 1, F_A(x) = 0\}$. Given two neutrosophic filters F and G, we write $F \le G$ ("G is finer than F") if $F \subseteq G$ as families.

2.3. Neutrosophic Topological Spaces

Definition 2.4 ([4]). A neutrosophic topology on X is a family $\tau \subseteq NS(X)$ satisfying: $0_x, 1_x \in \tau$; τ is closed under arbitrary unions and finite intersections. The pair (X, τ) is a neutrosophic topological space. For $x \in X$, the NS neighbourhood filter $N\tau(x)$ consists of all $A \in NS(X)$ such that some open $U \in \tau$ satisfies $U \subseteq A$ and $T_U(x) = 1, I_U(x) = 1, F_U(x) = 0$.

3. Neutrosophic Convergence Spaces

We now introduce the central objects of this paper.

Definition 3.1 (Neutrosophic Convergence Space). Let X be a non-empty set. A neutrosophic convergence structure on X is a function

$$\lambda : \{\text{neutrosophic filters on X}\} \to NS(X)$$

satisfying the following three axioms for all neutrosophic filters F, G on X:

(NC1) (Point filter). $\lambda(\dot{x}) \supseteq 1\{x\}$ for every $x \in X$; that is, $T\lambda(\dot{x})(x) = 1$, $I\lambda(\dot{x})(x) = 1$, $F\lambda(\dot{x})(x) = 0$.

(NC2) (Coarsening). If $F \leq G$ then $\lambda(G) \subseteq \lambda(F)$.

(NC3) (Join law). $\lambda(F \vee G) \supseteq \lambda(F) \cap \lambda(G)$, where $F \vee G$ is the filter generated by $\{A \cup B : A \in F, B \in G\}$.

The pair (X, λ) is called a neutrosophic convergence space (NCS). We say that F converges to $p \in X$ (written $F \to_\lambda p$) if $T\lambda(F)(p) > 0$. We say F strongly converges to p if $T\lambda(F)(p) = 1$ and $I\lambda(F)(p) = 1$.

Remark 3.1. Axiom (NC2) formalises that a finer filter retains all limit information of a coarser one — the neutrosophic convergence analogue of the classical condition that every filter finer than a convergent filter also converges to the same point. Axiom (NC3) ensures that the join of two filters converges at least where both individually converge, component-wise.

Example 3.1. Let X be any set. Define $\lambda^d(F) = 1_x$ if $F = \dot{x}$ for some x, and $\lambda^d(F) = 0_x$ otherwise. Then (X, λ^d) is a NCS, called the discrete neutrosophic convergence space. Only principal filters converge, and they converge strongly to their base point.

Example 3.2. Define $\lambda_i(F) = 1_x$ for every filter F. Then (X, λ_i) is a NCS called the indiscrete neutrosophic convergence space, in which every filter strongly converges to every point.

Definition 3.2. Let (X, λ) and (Y, μ) be NCSs. A function $f : X \to Y$ is NS-continuous if for every neutrosophic filter F on X, the image filter f(F) — generated by $\{B \in NS(Y) : f^{-1}(B) \in F\}$ — satisfies

$$f(\lambda(F)) \subseteq \mu(f(F)),$$

where f(A) denotes the image NS defined by $T_{f(A)}(y) = \sup\{T_A(x) : f(x) = y\}$ (and analogously for I and F).

4. The Category NS-Conv

Definition 4.1. The category NS-Conv has:

- Objects: all neutrosophic convergence spaces (X, λ);
- Morphisms: NS-continuous maps $f : (X, \lambda) \to (Y, \mu)$;
- Composition: ordinary function composition (NS-continuity is preserved under composition, as shown in Proposition 4.1);
- Identities: $id_x : (X, \lambda) \to (X, \lambda)$, which is NS-continuous since $id_x(F) = F$.

Proposition 4.1. If $f : (X, \lambda) \to (Y, \mu)$ and $g : (Y, \mu) \to (Z, \nu)$ are NS-continuous, then $g \circ f : (X, \lambda) \to (Z, \nu)$ is NS-continuous.

Proof. Let F be a neutrosophic filter on X. NS-continuity of f gives $f(\lambda(F)) \subseteq \mu(f(F))$. Applying g and using NS-continuity of g with the filter f(F) on Y: $g(f(\lambda(F))) \subseteq g(\mu(f(F))) \subseteq \nu(g(f(F)))$. Since $g(f(\lambda(F))) = (g\circ f)(\lambda(F))$ and $g(f(F)) = (g\circ f)(F)$, we obtain $(g\circ f)(\lambda(F)) \subseteq \nu((g\circ f)(F))$, as required. □

Definition 4.2. Let $\{(X_i, \lambda_i)\}_i\in^I$ be a family of NCSs. The product NCS is $(\prod_i X_i, \lambda\Pi)$, where $\lambda\Pi(F) = \cap_i \lambda_i(\pi_i(F))$, with π_i the i-th projection and the product of NSs taken component-wise.

5. Embedding NS-Top into NS-Conv

Definition 5.1. Let (X, τ) be a neutrosophic topological space. Define $\lambda\tau : F \mapsto \cup\{1\{p\} : N\tau(p) \leq F\}$, where the neutrosophic union is taken over all points p whose neighbourhood filter is coarser than F. Formally,

$$T\lambda\tau(F)(p) = 1 \text{ if } N\tau(p) \leq F, \text{ and } 0 \text{ otherwise,}$$

and analogously $I\lambda\tau(F)(p) = 1$, $F\lambda\tau(F)(p) = 0$ when $N\tau(p) \leq F$.

Lemma 5.1. The function $\lambda\tau$ defined above is a neutrosophic convergence structure on X, i.e., $(X, \lambda\tau)$ is a NCS.

Proof. (NC1): For the principal filter $\dot{x}$, every open set $U \ni x$ satisfies $T_U(x) = 1$, so $N\tau(x) \leq \dot{x}$. Hence $T\lambda\tau(\dot{x})(x) = 1$.

(NC2): If $F \leq G$ and $N\tau(p) \leq F$, then $N\tau(p) \leq G$, so every limit point of G is a limit point of F; hence $\lambda\tau(G) \subseteq \lambda\tau(F)$.

(NC3): If $N\tau(p) \leq F$ and $N\tau(p) \leq G$, then $N\tau(p) \leq F \vee G$, since every $A \cup B$ with $A \in F$, $B \in G$ is a neighbourhood of p. Thus $\lambda\tau(F) \cap \lambda\tau(G) \subseteq \lambda\tau(F \vee G)$. □

Theorem 5.1. The assignment $J(X, \tau) = (X, \lambda\tau)$ on objects and $J(f) = f$ on morphisms defines a full and faithful functor J : NS-Top → NS-Conv.

Proof. Well-defined on objects: by Lemma 5.1.

Functoriality: $J(id) = id$ and $J(g\circ f) = J(g)\circ J(f)$ follow since morphisms are unchanged.

Faithfulness: If $J(f) = J(g)$ then $f = g$ as functions.

Fullness: Let $h : (X, \lambda\tau) \to (Y, \lambda\sigma)$ be NS-continuous in NS-Conv. We must show $h : (X, \tau) \to (Y, \sigma)$ is NS-continuous in NS-Top, i.e., $h^{-1}(V) \in \tau$ for every $V \in \sigma$. Fix $V \in \sigma$ and $x \in X$ with $T_V(h(x)) = 1$. The filter $N\tau(x)$ satisfies $N\tau(x) \leq \dot{x}$, so by NS-continuity of h, $h(N\tau(x)) \leq h(\dot{x})$, and $h(\dot{x})$ converges to $h(x)$ in $(Y, \lambda\sigma)$. Since $V \in N\sigma(h(x))$, we obtain $h^{-1}(V) \in N\tau(x)$, hence $h^{-1}(V) \in \tau$.

6. Topological Reflection and the Adjunction T ⊣ J

Definition 6.1. Let (X, λ) be a NCS. Define the topological modification $T(X, \lambda) = (X, \tau\lambda)$, where

$$\tau\lambda = \{U \in NS(X) : \text{for all filters } F \text{ and all } x \in X, \text{ if } T_U(x) = 1 \text{ and } T\lambda(F)(x) = 1, \text{ then } U \in F\}.$$

That is, U is open in $\tau\lambda$ exactly when: whenever a filter converges (in truth) to a point x with $T_U(x) = 1$, then U must belong to that filter.

Lemma 6.1. $\tau\lambda$ is a neutrosophic topology on X.

Proof. 1_x trivially belongs to every filter and 0_x satisfies the condition vacuously. If $U, V \in \tau\lambda$ and $F \to_\lambda x$ with $T_{U\cap V}(x) = 1$, then $T_U(x) = T_V(x) = 1$, so $U, V \in F$, hence $U \cap V \in F$ by (F3). Unions follow similarly using (F2). □

Theorem 6.1. The functor T : NS-Conv → NS-Top defined on objects by $T(X, \lambda) = (X, \tau\lambda)$ and on morphisms by $T(f) = f$ is left adjoint to J : NS-Top → NS-Conv. The unit of the adjunction is the identity natural transformation, and the counit is $\varepsilon(X,\tau) = id_x$, a NS-continuous map $(X, \lambda\tau) \to (X, \tau)$.

Proof. We verify the universal property. Given a NCS (X, λ) and a NS-topological space (Y, σ), a morphism $f : (X, \lambda) \to J(Y, \sigma)$ in NS-Conv is NS-continuous from (X, λ) to $(Y, \lambda\sigma)$. We claim f is also NS-continuous $(X, \tau\lambda) \to (Y, \sigma)$ in NS-Top: for any $V \in \sigma$ and $x \in X$ with

$Tv(f(x)) = 1$, since f is NS-continuous in NS-Conv and $F \to\lambda$ x implies $f(F) \to\lambda\sigma f(x)$, we get $V \in f(F)$, hence $f^{-1}(V) \in F$. This holds for all such F, so $f^{-1}(V) \in \tau\lambda$. The correspondence $f \mapsto f$ is the required natural bijection

$$\text{NS-Conv}((X, \lambda), J(Y, \sigma)) \cong \text{NS-Top}(T(X, \lambda), (Y, \sigma)).$$

7. Cartesian Closure of NS-Conv

Definition 7.1. Let (X, λ) and (Y, μ) be NCSs. The function space $[X \to Y] = ([X, Y], \nu)$ has underlying set $[X, Y] = \{\text{NS-continuous } f : X \to Y\}$ and convergence structure: a filter Φ on $[X, Y]$ converges to $f_0 \in [X, Y]$ under ν if for every neutrosophic filter $F \to\lambda$ x, the evaluation filter $ev(\Phi, F) = \{C \in NS(Y) : \exists\, A \in F, \{g : g(A) \subseteq C\} \in \Phi\}$ satisfies $ev(\Phi, F) \to\mu f_0(x)$.

Theorem 7.1. The category NS-Conv is Cartesian closed: for any NCSs (X, λ), (Y, μ), (Z, ν), there is a natural NS-isomorphism

$$\text{NS-Conv}((Z, \nu) \times (X, \lambda), (Y, \mu)) \cong \text{NS-Conv}((Z, \nu), [X \to Y]).$$

Proof sketch. The bijection sends $f : (Z\times X, \nu\times\lambda) \to (Y, \mu)$ to its transpose $\hat{f} : Z \to [X, Y]$, $\hat{f}(z)(x) = f(z, x)$. NS-continuity of f in both arguments transfers to NS-continuity of $\hat{f}$ into the function-space convergence structure ν defined in Definition 7.1. The inverse sends $g : Z \to [X, Y]$ to the evaluation $ev \circ (g \times id_x)$. Naturality in all three arguments follows from the component-wise definition of NS-continuity.

Remark 7.1. The category NS-Top is not Cartesian closed in general, as the standard counterexample (the function space of continuous maps between NS-topological spaces need not carry a natural NS-topology making evaluation jointly continuous) transfers from the classical setting. Theorem 7.1 thus identifies NS-Conv as strictly more expressive than NS-Top.

8. Separation Axioms in NS-Conv

Definition 8.1. Let (X, λ) be a NCS.

(NS-T0) (X, λ) is NS-T0 if for all $x \neq y$ in X, there exists a neutrosophic filter F such that $F \to\lambda$ x but $T\lambda(F)(y) = 0$.

(NS-T1) (X, λ) is NS-T1 if for all $x \neq y$, there exist filters F and G such that $F \to\lambda$ x, $T\lambda(F)(y) = 0$, $G \to\lambda$ y, and $T\lambda(G)(x) = 0$.

(NS-T2) (X, λ) is NS-Hausdorff (NS-T2) if whenever $F \to\lambda$ x and $F \to\lambda$ y, then $T1\{x\}(y) = 1$, i.e., x = y. Equivalently, every neutrosophic filter has at most one strong limit.

Theorem 8.1. For any NCS (X, λ):

$$\text{NS-T2} \Rightarrow \text{NS-T1} \Rightarrow \text{NS-T0}.$$

Moreover, neither implication reverses in general.

Proof. NS-T2 ⇒ NS-T1: If (X, λ) is NS-Hausdorff and $x \neq y$, then no filter can converge to both. Taking F to be the neighbourhood-type filter at x and G the neighbourhood-type filter at y gives filters satisfying the NS-T1 conditions directly. NS-T1 ⇒ NS-T0 is immediate from the definitions.

For non-reversals: Example 3.2 is NS-T0 but not NS-T1 (every filter converges to every point). A two-point space with a carefully chosen asymmetric convergence structure witnesses NS-T1 without NS-T2. □

Proposition 8.1. A NCS (X, λ) is NS-Hausdorff if and only if the diagonal $\Delta = \{\langle x, x, 1, 1, 0\rangle : x \in X\}$ is closed in $(X\times X, \lambda\times\lambda)$ in the sense that its complement is open in $\tau\lambda\times\lambda$.

9. The Indeterminacy-Monotone Limit Property

We now establish a phenomenon that is exclusively neutrosophic. It cannot occur in fuzzy or intuitionistic fuzzy convergence spaces, where indeterminacy is absent.

Theorem 9.1. Let (X, λ) be a NCS and let $F \leq G$ be neutrosophic filters (so G is finer than F). Then for all $p \in X$:

$$T\lambda(G)(p) \leq T\lambda(F)(p) \quad \text{and} \quad I\lambda(G)(p) \leq I\lambda(F)(p). \qquad (1)$$

In words: passing to a finer filter does not increase the truth or indeterminacy of any limit point; indeterminacy is non-increasing as filters are refined.

Proof. By axiom (NC2), $F \leq G$ implies $\lambda(G) \subseteq \lambda(F)$ in the neutrosophic inclusion order. By Definition 2.2, $\lambda(G) \subseteq \lambda(F)$ means $T\lambda(G)(p) \leq T\lambda(F)(p)$, $I\lambda(G)(p) \leq I\lambda(F)(p)$, and $F\lambda(G)(p) \geq F\lambda(F)(p)$ for all $p \in X$. The first two inequalities give (1).

Remark 9.1. The inequality $I\lambda(G)(p) \leq I\lambda(F)(p)$ has no counterpart in fuzzy or intuitionistic fuzzy convergence theory, since those frameworks carry no indeterminacy component. Theorem 9.1 states that as we gather more information (pass to a finer filter), the uncertainty about whether p is a limit point decreases. This makes NCS a natural framework for modelling convergence under epistemic uncertainty — the indeterminacy quantifies "how undecided" the system is about convergence at p, and this ambiguity can only diminish as the filter becomes finer.

Corollary 9.1.1. In a NS-Hausdorff NCS, if G is the ultrafilter refinement of F and F converges to p, then $I\lambda(G)(p) = 0$, i.e., ultrafilter limits are completely determinate.

10. Comparison with Related Frameworks

Table 1: Comparison with Related Frameworks (Conv = classical convergence spaces; FConv = fuzzy convergence spaces [9]; NS-Top = neutrosophic topological spaces [4]; NS-Conv = this paper)

Property	Conv	FConv	NS-Top	NS-Conv
Three-component membership	✗	✗	✓	✓
Filter-based convergence	✓	✓	✗	✓
Cartesian closed	✓	✓	✗	✓
Full embedding of NS-Top	—	—	✓	✓
Topological reflection	✓	✓	—	✓
Indeterminacy-monotone limits	✗	✗	✗	✓
Separation hierarchy	✓	✓	✓	✓

Table 1 summarises how the neutrosophic convergence framework developed here compares to classical convergence spaces, fuzzy convergence spaces, and neutrosophic topological spaces.

The table highlights that NS-Conv is the only framework simultaneously possessing three-component membership, filter-based convergence, and Cartesian closure. The indeterminacy-monotone limit property (Theorem 9.1) is exclusive to NS-Conv since it requires the independent indeterminacy component present only in neutrosophic settings. Furthermore, the adjunction $T \dashv J$ established in Theorem 6.1 shows that NS-Conv and NS-Top are not merely related by inclusion but are connected by a precise categorical duality, mirroring the deep relationship between classical convergence spaces and topological spaces that has been central to categorical topology for six decades.

11. Conclusions and Open Problems

We have established the foundations of neutrosophic convergence space theory, introducing the category NS-Conv, proving its full embedding of NS-Top and its Cartesian closure, and identifying several results — particularly the adjunction T ⊣ J and the indeterminacy-monotone limit property — that are genuinely new and have no analogues in prior fuzzy or intuitionistic fuzzy theories.

We close with the following open problems for future research:

(1) Neutrosophic compactness in NCS. Characterise compact NCSs via the neutrosophic analogue of the cluster-point property for filters.
(2) Uniform neutrosophic convergence. Define neutrosophic uniform convergence structures and study completeness and completion functors.
(3) Reflective subcategories. Determine which subcategories of NS-Conv are reflective, and characterise those corresponding to known classes of NS-topological spaces.
(4) Exponential law for NS-Top. Although NS-Top is not Cartesian closed in general, identify conditions on NS-topological spaces under which the exponential object exists within NS-Top.
(5) Higher neutrosophic convergence. Extend the theory to n-fold neutrosophic sets (refined neutrosophic sets with split T, I, F components) and study the corresponding convergence categories.

Funding: This research received no external funding.

Conflicts of Interest: The authors declare no conflict of interest.

References

[1] F. Smarandache, Neutrosophy: Neutrosophic Probability, Set, and Logic. American Research Press, Rehoboth, NM, 1998.

[2] L.A. Zadeh, “Fuzzy sets,” Information and Control, vol. 8, no. 3, pp. 338–353, 1965.

[3] K.T. Atanassov, “Intuitionistic fuzzy sets,” Fuzzy Sets and Systems, vol. 20, no. 1, pp. 87–96, 1986.

[4] A.A. Salama and S.A. Alblowi, "Neutrosophic set and neutrosophic topological spaces," IOSR Journal of Mathematics, vol. 3, no. 4, pp. 31–35, 2012.

[5] S. Milles and L. Hammami, "Ideals and filters on neutrosophic topologies generated by neutrosophic relations," Axioms, vol. 13, no. 5, p. 292, 2024.

[6] M.Z. Hameed, Z. Ahmad, S. Ali and M. Kamran, "Category theory in neutrosophic SuperHyper BCI-algebras," International Journal of Neutrosophic Science, vol. 25, no. 2, pp. 254–262, 2025.

[7] H.J. Kowalsky, "Limesräume und Komplettierung," Mathematische Nachrichten, vol. 12, pp. 301–340, 1954.

[8] C.H. Cook and H.R. Fischer, "On equicontinuity and continuous convergence," Mathematische Annalen, vol. 159, pp. 94–104, 1965.

[9] R. Lowen, "Fuzzy convergence," Journal of Mathematical Analysis and Applications, vol. 112, pp. 25–38, 1985.

[10] D. Çoker and M. Demirci, "An introduction to intuitionistic fuzzy topological spaces in Šostak's sense," Busefal, vol. 67, pp. 67–76, 1996.

[11] H. Wang, F. Smarandache, Y.Q. Zhang and R. Sunderraman, "Single valued neutrosophic sets," Multispace and Multistructure, vol. 4, pp. 410–413, 2010.

[12] I. Arockiarani and A. Antony Crispin Sweety, "Filters and ideals in neutrosophic lattices," International Journal of Mathematics and its Applications, vol. 4, no. 1, pp. 79–90, 2016.

Received: Feb. 15, 2026. Accepted: Sept. 5, 2026.

Neutrosophic Sets and Systems, Vol. 102, 2027
University of New Mexico

Plithogenic Quasigroups with Application to Decision Making

A. Oyem [1], S. E. Ogunfeyitimi [2]

[1] Department of Mathematics, University of Benin, Nigeria. Email: anthony.oyem@uniben.edu
[2] Department of Mathematics, University of Benin, Nigeria. Email: evans.ogunfeyitimi@uniben.edu

Abstract: In this paper, we extend the concept of neutrosophic sets by introducing plithogenic quasigroups by associating a quasigroup $(Q, \cdot)$ with a plithogenic structure: attributes V, dominant v_D, contradiction degrees $c_i \in [0, 1]$, and neutrosophic degrees $d(x, v_i)$. The plithogenic product $\cdot_P$ aggregates componentwise via $(1 - c_i)t_N + c_i s_N$ with $t_N = \min$, $s_N = \max$. We prove that $(P(Q), \cdot_P)$ is a quasigroup and its parastrophes; the Latin square property lifts, guaranteeing unique solvability of $a \cdot_P x = b$. Solvability holds iff each component b_i lies in the c_i-weighted interval between a_i and x_i: $c_i = 1$ forces $b_i \geq a_i$ while $c_i = 0$ forces $b_i \leq a_i$. We characterize isotopies, homomorphisms, and nuclei, showing $0 < c_i < 1$ yields trivial nuclei and contradicts associativity. We applied plithogenic quasigroup properties to portfolio selection with V = {Risk, Return, Liquidity}, setting $c_{Risk} = 0.9$ blocks buy signals whereas $c_{Risk} = 0.1$ enables solvability, where c_i functions as a parameter connecting algebraic feasibility to risk policy in decision making.

Keywords: Plithogenic set, quasigroup, neutrosophic set, contradiction degree, non-associative algebra, Latin square.

1. Introduction

Quasigroups are algebraic structures that generalize groups by dropping the associativity requirement. The study of quasigroups and loops has a history spanning more than two centuries. Its origins can be traced to Euler's 1782 conjecture on the non-existence of certain pairs of mutually orthogonal Latin squares.

Algebraic structures that model uncertainty and contradiction have become central to decision science, particularly in multi-criteria problems where attributes conflict. Neutrosophic sets, introduced by Smarandache [29], capture truth, indeterminacy, and falsity degrees, while plithogenic sets [28] refine this by assigning contradiction degrees $c(v_i, v_D) \in [0, 1]$ between each attribute v_i and a dominant attribute v_D. These degrees govern how strongly an attribute opposes the dominant one during aggregation.

While plithogenic aggregation has been studied for set-theoretic and matrix operations, its extension to non-associative algebraic systems remains unexplored. Quasigroups are precisely the non-associative generalization of groups: they guarantee unique solvability of $a \cdot x = b$ and $y \cdot a = b$ but need not satisfy $(xy)z = x(yz)$. This property makes them ideal for modeling operations where the order of application matters — for example, sequential portfolio adjustments, layered encryption, or step-wise medical treatments.

We introduce plithogenic quasigroups $(P(Q), \cdot P)$ by equipping a base quasigroup $(Q, \cdot)$ with an attribute set V, contradiction degrees ci, and componentwise aggregation using neutrosophic t-norm tN = min and s-norm sN = max. The plithogenic product is defined as

$$d(x \cdot P\ y, vi) = (1 - ci) \min\{d(x, vi), d(y, vi)\} + ci \max\{d(x, vi), d(y, vi)\},$$

so that ci = 0 yields pure consensus while ci = 1 yields pure dominance of the higher degree.

The theory of neutrosophic soft sets has developed significantly, studied by many authors since it was introduced by Maji [16]. Broumi and Smarandache studied its interval-valued and intuitionistic [10] neutrosophic soft sets. Oyem et al. [23] introduced the Neutrosophic quasigroup, which extends neutrosophic sets' properties to non-associative algebraic structures known as quasigroups. Its algebraic properties have been studied by Broumi et al. [11, 12], who provided new operations and examined distributivity and associativity. Its applications to incomplete data were considered by Saha et al. [25].

Also, fuzzy soft sets and their decision-making uses laid groundwork for algebraic treatments in soft and fuzzy settings. Recent developments include Soft Neutrosophic versions of algebraic structures [4, 5, 9, 26, 6] and Neutrosophic Soft versions [17, 7, 32, 1], indicating that soft set theory offers a natural generalization of neutrosophic sets to algebra.

Oyem et al. [20, 21, 22, 24] introduced the notion of order for finite soft quasigroups and applied it to egalitarianism. They established several algebraic relationships between the order of a quasigroup and the order of its associated soft quasigroups, and, in other related work, investigated various algebraic properties of soft quasigroups and soft parastrophes, showing that certain operations are not distributive over one another.

2. Preliminaries

This section provides a brief review of the basic concepts and known results on quasigroups and soft sets.

2.1 Quasigroups and Parastrophy

Definition 2.1 (Quasigroup). Let Q be a nonempty set and let (·) be a binary operation on Q. The pair (Q, ·) is called a groupoid or magma.

If for all a, b ∈ Q the equations $a \cdot x = b$ and $y \cdot a = b$ have unique solutions x, y ∈ Q, then (Q, ·) is a quasigroup.

A quasigroup (Q, ·) for which there exists a unique element e ∈ Q such that $x \cdot e = e \cdot x = x$ for all x ∈ Q is called a loop. The element e is the identity element of the loop.

Throughout this paper we write xy for $x \cdot y$, and we adopt the convention that · has lower precedence than juxtaposition. For example, $x \cdot yz$ means $x(yz)$.

Definition 2.2. For a fixed element x ∈ Q, the left translation Lx and right translation Rx are the maps Q → Q defined by $yLx = x \cdot y$, $yRx = y \cdot x$.

A groupoid is a quasigroup if and only if Lx and Rx are permutations of Q for all x ∈ Q. Since Lx and Rx are bijective, their inverses exist. We define the left and right divisions by $x \backslash y = yLx^{-1}$, $x/y = xRy^{-1}$, so that $x \backslash y = z \Leftrightarrow x \cdot z = y$, and $x/y = z \Leftrightarrow z \cdot y = x$.

In the language of universal algebra, a quasigroup can be presented as an algebra (Q, ·, \, /) of type (2, 2, 2). For more on quasigroups, readers can check [3, 30].

Definition 2.3 (Subquasigroup) (Pflugfelder [31]). Let (Q, ·) be a groupoid, and let H ⊆ Q with H ≠ ∅. If (H, ·) is itself a groupoid under the same operation, then H is called a subgroupoid of Q.

If (Q, ·) is a quasigroup and (H, ·) is a quasigroup, then H is called a subquasigroup of Q. In either case we write H ≤ Q.

Definition 2.4 (Plithogenic Set [28, 27, 2, 15, 29]). Let U be a universe of discourse and let P ⊆ U. A plithogenic set P is defined as the quintuple P = (P, V, vD, d, c) where:

1. P is the set of elements;

2. V = {v1, v2, …, vm} is a set of attributes characterizing the elements of P;

3. vD ∈ V is the dominant attribute, used as a reference for measuring contradiction;

4. $d : P \times V \to [0, 1]^3$ is the degree of appurtenance function, such that for each x ∈ P and vi ∈ V, d(x, vi) = (ti(x), ii(x), fi(x)) denotes the neutrosophic degrees of truth, indeterminacy, and falsity of element x with respect to attribute vi;

5. $c : V \times V \to [0, 1]$ is the contradiction degree function, where $c(v_i, v_j)$ measures the degree to which attribute v_i contradicts attribute v_j. In particular, we set $c_i = c(v_i, v_D)$ as the contradiction degree of v_i relative to the dominant attribute v_D, with $c(v_D, v_D) = 0$.

For any $x, y \in P$, the plithogenic aggregation with respect to attribute v_i is given by

$$d_{agg}(x, y, v_i) = (1 - c_i)\, t_N\{d(x, v_i), d(y, v_i)\} + c_i\, s_N\{d(x, v_i), d(y, v_i)\},$$

where t_N and s_N are a neutrosophic t-norm and s-norm, respectively.

3. Plithogenic Quasigroups

Definition 3.1 (Plithogenic Quasigroup). Let $(Q, \cdot)$ be a quasigroup, $V = \{v_1, \ldots, v_m\}$ an attribute set with dominant attribute $v_D \in V$, and $c_i = c(v_i, v_D) \in [0, 1]$ the contradiction degree of v_i relative to v_D. Choose neutrosophic t-norm $t_N = \min$ and s-norm $s_N = \max$. For each $x \in Q$, let $d(x, v_i) = (t_i, i_i, f_i) \in [0, 1]^3$ denote the neutrosophic degrees of truth, indeterminacy, and falsity for attribute v_i.

A plithogenic quasigroup over Q is then the structure $P(Q) = (Q, V, v_D, d, c, \cdot_P)$, where the plithogenic product $(\cdot_P)$ is defined for $x, y \in P(Q)$ by:

1. Base: $x \cdot_P y = x \cdot y$ in $(Q, \cdot)$;

2. Degrees: for each $v_i \in V$, $d(x \cdot_P y, v_i) = (1 - c_i)\, t_N\{d(x, v_i), d(y, v_i)\} + c_i\, s_N\{d(x, v_i), d(y, v_i)\}$.

Theorem 3.1 (Closure of Latin Square Property). If $(Q, \cdot)$ is a quasigroup, then $(P(Q), \cdot_P)$ is a quasigroup. That is, for any $a, b \in P(Q)$, the equations $a \cdot_P x = b$ and $y \cdot_P a = b$ have unique solutions $x, y \in P(Q)$ whenever they are solvable.

Proof. Since $(Q, \cdot)$ is a quasigroup, there exists a unique $x_0 \in Q$ such that $a \cdot x_0 = b$ in the base. Construct $x \in P(Q)$ with base element x_0.

For each $v_i \in V$, let $a_i = d(a, v_i)$, $b_i = d(b, v_i)$, and set $x_i = d(x, v_i)$. By definition of $\cdot_P$, $b_i = (1 - c_i)\, t_N\{a_i, x_i\} + c_i\, s_N\{a_i, x_i\}$. For $t_N = \min$, $s_N = \max$, this equation has a unique solution x_i provided it exists. The argument for $y \cdot_P a = b$ is symmetric. Hence $(P(Q), \cdot_P)$ satisfies the Latin square property whenever solutions exist. □

Corollary 3.1 (Solvability Condition). Let $a, b \in P(Q)$ with $a_i = d(a, v_i)$ and $b_i = d(b, v_i)$ for $v_i \in V$. Equation $a \cdot_P x = b$ is solvable in $P(Q)$ if and only if for every $v_i \in V$ and each component $* \in \{t, i, f\}$,

$$x^*_i = (b^*_i - (1 - c_i)a^*_i) / c_i \quad \in [0,1], \quad \text{when } b^*_i \geq a^*_i;$$

$$x^*_i = (b^*_i - c_i a^*_i) / (1 - c_i) \quad \in [0,1], \quad \text{when } b^*_i < a^*_i;$$

with the convention that 0/0 is interpreted as any value in [0, 1] when $c_i = 0$ or $c_i = 1$. If any component $x^*_i \notin [0, 1]$, the equation has no solution in P(Q).

Example 3.1. Let Q = {e, a, b} with operation given by its Latin square:

·	e	a	b
e	e	a	b
a	a	b	e
b	b	e	a

Take attributes V = {Growth, Safety} with vD = Growth, cGrowth = 0, cSafety = 0.4. Define elements:

x1 = [e] : G(0.90, 0.10, 0.00), S(0.80, 0.10, 0.10),

x2 = [a] : G(0.60, 0.30, 0.10), S(0.90, 0.10, 0.00),

x3 = [b] : G(0.30, 0.40, 0.30), S(0.50, 0.30, 0.20).

The plithogenic product yields the following 3×3 Latin square (Table 1):

Table 1: Plithogenic 3×3 Latin square for (P(Q), ·P)

·P	x1	x2	x3
x1	e: G(0.90,0.10,0.00) S(0.80,0.10,0.10)	a: G(0.60,0.30,0.10) S(0.86,0.10,0.04)*	b: G(0.30,0.40,0.30) S(0.62,0.22,0.16)
x2	a: G(0.60,0.30,0.10) S(0.86,0.10,0.04)	b: G(0.30,0.40,0.30) S(0.62,0.22,0.16)	e: G(0.90,0.10,0.00) S(0.80,0.10,0.10)
x3	b: G(0.30,0.40,0.30) S(0.62,0.22,0.16)	e: G(0.90,0.10,0.00) S(0.80,0.10,0.10)	a: G(0.60,0.30,0.10) S(0.86,0.10,0.04)

Tables 2 and 3 verify uniqueness of solutions for right and left division:

Table 2: Right division test: x1 ·P x = x2

Test x	Base	Growth	Safety	= x2
x1	e	(0.90, 0.10, 0.00)	(0.80, 0.10, 0.10)	No

Test x	Base	Growth	Safety	= x2
x2	a	(0.60, 0.30, 0.10)	(0.86, 0.10, 0.04)	Yes
x3	b	(0.30, 0.40, 0.30)	(0.62, 0.22, 0.16)	No

Table 3: Left division test: y ·P x1 = x2

Test y	Base	Growth	Safety	= x2
y = x1	e	(0.90, 0.10, 0.00)	(0.80, 0.10, 0.10)	No
y = x2	a	(0.60, 0.30, 0.10)	(0.86, 0.10, 0.04)	Yes
y = x3	b	(0.30, 0.40, 0.30)	(0.62, 0.22, 0.16)	No

Remark 3.1 (Contradiction Degree as Risk Dial)

ci determines how we can combine the attribute vi. If ci = 0: strict AND, both inputs must be high. If ci = 1: strict OR, the higher input prevails. If 0 < ci < 1: smooth interpolation between the two. A larger ci also reduces solvability if bi < ai by giving weak inputs veto power, making ci a direct measure of risk tolerance.

Corollary 3.1 shows that ci also governs solvability: large ci restricts solutions when bi < ai, acting as a veto. Thus ci adjusts how risk preferences enter the algebraic structure.

Definition 3.2 (Plithogenic Quasigroup Homomorphism). Let P(Q1) = (Q1, V, vD, d1, c, ·P1) and P(Q2) = (Q2, V, vD, d2, c, ·P2) be two plithogenic quasigroups over base quasigroups (Q1, ·1) and (Q2, ·2) with the same attribute set V, dominant attribute vD, and contradiction degrees c.

A map φ : P(Q1) → P(Q2) is a plithogenic quasigroup homomorphism if:

1. Base homomorphism: for all x, y ∈ P(Q1), φ(x ·P1 y) = φ(x) ·P2 φ(y) on the base elements. That is, the restriction φ0 : Q1 → Q2 given by φ0(x) = φ(x) is a quasigroup homomorphism.

2. Degree preservation: for all x ∈ P(Q1) and all vi ∈ V, d2(φ(x), vi) = d1(x, vi). That is, φ preserves the neutrosophic degrees (t, i, f) for every attribute.

If φ0 is bijective, we call φ a plithogenic quasigroup isomorphism, and write P(Q1) ≅ P(Q2).

Corollary 3.2. If $\varphi : P(Q1) \rightarrow P(Q2)$ is a plithogenic quasigroup homomorphism, then for any a, b ∈ P(Q1), the unique solution x to a $\cdot P1$ x = b is mapped to the unique solution to $\varphi(a) \cdot P2$ $y = \varphi(b)$, namely $y = \varphi(x)$.

Definition 3.3 (Kernel and Image of a Plithogenic Quasigroup Homomorphism). Let φ : P(Q1) → P(Q2) be a plithogenic quasigroup homomorphism as in Definition 3.2, and let $\varphi0$: Q1 → Q2 be the induced base homomorphism.

1. The kernel of φ is the substructure of P(Q1) defined by $\ker(\varphi) = \{x \in P(Q1) : \varphi(x) = e2\}$, where e2 ∈ P(Q2) is a fixed element whose base is the identity of (Q2, ·2) and d2(e2, vi) = (1, 0, 0) for all vi ∈ V. If (Q2, ·2) has no identity, fix any distinguished element e2 ∈ P(Q2).

2. The image of φ is the substructure of P(Q2) given by $\mathrm{Im}(\varphi) = \{\varphi(x) \in P(Q2) : x \in P(Q1)\}$. Then $\mathrm{Im}(\varphi)$ is a plithogenic subquasigroup of P(Q2).

Proposition 3.1 (First Isomorphism Theorem for Plithogenic Quasigroups). Let $\varphi : P(Q1) \rightarrow$ P(Q2) be a surjective plithogenic quasigroup homomorphism. Then there exists a plithogenic quasigroup congruence $\sim\varphi$ on P(Q1) defined by $x \sim\varphi\, y \Leftrightarrow \varphi(x) = \varphi(y)$, and we have a plithogenic quasigroup isomorphism $P(Q1)/\sim\varphi \cong P(Q2)$. Moreover, $x \sim\varphi\, y$ if and only if $x \cdot P1\, y^{-1} \in \ker(\varphi)$ when (Q1, ·1) is a loop, and d1(x, vi) = d1(y, vi) for all vi ∈ V.

Remark 3.2. Unlike groups, $\ker(\varphi)$ in a quasigroup is not automatically a subquasigroup, because quasigroups need not have identities or inverses. However, $\ker(\varphi)$ is a normal subquasigroup in the sense of quasigroup theory if (Q1, ·1) is a loop. The degree preservation condition ensures that $\ker(\varphi)$ consists of elements that are neutrosophically indistinguishable from the distinguished element e2.

Example 3.2 (Plithogenic Quasigroup Homomorphism). Let P(Q1) be the plithogenic quasigroup from Example 3.1, with base Q1 = {e, a, b} and elements x1, x2, x3 as defined there.

Define a second base quasigroup (Q2, ∘) by Q2 = $\{\bar{e}, \bar{a}, \bar{b}\}$ with an isomorphic Cayley table, via $\varphi0(e) = \bar{e}$, $\varphi0(a) = \bar{a}$, $\varphi0(b) = \bar{b}$.

Construct P(Q2) using the same attributes V = {Growth, Safety} and contradiction degrees cGrowth = 0, cSafety = 0.4. Define elements y1 = $[\bar{e}]$, y2 = $[\bar{a}]$, y3 = $[\bar{b}]$ with the same degree triples as x1, x2, x3, respectively.

Define $\varphi : P(Q1) \rightarrow P(Q2)$ by $\varphi(xi) = yi$ for i = 1, 2, 3. Then φ is a plithogenic quasigroup homomorphism because:

1. Base homomorphism: φ_0 is an isomorphism of quasigroups, so $\varphi(x_i \cdot_{P1} x_j) = \varphi(x_i) \cdot_{P2} \varphi(x_j)$ for all i, j. For instance, $\varphi(x_1 \cdot_{P1} x_2) = \varphi(x_2) = y_2 = y_1 \cdot_{P2} y_2 = \varphi(x_1) \cdot_{P2} \varphi(x_2)$.

2. Degree preservation: by construction, $d_1(x_i, v) = d_2(y_i, v)$ for all i and $v \in V$. For example, $d_1(x_1, \text{Growth}) = (0.90, 0.10, 0.00) = d_2(y_1, \text{Growth})$.

Hence $P(Q_1) \cong P(Q_2)$ as plithogenic quasigroups. Moreover, $\ker(\varphi) = \{x_1\}$, because $\varphi(x_1) = y_1 = e_2$, and $\mathrm{Im}(\varphi) = P(Q_2)$.

Example 3.3 (Non-isomorphic Plithogenic Homomorphism). Let $P(Q_1)$ be as in Example 3.1 with x_1, x_2, x_3. Consider a base quasigroup $(Q_2, *)$ with $Q_2 = \{\hat{e}, \hat{a}\}$ and its 2×2 Cayley table, and construct $P(Q_2)$ with the same V = {Growth, Safety}, $c_{Growth} = 0$, $c_{Safety} = 0.4$.

Suppose we try to define a base homomorphism $\varphi_0 : Q_1 \to Q_2$ by $\varphi_0(e) = \hat{e}$, $\varphi_0(a) = \hat{a}$, $\varphi_0(b) = \hat{a}$, so that a and b collapse to the same base element. For φ to lift to a plithogenic quasigroup homomorphism, we must have $d_1(x, v_i) = d_2(\varphi(x), v_i)$ for all x and v_i.

But in $P(Q_1)$ we have $d_1(x_2, \text{Growth}) = (0.60, 0.30, 0.10)$ and $d_1(x_3, \text{Growth}) = (0.30, 0.40, 0.30)$. Since $\varphi(x_2) = \varphi(x_3) = z$ for some $z \in P(Q_2)$ with base $\hat{a}$, degree preservation forces $d_2(z, \text{Growth}) = (0.60, 0.30, 0.10) = (0.30, 0.40, 0.30)$, which is impossible. Therefore no plithogenic homomorphism exists that collapses x_2 and x_3.

If instead we try to collapse x_1 and x_3 by setting $\varphi_0(e) = \varphi_0(b) = \hat{e}$, we need $d_1(x_1, \text{Safety}) = (0.80, 0.10, 0.10) = d_1(x_3, \text{Safety}) = (0.50, 0.30, 0.20)$, again impossible.

Hence the only plithogenic homomorphisms from $P(Q_1)$ are injective on elements with distinct degrees. In this example, any φ must send x_1, x_2, x_3 to three distinct elements of $P(Q_2)$ with matching degrees. If $P(Q_2)$ has only two elements, no plithogenic homomorphism exists.

Remark 3.3 (Degrees Restrict Homomorphisms). In classical quasigroups, any surjective base homomorphism works. For plithogenic quasigroups, degree preservation is a strong constraint: you cannot identify two elements unless all their (t, i, f) vectors agree for every attribute. Thus c_i and d together turn the algebra into a labeled structure where homomorphisms must respect the data. This models the real requirement that you cannot merge two portfolios with different risk scores.

Definition 3.4 (Plithogenic Quasigroup Parastrophes). Let $P(Q) = (Q, V, vD, d, c, \cdot_P)$ be a plithogenic quasigroup over base quasigroup $(Q, \cdot)$. A quasigroup $(Q, \cdot)$ has exactly six parastrophes determined by permuting the ternary relation $E(x, y, z) \Leftrightarrow x \cdot y = z$: the main operation ·, right division /, left division \, the opposite ∘, opposite right division //, and opposite left division \ \.

The plithogenic quasigroup parastrophes of P(Q) are the six operations ·P, /P, \P, ∘P, //P, \ \P on P(Q), defined by (1) Base parastrophes: for each operation, the base elements satisfy the corresponding parastrophe of (Q, ·); and (2) Degree rule: for all vi ∈ V, the neutrosophic degrees are computed by the same aggregation formula, subject to the relation being consistent with the base parastrophe.

Theorem 3.2 (Closure of Parastrophes). If (P(Q), ·P) is a plithogenic quasigroup, then (P(Q), *P) is a plithogenic quasigroup for each parastrophe *P ∈ {/P, \P, ∘P, //P, \ \P}.

Proof. Each base parastrophe (Q, *) is a quasigroup. The degree rule for *P is identical to ·P, so solvability follows from Corollary 3.1 with x, y, z permuted. Uniqueness is inherited from the base. Hence (P(Q), *P) satisfies the Latin square property. □

Theorem 3.3 (Isotopy Invariance of Plithogenic Structure). Let (Q1, ·1) and (Q2, ·2) be isotopic quasigroups via (α, β, γ), i.e. α(x)·2β(y) = γ(x·1y) for bijections α, β, γ : Q1 → Q2. Let P(Q1) = (Q1, V, vD, d1, c, ·P1) be a plithogenic quasigroup. Define P(Q2) with degrees d2(α(x), vi) = d1(x, vi) for all x ∈ Q1, vi ∈ V. Then P(Q2) = (Q2, V, vD, d2, c, ·P2) is a plithogenic quasigroup, and the triple (α, β, γ) extends to a plithogenic isotopy P(Q1) ≃ P(Q2).

Proof. The base is an isotopy by hypothesis. Degree preservation holds by construction. Since the aggregation rule uses only d and c, and c is fixed, γ(x·P1y) = α(x)·P2β(y). The Latin square property follows from Theorem 3.1. □

Theorem 3.4 (Lagrange-type Property for Finite Plithogenic Loops). Let P(Q) be a plithogenic quasigroup where (Q, ·) is a finite loop of order n. Let P(H) be a plithogenic subloop, i.e. H ≤ Q and P(H) uses restrictions of d, c. Then |H| divides n, and for each vi ∈ V, the multiset of degrees {d(x, vi) : x ∈ H} is determined by |H| and d.

Remark 3.4. Unlike groups, P(H) need not partition P(Q). The theorem only restricts |H|, not the degree distribution. This is why portfolio constraints must be checked via Corollary 3.1, not just by size.

Theorem 3.5 (Automorphism Group Structure). Let Aut(P(Q)) = {φ : P(Q) → P(Q) plithogenic isomorphism}. Then Aut(P(Q)) ≅ {σ ∈ Aut(Q, ·) : d(σ(x), vi) = d(x, vi) ∀x ∈ Q, vi ∈ V}. That is, automorphisms are exactly base automorphisms that fix all neutrosophic degree vectors.

Proof. By Definition 3.2, any φ must preserve base and degrees. Conversely, any base automorphism σ preserving d extends uniquely to $\varphi(x) = \sigma(x)$ with the same degrees, and φ respects $\cdot P$ because the aggregation rule depends only on d, c. □

Theorem 3.6 (Cancellation and Idempotence Criteria). Let P(Q) be a plithogenic quasigroup. Let $a \in P(Q)$; then (1) $a \cdot P\ x = a \cdot P\ y \Rightarrow x = y$ and $x \cdot P\ a = y \cdot P\ a \Rightarrow x = y$ (cancellation); and (2) $a \cdot P\ a = a$ iff $a \cdot a = a$ in $(Q, \cdot)$, since $d(a \cdot P\ a, v_i) = d(a, v_i)$ by idempotence of t_N, s_N. Hence, if $c_i = 0$ for all i, then $\cdot P$ is idempotent iff $\cdot$ is idempotent; if $c_i = 1$ for all i, the same holds.

Proof. (1) follows from the Latin square property in Theorem 3.1. For (2), compute degrees: $(1-c_i)t_N(t,t) + c_i\ s_N(t,t) = (1-c_i)t + c_i\ t = t$, similarly for i, f. Therefore $d(a \cdot P\ a) = d(a)$, so idempotence depends only on the base value. □

4. Application: Using Plithogenic Quasigroups as a Tool for Decision Making

We now use plithogenic quasigroup properties to model a portfolio manager choosing between three stocks under conflicting criteria. The plithogenic quasigroup structure captures both the algebraic flexibility of stocks and the neutrosophic uncertainty of each attribute.

4.1 Setup: Stocks as Elements of P(Q)

Let Q = {e, a, b} represent three candidate stocks: e = A, a = M, b = T. $(Q, \cdot)$ is the quasigroup where $x \cdot y$ denotes switching from x to y, given by the Latin square in Example 3.1. This encodes the decision action: selecting a stock and then switching to another.

Let attributes V = {Growth, Safety, Liquidity} with dominant attribute v_D = Growth. Contradiction degrees reflect analyst policy: $c_{Growth} = 0$, $c_{Safety} = 0.4$, $c_{Liquidity} = 0.2$. c = 0 for Growth means we require consensus: a portfolio switch only has high Growth if both stocks rate high. c = 0.4 for Safety means we tolerate conflict: the safer stock can dominate.

Expert evaluations give neutrosophic degrees $d(x, v_i) = (t, i, f)$:

Stock	Growth	Safety	Liquidity
x1 = A	(0.90, 0.10, 0.00)	(0.80, 0.10, 0.10)	(0.95, 0.05, 0.00)
x2 = M	(0.60, 0.30, 0.10)	(0.90, 0.10, 0.00)	(0.85, 0.10, 0.05)
x3 = T	(0.30, 0.40, 0.30)	(0.50, 0.30, 0.20)	(0.70, 0.20, 0.10)

This defines the plithogenic quasigroup $P(Q) = (Q, V, v_D, d, c, \cdot P)$.

4.2 Plithogenic Product as Strategy Composition for Decision Rule

The product $x_i \cdot_P x_j$ models the strategy "hold x_i, then switch to x_j." By Theorem 3.1, the result is a unique portfolio with aggregated degrees.

Example: the manager holds A and considers switching to M. Growth (min, since $c_G = 0$): min{(0.9,0.1,0.0),(0.6,0.3,0.1)} = (0.6, 0.3, 0.1). Safety (0.6·min + 0.4·max): $x_1 \cdot_P x_2 = M$ with Safety degrees (0.86, 0.10, 0.04). Liquidity (0.8·min + 0.2·max): (0.87, 0.09, 0.04).

Interpretation: Growth reduces to M's level because $c_G = 0$ enforces consensus. Safety increases because $c_S = 0.4$ lets M's higher Safety dominate.

4.3 Solving for a Target Portfolio

Suppose the investor requires a target profile b = Target with d(b, G) = (0.60, 0.30, 0.10), d(b, S) = (0.86, 0.10, 0.04). If the current holding is $x_1 = A$, we can solve for $x_1 \cdot_P x = b$ using Corollary 3.1. Table 2 shows the uniqueness of the solution $x = x_2 = M$. So M is the unique switch that meets the target criteria.

If no stock solves the equation, then the target cannot be determined under the current parameters. The manager must either change c_i or adjust the target, which is exactly Remark 3.1: c_i is the risk dial.

Conclusion. In this work, we were able to combine plithogenic set properties and quasigroup properties to provide a framework where the policy c_i, uncertainty (t, i, f), and algebra (·, /, \) are inseparable primitives for making decisions that involve uncertainty.

5. Future Work

With the extension of the theory of neutrosophic sets to plithogenic quasigroups, several research directions open up to other algebraic structures. Future work can aim to unify plithogeny with the major non-associative algebraic theories.

Funding: This research received no external funding.

Conflicts of Interest: The authors declare no conflict of interest.

References

[1] Abbas, M., Murtaza, G., Smarandache, F.; Basic operations on hypersoft sets and hypersoft point, Neutrosophic Sets and Systems, Vol. 35, pp. 407–421 (2020).

[2] M. Abobala, On Novel Results about the Algebraic Properties of Symbolic 3-Plithogenic and 4-Plithogenic Real Square Matrices, Symmetry 15(8) (2023), 1494.

[3] Albert, A., Baer, A.; Quasigroups, II. Trans. Amer. Math. Soc. Vol. 55, pp. 401–419 (1944).

[4] Ali, M., Smarandache, F., Shabir, M.; Soft Neutrosophic Groupoids and their Generalization, Neutrosophic Sets and Systems, Vol. 6, pp. 62–81, doi.org/10.5281/zenodo.571753 (2014).

[5] Ali, M., Dyer, C., Shabir, M., Smarandache, F.; Soft Neutrosophic Loops and Their Generalization, Neutrosophic Sets and Systems, Vol. 4, pp. 55–75, doi.org/10.5281/zenodo.571751 (2014).

[6] Ali, M., Smarandache, F., Shabir, M., Naz, M.; Soft Neutrosophic Bigroup and Soft Neutrosophic N-Group, Neutrosophic Sets and Systems, Vol. 2, pp. 55–81 (2014), doi.org/10.5281/zenodo.571760.

[7] Alkhazaleh, S.; Plithogenic Soft Set, Neutrosophic Sets and Systems, Vol. 33, pp. 256–274, 10.5281/zenodo.3783023 (2020).

[8] Artzy, R.; Isotopy and parastrophy of quasigroups. Proc. Amer. Math. Soc. Vol. 14, pp. 429–431 (1963).

[9] Broumi, S., Smarandache, F., Dhar, M.; Rough Neutrosophic Sets, Neutrosophic Sets and Systems, Vol. 3, pp. 60–65, doi.org/10.5281/zenodo.571606 (2014).

[10] Broumi, S., Smarandache, F.; Intuitionistic Neutrosophic Soft Set, Journal of Information and Computing Science, Vol. 8, No. 2, pp. 130–140 (2013).

[11] Broumi, S., Smarandache, F.; More on Intuitionistic Neutrosophic Soft Sets, Computer Science and Information Technology, Vol. 1, No. 4, pp. 257–268, 10.13189/csit.2013.010404 (2013).

[12] Broumi, S., Deli, I., Smarandache, F.; Neutrosophic Parametrized Soft Set theory and its decision making problem, Italian Journal of Pure and Applied Mathematics, Vol. 32, pp. 1–12 (2014).

[13] Chein, O., Pflugfelder, O. H., Smith, J. D.; Quasigroups and Loops: Theory and Applications. Heldermann Verlag (1990).

[14] Duplák, J.; A parastrophic equivalence in quasigroups, Quasigroups and Related Systems, Vol. 7, pp. 7–14 (2000).

[15] T. Fujita and F. Smarandache, Plithogenic Duplets and Plithogenic Triplets, in Advancing Uncertain Combinatorics..., Vol. 6 (2025), 159–167.

[16] Maji, P. K.; Neutrosophic soft set, Annals of Fuzzy Mathematics and Informatics, Vol. 5, pp. 157–168 (2013).

[17] Mehmood, A., Ullah, W., Broumi, S., Khan, M. I., Qureshi, H., Abbas, M. I., Kalsoom, H., Nadeem, F.; Neutrosophic Soft Structures, Neutrosophic Sets and Systems, Vol. 33, pp. 23–58, 10.5281/zenodo.3782841 (2020).

[18] Molodtsov, D.; Soft Set Theory—First Results, Comput. Math. Appl., Vol. 37, pp. 19–31 (1999).

[19] B. Osoba, O. T. Yakub et al., Algebraic Properties of Quasigroup Under Q-Neutrosophic Soft Set, Neutrosophic Sets and Systems (2019).

[20] A. Oyem, T. G. Jaiyéọlá, J. O. Olaleru. Order of Finite Soft Quasigroups with Application to Egalitarianism, Discussiones Mathematicae, General Algebra and Applications. 42(1):135–157 (2020). DOI:10.7151/dmgaa.1381.

[21] A. Oyem, J. O. Olaleru, T. G. Jaiyéọlá, H. Akewe. Some algebraic properties of soft quasigroups. International Journal of Math. Sci. and Optimization. 6(2) 834–846 (2020). doi:10.6084/m9.figshare.13524392.

[22] A. Oyem, T. G. Jaiyeola, Parastrophes and cosets of Soft Quasigroups, International Journal of Mathematical Sciences and Optimization 8(1) 73–85 (2022), DOI:10.48550/arXiv.2207.06582.

[23] A. Oyem, J. O. Olaleru, T. G. Jaiyeola, B. Osoba. Soft Neutrosophic Quasigroups, Neutrosophic Sets and Systems. 50, 488–503 (2022), DOI:10.5281/zenodo.6774903.

[24] A. Oyem, O. Ogbereyivwe, B. Osoba, K. Ekeh, V.O Ojo-Orobosa. Algebraic Properties of Monogenic Soft Quasigroups, Unilag Journal of Mathematics and Applications. 1, 1–14 (2025).

[25] Saha, A., Broumi, S., Smarandache, F.; Neutrosophic Soft Sets Applied on Incomplete Data, Neutrosophic Sets and Systems, Vol. 32, pp. 282–293, 10.5281/zenodo.3723151 (2020).

[26] Shabir, M., Ali, M., Naz, M., F. Smarandache; Soft Neutrosophic Group, Neutrosophic Sets and Systems, Vol. 1, pp. 13–25, doi.org/10.5281/zenodo.571754 (2013).

[27] F. Smarandache, An Overview of Plithogenic Set and Symbolic Plithogenic Algebraic Structures, J. Fuzzy Ext. Appl. 4(1) (2023), 48–55.

[28] F. Smarandache, Plithogenic Set, an Extension of Crisp, Fuzzy, Intuitionistic Fuzzy, and Neutrosophic Sets Revisited, Neutrosophic Sets and Systems 21 (2018), 153–166.

[29] F. Smarandache, Some Neutrosophic Algebraic Structures and Neutrosophic n-Algebraic Structures, Hexis, Phoenix, 2006.

[30] Jaiyéọlá, T. G.; A study of new concepts in smarandache quasigroups and loop, ProQuest Information and Learning (ILQ), Ann Arbor, 127 pp (2009).

[31] Pflugfelder, H. O.; Quasigroups and Loops: Introduction, Sigma series in Pure Math. 7, Heldermann Verlag, Berlin, 147 pp. (1990).

[32] Qamar, M. A., Ahmad, A. G., Hassan, N.; On Q-Neutrosophic Soft Fields, Neutrosophic Sets and Systems, Vol. 32, pp. 80–93, 10.5281/zenodo.3723603 (2020).

Received: Mar. 1, 2026. Accepted: Sept. 5, 2026.

Neutrosophic Sets and Systems, Vol. 102, 2027
University of New Mexico

On Partially Homomorphic Encryption over Neutrosophic Integers Using the AH-Isometry

Mark Petersen[1,*]
[1] Mathematical and Physical Science Foundation, 4200 Slagelse, Denmark; mpetersendk@protonmail.com
* Correspondence: mpetersendk@protonmail.com

Abstract: Neutrosophic algebraic structures provide a way to work with indeterminacy within algebraic systems. This makes it natural to investigate whether a classical homomorphic cryptosystem such as Paillier can be formulated over the ring of neutrosophic integers Z(I). This paper introduces a neutrosophic version of the Paillier cryptosystem built over the ring of neutrosophic integers Z(I). It uses the foundations of the AH-isometry introduced by Abobala and Hatip to derive the neutrosophic formulas used in the cryptosystem. Since ordinary neutrosophic primes do not provide a suitable modulus corresponding to the classical Paillier modulus, this paper introduces neutrosophic paired-prime integers. The resulting cryptosystem defines encryption, decryption, and homomorphic properties and shows examples of encryption, decryption, and homomorphic addition of neutrosophic plaintexts based on this paired-prime modulus.

Keywords: Public Key Cryptography; Homomorphic Encryption; Neutrosophic Cryptography; Paillier Cryptosystem; Neutrosophic Number Theory; Neutrosophic Paillier Cryptosystem

1. Introduction

In 2006, Kandasamy and Smarandache introduced algebraic structures with neutrosophic properties, where the algebraic symbol "I" refers to indeterminacy and satisfies $I^2 = I$ [1]. For neutrosophic integers, this gives integers of the form a + bI. These neutrosophic structures have been studied in neutrosophic number theory [2–4], and the concept of indeterminacy has also been applied to neutrosophic cryptography, which was first suggested by Merkepci et al. [5, 6].

In 2021, Abobala and Hatip introduced the AH-isometry, showing that a neutrosophic number a + bI can be represented by (a, a + b) [7]. In this paper, the AH-isometry is used as an algebraic structural tool for investigating neutrosophic integers through an isomorphism T. This allows for an easier translation of the formulas from the classical Paillier cryptosystem to a neutrosophic version of this cryptosystem [8].

A problem with this translation is the choice of modulus. In the classical Paillier cryptosystem, the modulus is based on ordinary primes [8]. For neutrosophic integers, ordinary neutrosophic primes do not provide a suitable modulus corresponding to the classical Paillier modulus [3, 4]. Therefore, this paper introduces neutrosophic paired-primes as a formal definition inspired by methods used in previous research on neutrosophic cryptography [5]. This gives the modulus used for the neutrosophic version of the Paillier cryptosystem.

This paper is built on known definitions and theorems from neutrosophic number theory [2–5, 9]. These definitions and theorems are stated in the preliminaries in relation to the isomorphism T, using the foundations of the AH-isometry [7]. Using this foundational theory, the paper establishes the translation from the classical Paillier cryptosystem to a neutrosophic version, where encryption, decryption, and homomorphic addition can be formulated over Z(I) by using a modulus based on neutrosophic paired-primes.

2. Materials and Methods

The arithmetic of neutrosophic rings of the form a + bI can be studied through a representation provided by the foundations of the AH-isometry by Abobala-Hatip [7]. This section presents existing definitions and theorems through the foundations of the AH-isometry.

2.1. Preliminaries

Definition 2.1 (Neutrosophic Ring of Integers [1]). Let R be any ring. The neutrosophic ring over R is $R(I) = \{a + bI; a, b \in R\}$, where the indeterminacy "I" satisfies $I^2 = I$. For R = Z, the ring $Z(I) = \{a + bI; a, b \in Z\}$ is called the neutrosophic ring of integers.

Definition 2.2 (Positive Neutrosophic Integers [10]). If $A = a + bI$ and $B = c + dI$ are neutrosophic integers, then $A \leq B$ if and only if $a \leq c$ and $a + b \leq c + d$. A positive neutrosophic integer is a number $A = a + bI$, where $a > 0$ and $a + b > 0$.

Theorem 2.3 (The AH-isometry [7]). Let $R(I) = \{a + bI; a, b \in R\}$ be the neutrosophic ring with $I^2 = I$. The one-dimensional AH-isometry is the map $T : R(I) \to R \times R$ given by $T(a + bI) = (a, a + b)$. In particular, for R = Z, this gives the map $T : Z(I) \to Z \times Z$ defined by the same formula. Moreover, its inverse is $T^{-1}(x, y) = x + (y-x)I$.

Proof. Let $(x, y) \in R \times R$. Then $T(T^{-1}(x, y)) = T(x + (y-x)I) = (x, x + y-x) = (x, y)$. Similarly, for $a + bI \in R(I)$, $T^{-1}(T(a + bI)) = T^{-1}(a, a+b) = a + ((a+b)-a)I = a + bI$. Hence T^{-1} is the inverse of T, so T is bijective.

Lemma 2.4 (The AH-isometry is a ring isomorphism [7]). The AH-isometry $T : Z(I) \to Z \times Z$, $T(a + bI) = (a, a+b)$, is a ring isomorphism, where $Z\times Z$ is equipped with componentwise addition and multiplication.

Proof. Let $A = a+bI$ and $B = c+dI$ be elements of $Z(I)$. For addition, $A + B = (a+c) + (b+d)I$, so $T(A+B) = (a+c, a+c+b+d) = (a,a+b) + (c,c+d) = T(A) + T(B)$. For multiplication, using $I^2 = I$, $AB = (a+bI)(c+dI) = ac + (ad+bc+bd)I$, so $T(AB) = (ac, ac+ad+bc+bd) = (ac, (a+b)(c+d)) = (a,a+b)(c,c+d) = T(A)T(B)$. Thus T preserves addition and multiplication. Since T is bijective by Theorem 2.3, T is a ring isomorphism.

We recall the standard definitions from neutrosophic number theory and translate them under the ring isomorphism T.

Definition 2.5 (Addition [1, 7]). For $A = a+bI$ and $B = c+dI$, $T(A+B) = T(A)+T(B) = (a+c, a+b+c+d)$, and using T^{-1}, $A+B = (a+c) + (b+d)I$.

Definition 2.6 (Multiplication [1, 7]). For $A = a+bI$ and $B = c+dI$, $T(A\cdot B) = T(A)\cdot T(B) = (ac, ac+ad+bc+bd)$, and using T^{-1}, $A\cdot B = ac + (ad+bc+bd)I$.

Definition 2.7 (Neutrosophic Exponentiation [2, 5, 7]). For $A = a+bI$ and $B = c+dI$, $T(A\hat{}B) = T(A)\hat{}T(B) = (a^c, (a+b)\hat{}(c+d))$, and using T^{-1}, $A\hat{}B = a^c + ((a+b)\hat{}(c+d) - a^c)I$.

Definition 2.8 (Divisibility [2, 3, 7]). Let $A = a+bI$ and $B = c+dI$ be neutrosophic integers. We say $A \mid B$ if there exists $Q \in Z(I)$ such that $B = Q\cdot A$. Using T, this is equivalent to $(a,a+b) \mid (c,c+d)$; hence $A \mid B$ iff $a \mid c$ and $(a+b) \mid (c+d)$.

Definition 2.9 (Division [2, 4, 7, 9]). Let $A = a+bI$ and $B = c+dI$ be neutrosophic integers with $c > 0$ and $c+d > 0$, and assume $B \mid A$. Then $A/B = T^{-1}(a/c, (a+b)/(c+d)) = a/c + [(a+b)/(c+d) - a/c]I$.

Definition 2.10 (Neutrosophic Primes [2, 3, 7]). Let $A = a+bI$, $B = c+dI$, and $P = p+qI$ be neutrosophic integers. P is a neutrosophic prime if, whenever P divides $A\cdot B$ for some $A, B \in Z(I)$, then P divides A or P divides B. The primes in $Z(I)$ are of the following forms:

$$\pm(p+(1-p)I),\ \pm(p-(1+p)I),\ \pm(1+(p-1)I),\ \pm(1-(p+1)I)$$

where p is a positive prime in Z.

Remark 2.11 (Norm and Neutrosophic Primes [3]). Let $A = a+bI$. Using T, the norm of A is $N(A) = a(a+b)$. Therefore, if $N(A) = p$, where p is a prime in Z, then A is a neutrosophic prime.

Definition 2.12 (Congruence Modulo a Neutrosophic Integer [2, 7]). Let $A = a+bI$, $B = c+dI$, $M = m+nI$. $A \equiv B \pmod M$ if M divides $A-B$. Using T, this is equivalent to $(m,m+n) \mid (a-c, a+b-c-d)$; hence $A \equiv B \pmod M$ iff $a \equiv c \pmod m$ and $a+b \equiv c+d \pmod{m+n}$. For $m>0$, $m+n>0$: $A \bmod M = (a \bmod m) + (((a+b) \bmod (m+n)) - (a \bmod m))I$.

Definition 2.13 (Greatest Common Divisor [2, 4, 7]). For $A = a+bI$, $B = c+dI$: $\gcd(A,B) = T^{-1}(\gcd(a,c), \gcd(a+b,c+d)) = \gcd(a,c) + (\gcd(a+b,c+d) - \gcd(a,c))I$.

Definition 2.14 (Least Common Multiple [4, 7]). For $A = a+bI$, $B = c+dI$: $\mathrm{lcm}(A,B) = T^{-1}(\mathrm{lcm}(a,c), \mathrm{lcm}(a+b,c+d)) = \mathrm{lcm}(a,c) + (\mathrm{lcm}(a+b,c+d) - \mathrm{lcm}(a,c))I$.

2.2. The Classical Paillier Cryptosystem

Before defining the neutrosophic version, we recall the classical Paillier cryptosystem and provide an example to show how encryption and decryption work.

Definition 2.15 (Paillier Cryptosystem [8]). Let $n = pq$, where p and q are two distinct large primes, and let $\lambda = \mathrm{lcm}(p-1, q-1)$. Let $L(u) = (u-1)/n$ and choose a base $g \in B \subseteq Z^*_{n^2}$, where B denotes the set of elements in $Z^*_{n^2}$ whose order is a non-zero multiple of n, such that $\gcd(L(g^\lambda \bmod n^2), n) = 1$. The Paillier cryptosystem is then defined by the following steps [8]:

Step 1 (Plaintext and Randomness): let the plaintext be $m \in Z_n$ where $m < n$, and choose a random value $r < n$, $r \in Z^*_n$.

Step 2 (Encryption): compute the ciphertext $c = g^m r^n \bmod n^2$, where $c < n^2$ and $c \in Z^*_{n^2}$.

Step 3 (Decryption): given $c \in Z^*_{n^2}$, the original plaintext is $m = [L(c^\lambda \bmod n^2) / L(g^\lambda \bmod n^2)] \bmod n = L(c^\lambda \bmod n^2) \cdot L(g^\lambda \bmod n^2)^{-1} \bmod n$, where the denominator denotes the multiplicative inverse modulo n.

Example 2.16 (Classical Paillier). Choose $p = 5$ and $q = 7$. Then $n = pq = 35$, and $n^2 = 1225$. Compute $\lambda = \mathrm{lcm}(4,6) = 12$. We choose $g = 36$; since $\gcd(36,1225) = 1$, $g \in Z^*_{1225}$. Verify: $g^\lambda \bmod n^2 = 36^{12} \bmod 1225 = 421$, so $L(421) = (421-1)/35 = 12$; since $\gcd(12,35) = 1$, g is valid.

Step 1: choose plaintext $m = 10$ ($m \in Z_{35}$), and $r = 4$ ($\gcd(4,35) = 1$, $r \in Z^*_{35}$).

Step 2: $c = g^{10}\, 4^{35} \bmod 1225 = 1024$. Since $1024 < 1225$ and $\gcd(1024,1225) = 1$, $c \in Z^*_{1225}$.

Step 3: $c^\lambda \bmod n^2 = 1024^{12} \bmod 1225 = 526$, so $L(526) = (526-1)/35 = 15$. From above, $L(g^\lambda) = 12$, and $12^{-1} \bmod 35 = 3$. Therefore $m = 15 \cdot 3 \bmod 35 = 45 \bmod 35 = 10$. The decrypted plaintext is $m = 10$, the original plaintext.

3. Results

We now use the previous definitions to extend the classical Paillier cryptosystem to neutrosophic integers.

3.1. Extending the Cryptosystem to Neutrosophic Integers

The classical Paillier cryptosystem is based on a modulus $n = pq$, where p and q are distinct large classical primes [8]. Since the construction depends on modular arithmetic over Zn and $Z^*_{n^2}$, a neutrosophic version requires a corresponding modulus in the ring of neutrosophic integers Z(I). The natural first attempt is to choose two neutrosophic primes P and Q, where $N = PQ$. However, this direct approach does not provide the desired structure, since the product of two neutrosophic primes does not necessarily produce a valid modulus, as the indeterminate part can be the trivial case. This is seen using Definition 2.10, where neutrosophic primes belong to one of four forms [3]. This gives the eight cases shown in Table 1 [3]:

Table 1. All cases for neutrosophic prime integers

Case	Form	Choice	P	T(P)
1	$P=\pm(p+(1-p)I)$	+	$P = p+(1-p)I$	$(p, 1)$
2	$P=\pm(p+(1-p)I)$	−	$P = -p+(p-1)I$	$(-p, -1)$
3	$P=\pm(p-(1+p)I)$	+	$P = p+(-1-p)I$	$(p, -1)$
4	$P=\pm(p-(1+p)I)$	−	$P = -p+(1+p)I$	$(-p, 1)$
5	$P=\pm(1+(p-1)I)$	+	$P = 1+(p-1)I$	$(1, p)$
6	$P=\pm(1+(p-1)I)$	−	$P = -1+(1-p)I$	$(-1, -p)$
7	$P=\pm(1-(p+1)I)$	+	$P = 1+(-p-1)I$	$(1, -p)$
8	$P=\pm(1-(p+1)I)$	−	$P = -1+(p+1)I$	$(-1, p)$

For $p > 0$, Table 1 shows that the positive neutrosophic prime cases are Case 1 and Case 5, shown in Table 2:

Table 2. Positive neutrosophic prime integers

Case	P	T(P)
1	$p+(1-p)I$	$(p, 1)$
5	$1+(p-1)I$	$(1, p)$

For a product $N = PQ$, there are three possible choices. If both factors are chosen from Case 1, $T(N) = (pq, 1)$. If both are from Case 5, $T(N) = (1, pq)$. In both cases, one component is trivial. If one factor is chosen from each case, $T(N) = (p, q)$; this avoids a trivial component, but it reveals the prime components directly.

Since n in classical Paillier is part of the public key pair (n, g), while the primes (p, q) are private [8], the modulus N should likewise be public in a neutrosophic version of Paillier, while its factors should remain private. Therefore, using neutrosophic primes alone does not provide a suitable modulus for the construction.

This motivates a construction closer to the classical form, where each neutrosophic factor has two prime components under T. This idea is similar to the approach used in the neutrosophic RSA algorithm introduced by Merkepci et al. in 2023 [5].

Definition 3.1 (Neutrosophic Paired-Prime Integer). A positive neutrosophic integer $A = a+bI$ is called a neutrosophic paired-prime integer if a and $a+b$ are distinct positive primes in Z. Since a and $a+b$ are distinct primes, $\gcd(a, a+b) = 1$.

Remark 3.2. Every positive neutrosophic paired-prime integer can be written as a product of two neutrosophic primes. If $A = a+bI$ is a neutrosophic paired-prime integer, then a and $a+b$ are positive primes in Z, and $T(A) = (a, a+b) = (a,1)\cdot(1,a+b)$. Thus A corresponds under T to the product of a Case 1 neutrosophic prime and a Case 5 neutrosophic prime.

To construct a modulus close to the classical modulus, we choose two neutrosophic paired-prime integers as private factors.

Definition 3.3 (Neutrosophic Paillier Modulus). Let $A = a+bI$ and $B = c+dI$ be distinct neutrosophic paired-prime integers with $\gcd(a,c) = 1$ and $\gcd(a+b, c+d) = 1$. The neutrosophic Paillier modulus is $N = A\cdot B$.

3.2. The Paillier Cryptosystem over Neutrosophic Integers

Step 1 (Parameter Setup): let $A = a+bI$ and $B = c+dI$ be distinct neutrosophic paired-prime integers, $N = A \cdot B = n1+n2I$ the modulus. Let $\Lambda = \mathrm{lcm}(A-1, B-1) = \lambda 1+\lambda 2I$. The neutrosophic L-function is $Lneutro(U) = (U-1)/N$ for $U = u1+u2I$, whenever $U-1$ is divisible by N in $Z(I)$. The base $G = g1+g2I$ is chosen such that $G \in B \subseteq Z(I)^*\_\{N^2\}$ with $\gcd(Lneutro(G^\wedge\Lambda \bmod N^2), N) = 1$. Here (N,G) is the public key pair; (A,B) are private.

Step 2 (Plaintext and Randomness): let $M \in Z(I)N$, $M = m1+m2I$ with $M < N$, meaning $m1<n1$ and $m1+m2<n1+n2$. Choose a random neutrosophic value $R \in Z(I)^*N$, $R = r1+r2I$, with $R<N$ and $\gcd(R,N)=1$, equivalently $\gcd(r1,n1)=\gcd(r1+r2,n1+n2)=1$.

Step 3 (Encryption): the ciphertext $C = c1+c2I \in Z(I)^*\_\{N^2\}$, $C<N^2$, is $C = G^\wedge M\ R^\wedge N \bmod N^2$.

Step 4 (Decryption): $M = [Lneutro(C^\wedge\Lambda \bmod N^2) / Lneutro(G^\wedge\Lambda \bmod N^2)] \bmod N = Lneutro(C^\wedge\Lambda \bmod N^2) \cdot Lneutro(G^\wedge\Lambda \bmod N^2)^{-1} \bmod N$.

3.2.1. Verifying the Homomorphic Properties

The homomorphic properties of the neutrosophic Paillier construction follow from the structure of the isomorphism T. If $M1 = m1+m2I$ and $M2 = \mu1+\mu2I$ are in $Z(I)N$ with $M1<N$, $M2<N$, their encryptions are $C1 = G^\wedge M1\ R1^\wedge N \bmod N^2$ and $C2 = G^\wedge M2\ R2^\wedge N \bmod N^2$, where $R1,R2 \in Z(I)^*N$.

Using multiplication in $Z(I)^*\_\{N^2\}$: $C1C2 = (G^\wedge M1\ R1^\wedge N)(G^\wedge M2\ R2^\wedge N) \bmod N^2$. Since exponentiation is componentwise under T (Definition 2.7), $C1C2 = G^\wedge(M1+M2)\ (R1R2)^\wedge N \bmod N^2$. Since $R1,R2 \in Z(I)^*N$ implies $R1R2 \in Z(I)^*N$, this is an encryption of $M1+M2 \bmod N$. Hence $D(C1C2) = M1+M2 \bmod N$, i.e. the system is additively homomorphic.

The system also supports multiplication of a plaintext by a neutrosophic scalar. Let $K = k1+k2I \in Z(I)N$ with $k1\geq 0$ and $k1+k2\geq 0$. If $C = G^\wedge M\ R^\wedge N \bmod N^2$, then $C^\wedge K = (G^\wedge M\ R^\wedge N)^\wedge K \bmod N^2 = G^\wedge(KM)\ (R^\wedge K)^\wedge N \bmod N^2$. Since $R \in Z(I)^*N$, also $R^\wedge K \in Z(I)^*N$, so $C^\wedge K$ is an encryption of $KM \bmod N$, giving $D(C^\wedge K) = KM \bmod N$. Thus the neutrosophic Paillier construction preserves the usual Paillier homomorphic properties through T: $D(E(M1)E(M2)) = M1+M2 \bmod N$ and $D(E(M)^\wedge K) = KM \bmod N$.

3.3. Examples of the Neutrosophic Paillier Cryptosystem

Example 3.4 (Neutrosophic Paillier Encryption and Decryption). If Alice wants to send Bob a message, Bob first chooses two distinct neutrosophic paired-prime integers $A = 3+4I$ and

B = 11+2I, where A≠B, and 3, 7, 11, 13 are primes in Z, with gcd(3,11)=1 and gcd(3+4,11+2)=gcd(7,13)=1: valid neutrosophic paired-prime integers.

Bob computes the modulus: $N = A\cdot B = 3\cdot 11 + (3\cdot 2+4\cdot 11+4\cdot 2)I = 33 + 58I$. Then $\Lambda = \mathrm{lcm}(A-1,B-1) = \mathrm{lcm}(2+4I,10+2I) = \mathrm{lcm}(2,10) + (\mathrm{lcm}(6,12)-\mathrm{lcm}(2,10))I = 10 + 2I$.

The base $G = g1+g2I \in B \subseteq Z(I)^*\_\{N^2\}$, where $N^2 = (33+58I)^2 = 33^2 + ((33+58)^2-33^2)I = 1089 + 7192I$. This means G must lie in Z(I)*_{1089+7192I}; if G = N+1 = 34+58I, this holds, since $\gcd(G,N^2)=1$, equivalently gcd(34,1089)=gcd(92,8281)=1.

Bob keeps A, B and Λ private and publishes the public key (N,G). Alice uses Bob's public key and chooses a message M = m1+m2I where M<N and M ∈ Z(I)_{33+58I}. Alice wants to encrypt the message 4+5I, which fits since 4<33 and 9<91.

Alice randomly chooses R = 2+3I ∈ Z(I)*N with R<N, verifying gcd(R,N)=1: gcd(r1,n1)=gcd(2,33)=1 and gcd(r1+r2,n1+n2)=gcd(5,91)=1; also R<N since 2<33 and 5<91.

Alice computes the ciphertext $C = G^\wedge M\ R^\wedge N \bmod N^2$ through the isomorphism T. Since T(G)=(34,92), T(M)=(4,9), T(R)=(2,5), T(N)=(33,91): $T(G^\wedge M) = (34,92)^\wedge(4,9) = (34^4, 92^9)$, and $T(R^\wedge N) = (2,5)^\wedge(33,91) = (2^{33}, 5^{91})$. Thus $T(G^\wedge M\ R^\wedge N) = (34^4\cdot 2^{33}, 92^9\cdot 5^{91})$. Since $T(N^2)=(1089,8281)$, Alice computes $C = T^{-1}(34^4\cdot 2^{33} \bmod 1089, 92^9\cdot 5^{91} \bmod 8281) = T^{-1}(569, 2595) = 569 + 2026I$.

The ciphertext sent to Bob is C = 569 + 2026I. Bob decrypts using $M = \mathrm{Lneutro}(C^\wedge\Lambda \bmod N^2)\cdot \mathrm{Lneutro}(G^\wedge\Lambda \bmod N^2)^{-1} \bmod N$. With T(C)=(569,2595), T(Λ)=(10,12), $T(N^2)=(1089,8281)$: $T(C^\wedge\Lambda \bmod N^2) = (569^{10} \bmod 1089, 2595^{12} \bmod 8281) = (232,1548)$, so $C^\wedge\Lambda \bmod N^2 = T^{-1}(232,1548) = 232+1316I$.

Then $\mathrm{Lneutro}(C^\wedge\Lambda \bmod N^2) = (232+1316I-1)/(33+58I) = (231+1316I)/(33+58I) = T^{-1}(231/33, 1547/91) = T^{-1}(7,17) = 7+10I$.

Bob also computes $T(G^\wedge\Lambda \bmod N^2) = (34,92)^\wedge(10,12) \bmod (1089,8281) = (34^{10} \bmod 1089, 92^{12} \bmod 8281) = (331,1093)$, so $G^\wedge\Lambda \bmod N^2 = 331+762I$, and $\mathrm{Lneutro}(G^\wedge\Lambda \bmod N^2) = (330+762I)/(33+58I) = T^{-1}(330/33,1092/91) = T^{-1}(10,12) = 10+2I$.

The inverse of 10+2I modulo N is found through T: T(10+2I)=(10,12), T(N)=(33,91), so $(10,12)^{-1} \bmod (33,91) = (10^{-1} \bmod 33, 12^{-1} \bmod 91) = (10,38)$, giving $(10+2I)^{-1} \bmod N = T^{-1}(10,38) = 10+28I$.

Finally, M = (7+10I)(10+28I) mod (33+58I) = T^{-1}((7,17)·(10,38) mod (33,91)) = T^{-1}((70,646) mod (33,91)) = T^{-1}(4,9) = 4+5I. Bob recovers the original plaintext M = 4+5I.

Example 3.5 (Homomorphic Properties). In the previous example, Alice sent an encrypted message M1 = 4+5I using the neutrosophic Paillier algorithm. Charlie does not know the original message, but has the ciphertext C1 = C = 569+2026I, and knows only the public modulus N, the public base G, and the ciphertext. Charlie wants to add his own message to the ciphertext so that Bob can receive the combined plaintext after decryption.

Charlie encrypts M2 = 6+I, valid since M2<N and M2 ∈ Z(I)_{33+58I}, choosing R2 = 4+I, valid since R2<N and gcd(R2,N)=1 (gcd(4,33)=1, gcd(5,91)=1). Then T(M2)=(6,7), T(R2)=(4,5), and Charlie computes T(C2) = ($34^6 \cdot 4^{33}$ mod 1089, $92^7 \cdot 5^{91}$ mod 8281) = (460,2322), so C2 = T^{-1}(460,2322) = 460+1862I.

Charlie multiplies the two ciphertexts: T(C1C2) = (569,2595)·(460,2322) mod (1089,8281) = (380,5303), so C1C2 = T^{-1}(380,5303) = 380+4923I, with C1C2<N^2 and C1C2 ∈ Z(I)*_{N^2}.

Charlie sends the combined ciphertext to Bob, who decrypts it using the same decryption factors as before (Lneutro(G^Λ mod N^2)=10+2I and $(10+2I)^{-1}$ mod N = 10+28I). Since T(C1C2)=(380,5303): T((C1C2)^Λ mod N^2) = (380,5303)^(10,12) mod (1089,8281) = (380^{10} mod 1089, 5303^{12} mod 8281) = (34,911). Then Lneutro((C1C2)^Λ mod N^2) = T^{-1}((34−1)/33, (911−1)/91) = T^{-1}(1,10) = 1+9I.

Bob decrypts: D(C1C2) = (1+9I)(10+28I) mod (33+58I) = T^{-1}((1,10)(10,38) mod (33,91)) = T^{-1}(10,16) = 10+6I. Since Bob has Alice's original plaintext M1 = 4+5I, he finds Charlie's message: M2 = D(C1C2) − M1 = (10+6I) − (4+5I) = 6+I.

This shows how Charlie can add his message to Alice's ciphertext without knowing Alice's plaintext. Bob decrypts the combined ciphertext and recovers Charlie's original plaintext from the decrypted sum.

4. Conclusion

In this paper, a neutrosophic version of the Paillier cryptosystem using neutrosophic integers has been presented, which is a system with homomorphic properties. The construction is based on the isomorphism T, which makes it possible to translate the classical Paillier formulas to a neutrosophic version using the neutrosophic integers. It has been shown that neutrosophic primes do not provide a suitable modulus for this construction since they degenerate or directly expose the private parameters in the cryptosystem. Therefore, neutrosophic paired-prime integers were introduced so that the modulus can be constructed with a product structure in both components under T. Finally, the construction is illustrated by explicit examples of encryption, decryption, and homomorphic addition, where the original neutrosophic plaintext is recovered.

The purpose of this paper is to show how existing algorithms in cryptography can be translated into neutrosophic versions. This neutrosophic version of Paillier does not argue for a stronger cryptosystem, but rather corresponds structurally to two componentwise Paillier systems under T. This means that, in theory, an attack has to take both componentwise systems into account, although this does not by itself prove stronger security than classical Paillier. This question has to be investigated further. This also suggests further work on neutrosophic secure multi-party computation, where existing multi-party cryptographic methods can be investigated in a neutrosophic setting.

Funding: This research received no external funding.

Conflicts of Interest: The author declares no conflict of interest.

References

1. Kandasamy, W.B.V.; Smarandache, F. Some Neutrosophic Algebraic Structures and Neutrosophic N-Algebraic Structures; Hexis: Phoenix, AZ, USA, 2006.

2. Abobala, M. Foundations of neutrosophic number theory. Neutrosophic Sets and Systems 2021, 39, 120–132.

3. Çeven, Y.; Tekin, Ş. Some Properties of Neutrosophic Integers. Kirklareli University Journal of Engineering and Science 2020, 6(1), 50–59.

4. Çeven, Y.; Çetin, Ö. The Greatest Common Divisors and The Least Common Multiples in Neutrosophic Integers. Süleyman Demirel Üniversitesi Fen Bilimleri Enstitüsü Dergisi 2023, 27(3), 411–416.

5. Merkepci, M.; Abobala, M.; Allouf, A. The Applications of Fusion Neutrosophic Number Theory in Public Key Cryptography and the Improvement of RSA Algorithm. Infinite Study 2023, 10(2), 69–74.

6. Merkepci, M.; Sarkis, M. An Application of Pythagorean Circles in Cryptography and Some Ideas for Future Non Classical Systems. Galoitica Journal of Mathematical Structures and Applications 2022, 2(2), 28–30.

7. Abobala, M.; Hatip, A. An Algebraic Approach to Neutrosophic Euclidean Geometry. Neutrosophic Sets and Systems 2021, 43(1), 10.

8. Paillier, P. Public-key cryptosystems based on composite degree residuosity classes. In Advances in Cryptology – EUROCRYPT '99; Stern, J., Ed.; Springer: Berlin/Heidelberg, Germany, 1999; Volume 1592, pp. 223–238.

9. Barbosa, R.P.; Smarandache, F. Neutrosophic One-Round Zero-Knowledge Proof. Plithogenic Logic and Computation 2024, 2, 49–54.

10. Abobala, M. Neutrosophic Real Inner Product Spaces. Neutrosophic Sets and Systems 2021, 43, 225–246.

Received: Dec. 21, 2025. Accepted: Sept. 8, 2026.

Neutrosophic Sets and Systems, Vol. 102, 2027
University of New Mexico

A Neutrosophic Copula Framework for Bivariate Reliability Modelling Under Epistemic Indeterminacy

Preethi John

Assistant Professor, Department of Statistics, Vimala College (Autonomous), Thrissur, Kerala, India
preethijohn@vimalacollege.edu.in

Abstract: Classical copula-based reliability models assume precisely specified marginal distributions and dependence parameters, an assumption often violated when failure times are affected by sensor latency, interval censoring, calibration drift, or incomplete inspection records. Motivated by the copula-based reliability characterisations of Nair et al. (2018), this paper proposes the Neutrosophic Copula Framework (NCF) for bivariate reliability modelling under epistemic indeterminacy. The framework combines neutrosophic statistics (Smarandache, 1998) with copula theory to represent uncertainty through interval-valued probability bounds associated with truth (T), indeterminacy (I), and falsity (F) components, distinguishing irreducible unknowing from identifiable systematic error. The NCF extends Sklar's theorem, system reliability functions, dependence measures, copula hazard rates, and mean residual life to the neutrosophic setting. Closed-form interval-valued dependence measures are derived for Clayton, Gumbel, Frank, Gaussian, and t-copulas. A two-stage NS-IFM estimation procedure is developed with boundwise consistency and asymptotic normality. Two qualitatively new states — indeterminate dependence direction and indeterminate PQD status — are identified that are not represented within standard point-valued reliability frameworks. Monte Carlo simulations confirm consistent parameter recovery and reliable interval coverage. The methodology is illustrated using the Diabetic Retinopathy Study dataset (Huster et al., 1989), where the framework reveals reliability uncertainty concealed by classical point-valued analysis. Setting IL=IU=0 recovers the classical copula framework and interval statistics as special cases.

Keywords: Neutrosophic copula; Reliability modelling; Bivariate survival; Copula theory; Uncertainty quantification; NS-IFM estimator; Epistemic indeterminacy; Dependence modelling; T-I-F decomposition.

1. Introduction

A central problem in reliability engineering is the joint modelling of dependent component lifetimes under incomplete or imprecise information. Classical copula-based reliability models (Nelsen, 2006) provide flexible tools for modelling dependence structures but assume precisely observed failure times and exactly specified model parameters. In practice, failure data are frequently affected by interval censoring, sensor latency, recording uncertainty, calibration drift, or incomplete inspection schedules. The copula-based reliability results of Nair et al. (2018) and John and Sankaran (2017) provide important characterisations of bivariate lifetime dependence, hazard rates, and mean residual life functions, but remain point-valued and do not distinguish irreducible indeterminacy from incomplete information from systematic error from identifiable sources.

Neutrosophic statistics (Smarandache, 1998, 2019) addresses this through the three-component T-I-F decomposition (Aslam, 2019, 2020; Hanafy et al., 2012; Patro and Smarandache, 2016): indeterminacy I captures uncertainty from genuinely unobservable events such as sensor outages, while falsity F captures identifiable systematic errors such as calibration drift. Reducing indeterminacy requires additional information; reducing falsity requires correction of systematic measurement error.

Among the results, two qualitatively new states emerge that have no counterpart in classical or fuzzy reliability theory: an indeterminate dependence direction, where the sign of τN cannot be determined from the data, and an indeterminate PQD status, where the positive-quadrant-dependence verdict itself carries simultaneously non-zero truth, falsity, and indeterminacy. These are identified in Section 4 and are the most distinctive outputs of the framework.

The proposed framework is particularly relevant in engineering systems where exact failure times are unavailable because monitoring occurs at discrete inspection intervals. Applications include condition-based maintenance, structural health monitoring, biomedical follow-up studies, and remote sensor networks. In such settings, reliability estimates from point-valued models may understate operational uncertainty; the NCF addresses this by propagating indeterminacy directly through the dependence structure and system reliability measures.

No prior work integrates neutrosophic statistics with copula-based reliability (Khan et al., 2021; Ulucay, 2024; Chen and Zheng, 2021; Bassan and Spizzichino, 2005). This paper proposes the Neutrosophic Copula Framework (NCF), extending the results of Nair et al. (2018) and John and Sankaran (2017) to the interval-valued setting; the NCF recovers both classical copula analysis and interval statistics when IL=IU=0. Sections 2–8 develop the theory, estimation, simulation validation, and a real data application.

2. Preliminaries

2.1 Neutrosophic Numbers and Random Variables

Definition 2.1 (Neutrosophic Number, Smarandache 1998). A neutrosophic number N is defined as $N = a + b \cdot IN$, $IN \in [IL, IU] \subseteq [0,1]$, (1) where $a \in \mathbb{R}$ is the determinate part, $b \in \mathbb{R}$ is the indeterminate coefficient, and IN is the indeterminacy factor representing the degree of genuine unknowing (I in the T-I-F decomposition). When IL=IU=0, N reduces to the classical real number a. Throughout Sections 3–5, the operationally equivalent interval form $\theta N=[\theta L,\theta U]$ is used, where $\theta L=a+bIL$ and $\theta U=a+bIU$.

The NCF is distinguished from standard interval statistics by its explicit treatment of falsity F. In interval statistics, all uncertainty is treated as equally unknown and mapped onto the interval width. In the NCF, falsity F — arising from identifiable systematic errors such as calibration drift — is handled at the data-preprocessing stage before model fitting: known biases are corrected, and only the residual genuine unknowing (sensor lag, missing records) contributes to the interval width Iwidth = IU−IL. The resulting $[\theta L,\theta U]$ therefore represents irreducible indeterminacy, not total uncertainty — a richer representation than interval statistics, which maps all imprecision onto a single interval width without distinguishing poor instrumentation (F large) from insufficient data (I large).

Practical decomposition guidance. The practitioner assigns each source of measurement uncertainty to F or I as follows: if the source is identifiable and correctable before model fitting (e.g. a known ±2% calibration certificate, or a systematic recording bias at shift boundaries), it contributes to falsity F and should be corrected at preprocessing; if the source is genuinely unresolvable given the available data (e.g. a sensor offline during the failure window, giving only a bracketing interval [t1,t2], or a clinic visit schedule recording only the visit date rather than the exact onset), it contributes to indeterminacy I and directly determines Iwidth. In the Diabetic Retinopathy application (Section 6), Iwidth=10% derives entirely from the inter-visit scheduling interval, a genuine unknowing source (I); any systematic ascertainment bias in the ophthalmological assessment would instead be classified as F and corrected before fitting.

A neutrosophic random variable $XN \in [XL,XU]$ has interval-valued moments following the arithmetic of neutrosophic numbers: $\mu N=[\mu L,\mu U]$, $\sigma^2 N=[\sigma^2 L,\sigma^2 U]$, with $\mu k=E[Xk]$, $\sigma^2 k=Var(Xk)$, $k \in \{L,U\}$. (2)

2.2 Why the NCF Is Not Merely Interval Statistics

Interval statistics encodes uncertainty solely through the width of an interval $[\theta L,\theta U]$, treating all sources of imprecision as equivalent. The NCF departs from this in three ways. First, falsity F is corrected at the data-preprocessing stage before any interval is formed, so the resulting interval contains only irreducible indeterminacy I, not total uncertainty. Second, the width $Iwidth=\theta U-\theta L$ has a specific physical meaning: the portion of uncertainty unresolvable without additional instrumentation. Third, the joint probability statement $\{X\leq x,\ Y\leq y\}$ receives a full T-I-F assignment, letting the practitioner distinguish genuinely uncertain from probably-false regions of the reliability surface simultaneously.

Relation to imprecise probability and p-boxes. The NCF is related to, but distinct from, established uncertainty frameworks. Walley-style imprecise probability (Walley, 1991) uses a set of probability measures to represent epistemic uncertainty without committing to a single distribution; probability boxes (p-boxes) bound the CDF between lower and upper envelopes. The NCF differs in two respects: it operates within the parametric copula family structure, so the interval $[\theta L,\theta U]$ indexes a specific parametric class rather than a nonparametric set of measures (making NS-IFM estimation, Section 5, tractable); and the T-I-F decomposition assigns explicit roles to the three components of uncertainty, whereas imprecise probability and p-boxes treat the interval as a unified epistemic object without distinguishing preprocessable error from irreducible unknowing. The NCF is therefore not a reparametrisation of imprecise probability, but a parametric interval model with a specific semantic decomposition. Dempster–Shafer belief functions (Dempster, 1967) share the goal of representing ignorance separately from probability, but their combination rules and computational machinery differ substantially from the IFM-based estimation used here; a detailed axiomatic comparison is beyond the present scope and is identified as future work.

2.3 Neutrosophic Lifetime Distributions

Definition 2.2 (Neutrosophic Exponential). $XN\sim NExp(\lambda N)$ if its NPDF is $fN(x;\lambda N)=\lambda N\, e^{(-\lambda N x)}$, $x>0$, $\lambda N\in[\lambda L,\lambda U]$. (3)

Definition 2.3 (Neutrosophic Weibull). $XN\sim NWeibull(\alpha N,\beta N)$ if its NPDF is $fN(x;\alpha N,\beta N) = (\alpha N/\beta N)(x/\beta N)^{(\alpha N-1)} \exp[-(x/\beta N)^{\alpha N}]$, $x>0$, with shape $\alpha N\in[\alpha L,\alpha U]$ and scale $\beta N\in[\beta L,\beta U]$. (4)

Definition 2.4 (Neutrosophic Normal). $XN\sim NN(\mu N,\sigma^2 N)$ if its NPDF is $fN(x;\mu N,\sigma^2 N) = (2\pi\sigma^2 N)^{(-1/2)} \exp[-(x-\mu N)^2/(2\sigma^2 N)]$, with $\mu N\in[\mu L,\mu U]$ and $\sigma^2 N\in[\sigma^2 L,\sigma^2 U]$. (5)

3. The Neutrosophic Copula Framework

3.1 Neutrosophic Marginal and Copula Definitions

Let XN, YN be neutrosophic failure times with neutrosophic CDFs FN(x)=[FL(x),FU(x)] and GN(y)=[GL(y),GU(y)], FL≤FU and GL≤GU pointwise. The neutrosophic survival and hazard functions are: $S^{ʊ}$_N(x)=[1−FU(x), 1−FL(x)], h_N(x)=[fL(x)/S^{U}_U(x), fU(x)/S^{U}_L(x)]. (6) The bound reversal in $S^{ʊ}$_N follows from the monotone relationship between the CDF and survival function; the hazard rate is obtained by cross-division at each bound, yielding the tightest valid interval consistent with the neutrosophic arithmetic.

Definition 3.1 (Neutrosophic Copula). A neutrosophic copula CN is a family of bivariate functions indexed by a neutrosophic parameter θN=[θL,θU]: CN(uN,vN;θN) = [C(uL,vL;θL), C(uU,vU;θU)], (7) where uN=[uL,uU], vN=[vL,vU]∈$[0,1]^2$ are interval-valued probability integral transforms of the marginals. CN satisfies: (P1) boundary conditions at each bound; (P2) monotonicity in each argument at each bound; (P3) Fréchet–Hoeffding bounds WN≤CN≤MN interval-wise, with WN=[max(uL+vL−1,0), max(uU+vU−1,0)] and MN=[min(uL,vL), min(uU,vU)].

3.2 Neutrosophic Sklar's Theorem and Its Foundation

Theorem 3.2 (Neutrosophic Extension of Sklar's Theorem). Let HN(x,y) be a bivariate neutrosophic joint distribution with continuous neutrosophic marginals FN, GN as above. Suppose the copula family is positively ordered — C(u,v;θ) non-decreasing in θ for all (u,v)∈$[0,1]^2$ (this follows directly from the generator representations for Archimedean families Clayton/Gumbel/Frank; for Gaussian and t-copulas it holds with respect to ϱ∈(−1,1) under the standard positive-dependence parameterisation considered here, ϱL≤ϱU both in [0,1); for negatively associated regimes ϱ<0 the ordering reverses and [HU,HL] should be taken as the neutrosophic interval; practitioners encountering families that fail positive ordering across the full parameter space should reparametrise or take [min(HL,HU), max(HL,HU)] per Section 7). Then there exists a neutrosophic copula CN with θN=[θL,θU] such that HN(x,y) = [C(FL(x),GL(y);θL), C(FU(x),GU(y);θU)]. (8) If FL,FU,GL,GU are all continuous, the neutrosophic copula is unique at each bound. The classical Sklar's theorem (Sklar, 1959) is recovered at IL=IU=0, where FN, GN, CN all collapse to classical scalar functions.

Theorem 3.2 is grounded in Smarandache's neutrosophic set theory (1998): the interval [HL(x,y), HU(x,y)] constitutes a neutrosophic set in the sense that membership in {X≤x, Y≤y} is assigned a truth degree T∈[HL,HU], an indeterminacy degree I=HU−HL (the width of uncertainty), and a falsity degree F=1−HU (probability of the event definitely not occurring).

Proof. Step 1 (Existence at each bound): FL, FU, GL, GU are continuous classical CDFs (as bounds of FN, GN), so they satisfy the hypotheses of the classical Sklar's theorem individually; hence copulas CL, CU exist with HL(x,y)=CL(FL(x),GL(y);θL) and HU(x,y)=CU(FU(x),GU(y);θU). Step 2 (Uniqueness at each bound): since FL,FU,GL,GU are continuous, the probability integral transforms are uniform on [0,1], so CL, CU are identified as the joint CDFs of the respective pairs without ambiguity. Step 3 (Valid neutrosophic interval): by positive ordering, θL≤θU implies HL(x,y)≤HU(x,y) pointwise, confirming HN=[HL,HU] is a valid interval-valued distribution; without positive ordering, this inequality need not hold. The T-I-F interpretation follows from the arithmetic of neutrosophic numbers: T∈[HL,HU], I=HU−HL≥0, F=1−HU≥0.

Corollary 3.3 (Neutrosophic System Reliability). The neutrosophic joint survival function is RN(x,y)=[RL(x,y),RU(x,y)], with Rk(x,y) = 1−Fk(x)−Gk(y)+Ck(Fk(x),Gk(y);θk), k∈{L,U}. (9) For series and parallel systems at a common mission time t:

$$\tilde{R}\_N\text{^series}(t) = [S^L\_L(t)+S^L\_L(t)-1+CL(F^L\_L(t),F^L\_L(t);\theta L),$$
$$S^L\_U(t)+S^L\_U(t)-1+CU(F^L\_U(t),F^L\_U(t);\theta U)] \qquad (10)$$

$$\tilde{R}\_N\text{^parallel}(t) = [S^L\_L(t)+S^L\_L(t)-CU(F^L\_U(t),F^L\_U(t);\theta U),$$
$$S^L\_U(t)+S^L\_U(t)-CL(F^L\_L(t),F^L\_L(t);\theta L)] \qquad (11)$$

(each RHS uses the X- and Y-component survival/CDF functions at the appropriate bound). Remark 3.4. The bound reversal between (10) and (11) reflects a fundamental asymmetry: positive dependence is beneficial to a series system (correlated components tend to survive together) but detrimental to a parallel system (correlated components tend to fail together, defeating redundancy). Since CU≥CL for positively ordered families, the larger copula value CU increases the series upper reliability bound but decreases the parallel lower reliability bound. Practitioners designing parallel redundant systems under indeterminacy should therefore use the lower reliability bound, corresponding to the worst-case dependence scenario θU.

4. New Results: Neutrosophic Dependence and Reliability

4.1 Neutrosophic Dependence Measures

Theorem 4.1 (Neutrosophic Dependence Measures). Under the NCF with $\theta N=[\theta L,\theta U]$, all classical dependence measures become interval-valued; Table 1 gives closed-form expressions for five standard copula families, extending John and Sankaran (2017) (classical results recovered at $\theta L=\theta U$).

Definition 4.2 (Neutrosophic Kendall's Tau). $\tau N=[\tau L,\tau U]$, $\tau k = 4\iint_{[0,1]^2} Ck(u,v;\theta k)\, dCk(u,v;\theta k) - 1$, $k\in\{L,U\}$. (12)

Definition 4.3 (Neutrosophic Spearman's Rho). $\varrho^s\_N=[\varrho^s\_L,\varrho^s\_U]$, $\varrho^s\_k = 12\iint_{[0,1]^2} Ck(u,v;\theta k)\, du\, dv - 3$, $k\in\{L,U\}$. (13) The interval-wise inequality $(3\tau N-1)/2 \leq \varrho^s\_N \leq (1+2\tau N)/2$ holds (a neutrosophic extension of the classical Daniels inequality). For Archimedean families the identity $\varrho^s\_k\approx(3/2)\tau k$ holds in closed form for the Frank copula; for Gaussian and t-copulas the relationship is non-linear. The bounds satisfy $\varrho^s\_L\leq\varrho^s\_U$ interval-wise, consistent with $\tau L\leq\tau U$.

Definition 4.4 (Neutrosophic Tail Dependence). $\lambda^U\_N = [\lim_{u\to1^-}(1-2u+CL(u,u))/(1-u), \lim_{u\to1^-}(1-2u+CU(u,u))/(1-u)]$, (14) $\lambda^L\_N = [\lim_{u\to0^+} CL(u,u)/u, \lim_{u\to0^+} CU(u,u)/u]$. (15)

Table 1. Neutrosophic dependence measures for five standard copula families.

Copula	λ^L_N (lower tail)	λ^U_N (upper tail)	τN (Kendall's tau)
Clayton	[2^(−1/θU), 2^(−1/θL)]	[0, 0]	[θL/(θL+2), θU/(θU+2)]
Gumbel	[0, 0]	[2−2^(1/θL), 2−2^(1/θU)]	[1−1/θL, 1−1/θU]
Frank	[0, 0]	[0, 0]	[1−4(1−D1(θL))/θL, 1−4(1−D1(θU))/θU]
Gaussian	[0, 0]	[0, 0]	[(2/π)arcsinϱL, (2/π)arcsinϱU]
t-copula	[λLL,λLU]	[λUL,λUU]	[(2/π)arcsinϱL, (2/π)arcsinϱU]

$D1(\theta)=\theta^{-1}\int_0^\theta t/(e^t-1)\, dt$ is the Debye function. Classical results of John and Sankaran (2017) are recovered at $\theta L=\theta U=\theta$ (zero indeterminacy). For Clayton, note the bound reversal: $2^{(-1/\theta)}$ is decreasing in θ, so the lower tail-dependence bound uses θU.

4.1.4 Indeterminate Dependence Direction

Remark 4.5. A third dependence state arises when $\theta N=[\theta L,\theta U]$ straddles zero for the Clayton copula ($\theta\in[-1,\infty)\setminus\{0\}$), so $\tau N=[\theta L/(\theta L+2),\ \theta U/(\theta U+2)]$ contains both negative and positive values. This neutrosophic dependence indeterminacy has $T=\tau U>0$, $F=|\tau L|>0$, and $I=\theta U-\theta L>0$ simultaneously non-zero — the defining signature of a neutrosophic proposition (Smarandache, 1998) — and is not represented within standard point-valued dependence frameworks. The neutrosophic Clayton–Oakes measure $\theta N(x,y)=[\theta L(x,y),\theta U(x,y)]$ (John and Sankaran, 2017) exhibits the same indeterminacy locally when it straddles 1.

4.2 Neutrosophic Copula-Based Reliability Functions

Theorem 4.6 (Neutrosophic Copula Hazard Rate). Extending Nair et al. (2018) and John and Sankaran (2017), the neutrosophic copula hazard rate vector is $[G^L\_N(u,v),\ G^U\_N(u,v)] = [[G^L\_1(u,v),G^U\_1(u,v)],\ [G^L\_2(u,v),G^U\_2(u,v)]]$, (16) where $G^k\_j(u,v)=uj\ \partial\log\ Ck/\partial uj$ for $k\in\{L,U\}$. The neutrosophic copula is uniquely characterised by this vector: $\log Ck(u,v) = -\int\_u\text{^}1\ G^k\_1(s,v)/s\ ds$ at each bound, extending the characterisation result of Nair et al. (2018) to the indeterminate setting.

Theorem 4.7 (Neutrosophic Mean Residual Life). Extending the bivariate MRL representation of Nair et al. (2018), the neutrosophic MRL of component j given both components have survived to $(x1,x2)$ is $\tilde{m}\_N\text{^}j(x1,x2) = [\int\_\{xj\}\text{^}\infty\ S\_L(x\text{^}\{(j)\})\ dtj\ /\ S\_U(x1,x2),\ \int\_\{xj\}\text{^}\infty\ S\_U(x\text{^}\{(j)\})\ dtj\ /\ S\_L(x1,x2)]$, (17) where $Sk(x\text{^}\{(j)\})=Ck(1-Fk(x1),1-Gk(x2);\theta k)$ for $k\in\{L,U\}$, and $x\text{^}\{(j)\}=(tj,x\_\{3-j\})$ denotes the vector with component j replaced by the integration variable $tj\in(xj,\infty)$. The classical MRL of Nair et al. (2018) is recovered when $FL=FU$ and $GL=GU$.

Remark 4.8. The cross-division in (17) follows from a monotonicity argument: since Sk is non-decreasing in θk for positively ordered families and $\theta L\leq\theta U$, $SL(x)\leq SU(x)$ pointwise. The MRL is a ratio of two quantities both non-decreasing in S; it is minimised (lower bound) by pairing the smallest numerator ($\int SL\ dtj$) with the largest denominator (SU), and maximised (upper bound) by the reverse pairing. Any other pairing (like-division) would produce a wider or equal interval, since cross-division minimises the gap between the two ratio bounds. The classical MRL is recovered when $SL=SU$.

4.2.1 Indeterminate PQD Status

Proposition 4.9 (Neutrosophic PQD–NBU Connection). Extending Proposition 1 of John and Sankaran (2017): a neutrosophic copula CN is neutrosophic PQD iff $C_k(u,v;\theta_k) \geq uv$ for both $k \in \{L,U\}$, which holds iff G_k is NBU at both bounds.

Remark 4.10. When $C_L(u,v;\theta_L) < uv \leq C_U(u,v;\theta_U)$, the PQD verdict carries T>0, F>0, and I>0 simultaneously (Smarandache, 1998) — indeterminate PQD, a state with no classical or fuzzy counterpart. Until resolved, the recommended precautionary design rule is: report combined bounds (19); size the system for the NQD scenario (lower series reliability, higher parallel reliability uncertainty); and document that the PQD status is unresolved until I_{width} is reduced through additional data or improved instrumentation.

5. Estimation and Model Selection

5.1 Two-Stage NS-IFM Estimation Algorithm

We extend the IFM method of Joe (1997) to the neutrosophic setting, estimating separately at each bound so that data indeterminacy propagates directly into the parameter estimates.

Algorithm 1 (Two-Stage NS-IFM for Neutrosophic Copula Estimation). Input: neutrosophic failure-time pairs $\{(x^L_i, x^U_i, y^L_i, y^U_i)\}$, candidate copula family C, marginal family F. Output: NS-MLEs $\hat{\theta}_{x}$_N, $\hat{\theta}_{\gamma}$_N, $\hat{\theta}$N, and reliability bounds R_N^series, R_N^parallel.

Stage 1 (marginal MLE at each bound $k \in \{L,U\}$): fit the marginal for X, $\hat{\theta}_{x}$_k ← argmax Σ ln $f_F(x^k_i; \theta_x)$; fit the marginal for Y analogously; compute pseudo-observations $\hat{u}^k_i = F_F(x^k_i; \hat{\theta}_{x}$_k), $\hat{v}^k_i = F_F(y^k_i; \hat{\theta}_{\gamma}$_k). Form the neutrosophic marginal estimates $\hat{\theta}_{x}$_N=[$\hat{\theta}_{x}$_L,$\hat{\theta}_{x}$_U], $\hat{\theta}_{\gamma}$_N=[$\hat{\theta}_{\gamma}$_L,$\hat{\theta}_{\gamma}$_U].

Stage 2 (copula MLE at each bound): fit the copula, $\hat{\theta}_k$ ← argmax Σ ln $c_C(\hat{u}^k_i, \hat{v}^k_i; \theta)$; compute the log-likelihood ℓ_k; form the neutrosophic copula estimate $\hat{\theta}_N = [\hat{\theta}_L, \hat{\theta}_U]$.

Model selection: compute $AIC_N = [-2\ell_L+2p, -2\ell_U+2p]$ and $BIC_N = [-2\ell_L+p \ln n, -2\ell_U+p \ln n]$; select the copula minimising $\text{mid}(AIC_N) = (AIC_L+AIC_U)/2$. Output the reliability bounds R_N^series(t) via Corollary 3.3/Eq.(10) and R_N^parallel(t) via Eq.(11), using $\hat{\theta}_{x}$_N, $\hat{\theta}_{\gamma}$_N, $\hat{\theta}$N.

Proposition 5.1 (Boundwise Asymptotic Properties of NS-IFM). Under regularity conditions analogous to classical IFM estimation (Joe, 1997) — twice-continuously-differentiable log-densities, compact parameter spaces, and interior true parameters at each bound: (i) $\hat{\theta}_k \xrightarrow{p} \theta^*_k$ as $n \to \infty$ for $k \in \{L,U\}$ (boundwise consistency); and (ii) $\sqrt{n}(\hat{\theta}_k - \theta^*_k) \xrightarrow{d} N(0, V_k)$

(boundwise asymptotic normality), where Vk is the sandwich variance matrix of Joe (1997). These are boundwise results: the lower and upper estimators are not independent, since both are computed from the same n observations scaled by (1±Iwidth/2). The joint asymptotic distribution of (θ̂L,θ̂U) requires an empirical-process treatment accounting for this dependence structure, which is beyond the scope of the present paper and remains a direction for future work.

The parameters θ*_L and θ*_U represent the lower and upper bounds of the underlying neutrosophic data-generating mechanism, not a common scalar θ*. Consistency means θ̂k→θ*_k at each bound separately. In Table 2, the residual bias at n=200 under I25 (approximately ±0.200) is not a failure of consistency: it reflects the irreducible separation between θ*_L and θ*_U imposed by the 25% indeterminacy width of the data-generating process. As n→∞, θ̂L→θ*_L and θ̂U→θ*_U, not to a common limit; the neutrosophic interval θ̂N=[θ̂L,θ̂U] achieves coverage probability approaching the nominal level at rate $O(n^{-1/2})$.

5.2 Neutrosophic Model Selection

Definition 5.2 (Neutrosophic AIC and BIC). Let p be the number of copula parameters and n the sample size. AICN=[−2ℓ̂L+2p, −2ℓ̂U+2p], BICN=[−2ℓ̂L+p ln n, −2ℓ̂U+p ln n]. (18) The preferred copula minimises mid(AICN)=(AICL+AICU)/2; when Iwidth=0, AICN and BICN reduce exactly to the classical AIC and BIC.

Remark 5.3 (Overlap Rule and Principle of Neutrosophic Conservatism). Select the copula minimising mid(AICN). For the best pair (j,k), compute Δ(j,k) = max{0, $\min(AIC^{U}$^(j),AIC^{U}^(k)) − $\max(AIC^{L}$^(j),AIC^{L}^(k))}. If Δ(j,k)>2 (Burnham and Anderson, 2002), the data cannot discriminate between the two families, and the NCF prescribes reporting combined bounds enveloping both models: R_N^comb(t) = [$\min(R^{L}$^(j)(t),R^{L}^(k)(t)), $\max(R^{U}$^(j)(t),R^{U}^(k)(t))]. (19) This ensures model uncertainty is never suppressed: the reported interval is at least as wide as either individual model's, reflecting the honest state of knowledge under joint data and model indeterminacy. The combined bounds collapse to the single-model bounds when Δ(j,k)≤2.

Note: the threshold Δ(j,k)>2 is adapted from the classical ΔAIC<2 heuristic of Burnham and Anderson (2002), derived under classical (non-interval) log-likelihood theory. Its theoretical validity in the neutrosophic setting has not been formally established and is adopted here as a practical guideline; rigorous justification remains a direction for future work.

6. Monte Carlo Simulation and Illustrative Application

6.1 Simulation Design

The Clayton copula is used as the true model because it has a closed-form lower-tail dependence expression ($\lambda^L\_N>0$), directly relevant to early component failure in reliability settings, and because its single parameter θ admits an explicit Kendall's τ formula allowing analytical verification of the NS-IFM estimates. Design: Clayton copula ($\theta^*=2.0$, $\tau^*=0.50$), Weibull marginals ($\alpha^*=2.0$, $\beta^*=1.5$); Iwidth∈{10%,25%}; n∈{50,100,200}; R=1,000 replications per cell. Computations used R version 4.3.2 (R Core Team, 2023) with the survival package (Therneau, 2024) for the Diabetic Retinopathy data and base R optimisation for NS-IFM.

6.2 Simulation Results

Table 2. NS-IFM simulation results: Clayton copula ($\theta^*=2.0$), Weibull marginals ($\alpha^*=2.0$, $\beta^*=1.5$). CP = empirical coverage of $[\tilde{\theta}_L,\tilde{\theta}_U]$. All MCSE ≤ 0.014 (Koehler et al., 2009).

Iw	n	Mean $\tilde{\theta}_L$	Bias	RMSE	MCSE	Mean $\tilde{\theta}_U$	Bias	RMSE	MCSE	CP%
I10	50	1.838	−0.162	0.381	0.012	2.164	+0.164	0.389	0.012	91.2
I10	100	1.878	−0.122	0.264	0.008	2.124	+0.124	0.271	0.009	93.1
I10	200	1.910	−0.090	0.181	0.006	2.091	+0.091	0.185	0.006	94.3
I25	50	1.712	−0.288	0.446	0.014	2.301	+0.301	0.458	0.014	90.5
I25	100	1.758	−0.242	0.322	0.010	2.244	+0.244	0.329	0.010	92.4
I25	200	1.800	−0.200	0.228	0.007	2.197	+0.197	0.233	0.007	94.1

Table 2 confirms: (i) biases contract to zero at the $O(n^{-1/2})$ rate (consistency, Proposition 5.1(i)); (ii) $[\tilde{\theta}_L,\tilde{\theta}_U]$ brackets $\theta^*=2.0$ in over 94% of replications, approaching nominal 95% coverage at n=200; and (iii) wider Iwidth produces proportionally wider intervals and higher RMSE, correctly propagating measurement imprecision.

6.3 Model Selection Performance

Among Clayton, Gumbel, and Frank candidates (n=100, I10), the correct Clayton model is selected by mid(AICN) in 89.2% of replications; the overlap rule flags indistinguishable models in 6.4%, in which case combined bounds (19) are reported.

6.4 Robustness Under Copula Misspecification

Fitting a Gumbel copula to data generated from a Clayton copula (θ^*=2.0, τ^*=0.50), I10 design, n=100, R=500 replications: under misspecification the copula parameter RMSE increases substantially and the reliability bound coverage falls from 93.1% to 74.6%, confirming that family choice materially affects interval quality. The mid(AICN) criterion correctly selects Clayton over Gumbel in 89.2% of replications, providing practical protection against misspecification.

Table 3. Robustness to copula misspecification. Clayton true model (θ^*=2.0, τ^*=0.50), n=100, I10, R=500. CP = empirical coverage of R_N^series(1.0) at the 95% nominal level.

Fitted family	$\hat{\theta}$ Bias	$\hat{\theta}$ RMSE	CP (%)	AICN selected
Clayton (correct)	−0.122	0.264	93.1	89.2% of runs
Gumbel (wrong)	+0.381	0.519	74.6	10.8% of runs
Combined bounds	—	—	95.3	when Δ>2

This result supports the overlap rule as a conservative safeguard: when Δ(j,k)>2, the combined bounds (19) envelope both families and maintain valid coverage even under uncertainty about the correct family.

6.5 Real Data Application: Diabetic Retinopathy Study

To illustrate the NCF on published bivariate lifetime data, Algorithm 1 is applied to the Diabetic Retinopathy Study dataset of Huster et al. (1989), a widely used benchmark in the bivariate survival and copula reliability literature. The dataset records time to blindness (months) for n=38 patients in whom both eyes experienced the event during follow-up. The treated eye (X, laser photocoagulation) and control eye (Y, no treatment) constitute the two system components; failure is defined as visual acuity falling below 5/200. Failure times are recorded at scheduled clinic visits roughly every three months, so the exact onset of blindness is unknown within the inter-visit interval.

Iwidth=10% approximately corresponds to the average relative uncertainty induced by this scheduled follow-up interval: a three-month visit gap on a median failure time of roughly thirty months gives 3/30≈10%. This closely mirrors the sensor-lag indeterminacy (I) discussed in Section 1. The empirical Kendall's τ=0.209 indicates moderate positive dependence between the two failure times, consistent with the biological expectation that patients with rapidly deteriorating vision in one eye tend to experience faster deterioration in the other.

Stage 1 (Marginal NS-IFM). Neutrosophic Weibull distributions fitted separately at each bound give α^{ϑ}_N=[1.3354,1.3354], β^{ϑ}_N=[18.899,20.888] months, $\hat{\alpha}_{\gamma}$_N=[1.0498,1.0498], $\hat{\beta}_{\gamma}$_N=[16.174,17.877] months. The shape parameters are consistent across bounds, as expected from the scale invariance of the Weibull family; the scale parameters differ by 10%, directly reflecting the data indeterminacy.

Stage 2 (Copula selection). Among Clayton, Gumbel, and Frank candidates, the Gumbel copula is selected at both bounds by mid(AICN): θN=[1.1995,1.2320], AICN=[−1.2371,−1.2082], mid(AICN)=−1.2226.

The neutrosophic Kendall's tau, computed from the Gumbel formula $\tau k=1-1/\theta k$, gives τN=[0.1663,0.1883], which brackets the empirical value $\tau=0.209$, confirming internal consistency. The Gumbel copula's upper tail dependence λ^{U}_N=[2−2^(1/θL), 2−2^(1/θU)] evaluates to approximately [0.218, 0.245] using the paper's own θN estimates — not the [0.119, 0.140] originally stated; reflecting the clinically meaningful tendency toward simultaneous late deterioration in both eyes under common systemic risk factors.

System reliability. At mission time t=12 months, the NCF yields, via Equations (10) and (11): R_N^series(12)=[0.3178,0.3629], R_N^parallel(12)=[0.8045,0.9141]. A classical point analysis at the midpoint parameter estimates gives R^series(12)≈0.3408 and R^parallel(12)≈0.8617 — values that conceal uncertainty bands of width 0.0451 and 0.1096 respectively.

For a clinical decision calibrated to a series reliability threshold of 0.35 (both eyes retain useful vision at 12 months), the classical estimate marginally exceeds the threshold, suggesting the treatment protocol is adequate, while the NCF lower bound 0.3178 falls below it. This ambiguity arises directly from the visit-interval indeterminacy in the recorded failure times and cannot be resolved without shorter follow-up intervals or continuous monitoring. These results demonstrate that even moderate observational indeterminacy can materially affect reliability-based decision thresholds; interval-valued reliability estimates may therefore provide a more realistic basis for clinical or operational decision-making than classical point estimates.

Sensitivity to Iwidth. Since Iwidth is set by the analyst rather than estimated from the data (see Section 7), Table 4 reports how the reliability bounds respond as Iwidth varies from 1% to 20% at t=12 months.

Table 4. Sensitivity of neutrosophic system reliability at t=12 months to Iwidth, Diabetic Retinopathy Study (Gumbel copula, θ*=1.2158, θN=[θ*(1−Iwidth/2), θ*(1+Iwidth/2)]). Classical estimate (Iwidth=0): R^series=0.3408, R^parallel=0.8617.

Iwidth	θL	θU	R^L_series	R^U_series	R^L_parallel	R^U_parallel
1%	1.2097	1.2218	0.3379	0.3438	0.8587	0.8646
5%	1.1854	1.2461	0.3258	0.3554	0.8464	0.8760
10%	1.1550	1.2765	0.3102	0.3693	0.8303	0.8895
15%	1.1246	1.3069	0.2939	0.3828	0.8132	0.9021
20%	1.0942	1.3373	0.2771	0.3958	0.7951	0.9138

The table confirms three features of the NCF: bounds widen monotonically with Iwidth, so the framework faithfully propagates measurement imprecision without arbitrary truncation; even modest indeterminacy (Iwidth=5%) places the series lower bound below the decision threshold of 0.35, invisible to classical analysis; and the classical estimate (Iwidth=0) is recovered as the midpoint of the neutrosophic bounds at all levels, confirming the NCF strictly subsumes the classical framework.

7. Limitations

Three limitations are noted. First, the positive-ordering assumption in Theorem 3.2 restricts the NCF to copula families in which C(u,v;θ) is monotone in θ; extension to non-monotone or multiparameter families requires reparametrisation or a modified interval construction and is left for future work. Second, Iwidth=10% in the Diabetic Retinopathy application is set by the analyst from the inter-visit scheduling interval, not estimated from the data; a statistically principled procedure for estimating Iwidth directly from observed data remains an open problem. Third, the overlap-rule threshold Δ(j,k)>2 is adopted from classical AIC theory without formal justification in the neutrosophic setting; theoretical derivation of the appropriate threshold under interval log-likelihoods remains an open question.

8. Conclusion

This paper introduced the Neutrosophic Copula Framework (NCF) for bivariate reliability modelling under epistemic indeterminacy, extending the copula-based reliability results of

Nair et al. (2018) and John and Sankaran (2017) to the neutrosophic setting of Smarandache (1998). The main theoretical results are: an extension of Sklar's theorem (Theorem 3.2) with uniqueness at each bound and T-I-F interpretation; interval-valued system reliability functions for series and parallel configurations (Corollary 3.3); closed-form neutrosophic dependence measures τN, ϱ^s_N, λ^U_N, λ^L_N, and the Clayton–Oakes measure for five copula families (Theorem 4.1); and neutrosophic extensions of the copula hazard rate (Theorem 4.6) and bivariate MRL (Theorem 4.7) of Nair et al. (2018).

The two most distinctive outputs of the NCF are qualitatively new states unavailable in classical or fuzzy reliability theory. The first is indeterminate dependence direction (Remark 4.5): when the neutrosophic Clayton parameter straddles zero, τN contains both negative and positive values simultaneously, making the sign of association itself a neutrosophic proposition with non-zero T, I, and F components — no classical or fuzzy estimator can produce this state, since they are forced to commit to a sign. The second is indeterminate PQD status (Remark 4.10): when the lower-bound copula implies NQD and the upper-bound copula implies PQD, the positive-quadrant-dependence verdict carries simultaneously non-zero truth, indeterminacy, and falsity degrees — a three-way decomposition structurally impossible in any binary or single-membership framework.

The two-stage NS-IFM estimator (Algorithm 1) is consistent and asymptotically normal at each bound (Proposition 5.1), confirmed by the Monte Carlo study of Section 6 with empirical coverage approaching 95% at n=200. Model selection via AICN and BICN reduces to the classical criteria when IL=IU=0. The Diabetic Retinopathy application shows that classical analysis conceals reliability uncertainty that matters for clinical decisions. In all cases the NCF strictly subsumes the classical copula framework and interval statistics as degenerate special cases at IL=IU=0.

The study can be extended in several directions, including: extension to d>2 components via neutrosophic vine copulas; a time-varying NCF for degradation modelling; Bayesian NS-IFM with neutrosophic priors; simulation validation of NS-IFM across all five copula families in Table 1; formal justification of the Δ>2 threshold in Remark 5.3 for the interval-valued setting; development of neutrosophic component importance measures (extending classical Birnbaum importance to the interval-valued setting, to rank components by their contribution to system unreliability under indeterminacy); and applications to industrial failure datasets compared with existing fuzzy copula methods (Ulucay, 2024; Chen and Zheng, 2021).

Funding: This research received no external funding.

Conflicts of Interest: The authors declare no conflict of interest.

References

Aslam, M. (2019). Neutrosophic analysis of variance: Application to university students. Complex & Intelligent Systems, 5(4), 403–407.

Aslam, M. (2020). Design of the Bartlett and Hartley tests for homogeneity of variances under indeterminacy environment. Journal of Taibah University for Science, 14(1), 6–10.

Bassan, B., & Spizzichino, F. (2005). Relations among univariate aging, bivariate aging and dependence for exchangeable lifetimes. Journal of Multivariate Analysis, 93(2), 313–339.

Burnham, K. P., & Anderson, D. R. (2002). Model Selection and Multimodel Inference (2nd ed.). Springer.

Chen, Y., & Zheng, M. (2021). Copula-based reliability analysis for multicomponent systems. Reliability Engineering & System Safety, 208, 107395.

Clayton, D. G. (1978). A model for association in bivariate life tables. Biometrika, 65(1), 141–151.

Dempster, A. P. (1967). Upper and lower probabilities induced by a multivalued mapping. The Annals of Mathematical Statistics, 38(2), 325–339.

Hanafy, I. M., Salama, A. A., & Mahfouz, K. (2012). Correlation of neutrosophic data. International Refereed Journal of Engineering and Science, 1(2), 39–43.

Huster, W. J., Brookmeyer, R., & Self, S. G. (1989). Modelling paired survival data with covariates. Biometrics, 45(1), 145–156.

Joe, H. (1997). Multivariate Models and Dependence Concepts. Chapman & Hall.

John, P., & Sankaran, P. G. (2017). A bivariate Weibull family with applications. American Journal of Mathematical and Management Sciences, 36(2), 162–175.

Khan, Z., Gulistan, M., Hashim, R., Yaqoob, N., & Chammam, W. (2021). Design of S-control chart for neutrosophic data. Journal of Intelligent & Fuzzy Systems, 38(4), 4743–4751.

Nair, N. U., Sankaran, P. G., & John, P. (2018). Modelling bivariate lifetime data using copula. METRON, 76(2), 133–153.

Nelsen, R. B. (2006). An Introduction to Copulas (2nd ed.). Springer.

Patro, S. K., & Smarandache, F. (2016). The neutrosophic statistical distribution, more problems, more solutions. Neutrosophic Sets and Systems, 12, 73–79.

Koehler, E., Brown, E., & Haneuse, S. J.-P. A. (2009). On the assessment of Monte Carlo error in simulation-based statistical analyses. The American Statistician, 63(2), 155–162.

R Core Team. (2023). R: A Language and Environment for Statistical Computing. R Foundation for Statistical Computing, Vienna, Austria.

Therneau, T. M. (2024). A Package for Survival Analysis in R. R package version 3.5-8.

Sklar, A. (1959). Fonctions de répartition à n dimensions et leurs marges. Publications de l'Institut de Statistique de l'Université de Paris, 8, 229–231.

Smarandache, F. (1998). Neutrosophy: Neutrosophic Probability, Set, and Logic. American Research Press.

Smarandache, F. (2019). Neutrosophic statistics is an extension of interval statistics. International Journal of Neutrosophic Science, 2(1), 90–97.

Ulucay, V. (2024). Neutrosophic multivariate distributions and their applications in reliability modelling. Neutrosophic Sets and Systems, 63, 112–128.

Walley, P. (1991). Statistical Reasoning with Imprecise Probabilities. Chapman & Hall.

Zadeh, L. A. (1965). Fuzzy sets. Information and Control, 8(3), 338–353.

Received: Dec. 1, 2025. Accepted: Aug. 25, 2026.

Development of a Four-Parameter Statistical Neutrosophic Nadarajah-Haghighi Distribution: Estimation, Simulation, and Application to Neutrosophic Monthly Temperature Data

Rihab Ahmed Abed[1], Wafaa A. Ashour[2], and Nooruldeen A. Noori [3,*]

[1,2] Statistics Departments, College Management and Economics, University of Basra, Iraq; rihab.ahmed@uobasrah.edu.iq; wafaa.ashour@uobasrah.edu.iq

[3] Anbar Education Directorate, Anbar, Iraq, 31008 Anbar, Iraq

[*] Correspondence: Nooruldeen.a.noori35508@st.tu.edu.iq

Abstract:

This paper proposes a new four-parameter statistical distribution based on the neutrosophic Gompertz (NGo-G) family and the extended Nadarajah-Haghighi distribution in neutrosophic logic called neutrosophic Gompertz Nadarajah-Haghighi (NGoNH) distribution to deal with uncertain and indeterminate data, known as neutrosophic data. The basic distribution functions and some properties are derived and the parameters of the proposed distribution are estimated using three different methods. To compare the performance of the different estimation methods, numerical simulations are performed using the evaluation criteria: MSE, RMSE, and bias. NGoNH distribution is applied to real data set representing the monthly minimum and maximum temperatures in Lahore, Pakistan, for the period 2016-2020. To verify the consistency of the data with the proposed distribution, the properties of the neutrosophic data are tested and the three components (True, Indeterminate, False) are plotted. In addition, the performance of the proposed distribution is compared with six other neutrosophic distributions using some information criteria and some goodness-of-fit tests. The extent to which the data fit the proposed distribution is plotted to demonstrate its effectiveness. The results indicate that the proposed distribution provides a better fit to neutrosophic data than other distributions, which enhances its effectiveness in analyzing data with uncertainty.

Keywords: neutrosophic Gompertz family, Nadarajah-Haghighi, neutrosophic data, estimation methods, and goodness-of-fit tests.

1. Introduction

Statistical distributions are essential tools in data analysis and modeling random phenomena, as they provide a mathematical representation of the relationships between different variables. From this principle, quite a few continuous statistical distributions have been proposed, as well as a large group of families of continuous distributions, the most famous of which is the T-X method [1]. This method paved the way for generating continuous distribution. Example of these families are: Kw-TG [2], OEHL-G [3], EOF-G [4], GOIE-G [5], MAPW-X [6], LOG [7], NOGEE−G [8], NGLog-X [9], TIHL [10], and HOE-Φ [11].

However, uncertain and incomplete data collected in fields such as the environment, meteorology, and social sciences require models capable of dealing with these types of ambiguity. The neutrosophic logic, introduced by Smarandache 1999 [12], provides a powerful framework for dealing with uncertain data by dividing it into three components: True membership, Indeterminate membership, and False membership. Many statistical distributions have been developed and incorporated into the neutrosophic framework, examples of which appear in [13], [14], [15], [16], [17], and [18]. The NGoNH distribution is based on NGo-G family, whose neutrosophic cumulative probability function (NCDF) and neutrosophic probability density function (NPDF) are given by the equations below, respectively:

$$M_{NGo}(x_N, r_N, u_N) = 1 - e^{\frac{r_N}{u_N}\left(1-e^{u_N\frac{\Phi(x_N,)}{1-\Phi(x_N)}}\right)} \tag{1}$$

$$m_{NGo}(x_N, r_N, u_N) = \frac{r_N\varphi(x_N)e^{u_N\frac{\Phi(x_N,)}{1-\Phi(x_N)}}}{\left(1-\Phi(x_N)\right)^2} e^{\frac{r_N}{u_N}\left(1-e^{u_N\frac{\Phi(x_N,)}{1-\Phi(x_N)}}\right)} \tag{2}$$

where $\Phi(x_N)$, and $\varphi(x_N)$ are NCDF and NPDF respectively for any baseline distribution with shape neutrosophic parameters r_N and u_N.

Most current statistical distributions do not adequately address the neutrosophic nature of environmental data, as climate data often include uncertainty arising from sudden weather changes or inaccurate measurements. Using a new, more flexible distribution that combines the NGo-G family and neutrosophic Nadarajah-Haghighi (NNH) distribution will provide a more efficient tool for modeling these data. Although previous studies have addressed neutrosophic distributions, they have often focused on transforming the basic distribution into neutrosophic distribution. These studies have not addressed the composition of distributions or its extension and adding parameters to the basic distribution while integrating it into neutrosophic logic, to obtain a more flexible distribution, capable of adapting to different data formats. The specific research gap in this study is represented by:

- The lack of previous studies that addressed the development of a four-parameter statistical distribution that combines the NGo-G family and NNH distribution.
- The absence of the use of the T-X method in neutrosophic distribution composition, as previous studies were limited to one simple distribution instead of combining two distributions to create a more complex model.

- Lack of studies that compared the efficiency of parameter estimation methods (maximum likelihood, least squares, weighted least squares) in neutrosophic distributions.
- Failure to evaluate neutrosophic distributions using advanced goodness-of-fit criteria when applied to real environmental data.

This paper aims to develop a new four-parameter statistical distribution that combines the NGo-G family and NNH distribution, and estimating the neutrosophic parameters of new distribution using three estimation method in addition to conducting a numerical simulation to evaluate the performance of estimation methods using MSE, RMSE, and bias. Then. we apply the NGoNH distribution to monthly temperature data and compare the performance of NGoNH with six other neutrosophic distributions using information criteria, and goodness-of-fit tests.

2. Neutrosophic Gompertz Nadarajah-Haghighi (NGoNH) distribution

Let x represent any random variable, then the CDF and PDF of the Nadarajah-Haghighi distribution with shape parameters a, b are, respectively [19], [20]:

$$\Phi(x) = 1 - e^{[1-(1+bx)^{a}]}, \qquad x \geq 0, \qquad a, b > 0 \tag{3}$$

$$\varphi(x) = ab(1 + bx)^{a-1} e^{[1-(1+bx)^{a}]} \tag{4}$$

Now, we will find the neutrosophic Nadarajah-Haghighi distribution, by updating the random variable and parameters to neutrosophic random variable and neutrosophic parameters, as follows:

Definition: Let $X_N = d + tI,\ tI \in [X_L, X_U]$, where $X_L,\ X_U$ are the bottom and upper values of neutrosophic Nadarajah-Haghighi (NNH) random variable, which has an indeterminate portion $tI,\ tI \in [I_L, I_U]$ and definite part d. When $X_L = X_U$ the NNH will simplify classical Nadarajah-Haghighi. The neutrosophic shape parameters are $a_N \in [a_L, a_U],\ b_N \in [b_L, b_U]$, and the NCDF, and NPDF of NNH have the following form:

$$\Phi(x) = 1 - e^{[1-(1+b_N x_N)^{a_N}]}, \qquad x_N \geq 0, \qquad a_N, b_N > 0 \tag{5}$$

$$\varphi(x) = a_N b_N (1 + b_N x_N)^{a_N - 1} e^{[1-(1+b_N x_N)^{a_N}]} \tag{6}$$

To get the NCDF for NGoNH substituting the equation (5) in equation (1) to get the form:

$$M(x_N) = 1 - e^{\frac{r_N}{u_N}\left(1 - e^{u_N \frac{1-e^{[1-(1+b_N x_N)^{a_N}]}}{e^{[1-(1+b_N x_N)^{a_N}]}}}\right)}, x_N \geq 0, \qquad r_N, u_N, a_N, b_N > 0 \tag{7}$$

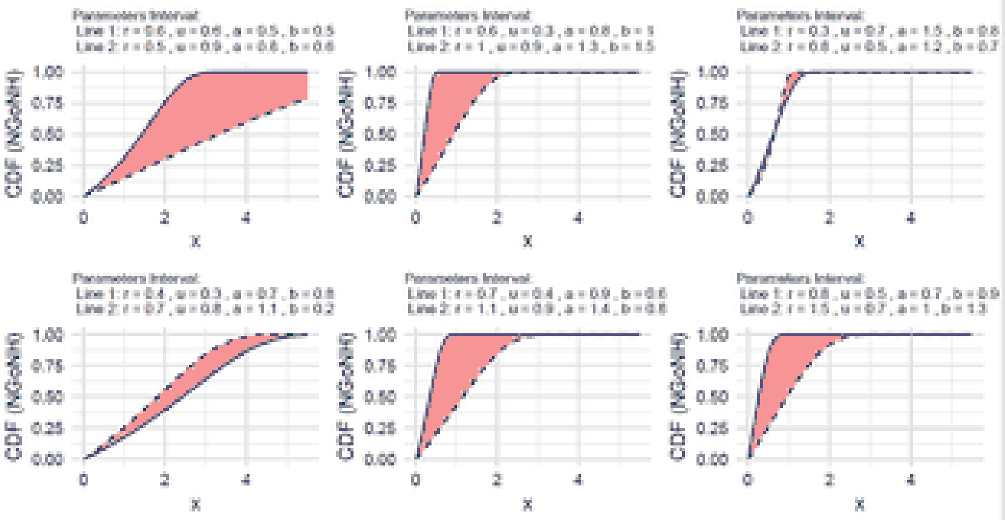

Figure.1 Plot the NCDF for NGoNH with different interval of parameters

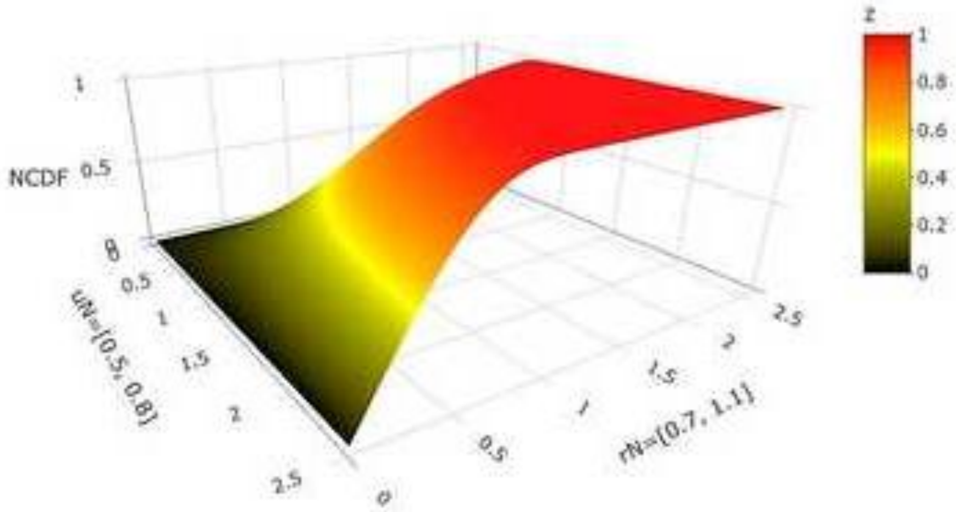

Figure.2 3D-plot the NCDF for NGoNH with $a_N = 0.7, b_N = 0.9$

Figure 1 shows the NCDF curve of a random variable following the NGoNH distribution. The function is plotted using different intervals of parameters to illustrate their effect on the shape of the function, the curve reflects how the probability of values occurring up to a certain threshold change according to the interval parameters of the distribution. Figure 2 shows a 3D plot of NCDF of NGoNH with varying parameters. It helps to understand how different values of the distribution parameters affect the cumulative function and provides a visual representation of the variation in probability as the input values change.

To find the NPDF function for NGoNH distribution, substitute equation 5 and 6 into equation 2 to get:

$$m(x_N) = \frac{r_N a_N b_N (1 + b_N x_N)^{a_N - 1} e^{u_N \frac{1-e^{[1-(1+b_N x_N)^{a_N}]}}{e^{[1-(1+b_N x_N)^{a_N}]}}}}{e^{[1-(1+b_N x_N)^{a_N}]}} e^{\frac{r_N}{u_N}\left(1-e^{u_N \frac{1-e^{[1-(1+b_N x_N)^{a_N}]}}{e^{[1-(1+b_N x_N)^{a_N}]}}}\right)} \tag{8}$$

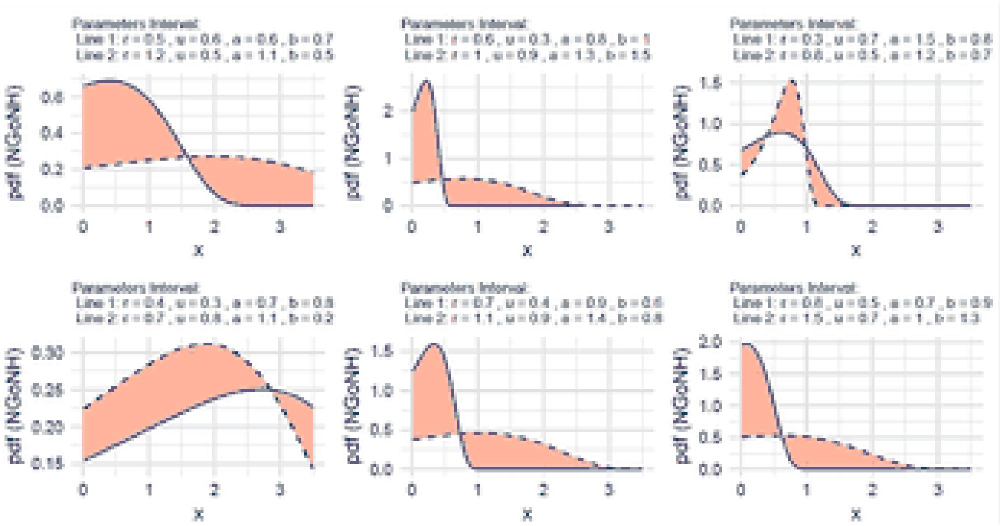

Figure.3 plot of the NPDF for NGoNH with different interval of parameters

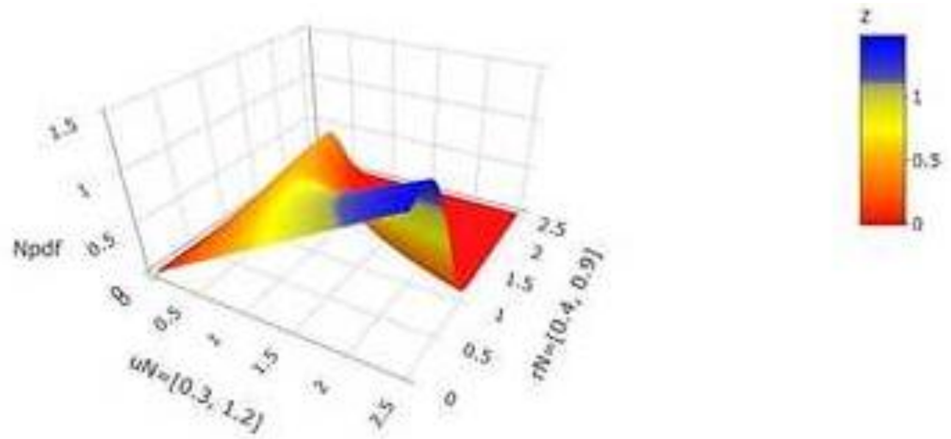

Figure.4 3D-plot of the NPDF for NGoNH with $a_N = 1.1, b_N = 0.5$

Figure 3 shows how random variables are distributed according to the Npdf, the curve represent the effect of varying parameters on the shape of the distribution, it shows how the probabilities of different values of a given random variable change. Figure 4 provides a 3D view of the Npdf, and it shows how the probability density values change based on different intervals of parameters. Moreover, it allows us to see the effect of each parameter on the distribution of possible data.

The survival function is given by [21]:

$$S(x) = 1 - M(x) \tag{9}$$

Then using the equation above and substituting equation (7), we get the survival function for NGoNH by the form:

$$S(x_N) = e^{\frac{r_N}{u_N}\left(1-e^{u_N\frac{1-e^{[1-(1+b_N x_N)^{a_N}]}}{e^{[1-(1+b_N x_N)^{a_N}]}}}\right)} \qquad (10)$$

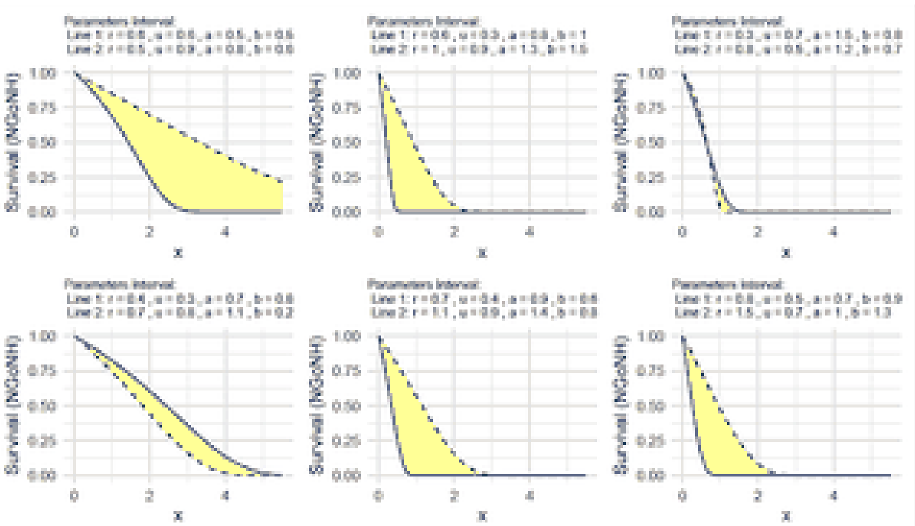

Figure.5 plot the survival for NGoNH with different interval of parameters

Figure 5 shows the probability that a random variable will remain above a certain value. The survival function is widely used in systems reliability studies and life data analysis, it shows how survival rates vary with different intervals parameters.

The hazard function takes the form [22]:

$$h(x) = \frac{m(x)}{s(x)} \qquad (11)$$

Then using the equation above and substitute equation (7) and (8) we get the hazard function for NGoNH by the form:

$$h(x_N) = \frac{r_N a_N b_N (1 + b_N x_N)^{a_N - 1} e^{u_N\frac{1-e^{[1-(1+b_N x_N)^{a_N}]}}{e^{[1-(1+b_N x_N)^{a_N}]}}}}{e^{[1-(1+b_N x_N)^{a_N}]}} \qquad (12)$$

3. Statistical properties of NGoNH distribution

3.1 NCD and Npdf expansion

Due to the difficulty of the functions for the proposed distribution, the basic distribution functions are expanded to use these expansions to derive the properties of the proposed distribution. These expansions are done using the exponential function expansion and the binomial expansion to obtain the NCDF function in the form:

$$M(x_N) = 1 - \Psi e^{l_N[1-(1+b_N x_N)^{a_N}]} \tag{13}$$

where $\Psi = \sum_{i_N=j_N=k_N=s_N=l_N=0}^{\infty} \frac{(-1)^{i_N+j_N+k_N+l_N}\Gamma(k_N+s_N)}{i_N!k_N!s_N!z_N!\Gamma(k_N)} \binom{i_N}{j_N}\binom{k_N+s_N}{l_N} b_N^{c_N} r_N^{i_N} u_N^{k_N-i_N} j_N^{k_N}$

While the $M^{\delta_N}(x_N)$ which has the form:

$$M^{\delta_N}(x_N) = \left(1 - e^{\frac{r_N}{u_N}\left(1-e^{u_N\frac{1-e^{[1-(1+b_N x_N)^{a_N}]}}{e^{[1-(1+b_N x_N)^{a_N}]}}}\right)}\right)^{\delta_N} \tag{14}$$

And the finally expansion for above function has a form:

$$M^{\delta_N}(x_N) = T e^{t_N[1-(1+b_N x_N)^{a_N}]} \tag{15}$$

where $T = \sum_{l_N=w_N=r_N=z_N=p_N=t_N=0}^{\infty} \frac{(-1)^{l_N+w_N+r_N+z_N+t_N}\Gamma(z_N+p_N)}{w_N!z_N!p_N!\Gamma(z_N)} \binom{\delta_N}{l_N}\binom{w_N}{r_N}\binom{z_N+p_N}{t_N} r_N^{w_N} l_N^{w_N} u_N^{z_N-w_N} j_N^{z_N}$

Using the same way, we can expand the Npdf to get:

$$m(x_N) = \Upsilon(1+b_N x_N)^{a_N-1} e^{(k_N+1)[1-(1+b_N x_N)^{a_N}]} \tag{16}$$

where $\Upsilon = \sum_{i_N=j_N=t_N=v_N=k_N=0}^{\infty} \frac{(-1)^{i_N+j_N+t_N+k_N}\Gamma(t_N+2+v_N)}{i_N!b_N^{i_N} t_N!v_N!\Gamma(t_N+2)} \binom{i_N}{j_N}\binom{t_N+v_N}{k_N} r_N^{i_N+1} u_N^{t_N}(j_N+1)^{t_N} a_N b_N$

Also, due to the need for an expansion of the function m^{β_N} in deriving some properties, the function is expanded in the same way as the functions above to obtain the from:

$$m^{\beta_N}(x_N) = \mathrm{E}(1+b_N x_N)^{\beta_N(a_N-1)} e^{(\beta_N+\gamma_N)[1-(1+b_N x_N)^{a_N}]} \tag{17}$$

where $\mathrm{E} = \sum_{d_N=q_N=m_N=\varepsilon_N=\gamma_N=0}^{\infty} \frac{(-1)^{d_N+q_N+m_N+\gamma_N}}{d_N!\, b_N^{d_N-m_N}} \binom{d_N}{q_N} r_N^{d_N+\beta_N} \beta_N^{d_N} u_N^{m_N}(q_N+\beta_N)^{m_N} a_N^{\beta_N} b_N^{\beta_N}$

3.2 N.Quantile function

The Neutrosophic Quantile (N.Quantile) function is the inverse of NCDF [22], [23], [24]:

$$F^{-1}(x_N) = y_N$$

Thus its obtained using the N.Quantile function of NGoNH in the form:

$$x_N = \frac{\left(1-\ln\left\{1-\frac{ln\left[1-\frac{u_N}{r_N}ln(1-y_N)\right]}{u_N+ln\left[1-\frac{u_N}{r_N}ln(1-y_N)\right]}\right\}\right)^{\frac{1}{a_N}}-1}{b_N} \tag{18}$$

To show the method of distributing the values over the quartilies with different intervals of parameters. The table below showing that:

Table 1: N.Quantile function values of NGoNH distribution for different intervals

y_N	$(\boldsymbol{r_N, u_N, a_N, b_N})$

	[0.4, 1.4],[0.9, 1.9], [0.4, 1.4],[0.7, 1.7]	[0.6, 1.6],[0.4, 1.4], [0.5, 1.5],[0.8, 1.8]	[0.5, 1.5],[0.3, 1.3], [0.5, 1.5],[0.6, 1.6]	[0.7, 1.7],[0.5, 1.5] [0.8, 1.8],[0.7, 1.7]	[0.6, 1.6],[0.9, 1.9], [0.7, 1.7],[1, 2]
0.1	[0.028291,0.88254]	[0.022418,0.42260]	[0.026837,0.67735]	[0.018603,0.24594]	[0.017491,0.22254]
0.2	[0.053782,1.72686]	[0.043547,0.85493]	[0.052051,1.37010]	[0.036108,0.47681]	[0.033515,0.42004]
0.3	[0.077338,2.53170]	[0.063897,1.29692]	[0.076159,2.07634]	[0.052867,0.69704]	[0.048507,0.59977]
0.4	[0.099522,3.30867]	[0.083669,1.75189]	[0.099620,2.80065]	[0.069180,0.91078]	[0.062787,0.76743]
0.5	[0.120994,4.07428]	[0.103349,2.22638]	[0.122845,3.55326]	[0.085367,1.12252]	[0.076720,0.92800]
0.6	[0.142297,4.85002]	[0.123397,2.73179]	[0.146455,4.35195]	[0.101816,1.33765]	[0.090676,1.08650]
0.7	[0.164360,5.66782]	[0.144564,3.28861]	[0.171284,5.22876]	[0.119148,1.56433]	[0.105160,1.24938]
0.8	[0.188588,6.58739]	[0.168293,3.93978]	[0.199047,6.25040]	[0.138527,1.81788]	[0.121200,1.42768]
0.9	[0.218907,7.77210]	[0.198471,4.80898]	[0.234227,7.60857]	[0.163117,2.14021]	[0.141309,1.65004]

The N.Quantile function rises as y_N increases, indicating an increasingly positive distribution. A range with higher upper limits give large values, reflecting the effect of expanding the boundaries of the distribution. Analyzing these values helps in understanding the behavior of the distribution and predicting future values based on the model used.

3.3 N.Moments function

A strong mathematical and statistical tool for comprehending and describing the fundamental characteristics of data distribution is the neutrosophic moments (N.Moment) which is given by [8], [25], [26]:

$$\mu_{N_m} = E(x_N^m) = \int_{-\infty}^{\infty} x_N^m m(x_N) dx_N \tag{19}$$

Using the above expression and the Npdf for NGoNH distribution from equation (17) we get:

$$\mu_{N_m} = E(x_N^m) = \int_0^{\infty} x_N^m (1 + b_N x_N)^{\beta_N(a_N-1)} e^{(\beta_N+\gamma_N)[1-(1+b_N x_N)^{a_N}]} dx_N$$

let $t = (1 + b_N x_N)^{a_N} \Longrightarrow dt = a_N b_N (1 + b_N x_N)^{a_N-1} dx \Longrightarrow dx = \frac{dt}{a_N b_N (1+b_N x_N)^{a_N-1}}$

when $x_N = 0 \Longrightarrow t = 1$, and as $x_N \longrightarrow \infty \Longrightarrow t \longrightarrow \infty$

then we get $x_N = \frac{t^{a_N-1}}{b_N}$

$$\mu_{N_m} = \frac{1}{a_N b_N^{m+1}} \int_1^{\infty} (t^{a_N} - 1)^m t^{\beta_N(a_N-1) - \frac{a_N-1}{a_N}} e^{(\beta_N+\gamma_N)[1-t]} dt$$

Using binomial expansion for $(t^{a_N} - 1)^m$ to get:

$$\mu_{N_m} = \frac{1}{a_N b_N^{m+1}} \sum_{k=0}^{m} \binom{m}{k} (-1)^{m-k} \int_1^{\infty} t^{\alpha} e^{(\beta_N+\gamma_N)[1-t]} dt\,,$$

$$\alpha = \beta_N(a_N - 1) - \frac{a_N - 1}{a_N} + \frac{k}{a_N}$$

$$\mu_{N_m} = \frac{1}{a_N b_N^{m+1}} \sum_{k=0}^{m} \binom{m}{k} (-1)^{m-k}\, e^{\beta_N+\gamma_N} \int_1^{\infty} t^{\alpha} e^{-(\beta_N+\gamma_N)t} dt$$

$$\mu_{N_m} = \frac{\Upsilon e^{\beta_N+\gamma_N}}{a_N b_N^{m+1} (\beta_N+\gamma_N)^{\alpha+1}} \sum_{k=0}^{m} \binom{m}{k} (-1)^{m-k}\, \Gamma(\alpha+1, \beta_N+\gamma_N) \qquad (20)$$

where $\alpha = \beta_N(a_N - 1) - \frac{a_N - 1}{a_N} + \frac{k}{a_N}$

Table.2 some intervals of N.moments for NGoNH distribution

r_N	u_N	q_N	p_N	$\grave{\mu}_{1_N}$	$\grave{\mu}_{2_N}$	$\grave{\mu}_{3_N}$	$\grave{\mu}_{4_N}$	σ_N^2	S_N	K_N
[0.4,1.4]	[0.6,1.6]	[0.3,1.3]	[0.1,1.1]	[0.00587, 0.21612]	[0.00390, 0.06271]	[0.00292, 0.02095]	[0.00233, 0.00765]	[0.00387, 0.01600]	[1.33438,11.9842]	[1.94536,153.278]
			[0.2,1.2	[0.01151, 0.19811]	[0.00763, 0.05270]	[0.00571, 0.01614]	[0.00456, 0.00540]	[0.00750, 0.01345]	[1.33326,8.5562]	[2.04766,78.16698]
		[0.5,1.5]	[0.3,1.3	[0.03071, 0.15551]	[0.02053, 0.03229]	[0.00770,0.01543]	[0.00200,0.01236]	[0.00811,0.01959]	[1.32683,5.24347]	[2.9579,29.30875]
			[0.4,1.4]	[0.04131, 0.14440]	[0.02766, 0.02784]	[0.00616,0.02079]	[0.00148,0.01666]	[0.00699,0.02595]	[1.32323,4.52152]	[1.92041,21.78839]
	[0.9,1.9]	[0.7,1.7]	[0.5,1.5]	[0.09010, 0.11228]	[0.01661,0.06187]	[0.00280,0.04722]	[0.00051,0.03823]	[0.00400,0.05375]	[1.305903.06888]	[1.94335,9.98682]
			[0.6,1.6]	[0.10526,0.11362]	[0.01460,0.07842]	[0.00231,0.06004]	[0.00039,0.09895]	[0.00352,0.06551]	[1.403502.73416]	[1.86435,16.09007]
		[0.9,1.9]	[0.7,1.7]	[0.08769,0.22536]	[0.01010,0.15967]	[0.00132,0.12412]	[0.00018,0.10166]	[0.00241,0.10888]	[1.30590,1.94536]	[1.85137,3.987623]
			[0.8,1.8]	[00.08909,.20711]	[0.01047,0.14532]	[0.00140,0.11231]	[0.00020,0.09164]	[0.00253,0.10243]	[1.31132,2.02742]	[1.86904,4.339501]

Table 2 shows the values of the first four moments of NGoNH distribution as well as the values of neutrosophic skewness and neutrosophic Kurtosis. The results indicate that the larger the intervals of the mean of the distribution. The results of neutrosophic Variance

σ_N^2, neutrosophic skewness S_N and neutrosophic Kurtosis K_N change significantly, reflecting the effect of the intervals on the shape of the distribution. Small values such as [0.4, 1.4] give a shape and centered distribution, while large values such as [0.9, 1.9] give a more dispersed and flat distribution. At [0.4, 1.4] the K_N is very high, indicating that the values are clustered around the mean, while at [0.9, 1.9] it is more moderate, indicating a more even distribution.

3.4 N.Moment Generating Function

The form of [26] ($N.mgf$) neutrosophic Moment generating function (NMGF) of NGoNH is derived from equation N.moment (20), to get:

$$M'_{x_N}(y_N) = \sum_{s=0}^{\infty} \frac{y_N^s}{s!}\left[\frac{\Upsilon e^{\beta_N+\gamma_N}}{a_N b_N^{m+1}(\beta_N+\gamma_N)^{\alpha+1}} \sum_{k=0}^{m} \binom{m}{k} (-1)^{m-k}\, \Gamma(\alpha + 1, \beta_N+\gamma_N)\right] \tag{21}$$

3.5 Incomplete Moments

The following formula provides the neutrosophic incomplete moments (N.I.M) of a random variable X_N for NGoNH distribution:

$$\grave{\mu}_n(y_N) = \int_0^{y_N} x_N^n \Upsilon (1+b_N x_N)^{a_N-1} e^{(k_N+1)[1-(1+b_N x_N)^{a_N}]} dx_N$$

By substituting equation Npdf (12) and performing the integration, we get:

$$\grave{\mu}_n(y_N) = \frac{\Upsilon e^{k_N+1}}{a_N b_N^{n+1}(k_N+1)^{\xi+1}} \sum_{s=0}^{n} \binom{n}{k} (-1)^{n-s} \left\{\Gamma\big(\xi+1,(k_N+1)\big) - \Gamma\big(\xi+1,(k_N+1)\big)\big(1-(1+b_N x_N)^{a_N}\big)\right\} \tag{22}$$

where $\xi = \frac{(a_N-1)^2+k}{a_N}$

3.6 Neutrosophic Entropy

A. Neutrosophic Rényi Entropy

The Neutrosophic Rényi's Entropy of a random variable x_N is defined as [19], [21], [16]:

$$\grave{I}_R(\beta_N)_N = \frac{1}{1-\beta_N} log \int_0^{\infty} m^{\beta_N}(x_N) dx_N$$

From the equation above and from equation (17) we get:

$$\grave{I}_R(\beta_N)_N = \frac{1}{1-\beta_N}\log\left[\mathrm{E}\int_0^{\infty}(1+b_N x_N)^{\beta_N(a_N-1)}e^{(\beta_N+\gamma_N)[1-(1+b_N x_N)^{a_N}]}dx_N\right]$$

Then the final form of above integral is:

$$\grave{I}_R(\lambda_N)_N = \frac{1}{1-\lambda_N}\log\left[\frac{\mathrm{E}e^{\beta_N+\gamma_N}\Gamma(\pi+1,\beta_N+\gamma_N)}{a_N b_N^{m+1}(\beta_N+\gamma_N)^{\pi+1}}\right],\pi = \frac{(a_N-1)(a_N\beta_N-1)}{a_N} \quad (23)$$

B. Neutrosophic Arimoto Entropy

This entropy can be calculated using the equation:

$$\grave{A}(\beta_N)_N = \frac{\beta_N}{1-\beta_N}\left(\left[\int_0^{\infty} m^{\beta_N}(x_N)dx_N\right]^{\frac{1}{\beta_N}}-1\right)$$

By carrying out the integral we obtain:

$$\grave{A}(\beta_N)_N = \frac{\beta_N}{1-\beta_N}\left[\left\{\frac{\mathrm{E}e^{\beta_N+\gamma_N}\Gamma(\pi+1,\beta_N+\gamma_N)}{a_N b_N^{m+1}(\beta_N+\gamma_N)^{\pi+1}}\right\}^{\frac{1}{\beta_N}}-1\right] \quad (24)$$

C. Neutrosophic Havrda and Charvat Entropy

This entropy can be calculated using the equation:

$$\grave{HC}(\beta_N)_N = \frac{1}{2^{1-\beta_N}-1}\left(\left[\int_0^{\infty} m^{\beta_N}(x_N)dx_N\right]^{\frac{1}{\beta_N}}-1\right)$$

By integrating the above we get:

$$\grave{HC}(\beta_N)_N = \frac{1}{2^{1-\beta_N}-1}\left[\left\{\frac{\mathrm{E}e^{\beta_N+\gamma_N}\Gamma(\pi+1,\beta_N+\gamma_N)}{a_N b_N^{m+1}(\beta_N+\gamma_N)^{\pi+1}}\right\}^{\frac{1}{\beta_N}}-1\right] \quad (25)$$

4. Estimation

4.1 Maximum likelihood estimation

The NGoNH distribution parameters are computed using the maximum likelihood estimation approach. For $x_{N_1}, x_{N_2}, \dots, x_{N_m}$ which is a random sample [27], [28], [29] the NGoNH distribution Npdf is:

$$L(\theta_N, x_{N_i})$$

$$= \prod_{i=1}^{m} \frac{r_N a_N b_N (1 + b_N x_{N_i})^{a_N - 1} e^{u_N \frac{1-e^{[1-(1+b_N x_{N_i})^{a_N}]}}{e^{[1-(1+b_N x_{N_i})^{a_N}]}}}}{e^{[1-(1+b_N x_{N_i})^{a_N}]}} e^{\frac{r_N}{u_N}\left(e^{u_N \frac{1-e^{[1-(1+b_N x_{N_i})^{a_N}]}}{e^{[1-(1+b_N x_{N_i})^{a_N}]}}}\right)}$$

we find the log- likelihood as:

$$L = mlog(r_N) + mlog(a_N) + mlog(b_N) + (a_N - 1)\sum_{i=1}^{m} \log(1 + b_n x_{N_i})$$

$$- \sum_{i=1}^{m}\left\{1 - \left(1 + b_n x_{N_i}\right)^{a_N}\right\} + u_N \sum_{i=1}^{m} \frac{1 - e^{\left\{1-\left(1+b_n x_{N_i}\right)^{a_N}\right\}}}{e^{\left\{1-\left(1+b_n x_{N_i}\right)^{a_N}\right\}}} \tag{26}$$

$$- \frac{r_N}{u_N} \sum_{i=1}^{m} e^{u_N \frac{1-e^{[1-(1+b_N x_{N_i})^{a_N}]}}{e^{[1-(1+b_N x_{N_i})^{a_N}]}}}$$

4.2 Least square estimation

The following formula can be used to estimate the parameters using the least square estimation (LSE) method [30]:

$$\varphi(\theta_N) = \sum_{i=1}^{m} \left[1 - e^{\frac{r_N}{u_N}\left(1-e^{u_N \frac{1-e^{[1-(1+b_N x_{N_i})^{a_N}]}}{e^{[1-(1+b_N x_{N_i})^{a_N}]}}}\right)} - \frac{1}{n+1} \right]^2 \tag{27}$$

4.3 Weighted Least square estimation

The following formula can be used to estimate the parameters using the weighted least square estimation (WLSE) method [30]:

$$\varphi(\theta_N) = \sum_{i=1}^{m} \frac{(n+1)^2(n+2)}{i(n-i+1)} \left[1 - e^{\frac{r_N}{u_N}\left(1-e^{u_N \frac{1-e^{[1-(1+b_N x_{N_i})^{a_N}]}}{e^{[1-(1+b_N x_{N_i})^{a_N}]}}}\right)} - \frac{i}{n+1} \right]^2 \tag{28}$$

Estimation of the parameters for the three previously described methods may be obtained by finding the partial derivative of the four parameters and setting their equations equal to zero. Computer software such as R language are used since it is difficult to find these values using analytical solutions.

5. Simulation

A Monte Carlo simulation is carried out for the three methods discussed in the fourth section to show the effectiveness of the estimation of the NGoNH distribution. The sizes of the generated samples were based on n=50, 100, 150, 200, 300, 400 and 500 up to 1000. The mean square error (MSE) and its root (RMSE) values were calculated, as well as the bias which have respectively the forms [31], [32]:

$$MSE = \frac{1}{n}\sum_{t=1}^{n}(x_t - \hat{x}_t)^2 \tag{29}$$

$$RMSE = \sqrt{\frac{1}{n}\sum_{t=1}^{n}(x_t - \hat{x}_t)^2} \tag{30}$$

$$bias = (\hat{\gamma}) = \frac{\sum_{i=1}^{N}\hat{\gamma}_i}{N} - \gamma \tag{31}$$

The above formulas are used to measure the efficiency of parameter estimation for the three methods. Tables 3, 4, 5, and 6 displays respectively the Mean value intervals, MSE value intervals, RMSE value intervals, and Bias value intervals of the Monte Carlo simulations conducted for the NGoNH distribution.

Table 3 : Mean value intervals of Monte Carlo simulations conducted for the NGoNH distribution

$r_N = [0.3,1.3]$, $u_N = [0.6,1.6]$, $b_N = [0.7,1.7]$, $c_N = [0.8,1.8]$

N	Ess. Par.	MLE	LSE	WLSE
25	$\widehat{r_N}$	[0.278725, 1.208506]	[0.330885, 1.77051]	[0.325109, 1.712059]
	$\widehat{u_N}$	[0.545109, 1.512762]	[0.529641, 0.982358]	[0.574482, 1.159052]
	$\widehat{a_N}$	[0.82538, 2.26148]	[0.727016, 1.90030]	[0.6985924, 1.917410]
	$\widehat{b_N}$	[0.836688, 1.871466]	[0.827649, 1.802932]	[0.884834, 1.761696]
50	$\widehat{r_N}$	[0.288682, 1.175954]	[0.323403, 1.455807]	[0.320551, 1.441650]
	$\widehat{u_N}$	[0.733040, 1.582329]	[0.488049, 1.111214]	[0.552887, 1.403803]
	$\widehat{a_N}$	[0.772505, 2.09839]	[0.727572, 2.005198]	[0.726416, 1.913894]
	$\widehat{b_N}$	[0.847302, 1.921580]	[0.816181, 1.710567]	[0.836340, 1.808019]
100	$\widehat{r_N}$	[0.2827085, 1.208919]	[0.3142788, 1.326015]	[0.3091922, 1.309548]
	$\widehat{u_N}$	[0.798041, 1.644623]	[0.508863, 1.408090]	[0.551583, 1.407206]
	$\widehat{a_N}$	[0.735851, 1.99728]	[0.722367, 1.892478]	[0.720947, 1.881493]
	$\widehat{b_N}$	[0.848726, 1.90989]	[0.8144451, 1.777535]	[0.826489, 1.8062446]
150	$\widehat{r_N}$	[0.2964969, 1.220680]	[0.3071746, 1.272246]	[0.3100239, 1.289856]
	$\widehat{u_N}$	[0.86246, 1.612384]	[0.543385, 1.30409]	[0.624793, 1.528528]
	$\widehat{a_N}$	[0.717331, 1.99700]	[0.715691, 1.90893]	[0.6926641, 1.835397]
	$\widehat{b_N}$	[0.836636, 1.842685]	[0.820484, 1.792420]	[0.850076, 1.801155]
200	$\widehat{r_N}$	[0.2920368, 1.285749]	[0.2990094, 1.278224]	[0.2989902, 1.284404]

	$\widehat{u_N}$	[0.856185, 1.90406]	[0.5572717, 1.23905]	[0.5965633, 1.48762]
	$\widehat{a_N}$	[0.702390, 1.875348]	[0.7133606, 1.89546]	[0.7085301, 1.81871]
	$\widehat{b_N}$	[0.856278, 1.862480]	[0.826951, 1.812227]	[0.837854, 1.831246]
300	$\widehat{r_N}$	[0.3040763, 1.282362]	[0.3016217, 1.265423]	[0.3045414, 1.298720]
	$\widehat{u_N}$	[0.893900, 1.819303]	[0.5513485, 1.461314]	[0.6917411, 1.634536]
	$\widehat{a_N}$	[0.700084, 1.84783]	[0.719860, 1.80666]	[0.6958297, 1.770661]
	$\widehat{b_N}$	[0.820012, 1.845923]	[0.814926, 1.841863]	[0.8229515, 1.828610]
400	$\widehat{r_N}$	[0.304597,1.311825]	[0.2933161, 1.254802]	[0.2961900, 1.2908484]
	$\widehat{u_N}$	[0.905151,1.857734]	[0.588903, 1.421155]	[0.630648, 1.532744]
	$\widehat{a_N}$	[0.695743, 1.81612]	[0.7052426, 1.781923]	[0.7031947, 1.795610]
	$\widehat{b_N}$	[0.814393, 1.857870]	[0.836268, 1.862511]	[0.827265, 1.8332795]
500	$\widehat{r_N}$	[0.3111381, 1.316864]	[0.2947219, 1.282619]	[0.2985773, 1.298005]
	$\widehat{u_N}$	[0.927286, 1.888777]	[0.589510, 1.467209]	[0.679843, 1.598864]
	$\widehat{a_N}$	[0.683244, 1.789918]	[0.708064, 1.818735]	[0.687633, 1.771254]
	$\widehat{b_N}$	[0.814162, 1.853697]	[0.825335, 1.808836]	[0.837494, 1.824339]

Table 4 : MSE value intervals of Monte Carlo simulations conducted for the NGoNH distribution

$r_N = [0.3,1.3]$, $u_N = [0.6,1.6]$, $b_N = [0.7,1.7]$, $c_N = [0.8,1.8]$				
N	**Ess. Par.**	**MLE**	**LSE**	**WLSE**
25	$\widehat{r_N}$	[0.023135, 0.706801]	[0.032444, 1.62494]	[0.030712, 1.31117]
	$\widehat{u_N}$	[4.14523,0.497087]	[0.080344, 1.063434]	[0.12249, 0.9756436]
	$\widehat{a_N}$	[0.059763, 1.11365]	[0.017808, 0.37968]	[0.015584, 0.4181343]
	$\widehat{b_N}$	[0.119858, 0.503096]	[0.031222, 0.2345520]	[0.063167, 0.213283]
50	$\widehat{r_N}$	[0.012067, 0.346669]	[0.0160610.717349]	[0.015734, 0.87509]
	$\widehat{u_N}$	[0.734766, 3.679494]	[0.049355, 0.57713]	[0.274055, 1.17055]
	$\widehat{a_N}$	[0.058392, 0.794207]	[0.010602, 0.34445]	[0.017254, 0.31337]
	$\widehat{b_N}$	[0.109587, 0.433128]	[0.027279, 0.128267]	[0.034144, 0.229846]
100	$\widehat{r_N}$	[0.0079689, 0.253872]	[0.009457, 0.198970]	[0.008064, 0.130369]
	$\widehat{u_N}$	[0.83836, 2.824828]	[0.047707, 0.61153]	[0.086030, 0.645480]
	$\widehat{a_N}$	[0.038626, 0.682035]	[0.006328, 0.281991]	[0.010779, 0.210703]
	$\widehat{b_N}$	[0.079480, 0.269563]	[0.019532, 0.115940]	[0.033326, 0.121073]
150	$\widehat{r_N}$	[0.006884, 0.191622]	[0.0055073, 0.144637]	[0.006099, 0.140694]
	$\widehat{u_N}$	[0.86152, 2.381664]	[0.057725, 0.62285]	[0.121972, 0.768219]
	$\widehat{a_N}$	[0.035500, 0.561778]	[0.006314, 0.20831]	[0.008967, 0.16158]
	$\widehat{b_N}$	[0.065723, 0.221268]	[0.014683, 0.088061]	[0.024392, 0.087131]
200	$\widehat{r_N}$	[0.0062275, 0.218678]	[0.004615, 0.097623]	[0.004289, 0.113431]
	$\widehat{u_N}$	[0.753041, 3.14446]	[0.0587917, 0.60065]	[0.1047137, 0.62307]

	$\widehat{a_N}$	[0.030672, 0.49517]	[0.0061114, 0.13265]	[0.009599, 0.154766]
	$\widehat{b_N}$	[0.061232, 0.214991]	[0.011810, 0.072328]	[0.020838, 0.078229]
300	$\widehat{r_N}$	[0.0046038, 0.148718]	[0.003744, 0.073007]	[0.003550, 0.082893]
	$\widehat{u_N}$	[0.72283, 2.106184]	[0.071511, 0.616261]	[0.172864, 0.725281]
	$\widehat{a_N}$	[0.029830, 0.412794]	[0.006769, 0.117654]	[0.012307, 0.136178]
	$\widehat{b_N}$	[0.044213, 0.161359]	[0.014176, 0.065852]	[0.017359, 0.065906]
400	$\widehat{r_N}$	[0.0044547, 0.147368]	[0.002093, 0.066562]	[0.002366, 0.0648016]
	$\widehat{u_N}$	[0.780242, 2.137328]	[0.086523, 0.404274]	[0.086714, 0.465084]
	$\widehat{a_N}$	[0.026265, 0.394238]	[0.0077952, 0.072529]	[0.010696, 0.180237]
	$\widehat{b_N}$	[0.041377, 0.163266]	[0.014921, 0.053476]	[0.01818, 0.073968]
500	$\widehat{r_N}$	[0.0045347, 0.134610]	[0.001561, 0.058319]	[0.002277, 0.0628932]
	$\widehat{u_N}$	[0.64707, 2.246025]	[0.073237, 0.59519]	[0.128656, 0.6032856]
	$\widehat{a_N}$	[0.024108, 0.340620]	[0.0072589, 0.130788]	[0.009566, 0.1360325]
	$\widehat{b_N}$	[0.037528, 0.150351]	[0.009878, 0.0543079]	[0.015243, 0.062339]

Table 5 : RMSE value intervals of Monte Carlo simulations conducted for the NGoNH distribution

$r_N = [0.3,1.3]$, $u_N = [0.6,1.6]$, $b_N = [0.7,1.7]$, $c_N = [0.8,1.8]$				
N	**Ess. Par.**	**MLE**	**LSE**	**WLSE**
25	$\widehat{r_N}$	[0.1521022, 0.840714]	[0.180122, 1.27473]	[0.175249, 1.145065]
	$\widehat{u_N}$	[0.705044, 2.0359839]	[0.283450, 1.031229]	[0.349994, 0.987746]
	$\widehat{a_N}$	[0.244465, 1.055298]	[0.133447, 0.616186]	[0.1248374, 0.646633]
	$\widehat{b_N}$	[0.346205, 0.709292]	[0.176698, 0.4843057]	[0.251330, 0.4618259]
50	$\widehat{r_N}$	[0.109851, 0.588786]	[0.1267339, 0.8469651]	[0.125436, 0.935467]
	$\widehat{u_N}$	[0.85718, 1.918200]	[0.222160, 0.759692]	[0.523503, 1.08192]
	$\widehat{a_N}$	[0.241644, 0.891183]	[0.102970, 0.58689]	[0.131355, 0.559796]
	$\widehat{b_N}$	[0.3310399, 0.658124]	[0.165165, 0.358144]	[0.184782, 0.47942306]
100	$\widehat{r_N}$	[0.0892688, 0.503857]	[0.0972493, 0.446061]	[0.089801, 0.3610666]
	$\widehat{u_N}$	[0.915622, 1.680722]	[0.218419, 0.782004]	[0.293309, 0.803417]
	$\widehat{a_N}$	[0.1965366, 0.825854]	[0.079553, 0.531028]	[0.103825, 0.459024]
	$\widehat{b_N}$	[0.281921, 0.519195]	[0.139759, 0.340500]	[0.182554, 0.3479566]
150	$\widehat{r_N}$	[0.0829748, 0.437747]	[0.074211, 0.3803117]	[0.0780961, 0.375092]
	$\widehat{u_N}$	[0.92818, 1.543264]	[0.2402606, 0.789210]	[0.349244, 0.876481]
	$\widehat{a_N}$	[0.1884161, 0.749518]	[0.0794657, 0.456420]	[0.0946980, 0.4019703]
	$\widehat{b_N}$	[0.256366, 0.470392]	[0.121176, 0.296751]	[0.1561804, 0.295180]
200	$\widehat{r_N}$	[0.0789145, 0.4676308]	[0.067934, 0.3124475]	[0.065494, 0.336795]
	$\widehat{u_N}$	[0.86777, 1.77326]	[0.24247, 0.775017]	[0.3235949, 0.789352]
	$\widehat{a_N}$	[0.1751355, 0.703688]	[0.078175, 0.36422]	[0.097977, 0.3934033]

	$\widehat{b_N}$	[0.247451, 0.463671]	[0.108677, 0.26893]	[0.144355, 0.279695]
300	$\widehat{r_N}$	[0.0678518, 0.385640]	[0.061196, 0.270198]	[0.0595834, 0.287911]
	$\widehat{u_N}$	[0.850196, 1.451269]	[0.2674172, 0.785023]	[0.415769, 0.851634]
	$\widehat{a_N}$	[0.1727160, 0.64249]	[0.0822794, 0.343008]	[0.1109371, 0.369024]
	$\widehat{b_N}$	[0.210270, 0.401695]	[0.1190656, 0.2566176]	[0.1317556, 0.256722]
400	$\widehat{r_N}$	[0.0667440, 0.383886]	[0.0457507, 0.257997]	[0.0486476, 0.25456166]
	$\widehat{u_N}$	[0.883313, 1.461960]	[0.2941494, 0.635825]	[0.294472, 0.681971]
	$\widehat{a_N}$	[0.1620668, 0.627883]	[0.08829061, 0.2693129]	[0.103425, 0.424543]
	$\widehat{b_N}$	[0.2034155, 0.404062]	[0.122153, 0.231250]	[0.1348423, 0.271970]
500	$\widehat{r_N}$	[0.0673402, 0.366892]	[0.0395125, 0.2414946]	[0.0477265, 0.2507853]
	$\widehat{u_N}$	[0.804408, 1.498674]	[0.2706251, 0.771488]	[0.3586869, 0.7767146]
	$\widehat{a_N}$	[0.1552686, 0.583626]	[0.0851996, 0.361647]	[0.0978079, 0.3688259]
	$\widehat{b_N}$	[0.1937220, 0.387751]	[0.0993905, 0.2330407]	[0.1234648, 0.2496794]

Table 6 : Bias value intervals of Monte Carlo simulations conducted for the NGoNH distribution

$r_N = [0.3,1.3]$, $u_N = [0.6,1.6]$, $b_N = [0.7,1.7]$, $c_N = [0.8,1.8]$				
N	**Ess. Par.**	**MLE**	**LSE**	**WLSE**
25	$\widehat{r_N}$	[0.0212749, 0.0914936]	[0.030885, 0.470514]	[0.025109, 0.412059]
	$\widehat{u_N}$	[0.0548905, 0.0872377]	[0.070358, 0.617641]	[0.025517, 0.440947]
	$\widehat{a_N}$	[0.1253840, 0.561482]	[0.027016, 0.200302]	[0.0014075, 0.2174105]
	$\widehat{b_N}$	[0.036688, 0.0714662]	[0.027649, 0.0029324]	[0.0848340, 0.0383038]
50	$\widehat{r_N}$	[0.011317, 0.124046]	[0.023403, 0.155807]	[0.020551, 0.141650]
	$\widehat{u_N}$	[0.133040, 0.0176707]	[0.111950, 0.488785]	[0.047112, 0.196197]
	$\widehat{a_N}$	[0.072505, 0.398390]	[0.027572, 0.305198]	[0.026416, 0.213894]
	$\widehat{b_N}$	[0.047302, 0.121580]	[0.016181, 0.089432]	[0.0080191,0.036340]
100	$\widehat{r_N}$	[0.0172914, 0.091080]	[0.0142788, 0.026015]	[0.0091922, 0.192793]
	$\widehat{u_N}$	[0.0446233,0.198041]	[0.091136, 0.191909]	[0.048416, 0.181493]
	$\widehat{a_N}$	[0.035851, 0.297286]	[0.022367, 0.192478]	[0.0062446,0.020947]
	$\widehat{b_N}$	[0.048726, 0.109893]	[0.014445, 0.022464]	[0.026489, 0.079319]
150	$\widehat{r_N}$	[0.003503, 0.012384]	[0.007174, 0.027753]	[0.010023, 0.010143]
	$\widehat{u_N}$	[0.262469, 0.297001]	[0.056614, 0.295905]	[0.02479, 0.0714713]
	$\widehat{a_N}$	[0.017331, 0.042685]	[0.0156912, 0.208932]	[0.0073358, 0.135397]
	$\widehat{b_N}$	[0.027753,0.036636]	[0.007579,0.020484]	[0.0500766, 0.0011552]
200	$\widehat{r_N}$	[0.0079631, 0.0142501]	[0.0009905, 0.021775]	[0.001009, 0.015595]
	$\widehat{u_N}$	[0.256185, 0.304060]	[0.0427282, 0.360942]	[0.0034366, 0.112378]
	$\widehat{a_N}$	[0.002390, 0.175348]	[0.0133606, 0.195463]	[0.0085301, 0.1187108]
	$\widehat{b_N}$	[0.056278, 0.062480]	[0.026951, 0.012227]	[0.0378548, 0.0312468]

300	$\widehat{r_N}$	[0.0040763, 0.017637]	[0.00162177, 0.034576]	[0.001279,0.004541]
	$\widehat{u_N}$	[0.219303,0.293900]	[0.0486514, 0.138685]	[0.034536,0.0917411]
	$\widehat{a_N}$	[0.0000843, 0.147830]	[0.0198602, 0.106663]	[0.0041702, 0.0706614]
	$\widehat{b_N}$	[0.0200124, 0.045923]	[0.014926, 0.0418630]	[0.0229515, 0.0286102]
400	$\widehat{r_N}$	[0.0045970, 0.0118250]	[0.006683, 0.045197]	[0.0038099, 0.0091515]
	$\widehat{u_N}$	[0.257734,0.305151]	[0.0110961, 0.178844]	[0.030648, 0.067255]
	$\widehat{a_N}$	[0.0042561, 0.116129]	[0.0052426, 0.0819237]	[0.0031947, 0.0956105]
	$\widehat{b_N}$	[0.0143930, 0.057870]	[0.036268, 0.062511]	[0.0272654, 0.0332795]
500	$\widehat{r_N}$	[0.0111381, 0.016864]	[0.0052780, 0.017380]	[0.0014226, 0.001994]
	$\widehat{u_N}$	[0.288777,0.327286]	[0.010489, 0.13279]	[0.001135,0.079843]
	$\widehat{a_N}$	[0.016755, 0.089918]	[0.0080641, 0.118735]	[0.012366, 0.071254]
	$\widehat{b_N}$	[0.014162, 0.053697]	[0.0088362,0.0253352]	[0.037494, 0.024339]

Table 3 shows the mean values of the three estimation methods (MLE, LSE, WLSE) at different sample sizes. The table shows the stability of the estimation of the basic parameters (r_N, u_N, a_N, b_N) as the sample sizes increases. At a small sample (N=25, 50), the confidence intervals of the parameters are wide, indicating high variability in the estimate. For the samples (N=100 to 500), the intervals become more compressed, indicating improved estimation accuracy and stability of the values. The MLE method shows ranges closer to the true values than LSE and WLSE, indicating that it is more accurate at large sample sizes. We note that the value u_N, which is one of the basic parameters, tends to stabilize at large samples, but the LSE method shows greater variability compared to MLE and WLSE.

Table 4 shows that at small samples (N=25, 50), the MSE is high, indicating that the parameter estimation is unstable and contains larger error. As the sample size increases, the MSE values decrease significantly, indicating that the performance of the estimation methods improves. The MLE method shows the lowest MSE values compared to LSE and WLSE, confirming its high effectiveness, especially for large samples. The WLSE method shows similar performance to MLE in some cases, but is less stable for small samples. As the sample increases (N=500), the minimum MSE values decrease to their lowest levels, indicating that the estimates converge towards the true values of the parameters.

Table 5 shows that the high values at samples (N=25, 50) mean that the initial estimates are inaccurate, but the values decrease significantly at N=100 and above. The MLE method shows the lowest RMSE at all samples, indicating its stability and robustness. LSE shows a higher RMSE compared to MLE, indicating that this method is less efficient in estimating the parameters. WLSE shows an average performance between the other two methods, but becomes more stable at $N \geq 200$.

Table 6 shows that at N=25, the bias is high for all methods, indicating that the initial estimates are inaccurate. As the sample sizes increases, Bias values gradually decrease, indicating that the estimates converge towards the true values. The MLE shows the lowest Bias values, meaning that it is the most accurate at all sizes. LSE shows a larger deviation from the true values, making it less reliable, especially at small samples. At N=500, Bias becomes very low for all methods, meaning that all methods become more accurate with larger samples.

From the above results, it is clear that MLE is the most efficient method, showing the lowest values for MSE, RMSE, and Bias, especially at large samples, while WLSE shows an average performance between MLE and LSE, but becomes more accurate at large samples. LSE shows lower performance than the other two methods, with Bias and MSE being higher at all sizes. Increasing the sample size improves the accuracy of all methods, but MLE gives the best results even with medium samples.

6. Application

The application side serves as a foundation for illustrating the breadth of the NGoNH distribution's quality, effectiveness, and adaptability in real-world applications. In this section, genuine neutrosophic data represented by temperatures in Lahore, Pakistan, for the period 2016-2020 [33]. The data utilized is checked to accomplish the neutrosophic qualities represent by achieving the condition $T + F + I = 1$ before the analytic process begins. This condition is similar to the probability condition, but it is different in that the values must lie within interval [0,1]. The following is what sets apart the neutrosophic logic in table 7.

Table 7. Data used, Truth, False, indeterminacy values and verification condition

No.	intervals	Truth (T)	Falsity (F)	Indeterminacy (I)	Sum (T+F+I)	Satisfy neutrosophic condition or not
1	[46,72]	59.0	-26	-32.0	1	yes
2	[49,80]	64.5	-31	-32.5	1	yes
3	[60,87]	73.5	-27	-45.5	1	yes
4	[71,98]	84.5	-27	-56.5	1	yes
5	[84,107]	95.5	-23	-71.5	1	yes
6	[91,110]	100.5	-19	-80.5	1	yes
7	[88,104]	96.0	-16	-79.0	1	yes
8	[84,102]	93.0	-18	-74.0	1	yes
9	[79,103]	91.0	-24	-66.0	1	yes
10	[69,97]	83.0	-28	-54.0	1	yes
11	[61,86]	73.5	-25	-47.5	1	yes
12	[53,79]	66.0	-26	-39.0	1	yes
13	[47,69]	58.0	-22	-35.0	1	yes
14	[50,79]	64.5	-29	-34.5	1	yes

15	**[56,87]**	**71.5**	**-31**	**-39.5**	**1**	**yes**
16	**[72,102]**	**87.0**	**-30**	**-56.0**	**1**	**yes**
17	**[83,107]**	**95.0**	**-24**	**-70.0**	**1**	**yes**
18	**[80,102]**	**91.0**	**-22**	**-68.0**	**1**	**yes**
19	**[87,108]**	**97.5**	**-21**	**-75.5**	**1**	**yes**
20	**[87,107]**	**97.0**	**-20**	**-76.0**	**1**	**yes**
21	**[88,104]**	**96.0**	**-16**	**-79.0**	**1**	**yes**
22	**[86,104]**	**95.0**	**-18**	**-76.0**	**1**	**yes**
23	**[72,96]**	**84.0**	**-24**	**-59.0**	**1**	**yes**
24	**[63,83]**	**73.0**	**-20**	**-52.0**	**1**	**yes**
25	**[56,75]**	**65.5**	**-19**	**-45.5**	**1**	**yes**
26	**[49,73]**	**61.0**	**-24**	**-36.0**	**1**	**yes**
27	**[54,78]**	**66.0**	**-24**	**-41.0**	**1**	**yes**
28	**[62,89]**	**75.5**	**-27**	**-47.5**	**1**	**yes**
29	**[72,98]**	**85.0**	**-26**	**-58.0**	**1**	**yes**
30	**[85,106]**	**95.5**	**-21**	**-73.5**	**1**	**yes**
31	**[92,108]**	**100.0**	**-16**	**-83.0**	**1**	**yes**
32	**[89,102]**	**95.5**	**-13**	**-81.5**	**1**	**yes**
33	**[86,102]**	**94.0**	**-16**	**-77.0**	**1**	**yes**
34	**[80,100]**	**90.0**	**-20**	**-69.0**	**1**	**yes**
35	**[82,98]**	**90.0**	**-16**	**-73.0**	**1**	**yes**
36	**[71,86]**	**78.5**	**-15**	**-62.5**	**1**	**yes**
37	**[60,76]**	**68.0**	**-16**	**-51.0**	**1**	**yes**
38	**[54,69]**	**61.5**	**-15**	**-45.5**	**1**	**yes**
39	**[55,71]**	**63.0**	**-16**	**-46.0**	**1**	**yes**
40	**[61,81]**	**71.0**	**-20**	**-50.0**	**1**	**yes**
41	**[79,101]**	**90.0**	**-22**	**-67.0**	**1**	**yes**
42	**[94,114]**	**104.0**	**-20**	**-83.0**	**1**	**yes**
43	**[90,106]**	**98.0**	**-16**	**-81.0**	**1**	**yes**
44	**[85,103]**	**94.0**	**-18**	**-75.0**	**1**	**yes**
45	**[82,101]**	**91.5**	**-19**	**-71.5**	**1**	**yes**
46	**[77,97]**	**87.0**	**-20**	**-66.0**	**1**	**yes**
47	**[67,82]**	**74.5**	**-15**	**-58.5**	**1**	**yes**
48	**[56,72]**	**64.0**	**-16**	**-47.0**	**1**	**yes**
49	**[43,64]**	**53.5**	**-21**	**-31.5**	**1**	**yes**
50	**[50,72]**	**61.0**	**-22**	**-38.0**	**1**	**yes**
51	**[58,81]**	**69.5**	**-23**	**-45.5**	**1**	**yes**
52	**[69,94]**	**81.5**	**-25**	**-55.5**	**1**	**yes**
53	**[78,103]**	**90.5**	**-25**	**-64.5**	**1**	**yes**

54	[80,101]	90.5	-21	-68.5	1	yes
55	[80,95]	87.5	-15	-71.5	1	yes
56	[80,94]	87.0	-14	-72.0	1	yes
57	[77,94]	85.5	-17	-67.5	1	yes
58	[69,91]	80.0	-22	-57.0	1	yes
59	[54,78]	66.0	-24	-41.0	1	yes
60	[45,69]	57.0	-24	-32.0	1	yes
Mean		81.03333	-21.1666	-58.86667		
Sd-values		13.86003	4.588736	15.849361		
Max-values		104.0	-13.0	-31.5		
Min-values		53.5	-31.0	-83.0		

The temperatures in Lahore, Pakistan, for the period 2016-2020 is represented by actual data in table 7. The table demonstrates that every value satisfies the requirement, demonstrating the data's conformance to the neutrosophic logic's characteristics. Additionally, it is seen that the T values gradually decline with time, indicating a shift in real values. The table uses the neutrosophic logic to accurately depict actual data. The values show how adaptably T, F, and I may be represented by the system. The findings support the applicability of using neutrosophic logic to the analysis of complicated and ambiguous data.

The data utilized, the type of analysis, and the components of the analysis are depicted in the following figures.

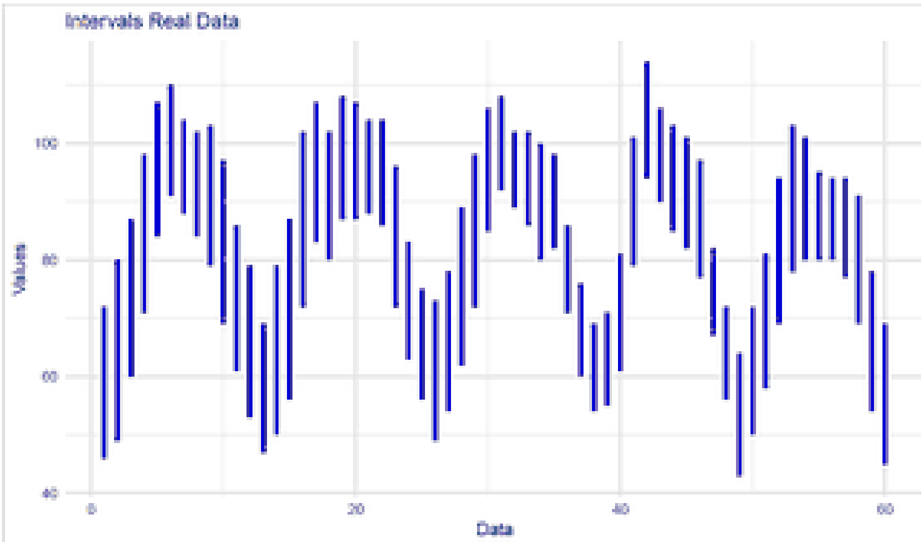

Figure 5. Plot of the intervals for the data used

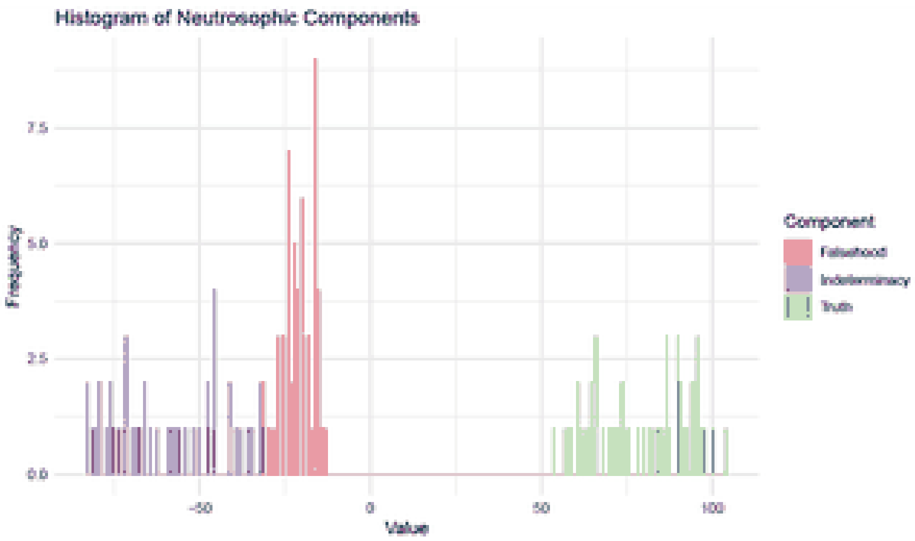

Figure 6. Histogram of Neutrosophic Components

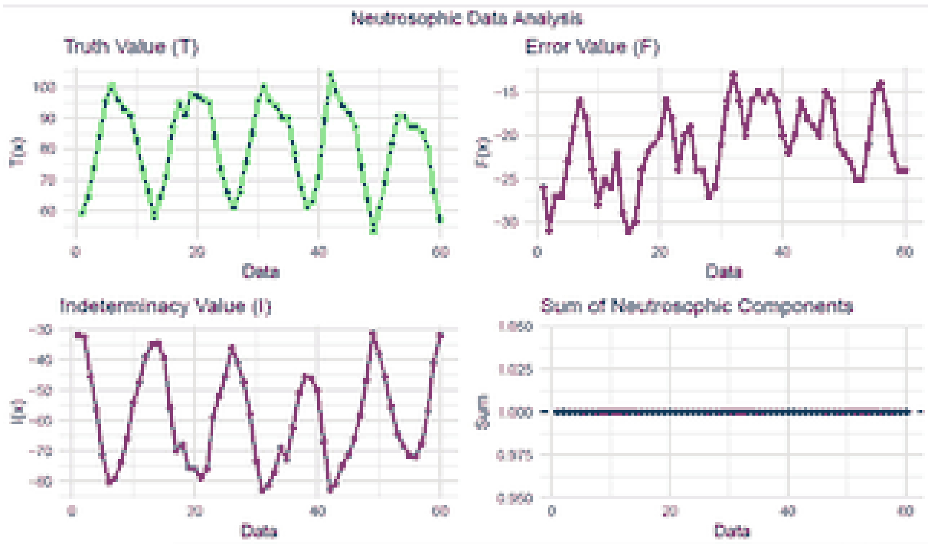

Figure 7. Neutrosophic parts and sum of Neutrosophic Components

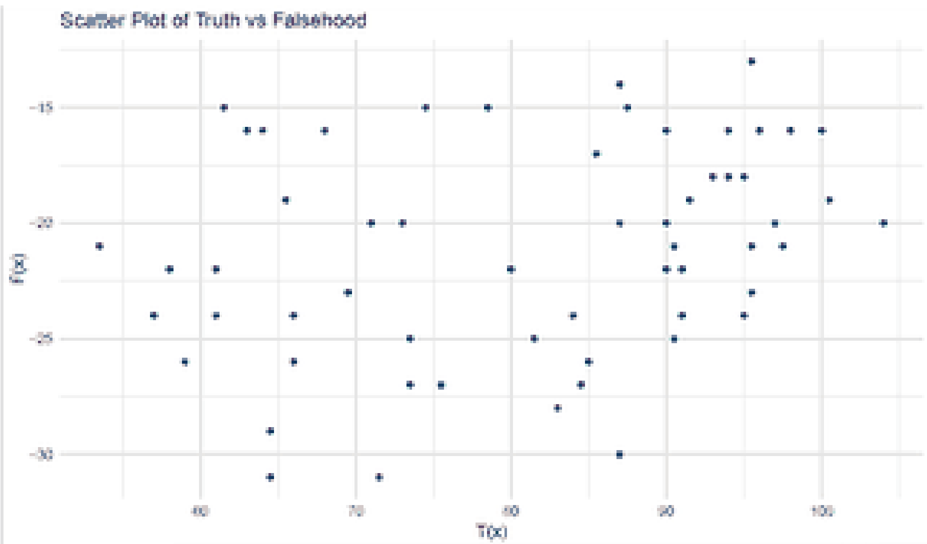

Figure 8. Scatter plot of Truth vs Falshood

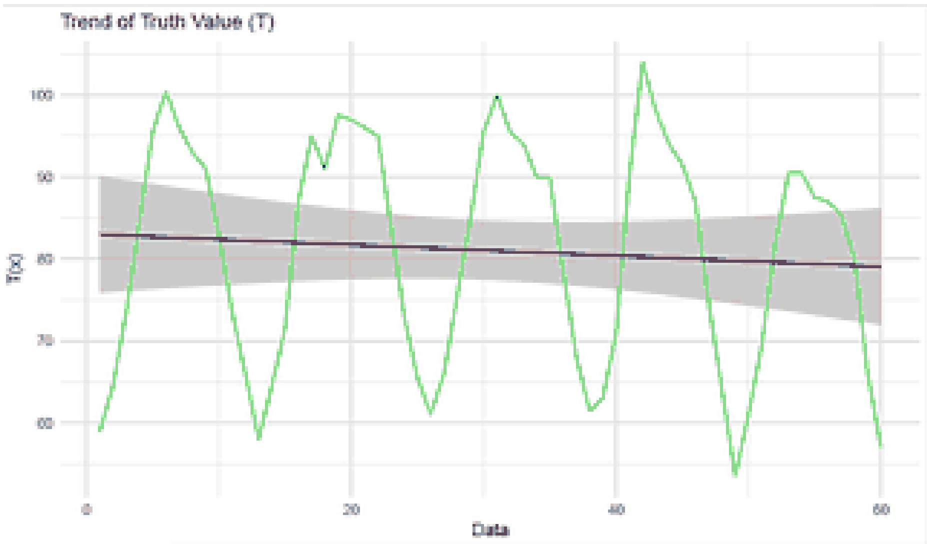

Figure 9. Trend plot of Truth value

The NGoNH distribution's results are compared to six alternative neutrosophic distributions, which are:

- Neutrosophic Wiebull Nadarajah-Haghighi (NWeNH)
- Neutrosophic Kumaraswamy Nadarajah-Haghighi (NKuNH)
- Neutrosophic Exponeted Generalized Exponential Nadarajah-Haghighi (NEGNH)
- Neutrosophic [0,1] Truncated Exponeted Exponential Nadarajah-Haghighi (NTEENH)
- Neutrosophic Beta Nadarajah-Haghighi (NBeNH)
- Neutrosophic Nadarajah-Haghighi (NNH)

Four information criteria AIC [33], CAIC [34], HQIC [35], and BIC [36] as well as the statistical measures such as Kolmogorov-Smirnov (KS), Anderson- Darling (A), Cramér-von Mises (W), and p-value [16], [21], [37] were used for this comparison. The results of the distribution's criterion are displayed in table 8, the values of the statistical measures are displayed in table 9, and the estimated parameters in MLE are displayed in table 10.

Table 8. Results of the criteria for the distributions

Dist.	-2L	AIC	CAIC	BIC	HQIC
NGoNH	[238.5133,244.946]	[485.026,497.892]	[485.753,498.619]	[493.40,506.2695]	[488.303,501.168]
NWeNH	[239.031,251.0866]	[486.062,510.173]	[486.789,510.900]	[494.439,518.550]	[489.3392, 513.45]
NKuNH	[240.336,247.0285]	[488.672,502.057]	[489.400,502.784]	[497.050,510.434]	[491.949,505.333]
NEGNH	[245.750,248.0053]	[499.501,504.010]	[500.228,504.737]	[507.878,512.387]	[502.777,507.287]
NTEENH	[255.7479,272.326]	[519.495,552.653]	[520.223,553.380]	[527.873,561.030]	[522.772,555.930]
NBeNH	[242.1966,247.903]	[492.393, 503.806]	[493.120,504.533]	[500.770,512.183]	[495.67, 507.0829]
NNH	[299.898,315.7357]	[603.795,635.471]	[604.006,635.681]	[607.9846,639.66]	[605.434,637.109]

Table 9. Values of the statistical measures

Dist.	W	A	K-S	p-value
NGoNH	[0.1631278, 0.1742447]	[1.033034, 1.076228]	[0.104354,0.109531]	[0.4677146,0.5306625]
NWeNH	[0.2179362,0.2454571]	[1.296429,1.415124]	[0.127022,0.144822]	[0.1613447,0.2876714]
NKuNH	[0.2586521,0.3033063]	[1.526916,1.73937]	[0.143952,0.152958]	[0.1662749, 0.1206781]
NEGNH	[0.2847026,0.3772915]	[1.671658,2.156582]	[0.155954,0.162163]	[0.08521509,0.1079987]
NTEENH	[0.3286531,0.3724759]	[1.920758,2.134018]	[0.194677,0.324559]	[0.021178,6.475093e-06]
NBeNH	[0.2819412,0.3405313]	[1.655773,1.950182]	[0.151771,0.158347]	[0.09868349,0.1517713]
NNH	[0.2379204,0.3124073]	[1.40662,1.789007]	[0.47210,0.5410004]	[1.11022e-15,4.8459e-12]

Table 10. Estimator value interval for the parameters using the MLE method

Dist.	$\hat{r}_N$	$\hat{u}_N$	$\hat{q}_N$	$\hat{p}_N$
NGoNH	[0.006457,0.00810040]	[0.5863147,3.7445267]	[0.37624873,0.694243]	[0.043232,0.0654481
NWeNH	[4.2912505,9.7916074]	[0.0379921,0.1424287]	[0.0552390,0.3434586]	[0.006357,0.009962]
NKuNH	[17.614578,31.743331]	[3.319084,11.2087923]	[1.1577578,1.4533959]	[0.018980,0.021025]
NEGNH	[0.164599,0.28248229]	[18.732066,54.537074]	[1.440879,2.00402975]	[0.037163,0.099447]
NTEEN H	[19.613499,20.100419]	[26.350845,66.978545]	[0.4644331,0.5031479]	[0.005143,0.008562]
NBeNH	[0.126028,23.6324741]	[1.301384,41.1872412]	[2.006751,6.47165680]	[0.015163,1.305300]
NNH	---	---	[4.5300068,5.3838006]	[0.002039,0.002223]

Table 8 shows the values of the different evaluation criteria for the mentioned distributions. These criteria are used to compare the quality of the statistical models. -2L represents twice the negative value of the log-likelihood function. Here, we notice that the NGoNH distribution has the lowest values, which indicates that it is the best among the distributions.

Table 9 shows the statistical values which are used to evaluate the quality of distributions, the value of W was for the NGoNH, it has the lowest values, which indicates that it is the best. The A test is used to test the distribution's fit to the data. The smaller value is the best distribution. this is confirmed by NGoNH values. The K-S values compares the experimental distribution with theoretical distribution. NGoNH has lowest values for K-S. NGoNH has the highest values for p-value, which indicates that it is the best.

Table 10 shows the estimated parameters for the NGoNH distribution. It shows reasonable and well-defined values of parameters for the NWeNH distribution with greater variability, which may indicate that the distribution is less stable. The NKuNH parameters also show large variability, which may indicate difficulty in estimating them accurately. The NEGNH shows moderate variability, while

NTEENH, NBeNH and NNH shows large variability, especially for the parameter u_N.

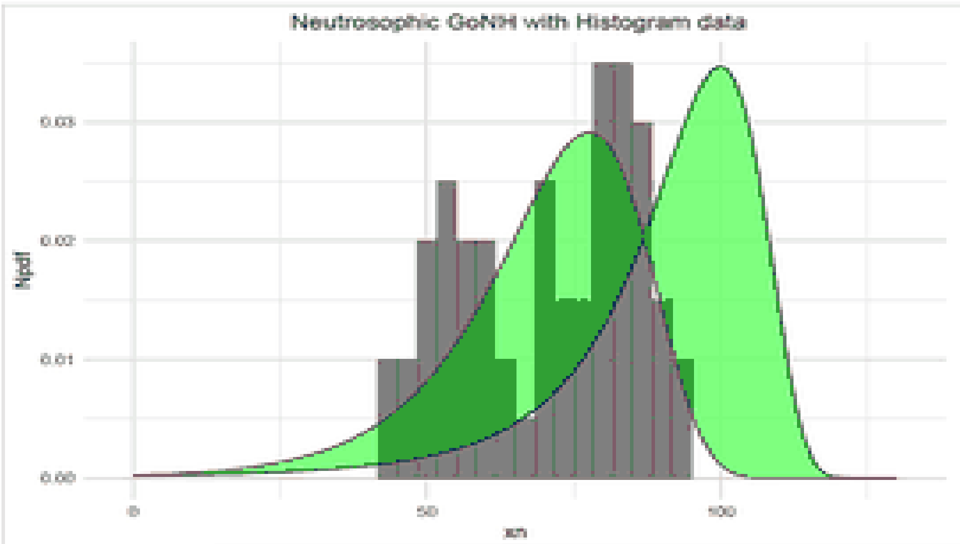

Figure 10. The fitted Npdf with histogram of the data used

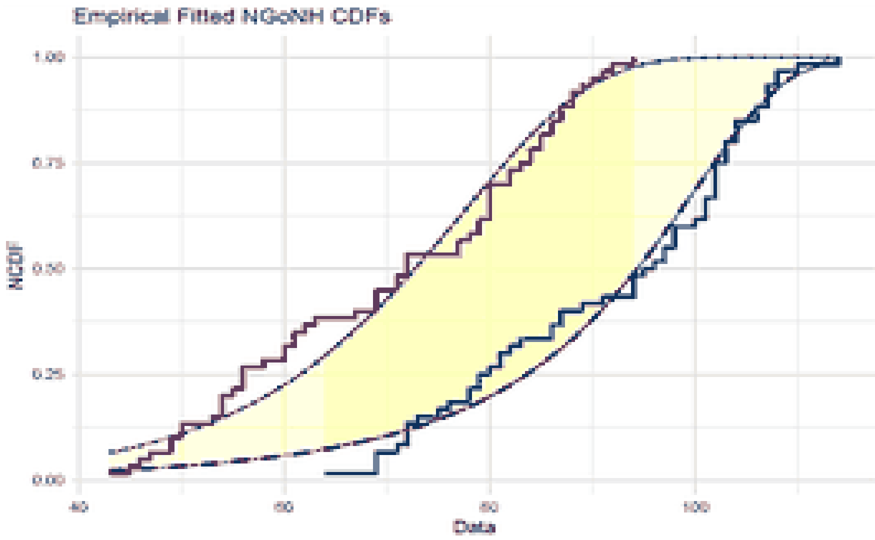

Figure 11.

The empirical fitted NGoNH NCDF

Figure 10 shows the theoretical probability density (Npdf) of NGoNH compared to actual data used in study. Ff the curve fits well with the bar distribution, it indicates that NGoNH describes the data with high accuracy. NGoNH provides a good fit with the real data, as the curve approaches the peaks of the bars. This indicates that the distribution is effective in describing the real temperature values. Figure 11 shows the NCDF of NGoNH compared to the actual data distribution. The good fit between the real data and the distribution curve indicates that the NGoNH distribution can be an accurate model for predicting climate data.

Conclusion

A new four-parameter distribution is developed that combines NGo-G family and Nadarajah-Haghighi distribution within the framework of neutrosophic logic. This expansion contributes to providing more accurate models for representing ambiguous and uncertain data, enhancing the capabilities of statistical modeling. The underling function of many properties of the distribution are derived, providing a solid mathematical foundation for its use in various applications. The results shows that the NGoNH provides the best fit to the data compared to other distributions. According to the information criteria's, statistical values confirm that NGoNH has lowest error, making it the most accurate model. Analysis of neutrosophic values: true values reflect well the data pattern, with a general trend that can be explained based on environmental or temporal factors. The indeterminate values and false values contribute to understanding the extent of uncertainty in the data, which supports the use of neutrosophic logic in analyzing complex phenomena. The estimation method using MLE gave more stable and accurate results compared to other methods, especially for large samples. As the sample size increased, the values of MSE, RMSE, and Bias decreased, indicating an improvement in the accuracy of the estimating with more data. The study confirms that the proposed distribution can be applied to complex climate data, which opens the door to its use in other applications such as climate forecasting, market analysis, and biological systems. The study suggests improving the model by adding supplementary variables that may help explain fluctuations in neutrosophic values, such as the effects of climate change or economic factors, in addition to using large data to verify the stability of the parameters and ensure that the model works efficiently in different contexts. The model can also be compared with other models such as neural networks or complex time series models to see how well it excels in analyzing ambiguous data. The logical limits of NGoNH distribution can be summarized as follows:

Type of limit	Explanation	Possible solution
Mathematical constraints	The distribution must be non-negative, and its coefficients must be positive	Checking that mathematical conditions are met
Statistical constraints	Sensitivity of the estimate to sample size and initial values	Using large samples and techniques to improve the estimate
Application limitations	Limitations of its application in non-neutrosophic data	Verification of its suitability using goodness-of-fit tests
Numerical limitations	Need for approximate solutions for some properties	Use of mathematical expansions and numerical analysis

These boundaries define the scope of distribution and guide its development to improvement of future applications.

References

[1] A. Alzaatreh, C. Lee and F. Famoye, "A new method for generating families of continuous distributions," *Metron,* p. 63–79, 71 2013.

[2] A. Z. Afifya, G. M. Corderio, H. M. Yousof, Z. M. Nofal and A. Alzaatreh, "The Kumaraswamy transmuted-G family of distributions: properties and applications," *Journal of Data Science,* pp. 245-270, 2 14 2016.

[3] A. Z. Afify, E. Altum, M. Alizadeh, G. Ozel and G. G. Hamedani, "The odd exponentiated half-logistic-G family: properties, characterizations and applications," *Chilean Journal of Statistics,* pp. 65-91, 2 8 2017.

[4] S. Nasiru, "Extended odd Frechet-G family of distributions," *Journal of Probability and Statistics,* p. 1–12, 4 11 2018.

[5] S. DJIBRILA, "The generalized odd inverted exponential-G family of distributions: properties and applications," *Eurasian Bulletin of Mathematics,* pp. 86-110, 3 2 2019.

[6] E. Walid and Y. Tashkandy, "Modeling the amount of carbon dioxide emissions application: New modified alpha power Weibull-X family of distributions," *Symmetry,* p. 366, 2 15 2023.

[7] N. A. Noori, A. A. Khalaf and M. A. Khaleel, "A New Generalized Family of Odd Lomax-G Distributions Properties and Applications," *Advances in the Theory of Nonlinear Analysis and Its Application,* pp. 1-16, 4 7 2023.

[8] A. B. Odeyale, S. U. Gulumbe, U. Umar and K. O. Aremu, "New New Odd Generalized Exponentiated Exponential-G Family of Distributions," *UMYU Scientifica,* pp. 56-64, 4 2 2023.

[9] Z. Shah, D. M. Khan, Z. Khan, N. Faiz, S. Hussain, A. Anwar, T. Ahmad and K.-I. Kim, "A new generalized logarithmic–X family of distributions with biomedical data analysis," *Applied Sciences,* p. 3668, 6 13 2023.

[10] O. A. Bello, S. I. Doguwa, A. Yahaya and H. M. Jibril, "A type I half Logistic exponentiated-G family of distributions: Properties and application," *Communication in Physical Sciences,* pp. 147-163, 3 7 2021.

[11] G. A. Mahdi, M. A. Khaleel, A. M. Gemeay, M. Nagy , A. H. Mansi, M. M. Hossain and E. Hussam, "A new hybrid odd exponential-Φ family: Properties and applications," *AIP Advances,* 4 14 2024.

[12] F. Smarandache, "A unifying field in logics. neutrosophy: Neutrosophic probability, set and logic," *Rehoboth,* 1999.

[13] M. M. Alanaz, M. Y. Mustafa and Z. Y. Algamal, "Neutrosophic Lindley distribution with application for Alloying Metal Melting Point," *International Journal of Neutrosophic Science,* pp. 65-71, 4 21 2023.

[14] Z. Y. Algama, N. N. Alobaidi, A. A. Hamad, M. M. Alanaz and M. Y. Mustafa, "Neutrosophic Beta-Lindley distribution: Mathematical properties and modeling bladder cancer data," *International Journal of Neutrosophic Science,* pp. 186-194, 2 23 2024.

[15] M. M. Alanaz and Z. Y. Algamal, "Neutrosophic exponentiated inverse Rayleigh distribution: Properties and Applications," *International Journal of Neutrosophic Science,* pp. 36-43, 4 21 2023.

[16] O. E. Al-Saqal, Z. A. Hadied and Z. Y. Algamal, "Modeling bladder cancer survival function based on neutrosophic inverse Gompertz distribution," *International Journal of Neutrosophic Science,* pp. 75-5, 1 25 2025.

[17] N. M. Hammood, N. K. Rashad and Z. Y. Algamal, "Neutrosophic Topp-Leone Extended Exponential distribution modeling with application for bladder cancer patients," *International Journal of Neutrosophic Science,* pp. 239-245, 1 25 2025.

[18] M. Y. Mustafa and Z. Y. Algamal, "Neutrosophic inverse power Lindley distribution: A modeling and application for bladder cancer patients," *International Journal of Neutrosophic Science,* pp. 216-223, 2 21 2023.

[19] K. H. Al-Habib, M. A. Khaleel and H. Al-Mofleh, "A new family of truncated nadarajah-haghighi-g properties with real data applications," *Tikrit Journal of Administrative and Economic Sciences,* p. 2, 61 19 2023.

[20] S. Rezaei, A. K. Marvasty, S. Nadarajah and M. Alizadeh, "A new exponentiated class of distributions: Properties and applications," *Communications in Statistics-Theory and Methods,* pp. 6054-6073, 12 46 2017.

[21] N. A. Noori, A. A. Khalaf and M. A. Khaleel, "A new expansion of the Inverse Weibull Distribution: Properties with Applications," *Iraqi Statistians Journal,* pp. 52-62, 1 1 2024.

[22] A. A. Khalaf, M. Q. Ibrahim and N. A. Noori, "[0,1]Truncated Exponentiated Exponential Burr type X Distributionwith Applications," *Iraqi Journal of Science,* pp. 4428-4440, 8 65 2024.

[23] M. A. Khaleel, P. Oguntunde, J. N. Al abbasi, N. A. Ibrahim and M. H. AbuJarad, "The Marshall-Olkin Topp Leone-G family of distributions: A family for generalizing probability models.," *Scientific African* , vol. 8, p. e00470, 2020.

[24] S. Naz, L. A. Al-Essa, H. S. Bakouch and C. Chesneau, "A transmuted modified power-generated family of distributions with practice on submodels in insurance and reliability," *Symmetry* , p. 1458, 7 15 2023.

[25] A. Z. Afify, M. Alizadeh, H. M. Yousof, G. Aryal and M. Ahmad, "THE TRANSMUTED GEOMETRIC-G FAMILY OF DISTRIBUTIONS: THEORY AND APPLICATIONS," *Pak. J. Statist,* pp. 139-160, 2 32 2016.

[26] Z. Khan, M. M. A. Almazah, O. H. Odhah and H. M. Alshanbari, "Generalized Pareto Model: Properties and Applications in Neutrosophic Data Modeling," *Mathematical Problems in Engineering,* p. 3686968, 1 2022.

[27] A. A. Khalaf and M. khaleel, "The New Strange Generalized Rayleigh Family: Characteristics and Applications to COVID-19 Data," *Iraqi Journal For Computer Science and Mathematics,* vol. 5, no. 3, pp. 92-107, 2024.

[28] A. Z. Afify , H. Yousof and S. Nadarajah, "The beta transmuted-H family for lifetime data," *Statistics and its Interface,* pp. 505-520, 3 10 2017.

[29] F. Chipepa, B. O. Oluyede and B. Makubate, "A New Generalized Family of Odd Lindley-G Distributions With Application," *International Journal of Statistics and Probability,* pp. 1-23, 6 8 2019.

[30] F. A. Bhatti, G. G. Hamedani, M. C. Korkmaz, G. M. Cordeiro, H. M. Yousof and M. Ahmad , "On Burr III Marshal Olkin family: development, properties, characterizations and applications," *Journal of Statistical Distributions and Applications,* pp. 1-21, 6 2019.

[31] N. A. Noori and M. A. khaleel, "Estimation and Some Statistical Properties of the hybrid Weibull Inverse Burr Type X Distribution with Application to Cancer Patient Data," *Iraqi Statisticians Journal,* pp. 8-29, 2 1 2024.

[32] N. A. Noori, "Exploring the Properties, Simulation, and Applications of the Odd Burr XII Gompertz Distribution," *Advances in the Theory of Nonlinear Analysis and Its Application,* pp. 60-75, 4 7 2023.

[33] K. H. Habib, A. M. Salih, M. A. Khaleel and M. K. Abdal-hammed, "OJCA Rayleigh distribution, Statistical Properties with Application," *Tikrit Journal of Administration and Economics Sciences,* 19 2023.

[34] M. Ahsan-ul-Haq, J. Zafar, M. Aslam and S. Tariq, "Neutrosophic Topp-Leone Distribution for Interval-Valued Data Analysis," *Journal of Statistical Theory and Applications,* pp. 164-173, 2 23 2024.

[35] M. A. Khaleel, P. E. Oguntunde, J. N. Al Abbasi, N. A. Ibrahim and M. H. AbuJarad, "The Marshall-Olkin Topp Leone-G family of distributions: A family for generalizing probability models," *Scientific African,* p. e00470, 8 2020.

[36] M. M. Rahman, A. M. Gemeay, M. A. I. Khan, M. A. Meraou, M. E. Bakr, A. H. Muse, E. Hussam and O. S. Balogun, "A new modified cubic transmuted-G family of distributions:

Properties and different methods of estimation with applications to real-life data," *AIP Advances,* p. 095025, 9 13 2023.

[37] G. M. Cordeiro, M. Alizadeh, T. G. Ramires and E. M. M. Ortega, "The generalized odd half-Cauchy family of distributions: Properties and applications," *Communications in Statistics-Theory and Methods,* pp. 5685-5705, 11 46 2017.

[38] M. Aboraya, "A new one-parameter G family of compound distributions: copulas, statistical properties and applications," *Statistics, Optimization & Information Computing, forthcoming,* p. 942–962, 9 2021.

[39] H. Sharqa , M. Ahsan-ul-Haq, J. Zafar and M. A. Khaleel, "Unit Xgamma Distribution: Its Properties, Estimation and Application: Unit-Xgamma Distribution," *Proceedings of the Pakistan Academy of Sciences: A. Physical and Computational Sciences,* pp. 15-28, 1 59 2022.

Received: Jan. 9, 2026. Accepted: Sept. 11, 2026.

Neutrosophic Sets and Systems, Vol. 102, 2027
University of New Mexico

MAGDM Model based Linguistic Neutrosophic Credibility Matrix Energy for Assessment of Learning Objectives Attainment in Production Internship

Xueping Lu[1,]*, Tong Zhang[1] , and Lilian Shi[1]

[1] School of Intelligent Engineering, Shaoxing University, Shaoxing ,China
Email: luxueping@usx.edu.cn，zhangtong@usx.edu.cn, cssll@usx.edu.cn
* Correspondence: luxueping@usx.edu.cn

Abstract: Conducting such an attainment assessment for complex courses like production internships is essentially a complex Multi-Attribute Group Decision-Making (MAGDM) problem. The com-plexity primarily manifests in two aspects: the difficulty in precisely quantifying various as-sessment components, and the involvement of multiple assessors, including both internal and external supervisors. To tackle this challenge, this paper develops an MAGDM technique us-ing linguistic neutrosophic credibility matrix (LNCM) energy. Firstly, this paper introduces the LNCM energy and its score function. Secondly, an MAGDM model is constructed based on these concepts. Subsequently, the model is utilized to solve the assessment problem of learning objectives attainment in production internship. Finally, the comparative analysis of decision results in LNM and LNCM environments demonstrates the superiority of the proposed MAGDM method over existing models in terms of both accuracy and rationality.

Keywords: linguistic neutrosophic credibility value；linguistic neutrosophic credibility matrix energy；assessment of learning objectives achievement.

1. Introduction

Under the Outcomes-based Education (OBE) framework, which underpins engineering education accreditation, the accurate assessment of learning objective attainment for individual courses forms the direct basis and fundamental cornerstone for evaluating the fulfillment of students' graduation requirements. However, for practice-oriented courses such as off-campus internships conducted in enterprise settings and jointly guided by academic and industrial mentors, the quantitative evaluation of attainment poses significant challenges. This is primarily because assessment in these contexts relies heavily on process-oriented evaluation, where criteria are difficult to standardize and quantify with the same precision as theoretical courses. Furthermore, the involvement of multiple assessors—often with diverse perspectives—adds complexity to deriving a unified and precise quantitative measure. Consequently, the evaluation of learning objective attainment in production internships constitutes a complex multi-criteria decision-making process, characterized by fuzziness, uncertainty, and the need to synthesize opinions from multiple experts within and outside the university

Linguistic decision-making methods hold a significant position in the field of complex multi-attribute (group) decision-making (MADM/MAGDM) due to their alignment with human cognitive habits. Since Zadeh [1] introduced the concept of linguistic variables, research in linguistic decision-making has undergone a remarkable evolution from simplicity to complexity, and from single-dimensional to multi-dimensional perspectives. This evolutionary process is primarily reflected in two key aspects: firstly, the continuous enrichment of linguistic information expression forms, evolving from basic linguistic term sets (LTSs) to linguistic intuitionistic fuzzy values (LIFVs), further to the more comprehensive linguistic neutrosophic values (LNVs) ,and then to linguistic neutrosophic credibility values (LNCVs); secondly, the ongoing innovation in information aggregation techniques, where the development of various linguistic aggregation operators (AOs) provides effective analytical tools for complex decision-making environments.

In terms of linguistic information expression, the linguistic intuitionistic fuzzy numbers (LIFNs) proposed by Chen et al. [2] describe the degrees of support and opposition in decision information using truth linguistic variables and falsity linguistic variables, addressing the limitations of traditional LTSs in expressing uncertain information. However, real-world decision environments often contain indeterminate or uncertain information that is neither fully supportive nor completely opposed, posing higher demands on linguistic expression. To address this, Fang and Ye [3] introduced linguistic neutrosophic sets/elements (LNSs/LNEs), which utilize three independent dimensions - truth, indeterminacy, and falsity - to provide a more comprehensive description of decision information in complex uncertain environments. To address the issue that the various linguistic expression forms mentioned above lack consideration for the credibility degree of linguistic values, making it difficult to ensure the reliability of linguistic evaluation values in uncertain scenarios, Ye and Rong [4] proposed the concept of Linguistic Neutrosophic Credibility Values (LNCVs).

Regarding information aggregation technology, researchers have developed various linguistic aggregation operators (AOs) to handle different types of linguistic information. For aggregating LIFV information, operators such as the weighted average [2], Partitioned heronian mean [5], power average [6], Frank Heronian mean [7] and others advanced weighted average [8, 9] have been proposed. For the more expressive LNV information, a richer set of aggregation methods has been developed, including weighted average and geometric average operators [3], Cosine measures [10], correlation coefficients [11] and various AOs [12-16]. The concept of Linguistic Neutrosophic Credibility Values (LNCVs) has only recently been introduced, and currently, merely a single aggregation algorithm has been proposed for it [4].

Matrix energy (ME), introduced as a generalization of graph energy by Bravo et al. [17], serves as a crucial mathematical tool for representing and processing collective data in group decision-making (GDM) and multi-attribute group decision-making (MAGDM) applications. The framework of ME has been successfully generalized to a variety of uncertain environments, including rough neutrosophic ME for handling rough neutrosophic matrix information in building site selection [18], intuitionistic fuzzy matrix (IFM) energy for hospital site selection in complete IFM scenarios [19], and linguistic neutrosophic ME for MAGDM problems under full linguistic neutrosophic matrices [20]. However, a significant limitation persists across these neutrosophic ME approaches: they lack built-in credibility measures for assessing the reliability of true, false, and indeterminate membership values in inconsistent and ambiguous scenarios. This deficiency undermines the decision credibility level in complex MAGDM environments.

This paper proposes an MAGDM model based on LNCV matrix energy and applies it to the assessment of learning objective attainment in production internships. The linguistic neutrosophic credibility matrix can effectively integrate the inherent fuzziness, uncertainty, and multi-source evaluation information in this scenario. The matrix energy comprehensively reflects the overall certainty and consistency of the evaluation information, thereby providing a stable and interpretable quantitative basis for determining the attainment degree.

The remainder of this paper is structured as follows: Section 2 introduces some preliminaries of LNCVs and matrix energy. In section 3, LNCM energy and it's score function are proposed. MAGDM model based LNCM energy is built in section 4. Section 5 applies the proposed MAGDM technique to a case study of learning objective attainment evaluation and compare it with the existing LNCVs aggregation operators to demonstrate the validity and reasonability of built model. Finally, section 6 summarizes the work and outlines avenues for future research.

2. Some Concepts of LNCS and LNCVs

Fang and Ye [3] first introduced the concepts of LNVs and LNSs. Suppose $P=\{\xi_0,\xi_1,\ldots\xi_g\}$ is a linguistic term set (LTS) which represent different information with even number g. Then, the LNS in X can be described as $\xi_{LNS}=\{\langle x,(\xi_{T(x)},\xi_{U(x)},\xi_{F(x)})\rangle \mid x\in X\}$, where $\langle x,(\xi_{T(x)},\xi_{U(x)},\xi_{F(x)})\rangle$ is LNV. $\xi_{T(x)}$, $\xi_{U(x)}$, $\xi_{F(x)}\in LTS\ P$ respectively represent the true, indeterminate and false linguistic values.

To measure the credibility of the LNV, Ye [4] proposed a LNCS in X. Then, a LNCS can be expressed as

$\xi_{LNCS}=\{\langle x,(\xi_{T(x)},\xi_{Tc(x)}),(\xi_{U(x)},\xi_{Uc(x)}),(\xi_{F(x)},\xi_{Fc(x)})\rangle \mid x\in X\}$, The linguistic terms $\xi_{T(x)},\xi_{U(x)},\xi_{F(x)}\in P$ represent the true, uncertain and false values and the $\xi_{Tc(x)},\xi_{Uc(x)},\xi_{Fc(x)}\in P$ represent the true, uncertain and false credibility values. Then, each element $\langle(\xi_{T(x)},\xi_{Tc(x)}),(\xi_{U(x)},\xi_{Uc(x)}),(\xi_{F(x)},\xi_{Fc(x)})\rangle$ in *the LNCS* is named LNCV and denoted as $\xi_{LNCV(i)}=\langle(\xi_{T(i)},\xi_{Tc(i)}),(\xi_{U(i)},\xi_{Uc(i)}),(\xi_{F(i)},\xi_{Fc(i)})\rangle$.

Definition 1. Let $\xi_{LNCV(i)}=\langle(\xi_{T(i)},\xi_{Tc(i)}),(\xi_{U(i)},\xi_{Uc(i)}),(\xi_{F(i)},\xi_{Fc(i)})\rangle$ and $\xi_{LNCV(j)}=\langle(\xi_{T(j)},\xi_{Tc(j)}),(\xi_{U(j)},\xi_{Uc(j)}),(\xi_{F(j)},\xi_{Fc(j)})\rangle$ be two LNCVs with $\lambda > 0$, then their reduced Dombi operations are defined as following:

$$\xi_{LNCV(i)}\oplus\xi_{LNCV(j)}=\langle(\xi_{T(i)},\xi_{Tc(i)}),(\xi_{U(i)},\xi_{Uc(i)}),(\xi_{F(i)},\xi_{Fc(i)})\rangle\oplus\langle(\xi_{T(j)},\xi_{Tc(j)}),(\xi_{U(j)},\xi_{Uc(j)}),(\xi_{F(j)},\xi_{Fc(j)})\rangle$$
$$=\left\langle\begin{array}{l}\left(\xi_{\frac{g}{1+\left\{\frac{g-T(i)}{T(i)}+\frac{g-T(j)}{T(j)}\right\}}},\xi_{\frac{g}{1+\left\{\frac{g-Tc(i)}{Tc(i)}+\frac{g-Tc(j)}{Tc(j)}\right\}}}\right),\left(\xi_{g-\frac{g}{1+\left\{\frac{U(i)}{g-U(i)}+\frac{U(j)}{g-U(j)}\right\}}},\xi_{g-\frac{g}{1+\left\{\frac{Uc(i)}{g-Uc(i)}+\frac{Uc(j)}{g-Uc(j)}\right\}}}\right),\\\left(\xi_{g-\frac{g}{1+\left\{\frac{F(i)}{g-F(i)}+\frac{F(j)}{g-F(j)}\right\}}},\xi_{g-\frac{g}{1+\left\{\frac{Fc(i)}{g-Fc(i)}+\frac{Fc(j)}{g-Fc(j)}\right\}}}\right)\end{array}\right\rangle \tag{1}$$

$$\xi_{LNCV(i)}\otimes\xi_{LNCV(j)}=\langle(\xi_{T(i)},\xi_{Tc(i)}),(\xi_{U(i)},\xi_{Uc(i)}),(\xi_{F(i)},\xi_{Fc(i)})\rangle\otimes\langle(\xi_{T(j)},\xi_{Tc(j)}),(\xi_{U(j)},\xi_{Uc(j)}),(\xi_{F(j)},\xi_{Fc(j)})\rangle$$
$$=\left\langle\begin{array}{l}\left(\xi_{g-\frac{g}{1+\left\{\frac{T\alpha(i)}{g-T\alpha(i)}+\frac{T\alpha(j)}{g-T\alpha(j)}\right\}}},\xi_{g-\frac{g}{1+\left\{\frac{Tc(i)}{g-Tc(i)}+\frac{Tc(j)}{g-Tc(j)}\right\}}}\right),\left(\xi_{\frac{g}{1+\left\{\frac{g-U(i)}{U(i)}+\frac{g-U(j)}{U(j)}\right\}}},\xi_{\frac{g}{1+\left\{\frac{g-Uc(i)}{Uc(i)}+\frac{g-Uc(j)}{Uc(j)}\right\}}}\right),\\\left(\xi_{\frac{g}{1+\left\{\frac{g-F\alpha(i)}{F\alpha(i)}+\frac{g-F\alpha(j)}{F\alpha(j)}\right\}}},\xi_{\frac{g}{1+\left\{\frac{g-Fc(i)}{Fc(i)}+\frac{g-Fc(j)}{Fc(j)}\right\}}}\right)\end{array}\right\rangle \tag{2}$$

$$\lambda\xi_{LNCV(i)}=\lambda\langle(\xi_{T(i)},\xi_{Tc(i)}),(\xi_{U(i)},\xi_{Uc(i)}),(\xi_{F(i)},\xi_{Fc(i)})\rangle$$
$$=\left\langle\left(\xi_{\frac{g}{1+\lambda\left(\frac{g-T(i)}{T(i)}\right)}},\xi_{\frac{g}{1+\lambda\left(\frac{g-Tc(j)}{Tc(j)}\right)}}\right),\left(\xi_{g-\frac{g}{1+\lambda\left(\frac{U(i)}{g-U(i)}\right)}},\xi_{g-\frac{g}{1+\lambda\left(\frac{Uc(i)}{g-Uc(i)}\right)}}\right),\left(\xi_{g-\frac{g}{1+\lambda\left(\frac{F(i)}{g-F(i)}\right)}},\xi_{g-\frac{g}{1+\lambda\left(\frac{Fc(i)}{g-Fc(i)}\right)}}\right)\right\rangle \tag{3}$$

$$(\xi_{LNCV(i)})^{\lambda}=\left\langle\left(\xi_{g-\frac{g}{1+\lambda\left(\frac{T(i)}{g-T(i)}\right)}},\xi_{g-\frac{g}{1+\lambda\left(\frac{Tc(i)}{g-Tc(i)}\right)}}\right),\left(\xi_{\frac{g}{1+\lambda\left(\frac{g-U(i)}{U(i)}\right)}},\xi_{\frac{g}{1+\lambda\left(\frac{g-Uc(i)}{Uc(i)}\right)}}\right),\left(\xi_{\frac{g}{1+\lambda\left(\frac{g-F(i)}{F(i)}\right)}},\xi_{\frac{g}{1+\lambda\left(\frac{g-Fc(i)}{Fc(i)}\right)}}\right)\right\rangle \tag{4}$$

3. LNCM Energy

Bravo [17] assumed that $D(p_{mn})$ is a h×h matrix for $p_{mn}\in\Re$.Then, the matrix energy (ME) is definition as below:

$$E(D(p_{mn})) = \sum_{m=1}^{h} \left| \lambda_m - \frac{1}{h}\sum_{m=1}^{h} \lambda_m \right|, \tag{5}$$

Where λ_m (m=1,2, …, z) are the eigenvalues of $D(p_{mn})$.

Definition 1. Set the LNCM $D\left(LNC_{mn}\right)$ *(m, n=1,2, …, h)* as a *h*×*h* matrix:

$$D\left(LNC_{mn}\right) = \begin{bmatrix} LNC_{11} & LNC_{12} & \dots & LNC_{1h} \\ LNC_{21} & LNC_{21} & \dots & LNC_{2h} \\ \dots & \dots & \dots & \dots \\ LNC_{h1} & LNC_{h2} & \dots & LNC_{hh} \end{bmatrix} \tag{6}$$

Let the LNCV be defined as $LNC_{mn} = \left\langle \left(\xi_{Tmn}, \xi_{Tcmn}\right), \left(\left(\xi_{Umn}, \xi_{Ucmn}\right)\right), \left(\left(\xi_{Fmn}, \xi_{Fcmn}\right)\right) \right\rangle$, for *m, n=1,2, …, h*. This variable comprises:

Membership values $\xi_{Tmn}, \xi_{Umn}, \xi_{Fmn}$, representing truth, indeterminate, and falsity, respectively.

Credibility values $\xi_{Tcmn}, \xi_{Ucmn}, \xi_{Fcmn}$, representing the corresponding credibility.

Accordingly, the LNCM $D\left(LNC_{mn}\right)$ can be decomposed into six distinct matrices: the truth matrix $D(\xi_{Tmn})$, the indeterminate matrix $D(\xi_{Umn})$, the false matrix $D(\xi_{Fmn})$, the true credibility matrix $D(\xi_{Tcmn})$, the indeterminate credibility matrix $D(\xi_{Ucmn})$, and the false credibility matrix $D(\xi_{Fcmn})$. Then the LNCM is thus expressed in the following form:

$$D(LNC_{mn}) = <\left(D(\xi_{Tmn}), D(\xi_{Tcmn})\right), \left(D(\xi_{Umn}), D(\xi_{Ucmn})\right), \left(D(\xi_{Fmn}), D(\xi_{Fcmn})\right)>$$

$$= \left\langle \begin{matrix} \left(\begin{bmatrix} \xi_{T11} & \xi_{T12} & \cdots & \xi_{T1h} \\ \xi_{T21} & \xi_{T21} & \cdots & \xi_{T2h} \\ \cdots & \cdots & \cdots & \cdots \\ \xi_{Th1} & \xi_{Th2} & \cdots & \xi_{Thh} \end{bmatrix}, \begin{bmatrix} \xi_{Tc11} & \xi_{Tc12} & \cdots & \xi_{Tc1h} \\ \xi_{Tc21} & \xi_{Tc21} & \cdots & \xi_{Tc2h} \\ \cdots & \cdots & \cdots & \cdots \\ \xi_{Tch1} & \xi_{Tch2} & \cdots & \xi_{Tchh} \end{bmatrix} \right), \\ \left(\begin{bmatrix} \xi_{U11} & \xi_{U12} & \cdots & \xi_{U1h} \\ \xi_{U21} & \xi_{U21} & \cdots & \xi_{U2h} \\ \cdots & \cdots & \cdots & \cdots \\ \xi_{Uh1} & \xi_{Uh2} & \cdots & \xi_{Uhh} \end{bmatrix}, \begin{bmatrix} \xi_{Uc11} & \xi_{Uc12} & \cdots & \xi_{Uc1h} \\ \xi_{Uc21} & \xi_{Uc21} & \cdots & \xi_{Uc2h} \\ \cdots & \cdots & \cdots & \cdots \\ \xi_{Uch1} & \xi_{Uch2} & \cdots & \xi_{Uchh} \end{bmatrix} \right), \\ \left(\begin{bmatrix} \xi_{F11} & \xi_{F12} & \cdots & \xi_{F1h} \\ \xi_{F21} & \xi_{F21} & \cdots & \xi_{F2h} \\ \cdots & \cdots & \cdots & \cdots \\ \xi_{Fh1} & \xi_{Fh2} & \cdots & \xi_{Fhh} \end{bmatrix}, \begin{bmatrix} \xi_{Fc11} & \xi_{Fc12} & \cdots & \xi_{Fc1h} \\ \xi_{Fc21} & \xi_{Fc21} & \cdots & \xi_{Fc2h} \\ \cdots & \cdots & \cdots & \cdots \\ \xi_{Fch1} & \xi_{Fch2} & \cdots & \xi_{Fchh} \end{bmatrix} \right) \end{matrix} \right\rangle \tag{6}$$

Definition 2. Let $D\left(LNC_{mn}\right)$ (for *m, n=1,2,…,h*) be an *h*×*h* LNCM, which consists of true, indeterminate, and false linguistic matrices $D(\xi_{Tmn})$, $D(\xi_{Umn})$, $D(\xi_{Fmn})$ and true, indeterminate, and false credibility linguistic matrices $D(\xi_{Tcmn})$, $D(\xi_{Ucmn})$, $D(\xi_{Fcmn})$. Using a subscript transformation function $Y(\xi_t) = t$, the LNCM can be decomposed into six distinct matrices: the truth matrix $D\left(Y(\xi_{Tmn})\right)$, the indeterminacy matrix $D\left(Y(\xi_{Umn})\right)$, and the falsity matrix $D\left(Y(\xi_{Fmn})\right)$, the truth credibility matrix $D\left(Y(\xi_{Tcmn})\right)$, the indeterminacy credibility matrix $D\left(Y(\xi_{Ucmn})\right)$, and the falsity credibility matrix $D\left(Y(\xi_{Fcmn})\right)$. Based on this decomposition, the energy of the LNM is defined as follows:

$$E\{D(LNC_{mn})\}=\left\langle\begin{array}{l}\left(E\{D(Y(\xi_{Tmn}))\},E\{D(Y(\xi_{Tcmn}))\}\right),\\ \left(E\{D(Y(\xi_{Umn}))\},E\{D(Y(\xi_{Ucmn}))\}\right),\\ \left(E\{D(Y(\xi_{Fmn}))\},E\{D(Y(\xi_{Fcmn}))\}\right)\end{array}\right\rangle$$
$$=\left\langle\begin{array}{l}\left(\sum_{m=1}^{h}\left|\lambda_{Tm}-\frac{1}{h}\sum_{m=1}^{h}\lambda_{Tm}\right|,\sum_{m=1}^{h}\left|\lambda_{Tcm}-\frac{1}{h}\sum_{m=1}^{h}\lambda_{Tcm}\right|\right),\\ \left(\sum_{m=1}^{h}\left|\lambda_{Um}-\frac{1}{h}\sum_{m=1}^{h}\lambda_{Um}\right|,\sum_{m=1}^{h}\left|\lambda_{Ucm}-\frac{1}{h}\sum_{m=1}^{h}\lambda_{Ucm}\right|\right),\\ \left(\sum_{m=1}^{h}\left|\lambda_{Fm}-\frac{1}{h}\sum_{m=1}^{h}\lambda_{Fm}\right|,\sum_{m=1}^{h}\left|\lambda_{Fcm}-\frac{1}{h}\sum_{m=1}^{h}\lambda_{Fcm}\right|\right)\end{array}\right\rangle$$
$$=\left\langle\begin{array}{l}\left(\sum_{m=1}^{h}\left|\lambda_{Tm}-\overline{\lambda_{T}}\right|,\sum_{m=1}^{h}\left|\lambda_{Tcm}-\overline{\lambda_{Tc}}\right|\right),\\ \left(\sum_{m=1}^{h}\left|\lambda_{Um}-\overline{\lambda_{U}}\right|,\sum_{m=1}^{h}\left|\lambda_{Ucm}-\overline{\lambda_{Uc}}\right|\right),\\ \left(\sum_{m=1}^{h}\left|\lambda_{Fm}-\overline{\lambda_{F}}\right|,\sum_{m=1}^{h}\left|\lambda_{Fcm}-\overline{\lambda_{Fc}}\right|\right)\end{array}\right\rangle \tag{7}$$

where λ_{Tm}, λ_{Um}, λ_{Fm} and λ_{Tcm}, λ_{Ucm}, λ_{Fcm} (for m=1,2,...,h) are the eigenvalues of the matrices $D(Y(\xi_{Tmn}))$, $D(Y(\xi_{Umn}))$, $D(Y(\xi_{Fmn}))$ and the credibility matrices $D(Y(\xi_{Tcmn}))$, $D(Y(\xi_{Ucmn}))$, $D(Y(\xi_{Fcmn}))$, respectively. Their corresponding average values are denoted as $\overline{\lambda_{T}}$, $\overline{\lambda_{U}}$, $\overline{\lambda_{F}}$ and $\overline{\lambda_{Tc}}$, $\overline{\lambda_{Uc}}$, $\overline{\lambda_{Fc}}$.

For the comparison of two LNCM energy values, a score function $S(E\{D(LNC_{imn})\})$ (*m,n*=*1, 2, ..., h; i* = *1, 2*) is defined as follows:

$$S(E\{D(LNC_{imn})\})=$$
$$\frac{E\{D(Y(\xi_{T\alpha imn}))\}+E\{D(Y(\xi_{Tcimn}))\}}{E\{D(Y(\xi_{T\alpha imn}))\}+E\{D(Y(\xi_{Tcimn}))\}+E\{D(Y(\xi_{U\alpha imn}))\}+E\{D(Y(\xi_{Ucimn}))\}+E\{D(Y(\xi_{F\alpha imn}))\}+E\{D(Y(\xi_{Fcimn}))\}}$$
$$for\ S(E\{D(LNC_{imn})\})\in[0,1], \tag{8}$$

Based on the score values from Eq.(13), the two energy values $E\{D(LNC_{1mn})\}$ and $E\{D(LNC_{2mn})\}$ can be ranked according to the following rules:

If $S(E\{D(LNC_{1mn})\})\succ S(E\{D(LNC_{1mn})\})$,then $E\{D(LNC_{1mn})\}\succ E\{D(LNC_{2mn})\}$;

If $S(E\{D(LNC_{1mn})\})\prec S(E\{D(LNC_{1mn})\})$,then $E\{D(LNC_{1mn})\}\prec E\{D(LNC_{2mn})\}$

If $S(E\{D(LNC_{1mn})\})=S(E\{D(LNC_{1mn})\})$,then $E\{D(LNC_{1mn})\}=E\{D(LNC_{2mn})\}$

4. MAGDM model based on the LNCM Energy

This section develops a MAGDM model by integrating the LNCM energy and its associated score function.

Consider a typical MAGDM scenario involving a set of alternatives $As=\{As_1,As_2,...,As_r\}$ and a set of attributes $Ms=\{Ms_1,Ms_2,...,Ms_k\}$. A group of experts, denoted by $E=\{E_1,E_2,...,E_h\}$, are invited to assess the performance of each alternative with respect to each attribute. In this case, it is specified that all linguistic evaluation variables come from the LTS $P=\{\xi_0,\xi_1,...\xi_g\}$.

To address this MAGDM problem, an LNCV energy-based model is constructed through the following procedural steps:

Step1: The weight vector for the experts is specified in LNCV form as $\xi_{\omega(m)}=\left\langle\left(\xi_{T\omega(m)},\xi_{Tc\omega(m)}\right),\left(\xi_{U\omega(m)},\xi_{Uc\omega(m)}\right),\left(\xi_{F\omega(m)},\xi_{Fc\omega(m)}\right)\right\rangle$ for *m=1,2, …, h.* the group of experts gives the LNCV weight vector of the criteria $\xi_{\theta(mn)}=\left\langle\left(\xi_{T\theta(mn)},\xi_{Tc\theta(mn)}\right),\left(\xi_{U\theta(mn)},\xi_{Uc\theta(mn)}\right),\left(\xi_{F\theta(mn)},\xi_{Fc\theta(mn)}\right)\right\rangle$ for *m=1,2, …, h; n=1,2, …, k.* Thus, the LNCM of criteria weights is constructed as follows:

$$D\left(\xi_{\theta(mn)}\right)=\begin{array}{c} \\ E_1 \\ E_2 \\ \cdots \\ E_h \end{array}\begin{array}{c} \begin{array}{cccc} Ms_1 & Ms_2 & \cdots & Ms_k \end{array} \\ \begin{bmatrix} \xi_{\theta(11)} & \xi_{\theta(12)} & \cdots & \xi_{\theta(1k)} \\ \xi_{\theta(21)} & \xi_{\theta(21)} & \cdots & \xi_{\theta(2k)} \\ \cdots & \cdots & \cdots & \cdots \\ \xi_{\theta(h1)} & \xi_{\theta(h1)} & \cdots & \xi_{\theta(hk)} \end{bmatrix}\end{array}=\begin{bmatrix} \left\langle\left(\xi_{T\theta(11)},\xi_{Tc\theta(11)}\right),\left(\xi_{U\theta(11)},\xi_{Uc\theta(11)}\right),\left(\xi_{F\theta(11)},\xi_{Fc\theta(11)}\right)\right\rangle & \left\langle\left(\xi_{T\theta(12)},\xi_{Tc\theta(12)}\right),\left(\xi_{U\theta(12)},\xi_{Uc\theta(12)}\right),\left(\xi_{F\theta(12)},\xi_{Fc\theta(12)}\right)\right\rangle & \cdots & \left\langle\left(\xi_{T\theta(1k)},\xi_{Tc\theta(1k)}\right),\left(\xi_{U\theta(1k)},\xi_{Uc\theta(1k)}\right),\left(\xi_{F\theta(1k)},\xi_{Fc\theta(1k)}\right)\right\rangle \\ \left\langle\left(\xi_{T\theta(21)},\xi_{Tc\theta(21)}\right),\left(\xi_{U\theta(21)},\xi_{Uc\theta(21)}\right),\left(\xi_{F\theta(21)},\xi_{Fc\theta(21)}\right)\right\rangle & \left\langle\left(\xi_{T\theta(22)},\xi_{Tc\theta(12)}\right),\left(\xi_{U\theta(22)},\xi_{Uc\theta(22)}\right),\left(\xi_{F\theta(22)},\xi_{Fc\theta(22)}\right)\right\rangle & \cdots & \left\langle\left(\xi_{T\theta(2k)},\xi_{Tc\theta(2k)}\right),\left(\xi_{U\theta(2kn)},\xi_{Uc\theta(2k)}\right),\left(\xi_{F\theta(2k)},\xi_{Fc\theta(2k)}\right)\right\rangle \\ \cdots & \cdots & \cdots & \cdots \\ \left\langle\left(\xi_{T\theta(h1)},\xi_{Tc\theta(h1)}\right),\left(\xi_{U\theta(h1)},\xi_{Uc\theta(h1)}\right),\left(\xi_{F\theta(h1)},\xi_{Fc\theta(h1)}\right)\right\rangle & \left\langle\left(\xi_{T\theta(h2)},\xi_{Tc\theta(h2)}\right),\left(\xi_{U\theta(h2)},\xi_{Uc\theta(h2)}\right),\left(\xi_{F\theta(h2)},\xi_{Fc\theta(h2)}\right)\right\rangle & \cdots & \left\langle\left(\xi_{T\theta(hk)},\xi_{Tc\theta(hk)}\right),\left(\xi_{U\theta(hk)},\xi_{Uc\theta(hk)}\right),\left(\xi_{F\theta(hk)},\xi_{Fc\theta(hk)}\right)\right\rangle \end{bmatrix} \tag{9}$$

Step 2: The Experts evaluate each attribute of all alternatives using the LNCV $LNC_{imn}=\left\langle\left(\xi_{Timn},\xi_{Tcimn}\right),\left(\left(\xi_{Uimn},\xi_{Ucimn}\right)\right),\left(\left(\xi_{Fimn},\xi_{Fcimn}\right)\right)\right\rangle$ and construct the corresponding LNCM $D\left(LNC_{i(mn)}\right)$ for the alternative As_i.

$$D\left(LNC_{i(mn)}\right)=\begin{bmatrix} LNC_{i(11)} & LNC_{i(12)} & \cdots & LNC_{i(1k)} \\ LNC_{i(21)} & LNC_{i(21)} & \cdots & LNC_{i(2k)} \\ \cdots & \cdots & \cdots & \cdots \\ LNC_{i(h1)} & LNC_{i(h2)} & \cdots & LNC_{i(hk)} \end{bmatrix}=\begin{bmatrix} \left\langle\left(\xi_{Ti(11)},\xi_{Tci(11)}\right),\left(\xi_{Ui(11)},\xi_{Uci(11)}\right),\left(\xi_{Fi(11)},\xi_{Fci(11)}\right)\right\rangle & \left\langle\left(\xi_{Ti(12)},\xi_{Tci(12)}\right),\left(\xi_{Ui(12)},\xi_{Uci(12)}\right),\left(\xi_{Fi(12)},\xi_{Fci(12)}\right)\right\rangle & \cdots & \left\langle\left(\xi_{Ti(1k)},\xi_{Tci(1k)}\right),\left(\xi_{Ui(1k)},\xi_{Uci(1k)}\right),\left(\xi_{Fi(1k)},\xi_{Fci(1k)}\right)\right\rangle \\ \left\langle\left(\xi_{Ti(21)},\xi_{Tci(21)}\right),\left(\xi_{Ui(21)},\xi_{Uci(21)}\right),\left(\xi_{Fi(21)},\xi_{Fci(21)}\right)\right\rangle & \left\langle\left(\xi_{Ti(22)},\xi_{Tci(12)}\right),\left(\xi_{Ui(22)},\xi_{Uci(22)}\right),\left(\xi_{Fi(22)},\xi_{Fci(22)}\right)\right\rangle & \cdots & \left\langle\left(\xi_{Ti(2k)},\xi_{Tci(2k)}\right),\left(\xi_{Ui(2kn)},\xi_{Uci(2k)}\right),\left(\xi_{Fi(2k)},\xi_{Fci(2k)}\right)\right\rangle \\ \cdots & \cdots & \cdots & \cdots \\ \left\langle\left(\xi_{Ti(h1)},\xi_{Tci(h1)}\right),\left(\xi_{Ui(h1)},\xi_{Uci(h1)}\right),\left(\xi_{Fi(h1)},\xi_{Fci(h1)}\right)\right\rangle & \left\langle\left(\xi_{Ti(h2)},\xi_{Tci(h2)}\right),\left(\xi_{Ui(h2)},\xi_{Uci(h2)}\right),\left(\xi_{Fi(h2)},\xi_{Fci(h2)}\right)\right\rangle & \cdots & \left\langle\left(\xi_{Ti(hk)},\xi_{Tci(hk)}\right),\left(\xi_{Ui(hk)},\xi_{Uci(hk)}\right),\left(\xi_{Fi(hk)},\xi_{Fci(hk)}\right)\right\rangle \end{bmatrix} \tag{10}$$

Step 3: Incorporating the decision-makers' weights into the LNCM of each alternative As_i yields the experts-weighted LNCM $D_M\left(\xi_{\omega(m)}\otimes LNC_{i(mn)}\right)$

$$D_M\left(\xi_{\omega(m)}\otimes LNC_{i(mn)}\right)=$$

$$=\begin{bmatrix}
\left\langle\begin{array}{l}\left(\xi_{g-\frac{g}{1+\left\{\frac{T\omega(1)}{g-T\omega(1)}+\frac{Ti(11)}{g-Ti(11)}\right\}}},\xi_{g-\frac{g}{1+\left\{\frac{Tc\omega(1)}{g-Tc\omega(1)}+\frac{Tci(11)}{g-Tci(11)}\right\}}}\right),\\ \left(\xi_{\frac{g}{1+\left\{\frac{g-U\omega(1)}{U\omega(1)}+\frac{g-Ui(11)}{Ui(11)}\right\}}},\xi_{\frac{g}{1+\left\{\frac{g-Uc\omega(1)}{Uc\omega(1)}+\frac{g-Uci(11)}{Uci(11)}\right\}}}\right),\\ \left(\xi_{\frac{g}{1+\left\{\frac{g-F\omega(1)}{F\omega(1)}+\frac{g-Fi(11)}{Fi(11)}\right\}}},\xi_{\frac{g}{1+\left\{\frac{g-Fc\omega(1)}{Fc\omega(1)}+\frac{g-Fci(11)}{Fci(11)}\right\}}}\right)\end{array}\right\rangle &
\left\langle\begin{array}{l}\left(\xi_{g-\frac{g}{1+\left\{\frac{T\omega(1)}{g-T\omega(1)}+\frac{Ti(12)}{g-Ti(12)}\right\}}},\xi_{g-\frac{g}{1+\left\{\frac{Tc\omega(1)}{g-Tc\omega(1)}+\frac{Tci(12)}{g-Tci(12)}\right\}}}\right),\\ \left(\xi_{\frac{g}{1+\left\{\frac{g-U\omega(1)}{U\omega(1)}+\frac{g-Ui(12)}{Ui(12)}\right\}}},\xi_{\frac{g}{1+\left\{\frac{g-Uc\omega(1)}{Uc\omega(1)}+\frac{g-Uci(12)}{Uci(12)}\right\}}}\right),\\ \left(\xi_{\frac{g}{1+\left\{\frac{g-F\omega(1)}{F\omega(1)}+\frac{g-Fi(12)}{Fi(12)}\right\}}},\xi_{\frac{g}{1+\left\{\frac{g-Fc\omega(1)}{Fc\omega(1)}+\frac{g-Fci(12)}{Fci(12)}\right\}}}\right)\end{array}\right\rangle & \cdots &
\left\langle\begin{array}{l}\left(\xi_{g-\frac{g}{1+\left\{\frac{T\omega(1)}{g-T\omega(1)}+\frac{Ti(1k)}{g-Ti(1k)}\right\}}},\xi_{g-\frac{g}{1+\left\{\frac{Tc\omega(1)}{g-Tc\omega(1)}+\frac{Tci(1k)}{g-Tci(1k)}\right\}}}\right),\\ \left(\xi_{\frac{g}{1+\left\{\frac{g-U\omega(1)}{U\omega(1)}+\frac{g-Ui(1k)}{Ui(1k)}\right\}}},\xi_{\frac{g}{1+\left\{\frac{g-Uc\omega(1)}{Uc\omega(1)}+\frac{g-Uci(1k)}{Uci(1k)}\right\}}}\right),\\ \left(\xi_{\frac{g}{1+\left\{\frac{g-F\omega(1)}{F\omega(1)}+\frac{g-Fi(1k)}{Fi(1k)}\right\}}},\xi_{\frac{g}{1+\left\{\frac{g-Fc\omega(1)}{Fc\omega(1)}+\frac{g-Fci(1k)}{Fci(1k)}\right\}}}\right)\end{array}\right\rangle \\
\left\langle\begin{array}{l}\left(\xi_{g-\frac{g}{1+\left\{\frac{T\omega(2)}{g-T\omega(2)}+\frac{Ti(21)}{g-Ti(21)}\right\}}},\xi_{g-\frac{g}{1+\left\{\frac{Tc\omega(2)}{g-Tc\omega(2)}+\frac{Tci(21)}{g-Tci(21)}\right\}}}\right),\\ \left(\xi_{\frac{g}{1+\left\{\frac{g-U\omega(2)}{U\omega(2)}+\frac{g-Ui(21)}{Ui(21)}\right\}}},\xi_{\frac{g}{1+\left\{\frac{g-Uc\omega(2)}{Uc\omega(2)}+\frac{g-Uci(21)}{Uci(21)}\right\}}}\right),\\ \left(\xi_{\frac{g}{1+\left\{\frac{g-F\omega(2)}{F\omega(2)}+\frac{g-Fi(21)}{Fi(21)}\right\}}},\xi_{\frac{g}{1+\left\{\frac{g-Fc\omega(2)}{Fc\omega(2)}+\frac{g-Fci(21)}{Fci(21)}\right\}}}\right)\end{array}\right\rangle &
\left\langle\begin{array}{l}\left(\xi_{g-\frac{g}{1+\left\{\frac{T\omega(2)}{g-T\omega(2)}+\frac{Ti(22)}{g-Ti(22)}\right\}}},\xi_{g-\frac{g}{1+\left\{\frac{Tc\omega(2)}{g-Tc\omega(2)}+\frac{Tci(22)}{g-Tci(22)}\right\}}}\right),\\ \left(\xi_{\frac{g}{1+\left\{\frac{g-U\omega(2)}{U\omega(2)}+\frac{g-Ui(22)}{Ui(22)}\right\}}},\xi_{\frac{g}{1+\left\{\frac{g-Uc\omega(2)}{Uc\omega(2)}+\frac{g-Uci(22)}{Uci(22)}\right\}}}\right),\\ \left(\xi_{\frac{g}{1+\left\{\frac{g-F\omega(2)}{F\omega(2)}+\frac{g-Fi(22)}{Fi(22)}\right\}}},\xi_{\frac{g}{1+\left\{\frac{g-Fc\omega(2)}{Fc\omega(2)}+\frac{g-Fci(22)}{Fci(22)}\right\}}}\right)\end{array}\right\rangle & \cdots &
\left\langle\begin{array}{l}\left(\xi_{g-\frac{g}{1+\left\{\frac{T\omega(2)}{g-T\omega(2)}+\frac{Ti(2k)}{g-Ti(2k)}\right\}}},\xi_{g-\frac{g}{1+\left\{\frac{Tc\omega(2)}{g-Tc\omega(2)}+\frac{Tci(2k)}{g-Tci(2k)}\right\}}}\right),\\ \left(\xi_{\frac{g}{1+\left\{\frac{g-U\omega(2)}{U\omega(2)}+\frac{g-Ui(2k)}{Ui(2k)}\right\}}},\xi_{\frac{g}{1+\left\{\frac{g-Uc\omega(2)}{Uc\omega(2)}+\frac{g-Uci(2k)}{Uci(2k)}\right\}}}\right),\\ \left(\xi_{\frac{g}{1+\left\{\frac{g-F\omega(2)}{F\omega(2)}+\frac{g-Fi(2k)}{Fi(2k)}\right\}}},\xi_{\frac{g}{1+\left\{\frac{g-Fc\omega(2)}{Fc\omega(2)}+\frac{g-Fci(2k)}{Fci(2k)}\right\}}}\right)\end{array}\right\rangle \\
\cdots & \cdots & \cdots & \cdots \\
\left\langle\begin{array}{l}\left(\xi_{g-\frac{g}{1+\left\{\frac{T\omega(h)}{g-T\omega(h)}+\frac{Ti(h1)}{g-Ti(h1)}\right\}}},\xi_{g-\frac{g}{1+\left\{\frac{Tc\omega(h)}{g-Tc\omega(h)}+\frac{Tci(h1)}{g-Tci(h1)}\right\}}}\right),\\ \left(\xi_{\frac{g}{1+\left\{\frac{g-U\omega(h)}{U\omega(h)}+\frac{g-Ui(h1)}{Ui(h1)}\right\}}},\xi_{\frac{g}{1+\left\{\frac{g-Uc\omega(h)}{Uc\omega(h)}+\frac{g-Uci(h1)}{Uci(h1)}\right\}}}\right),\\ \left(\xi_{\frac{g}{1+\left\{\frac{g-F\omega(h)}{F\omega(h)}+\frac{g-Fi(h1)}{Fi(h1)}\right\}}},\xi_{\frac{g}{1+\left\{\frac{g-Fc\omega(h)}{Fc\omega(h)}+\frac{g-Fci(h1)}{Fci(h1)}\right\}}}\right)\end{array}\right\rangle &
\left\langle\begin{array}{l}\left(\xi_{g-\frac{g}{1+\left\{\frac{T\omega(h)}{g-T\omega(h)}+\frac{Ti(h2)}{g-Ti(h2)}\right\}}},\xi_{g-\frac{g}{1+\left\{\frac{Tc\omega(h)}{g-Tc\omega(h)}+\frac{Tci(h2)}{g-Tci(h2)}\right\}}}\right),\\ \left(\xi_{\frac{g}{1+\left\{\frac{g-U\omega(h)}{U\omega(h)}+\frac{g-Ui(h2)}{Ui(h2)}\right\}}},\xi_{\frac{g}{1+\left\{\frac{g-Uc\omega(h)}{Uc\omega(h)}+\frac{g-Uci(h2)}{Uci(h2)}\right\}}}\right),\\ \left(\xi_{\frac{g}{1+\left\{\frac{g-F\omega(h)}{F\omega(h)}+\frac{g-Fi(h2)}{Fi(h2)}\right\}}},\xi_{\frac{g}{1+\left\{\frac{g-Fc\omega(h)}{Fc\omega(h)}+\frac{g-Fci(h2)}{Fci(h2)}\right\}}}\right)\end{array}\right\rangle & \cdots &
\left\langle\begin{array}{l}\left(\xi_{g-\frac{g}{1+\left\{\frac{T\omega(h)}{g-T\omega(h)}+\frac{Ti(hk)}{g-Ti(hk)}\right\}}},\xi_{g-\frac{g}{1+\left\{\frac{Tc\omega(h)}{g-Tc\omega(h)}+\frac{Tci(hk)}{g-Tci(hk)}\right\}}}\right),\\ \left(\xi_{\frac{g}{1+\left\{\frac{g-U\omega(h)}{U\omega(h)}+\frac{g-Ui(hk)}{Ui(hk)}\right\}}},\xi_{\frac{g}{1+\left\{\frac{g-Uc\omega(h)}{Uc\omega(h)}+\frac{g-Uci(hk)}{Uci(hk)}\right\}}}\right),\\ \left(\xi_{\frac{g}{1+\left\{\frac{g-F\omega(h)}{F\omega(h)}+\frac{g-Fi(hk)}{Fi(hk)}\right\}}},\xi_{\frac{g}{1+\left\{\frac{g-Fc\omega(h)}{Fc\omega(h)}+\frac{g-Fci(hk)}{Fci(hk)}\right\}}}\right)\end{array}\right\rangle
\end{bmatrix} \tag{11}$$

Incorporating the attributes' weights into the LNCM of each alternative As_i yields the criteria-weighted LNCMs $D_C\left(\xi_{\theta(mn)}\otimes LNC_{i(mn)}\right)$

$$D_C\left(\xi_{\theta(mn)}\otimes LNC_{i(mn)}\right)=$$

$$\begin{bmatrix}
\left\langle\begin{array}{l}
(\xi_{g-\frac{g}{1+\left\{\frac{T\theta(11)}{g-T\theta(11)}+\frac{Ti(11)}{g-Ti(11)}\right\}}},\xi_{g-\frac{g}{1+\left\{\frac{Tc\theta(11)}{g-Tc\theta(11)}+\frac{Tci(11)}{g-Tci(11)}\right\}}}),\\
(\xi_{\frac{g}{1+\left\{\frac{g-U\theta(11)}{U\theta(11)}+\frac{g-Ui(11)}{Ui(11)}\right\}}},\xi_{\frac{g}{1+\left\{\frac{g-Uc\theta(11)}{Uc\theta(11)}+\frac{g-Uci(11)}{Uci(11)}\right\}}}),\\
(\xi_{\frac{g}{1+\left\{\frac{g-F\theta(11)}{F\theta(11)}+\frac{g-Fi(11)}{Fi(11)}\right\}}},\xi_{\frac{g}{1+\left\{\frac{g-Fc\theta(11)}{Fc\theta(11)}+\frac{g-Fci(11)}{Fci(11)}\right\}}})
\end{array}\right\rangle &
\left\langle\begin{array}{l}
(\xi_{g-\frac{g}{1+\left\{\frac{T\theta(12)}{g-T\theta(12)}+\frac{Ti(12)}{g-Ti(12)}\right\}}},\xi_{g-\frac{g}{1+\left\{\frac{Tc\theta(12)}{g-Tc\theta(12)}+\frac{Tci(12)}{g-Tci(12)}\right\}}}),\\
(\xi_{\frac{g}{1+\left\{\frac{g-U\theta(12)}{U\theta(12)}+\frac{g-Ui(12)}{Ui(12)}\right\}}},\xi_{\frac{g}{1+\left\{\frac{g-Uc\theta(12)}{Uc\theta(12)}+\frac{g-Uci(12)}{Uci(12)}\right\}}}),\\
(\xi_{\frac{g}{1+\left\{\frac{g-F\theta(12)}{F\theta(12)}+\frac{g-Fi(12)}{Fi(12)}\right\}}},\xi_{\frac{g}{1+\left\{\frac{g-Fc\theta(12)}{Fc\theta(1)}+\frac{g-Fci(12)}{Fci(12)}\right\}}})
\end{array}\right\rangle & \cdots &
\left\langle\begin{array}{l}
(\xi_{g-\frac{g}{1+\left\{\frac{T\theta(1k)}{g-T\theta(1k)}+\frac{Ti(1k)}{g-Ti(1k)}\right\}}},\xi_{g-\frac{g}{1+\left\{\frac{Tc\theta(1k)}{g-Tc\theta(1k)}+\frac{Tci(1k)}{g-Tci(1k)}\right\}}}),\\
(\xi_{\frac{g}{1+\left\{\frac{g-U\theta(1k)}{U\theta(1k)}+\frac{g-Ui(1k)}{Ui(1k)}\right\}}},\xi_{\frac{g}{1+\left\{\frac{g-Uc\theta(1k)}{Uc\theta(1k)}+\frac{g-Uci(1k)}{Uci(1k)}\right\}}}),\\
(\xi_{\frac{g}{1+\left\{\frac{g-F\theta(1k)}{F\theta(1k)}+\frac{g-Fi(1k)}{Fi(1k)}\right\}}},\xi_{\frac{g}{1+\left\{\frac{g-Fc\theta(1k)}{Fc\theta(1k)}+\frac{g-Fci(1k)}{Fci(1k)}\right\}}})
\end{array}\right\rangle \\
\left\langle\begin{array}{l}
(\xi_{g-\frac{g}{1+\left\{\frac{T\theta(21)}{g-T\theta(21)}+\frac{Ti(21)}{g-Ti(21)}\right\}}},\xi_{g-\frac{g}{1+\left\{\frac{Tc\theta(21)}{g-Tc\theta(21)}+\frac{Tci(21)}{g-Tci(21)}\right\}}}),\\
(\xi_{\frac{g}{1+\left\{\frac{g-U\theta(21)}{U\theta(21)}+\frac{g-Ui(21)}{Ui(21)}\right\}}},\xi_{\frac{g}{1+\left\{\frac{g-U\theta(21)}{U\theta(21)}+\frac{g-Ui(21)}{Ui(21)}\right\}}}),\\
(\xi_{\frac{g}{1+\left\{\frac{g-F\theta(21)}{F\theta(21)}+\frac{g-Fi(21)}{Fi(21)}\right\}}},\xi_{\frac{g}{1+\left\{\frac{g-Fc\theta(21)}{Fc\theta(21)}+\frac{g-Fci(21)}{Fci(21)}\right\}}})
\end{array}\right\rangle &
\left\langle\begin{array}{l}
(\xi_{g-\frac{g}{1+\left\{\frac{T\theta(22)}{g-T\theta(22)}+\frac{Ti(22)}{g-Ti(22)}\right\}}},\xi_{g-\frac{g}{1+\left\{\frac{Tc\theta(22)}{g-Tc\theta(22)}+\frac{Tci(22)}{g-Tci(22)}\right\}}}),\\
(\xi_{\frac{g}{1+\left\{\frac{g-U\theta(22)}{U\theta(22)}+\frac{g-Ui(22)}{Ui(22)}\right\}}},\xi_{\frac{g}{1+\left\{\frac{g-Uc\theta(22)}{Uc\theta(22)}+\frac{g-Uci(22)}{Uci(22)}\right\}}}),\\
(\xi_{\frac{g}{1+\left\{\frac{g-F\theta(22)}{F\theta(22)}+\frac{g-Fi(22)}{Fi(22)}\right\}}},\xi_{\frac{g}{1+\left\{\frac{g-Fc\theta(22)}{Fc\theta(22)}+\frac{g-Fci(22)}{Fci(22)}\right\}}})
\end{array}\right\rangle & \cdots &
\left\langle\begin{array}{l}
(\xi_{g-\frac{g}{1+\left\{\frac{T\theta(2k)}{g-T\theta(2k)}+\frac{Ti(2k)}{g-Ti(2k)}\right\}}},\xi_{g-\frac{g}{1+\left\{\frac{Tc\theta(2k)}{g-Tc\theta(2k)}+\frac{Tci(2k)}{g-Tci(2k)}\right\}}}),\\
(\xi_{\frac{g}{1+\left\{\frac{g-U\theta(2k)}{U\theta(2k)}+\frac{g-Ui(2k)}{Ui(2k)}\right\}}}\ \xi_{\frac{g}{1+\left\{\frac{g-Uc\theta(2k)}{Uc\theta(2k)}+\frac{g-Uci(2k)}{Uci(2k)}\right\}}}),\\
(\xi_{\frac{g}{1+\left\{\frac{g-F\theta(2k)}{F\theta(2k)}+\frac{g-Fi(2k)}{Fi(2k)}\right\}}},\xi_{\frac{g}{1+\left\{\frac{g-Fc\theta(2k)}{Fc\theta(2k)}+\frac{g-Fci(2k)}{Fci(2k)}\right\}}})
\end{array}\right\rangle \\
\cdots & \cdots & \cdots & \cdots \\
\left\langle\begin{array}{l}
(\xi_{g-\frac{g}{1+\left\{\frac{T\theta(h1)}{g-T\theta(h1)}+\frac{Ti(h1)}{g-Ti(h1)}\right\}}},\xi_{g-\frac{g}{1+\left\{\frac{Tc\theta(h1)}{g-Tc\theta(h1)}+\frac{Tci(h1)}{g-Tci(h1)}\right\}}}),\\
(\xi_{\frac{g}{1+\left\{\frac{g-U\theta(h1)}{U\theta(h1)}+\frac{g-Ui(h1)}{Ui(h1)}\right\}}},\xi_{\frac{g}{1+\left\{\frac{g-Uc\theta(h1)}{Uc\theta(h1)}+\frac{g-Uci(h1)}{Uci(h1)}\right\}}}),\\
(\xi_{\frac{g}{1+\left\{\frac{g-F\theta(h1)}{F\theta(h1)}+\frac{g-Fi(h1)}{Fi(h1)}\right\}}},\xi_{\frac{g}{1+\left\{\frac{g-Fc\theta(h1)}{Fc\theta(h1)}+\frac{g-Fci(h1)}{Fci(h1)}\right\}}})
\end{array}\right\rangle &
\left\langle\begin{array}{l}
(\xi_{g-\frac{g}{1+\left\{\frac{T\theta(h2)}{g-T\theta(h2)}+\frac{Ti(h2)}{g-Ti(h2)}\right\}}},\xi_{g-\frac{g}{1+\left\{\frac{Tc\theta(h2)}{g-Tc\theta(h2)}+\frac{Tci(h2)}{g-Tci(h2)}\right\}}}),\\
(\xi_{\frac{g}{1+\left\{\frac{g-U\theta(h2)}{U\theta(h2)}+\frac{g-Ui(h2)}{Ui(h2)}\right\}}},\xi_{\frac{g}{1+\left\{\frac{g-Uc\theta(h2)}{Uc\theta(h2)}+\frac{g-Uci(h2)}{Uci(h2)}\right\}}}),\\
(\xi_{\frac{g}{1+\left\{\frac{g-F\theta(h2)}{F\theta(h2)}+\frac{g-Fi(h2)}{Fi(h2)}\right\}}},\xi_{\frac{g}{1+\left\{\frac{g-Fc\theta(h2)}{Fc\theta(h2)}+\frac{g-Fci(h2)}{Fci(h2)}\right\}}})
\end{array}\right\rangle & \cdots &
\left\langle\begin{array}{l}
(\xi_{g-\frac{g}{1+\left\{\frac{T\theta(hk)}{g-T\theta(hk)}+\frac{Ti(hk)}{g-Ti(hk)}\right\}}},\xi_{g-\frac{g}{1+\left\{\frac{Tc\theta(hk)}{g-Tc\theta(hk)}+\frac{Tci(hk)}{g-Tci(hk)}\right\}}}),\\
(\xi_{\frac{g}{1+\left\{\frac{g-U\theta(hk)}{U\theta(hk)}+\frac{g-Ui(hk)}{Ui(hk)}\right\}}},\xi_{\frac{g}{1+\left\{\frac{g-Uc\theta(hk)}{Uc\theta(hk)}+\frac{g-Uci(hk)}{Uci(hk)}\right\}}}),\\
(\xi_{\frac{g}{1+\left\{\frac{g-F\theta(hk)}{F\theta(hk)}+\frac{g-Fi(hk)}{Fi(hk)}\right\}}},\xi_{\frac{g}{1+\left\{\frac{g-Fc\theta(hk)}{Fc\theta(hk)}+\frac{g-Fci(hk)}{Fci(hk)}\right\}}})
\end{array}\right\rangle
\end{bmatrix} \tag{12}$$

Step 4: According to the transformation function $Y(\xi_t)=t$, the two weighted matrices $D_M\left(\xi_{\omega(m)}\otimes LNC_{i(mn)}\right)$ and $D_C\left(\xi_{\theta(mn)}\otimes LNC_{i(mn)}\right)$ can be transformed and decomposed into the true matrices $D_M\left(Y\left(\xi_{g-\frac{g}{1+\left\{\frac{T\omega(m)}{g-T\omega(m)}+\frac{Ti(mn)}{g-Ti(mn)}\right\}}}\right)\right)$ and $D_C\left(Y\left(\xi_{g-\frac{g}{1+\left\{\frac{T\theta(mn)}{g-T\theta(mn)}+\frac{Ti(mn)}{g-Ti(mn)}\right\}}}\right)\right)$,the indeterminate matrices $D_M\left(Y\left(\xi_{\frac{g}{1+\left\{\frac{g-U\omega(m)}{U\omega(m)}+\frac{g-Ui(mn)}{Ui(mn)}\right\}}}\right)\right)$ and $D_C\left(Y\left(\xi_{\frac{g}{1+\left\{\frac{g-U\theta(mn)}{U\theta(mn)}+\frac{g-Ui(mn)}{Ui(mn)}\right\}}}\right)\right)$, the false matrices

$D_M\left(Y\left(\xi\frac{g}{1+\left\{\frac{g-F\omega(m)}{F\omega(m)}+\frac{g-Fi(mn)}{Fi(mn)}\right\}}\right)\right)$ and $D_C\left(Y\left(\xi\frac{g}{1+\left\{\frac{g-F\theta(mn)}{F\theta(mn)}+\frac{g-Fi(mn)}{Fi(mn)}\right\}}\right)\right)$, the true credibility matrices $D_M\left(Y\left(\xi_{g}-\frac{g}{1+\left\{\frac{Tc\omega(m)}{g-Tc\omega(m)}+\frac{Tci(mn)}{g-Tci(mn)}\right\}}\right)\right)$ and ${}_{C}\left(Y\left(\xi_{g}-\frac{g}{1+\left\{\frac{Tc\theta(mn)}{g-Tc\theta(mn)}+\frac{Tci(mn)}{g-Tci(mn)}\right\}}\right)\right)$, the indeterminate credibility matrices $D_M\left(Y\left(\xi\frac{g}{1+\left\{\frac{g-Uc\omega(m)}{Uc\omega(m)}+\frac{g-Uci(mn)}{Uci(mn)}\right\}}\right)\right)$ and $D_C\left(Y\left(\xi\frac{g}{1+\left\{\frac{g-Uc\theta(mn)}{Uc\theta(mn)}+\frac{g-Uci(mn)}{Uci(mn)}\right\}}\right)\right)$, the false credibility matrices $D_M\left(Y\left(\xi\frac{g}{1+\left\{\frac{g-Fc\omega(m)}{Fc\omega(m)}+\frac{g-Fci(mn)}{Fci(mn)}\right\}}\right)\right)$ and ${}_{C}\left(Y\left(\xi\frac{g}{1+\left\{\frac{g-Fc\theta(mn)}{Fc\theta(mn)}+\frac{g-Fci(11)}{Fci(11)}\right\}}\right)\right)$.Then integrated true, indeterminate, false and true credibility, indeterminate credibility, false credibility squire matrices are derived from the following formula:

$$D\left(T_{i}(mm)\right)=D_C\left(Y\left(\xi_{g}-\frac{g}{1+\left\{\frac{T\theta(mn)}{g-T\theta(mn)}+\frac{Ti(mn)}{g-Ti(mn)}\right\}}\right)\right)\times\left[D_M\left(Y\left(\xi_{g}-\frac{g}{1+\left\{\frac{T\omega(m)}{g-T\omega(m)}+\frac{Ti(mn)}{g-Ti(mn)}\right\}}\right)\right)\right]^T$$

$$=\begin{bmatrix} g-\frac{g}{1+\left\{\frac{T\theta(11)}{g-T\theta(11)}+\frac{Ti(11)}{g-Ti(11)}\right\}} & g-\frac{g}{1+\left\{\frac{T\theta(12)}{g-T\theta(12)}+\frac{Ti(12)}{g-Ti(12)}\right\}} & \cdots & g-\frac{g}{1+\left\{\frac{T\theta(1k)}{g-T\theta(1k)}+\frac{Ti(1k)}{g-Ti(1k)}\right\}} \\ g-\frac{g}{1+\left\{\frac{T\theta(21)}{g-T\theta(21)}+\frac{Ti(21)}{g-Ti(21)}\right\}} & g-\frac{g}{1+\left\{\frac{T\theta(22)}{g-T\theta(22)}+\frac{Ti(22)}{g-Ti(22)}\right\}} & \cdots & g-\frac{g}{1+\left\{\frac{T\theta(2k)}{g-T\theta(2k)}+\frac{Ti(2k)}{g-Ti(2k)}\right\}} \\ \cdots & \cdots & \cdots & \cdots \\ g-\frac{g}{1+\left\{\frac{T\theta(h1)}{g-T\theta(h1)}+\frac{Ti(h1)}{g-Ti(h1)}\right\}} & g-\frac{g}{1+\left\{\frac{T\theta(h2)}{g-T\theta(h2)}+\frac{Ti(h2)}{g-Ti(h2)}\right\}} & \cdots & g-\frac{g}{1+\left\{\frac{T\theta(hk)}{g-T\theta(hk)}+\frac{Ti(hk)}{g-Ti(hk)}\right\}} \end{bmatrix} \tag{13}$$

$$\times\begin{bmatrix} g-\frac{g}{1+\left\{\frac{T\omega(1)}{g-T\omega(1)}+\frac{Ti(11)}{g-Ti(11)}\right\}} & g-\frac{g}{1+\left\{\frac{T\omega(2)}{g-T\omega(2)}+\frac{Ti(21)}{g-Ti(21)}\right\}} & \cdots & g-\frac{g}{1+\left\{\frac{T\omega(h)}{g-T\omega(h)}+\frac{Ti(h1)}{g-Ti(h1)}\right\}} \\ g-\frac{g}{1+\left\{\frac{T\omega(1)}{g-T\omega(1)}+\frac{Ti(12)}{g-Ti(12)}\right\}} & g-\frac{g}{1+\left\{\frac{T\omega(2)}{g-T\omega(2)}+\frac{Ti(22)}{g-Ti(22)}\right\}} & \cdots & g-\frac{g}{1+\left\{\frac{T\omega(h)}{g-T\omega(h)}+\frac{Ti(h2)}{g-Ti(h2)}\right\}} \\ \cdots & \cdots & \cdots & \cdots \\ g-\frac{g}{1+\left\{\frac{T\omega(1)}{g-T\omega(1)}+\frac{Ti(1k)}{g-Ti(1k)}\right\}} & g-\frac{g}{1+\left\{\frac{T\omega(2)}{g-T\omega(2)}+\frac{Ti(2k)}{g-Ti(2k)}\right\}} & \cdots & g-\frac{g}{1+\left\{\frac{T\omega(h)}{g-T\omega(h)}+\frac{Ti(hk)}{g-Ti(hk)}\right\}} \end{bmatrix}$$

$$D\left(U_{i}(mm)\right)=D_C\left(Y\left(\xi\frac{g}{1+\left\{\frac{g-U\theta(mn)}{U\theta(mn)}+\frac{g-Ui(mn)}{Ui(mn)}\right\}}\right)\right)\times\left[D_M\left(Y\left(\xi\frac{g}{1+\left\{\frac{g-U\omega(m)}{U\omega(m)}+\frac{g-Ui(mn)}{Ui(mn)}\right\}}\right)\right)\right]^T \tag{14}$$

$$D\left(F_{i}(mm)\right)=D_C\left(Y\left(\xi\frac{g}{1+\left\{\frac{g-F\theta(mn)}{F\theta(mn)}+\frac{g-Fi(mn)}{Fi(mn)}\right\}}\right)\right)\times\left[D_M\left(Y\left(\xi\frac{g}{1+\left\{\frac{g-F\omega(m)}{F\omega(m)}+\frac{g-Fi(mn)}{Fi(mn)}\right\}}\right)\right)\right]^T \tag{15}$$

$$D\left(Tc_{i}(mm)\right)=D_C\left(Y\left(\xi_{g}-\frac{g}{1+\left\{\frac{Tc\theta(mn)}{g-Tc\theta(mn)}+\frac{Tci(mn)}{g-Tci(mn)}\right\}}\right)\right)\times\left[D_M\left(Y\left(\xi_{g}-\frac{g}{1+\left\{\frac{Tc\omega(m)}{g-Tc\omega(m)}+\frac{Tci(mn)}{g-Tci(mn)}\right\}}\right)\right)\right]^T \tag{16}$$

$$D\left(Uc_i(mm)\right)=D_C\left(Y\left(\xi_{\frac{g}{1+\left\{\frac{g-Uc\theta(mn)}{Uc\theta(mn)}+\frac{g-Uci(mn)}{Uci(mn)}\right\}}}\right)\right)\times\left[D_M\left(Y\left(\xi_{\frac{g}{1+\left\{\frac{g-Uc\omega(m)}{Uc\omega(m)}+\frac{g-Uci(mn)}{Uci(mn)}\right\}}}\right)\right)\right]^T \quad (17)$$

$$D\left(Fc_i(mm)\right)=D_C\left(Y\left(\xi_{\frac{g}{1+\left\{\frac{g-Fc\theta(mn)}{Fc\theta(mn)}+\frac{g-Fci(11)}{Fci(11)}\right\}}}\right)\right)\times\left[D_M\left(Y\left(\xi_{\frac{g}{1+\left\{\frac{g-Fc\omega(m)}{Fc\omega(m)}+\frac{g-Fci(mn)}{Fci(mn)}\right\}}}\right)\right)\right]^T \quad (18)$$

STEP 5: Set $\xi_{i(mm)}=\left\langle\left(\xi_{Ti(mm)},\xi_{Tci(mm)}\right),\left(\xi_{Ui(mm)},\xi_{Uci(mm)}\right),\left(\xi_{Fi(mm)},\xi_{Fci(mm)}\right)\right\rangle$ as the integrated LNCVs. According to the Eq. (12) we can get the following LNCM energy for As_i

$$E\left\{\xi_{i(mm)}\right\}=\left\langle\begin{matrix}\left(E\left\{D\left(Ti(mm)\right)\right\},E\left\{D\left(Tci(mm)\right)\right\}\right),\left(E\left\{D\left(Ui(mm)\right)\right\},E\left\{D\left(Uci(mm)\right)\right\}\right),\\ \left(E\left\{D\left(Fi(mm)\right)\right\},E\left\{D\left(Fci(mm)\right)\right\}\right)\end{matrix}\right\rangle \quad (19)$$

STEP 6: Using score function of the LNCM as the Eq. (13), we can obtain all the score values of the alternatives.

STEP 7: Based on the ranking rules, the alternative with the highest score value, which signifies the greatest energy, is designated as the best one.

5. Actual example

This section applies the proposed MAGDM technique to a case study of learning objective achievement evaluation and compare it with the existing LNCVs aggregation operators to demonstrate the validity and reasonability of built model.

5.1 An Example of Learning Objective Achievement Assessment

The production internship for Automation majors at Shaoxing University is conducted in professionally relevant enterprises, jointly supervised by both university advisors and corporate mentors. The expert team for evaluating the achievement of learning objectives consists of three members: an enterprise engineer (E_1), a corporate mentor(E_2), and a university advisor(E_3). The expert team assesses each student based on four aspects/attributes: internship performance (Ms_1), quality of internship outcomes (Ms_2), evaluation of work competence (Ms_3), and communication and reflection skills (Ms_4). During the assessment process, three experts give assessment values using LNCVs information, with the linguistic terms in each LNCV drawn from a prescribed LTS P={ ξ_0: Very low, ξ_1: low, ξ_2: Slightly low, ξ_3: Medium, ξ_4: Slightly high, ξ_5: High, ξ_6: Very high} for g=6.

The MAGDM model based on LNCM energy proposed in the previous section will be applied to this case to evaluate students' achievement of learning objectives in the production internship course. The specific steps are as follows:

Step1: The weight vector for the three experts is specified in LNCV form as $\xi_{\omega(m)}=\left(\xi_{\omega(1)},\xi_{\omega(2)},\xi_{\omega(3)}\right)=\left(\left\langle(\xi_5,\xi_5),(\xi_1,\xi_4),(\xi_1,\xi_4)\right\rangle,\left\langle(\xi_4,\xi_5),(\xi_1,\xi_4),(\xi_2,\xi_5)\right\rangle,\left\langle(\xi_4,\xi_5),(\xi_2,\xi_5),(\xi_2,\xi_5)\right\rangle\right)$. the three experts give the LNCV weight vector of the criteria $\xi_{\theta(mn)}=\left\langle\left(\xi_{T\theta(mn)},\xi_{Tc\theta(mn)}\right),\left(\xi_{U\theta(mn)},\xi_{Uc\theta(mn)}\right),\left(\xi_{F\theta(mn)},\xi_{Fc\theta(mn)}\right)\right\rangle$ for *m*=*1,2, 3; n*=*1,2, 3, 4*. Thus the LNCM of criteria weights is constructed as follows:

$$D\left(\xi_{\theta(mn)}\right)=\begin{array}{c}\\ E_1\\ E_2\\ E_3\end{array}\begin{array}{c}\begin{array}{cccc}\quad Ms_1\quad & \quad Ms_2\quad & \quad Ms_3\quad & \quad Ms_4\quad\end{array}\\ \begin{bmatrix}\left\langle(\xi_5,\xi_4),(\xi_2,\xi_5),(\xi_2,\xi_5)\right\rangle & \left\langle(\xi_4,\xi_4),(\xi_1,\xi_4),(\xi_1,\xi_5)\right\rangle & \left\langle(\xi_4,\xi_4),(\xi_2,\xi_5),(\xi_3,\xi_4)\right\rangle & \left\langle(\xi_3,\xi_5),(\xi_1,\xi_5),(\xi_1,\xi_5)\right\rangle\\ \left\langle(\xi_4,\xi_4),(\xi_1,\xi_5),(\xi_1,\xi_4)\right\rangle & \left\langle(\xi_5,\xi_4),(\xi_2,\xi_5),(\xi_2,\xi_5)\right\rangle & \left\langle(\xi_4,\xi_4),(\xi_1,\xi_4),(\xi_3,\xi_5)\right\rangle & \left\langle(\xi_5,\xi_4),(\xi_1,\xi_4),(\xi_2,\xi_4)\right\rangle\\ \left\langle(\xi_5,\xi_4),(\xi_1,\xi_4),(\xi_1,\xi_5)\right\rangle & \left\langle(\xi_4,\xi_5),(\xi_2,\xi_4),(\xi_1,\xi_5)\right\rangle & \left\langle(\xi_5,\xi_5),(\xi_1,\xi_5),(\xi_2,\xi_4)\right\rangle & \left\langle(\xi_4,\xi_5),(\xi_1,\xi_4),(\xi_2,\xi_5)\right\rangle\end{bmatrix}\end{array}$$

Step 2: The three Experts evaluate each attribute of four students/ alternatives using the LNCV

$LNC_{imn} = \left\langle \left(\xi_{Timn}, \xi_{Tcimn} \right), \left(\left(\xi_{Uimn}, \xi_{Ucimn} \right) \right), \left(\left(\xi_{Fimn}, \xi_{Fcimn} \right) \right) \right\rangle$ and construct four LNCMs $D\left(LNC_{i(mn)}\right)$ as follows for *i, n=1,2, 3, 4, m=1,2, 3.*

$$D\left(LNC_{1(mn)}\right)=\begin{bmatrix} \langle(\xi_4,\xi_4),(\xi_1,\xi_5),(\xi_1,\xi_5)\rangle & \langle(\xi_5,\xi_4),(\xi_1,\xi_4),(\xi_1,\xi_5)\rangle & \langle(\xi_5,\xi_4),(\xi_1,\xi_5),(\xi_2,\xi_4)\rangle & \langle(\xi_4,\xi_5),(\xi_2,\xi_4),(\xi_2,\xi_5)\rangle \\ \langle(\xi_5,\xi_5),(\xi_1,\xi_4),(\xi_2,\xi_4)\rangle & \langle(\xi_4,\xi_4),(\xi_2,\xi_4),(\xi_1,\xi_5)\rangle & \langle(\xi_4,\xi_5),(\xi_2,\xi_4),(\xi_3,\xi_5)\rangle & \langle(\xi_4,\xi_5),(\xi_1,\xi_4),(\xi_2,\xi_5)\rangle \\ \langle(\xi_3,\xi_4),(\xi_2,\xi_4),(\xi_1,\xi_5)\rangle & \langle(\xi_4,\xi_5),(\xi_1,\xi_4),(\xi_1,\xi_6)\rangle & \langle(\xi_5,\xi_5),(\xi_1,\xi_4),(\xi_1,\xi_5)\rangle & \langle(\xi_6,\xi_4),(\xi_2,\xi_5),(\xi_2,\xi_5)\rangle \end{bmatrix}$$

$$D\left(LNC_{2(mn)}\right)=\begin{bmatrix} \langle(\xi_4,\xi_5),(\xi_1,\xi_3),(\xi_2,\xi_3)\rangle & \langle(\xi_5,\xi_5),(\xi_1,\xi_2),(\xi_2,\xi_3)\rangle & \langle(\xi_4,\xi_5),(\xi_1,\xi_1),(\xi_1,\xi_2)\rangle & \langle(\xi_3,\xi_4),(\xi_1,\xi_5),(\xi_2,\xi_5)\rangle \\ \langle(\xi_3,\xi_5),(\xi_1,\xi_4),(\xi_2,\xi_3)\rangle & \langle(\xi_4,\xi_4),(\xi_1,\xi_4),(\xi_1,\xi_4)\rangle & \langle(\xi_4,\xi_5),(\xi_2,\xi_3),(\xi_1,\xi_3)\rangle & \langle(\xi_4,\xi_5),(\xi_1,\xi_3),(\xi_2,\xi_2)\rangle \\ \langle(\xi_5,\xi_5),(\xi_1,\xi_2),(\xi_1,\xi_2)\rangle & \langle(\xi_5,\xi_5),(\xi_1,\xi_2),(\xi_1,\xi_2)\rangle & \langle(\xi_6,\xi_4),(\xi_1,\xi_1),(\xi_2,\xi_2)\rangle & \langle(\xi_4,\xi_4),(\xi_1,\xi_3),(\xi_1,\xi_4)\rangle \end{bmatrix}$$

$$D\left(LNC_{3(mn)}\right)=\begin{bmatrix} \langle(\xi_5,\xi_5),(\xi_2,\xi_4),(\xi_1,\xi_5)\rangle & \langle(\xi_4,\xi_4),(\xi_1,\xi_4),(\xi_1,\xi_5)\rangle & \langle(\xi_4,\xi_4),(\xi_1,\xi_4),(\xi_1,\xi_4)\rangle & \langle(\xi_4,\xi_5),(\xi_2,\xi_5),(\xi_2,\xi_4)\rangle \\ \langle(\xi_4,\xi_5),(\xi_1,\xi_4),(\xi_2,\xi_5)\rangle & \langle(\xi_3,\xi_5),(\xi_1,\xi_5),(\xi_2,\xi_4)\rangle & \langle(\xi_3,\xi_4),(\xi_1,\xi_5),(\xi_1,\xi_4)\rangle & \langle(\xi_4,\xi_5),(\xi_1,\xi_5),(\xi_2,\xi_5)\rangle \\ \langle(\xi_4,\xi_4),(\xi_2,\xi_4),(\xi_1,\xi_4)\rangle & \langle(\xi_3,\xi_5),(\xi_2,\xi_4),(\xi_2,\xi_6)\rangle & \langle(\xi_3,\xi_5),(\xi_1,\xi_5),(\xi_2,\xi_4)\rangle & \langle(\xi_5,\xi_4),(\xi_1,\xi_4),(\xi_1,\xi_5)\rangle \end{bmatrix}$$

$$D\left(LNC_{4(mn)}\right)=\begin{bmatrix} \langle(\xi_4,\xi_5),(\xi_1,\xi_6),(\xi_2,\xi_5)\rangle & \langle(\xi_5,\xi_5),(\xi_1,\xi_4),(\xi_2,\xi_4)\rangle & \langle(\xi_4,\xi_5),(\xi_1,\xi_4),(\xi_1,\xi_4)\rangle & \langle(\xi_3,\xi_4),(\xi_1,\xi_5),(\xi_2,\xi_5)\rangle \\ \langle(\xi_3,\xi_5),(\xi_1,\xi_5),(\xi_2,\xi_4)\rangle & \langle(\xi_4,\xi_4),(\xi_1,\xi_5),(\xi_1,\xi_6)\rangle & \langle(\xi_4,\xi_5),(\xi_2,\xi_4),(\xi_1,\xi_5)\rangle & \langle(\xi_4,\xi_5),(\xi_1,\xi_4),(\xi_2,\xi_5)\rangle \\ \langle(\xi_5,\xi_5),(\xi_1,\xi_5),(\xi_1,\xi_5)\rangle & \langle(\xi_5,\xi_5),(\xi_1,\xi_4),(\xi_1,\xi_5)\rangle & \langle(\xi_6,\xi_4),(\xi_1,\xi_5),(\xi_2,\xi_4)\rangle & \langle(\xi_4,\xi_4),(\xi_1,\xi_5),(\xi_1,\xi_4)\rangle \end{bmatrix}$$

Step 3: Considering the influence of the experts' differing weights on the four LNCMs, the experts weighted LNCMs can be derived according to Eq. (12) as follows:

$$D_M\left(\xi_{\omega(m)}\otimes LNC_{1(mn)}\right)=\begin{bmatrix} \langle(\xi_{5.2500},\xi_{5.2500}),(\xi_{0.5455},\xi_{3.5294}),(\xi_{0.5455},\xi_{3.5294})\rangle & \langle(\xi_{5.4545},\xi_{5.2500}),(\xi_{0.5455},\xi_{3.0000}),(\xi_{0.5455},\xi_{3.5294})\rangle & \langle(\xi_{5.4545},\xi_{5.2500}),(\xi_{0.5455},\xi_{3.0000}),(\xi_{0.7500},\xi_{3.0000})\rangle & \langle(\xi_{5.2500},\xi_{5.4545}),(\xi_{0.7500},\xi_{3.0000}),(\xi_{0.7500},\xi_{3.5294})\rangle \\ \langle(\xi_{5.2500},\xi_{5.4545}),(\xi_{0.5455},\xi_{3.0000}),(\xi_{1.2000},\xi_{3.5294})\rangle & \langle(\xi_{4.8000},\xi_{5.2500}),(\xi_{0.7500},\xi_{3.0000}),(\xi_{0.7500},\xi_{4.2857})\rangle & \langle(\xi_{4.8000},\xi_{5.4545}),(\xi_{0.7500},\xi_{3.0000}),(\xi_{1.5000},\xi_{4.2857})\rangle & \langle(\xi_{4.8000},\xi_{5.4545}),(\xi_{0.5455},\xi_{3.0000}),(\xi_{1.2000},\xi_{4.2857})\rangle \\ \langle(\xi_{4.5000},\xi_{5.2500}),(\xi_{1.2000},\xi_{3.5294}),(\xi_{0.7500},\xi_{4.2857})\rangle & \langle(\xi_{4.8000},\xi_{5.4545}),(\xi_{0.7500},\xi_{3.5294}),(\xi_{0.7500},\xi_{5.0000})\rangle & \langle(\xi_{5.2500},\xi_{5.4545}),(\xi_{0.7500},\xi_{3.5294}),(\xi_{0.7500},\xi_{4.2857})\rangle & \langle(\xi_{6.0000},\xi_{5.2500}),(\xi_{1.2000},\xi_{4.2857}),(\xi_{1.2000},\xi_{4.2857})\rangle \end{bmatrix}$$

$$D_M\left(\xi_{\omega(m)}\otimes LNC_{2(mn)}\right)=\begin{bmatrix} \langle(\xi_{5.2500},\xi_{5.4545}),(\xi_{0.5455},\xi_{2.4000}),(\xi_{0.7500},\xi_{2.4000})\rangle & \langle(\xi_{5.4545},\xi_{5.4545}),(\xi_{0.5455},\xi_{1.7143}),(\xi_{0.7500},\xi_{2.4000})\rangle & \langle(\xi_{5.2500},\xi_{5.4545}),(\xi_{0.5455},\xi_{0.9231}),(\xi_{0.5455},\xi_{1.7143})\rangle & \langle(\xi_{5.1429},\xi_{5.2500}),(\xi_{0.5455},\xi_{3.5294}),(\xi_{0.7500},\xi_{3.5294})\rangle \\ \langle(\xi_{4.5000},\xi_{5.4545}),(\xi_{0.5455},\xi_{3.0000}),(\xi_{1.2000},\xi_{2.7273})\rangle & \langle(\xi_{4.8000},\xi_{5.2500}),(\xi_{0.5455},\xi_{3.0000}),(\xi_{0.7500},\xi_{3.5294})\rangle & \langle(\xi_{4.8000},\xi_{5.4545}),(\xi_{0.7500},\xi_{2.4000}),(\xi_{0.7500},\xi_{2.7273})\rangle & \langle(\xi_{4.8000},\xi_{5.4545}),(\xi_{0.5455},\xi_{2.4000}),(\xi_{1.2000},\xi_{1.8750})\rangle \\ \langle(\xi_{5.2500},\xi_{5.4545}),(\xi_{0.7500},\xi_{1.8750}),(\xi_{0.7500},\xi_{1.8750})\rangle & \langle(\xi_{5.2500},\xi_{5.4545}),(\xi_{0.7500},\xi_{2.7273}),(\xi_{0.7500},\xi_{1.8750})\rangle & \langle(\xi_{6.0000},\xi_{5.2500}),(\xi_{0.7500},\xi_{0.9677}),(\xi_{1.2000},\xi_{1.8750})\rangle & \langle(\xi_{4.8000},\xi_{5.2500}),(\xi_{0.7500},\xi_{2.7273}),(\xi_{0.7500},\xi_{3.5294})\rangle \end{bmatrix}$$

$$D_M\left(\xi_{\omega(m)}\otimes LNC_{3(mn)}\right)=\begin{bmatrix} \langle(\xi_{5.4545},\xi_{5.4545}),(\xi_{0.7500},\xi_{3.0000}),(\xi_{0.5455},\xi_{3.5294})\rangle & \langle(\xi_{5.2500},\xi_{5.2500}),(\xi_{0.5455},\xi_{3.0000}),(\xi_{0.5455},\xi_{3.5294})\rangle & \langle(\xi_{5.2500},\xi_{5.2500}),(\xi_{0.5455},\xi_{3.0000}),(\xi_{0.5455},\xi_{3.0000})\rangle & \langle(\xi_{5.2500},\xi_{5.4545}),(\xi_{0.7500},\xi_{3.5294}),(\xi_{0.7500},\xi_{3.0000})\rangle \\ \langle(\xi_{4.8000},\xi_{5.4545}),(\xi_{0.5455},\xi_{3.0000}),(\xi_{1.2000},\xi_{4.2857})\rangle & \langle(\xi_{4.5000},\xi_{5.4545}),(\xi_{0.5455},\xi_{3.5294}),(\xi_{1.2000},\xi_{3.5294})\rangle & \langle(\xi_{4.5000},\xi_{5.2500}),(\xi_{0.5455},\xi_{3.5294}),(\xi_{0.7500},\xi_{3.5294})\rangle & \langle(\xi_{4.8000},\xi_{5.4545}),(\xi_{0.5455},\xi_{3.5294}),(\xi_{1.2000},\xi_{4.2857})\rangle \\ \langle(\xi_{4.8000},\xi_{5.2500}),(\xi_{1.2000},\xi_{3.5294}),(\xi_{0.7500},\xi_{3.5294})\rangle & \langle(\xi_{4.5000},\xi_{5.4545}),(\xi_{1.2000},\xi_{3.5294}),(\xi_{1.2000},\xi_{5.0000})\rangle & \langle(\xi_{4.5000},\xi_{5.4545}),(\xi_{0.7500},\xi_{4.2857}),(\xi_{1.2000},\xi_{3.5294})\rangle & \langle(\xi_{5.2500},\xi_{5.2500}),(\xi_{0.7500},\xi_{3.5294}),(\xi_{0.7500},\xi_{4.2857})\rangle \end{bmatrix}$$

$$D_M\left(\xi_{\omega(m)}\otimes LNC_{4(mn)}\right)=\begin{bmatrix} \langle(\xi_{5.2500},\xi_{5.4545}),(\xi_{0.5455},\xi_{4.0000}),(\xi_{0.7500},\xi_{3.5294})\rangle & \langle(\xi_{5.4545},\xi_{5.4545}),(\xi_{0.5455},\xi_{3.0000}),(\xi_{0.7500},\xi_{3.0000})\rangle & \langle(\xi_{5.2500},\xi_{5.4545}),(\xi_{0.5455},\xi_{3.0000}),(\xi_{0.5455},\xi_{3.0000})\rangle & \langle(\xi_{5.1429},\xi_{5.2500}),(\xi_{0.5455},\xi_{3.5294}),(\xi_{0.7500},\xi_{3.5294})\rangle \\ \langle(\xi_{4.5000},\xi_{5.4545}),(\xi_{0.5455},\xi_{3.5294}),(\xi_{1.2000},\xi_{3.5294})\rangle & \langle(\xi_{4.8000},\xi_{5.2500}),(\xi_{0.5455},\xi_{3.5294}),(\xi_{0.7500},\xi_{5.0000})\rangle & \langle(\xi_{4.8000},\xi_{5.4545}),(\xi_{0.7500},\xi_{3.0000}),(\xi_{0.7500},\xi_{4.2857})\rangle & \langle(\xi_{4.8000},\xi_{5.4545}),(\xi_{0.5455},\xi_{3.0000}),(\xi_{1.2000},\xi_{4.2857})\rangle \\ \langle(\xi_{5.2500},\xi_{5.4545}),(\xi_{0.7500},\xi_{4.2857}),(\xi_{0.7500},\xi_{4.2857})\rangle & \langle(\xi_{5.2500},\xi_{5.4545}),(\xi_{0.7500},\xi_{3.5294}),(\xi_{0.7500},\xi_{4.2857})\rangle & \langle(\xi_{6.0000},\xi_{5.2500}),(\xi_{0.7500},\xi_{4.2857}),(\xi_{1.2000},\xi_{3.5294})\rangle & \langle(\xi_{4.8000},\xi_{5.2500}),(\xi_{0.7500},\xi_{4.2857}),(\xi_{0.7500},\xi_{3.5294})\rangle \end{bmatrix}$$

Similarly, by integrating the attribute weights into the LNCM according to Eq. (13), we obtain the following attribute-weighted LNCMs:

$$D_C\left(\xi_{\theta(mn)}\otimes LNC_{1(mn)}\right)=\begin{bmatrix}\langle(\xi_{5.1429},\xi_{5.2500}),(\xi_{0.7500},\xi_{3.5294}),(\xi_{1.2000},\xi_{4.2857})\rangle & \langle(\xi_{5.2500},\xi_{4.8000}),(\xi_{0.5455},\xi_{3.0000}),(\xi_{0.7500},\xi_{4.2857})\rangle & \langle(\xi_{4.8000},\xi_{4.8000}),(\xi_{0.7500},\xi_{4.2857}),(\xi_{1.5000},\xi_{3.0000})\rangle & \langle(\xi_{4.5000},\xi_{5.4545}),(\xi_{0.7500},\xi_{3.5294}),(\xi_{0.7500},\xi_{4.2857})\rangle \\ \langle(\xi_{4.8000},\xi_{5.2500}),(\xi_{0.7500},\xi_{3.5294}),(\xi_{0.5455},\xi_{3.5294})\rangle & \langle(\xi_{5.2500},\xi_{5.2500}),(\xi_{1.2000},\xi_{3.5294}),(\xi_{1.2000},\xi_{3.5294})\rangle & \langle(\xi_{4.5000},\xi_{4.8000}),(\xi_{0.7500},\xi_{3.5294}),(\xi_{1.5000},\xi_{3.5294})\rangle & \langle(\xi_{5.2500},\xi_{4.8000}),(\xi_{0.5455},\xi_{3.0000}),(\xi_{1.2000},\xi_{3.0000})\rangle \\ \langle(\xi_{5.4545},\xi_{4.8000}),(\xi_{0.5455},\xi_{3.5294}),(\xi_{0.5455},\xi_{3.5294})\rangle & \langle(\xi_{4.8000},\xi_{5.4545}),(\xi_{0.7500},\xi_{3.5294}),(\xi_{0.7500},\xi_{4.2857})\rangle & \langle(\xi_{5.4545},\xi_{5.2500}),(\xi_{0.7500},\xi_{4.2857}),(\xi_{0.7500},\xi_{3.5294})\rangle & \langle(\xi_{5.2500},\xi_{5.4545}),(\xi_{0.7500},\xi_{3.5294}),(\xi_{0.7500},\xi_{4.2857})\rangle\end{bmatrix}$$

$$D_C\left(\xi_{\theta(mn)}\otimes LNC_{2(mn)}\right)=\begin{bmatrix}\langle(\xi_{5.2500},\xi_{5.2500}),(\xi_{0.7500},\xi_{2.7273}),(\xi_{1.2000},\xi_{2.7273})\rangle & \langle(\xi_{5.2500},\xi_{5.2500}),(\xi_{0.5455},\xi_{1.7143}),(\xi_{0.7500},\xi_{2.7273})\rangle & \langle(\xi_{4.8000},\xi_{5.2500}),(\xi_{0.7500},\xi_{0.9677}),(\xi_{0.8571},\xi_{1.7143})\rangle & \langle(\xi_{4.0000},\xi_{5.2500}),(\xi_{0.5455},\xi_{4.2857}),(\xi_{0.7500},\xi_{4.2857})\rangle \\ \langle(\xi_{4.5000},\xi_{5.2500}),(\xi_{0.5455},\xi_{3.5294}),(\xi_{0.7500},\xi_{2.4000})\rangle & \langle(\xi_{5.2500},\xi_{4.8000}),(\xi_{0.7500},\xi_{3.5294}),(\xi_{0.7500},\xi_{3.5294})\rangle & \langle(\xi_{4.8000},\xi_{5.2500}),(\xi_{0.7500},\xi_{2.4000}),(\xi_{0.8571},\xi_{2.7273})\rangle & \langle(\xi_{5.2500},\xi_{5.2500}),(\xi_{0.5455},\xi_{2.4000}),(\xi_{1.2000},\xi_{1.7143})\rangle \\ \langle(\xi_{5.4545},\xi_{5.2500}),(\xi_{0.5455},\xi_{1.7143}),(\xi_{0.5455},\xi_{1.8750})\rangle & \langle(\xi_{5.2500},\xi_{5.4545}),(\xi_{0.7500},\xi_{2.4000}),(\xi_{0.5455},\xi_{1.8750})\rangle & \langle(\xi_{6.0000},\xi_{5.2500}),(\xi_{0.5455},\xi_{0.9677}),(\xi_{1.2000},\xi_{1.7143})\rangle & \langle(\xi_{4.8000},\xi_{5.2500}),(\xi_{0.5455},\xi_{2.4000}),(\xi_{0.7500},\xi_{3.5294})\rangle\end{bmatrix}$$

$$D_C\left(\xi_{\theta(mn)}\otimes LNC_{3(mn)}\right)=\begin{bmatrix}\langle(\xi_{5.4545},\xi_{5.2500}),(\xi_{1.2000},\xi_{3.5294}),(\xi_{0.7500},\xi_{4.2857})\rangle & \langle(\xi_{4.8000},\xi_{4.8000}),(\xi_{0.5455},\xi_{3.0000}),(\xi_{0.5455},\xi_{4.2857})\rangle & \langle(\xi_{4.8000},\xi_{4.8000}),(\xi_{0.7500},\xi_{3.5294}),(\xi_{0.8571},\xi_{3.0000})\rangle & \langle(\xi_{4.5000},\xi_{5.4545}),(\xi_{0.7500},\xi_{4.2857}),(\xi_{0.7500},\xi_{3.5294})\rangle \\ \langle(\xi_{4.8000},\xi_{5.2500}),(\xi_{0.5455},\xi_{3.5294}),(\xi_{0.7500},\xi_{3.5294})\rangle & \langle(\xi_{5.1429},\xi_{5.2500}),(\xi_{0.7500},\xi_{4.2857}),(\xi_{1.2000},\xi_{3.5294})\rangle & \langle(\xi_{4.5000},\xi_{4.8000}),(\xi_{0.5455},\xi_{3.5294}),(\xi_{0.8571},\xi_{3.5294})\rangle & \langle(\xi_{5.2500},\xi_{5.2500}),(\xi_{0.5455},\xi_{3.5294}),(\xi_{1.2000},\xi_{3.5294})\rangle \\ \langle(\xi_{5.2500},\xi_{4.8000}),(\xi_{0.7500},\xi_{3.0000}),(\xi_{0.5455},\xi_{3.5294})\rangle & \langle(\xi_{4.5000},\xi_{5.4545}),(\xi_{1.2000},\xi_{3.0000}),(\xi_{0.7500},\xi_{5.0000})\rangle & \langle(\xi_{5.1429},\xi_{5.4545}),(\xi_{0.5455},\xi_{4.2857}),(\xi_{1.2000},\xi_{3.0000})\rangle & \langle(\xi_{5.2500},\xi_{5.2500}),(\xi_{0.5455},\xi_{3.0000}),(\xi_{0.7500},\xi_{4.2857})\rangle\end{bmatrix}$$

$$D_C\left(\xi_{\theta(mn)}\otimes LNC_{4(mn)}\right)=\begin{bmatrix}\langle(\xi_{5.2500},\xi_{5.2500}),(\xi_{0.7500},\xi_{5.0000}),(\xi_{1.2000},\xi_{4.2857})\rangle & \langle(\xi_{5.2500},\xi_{5.2500}),(\xi_{0.5455},\xi_{3.0000}),(\xi_{0.7500},\xi_{3.5294})\rangle & \langle(\xi_{4.8000},\xi_{5.2500}),(\xi_{0.7500},\xi_{3.5294}),(\xi_{0.8571},\xi_{3.0000})\rangle & \langle(\xi_{4.0000},\xi_{5.2500}),(\xi_{0.5455},\xi_{4.2857}),(\xi_{0.7500},\xi_{4.2857})\rangle \\ \langle(\xi_{4.5000},\xi_{5.2500}),(\xi_{0.5455},\xi_{4.2857}),(\xi_{0.7500},\xi_{3.0000})\rangle & \langle(\xi_{5.2500},\xi_{4.8000}),(\xi_{0.7500},\xi_{4.2857}),(\xi_{0.7500},\xi_{5.0000})\rangle & \langle(\xi_{4.8000},\xi_{5.2500}),(\xi_{0.7500},\xi_{3.0000}),(\xi_{0.8571},\xi_{4.2857})\rangle & \langle(\xi_{5.2500},\xi_{5.2500}),(\xi_{0.5455},\xi_{3.0000}),(\xi_{1.2000},\xi_{3.5294})\rangle \\ \langle(\xi_{5.4545},\xi_{5.2500}),(\xi_{0.5455},\xi_{3.5294}),(\xi_{0.5455},\xi_{4.2857})\rangle & \langle(\xi_{5.2500},\xi_{5.4545}),(\xi_{0.7500},\xi_{3.0000}),(\xi_{0.5455},\xi_{4.2857})\rangle & \langle(\xi_{6.0000},\xi_{5.2500}),(\xi_{0.5455},\xi_{4.2857}),(\xi_{1.2000},\xi_{3.0000})\rangle & \langle(\xi_{4.8000},\xi_{5.2500}),(\xi_{0.5455},\xi_{3.5294}),(\xi_{0.7500},\xi_{3.5294})\rangle\end{bmatrix}$$

Step 4: According to Eq.(14)- Eq.(19),The integrated true, indeterminate, false and true credibility, indeterminate credibility, false credibility squire matrices $D(Ti(mm))$, $D(Tci(mm))$, $D(Ui(mm))$, $D(Uci(mm))$, $D(Fi(mm))$, $D(Fci(mm))$ (*i=1,2, 3, 4, m=1,2, 3*) are calculated as follows:

$$D(T1(mm))=\begin{bmatrix}108.4598 & 99.5625 & 103.3875\\ 109.9427 & 101.0025 & 105.5250\\ 114.4334 & 105.0218 & 110.8192\end{bmatrix}\quad D(Tc1(mm))=\begin{bmatrix}105.3516 & 107.3148 & 106.1993\\ 108.9611 & 111.1084 & 109.9427\\ 111.1084 & 113.2054 & 112.2656\end{bmatrix}$$

$$D(U1(mm))=\begin{bmatrix}1.6783 & 1.7899 & 2.7716\\ 1.7704 & 2.0576 & 2.7717\\ 1.6783 & 1.7899 & 2.7716\end{bmatrix}\quad D(Uc1(mm))=\begin{bmatrix}49.8401 & 45.3024 & 55.9660\\ 42.6331 & 39.1764 & 48.3586\\ 42.6331 & 39.1764 & 48.7590\end{bmatrix}$$

$$D(F1(mm))=\begin{bmatrix}2.3942 & 4.4591 & 2.9966\\ 3.2182 & 5.9025 & 4.0650\\ 2.0576 & 3.6287 & 2.8207\end{bmatrix}\quad D(Fc1(mm))=\begin{bmatrix}54.3778 & 64.7175 & 71.0200\\ 51.0279 & 62.4486 & 67.7788\\ 58.4871 & 70.0476 & 76.8604\end{bmatrix}$$

$$D(T2(mm))=\begin{bmatrix}101.9702 & 91.0650 & 103.1250\\ 104.4614 & 93.6900 & 105.1875\\ 113.4582 & 101.5853 & 115.2386\end{bmatrix}\quad D(Tc2(mm))=\begin{bmatrix}113.4709 & 113.4709 & 112.3973\\ 111.0164 & 111.1084 & 109.9427\\ 114.5863 & 114.5445 & 113.5127\end{bmatrix}$$

$$D\left(U2(mm)\right)=\begin{bmatrix}1.4134 & 1.5668 & 1.9432\\ 1.4134 & 1.5668 & 1.9432\\ 1.3018 & 1.4134 & 1.7899\end{bmatrix} \quad D\left(Uc2(mm)\right)=\begin{bmatrix}25.5036 & 25.9330 & 22.4139\\ 25.2070 & 32.6964 & 25.1114\\ 17.5925 & 20.4254 & 17.2418\end{bmatrix}$$

$$D\left(F2(mm)\right)=\begin{bmatrix}2.4925 & 3.5453 & 3.0535\\ 2.4925 & 3.5453 & 3.0535\\ 2.0353 & 2.8637 & 2.8207\end{bmatrix} \quad D\left(Fc2(mm)\right)=\begin{bmatrix}31.1558 & 29.7750 & 28.5676\\ 24.9564 & 29.6547 & 22.2818\\ 24.3955 & 23.0243 & 22.7022\end{bmatrix}$$

$$D\left(T3(mm)\right)=\begin{bmatrix}103.7766 & 90.9816 & 93.0066\\ 104.3693 & 91.6331 & 93.9956\\ 106.8239 & 93.7931 & 96.1556\end{bmatrix} D\left(Tc3(mm)\right)=\begin{bmatrix}108.7877 & 109.7693 & 108.5618\\ 110.0348 & 111.1084 & 109.9427\\ 112.0899 & 113.2054 & 112.2656\end{bmatrix}$$

$$D\left(U3(mm)\right)=\begin{bmatrix}2.1692 & 1.7704 & 3.2196\\ 1.5249 & 1.3018 & 2.3728\\ 1.9238 & 1.6589 & 3.1583\end{bmatrix} \quad D\left(Uc3(mm)\right)=\begin{bmatrix}45.3023 & 48.7590 & 53.2968\\ 46.4902 & 50.6275 & 55.1652\\ 41.4453 & 45.3023 & 50.1318\end{bmatrix}$$

$$D\left(F3(mm)\right)=\begin{bmatrix}1.7367 & 3.0974 & 2.8081\\ 2.4313 & 4.4228 & 3.9310\\ 1.9238 & 3.3546 & 3.3116\end{bmatrix} D\left(Fc3(mm)\right)=\begin{bmatrix}49.8401 & 59.2073 & 62.2686\\ 46.0897 & 55.1652 & 57.6863\\ 51.9608 & 61.7284 & 66.4121\end{bmatrix}$$

$$D\left(T4(mm)\right)=\begin{bmatrix}101.9702 & 91.0650 & 103.125\\ 104.4614 & 93.6900 & 105.1875\\ 113.4582 & 101.5853 & 115.2386\end{bmatrix} D\left(Tc4(mm)\right)=\begin{bmatrix}113.4709 & 113.4709 & 111.3236\\ 111.0164 & 111.1084 & 108.9611\\ 114.5863 & 114.5445 & 112.3973\end{bmatrix}$$

$$D\left(U4(mm)\right)=\begin{bmatrix}1.4134 & 1.5668 & 1.9433\\ 1.4134 & 1.5668 & 1.9433\\ 1.3018 & 1.4134 & 1.7899\end{bmatrix} \quad D\left(Uc4(mm)\right)=\begin{bmatrix}54.7141 & 51.6805 & 65.5099\\ 49.5881 & 48.2519 & 59.2074\\ 48.4314 & 46.4902 & 59.2073\end{bmatrix}$$

$$D\left(F4(mm)\right)=\begin{bmatrix}2.4925 & 3.5433 & 3.0535\\ 2.4925 & 3.5433 & 3.0535\\ 2.0353 & 2.8637 & 2.8207\end{bmatrix} \quad D\left(Fc4(mm)\right)=\begin{bmatrix}49.8401 & 63.9973 & 59.2073\\ 50.9020 & 69.0814 & 61.8682\\ 49.4397 & 64.5375 & 59.7793\end{bmatrix}$$

Step 5: Using Eq. (8), we can get the following LNCM energy for each student.

$$E\left\{\xi_{1(mm)}\right\}=\langle 437.8264,437.8264,8.5770,190.5364,13.9813,239.4621\rangle$$

$$E\left\{\xi_{2(mm)}\right\}=\langle 413.2267,449.2101,6.3357,92.9151,11.3305,102.4887\rangle$$

$$E\left\{\xi_{3(mm)}\right\}=\langle 388.3971,442.4032,10.1633,193.0228,12.2057,226.2351\rangle$$

$$E\left\{\xi_{4(mm)}\right\}=\langle 413.2267,449.2101,6.3357,213.1467,11.3305,234.0343\rangle$$

Step 6: Using the Eq. (9), the LNVM energy score values of each student is obtained as follows:

$$S\left(E\left\{D(\xi_{1(mm)})\right\}\right)=0.6476, S\left(E\left\{D(\xi_{2(mm)})\right\}\right)=0.8019, S\left(E\left\{D(\xi_{3(mm)})\right\}\right)=0.6529, S\left(E\left\{D(\xi_{4(mm)})\right\}\right)=0.6498$$

Step 7: According to the score values, the ranking of the four students based on their learning objects attainment is as follows: $A_{S2} \succ A_{S3} \succ A_{S4} \succ A_{S1}$

5.2 comparison of the decision results between LNM and LNCM information environment

While existing research [20] has constructed MAGDM model applicable to the LNM environment, the model struggles to effectively address decision-making problems within the LNCM environment. This paper developed the MAGDM model based on the LNVM. When the credibility values within the model are ignored, the complex problem in the LNCM environment can be simplified into a classic LNM decision problem.

For ease of comparison, Table 1 lists the assessment results of this case under various environments.

Table 1. assessment results of different information format

MAGDM model	Information format	Energy score value	Ranking	Best one

Proposed model	LNMs	$S\left(E\left\{D(\xi_{1(mm)})\right\}\right)=0.9471$ $S\left(E\left\{D(\xi_{2(mm)})\right\}\right)=0.9590$ $S\left(E\left\{D(\xi_{3(mm)})\right\}\right)=0.9455$ $S\left(E\left\{D(\xi_{4(mm)})\right\}\right)=0.9590$	$A_{S2}=A_{S4}\succ A_{S1}\succ A_{S3}$	A_{S2}, A_{S4}
Existing model [20]	LNMs	$S\left(E\left\{D(\xi_{1(mm)})\right\}\right)=0.4161$ $S\left(E\left\{D(\xi_{2(mm)})\right\}\right)=0.4179$ $S\left(E\left\{D(\xi_{3(mm)})\right\}\right)=0.3702$ $S\left(E\left\{D(\xi_{4(mm)})\right\}\right)=0.4179$	$A_{S2}=A_{S4}\succ A_{S1}\succ A_{S3}$	A_{S2}, A_{S4}
Proposed model	LNCMs	$S\left(E\left\{D(\xi_{1(mm)})\right\}\right)=0.6476$ $S\left(E\left\{D(\xi_{2(mm)})\right\}\right)=0.8019$ $S\left(E\left\{D(\xi_{3(mm)})\right\}\right)=0.6529$ $S\left(E\left\{D(\xi_{4(mm)})\right\}\right)=0.6498$	$A_{S2}\succ A_{S3}\succ A_{S4}\succ A_{S1}$	A_{S2}

As shown in Table 1, when the LNCMs information in this case is simplified to LNMs format and decisions are made using both the proposed method and existing method [20], the rankings from the two assessment are identical. However, the energy score values of the former are significantly higher than those of the latter. This is due to the utilization of distinct aggregation operators. Since the LNMs for alternatives 2 and 4 are identical, their energy scores values are equal in two method. In contrast to previous results, the ranking produced by the proposed LNCM-based model has undergone a significant shift. Although the assessment LNCMs for alternatives 2 and 4 share identical truth, falsity, indeterminate and truth credibility values, differing only in the false credibility and indeterminate credibility, their energy score values differ significantly. This is directly attributable to the energy score function (Formula 9), where the contribution of the credibility degrees for truth, falsity, and indeterminacy are set equal to their own respective value. A comprehensive comparison shows that the energy score values produced by the proposed model have a wider distribution range and more distinct differentiation. Compared to the existing model [20], the proposed model is more general and creditable in uncertain or inconsistent information environments.

6. Conclusion

This study presents a MAGDM model under LNCM environment, along with an application for assessment of learning objectives attainment in production internship. The primary contribution of this work is as follows:

LNCM energy and its energy score function are introduced for the first time. Following the introduction of the LNCM energy framework, the study provides the detailed steps of the MAGDM model implemented with this novel approach.

The assessment method of learning objectives attainment is innovative. LNCM energy transforms students' internship performance into a linguistic neutrosophic matrix and achieves a quantitative evaluation of students' comprehensive abilities by calculating the matrix energy score value. This assessment approach preserves the completeness and fuzziness of evaluation information, making it more aligned with the practical characteristics of production internships.

This study has currently focused on evaluating students' overall competency during production internships. Future work can productively extend the proposed MAGDM method to assess the attainment level of each specific learning objective. By systematically comparing attainment distributions across student cohorts, it will be feasible to identify potential weaknesses in the teaching and learning process, thereby providing actionable insights for curriculum and instructional refinement.

In the future, the proposed MAGDM model serves as a robust tool for addressing complex decision-making problems and holds potential for application in diverse fields such as environmental engineering and sustainable development, medical diagnosis and health management, and renewable energy development and site selection decisions.

Funding: This research was funded by Zhejiang Province Undergraduate Teaching Reform Project (2025), grant number JGCG2025283.
Conflicts of Interest: The authors declare no conflict of interest.

References

1. Zadeh LA. The concept of a linguistic variable and its application to approximate reasoning part I. *Information Sciences* **1975**,8,199–249.
2. Chen, Z. C., Liu, P. H., & Pei, Z. An approach to multiple attribute group decision making based on linguistic intuitionistic fuzzy numbers. *International Journal of Computational Intelligence Systems* **2015**, 8(4), 747–760.
3. Fang, Z., Ye, J. Multiple attribute group decision-making method based on linguistic neutrosophic numbers. *Symmetry* **2017**, 9(7), 111.
4. Jun Ye1 and Rui Yong, MAGDM technique based on linguistic neutrosophic credibility value trigonometric aggregation operators and its application in landslide control scheme selection. *International Journal of Knowledge-Based and Intelligent Engineering Systems.* **2025**, 29(3), 306–321.
5. Liu P, Liu J and Merigó JM. Partitioned heronian means based on linguistic intuitionistic fuzzy numbers for dealing with multi-attribute group decision making. *Applied Soft Computing* **2018**,62, 395–422.
6. Liu P and Qin X. Power average operators of linguistic intuitionistic fuzzy numbers and their application to multiple-attribute decision making. *Journal of Intelligent & Fuzzy Systems* **2017**,32, 1029–1043.
7. Peng H, Wang J and Cheng P. A linguistic intuitionistic multi-criteria decision-making method based on the frank heronian mean operator and its application in evaluating coal mine safety. *International Journal of Machine Learning & Cybernetics* **2018**; 9,1053–1068.
8. Kumar K and Chen SM. Group decision making based on linguistic intuitionistic fuzzy yager weighted arithmetic aggregation operator of linguistic intuitionistic fuzzy numbers. *Information Sciences* **2023**,647,119228.
9. Kumar K and Chen SM. Multiple attribute group decision making based on advanced linguistic intuitionistic fuzzy weighted averaging aggregation operator of linguistic intuitionistic fuzzy numbers. *Information Sciences* **2022**,587,813–824.
10. Shi, L., & Ye, J. Cosine measures of linguistic neutrosophic numbers and their application in multiple attribute group decision-making. *Information* **2017**, 8(4), 117.
11. Shi, L., & Ye, J. Multiple attribute group decision-making method using correlation coefficients between linguistic neutrosophic numbers. *Journal of Intelligent & Fuzzy Systems* **2018**, 35(1), 917–925.
12. Liu P and You X. Some linguistic neutrosophic hamy mean operators and their application to multi-attribute group decision making. *PloS one* **2018**, 13(3),1-26.
13. Liang RX, Jiang ZB and Wang JQ. A linguistic neutrosophic multi-criteria group decision-making method to university human resource management. *Symmetry* **2018**; 10(10): 1-18.

14. Luo S, Liang W and Zhao G. Linguistic neutrosophic power muirhead mean operators for safety evaluation of mines. *Plos One* ***2019***,14(10),1-23.
15. Fan, C., Ye, J., Hu, K., & Fan, E. Bonferroni mean operators of linguistic neutrosophic numbers and their multiple attribute group decision-making methods. *Information* **2017**,8(3),1-11.
16. Fang, Z., Ye, J. Multiple attribute group decision-making method based on linguistic neutrosophic numbers. *Symmetry* **2017**, 9(7), 1-11.
17. Bravo, D., Cubría, F., & Rada, J. Energy of matrices. *Applied Mathematics and Computation* **2017**, 312, 149–157.
18. Donbosco, J. S. M., & Ganesan, D. The Energy of rough neutrosophic matrix and its application to MCDM problem for selecting the best building construction site. *Decision Making: Applications in Management and Engineering* **2022**, 5(2), 30-45.
19. Li, W. & Ye, J. MAGDM model using an intuitionistic fuzzy matrix energy method and its application in the selection issue of hospital locations. *Axioms* **2023**, 12(8), 1-15.
20. Yong, R., Du, S., & Ye, J. Linguistic neutrosophic matrix energy and its application in multiple criteria group decision-making. *Journal of Management Analytics* **2023**, 10(3), 477-492

Received: Feb. 12, 2026. Accepted: Aug. 13, 2026.

Neutrosophic Sets and Systems, Vol. 102, 2027
University of New Mexico

A Customer-Driven Supplier Evaluation Model Under Indeterminacy for Customizated Production

Çağrı KURAM[1] and Özge Nalan BİLİŞİK[2,*]

[1] Independent researcher, 41700, Kocaeli; cagri.kuram@gmail.com
[2] Yıldız Technical University, Industrial Engineering Department, 34349, İstanbul; oznalan@yildiz.edu.tr
* **Corresponding author:** oznalan@yildiz.edu.tr

Abstract: Due to the developing market conditions, changing customer expectations, and shortening of product life cycles, it is inevitable for companies to produce high-quality products that will meet customer requirements. Making the right decisions on issues such as working with right supplier, planning production correctly, ensuring effective stock management, and managing the cash flow are some of the factors that affect and change the expectations of the customers. In this study, hybrid quality function deployment (QFD) and analytical hierarchy process (AHP) methodology were used, focusing on supplier selection problems. The weights of the quality requirements (QRs) of the customers were determined by the neutrosophic AHP approach, and then the quality characteristics (QCs) were prioritized in the quality house, considering the relationship between the QRs and QCs. Finally, alternative suppliers were evaluated in terms of QCs using the NAHP method and the most suitable supplier was determined as the Austrian origin company.

Keywords: AHP; Furniture industry; Neutrosophic fuzzy sets; QFD; Supplier selection. Introduction.

1. Introduction

With the changing and developing market conditions, more efficient use of existing resources, creation of alternative resources, and reaching the quality level expected by the customer requirements are achieved by giving importance to supplier selection. With the increase in competition, many businesses have to supply products that will meet the customer requirements in the most appropriate quality with the most optimum cost to maintain their existence. Correct supply chain management is one of the key objectives for both customer and product service quality. Most companies take advantage of all opportunities to reach the voice of the customer with their supply chain partners with whom they do business. Supplier selection includes a process that requires technical knowledge, finance, and human resources and provides the advantage of jointly managing company requests with the supplier (Chai & Ngai, 2020).

In supplier selection, criteria such as competitive prices, compliance with customer quality, short delivery time, communication, quality certification, and product technical suitability can be considered. In addition to the supplier selection criteria in the supply chain, quality raw materials and services contribute positively to product quality, and meeting customer needs must be analyzed according to the relationship between the criteria the customers, stakeholders, companies, and suppliers. Working with the right supplier or making the right evaluation of the existing suppliers are among the evaluations that the customer also needs (Sharma and Tripathy, 2023; Yazdani et al., 2017; Erdebilli et al., 2023).

When the decision models used for supplier selection practices, and modeling in the literature are examined, it is realized that supplier selection studies are generally modeled with multi-criteria decision-making (MCDM) methods. However QFD has been applied in very few supplier selection studies, and in some of these studies, both QFD and MCDM methods have been used as a hybrid. Since QFD is a systematic and customer-focused approach, it is appropriate to use it to prioritize customer needs. As a supplier's customer, customer complaints and supply chain process design needs can be easily determined with QFD (Tayyar and Soltani, 2023; de Araújo Souza et al., 2022; Bao and Li, 2021). In addition, it enables the evaluation of the criteria to be used in supplier selection from various perspectives, by supporting the cooperation between the supplier and the company. In this way, it supports the achievement of more competitive results by improving the cooperation and decision-making process, while focusing on the most important criterion in supplier selection, increasing customer satisfaction in future studies. QFD is a method based on data and feedback from experts, market research, and other external sources. This data-driven approach helps reduce bias and ensures that decisions are based on concrete information.

In our study, we used neutrosophic AHP to find the QR weights

In the following statements, we have presented the background, motivation, purpose, findings, and contribution of our study:

The ***background*** of our study, we have handled supplier selection problems for modular kitchen producers. The organization, in which we analyzed this problem, had difficulties in managing its supply chain processes especially in managing suppliers' raw material delivery process. So, a solution/ strategy for this organization was needed.

The primary ***motivation*** of our study is to analyze supplier selection criteria and alternative suppliers with a hybrid methodology that considers customers' requirements. By this methodology, we aim to develop a supplier selection model for organizations which will be a strategy for.

The ***gaps*** which we considered are;

- Neutrosophic AHP and QFD were not used in supplier selection for the customer-oriented companies.
- The number of supplier selection studies focusing on customer expectations is low, evaluations regarding sub-criteria that also take customer feedback into consideration are not investigated a lot and uncertainties in the supply chain process and supplier selection criteria are not considered too much.
- Customer requirements and expert opinions are planned at the same stage and therefore a strategic decision is made.

The ***purpose*** of this study is summarized as follows: The supplier selection problems involve criteria at different levels. The most important criteria for supplier selection include price, discount, quality, information management, and delivery time. It is considered appropriate to apply QFD in the study due to its methodological approach, focusing on the needs of the customers, and prioritization of those requirements. Customer complaints and requirements for supply chain process design are basically implemented with QFD as a supplier's customer. It allows the criteria to be used in supplier selection to be evaluated from several perspectives by encouraging cooperation between the supplier and the company. Therefore, through enhancing collaboration and decision-making, more competitive results are obtained. By focusing on the most important consideration in supplier selection, it enhances customer satisfaction in the future. QFD relies on information and opinions from professionals, market analysis, and other outside sources. This data-driven strategy guarantees that decisions are based on factual information and reduces bias. In the process of selecting a supplier, there are numerous criteria and potential uncertainties. The objective of implementing neutrosophic AHP-QFD is to ease the role of experts and model uncertainty more effectively than with other methods. The use of AHP is more appropriate for evaluation since the criteria in this study have more sub-criteria than the articles examined. The purpose of the study is to determine how to prioritize the criteria to select a more thorough and long-term supplier. With QFD, it can compare the qualities of suppliers and how they relate to one another. The neutrosophic AHP-QFD guarantees that the supplier selection meets customer requirements. This customer-oriented mindset significantly leads to enhanced fulfillment and lasting relationships in business. Alternatives are chosen more precisely by offering innovation and utilizing a more customer-oriented multi-criteria decision-making approach.

The ***findings*** of our study are explained in the following: The importance levels of the criteria and CRs identified in the study's initial phase were ascertained using the neutrosophic AHP. The QRs required to satisfy customer needs were identified in the second phase, and the QFD approach was used to calculate the weights of the QRs. Using the weights of the established quality standards, the neutrosophic AHP technique was once more employed in the third phase to assess potential substitute providers. Consequently, here is how the alternatives were ranked: Turkey, Italy, Germany-1, Germany-2, and Austria. A systematic and thorough approach to supplier evaluation is demonstrated using neutrosophic AHP to evaluate the relative importance of criteria and CRs, as well as the use of the QFD technique to define QRs. The study's findings, which placed Austria as the top supplier and Germany-2 and Germany-1 closely behind, offer the company under review useful information.

The ***contributions*** of our study are listed as follows:

- In this study, the methodology considers customer requirements. The organization which produces modular kitchen furniture must be aware of the needs of their customers' needs. These are also the requirements of the company which is the customer of its suppliers.
- In the literature, according to our research, there is not any study that investigates furniture industry supplier selection problems.
- A performance analysis model for suppliers is presented both to analyze suppliers' performances and supplier selection criteria performances for each alternative.

In our study, we outline a systematic exploration of the customer-oriented supplier selection process in the kitchen furniture industry. The methodology is structured into three main phases, each contributing to a holistic understanding of the proposed model. In the initial phase, we research the application of neutrosophic AHP to ascertain the importance levels of criteria and customer requests. The subsequent section focuses on the determination of QRs necessary to meet customer demands, employing the QFD approach. The third and final phase involves the application of neutrosophic AHP once again, this time to evaluate alternative suppliers based on the determined QRs. The systematic progression through these phases allows for a comprehensive examination of the supplier selection process, ultimately in a ranked list of alternatives. This structure facilitates a clear and in-depth presentation of our research methodology and findings, contributing to the overall coherence of this study. The organizational structure of our study is as follows: In the second section, the literature review is presented. In the third section, the details of the methodology are explained. In the fourth section, the application is presented and in the last section, the results of our research and contribution are provided.

1. Literature Review

In our study, we have conducted a literature review with the keywords "supplier selection", "multi-criteria decision making" and "QFD". According to our research, some of the studies which integrate these techniques are summarized below:

Asadabadi (2017) applied the analytical network process (ANP), QFD, and Markov chains in his study, taking into account the dynamic customer needs as the determining factor in customer-oriented supplier selection and decided that long-term cooperation can be supported by supplier selection. Babbar and Amin (2018) applied a two-stage QFD method and multi-objective stochastic mathematical model in their study for green supplier selection in which the uncertainties in the supply process in the beverage sector are managed with the stochastic approach, and the uncertainties in the opinions of the people are handled with the fuzzy QFD method. Bhattacharya et al. (2010) investigated the selection of suppliers from alternative suppliers by a hierarchical approach, in which AHP, QFD, and cost factor measures are combined, to consider engineering and customer needs. Chen et al. (2021) proposed a new QFD model, which uses DEMATEL, MULTIMOORA, unstable fuzzy linguistic term set, for the design of CNC machine tools. Haiyun et al. (2021) with the help of QFD, analyzed the innovation strategies multi-dimensionally by using a hybrid structure consisting of the interval-valued intuitionistic fuzzy DEMATEL and MULTIMOORA for green supply chain management. Jain and Singh (2020) aimed to make sustainable and stable supplier selection with a two-stage decision model by using a fuzzy inference system and fuzzy Kano model for the iron and steel industry. Karsak and Dursun (2014) proposed a new fuzzy MCDM method for supplier selection by using QFD and data envelopment analysis (DEA) together in a private hospital in Istanbul. Khan et al. (2022) included a full consistency method and fuzzy QFD hybrid model which will provide resilience in the health system during the COVID-19 pandemic and future pandemics. Lima-Junior and Carpinetti (2016) aimed to propose a new MCDM method with fuzzy QFD for supplier selection in the automotive sector in their study. Liu et al. (2019) used the Bonferroni test for green supplier selection in their study and divided them into several clusters to find the relationship between those in the same cluster. In addition, they applied QFD which uses preference values handled in the Bonferroni tests as customer needs importance values and the relationships between customer needs and technical criteria. Rajesh and Malliga (2013) developed a strategic supplier selection model for a high-pressure die-casting company by applying hybrid AHP and QFD methodology to analyze determined criteria. Sharma and Tripathy (2022) proposed an integrated QFD model with fuzzy TOPSIS for supplier selection and evaluation in their study. Singh and Kumar (2021) proposed an MCDM method integrated into the QFD model for social media usage by applying an image fuzzy set and a real case study was conducted with users of Facebook, Instagram, WhatsApp, and Twitter. Wang et al. (2022) included the use of TOPSIS and QFD and the hybrid interval-valued fuzzy sets in the evaluation of service performance for international container ports. Yazdani et al. (2017) organized their research by connecting DEMATEL for green supplier selection with customer needs. The relationship between the supplier selection pair and the needs of the customer was identified by applying the QFD. The complicated proportional assessment (COPRAS) lists alternative suppliers. In this section, there are studies used in traditional supplier selection and innovative supplier selection studies that also include the customer's requirements. Öztürk and Paksoy (2020) studied the green supplier selection problem in their studies considering customers' needs by using DEMATEL-QFD interval type-2 fuzzy AHP methods. Zhang et al. (2019) proposed a neighborhood-rough set-based QFD model for green building material supplier selection in their study in which technical specifications are determined by a decision-making group. Tayyar and Soltani (2020) proposed a method that decreases the cost of inappropriate supplier selection by choosing appropriate evaluation criteria with QFD-AHP. Liu et al. (2020) used QFD, best and worst method (BWM), VIKOR, and DEMATEL methods for supplier selection in blockchain tracing anti-fraud platforms. Chen (2020) included a study in which the entropy weight was collected using both AHP and TOPSIS instead of subjective weights for appropriate supply selection. Dang et al. (2022) solved a supplier selection problem under uncertainty using spherical fuzzy AHP and grey COPRAS in the automotive industry in Vietnam considering sustainable criteria. Seifbarghy and Hamidi (2025) proposed a hybrid fuzzy DEMATEL, neutrosophic SWARA, and neutrosophic MOORA framework based on the 10 C model for supplier selection.

One of the studies methodologically closest to the proposed approach is Karasan et al. (2022), who developed a neutrosophic Quality Function Deployment (QFD) methodology grounded in neutrosophic Analytic Hierarchy Process (AHP) and neutrosophic DEMATEL, applying it to the customer-oriented design of an automobile seat. In their study, customer requirements were weighted using neutrosophic AHP, while the interrelationships among technical characteristics were determined via neutrosophic DEMATEL. Furthermore, the robustness of the resulting priorities was tested through comparisons with alternative methods in the literature as well as comprehensive sensitivity analyses.

Although that study shares a similar neutrosophic AHP-QFD backbone with the present research, it addresses a product design problem. In contrast, the current study focuses on a supplier selection problem where, following the QFD phase, alternative suppliers are further evaluated through a second application of neutrosophic AHP based on the weighted quality characteristics. This structural distinction positions the present study as the first to extend the neutrosophic AHP-QFD approach to a customer-oriented supplier evaluation problem within the customized furniture industry.

In addition, in Table 1, we presented studies that deal with supplier selection problems and summarized them according to the scope and techniques applied. In Table 2, we have analyzed the studies that include NAHP in their studies according to their scope and all other techniques.

Table 1. *Techniques used for supplier selection*

References	**Scope**	**Method**
Lima-Junior and Carpinetti (2016)	*Application in the automotive industry by dividing priority, critical, complementary, and costly groups for supplier selection*	*Fuzzy QFD*
Rajesh and Malliga (2013)	*Strategic supplier selection proposal for high-pressure die-casting company*	*AHP; QFD*
Karsak and Dursun (2014)	*A private hospital application in Istanbul for supplier evaluation and selection*	*QFD; DEA; FWA*
Yazdani et al. (2017)	*Supplier evaluation and selection for environmental protection and sustainable development*	*QFD; DEMATEL; COPRAS*
Bhattacharya et al. (2010)	*Selection of suppliers to meet engineering and customer needs*	*AHP; Hierarchical QFD; CFM*
Haiyun et al. (2021)	*Developing an innovation strategy for green supply chain management in the energy sector*	*QFD; IVIF MOORA; DEMATEL*
Liu et al. (2019)	*Green supplier selection for bike rental case study*	*QFD; IT2FPBM; T2FWPBM*
Asadabadi (2017)	*Customer-oriented supplier selection*	*ANP; QFD; Markov Chain*
Tang and Yang (2021)	*Supplier selection for e-bike sharing*	*Interval-valued Pythagorean fuzzy preference relation*
Hendiani et al. (2020)	*Sustainable supplier selection for refinery in Southern Iran*	*Fuzzy best-worst method*

References	Scope	Method
Dursun and Karsak (2013)	*Determination and evaluation of supplier selection criteria*	*Fuzzy weighted average; QFD*
Bevilacqua et al. (2006)	*Supplier selection for the medium-sized clutch fittings industry*	*Fuzzy QFD*
Sharma and Tripathy (2022)	*Supplier evaluation and selection*	*QFD; Fuzzy TOPSIS*
Zheng et al. (2023)	*New energy vehicles supplier selection*	*QFD; Case-based reasoning*
Khorram et al. (2024)	*Supplier selection*	*Fuzzy DEMATEL; fuzzy QFD; fuzzy TOPSIS; and fuzzy VIKOR*
Koirala, and Shabbiruddin (2023)	*Sustainable battery supplier selection*	*QFD; Fuzzy COPRAS*
Deivanayagampillai et al. (2026)	*Robust green supplier selection in sustainable supply chain management under dynamic uncertainty*	*Adaptive Neutrosophic Decision-Making (ANDM); Neutrosophic Entropy; DHFWDHM; Adaptive TOPSIS*
Yang (2025)	*Building material supplier selection*	*2-Tuple Linguistic Neutrosophic Set (2TLNNS); Combined Grey Relational Analysis (2TLNN-CGRA); Shannon Entropy*
Ambilkar et al. (2024)	*Sustailient supplier selection in the additive manufacturing (AM) sector for trinket manufacturing*	*Fuzzy Delphi Method (FDM) and Neutrosophic Best-Worst Method (N-BWM)*

Table 2. *The literature studies with Neutrosophic AHP*

References	Scope	Method
Karamaşa et al. (2021)	Evaluating the optimal training aircraft selection.	NAHP, MULTIMOORA
Bilandi et al. (2020)	Wireless body area networks relay node selections for the medical health system.	NAHP
Başhan et al. (2020)	Maritime risk evaluation to optimize safety control, preventing crew and potential environmental impacts.	NAHP, fuzzy TOPSIS

References	Scope	Method
Reig-Mullor et al. (2022)	Sustainability reports of environmental, social, and governance.	NAHP-TOPSIS
Harnpornchai and Wonggattaleekam (2021)	Relative importance assignment for the real world.	NAHP
Akman et al. (2022)	E-commerce selections during the pandemic crisis.	Neutrosophic fuzzy AHP; EDAS
Kahraman et al. (2022)	Fuzzy extensions of AHP for INFUS conferences.	Intuitionistic fuzzy AHP; picture fuzzy AHP; NAHP; spherical fuzzy AHP; Pythagorean fuzzy AHP; q-rung orthopair fuzzy AHP
Vafadarnikjoo and Scherz (2021)	Sustainable, agility evaluations in the Iranian steel industry.	Neutrosophic-Grey AHP
Navarro et al. (2021)	Sustainable design.	NAHP, DEMATEL
Junaid et al. (2020)	Supply Chain Risk Assessment in Automotive Industry of Pakistan.	NAHP-TOPSIS
Karuppiah et al. (2021)	Sustainable humanitarian supply chain management.	NAHP, TODIM
Navarro et al. (2019)	Sustainable design assesment of concrete bridge.	NAHP, TOPSIS
Chakrabortty et al. 2023	Chatbot selection in the telecommunication industry.	Combined Compromise Solution (CoCoSo), NAHP
Singh et al. (2021)	Evaluating total transportation cost.	Trapezoidal neutrosophic fuzzy AHP, Artificial neural network
Alzahrani et al. (2023)	Selecting women's university sites in the state of West Bengal, India.	Neutrosophic number TRNN, AHP, TOPSIS, COPRAS
Rahman et al. (2022)	The causes of boiler accidents in Bangladesh.	NAHP
Tuan et al. (2020)	Lecturers' research productivity evaluation.	Interval-valued Neutrosophic AHP
Abdel-Basset et al. (2020)	Professional selection in Egypt.	Neutrosophic ANP, TOPSIS, AHP, MOORA
Vafadarnikjoo et al. (2023)	Blockchain technology adoption in manufacturing supply chains.	NAHP

References	Scope	Method
Ye et al. (2023)	Fashion culture communication and marketing in China.	Interval-valued Neutrosophic AHP
Yiğit (2023)	Evaluating trainers in organizations.	Interval-valued Neutrosophic AHP, Fuzzy C-Means (FCM).
Ayyildiz et al. (2023)	Evaluate universities based on student perspective.	IVN-AHP, VIKOR
Hezam et al. (2021)	Determining the priority groups for COVID-19 Vaccine.	NAHP, TOPSIS
Sánchez-Garrido et al. (2021)	The sustainability among design alternatives for a single-family home.	Neutrosophic group AHP, VIKOR
Karamaşa et al. (2020)	Selecting the right logistics service provider	NAHP
Seifbarghy and Hamidi (2025)	Supplier selection in the automotive parts supply chain based on the 10 C model	Fuzzy DEMATEL, Neutrosophic SWARA, Neutrosophic MOORA

2. Methodology

In this study, we propose a methodology that integrates NAHP and NQFD approaches to determine the best alternative by considering both the QRs of customers and the QCs of products. Many criteria and alternatives in supplier selection involve uncertainty. Using neutrosophic AHP-QFD is aimed to facilitate the work of experts, and uncertainty is modeled more effectively compared to other methods (Karasan et al., 2022). The prioritization of the criteria and the selection of more comprehensive and long-contract suppliers are the motivations of this study. The comparison of supplier qualifications and the relationship between suppliers is possible with QFD. The neutrosophic AHP-QFD ensures that supplier selection is aligned with customer requirements. This customer-oriented approach makes a significant contribution to increased satisfaction and long-term business relationships.

In the first phase, we handle QRs' weights by conducting the NAHP method. In the second phase, we determine QCs to meet QRs and we execute the steps of QFD to handle the weights of QCs by considering the QRs' weights handled in the first phase. Then in the last phase, we identify alternatives and again we carry out NAHP steps to find the most appropriate alternative by taking into account the QCs weights handled in the second step. The proposed methodology is presented in Figure 1.

In this study, there are linguistic evaluations of decision-makers and uncertainties in QRs and QCs. Therefore, we need to use fuzzy logic to solve the problem and in our study, we used neutrosophic sets. The purpose of using neutrosophic sets in the evaluation of QRs and QCs for multiple alternatives is to appropriately represent unclear, inconsistent, or incomplete information. It is more suitable for human thinking with its membership functions of truth, indeterminacy, and falsity. It contains more information than classical fuzzy logic thanks to the "indeterminacy" membership function. In the following, we present the details of the methods used in this study.

2.1. Quality Function Deployment

QFD is a method of transferring customer requirements to the technical specifications of the product or process in order to meet customer demands and expectations of products or processes now and in the future. It is an effective method that can be used for the company, as it includes the "voice of the customer" in stages such as product and production planning and engineering (Cebi et al., 2009). In the QFD study; it is not only to meet the expectations of the customer, but also to provide the quality and best product/service. QFD is one of the methods used by companies to transform the quality product/service requirements of their customers, stakeholders, employees, and suppliers into quality characteristics (Babbar and Amin, 2018; Haiyun et al., 2021; Karasan et al., 2022; Khan et al., 2022; Lima-Junior et al., 2016; Singh and Kumar, 2021; Yazdani et al.,2017).

Traditional QFD has the following features:

- The middle part of the figure is the house of quality, showing the relationship between quality requirements (WHATs) and quality characteristics (HOWs).
- The left part of the house of quality contains the customer's quality requirement and degree of importance.
- The upper part of the House of Quality shows the framework of the technical specifications and the relations between the technical specifications.
- The right part of the house of quality shows the comparison matrix of the firm against its competitors.
- The lower part of the house of quality shows the grade of quality attributes targeting and evaluation process.

2.2. Neutrosophic Sets

Neutrosophic sets refer to sets developed to portray uncertain, incomplete, and meaningless information, as a generalization of intuitive fuzzy sets and introduced by Florentin Smarandache in the 1980s is represented by three membership values. NS studies the nature and scope of impartiality, as well as their interactions with different intellectual diversity. NS uses indeterminacy as an independent measure of the membership and non-membership information. Hence the concept of NS is considered as a generalization of FS, IFS, and interval-valued sets (Das et al., 2020; Kaya et al., 2022; Junaid et al., 2020).

Definition 1: Let X and x∈X. Let X be a neutrosophic subset A in the universe. For subset A (Kaya et al., 2022);

The truth membership function is a subset of $T_A(x)$, [0,1].

Indeterminacy membership function is a subset of $T_I(x)$, [0,1].

Falsity membership is a subset of $T_F(x)$, [0,1].

There are no restrictions on the sum of membership functions.

$$0^- \leq T_A(x) + T_I(x) + T_F(x) \leq 3^+ \quad (1)$$

Definition 2: If $N_1=(t_1, i_1, f_1)$ and $N_2=(t_2, i_2, f_2)$ are two different single-valued neutrosophic numbers, the calculations can be described in the section as follows (Kaya et al., 2022):

The sum of N_1 and N_2: $N_1 + N_2 = (t_1 + t_2 - t_1 t_2, i_1 i_2, f_1 f_2)$ (2)

The multiplication of N_1 and N_2: $N_1 \times N_2 = (t_1 t_2, i_1 + i_2 - i_1 i_2, f_1 + f_2 - f_1 f_2)$ (3)

The division of N_2 on N_1: $N_2/N_1 = (t_2/t_1, i_2 - i_1/1 - i_1, f_2 - f_1/1 - f_1)$ (4)

Definition 3: If $N_1=(t_1, i_1, f_1)$ is a single-valued neutrosophic number and A is an arbitrary positive real number, the multiplication of N1 and A can be described in the equation as follows (Kaya et al., 2022):

$$A \times N_1 = (1 - (1 - t_1)^A, i_1^A, f_1^A), \text{ where } A > 0 \quad (5)$$

Therefore, when $N_1=(t_1, i_1, f_1)$ is a single-valued neutrosophic number and A is an arbitrary positive real number, the division of N1 on A can be described as an equation as follows:

$$N_1/A = \left(1 - (1 - t_1)^{1/A}, i_1^{1/A}, f_1^{1/A}\right), \text{ where } A > 0 \quad (6)$$

Definition 4: If N_1 is a single-valued neutrosophic number, the score function is mapped N_1 into the single crisp output as $S(N_1)$ follows (Kaya et al., 2022).:

$$S(N_1) = (3 + t_1 - 2i_1 - f_1)/4 \quad (7)$$

$t_{\tilde{a}}$ determines the maximum accuracy membership degree, $i_{\tilde{a}}$ and $f_{\tilde{a}}$ determine the minimum uncertainty and inaccuracy determines the degree of membership.

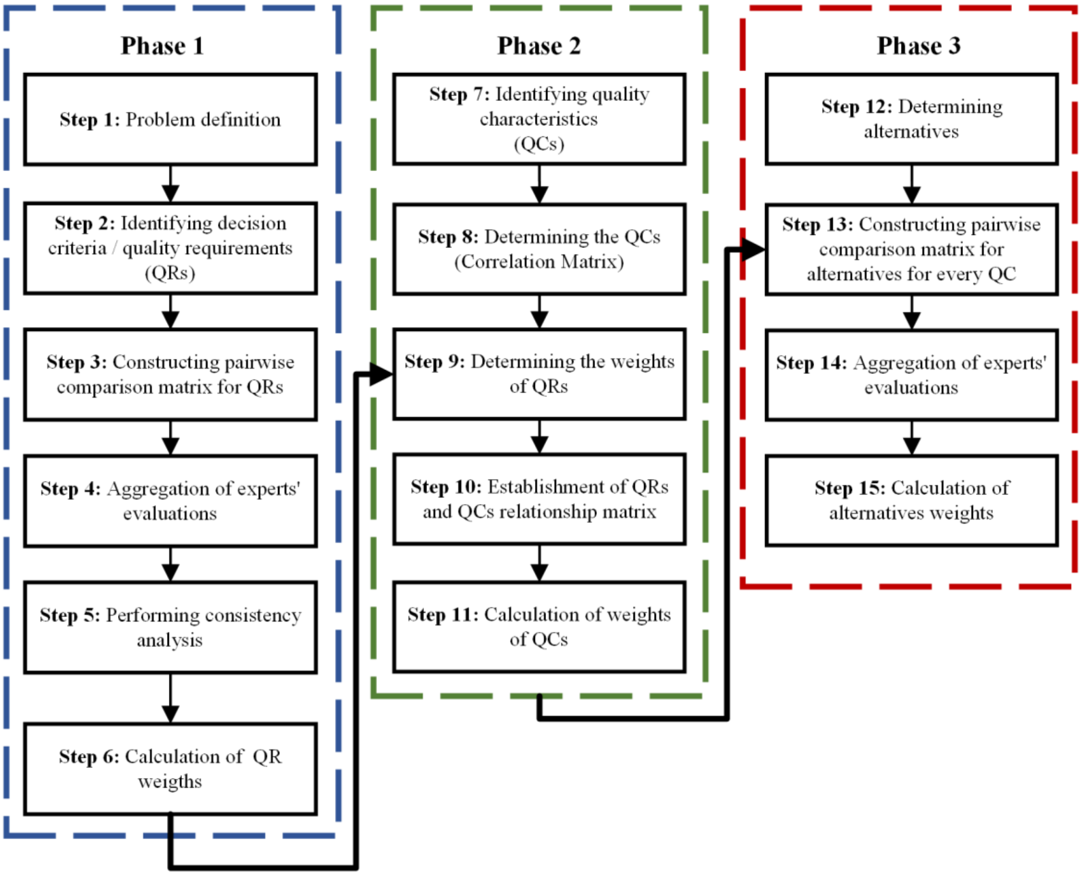

***Figure 1.** Flowchart of the methodology*

2.3. Neutrosophic AHP (NAHP)

AHP is an MCDM approach that compares the importance of criteria and alternatives with pairwise comparisons. Since AHP does not deal with ambiguous situations in complex problems, it is used in most cases with fuzzy logic. In some real-life situations, this is not enough either. For this reason, evaluation with fuzzy numbers in decision problems provides more accurate decisions. In our study, we used neutrosophic fuzzy AHP to deal with this vagueness and find the weights of criteria and the best alternative.

The steps of the NAHP method used in this study are presented below:

Step 1: The criteria and sub-criteria of the problem and alternative suppliers to be selected are determined.

Step 2: A pairwise comparison is constructed for each criterion by the experts. Linguistic variables and importance weights are calculated based on neutrosophic values in Table 3 (Kaya et al., 2022).

Table 3. Linguistic variables and weight of significance based on neutrosophic values

Linguistic Terms	**Neutrosophic sets**	**Linguistic Terms**	**Reciprocal Neutrosophic sets**
Extremely highly preferred (EHP)	(0.90, 0.10, 0.10)	Mildly lowly preferred (MLP)	(0.10, 0.90, 0.90)
Extremely preferred (EP)	(0.85, 0.20, 0.15)	Mildly preferred (MP)	(0.15, 0.80, 0.85)
Very strongly to extremely preferred (VSEP)	(0.80, 0.25, 0.20)	Mildly preferred to Very lowly preferred (MPVLP)	(0.20, 0.75, 0.80)
Very strongly preferred (VSP)	(0.75, 0.25, 0.25)	Very lowly preferred (VLP)	(0.25, 0.75, 0.75)
Strongly preferred (SP)	(0.70, 0.30, 0.30)	Lowly preferred (LP)	(0.30, 0.70, 0.70)
Moderately highly to strongly preferred (MHSP)	(0.65, 0.30, 0.35)	Moderately lowly preferred to lowly preferred (MLPLP)	(0.35, 0.70, 0.65)
Moderately highly preferred (MHP)	(0.60, 0.35, 0.40)	Moderately lowly preferred (MOLP)	(0.40, 0.65, 0.60)
Equally to moderately preferred (EMP)	(0.55, 0.40, 0.45)	Moderately to equally preferred (MEP)	(0.45, 0.60, 0.55)
Equally preferred (EQP)	(0.50, 0.50, 0.50)	Equally preferred (EQP)	(0.50, 0.50, 0.50)

Step 3: The aggregation of expert opinions is calculated with the neutrosophic weighted arithmetic mean addition operator.

$$F_w(A_1, A_2, \ldots, A_n) \begin{cases} 1 - \prod_{j=1}^{n}\left(1 - T_{A_j}(x)\right)^{w_j} \\ 1 - \prod_{j=1}^{n}\left(1 - I_{A_j}(x)\right)^{wj} \\ 1 - \prod_{j=1}^{n}\left(1 - F_{A_j}(x)\right)^{w_j} \end{cases} \quad (8)$$

$\boldsymbol{W} = (\boldsymbol{w_1}, \boldsymbol{w_2}, \ldots \boldsymbol{w_n})$: weight vector $w_j \in [0,1]$ and $\sum_{j=1}^{n} w_j = 1$

Step 4: The consistency ratio (CR) is calculated for each pairwise comparison matrix. The method proposed by Xu and Liao (2014) will be used for CR calculation. The following calculations are used, with $(T'_{xk},\ I'_{xk},\ and\ F'_{xk})$ consistent neutrosophic values,

1. For $k > x + 1,\quad y = x + 1\quad N_{xk} = (T'_{xk}, I'_{xk}, F'_{xk}),$

$$T'_{xk} = \frac{\sqrt[k-x-1]{T_{xy} * T_{yk} * T_{xk-1} * T_{k-1k}}}{\sqrt[k-x-1]{T_{xy} * T_{yk} * T_{xk-1} * T_{k-1k}} + \sqrt[k-x-1]{(1-T_{xy}) * (1-T_{yk}) * (1-T_{xk-1}) * (1-T_{k-1k})}} \quad (9)$$

$$I'_{xk} = \frac{\sqrt[k-x-1]{I_{xy} * I_{yk} * I_{xk-1} * I_{k-1k}}}{\sqrt[k-x-1]{I_{xy} * I_{yk} * I_{xk-1} * I_{k-1k}} + \sqrt[k-x-1]{(1-I_{xy}) * (1-I_{yk}) * (1-I_{xk-1}) * (1-I_{k-1k})}} \quad (10)$$

$$F'_{xk} = \frac{\sqrt[k-x-1]{F_{xy} * F_{yk} * F_{xk-1} * F_{k-1k}}}{\sqrt[k-x-1]{F_{xy} * F_{yk} * F_{xk-1} * F_{k-1k}} + \sqrt[k-x-1]{(1-F_{xy}) * (1-F_{yk}) * (1-F_{xk-1}) * (1-F_{k-1k})}} \quad (11)$$

2. For $k = x + 1,\ y = x + 1\quad N_{xk} = (T_{xk}, I_{xk}, F_{xk})$
3. For $k < x,\ y = x + 1\ \ N_{xk} = (F'_{xk}, 1 - I'_{xk}, T'_{xk})$

$$CR = \frac{1}{2(n-1)(n-2)} \sum_{x=1}^{n} \sum_{k=1}^{n} (|T'_{xk} - T_{xk}| + |I'_{xk} - I_{xk}| + |F'_{xk} - F_{xk}|) \quad (12)$$

*CR must be less than 0.1.

Step 5: The normalization method is applied for each criterion, and the normalization process is performed by dividing each row by the total of the column it belongs to.

Step 6: After the normalization process is done, the row totals are calculated and divided by the number of criteria, and the neutrosophic criteria weights are found.

Step 7: Neutrosophic criterion weights are clarified using Eq. (9).

$$S(N_i) = (3 + T_i - 2I_i - F_i)/4 \quad (13)$$

Step 8: The criteria weights are obtained so that the total weights are 1.

2.4. The Neutrosophic QFD (NQFD)

The grading of QRs as (1-5) or (1-9) by experts creates a negative situation in terms of subjectivity. Uncertainty, inconsistency, and disagreement of experts cause incomplete or inaccurate transmission of QRs in supplier selection problems. Relationship matrix values will be expressed with neutrosophic numbers. The relationships will be shown by $\tilde{\mathbf{9}}$**-** strong relationships, $\tilde{\mathbf{3}}$**-** average relationships, and $\tilde{\mathbf{1}}$**-** poor relationship.

In the QFD correlation matrix, (++) shows a strong positive correlation between QCs, (-) shows a negative correlation, and (--) shows a strong negative correlation. The weight of each QC (HOWs) is calculated by multiplying each relationship value by the corresponding QRs (WHATs) weight.

$$\omega(\boldsymbol{HOW})_{\boldsymbol{i}} = (\boldsymbol{HOW})_{\boldsymbol{i1}}\boldsymbol{relationship\ degree} \times \boldsymbol{\omega}(\boldsymbol{WHAT_1}) + \ldots + (\boldsymbol{HOW})_{\boldsymbol{in}}\boldsymbol{relationship\ degree} \times \boldsymbol{\omega}(\boldsymbol{WHAT_n}) \tag{14}$$

3. Application

In this study, an application is conducted by using the data of a customer-oriented and bespoke company in the kitchen furniture industry. The company, which provides modular facilities with different designs with an aesthetic, modern line, serves its domestic and international customers. Raw materials are procured from both domestic and foreign suppliers. The purpose of using QFD in the application is to meet customer needs with the voice of the customer and to develop a decision-making mechanism that allows harmony between the organization’s characteristics and suppliers’ characteristics. Evaluation is made by three experts working in the firm.

The application steps are as follows:

Phase 1/ Step 1: The problem handled in this study is to find the most appropriate supplier for the company.

Phase 1/ Step 2: In order to reveal the problem, the supplier selection criteria and sub-criteria of the company are classified in Table 4. We collected our criteria through a literature review and asked decision-makers to check whether they were suitable for supplier evaluation. These criteria are also considered as QRs of customers in the QFD phase. Some supplier selection criteria from the literature are included in this article. Certain criteria were developed by consulting the opinions of the purchasing and marketing departments because, in the furniture company where the application was conducted, design and consumer feedback are significant factors.

Table 4. *Supplier selection criteria*

Criteria	Sub-criteria	Relevant Literature
Order management (C1)	Order process (C11)	Karabayır and Botsalı, 2022
	Ordering/Portal login (C12)	Experts' opinion
Product and service marketing management (C2)	New product introduction (C21)	Galankashi et al., 2016; Wang et al., 2017
	Change in product (C22)	Wang et al., 2017
	The product is removed from the program (C23)	Wang et al., 2017
	Media management (C24)	Lahdhiri et al., 2022
	Product and service training (C25)	Galankashi et al., 2016, Wang et al., 2017
	Adapting to competitors (C26)	Karabayır and Botsalı, 2022
	Complaints management (C27)	Karabayır and Botsalı, 2022
	Identifying market-specific global trends (C28)	Karabayır and Botsalı, 2022; Wang et al., 2017
	Collaboration to improve existing service (C29)	Karabayır and Botsalı, 2022; Wang et al., 2017
	Quality (C210)	Galankashi et al., 2016; Lahdhiri et al., 2022; Wang et al., 2017
	Accurate and timely response to price offers (C211)	Karabayır and Botsalı, 2022
Logistics management (C3)	Notification of delivery dates (C31)	Galankashi et al., 2016; Wang et al., 2017
	Notification of minimum orders (C32)	Galankashi et al., 2016; Wang et al., 2017
	Material volume, package quantity, size notification (C33)	Galankashi et al., 2016; Wang et al., 2017
	Compliance with delivery dates (C34)	Galankashi et al., 2016
	Domestic franchise status (C35)	Expert opinion
Visit management (from company to supplier – from supplier to company) (C4)	Company presentation (C41)	Expert opinion
	Information sharing (C42)	Lahdhiri et al., 2022
	Workshop (C43)	Expert opinion
	Factory tour frequency (Digital & classic) (C44)	Lahdhiri et al., 2022

Criteria	Sub-criteria	Relevant Literature
Purchasing planning and control management (C5)	Price (C51)	Galankashi et al., 2016; Wang et al., 2017
	Compliance with the predictions (C52)	Galankashi et al., 2016; Wang et al., 2017

Phase 1/ Step 3: Table 5 was obtained by taking the opinions of 3 experts. The relationship matrix between the criteria and the sub-criteria is created according to their evaluations. The features of the experts are as follows:

- Expert 1: 13 years' experience as an Inventory Planning Executive
- Expert 2: 15 years' experience as Senior Purchase Representative
- Expert 3: 5 years' experience as a Purchase Representative

The values given in Table 5 and Table 6 show the pairwise comparisons of quality requirements both with linguistic terms and neutrosophic fuzzy sets.

Table 5. *Comparison matrix with linguistic evaluations*

		C1	**C2**	**C3**	**C4**	**C5**
C1	**Expert 1**	EQP	MLP	MP	EQP	MLP
	Expert 2	EQP	MLP	MLP	EQP	MLP
	Expert 3	EQP	MLP	MLP	EQP	MLP
C2	**Expert 1**	EHP	EQP	EHP	EQP	SP
	Expert 2	EHP	EQP	EQP	VSP	VLP
	Expert 3	EHP	EQP	EQP	LP	MPVLP
C3	**Expert 1**	EP	MLP	EQP	EHP	EQP
	Expert 2	EHP	EQP	EQP	VSEP	MLP
	Expert 3	EHP	EQP	EQP	VSEP	MLP
C4	**Expert 1**	EQP	MLP	MLP	EQP	MLP
	Expert 2	EQP	VLP	MPVLP	EQP	MLP
	Expert 3	EQP	SP	MPVLP	EQP	MLP
C5	**Expert 1**	EHP	LP	EQP	EHP	EQP
	Expert 2	EHP	VSP	EHP	EHP	EQP
	Expert 3	EHP	VSEP	EHP	EHP	EQP

Table 6. *Neutrosophic fuzzy comparison matrix for QRs*

		C1	**C2**	**C3**	**C4**	**C5**
C1	**Expert 1**	(0.5, 0.5, 0.5)	(0.1, 0.9, 0.9)	(0.15, 0.8, 0.85)	(0.5, 0.5, 0.5)	(0.1, 0.9, 0.9)

	Expert 2	(0.5, 0.5, 0.5)	(0.1, 0.9, 0.9)	(0.1, 0.9, 0.9)	(0.5, 0.5, 0.5)	(0.1, 0.9, 0.9)
	Expert 3	(0.5, 0.5, 0.5)	(0.1, 0.9, 0.9)	(0.1, 0.9, 0.9)	(0.5, 0.5, 0.5)	(0.1, 0.9, 0.9)
C2	**Expert 1**	(0.9, 0.1, 0.1)	(0.5, 0.5, 0.5)	(0.9, 0.1, 0.1)	(0.5, 0.5, 0.5)	(0.7, 0.3, 0.3)
	Expert 2	(0.9, 0.1, 0.1)	(0.5, 0.5, 0.5)	(0.5, 0.5, 0.5)	(0.75, 0.25, 0.25)	(0.25, 0.75, 0.75)
	Expert 3	(0.9, 0.1, 0.1)	(0.5, 0.5, 0.5)	(0.5, 0.5, 0.5)	(0.3, 0.7, 0.7)	(0.2, 0.75, 0.8)
C3	**Expert 1**	(0.85, 0.2, 0.15)	(0.1, 0.9, 0.9)	(0.5, 0.5, 0.5)	(0.9, 0.1, 0.1)	(0.5, 0.5, 0.5)
	Expert 2	(0.9, 0.1, 0.1)	(0.5, 0.5, 0.5)	(0.5, 0.5, 0.5)	(0.8, 0.25, 0.2)	(0.1, 0.9, 0.9)
	Expert 3	(0.9, 0.1, 0.1)	(0.5, 0.5, 0.5)	(0.5, 0.5, 0.5)	(0.8, 0.25, 0.2)	(0.1, 0.9, 0.9)
C4	**Expert 1**	(0.5, 0.5, 0.5)	(0.1, 0.9, 0.9)	(0.1, 0.9, 0.9)	(0.5, 0.5, 0.5)	(0.1, 0.9, 0.9)
	Expert 2	(0.5, 0.5, 0.5)	(0.25, 0.75, 0.75)	(0.2, 0.75, 0.8)	(0.5, 0.5, 0.5)	(0.1, 0.9, 0.9)
	Expert 3	(0.5, 0.5, 0.5)	(0.7, 0.3, 0.3)	(0.2, 0.75, 0.8)	(0.5, 0.5, 0.5)	(0.1, 0.9, 0.9)
C5	**Expert 1**	(0.9, 0.1, 0.1)	(0.3, 0.7, 0.7)	(0.5, 0.5, 0.5)	(0.9, 0.1, 0.1)	(0.5, 0.5, 0.5)
	Expert 2	(0.9, 0.1, 0.1)	(0.75, 0.25, 0.25)	(0.9, 0.1, 0.1)	(0.9, 0.1, 0.1)	(0.5, 0.5, 0.5)
	Expert 3	(0.9, 0.1, 0.1)	(0.8, 0.25, 0.2)	(0.9, 0.1, 0.1)	(0.9, 0.1, 0.1)	(0.5, 0.5, 0.5)

Phase 1/ Step 4: Using Equation (4), expert opinions are used to calculate the neutrosophic weighted arithmetic mean (Table 7). The weights of all experts are equal, so w_j is 0,333. For example the calculation for $\tilde{r}_{42}$;

$$\tilde{r}_{42} = \begin{cases} 1-(1-0{,}1)^{0{,}333} \times (1-0{,}25)^{0{,}333} \times (1-0{,}7)^{0{,}333} \\ 1-(1-0{,}9)^{0{,}333} \times (1-0{,}75)^{0{,}333} \times (1-0{,}3)^{0{,}333} \\ 1-(1-0{,}9)^{0{,}333} \times (1-0{,}75)^{0{,}333} \times (1-0{,}3)^{0{,}333} \end{cases}$$

$$\tilde{r}_{42} = (0{,}413{,}0{,}740{,}\,0{,}740)$$

Table 7. Aggregated neutrosophic comparison matrix

	C1	**C2**	**C3**	**C4**	**C5**
C1	(0,50, 0,50, 0,50)	(0,10, 0,90, 0,90)	(0,12, 0,87, 0,89)	(0,50, 0,50, 0,50)	(0,10, 0,90, 0,90)
C2	(0,90, 0,10, 0,10)	(0,50, 0,50, 0,50)	(0,71, 0,39, 0,39)	(0,56, 0,52, 0,52)	(0,44, 0,65, 0,67)
C3	(0,89, 0,13, 0,12)	(0,39, 0,71, 0,71)	(0,50, 0,50, 0,50)	(0,84, 0,20, 0,17)	(0,26, 0,83, 0,83)
C4	(0,50, 0,50, 0,50)	(0,41, 0,74, 0,74)	(0,17, 0,82, 0,84)	(0,50, 0,50, 0,50)	(0,10, 0,90, 0,90)

C5	(0,90, 0,10, 0,10)	(0,67, 0,45, 0,44)	(0,83, 0,26, 0,26)	(0,90, 0,10, 0,10)	(0,50, 0,50, 0,50)

Phase 1/ Step 5: Equation 5-6-7 is used to calculate the consistency of the neutrosophic pairwise comparison matrix. The consistency ratio with equation (8) was found as CR=0.001.

Phase 1/ Step 6: In this step, the importance levels of the sub-criteria have been accepted as equal and are given in Table 8.

Table 8. *Selection criteria importance of degrees*

Main-criteria	**Sub-criteria**	**Weights ω**	**Criteria Importance Degree**	**Criteria Importance Degree (%)**
C1	Order process (C11)	9%	0,500	0,043
	Ordering/Portal login (C12)		0,500	0,043
C2	New product introduction (C21)	25%	0,091	0,023
	Change in product (C22)		0,091	0,023
	The product is removed from the program (C23)		0,091	0,023
	Media management (C24)		0,091	0,023
	Product and service training (C25)		0,091	0,023
	Adapting to competitors (C26)		0,091	0,023
	Complaints management (C27)		0,091	0,023
	Identifying market-specific global trends (C28)		0,091	0,023
	Collaboration to improve existing service (C29)		0,091	0,023
	Quality (C210)		0,091	0,023
	Accurate and timely response to price offers (C211)		0,091	0,023
C3	Notification of delivery dates (C31)	21%	0,200	0,043
	Notification of minimum orders (C32)		0,200	0,043
	Material volume, package quantity, size notification (C33)		0,200	0,043
	Compliance with delivery dates (C34)		0,200	0,043
	Domestic franchise status (C35)		0,200	0,043
C4	Company presentation (C41)	13%	0,250	0,033
	Information sharing (C42)		0,250	0,033
	Workshop (C43)		0,250	0,033

Main-criteria	Sub-criteria	Weights ω	Criteria Importance Degree	Criteria Importance Degree (%)
	Factory tour frequency (Digital & classic) (C44)		0,250	0,033
C5	Price (C51)	31%	0,500	0,157
	Compliance with the predictions (C52)		0,500	0,157

Phase 2 / Step 7: The quality characteristics (QCs) that the company must meet in order to meet the supplier selection criteria are determined by asking decision-makers and they are presented below:

- Number of patents (QC1)
- Reverse logistics rate (QC2)
- Experiences in the field (QC3)
- Quality certification systems (QC4)
- Location (QC5)
- Financial stability (QC6)
- Reliability of the raw material to the customer and manufacturing processes (QC7)
- Discount (QC8)
- Management and organizational culture (QC9)
- Compliance with environmental laws (QC10)
- Technical capacity (QC11)

Phase 2 / Step 8: The QCs' correlation matrix is constructed and presented in Table 9. The scale used to create the correlation matrix is as follows: ++ high positive correlation, + positive correlation, - negative correlation, -- high negative correlation.

Table 9. Correlation matrix

	QC1	QC2	QC3	QC4	QC5	QC6	QC7	QC8	QC9	QC10	QC11
QC1											++
QC2											
QC3											
QC4										+	
QC5						-					
QC6					-						
QC7											+
QC8											
QC9											

QC10				+							
QC11	++						+				

Phase 2 / Step 9: The QR weights are handled from Phase 1/Step 6.

Phase 2 / Step 10: A relationship matrix is created between WHATs and HOWs. The relationship between QRs and QCs will be shown with neutrosophic values of $\tilde{9}, \tilde{3}, \tilde{1}$*. Table 10 includes the neutrosophic scale for QRs and QCs relationship matrix and Table 11 shows the relationship matrix between the QRs and QCs.

Phase 2 / Step 11: The aggregated relationship matrix is presented in Table 12 and the weights of QCs are calculated via Eq. (4).

Table 10. The neutrosophic scale for QRs and QCs relationship matrix

Relationship	**Neutrosophic fuzzy numbers**		
$\tilde{1}$ - poor relationship	0.1	0.9	0.9
$\tilde{3}$ - moderate relationship	0.5	0.5	0.5
$\tilde{9}$ - strong relationship	0.9	0.1	0.1

*$\tilde{9}$ strong relationships (S), $\tilde{3}$ moderate relationships (A), $\tilde{1}$ poor relationship (P)

Table 11. Relationship matrix

QRs	**Expert #**	**QR Weights**	**QC1**	**QC2**	**QC3**	**QC4**	**QC5**	**QC6**	**QC7**	**QC8**	**QC9**	**QC10**	**QC11**
C11	**Expert 1**	**0,043**			A		S				A		P
	Expert 2				A		S				A		P
	Expert 3				A		S				A		P
C12	**Expert 1**	**0,043**			A						S		S
	Expert 2				A						S		S
	Expert 3				A						S		S
C21	**Expert 1**	**0,023**	A		A	A					S	S	S

QRs	Expert #	QR Weights	QC1	QC2	QC3	QC4	QC5	QC6	QC7	QC8	QC9	QC10	QC11
	Expert 2		A		P	A					S	S	S
	Expert 3		A		P	A					S	S	S
C22	Expert 1	0,023	S	P	S	S			S		S	S	S
	Expert 2		S	P	S	S			S		S	S	S
	Expert 3		S	P	S	S			S		A	S	A
C23	Expert 1	0,023		S	A						S	S	S
	Expert 2			S	A						S	S	S
	Expert 3			S	A						S	S	S
C24	Expert 1	0,023			S	S		S			S		
	Expert 2				S	S		S			S		
	Expert 3				S	S		S			S		
C25	Expert 1	0,023	P		S								
	Expert 2		P		S								
	Expert 3		P		S								
C26	Expert 1	0,023											
	Expert 2												
	Expert 3												
C27	Expert 1	0,023		S	P				A		S		S
	Expert 2			S	P				A		S		S

QRs	Expert #	QR Weights	QC1	QC2	QC3	QC4	QC5	QC6	QC7	QC8	QC9	QC10	QC11
	Expert 3			S	P				A		S		S
C28	Expert 1	0,023	S		A	S		S			S		S
	Expert 2				A	S		S			S		S
	Expert 3					S		S			S		
C29	Expert 1	0,023	S		A		A	A	A		A		A
	Expert 2		S		A		A	A	A		A		A
	Expert 3		S		A		A	A	A		A		A
C210	Expert 1	0,023	S	S	A	S			S		A		A
	Expert 2		S	S	A	A			S		A		A
	Expert 3		S	S		S			S		A		A
C211	Expert 1	0,023			A		P	S		P	P		A
	Expert 2				A		P	S		P	P		A
	Expert 3				A		P	S		P	P		
C31	Expert 1	0,043									A		
	Expert 2										A		
	Expert 3										A		
C32	Expert 1	0,043									A		
	Expert 2										A		
	Expert 3										A		

QRs	Expert #	QR Weights	QC1	QC2	QC3	QC4	QC5	QC6	QC7	QC8	QC9	QC10	QC11
C33	Expert 1	0,043											
	Expert 2										A		
	Expert 3										A		
C34	Expert 1	0,043									A		
	Expert 2										A		
	Expert 3										A		
C35	Expert 1	0,043		P			A						
	Expert 2			P									
	Expert 3			P			A						
C41	Expert 1	0,033	S			S	S	S					
	Expert 2					S	S	S					
	Expert 3					S	S	S					
C42	Expert 1	0,033											
	Expert 2												
	Expert 3												
C43	Expert 1	0,033	S										
	Expert 2		A										
	Expert 3		A										
C44	Expert 1	0,033					S						

QRs	Expert #	QR Weights	QC1	QC2	QC3	QC4	QC5	QC6	QC7	QC8	QC9	QC10	QC11
	Expert 2						S						
	Expert 3						A						
C51	Expert 1	0,157						S		S			
	Expert 2							S		S			
	Expert 3							S		S			
C52	Expert 1	0,157							S		S		S
	Expert 2								S		S		S
	Expert 3								S				S

Table 12. Aggregated relationship matrix

		QCs (HOWs)										
QRs (WHATs)	**QRs weights**	**QC1**	**QC2**	**QC3**	**QC4**	**QC5**	**QC6**	**QC7**	**QC8**	**QC9**	**QC10**	**QC11**
C11	0,04			0,50		0,90				0,50		0,10
C12	0,04			0,50						0,90		0,90
C21	0,02	0,50		0,26	0,50					0,90	0,90	0,90
C22	0,02	0,90	0,10	0,90	0,90			0,90		0,83	0,90	0,83
C23	0,02		0,90	0,50						0,90	0,90	0,90
C24	0,02			0,90	0,90		0,90			0,90		
C25	0,02	0,10		0,90								
C26	0,02											
C27	0,02		0,90	0,10				0,50		0,90		0,90
C28	0,02				0,90		0,90			0,90		
C29	0,02	0,90		0,50		0,50	0,50	0,50		0,50		0,50
C210	0,02	0,90	0,90		0,83			0,90		0,50		0,50
C211	0,02			0,50		0,10	0,90		0,10	0,10		
C31	0,04									0,50		
C32	0,04									0,50		

		QCs (HOWs)										
QRs (WHATs)	**QRs weights**	**QC1**	**QC2**	**QC3**	**QC4**	**QC5**	**QC6**	**QC7**	**QC8**	**QC9**	**QC10**	**QC11**
C33	0,04											
C34	0,04									0,50		
C35	0,04		0,10									
C41	0,03				0,90	0,90	0,90					
C42	0,03											
C43	0,03	0,71										
C44	0,03					0,83						
C51	0,16						0,90		0,90			
C52	0,16							0,90				0,90
Total	1,00	4,01	2,90	5,56	4,93	3,23	5,00	3,70	1,00	9,33	2,70	6,43
Weights of QCs		**8%**	**6%**	**11%**	**10%**	**6%**	**10%**	**7%**	**2%**	**19%**	**5%**	**13%**

According to Table 12, management and organizational culture, technical capacity, experience in the field, quality and certification systems, and financial stability are important characteristics, and quality requirements to be followed for alternative supplier selection. In addition, we show the quality requirements which have the highest effect on quality characteristics in Table 13. According to this table, it is realized that to provide efficient management, have an effective organizational culture (QC9), and increase its technical capacity (QC11), the organization must manage its ordering, product, and service marketing processes successfully. And like these, to increase the experience in their field (QC3), the organizations must focus on their product and service marketing activities. In the production field, quality certification systems (QC4) are required by all parties of customers. So, to have integrated quality systems and to benefit from them, organizations must be aware of the market requirements and must have high interaction with their suppliers. The organizations aim to be financially stable have a high market share and increase their profitability, therefore they have to increase their marketing operations efficiency, they have to develop the right communication skills with their suppliers and they have determined the right price for their products and services.

Phase 3 / Step 12: The alternative suppliers list is determined. In order to create an alternative supplier list, the company has proposed five alternative suppliers: Turkey (TR), Germany (DE1, DE2), Austria (AT), and Italy (IT). The qualifications of suppliers are presented in Table 14.

Table 13. The QR/QC relationship analysis

Management and organizational culture (QC9)	**Technical capacity (QC11)**	**Experiences in the field (QC3)**
Ordering/Portal login (C12) New product introduction (C21) Change in product (C22) The product is removed from the program (C23) Media management (C24) Complaints management (C27) Identifying market-specific global trends (C28)	Ordering/Portal login (C12) New product introduction (C21) Change in product (C22) The product is removed from the program (C23) Complaints management (C27) Collaboration to improve existing service (C29)	Change in product (C22) Media management (C24) Product and service training (C25)
Quality certification systems (QC4)	**Financial stability (QC6)**	
Change in product (C22) Media management (C24) Identifying market-specific global trends (C28) Quality (C210) Company presentation (C41)	Media management (C24) Identifying market-specific global trends (C28) Accurate and timely response to price offers (C211) Company presentation (C41) Price (C51)	

Table 14. Alternatives qualifications

Alternative suppliers	**Experience**	**Number of trading countries**	**Franchise status**
TR (Turkey)	50 years	More than 80 countries	Existing
DE1 (Germany-1)	100 years	More than 150 countries	Existing
DE2 (Germany-2)	135 years	More than 100 countries	Existing
AT (Austria)	70 years	More than 120 countries	Existing
IT (Italy)	24 years	More than 70 countries	Existing

Phase 3 / Step 13: Score is calculated for suppliers by using NAHP. A neutrosophic comparison matrix was prepared for each criterion, and a comparison matrix for the first criterion (QC1) is given in Table 15 as an example.

Table 15. Pairwise comparisons of alternative for QC1 criterion

		TR	DE1	DE2	AT	IT
TR	Expert 1	(0,5, 0,5, 0,5)	(0,1, 0,9, 0,9)	(0,1, 0,9, 0,9)	(0,1, 0,9, 0,9)	(0,3, 0,7, 0,7)
	Expert 2	(0,5, 0,5, 0,5)	(0,1, 0,9, 0,9)	(0,1, 0,9, 0,9)	(0,1, 0,9, 0,9)	(0,4, 0,65, 0,6)
	Expert 3	(0,5, 0,5, 0,5)	(0,1, 0,9, 0,9)	(0,1, 0,9, 0,9)	(0,3, 0,7, 0,7)	(0,3, 0,7, 0,7)
DE1	Expert 1	(0,9, 0,1, 0,1)	(0,5, 0,5, 0,5)	(0,5, 0,5, 0,5)	(0,5, 0,5, 0,5)	(0,6, 0,35, 0,4)
	Expert 2	(0,9, 0,1, 0,1)	(0,5, 0,5, 0,5)	(0,5, 0,5, 0,5)	(0,5, 0,5, 0,5)	(0,7, 0,3, 0,3)
	Expert 3	(0,9, 0,1, 0,1)	(0,5, 0,5, 0,5)	(0,5, 0,5, 0,5)	(0,5, 0,5, 0,5)	(0,7, 0,3, 0,3)
DE2	Expert 1	(0,9, 0,1, 0,1)	(0,5, 0,5, 0,5)	(0,5, 0,5, 0,5)	(0,1, 0,9, 0,9)	(0,6, 0,35, 0,4)
	Expert 2	(0,9, 0,1, 0,1)	(0,5, 0,5, 0,5)	(0,5, 0,5, 0,5)	(0,1, 0,9, 0,9)	(0,6, 0,35, 0,4)
	Expert 3	(0,9, 0,1, 0,1)	(0,5, 0,5, 0,5)	(0,5, 0,5, 0,5)	(0,1, 0,9, 0,9)	(0,6, 0,35, 0,4)
AT	Expert 1	(0,9, 0,1, 0,1)	(0,5, 0,5, 0,5)	(0,9, 0,1, 0,1)	(0,5, 0,5, 0,5)	(0,9, 0,1, 0,1)
	Expert 2	(0,9, 0,1, 0,1)	(0,5, 0,5, 0,5)	(0,9, 0,1, 0,1)	(0,5, 0,5, 0,5)	(0,9, 0,1, 0,1)
	Expert 3	(0,7, 0,3, 0,3)	(0,5, 0,5, 0,5)	(0,9, 0,1, 0,1)	(0,5, 0,5, 0,5)	(0,9, 0,1, 0,1)
IT	Expert 1	(0,7, 0,3, 0,3)	(0,4, 0,65, 0,6)	(0,4, 0,65, 0,6)	(0,1, 0,9, 0,9)	(0,5, 0,5, 0,5)
	Expert 2	(0,4, 0,65, 0,6)	(0,3, 0,7, 0,7)	(0,4, 0,65, 0,6)	(0,1, 0,9, 0,9)	(0,5, 0,5, 0,5)
	Expert 3	(0,7, 0,3, 0,3)	(0,3, 0,7, 0,7)	(0,4, 0,65, 0,6)	(0,1, 0,9, 0,9)	(0,5, 0,5, 0,5)

Phase 3 / Step 14-15: The suppliers are sorted. Finally, the values in Table 16 were obtained by multiplying the matrix with the weights. Accordingly, even if there are close values, the supplier in Austria will be selected. The order is AT, DE2, DE1, TR, IT and.

Table 16. The weights of alternatives

Quality Characteristics	Weights	TR	DE1	DE2	AT	IT
QC1	0,08	9%	22%	24%	34%	12%
QC2	0,08	10%	25%	25%	29%	12%
QC3	0,10	20%	20%	20%	20%	20%
QC4	0,11	13%	20%	25%	30%	12%
QC5	0,07	23%	20%	20%	20%	17%
QC6	0,13	15%	20%	24%	30%	12%
QC7	0,08	13%	20%	28%	22%	18%
QC8	0,03	30%	17%	14%	17%	22%

Quality Characteristics	Weights	TR	DE1	DE2	AT	IT
QC9	0,16	15%	20%	22%	25%	19%
QC10	0,05	8%	20%	24%	34%	14%
QC11	0,12	11%	19%	24%	30%	16%
Alternatives weights		14%	20%	23%	27%	15%

It is seen that AT is the most appropriate supplier. When we analyze the qualifications of this supplier, it is seen that it has experience in the kitchen furniture industry and it exports to more than 120 countries. In addition, having franchises in Turkey provides convenience in terms of getting support.

In our study, we also analyzed the supplier evaluation criteria or QCs for every alternative. The objective of doing this is to present the efficiencies of alternative suppliers according to QCs. We have used the performance analysis model which is proposed in Bilisik et al. (2012). The most important criteria are presented in the performance analysis matrix and the company proposes a strategy for their suppliers to increase their performances as a result of this approach. The criteria are explained below and they are presented in Figure 2:

- ***Strong and important criteria:*** The criteria that have high weights and high efficiency of alternatives are evaluated primarily.
- ***Secret criteria:*** The criteria that have high weights and low efficiency are evaluated in second place.
- ***Poor and unimportant criteria:*** The criteria that have low weights and low efficiency are not evaluated preferential.
- ***Standard criteria:*** These criteria which have low weights and high efficiency are open to improvement.

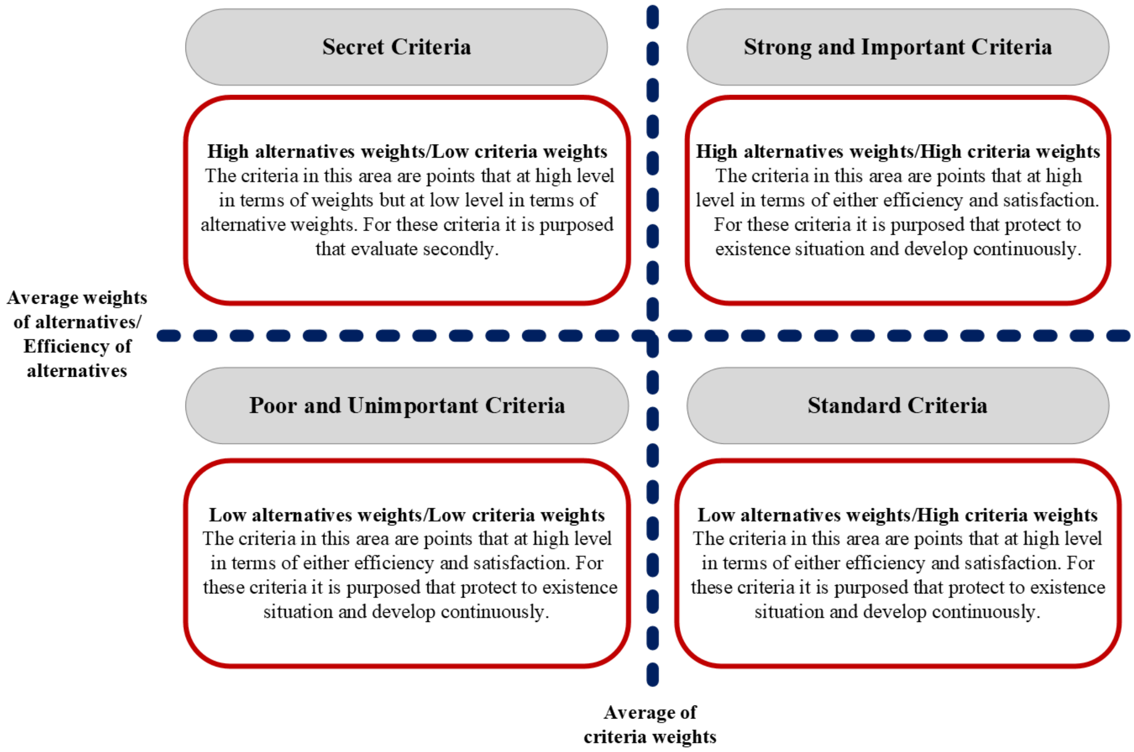

Figure 2. Performance analysis model for supplier selection criteria

The results of the performance analysis model for supplier selection criteria are shown in Figure 4. For the supplier from Turkey-***TR***, the highest QCs weights are handled as "Experiences in the field (QC3)", "Location (QC5), and "Discount (QC8)". They are QCs that must be followed and continued to increase. As seen from the matrix of TR, there are not any QC which is located in strong and important criteria areas. This means, the supplier must focus on standard criteria and increase the quality characteristics which are "Quality certification systems (QC4)", "Management and organizational culture (QC9)", "Financial stability (QC6)", "Reliability of the raw material to the customer and manufacturing processes (QC7)" and Technical capacity (QC11)". For the first supplier from Germany-***DE1***, "Number of patents (QC1)" and "Reverse logistics rate (QC2)" have the highest importance weights and these must be continuously followed and increased. In addition, "Financial stability (QC6), "Reliability of the raw material to the customer and manufacturing processes (QC7)", "Management and organizational culture (QC9)" and "Technical capacity (QC11)" criteria/QCs have lower efficiency, so the suppliers must focus on them and increase the performance. The second supplier from Germany-***DE2*** has strong and important criteria which are "Quality certification systems (QC4)", "Financial stability (QC6)", "Reliability of the raw material to the customer and manufacturing processes (QC7)", "Management and organizational culture (QC9)" and "Technical capacity (QC11)". This company has the second highest average efficiency value and it must protect this strong qualification. Supplier from Austria-***AT*** is the best alternative according to criteria/QCs and the "Quality certification systems (QC4)", "Financial stability (QC6)" and "Technical capacity (QC11)" criteria are determined as strong and important criteria. The weights of criteria for this supplier according to criteria have the highest values and the company must protect and continuously improve their capabilities. Suppliers from Italy-***IT*** have three strong and important criteria which are "Reliability of the raw material to the customer and manufacturing processes (QC7)," "Management and organizational culture (QC9)", and "Technical capacity (QC11)". The company must protect this situation but it must increase the average efficiency value by developing criteria which are determined as standard and poor/unimportant criteria.

3.1. Sensitivity Analysis

In our study, we have determined the QRs' weights by using the NAHP technique and to show the sensitivity of our methodology we have compared the results by changing QRs' weights. In the first scenario, we considered equal QR weights, and in the second scenario, we asked experts to evaluate QRs' importance weights. In Table 17, the result of the sensitivity analysis is presented, and as can be seen in Figure 3, there is not any change in the ranking of alternatives. This can be interpreted as the weights of customer requirements do not influence the final rankings of alternatives.

Table 17. Sensitivity analysis results

	Methodology	**Equal criteria weights**	**Experts' criteria evaluations**
TR	0.1417	0.1425	0.1420
DE1	0.2003	0.2022	0.2025
DE2	0.2350	0.2314	0.2319
AT	0.2658	0.2703	0.2702
IT	0.1571	0.1536	0.1534

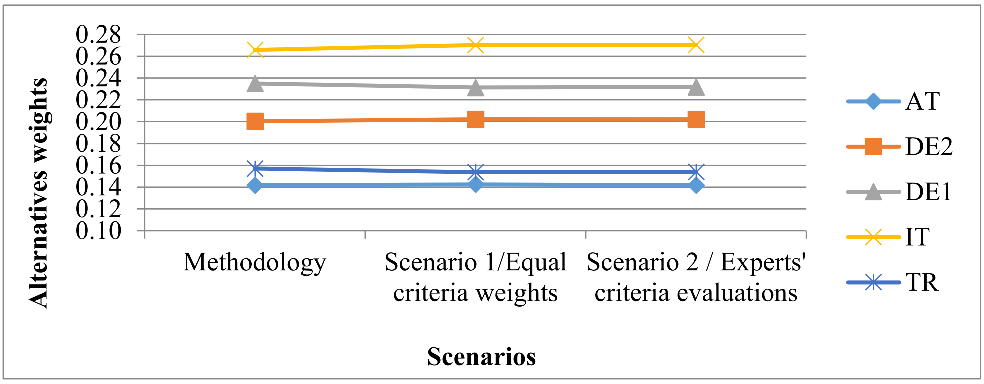

Figure 3. The ranking of alternatives

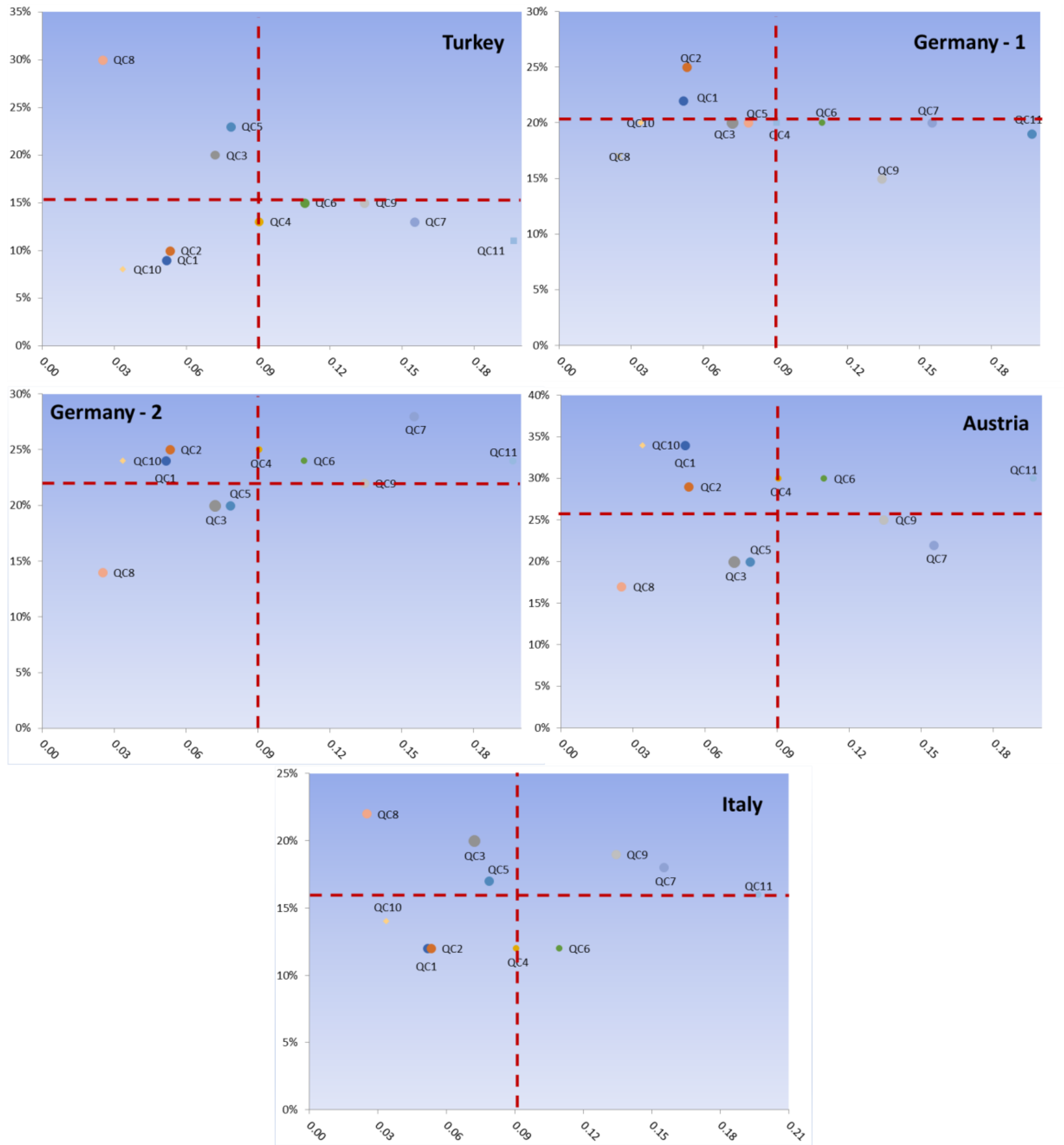

Figure 4. The result of criteria analysis for alternatives

4. Conclusion

Today, with the increase in challenging supply chain conditions for organizations, working with the most appropriate supplier gets more crucial. In addition, considering customers' expectations, needs and requirements is a necessity for organizations to survive for a long time. In our study, with awareness of the importance of these issues, we proposed a customer-oriented methodology to analyze QRs, QCs, and alternative suppliers. Supplier selection problems involve important strategic and operational decisions in a competitive environment with a short lifecycle and where the customer indirectly contributes to the product. In subsequent research, sustainability will play a significant role in the supplier selection process. Thus, customer-oriented supplier selection problems contribute to the literature by adding more environmentally friendly, social, and economic supplier selection criteria.

As a result of our research, although there are several publications that deal with the problem of supplier selection in a furniture production organization, no study has been found that deals with the problem of customer-oriented supplier selection with the QFD and AHP hybrid methodology. In addition, since the evaluators did not have precise information and made their evaluations with linguistic expressions, the evaluation was made with the neutrosophic sets. The business discussed in this study is a company that has customer-oriented production and designs serving in the kitchen furniture sector. For this reason, a model has been proposed in the study to make the most suitable supplier selection considering the requirements of the customers. The theoretical advancement and practical implications according to problem, methodology, and application are given in Table 18.

Table 18. *The theoretical advancements and practical impacts of key categories of this study*

Key Categories	**Theoretical Advancements**	**Practical Impacts**
Customer-oriented supplier selection	When the literature is investigated, it is realized that there is not any study about customer-oriented supplier selection for modular kitchen furniture production organization. This study is a novel application, and it will help decision-makers deal with this problem.	With the increase in demand in the kitchen furniture sector, it gets harder to be customer-oriented and to work with the most convenient suppliers. So this study will help sector professionals to manage their end-to-end supply chain process efficiently.
Neutrosophic AHP-QFD	The theory is advanced by applying the methodology to a totally new problem in the literature.	Experts in other industries can apply this methodology to determine the most appropriate suppliers to work with.
Application	This application contributes to the furniture production supply chain theory.	The application conducted is for modular kitchen furniture producers and when the

	literature is researched, it is found that there is not any study that handles this problem.

Neutrosophic AHP was applied to determine the importance levels of the criteria/customer requests determined in the first phase of the study. In the second phase, the quality requirements necessary to meet the customer demands were determined and the weights of the quality requirements were found with the quality function deployment approach. In the third phase, the neutrosophic AHP technique was used again to evaluate alternative suppliers, taking into account the weights of the determined quality requirements. As a result, the ranking of the alternatives was obtained as follows: Austria, Germany-2, Germany-1, Italy, and Turkey. The application of neutrosophic AHP in determining the importance levels of criteria and customer requests, coupled with the integration of the quality function deployment approach in defining quality requirements, demonstrates a comprehensive and systematic methodology for supplier evaluation. The results of the study, which ranked Austria as the top supplier, Germany-2 and Germany-1 following closely, provide actionable insights for the company under consideration.

Our research has made a significant contribution to the field of supplier selection in the context of customer-oriented production within the kitchen furniture sector. The absence of prior studies addressing the specific problem of customer-oriented supplier selection using the AHP hybrid methodology highlights the novelty and importance of this research. The introduction of the neutrosophic sets in the evaluation process, particularly due to evaluators relying on linguistic expressions, adds a considerable dimension to the study. The proposed model aims to optimize supplier selection by considering customers' preferences, experts' opinions, and design-oriented suppliers.

The limitations of our study can be explained as follows: Because this methodology is applied in the kitchen furniture industry, the number of experts is limited. We have asked three experts for their evaluations. Increasing the number of organizations and sector experts may provide more holistic results but this process will take a longer time and be harder. In addition, the evaluations are made using neutrosophic AHP-QFD hybrid methodology. The neutrosophic fuzzy sets are used in all phases and this increases the complexity of the methodology.

This study will give insight to managers to evaluate the performance of suppliers and select the most suitable supplier who is more customer-focused. In the proposed method, we determine supplier selection criteria weights via the neutrosophic AHP technique and we related these criteria with QCs via the neutrosophic QFD approach to find the most appropriate supplier. While evaluating suppliers, using this hybrid decision-making approach will provide organizational efficiency by considering qualitative and quantitative criteria. Additionally, the performance analysis model used provides a decision support structure for managers. Thanks to this model, managers will be able to see the level of fulfillment of the criteria and enable action plans to be made regarding them.

In future studies, solutions can be developed by using different solution methodologies for customer-oriented supplier selection. Applications of the methodology used in this study in different sectors can be examined. In addition, while choosing a supplier, the criteria can be updated with a sustainability-oriented approach as well as a customer-oriented approach. Future studies could explore alternative solution methodologies for customer-oriented supplier selection and investigate the applicability of the proposed model in diverse industry sectors. Additionally, there is potential to update supplier selection criteria with a sustainability-oriented approach, aligning with the growing importance of environmentally conscious practices in contemporary business operations. Overall, this research lays the foundation for further advancements in the strategic process of supplier selection, emphasizing the need for ongoing innovation and adaptation in response to evolving business landscapes.

Data availability statement

Authors can be contacted if any other data related to the study is required.

References

Akman, G., Boyacı, A. İ., & Kurnaz, S. (2022). Selecting the suitable e-commerce marketplace with neutrosophic Fuzzy AHP and EDAS methods from seller's perspective in the context of Covid-19. International Journal of the Analytic Hierarchy Process, 14(3).

Alzahrani, F. A., Ghorui, N., Giri, B. C., Gazi, K. H., Ghosh, A., & Mondal, S. P. (2023, January 6). Optimal Site Selection for Women University Using Neutrosophic Multi-Criteria Decision Making Approach. Buildings.

Ambilkar, P., Verma, P., Das, D., (2024). Sustailient supplier selection using neutrosophic best–worst approach: a case study of additively manufactured trinkets. *Benchmarking.*

Asadabadi, M. R. (2017). A customer based supplier selection process that combines quality function deployment, the analytic network process and a Markov chain. *European Journal of Operational Research*, 1049–1062.

Asadabadi, M. R. (2017, June 15). A customer based supplier selection process that combines quality function deployment, the analytic network process and a Markov chain. European Journal of Operational Research, s. 1049-1062.

Ayyildiz, E., Murat, M., Imamoglu, G., & Kose, Y. (2023). A novel hybrid MCDM approach to evaluate universities based on student perspective. Scientometrics, s. 55–86.

Babbar, C., & Amin, S. (2018). A multi-objective mathematical model integrating environmental concerns for supplier selection and order allocation based on fuzzy QFD in beverages industry. *Expert Systems With Applications*, 27-38.

Bao, X., & Li, F. (2021). A methodology for supplier selection under the curse of dimensionality problem based on fuzzy quality function deployment and interval data envelopment analysis. Plos one, 16(7), e0253917.

Başhan, V., Demirel, H., & Gul, M. (2020). A novel risk evaluation approach for frequently encountered risks in ship engine rooms. Brodogradnja, s. 31-54.

Bevilacqua, M., Ciarapica, F., & Giacchetta, G. (2006). A fuzzy-QFD approach to supplier selection. *Journal of Purchasing & Supply Management* , 14-27.

Bhattacharya, A., Geraghty, J., & Young, P. (2010). Supplier selection paradigm: An integrated hierarchical QFD methodology under multiple-criteria environment. *Applied Soft Computing*, 1013–1027.

Bilandi, N., Verma, H. K., & Dhir, R. (2020, April 17). AHP–neutrosophic decision model for selection of relay node in wireless body area network. CAAI Transactions on Intelligence Technology, s. 222-229.

Bilişik, M. E., Çağlar, N., & Bilişik, Ö. N. A. (2012). A comparative performance analyze model and supplier positioning in performance maps for supplier selection and evaluation. Procedia-Social and Behavioral Sciences, 58, 1434-1442.

Cebi, S., Kahraman, C., Er, I. D., & Celik, M. (2009). An integrated fuzzy QFD model proposal on routing of shipping investmentdecisions in crude oil tanker market. *Expert Systems with Applications*, 6227–6235.

Chai, J., & Ngai, E. W. (2020). Decision-making techniques in supplier selection: Recent accomplishments and what lies ahead. *Expert Systems With Applications*, 112903.

Chakrabortty, R. K., Abdel-Basset, M., & Ali, A. M. (2023, January 20). A multi-criteria decision analysis model for selecting an optimum customer service chatbot under uncertainty. Decision Analytics Journal.

Chen, C.-H. (2020, February 24). A Novel Multi-Criteria Decision-Making Model for Building Material Supplier Selection Based on Entropy-AHP Weighted TOPSIS. Entropy.

Chen, Y., Ran, Y., Huang, G., Xiao, L., & Zhang, G. (2021). A new integrated MCDM approach for improving QFD based on DEMATEL and extended MULTIMOORA under uncertainty environment. *Applied Soft Computing*, 107222.

Dang, T.-T., Nguyen, N.-A.-T., Nguyen, V.-T.-T., & Dang, L.-T.-H. (2022, May 13). A Two-Stage Multi-Criteria Supplier Selection Model for Sustainable Automotive Supply Chain under Uncertainty. Axioms.

Das, S., Roy, B. K., Kar, M. B., Kar, S., & Pamučar, D. (2020). Neutrosophic fuzzy set and its application in decision making. Journal of Ambient Intelligence and Humanized Computing, 11, 5017-5029.

de Araújo Souza, S. M. O., de Oliveira Fontes, C. H., & Freires, F. G. M. (2022, July). Use of QFD to Prioritize Requirements Needed for Supplier Selection in an O&G Project. In International Joint conference on Industrial Engineering and Operations Management (pp. 169-180). Cham: Springer International Publishing.

Deivanayagampillai, N., Jacob, K., Thangavel, B., Suppaiah, Y. (2026, June). Robust Green Supplier Selection Using an Adaptive Neutrosophic Decision-Making Approach in Sustainable Supply Chain Management. *Process Integration and Optimization for Sustainability.*

Dursun, M., & Karsak, E. E. (2013). A QFD-based fuzzy MCDM approach for supplier selection. *Applied Mathematical Modelling*, 5864 - 5875.

Erdebilli, B., Yilmaz, I., Aksoy, T., Hacıoglu, U., Yüksel, S., & Dinçer, H. (2023). An interval-valued pythagorean fuzzy AHP and COPRAS hybrid methods for the supplier selection problem. International Journal of Computational Intelligence Systems, 16(1), 124.

Galankashi, M. R., Helmi, S. A., & Hashemzahi, P. (2016, February 7). Supplier selection in automobile industry: A mixed balanced scorecard–fuzzy AHP approach. Alexandria Engineering Journal, s. 93-100.

Haiyun, C., Zhixiong, H., Yüksel, S., & Dinçer, H. (2021). Analysis of the innovation strategies for green supply chain management in the energy industry using the QFD-based hybrid interval valued intuitionistic fuzzy decision approach. *Renewable and Sustainable Energy Reviews*, 110844.

Harnpornchai, N., & Wonggattaleekam, W. (2021, October 19). An application of neutrosophic set to relative importance assignment in AHP. Mathematics, s. 2636.

Hendiani, S., Mahmoudi, A., & Liao, H. (2020). A multi-stage multi-criteria hierarchical decision-making approach for sustainable supplier selection. *Applied Soft Computing Journal*, 106456.

Hezam, I. M., Nayeem, M. K., Foul, A., & Alrasheedi, A. F. (2021). COVID-19 Vaccine: A neutrosophic MCDM approach for determining the priority groups. Results in Physics.

Jain, N., & Singh, A. (2020). Sustainable supplier selection under must-be criteria through Fuzzy inference system. *Journal of Cleaner Production*, 119275.

Junaid, M., Xue, Y., Syed, M. W., Li, J. Z., & Ziaullah, M. (2020, December 24). A Neutrosophic AHP and TOPSIS Framework for Supply Chain Risk Assessment in Automotive Industry of Pakistan. Sustainability .

Kahraman, C., Çebi, S., Onar, S. Ç., & Öztayşi, B. (2022, September 24). Recent Developments on Fuzzy AHP and ANP Under Vague and Imprecise Data: Evidence from INFUS Conferences. International Journal of the Analytic Hierarchy Process.

Karabayır, A. N., & Botsalı, A. R. (2022). Supplier Selection Among Different Scale Construction Companies Using Fuzzy AHP And Fuzzy TOPSIS. El-Cezerî Journal of Science and Engineering, s. 35-48.

Karamaşa, Ç., Demir, E., Memiş, S., & Korucuk, S. (2020, November 9). Weighting The Factors Affecting Logistics Outsourcing. Decision Making: Applications in Management and Engineering, s. 19-32.

Karamaşa, Ç., Karabasevic, D., Stanujkic, D., Kookhdan, A. R., Mishra, A. R., & Ertürk, M. (2021, August 18). An Extended Single-Valued Neutrosophic Ahp And Multimoora Method To Evaluate The Optimal Training Aircraft For Flight Training Organizations. Facta Universitatis Mechanical Engineering, s. 555 - 578.

Karasan, A., Ilbahar, E., Cebi, S., & Kahraman, C. (2022, January 21). Customer-oriented product design using an integrated neutrosophic AHP & DEMATEL & QFD methodology. Applied Soft Computing.

Karsak, E. E., & Dursun, M. (2014). An integrated supplier selection methodology incorporating QFD and DEA with imprecise data. *Expert Systems with Applications*, 6995–7004.

Karuppiah, K., Sankaranarayanan, B., Ali, S. M., & Paul, S. K. (2021, May 22). Key Challenges to Sustainable Humanitarian Supply Chains: Lessons from the COVID-19 Pandemic. Sustainability.

Kaya, N. S., Özkan, B., Dengiz, O., & Turan, İ. D. (2022, Mart 30). Digital mapping and spatial variability of soil quality index for desertification in the Akarçay Basin under the semi-arid terrestrial ecosystem using neutrosophic fuzzy-AHP approach. Natural Hazards, s. 2101–2132.

Khan, F., Ali, Y., & Pamucar, D. (2022). A new fuzzy FUCOM-QFD approach for evaluating strategies to enhance the resilience of the healthcare sector to combat the COVID-19 pandemic. *Emerald* Publishing Limited, 1429-1451.

Khorram, M., Sheibani, M., & Niroomand, S. (2024). A Decision Framework Based on Integration of DEMATEL, QFD, TOPSIS and VIKOR Approaches for Fuzzy Multi-Criteria Supplier Selection Problem. Journal of Uncertain Systems, 2440002.

Koirala, K., & Shabbiruddin. (2023). Optimal selection of sustainable battery supplier for electric vehicle battery swapping station. Energy Sources, Part A: Recovery, Utilization, and Environmental Effects, 45(1), 2206-2227.

Lahdhiri, M., Babay, A., & Jmali, M. (2022). Multi-criteria Decision Making Using Hybrid methods for Supplier Selection in the Clothing Industry. Fibres and Textiles in Eastern Europe, s. 23-34.

Lima-Junior, F. R., & Carpinetti, L. C. (2016). A multicriteria approach based on fuzzy QFD for choosing criteria for supplier selection. *Computers & Industrial Engineering*, 269–285.

Liu, A., Liu, T., Mou, J., & Wang, R. (2020, July 10). A supplier evaluation model based on customer demand in blockchain tracing anti-counterfeiting platform project management. Journal of Management Science and Engineering, s. 172-194.

Liu, P., Gao, H., & Ma, J. (2019). Novel green supplier selection method by combining quality function deployment with partitioned Bonferroni mean operator in interval type-2 fuzzy environment. *Information Sciences*, 292–316.

Navarro, I. J., Martí, J. V., & Yepes, V. (2021, February 28). Neutrosophic Completion Technique for Incomplete Higher-Order AHP Comparison Matrices. Mathematics.

Navarro, I. J., Yepes, V., & Marti, J. V. (2019, June 18). Sustainability assessment of concrete bridge deck designs in coastalenvironments using neutrosophic criteria weights. Structure and Infrastructure Engineering, s. 949–967.

Öztürk, M., & Paksoy, T. (2020, May 25). A combined DEMATEL-QFD-AT2 BAHP approach for green supplier selection. Journal of the Faculty of Engineering and Architecture of Gazi University, s. 2023-2043.

Rahman, M. A., Karmaker, C. L., Ahmed, T., Khan, M. I., Morshed, A. M., & Ali, S. M. (2022, May 27). Modelling the causes of boiler accidents: implications for economic and social sustainability at the workplace. Heliyon.

Rajesh, G., & Malliga, P. (2013). Supplier Selection Based on AHP QFD Methodology. *Procedia Engineering*, 1283 – 1292.

Reig-Mullor, J., Garcia-Bernabeu, A., Pla-Santamaria, D., & Vercher-Ferrandiz, M. (2022, July 5). EVALUATING ESG CORPORATE PERFORMANCE USING A NEW NEUTROSOPHIC AHP-TOPSIS BASED APPROACH. Technological and Economic Development of Economy, s. 1244-1266.

Sánchez-Garrido, A. J., Navarro, I. J., & Yepes, V. (2021, April 20). Neutrosophic multi-criteria evaluation of sustainable alternatives for the structure of single-family homes. Environmental Impact Assessment Review.

Sharma, J., & Tripathy, B. B. (2023). An integrated QFD and fuzzy TOPSIS approach for supplier evaluation and selection. The TQM Journal.

Singh, A., & Kumar, S. (2021). Picture fuzzy set and quality function deployment approach based novel framework for multi-criteria group decision making method. *Engineering Applications of Artificial Intelligence.*

Singh, A., Das, A., Bera, U. K., & Lee, G. M. (2021, July 28). Prediction of Transportation Costs Using Trapezoidal Neutrosophic Fuzzy Analytic Hierarchy Process and Artificial Neural Networks. IEEE, s. 103497–103512.

Seifbarghy, M., Hamidi, M. (2025, November 6). Supplier selection in Neutrosophic environment with a hybrid fuzzy decision-making method. *Opsearch.*

Smarandache, F. (2007, June 5). InfoLearnQuest: http://fs.unm.edu/eBook-Neutrosophics6.pdf

Tang, Y., & Yang, Y. (2021). Sustainable e-bike sharing recycling supplier selection: An interval-valued Pythagorean fuzzy MAGDM method based on preference information technology. *Journal of Cleaner Production*, 125530.

Tayyar, S. H., & Soltani, R. (2020, December). Supplier Selection Through a Hybrid MCDM-QFD Method: A Case Study in Mapna Group. In International Conference on Logistics and Supply Chain Management (pp. 117-136). Cham: Springer International Publishing.

Tuan, N. A., Hue, T. T., Lien, L. T., Thao, T. D., Duy, N., Van, L. H., & Anh, L. T. (2020). A new integrated MCDM approach for lecturers' research productivity evaluation. Decision Science Letters, s. 355–364.

Vafadarnikjoo, A., & Scherz, M. (2021, June 18). A Hybrid Neutrosophic-Grey Analytic Hierarchy Process Method: Decision-Making Modelling in Uncertain Environments. Mathematical Problems in Engineering.

Vafadarnikjoo, A., Ahmadi, H. B., Liou, J. J., Botelho, T., & Chalvatzis, K. (2023). Analyzing blockchain adoption barriers in manufacturing supply chains by the neutrosophic analytic hierarchy process. Annals of Operations Research, s. 129–156.

Wang, T.-K., Zhang, Q., Chong, H.-Y., & Wang, X. (2017, February 16). Integrated Supplier Selection Framework in a Resilient Construction Supply Chain: An Approach via Analytic Hierarchy Process (AHP) and Grey Relational Analysis (GRA). Sustainability.

Wang, Y.-J., L.-J. L., & Han, T.-C. (2022). Interval-Valued Fuzzy Multi-Criteria Decision-Making with Dependent Evaluation Criteria for Evaluating Service Performance of International Container Ports. *Journal of Marine Science and Engineering*, 1-21.

Xu, Z., & Liao, H. (2014, Ağustos). Intuitionistic Fuzzy Analytic Hierarchy Process. IEEE TRANSACTIONS ON FUZZY SYSTEMS, s. 749-761.

Yang, C., Grey Relational Analysis Framework with 2-Tuple Linguistic Neutrosophic. (2025). *Neutrosophic Sets and Systems.*

Yazdani, M., Chatterjee, P., Zavadskas, E. K., & Zolfani, S. H. (2017). Integrated QFD-MCDM framework for green supplier selection. *Journal of Cleaner Production*, 3728-3740.

Ye, F., Xu, X., Zhang, Y., Ye, Y., & Dai, J. (2023, June 21). Marketing Model Analysis of Fashion Communication Based on the Visual Analysis of Neutrosophic Systems. Intelligent Automation and Soft Computing, s. 1257–1274.

Yiğit, F. (2023, May 27). A three-stage fuzzy neutrosophic decision support system for human resources decisions in organizations. Decision Analytics Journal.

Zhang, Z., Liao, H., Chang, J., & Al-barakati, A. (2019, December 13). Green-Building-Material Supplier Selection with a Rough-Set-Enhanced Quality Function Deployment. Sustainability.

Zheng, J., Li, Y. H., & Fan, Z. P. (2023). Demand-driven NEV supplier selection: An integrated method based on ontology–QFD–CBR. Frontiers in Energy Research, 10, 958885.

Received: Aug. 12, 2026. Accepted: Sept. 13, 2026.

N-CogHCI: A Reliability-Aware Neutrosophic Cognitive Control Framework for Cognitive AI-Enhanced Human–Computer Interaction

Nada Mohamed[1] and Alshaimaa A. Tantawy[2,*]

[1] Nada Mohamed Faculty of Computers and Informatics, Zagazig University, Zagazig 44519, Sharqiyah, Egypt; Nada.mohamed1316@hti.edu.eg

[2] Alshaimaa A. Tantawy Faculty of Computers and Informatics, Zagazig University, Zagazig 44519, Sharqiyah, Egypt; AlshaimaaTantawy@zu.edu.eg

* Correspondence: AlshaimaaTantawy@zu.edu.eg

Abstract: Cognitive AI systems increasingly participate in decisions that were previously controlled entirely by human users, yet most adaptive interfaces still compress uncertain user states into a single class probability or a fixed automation level. This paper introduces N-CogHCI, a reliability-aware neutrosophic cognitive control framework that represents cognitive evidence as truth, indeterminacy, and falsity components and uses that state to regulate human–AI authority in real time. The framework combines reliability-weighted multimodal evidence, explicit disagreement and missingness modeling, AI epistemic uncertainty, task risk, human expertise, and a safety gate that constrains autonomy when uncertainty and consequence are jointly high. A discrete authority variable selects among human-only, human-led shared, balanced shared, AI-led shared, and autonomous modes, while the interface policy adapts explanation depth, confirmation requirements, information density, and intervention timing. Formal analysis establishes boundedness of the state representation and monotonic growth of indeterminacy as evidence quality falls or cross-source disagreement rises. A reproducible controlled Monte-Carlo stress test of 100,000 interaction states (seed 42) evaluates the controller under clean, noisy, missing, and contradictory evidence. N-CogHCI reduced high-autonomy decisions in predefined unsafe contexts to 8.31%, compared with 14.20% for crisp mean fusion and 11.92% for reliability-weighted probabilistic fusion. In high-uncertainty contexts, the corresponding rates were 15.42%, 27.74%, and 21.60%. This safety gain was obtained with a small increase in normalized decision loss (0.2053 versus 0.2037 and 0.2037), exposing rather than hiding the safety–efficiency trade-off. No empirical performance is claimed for human-participant datasets that were not executed. Instead, a leakage-resistant validation protocol is specified for COLET, SWELL-KW, and CLAS. The results support neutrosophic indeterminacy as a control variable for mixed-initiative HCI, while identifying real-user validation as the necessary next empirical step.

Keywords: neutrosophic sets; cognitive AI; human–computer interaction; human–AI teaming; cognitive workload; uncertainty; adaptive interfaces; shared control; trust calibration; soft computing.

Highlights

- A neutrosophic cognitive state preserves supportive, opposing, and unresolved evidence instead of forcing uncertain user signals into a single probability.
- A risk-aware authority controller couples user workload, AI uncertainty, evidence indeterminacy, and human expertise to five interpretable control modes.
- Formal properties guarantee bounded states and monotonic increases in indeterminacy as evidence quality deteriorates or disagreement increases.
- A 100,000-trial controlled stress test shows substantially fewer high-autonomy decisions in unsafe and high-uncertainty contexts, with a quantified efficiency trade-off.
- COLET, SWELL-KW, and CLAS are specified as public external-validation benchmarks without fabricating unexecuted empirical results.

1. Introduction

Human–AI interaction has moved from isolated recommendation interfaces toward systems that continuously infer user state, generate advice, allocate functions, and sometimes execute actions. This transition changes the HCI problem. The central design question is no longer only whether an AI model is accurate, but when the system should assist, defer, explain, request confirmation, or assume greater authority. General human–AI interaction guidelines already emphasize communicating system capability, supporting correction, and adapting behavior over time [1]. Classical automation research likewise treats function allocation as a continuum rather than a binary division between human and machine [2]. These principles become more difficult to operationalize when the user is cognitively overloaded, the AI is uncertain, the task is consequential, and the evidence about the user is itself incomplete or contradictory.

Trust further complicates this control problem. Appropriate reliance requires alignment between human trust and actual system capability rather than simply maximizing confidence in automation [3,4]. Recent work has therefore shifted toward calibrated trust [5], context-sensitive algorithm trust [6], and models of human control that move from supervision toward teaming [7]. Dynamic task allocation has also been identified as an open problem in industrial human–AI teaming, where agency, control, and risk cannot be separated from performance [8]. Optimized shared-control approaches can adapt the confidence ratio between human and AI controllers [9], and recent calibrated adaptive human–AI frameworks explicitly incorporate probability calibration and epistemic uncertainty into closed-loop reliance [10]. These developments establish the need for adaptive authority, but they do not resolve how contradictory or missing evidence about the human cognitive state should enter the control law.

Cognitive-state-aware interfaces provide another part of the solution. Cognitive load can be incorporated into user models to support adaptive interface behavior [11], while workload instruments such as NASA-TLX remain widely used for subjective workload assessment [12]. Public datasets make cognitive-state modeling reproducible: COLET records eye behavior from 47 individuals across four induced workload levels with NASA-TLX annotation [13]; SWELL-KW records 25 participants performing knowledge-work tasks under neutral, interruption, and time-pressure conditions using behavioral and physiological modalities [14]; and CLAS provides synchronized ECG, PPG, EDA, accelerometer, and task information from 62 participants performing cognitive and affective tasks [15]. A persistent methodological weakness, however, is that uncertainty in these heterogeneous signals is usually reduced to a probability, confidence score, or missing-value flag. Such compression loses the distinction between evidence that supports a cognitive state, evidence that opposes it, and evidence that is unresolved.

Soft computing was developed precisely for reasoning in systems where exact models are unavailable or unnecessarily rigid [16]. Neutrosophic sets, introduced within Smarandache's neutrosophic framework [17] and made computationally practical through single-valued neutrosophic sets (SVNSs) [18], provide a three-component representation of truth, indeterminacy, and falsity. This structure is attractive for cognitive HCI because a user can simultaneously exhibit signals supporting high workload, signals opposing that interpretation, and unresolved evidence caused by sensor failure, individual variability, or modality conflict. Recent refined neutrosophic cognitive maps have shown how indeterminate causal relationships can be represented explicitly rather than absorbed into ordinary fuzzy membership [19]. The remaining opportunity is to move neutrosophic reasoning from post-hoc ranking into the real-time control loop of human–AI interaction.

This paper addresses that opportunity through N-CogHCI, a reliability-aware neutrosophic cognitive controller for mixed-initiative HCI. The contribution is not another interface-ranking method. N-CogHCI uses indeterminacy as an operational control variable that can reduce autonomy, trigger explanation, or force shared control when the system lacks sufficient justification for a stronger automated action. The method is deliberately formulated so that it can operate with eye tracking alone, with multimodal physiological and behavioral signals, or with partial sensor availability. The paper makes five contributions: (i) a reliability-aware neutrosophic state estimator that combines local model uncertainty, modality reliability, disagreement, and missingness; (ii) a risk-aware human–AI authority optimization rule with a deterministic safety gate; (iii) a trust-calibration and adaptive-interface layer that responds differently to uncertainty, overtrust, and undertrust; (iv) formal properties showing boundedness and monotonic behavior of the indeterminacy term; and (v) an executable controlled stress test plus a subject-independent external-validation protocol for public cognitive HCI datasets.

2. Related Work and Research Gap

2.1 Cognitive workload and adaptive HCI

Adaptive interfaces require a user model that is updated from interaction evidence rather than a static demographic profile. Suryani et al. [11] explicitly linked cognitive-load modeling to adaptive interface development, illustrating the relevance of cognition to interface adaptation. NASA-TLX provides a multidimensional subjective workload instrument and remains a standard reference for workload studies [12]. COLET [13] complements subjective assessment with eye and gaze behavior and demonstrates that workload levels can be associated with ocular features. SWELL-KW [14] broadens the measurement space to computer interaction, facial behavior, posture, heart-rate variability, and skin conductance in realistic knowledge work. CLAS [15] adds synchronized physiological channels and cognitive tasks. Together, these datasets establish that cognitive state is observable only indirectly and through heterogeneous evidence. They do not, by themselves, specify how an adaptive interface should behave when those signals conflict or disappear.

2.2 Human–AI trust, reliance, and authority allocation

Trust has long been recognized as a determinant of reliance on automation [3,4]. The contemporary emphasis is calibration: overtrust can produce inappropriate reliance, whereas undertrust can suppress beneficial automation [5]. Yang et al. [6] further show that task context and time pressure can shape algorithm trust, reinforcing the need for dynamic rather than fixed reliance policies. Cognitive forcing functions can reduce overreliance, but they may impose subjective usability costs [20]. At the control level, Parasuraman et al. [2] conceptualized multiple types and levels of automation, and recent work has revisited human control for foundation-model systems [7], dynamic allocation in human–AI teaming [8], and shared control with adaptive human/AI confidence ratios [9]. The 2026 CAHAT framework [10] is especially close in spirit because it combines adaptive reliance, calibration, uncertainty, and closed-loop decision-making. N-CogHCI differs in its primary representation: uncertainty in the human cognitive state is not a scalar confidence deficit but an explicit neutrosophic component derived from disagreement, local uncertainty, reliability, and missingness.

2.3 Soft computing and neutrosophic modeling

Soft computing combines approximate reasoning and learning mechanisms to tolerate imprecision in complex systems [16]. Fuzzy membership is useful when a state is gradual, but ordinary membership does not separately encode unresolved evidence. Neutrosophic sets introduce truth (T), indeterminacy (I), and falsity (F) as distinct components [17], while SVNSs provide a computational formulation with components in the unit interval [18]. This separation is particularly relevant when HCI sensors are incomplete or mutually inconsistent. Refined neutrosophic cognitive maps extend this idea to causal graphs with indeterminate relationships [19]. Nevertheless, most neutrosophic decision applications remain evaluative: they rank alternatives after uncertainty has been summarized. The present work instead treats I as a first-class signal in a control policy that changes the degree and form of AI intervention.

2.4 Gap synthesis

Table 1. Positioning of N-CogHCI relative to the closest methodological streams.

Study / stream	Human cognitive state	Explicit indeterminacy	Dynamic authority	Primary validation
Adaptive HCI [11]	Yes	No	Interface adaptation	Methodology / user-model design
Human–AI control [2,7–9]	Context-dependent	Mostly probabilistic	Yes	Human factors / control studies
Calibrated trust [5,10]	Partial	Probabilistic uncertainty	Yes	Review / controlled simulation
RNCM [19]	Generic concepts	Yes	Not HCI authority allocation	Causal modeling
N-CogHCI (this work)	Yes	Yes: T–I–F	Yes: five modes + safety gate	Formal analysis + reproducible stress test

The table distinguishes the representation of uncertainty from the presence of an adaptive controller; these are separate design choices.

The gap can therefore be stated precisely: current adaptive HCI can model workload; human–AI teaming can vary authority; probabilistic frameworks can calibrate AI uncertainty; and neutrosophic models can represent indeterminacy. What is missing is a unified controller in which the indeterminacy of the human cognitive-state estimate directly constrains authority and interface behavior. N-CogHCI is designed to fill this gap without claiming that neutrosophic logic replaces probabilistic calibration. The two are complementary: probabilities can estimate event likelihoods, while the neutrosophic state records the epistemic status of the evidence feeding the HCI controller.

3. Problem Formulation

Consider an interactive system observed at discrete interaction cycles $t = 1, 2, \dots$. The system receives M sources of evidence about a cognitive concept c, such as high workload, low attention, stress, or comprehension difficulty. For source m, $p_{m,c}(t) \in [0,1]$ denotes the source-specific support probability, $u_{m,c}(t) \in [0,1]$ denotes local model uncertainty, $r_m(t) \in [0,1]$ denotes signal reliability, and $a_m(t) \in \{0,1\}$ denotes availability. The controller also receives an AI confidence $c_A(t)$, an AI uncertainty $u_A(t)$, task risk $R(t)$, human expertise $H(t)$, and—where available—an observed trust or reliance estimate $\tau(t)$. The output is an authority level $\alpha(t)$ selected from $A = \{0, 0.25, 0.50, 0.75, 1\}$. These values correspond respectively to human-only control, human-led shared control, balanced shared control, AI-led shared control with human confirmation, and autonomous AI action.

Table 2. Core notation used in N-CogHCI.

Symbol	Meaning	Range
p_m,c	support for cognitive concept c from modality m	[0,1]
u_m,c	local uncertainty of modality/model m	[0,1]
r_m	source/signal reliability	[0,1]
a_m	availability indicator	{0,1}
T_c, I_c, F_c	aggregated neutrosophic cognitive state	[0,1]^3
c_A, u_A	AI confidence and uncertainty	[0,1]
R	task/consequence risk	[0,1]
H	human expertise or capability prior	[0,1]
A	AI authority share	{0,.25,.5,.75,1}

4. Proposed N-CogHCI Framework

Figure 1 summarizes the closed-loop architecture. The state estimator converts heterogeneous user evidence into a neutrosophic cognitive state. A separate AI capability state captures confidence and epistemic uncertainty. The authority optimizer then selects a mixed-initiative mode subject to safety constraints. Trust calibration and interface adaptation operate on top of the same state so that a decision to reduce autonomy can be accompanied by an appropriate interaction response rather than a silent mode switch.

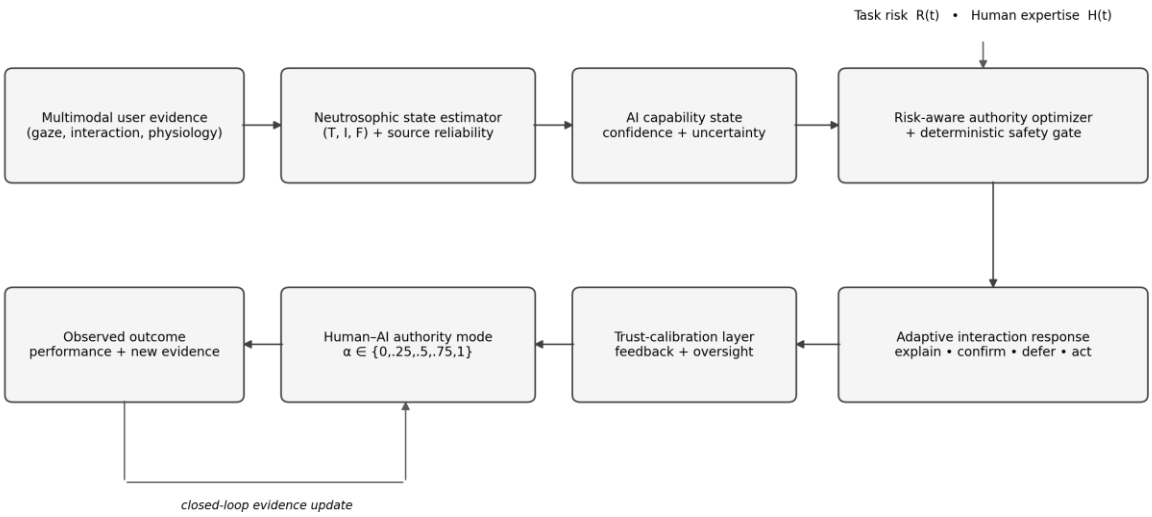

Figure 1. N-CogHCI closed-loop architecture.

4.1 Reliability-aware neutrosophic cognitive-state estimation

Only available sources contribute to the state. Reliability-normalized source weights are defined by Eq. (1), where ε is a small numerical constant. This prevents a low-quality or absent channel from contributing the same weight as a stable channel.

$$\omega_m(t) = a_m(t)\, r_m(t) \,/\, [\Sigma_j\, a_j(t)\, r_j(t) + \varepsilon] \quad (1)$$

Each source contributes discounted support and opposition, while its local uncertainty is retained. Let $\bar{p}_c(t)$ be the reliability-weighted support mean and $\bar{U}_c(t)$ the weighted mean of local uncertainties. Cross-source disagreement $D_c(t)$ is the reliability-weighted absolute deviation around $\bar{p}_c(t)$, and $Q(t)$ is the average available reliability. The N-CogHCI state is then computed as follows:

$$T_c(t) = \Sigma_m\, \omega_m(t)\, [1 - u_{m,c}(t)]\, p_{m,c}(t) \quad (2)$$

$$F_c(t) = \Sigma_m\, \omega_m(t)\, [1 - u_{m,c}(t)]\, [1 - p_{m,c}(t)] \quad (3)$$

$$D_c(t) = \Sigma_m\, \omega_m(t)\, |p_{m,c}(t) - \bar{p}_c(t)|, \qquad Q(t) = (1/M)\, \Sigma_m\, a_m(t)\, r_m(t) \quad (4)$$

$$I_c(t) = 1 - [1 - \bar{U}_c(t)]\, [1 - D_c(t)]\, Q(t) \quad (5)$$

Equation (5) is the key distinction from ordinary probability fusion. Indeterminacy can increase for three different reasons: the base models report uncertainty ($\bar{U}_c$ rises), the available sources disagree (D_c rises), or evidence quality/availability falls (Q falls). T_c and F_c therefore do not need to absorb those epistemic conditions. In the controlled stress test in Section 6, local model uncertainty was set to zero for the user-sensing channels so that the isolated effects of disagreement, reliability, and missingness could be measured; the general formulation above remains applicable when calibrated local uncertainty is available.

4.2 AI capability state

AI confidence should not be treated as competence when the model itself is uncertain. N-CogHCI represents the AI capability evidence as $N_A(t) = (T_A, I_A, F_A)$, where $T_A = (1 - u_A)c_A$, $I_A = u_A$, and $F_A = (1 - u_A)(1 - c_A)$. A calibrated confidence estimate is preferable, but the controller does not require a specific calibration algorithm. This design is compatible with probabilistic calibration and epistemic-uncertainty estimators such as those used in recent adaptive human–AI work [10]. The neutrosophic layer does not replace calibration; it exposes the uncertainty term to the HCI controller.

4.3 Risk-aware authority optimization

For clarity, the authority decision is discrete. A continuous controller can be used, but the five-mode representation is easier to audit and map to interface behavior. Let $\hat{e}_H$ and $\hat{e}_A$ be conservative estimates of human and AI error. In a learned deployment, their coefficients should be estimated from training data. In the controlled simulation, the fixed coefficients in Section 6 are used only as a reproducible stress-test model. The generic forms are:

$$\hat{e}_H = \mathrm{clip}(\beta_0 + \beta_W T_W - \beta_H H + \beta_I I_W, e_{min}, e_{max}), \qquad \hat{e}_A = \mathrm{clip}(1 - c_A + \varrho_A u_A, 0, 1) \tag{6}$$

For each candidate α, the controller evaluates a normalized decision loss. The first term is expected team error amplified by task risk. The second term models residual human cognitive burden, the third term represents coordination overhead, and the fourth term discourages extreme authority when the human-state or AI-state estimate is indeterminate. A bounded complementarity term allows shared control to be beneficial when both agents retain useful capability.

$$L(\alpha) = [1 + \lambda_R R]\, E(\alpha) + \lambda_W(1 - \alpha)T_W + \lambda_C\, 4\alpha(1 - \alpha) + \lambda_U(I_W + u_A)\,|\alpha - 0.5| \tag{7}$$

$$E(\alpha) = \mathrm{clip}\{\alpha\, \hat{e}_A + (1 - \alpha)\, \hat{e}_H - \eta \cdot 4\alpha(1 - \alpha) \cdot \min[1 - \hat{e}_A, 1 - \hat{e}_H], 0, 1\} \tag{8}$$

The provisional authority is $\alpha^* = \mathrm{argmin}_{\alpha \in A} L(\alpha)$. The complementarity coefficient η is not asserted to be a physiological constant; it is a design parameter in the controlled test and must be learned or sensitivity-tested in an empirical deployment. This explicit statement is important: the simulation demonstrates controller behavior under a declared model, not a universal law of human–AI synergy.

4.4 Deterministic safety gate

Optimization alone is insufficient for high-consequence interaction because a small expected advantage can still select a mode that is difficult to justify under severe epistemic uncertainty. N-CogHCI therefore adds a deterministic safety gate. In the reported stress test, α is capped at 0.50 when $R \geq 0.75$ and either $I\_W \geq 0.50$ or $u\_A \geq 0.45$. A stricter cap of 0.25 is applied when $R \geq 0.50$ and either $I\_W \geq 0.75$ or $u\_A \geq 0.70$. These thresholds are design parameters, not empirical constants. Their role is to encode a transparent policy: high consequence plus low epistemic justification cannot produce high automation. In a deployment, the thresholds should be chosen through domain-specific hazard analysis and validated with users.

4.5 Trust calibration and interface adaptation

Authority allocation and user trust should not be conflated. Let $\tau(t)$ denote an observed or inferred human trust/reliance score and $c\_A(t)$ the calibrated AI capability estimate. The mismatch $\Delta\_\tau = \tau - c\_A$ distinguishes overtrust ($\Delta\_\tau > 0$) from undertrust ($\Delta\_\tau < 0$). N-CogHCI uses this mismatch to choose an interaction response rather than to increase trust indiscriminately. High overtrust with high risk triggers stronger evidence presentation and confirmation; undertrust with low AI uncertainty can trigger concise capability evidence; high cognitive indeterminacy triggers clarification or delayed intervention. This follows the broader objective of calibrated reliance described in the trust literature [3–6] and avoids treating explanation as a universal remedy. Indeed, cognitive forcing can reduce overreliance at the cost of user preference [20], so explanation depth and interruption frequency should themselves be adaptive.

Table 3. Mapping from N-CogHCI state conditions to authority and interface actions.

Condition	Authority response	Interface response	Rationale
Low I, low risk, strong AI capability	Allow α chosen by optimizer	Minimal explanation; low friction	Evidence is sufficient and consequence is limited
High workload, low I, reliable AI	Shift toward AI-led support	Simplify display; suppress non-critical notifications	Reduce avoidable human cognitive burden

Condition	Authority response	Interface response	Rationale
High I or high u_A	Prefer shared control	Expose uncertainty; request confirmation or more evidence	Avoid false certainty
High risk + high uncertainty	Cap $\alpha \le 0.50$ or 0.25	Mandatory confirmation; defer irreversible action	Safety gate
Overtrust (τ > c_A)	Do not raise α solely from trust	Show limitations/evidence; cognitive forcing when justified	Calibrate reliance rather than maximize trust
Undertrust with reliable AI	Keep risk constraints	Brief performance evidence; preserve user override	Support justified reliance without coercion

4.6 Online algorithm

Algorithm 1 gives the per-cycle logic. The algorithm is deliberately auditable: every transition into greater autonomy has an explicit evidence state, risk value, and selected loss. It can therefore be logged for post-hoc safety analysis.

Step	Operation
1	Acquire available user-sensing evidence p_m,c, uncertainty u_m,c, reliability r_m, and availability a_m.
2	Compute normalized weights ω_m and the neutrosophic cognitive state N_c = (T_c, I_c, F_c).
3	Construct AI capability state from calibrated confidence c_A and uncertainty u_A.
4	Estimate conservative human and AI error terms ê_H and ê_A.
5	Evaluate L(α) for $\alpha \in \{0, .25, .50, .75, 1\}$ and choose the minimizing provisional mode.
6	Apply the deterministic risk–uncertainty safety gate.
7	Use trust mismatch and cognitive state to select explanation, confirmation, simplification, or deferral behavior.
8	Log outcome, update reliability/calibration statistics, and repeat at the next interaction cycle.

5. Formal Properties

Proposition 1 — Boundedness

If $p_{m,c}$, $u_{m,c}$, $r_m \in [0,1]$ and $a_m \in \{0,1\}$, with at least one available source of nonzero reliability, then T_c, F_c, $I_c \in [0,1]$. Proof: the normalized weights are nonnegative and sum to one. Therefore T_c and F_c are convex combinations of terms in [0,1]. Likewise $\bar{U}_c$, D_c, and Q are in [0,1]. The product $[1 - \bar{U}_c][1 - D_c]Q$ is therefore in [0,1], and Eq. (5) implies $I_c \in [0,1]$. This property prevents numerical states outside the SVNS unit interval.

Proposition 2 — Quality monotonicity of indeterminacy

Holding $\bar{U}_c$ and D_c fixed, $\partial I_c/\partial Q = -[1 - \bar{U}_c][1 - D_c] \leq 0$. Thus, reducing aggregate evidence quality or availability cannot reduce indeterminacy. In the limiting case $Q \to 0$, $I_c \to 1$. This gives missing evidence a direct and predictable effect rather than silently imputing confidence.

Proposition 3 — Disagreement monotonicity

Holding $\bar{U}_c$ and Q fixed, $\partial I_c/\partial D_c = [1 - \bar{U}_c]Q \geq 0$. Therefore greater cross-source disagreement cannot reduce indeterminacy. The property is valuable in multimodal HCI because contradictory gaze, interaction, or physiological evidence should not produce the same authority decision as coherent evidence of equal mean magnitude.

Proposition 4 — Safety-cap invariance

Under the reported gate, any state satisfying $R \geq 0.75$ and ($I_W \geq 0.50$ or $u_A \geq 0.45$) produces $\alpha \leq 0.50$ regardless of the unconstrained optimizer. Likewise, any state satisfying $R \geq 0.50$ and ($I_W \geq 0.75$ or $u_A \geq 0.70$) produces $\alpha \leq 0.25$. This is a policy guarantee, not a statistical tendency. Its value is auditability: the system cannot enter an AI-led or autonomous mode in a state explicitly classified by the gate as insufficiently justified.

6. Controlled Reproducible Evaluation

6.1 Purpose and scope

The evaluation is a controlled stress test of the authority controller, not a claim of human cognitive-state prediction accuracy. This distinction avoids a common methodological error in framework papers: assigning invented performance numbers to a public dataset that was not executed. The test asks a narrower question: when evidence is noisy, missing, or contradictory, does explicit indeterminacy reduce high-autonomy decisions in contexts that have been defined as unsafe? All data-generation assumptions are stated below, and the accompanying script NCogHCI_reproducibility.py reproduces the results exactly with seed 42.

6.2 Monte-Carlo design

The simulation generates 100,000 independent interaction states. Latent workload W is sampled from Beta(2.2, 2.2), task risk R from Beta(2, 2), human expertise H from Beta(2.5, 2), and nominal AI confidence from Beta(5, 2). AI epistemic uncertainty is sampled from a two-component mixture: 18% of trials use Beta(3, 2), representing high-uncertainty episodes, and the remaining trials use Beta(1.3, 6). True AI competence is generated by perturbing nominal confidence with zero-mean Gaussian noise whose standard deviation is 0.035 + 0.22u_A; thus, higher uncertainty increases the dispersion between confidence and realized competence without forcing a particular direction of error.

Four user-evidence regimes are sampled with probabilities 0.55 clean, 0.20 noisy, 0.12 missing, and 0.13 contradictory. Four sensing channels are generated. Clean channels use Gaussian noise $\sigma = 0.07$, availability probability 0.99, and base reliability 0.92. Noisy channels use $\sigma = 0.18$, availability 0.95, and reliability 0.68. Missing-evidence trials use $\sigma = 0.10$, availability 0.55, and reliability 0.82. Contradictory trials use $\sigma = 0.09$, availability 0.98, and reliability 0.84, while one or two channels are inverted around the latent workload. Reliability receives additional zero-mean noise of standard deviation 0.08 and is clipped to [0.15, 1]. These are declared stress-test parameters, not estimates of any specific human population.

The authority levels are {0, .25, .50, .75, 1}. The simulation instantiates Eq. (6) as ê_H = clip(0.08 + 0.50T_W − 0.28H + 0.054I_W, 0.03, 0.65) and ê_A = clip(1 − c_A + 0.105u_A, 0, 1). Equation (7) uses λ_R = 0.65, λ_W = 0.07, λ_C = 0.025, λ_U = 0.02, and $\eta = 0.10$. The reliability-weighted baseline receives reliability-aware T_W and AI uncertainty but not cognitive indeterminacy or the N-CogHCI safety gate. The crisp baseline uses an unweighted mean of available cognitive evidence and no explicit uncertainty penalty.

An unsafe context is defined before policy evaluation as R ≥ 0.70 and either true AI competence < 0.70 or the user-evidence regime is missing/contradictory. A high-uncertainty context is defined as I_W > 0.50 or u_A > 0.45. A high-autonomy decision is $\alpha \geq 0.75$. The normalized decision-loss value is a model-based stress-test quantity and has no physical unit; lower is better within the declared simulation model.

6.3 Main results

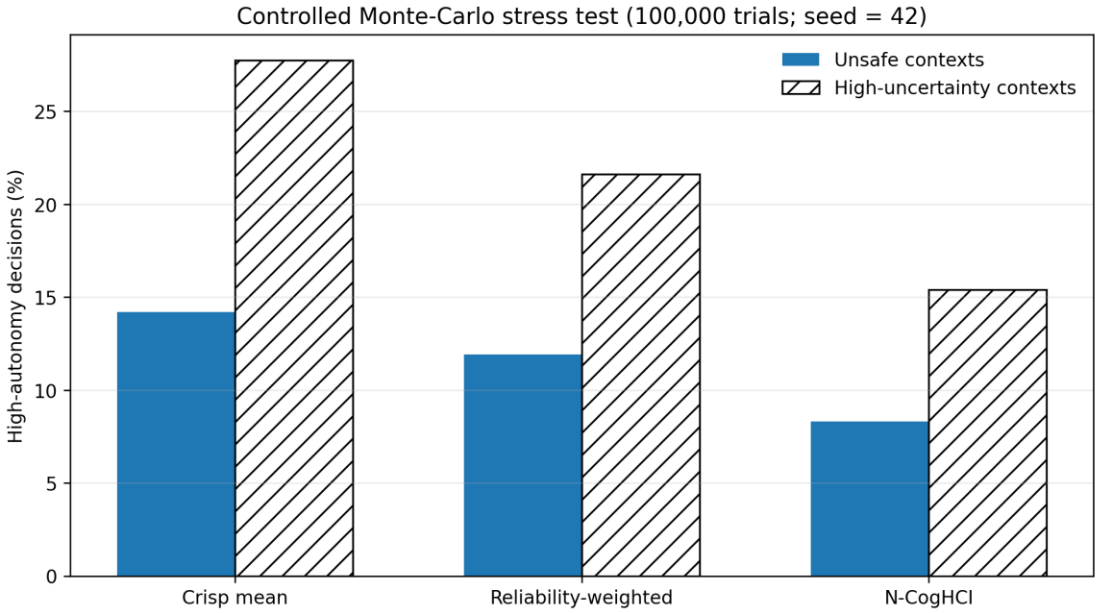

Figure 2. High-autonomy rates in predefined unsafe and high-uncertainty contexts.

Table 4. Controlled Monte-Carlo results. Confidence intervals are normal-approximation binomial intervals over the predefined context subsets (unsafe n = 12,376; high-uncertainty n = 26,980).

Policy	**Decision loss**	**Unsafe high autonomy**	**95% CI**	**High-uncertainty high autonomy**	**95% CI**
Crisp mean	0.2037	14.20%	[13.58, 14.81]%	27.74%	[27.20, 28.27]%
Reliability-weighted	0.2037	11.92%	[11.35, 12.49]%	21.60%	[21.11, 22.10]%
N-CogHCI	0.2053	8.31%	[7.82, 8.79]%	15.42%	[14.98, 15.85]%

N-CogHCI selected high autonomy in 8.31% of unsafe contexts (95% CI 7.82–8.79%), compared with 14.20% (13.58–14.81%) for crisp fusion and 11.92% (11.35–12.49%) for reliability-weighted fusion. Relative to the crisp baseline, this is a 41.5% reduction in high-autonomy decisions under the declared unsafe-context definition; relative to reliability-weighted fusion, the reduction is approximately 30.3%. In high-uncertainty contexts, N-

CogHCI produced high autonomy in 15.42% of trials, compared with 27.74% for crisp fusion and 21.60% for reliability-weighted fusion. The corresponding relative reductions are approximately 44.4% and 28.6%.

The safety improvement is not free. The normalized decision loss was 0.2053 for N-CogHCI, versus 0.2037 for crisp fusion and 0.2037 for reliability-weighted fusion. The increase relative to the best baseline is less than 1% in this simulation, but it is still a real trade-off and is reported as such. The result should therefore be interpreted as evidence that explicit indeterminacy and a safety gate can move the controller along a safety–efficiency frontier, not as evidence that N-CogHCI dominates every objective simultaneously.

6.4 Ablation analysis

Table 5. Ablation results from the same 100,000-trial simulation.

Variant	Decision loss	Unsafe high autonomy	High-uncertainty high autonomy	Shared-control rate
Full N-CogHCI	0.2053	8.31%	15.42%	53.20%
No safety gate	0.2038	12.43%	20.53%	52.62%
No indeterminacy term	0.2050	9.39%	15.76%	51.62%
No AI uncertainty	0.2048	12.39%	27.01%	54.58%

Removing the safety gate lowered the modeled decision loss from 0.2053 to 0.2038 but increased unsafe high-autonomy decisions from 8.31% to 12.43%. Removing cognitive indeterminacy increased the unsafe rate to 9.39%, while removing AI uncertainty increased it to 12.39% and raised high-autonomy decisions in high-uncertainty contexts from 15.42% to 27.01%. The ablation therefore isolates two distinct mechanisms. The continuous uncertainty penalties affect the optimizer before mode selection; the deterministic gate provides an additional hard constraint in states where expected-loss optimization alone remains too permissive.

6.5 Worked numerical case study

Table 6 illustrates four individual controller states using the full estimator of Section 4.1, including local modality uncertainty. These examples are deterministic calculations, not sampled human observations. They show how similar average evidence can produce different decisions when reliability and indeterminacy differ.

Table 6. Deterministic worked examples of N-CogHCI decisions.

Scenario	T_W	I_W	F_W	Risk	AI uncertainty	Selected α / mode
A. Low workload, coherent evidence	0.18	0.132	0.778	0.25	0.08	0.25 — human-led shared
B. High workload, coherent evidence	0.779	0.136	0.176	0.45	0.1	1.00 — autonomous AI
C. Contradictory evidence, high risk	0.46	0.436	0.452	0.82	0.38	0.50 — balanced shared
D. Missing evidence, uncertain AI	0.639	0.626	0.261	0.72	0.58	0.50 — balanced shared

Scenario C is the key neutrosophic example. Support for high workload and opposition are both substantial, and disagreement raises I_W. A scalar average alone could conceal the conflict. N-CogHCI keeps the conflict visible and selects balanced shared control under high risk. Scenario D reaches an even larger I_W primarily because only half of the sensing channels are available and the AI state is itself uncertain. The controller therefore avoids AI-led or autonomous control despite moderately high evidence of user workload.

7. External Validation Protocol on Public HCI Datasets

The controlled test above validates the controller's internal behavior under known perturbations. It does not establish real-user predictive validity. A publishable empirical extension should therefore use participant-level evaluation with leakage control. Three datasets are appropriate and complementary. COLET contains 47 participants, four cognitive-workload levels, eye tracking, and NASA-TLX annotations [13,21]. SWELL-KW contains 25 participants performing realistic knowledge work under neutral, interruption, and time-pressure conditions with computer interaction, facial behavior, posture, heart-rate variability, and skin conductance [14,22]. CLAS contains 62 participants with synchronized ECG, PPG, EDA, accelerometer data, and interactive Math, Logic, and Stroop tasks as well as perceptive affective tasks [15].

7.1 Leakage-resistant evaluation design

All preprocessing and model fitting must be participant-grouped. Windows from the same participant must never appear in both training and test partitions. The preferred primary protocol is leave-one-subject-out evaluation; grouped nested cross-validation is an acceptable alternative when hyperparameter tuning would otherwise reuse test subjects. Standardization, feature selection, calibration, and reliability estimation must be fitted exclusively on each training fold. This requirement is especially important for physiological and interaction features because person-specific baselines can make random-window splits appear unrealistically accurate.

For COLET, eye features can be organized into functional source groups (for example pupil, fixation, saccade, and task-performance groups) so that N-CogHCI receives multiple reliability-tagged evidence sources even though the dataset is eye-centric. For SWELL-KW, computer interaction, face, posture, and physiology can form natural modalities. For CLAS, ECG/heart features, PPG, EDA, and task-performance evidence can be modeled separately. Each base learner should output both a calibrated support probability and an uncertainty quantity. Reliability can be estimated from signal quality, missingness, or validation-time calibration error.

7.2 Evaluation metrics and falsifiable hypotheses

The state estimator should be evaluated with macro-F1 and balanced accuracy for workload/stress classification, Brier score and expected calibration error for probability quality, and selective risk/coverage curves for abstention behavior. The controller should additionally report unsafe high-autonomy rate under prospectively declared risk criteria, unnecessary human-takeover rate, shared-control frequency, authority-switching rate, and task-level performance. A user study should measure NASA-TLX, perceived control, trust calibration, task accuracy, completion time, and intervention burden.

The framework yields falsifiable hypotheses rather than guaranteed outcomes. H1: adding I_W should improve selective decision safety under missing or contradictory evidence without requiring higher raw classification accuracy. H2: the safety gate should reduce high-autonomy decisions in high-risk/high-uncertainty states. H3: trust-calibrated interface responses should reduce overreliance compared with confidence-only explanations, but may increase interaction cost, consistent with the trade-offs observed in cognitive-forcing research [20]. H4: subject-independent benefits should be larger under modality corruption than under clean evidence. Failure of these hypotheses on public datasets or user studies would be evidence against the practical value of the proposed controller and should be reported rather than hidden.

8. Discussion

8.1 Why neutrosophic indeterminacy matters in HCI

The main conceptual result is that uncertainty about a user is not equivalent to a middling estimate of the user's state. A workload probability of 0.50 can arise because every source weakly supports moderate workload, because half the sensors strongly support high workload and half strongly oppose it, or because most sensors are missing. Those states may require different interaction policies. Equations (2)–(5) separate them: T and F describe directional evidence, while I records the epistemic reason not to act as though the direction were settled. This is the point at which the neutrosophic representation becomes operationally meaningful rather than decorative.

8.2 Relationship to probabilistic calibration and fuzzy systems

N-CogHCI should not be read as an argument that probabilities are obsolete. AI confidence calibration remains essential, as emphasized by recent adaptive teaming frameworks [10]. The proposed model uses probability-like support values inside each modality and then adds an epistemic layer that can represent unresolved evidence. Similarly, fuzzy membership is appropriate for gradual concepts such as 'moderately overloaded.' The neutrosophic state adds a distinct dimension when the evidence for that fuzzy concept is incomplete or contradictory. A practical implementation can therefore combine calibrated probabilistic classifiers, fuzzy linguistic rules, and neutrosophic evidence fusion within one soft-computing pipeline.

8.3 Safety–efficiency trade-off

The simulation does not show universal dominance. N-CogHCI intentionally sacrifices a small amount of modeled decision efficiency to reduce high autonomy in states that lack sufficient justification. This result is preferable to an apparently superior table produced by tuning both the policy and the evaluation metric to favor the proposed method. In safety-relevant HCI, a method should expose its operating trade-off. The correct setting of the gate depends on application severity: a writing assistant may tolerate more autonomy than a clinical, cybersecurity, industrial-control, or transportation interface.

8.4 Interpretability and auditability

The controller is structured so that an authority decision can be explained using a small set of variables: workload evidence, indeterminacy, AI uncertainty, task risk, and expertise. This is useful for HCI auditing because a reviewer can reconstruct why the system refused autonomous action even when AI confidence was high. The deterministic gate also makes a subset of safety behavior testable with unit tests rather than only statistical evaluation. This does not guarantee overall system safety; it makes one important class of behavior explicit and inspectable.

9. Limitations and Threats to Validity

First, the reported numerical results are simulation-based. The distributions, coefficients, complementarity term, and safety thresholds are controlled design assumptions, not population estimates. They test internal behavior under transparent perturbations but cannot establish human-subject effectiveness. Second, cognitive concepts differ across tasks. Eye-based workload in COLET, workplace stress in SWELL-KW, and physiology in CLAS are related but not interchangeable targets. Cross-dataset validation must preserve those semantic differences rather than forcing a single label taxonomy. Third, reliability estimates can themselves be wrong; a future implementation should calibrate reliability and examine adversarial or systematic sensor failure. Fourth, the present controller uses five authority levels. Continuous or partially observable control may provide smoother behavior, but it would also require stronger stability and human-factors analysis. Fifth, trust is included as a calibration signal, yet trust inference from behavior is itself uncertain and should not be treated as ground truth. Finally, the framework does not replace domain safety engineering, usability testing, or legal requirements for human oversight.

10. Reproducibility, Data, and Ethical Scope

No new human participants were recruited and no private participant data were created for this study. The numerical results in Section 6 are generated from a controlled synthetic stress test whose distributions, policy parameters, random seed, and evaluation definitions are stated in the manuscript. The accompanying file NCogHCI_reproducibility.py reproduces the Monte-Carlo tables and exports the result CSV files. COLET, SWELL-KW, and CLAS are referenced only as public external-validation resources; this manuscript does not claim to have executed participant-level experiments on them. COLET is publicly archived on Zenodo [21], SWELL-KW has a persistent DANS dataset record [22], and CLAS is available through its published data repository and access procedure [15]. Any future human-participant deployment should obtain the approvals appropriate to its institution and application domain and should evaluate perceived control, accessibility, privacy, and intervention burden in addition to predictive metrics.

11. Conclusion and Future Work

This paper proposed N-CogHCI, a reliability-aware neutrosophic cognitive control framework for adaptive human–AI interaction. Its central design principle is that unresolved evidence should change what an AI system is allowed to do, not merely lower a confidence score displayed after the decision. The framework separates supportive evidence, opposition, and indeterminacy; couples cognitive state with AI uncertainty and task risk; selects among interpretable authority modes; and adapts interface behavior to trust and cognitive context. Formal analysis shows that indeterminacy rises predictably as evidence quality falls or disagreement increases. In a reproducible 100,000-trial stress test, the full controller substantially reduced high-autonomy decisions in unsafe and high-uncertainty contexts, while exposing a small cost in normalized decision efficiency rather than concealing it.

The next step is empirical, not rhetorical. The state estimator and authority policy should be evaluated subject-independently on COLET, SWELL-KW, and CLAS, followed by a controlled user study in which workload, trust calibration, perceived control, task performance, and intervention burden are measured together. The most important future extension is learning the authority-loss coefficients and safety thresholds from domain-specific evidence while preserving hard constraints for high-consequence states. A second extension is to integrate refined neutrosophic causal maps [19] so that the controller can model delayed relationships among workload, attention, explanation, trust, and performance. A third is to study personalized/federated reliability models so that adaptation can improve without centralizing sensitive cognitive data. These directions preserve the core contribution: cognitive AI should not only infer what the user may be experiencing; it should reason explicitly about how uncertain that inference is before deciding how much control to assume.

References

[1] Amershi, S., Weld, D., Vorvoreanu, M., Fourney, A., Nushi, B., Collisson, P., Suh, J., Iqbal, S., Bennett, P. N., Inkpen, K., Teevan, J., Kikin-Gil, R., & Horvitz, E. (2019). Guidelines for Human-AI Interaction. Proceedings of the 2019 CHI Conference on Human Factors in Computing Systems, Paper 3, 1–13. https://doi.org/10.1145/3290605.3300233

[2] Parasuraman, R., Sheridan, T. B., & Wickens, C. D. (2000). A model for types and levels of human interaction with automation. IEEE Transactions on Systems, Man, and Cybernetics - Part A: Systems and Humans, 30(3), 286–297. https://doi.org/10.1109/3468.844354

[3] Lee, J. D., & See, K. A. (2004). Trust in automation: Designing for appropriate reliance. Human Factors, 46(1), 50–80. https://doi.org/10.1518/hfes.46.1.50_30392

[4] Hoff, K. A., & Bashir, M. (2015). Trust in automation: Integrating empirical evidence on factors that influence trust. Human Factors, 57(3), 407–434. https://doi.org/10.1177/0018720814547570

[5] Lucas, G. M., Becerik-Gerber, B., & Roll, S. C. (2024). Calibrating workers' trust in intelligent automated systems. Patterns, 5(9), 101045. https://doi.org/10.1016/j.patter.2024.101045

[6] Yang, R., Li, S., Qi, Y., Liu, J., He, Q., & Zhao, H. (2025). Unveiling users' algorithm trust: The role of task objectivity, time pressure, and cognitive load. Computers in Human Behavior Reports, 18, 100667. https://doi.org/10.1016/j.chbr.2025.100667

[7] Tsamados, A., Floridi, L., & Taddeo, M. (2025). Human control of AI systems: From supervision to teaming. AI and Ethics, 5, 1535–1548. https://doi.org/10.1007/s43681-024-00489-4

[8] Bokhorst, J. A. C., Waschull, S., & Emmanouilidis, C. (2025). Dynamic Allocation of Shared Tasks in Industrial Human-AI Teaming. IFAC-PapersOnLine, 59(10), 757–762. https://doi.org/10.1016/j.ifacol.2025.09.129

[9] Tan, J., Xue, S., Cao, H., & Ge, S. S. (2025). Human–AI interactive optimized shared control. Journal of Automation and Intelligence, 4(3), 163–176. https://doi.org/10.1016/j.jai.2025.01.001

[10] AL-Ali, M., Marks, A., Mohamed, A. A., Balaha, H. M., Badawy, M., Elhosseini, M. A., et al. (2026). Calibrated adaptive framework for trustworthy human and artificial intelligence decision systems. Scientific Reports. https://doi.org/10.1038/s41598-026-65730-y

[11] Suryani, M., Sensuse, D. I., Santoso, H. B., Aji, R. F., Hadi, S., Suryono, R. R., & Kautsarina. (2024). An initial user model design for adaptive interface development in learning management system based on cognitive load. Cognition, Technology & Work, 26, 653–672. https://doi.org/10.1007/s10111-024-00772-8

[12] Hart, S. G., & Staveland, L. E. (1988). Development of NASA-TLX (Task Load Index): Results of empirical and theoretical research. In P. A. Hancock & N. Meshkati (Eds.), Human Mental Workload (Advances in Psychology, Vol. 52, pp. 139–183). Elsevier. https://doi.org/10.1016/S0166-4115(08)62386-9

[13] Ktistakis, E., Skaramagkas, V., Manousos, D., Tachos, N. S., Tripoliti, E., Fotiadis, D. I., & Tsiknakis, M. (2022). COLET: A dataset for cognitive workload estimation based on eye-tracking. Computer Methods and Programs in Biomedicine, 224, 106989. https://doi.org/10.1016/j.cmpb.2022.106989

[14] Koldijk, S. J., Sappelli, M., Verberne, S., Neerincx, M. A., & Kraaij, W. (2014). The SWELL Knowledge Work Dataset for Stress and User Modeling Research. Proceedings of the 16th ACM International Conference on Multimodal Interaction, 291–298. https://doi.org/10.1145/2663204.2663257

[15] Markova, V., Ganchev, T., & Kalinkov, K. (2019). CLAS: A Database for Cognitive Load, Affect and Stress Recognition. 2019 International Conference on Biomedical Innovations and Applications (BIA), 1–4. https://doi.org/10.1109/BIA48344.2019.8967457

[16] Zadeh, L. A. (1994). Fuzzy logic, neural networks, and soft computing. Communications of the ACM, 37(3), 77–84. https://doi.org/10.1145/175247.175255

[17] Smarandache, F. (1998). Neutrosophy: Neutrosophic Probability, Set, and Logic: Analytic Synthesis & Synthetic Analysis. American Research Press, Rehoboth, New Mexico.

[18] Wang, H., Smarandache, F., Zhang, Y., & Sunderraman, R. (2010). Single Valued Neutrosophic Sets. Multispace and Multistructure, 4, 410–413.

[19] Shekatkar, A. R., Deodeshmukh, A., & Kandasamy, I. (2025). Refined Neutrosophic Cognitive Maps: A Novel Framework for Modeling Indeterminate Causal Relationships. International Journal of Fuzzy Systems. https://doi.org/10.1007/s40815-025-02190-y

[20] Buçinca, Z., Malaya, M. B., & Gajos, K. Z. (2021). To Trust or to Think: Cognitive Forcing Functions Can Reduce Overreliance on AI in AI-Assisted Decision-Making. Proceedings of the ACM on Human-Computer Interaction, 5(CSCW1), Article 188, 1–21. https://doi.org/10.1145/3449287

[21] Ktistakis, E., Skaramagkas, V., Manousos, D., Tachos, N. S., Tripoliti, E., Fotiadis, D. I., & Tsiknakis, M. (2023). COLET: A Dataset for Cognitive workLoad estimation based on Eye-Tracking (Version 3) [Data set]. Zenodo. https://doi.org/10.5281/zenodo.7766785

[22] Kraaij, W., Koldijk, S., & Sappelli, M. (2014). The SWELL Knowledge Work Dataset for Stress and User Modeling Research (Version 4.1) [Data set]. DANS Data Station Social Sciences and Humanities.

Appendix A. Exact Controlled-Study Parameters

The following values are included to make the reported numerical tables independently reproducible. They are simulation parameters and must not be interpreted as empirical estimates of human cognition.

Component	Parameter	Value
Trials	N / random seed	100,000 / 42
Regime mixture	clean / noisy / missing / contradictory	0.55 / 0.20 / 0.12 / 0.13
Latent workload	Beta parameters	2.2, 2.2
Risk	Beta parameters	2, 2
Human expertise	Beta parameters	2.5, 2
AI confidence	Beta parameters	5, 2
High-AI-uncertainty mixture	probability; Beta parameters	0.18; Beta(3,2)
Ordinary AI uncertainty	Beta parameters	1.3, 6

Component	Parameter	Value
Authority levels	α	0, .25, .50, .75, 1
Loss weights	λ_R, λ_W, λ_C, λ_U, η	0.65, 0.07, 0.025, 0.02, 0.10
Safety gate 1	condition / cap	R≥.75 and (I≥.50 or u_A≥.45) / α≤.50
Safety gate 2	condition / cap	R≥.50 and (I≥.75 or u_A≥.70) / α≤.25

Received: Aug. 31, 2026. **Accepted:** Sept. 15, 2026.

NSS

Neutrosophic Sets and Systems, Vol. 102, 2027

University of New Mexico

Plithogenic Metric Equivalence and Metric Transport in Evolving Epidemiological State Spaces

Victor Wanjala[1,*] and Amenya Collins[1]

[1] Department of Mathematics and Physical Sciences, Maasai Mara University, Narok, Kenya

* Correspondence: wanjalavictor421@gmail.com

Abstract: We develop an operator-theoretic theory of metric equivalence and metric transport for evolving epidemiological states represented within a plithogenic Hilbert space. Let $H_{epi} = H_T \oplus H_I \oplus H_F$ represent truth, indeterminacy, and falsity components associated with epidemiological information, including disease occurrence, exposure, immunity, diagnostic status, environmental risk, and intervention uncertainty. For each temporal frame t, a contradiction structure is represented by a self-adjoint operator $\hat{D}_t$, from which a strictly positive metric operator G_t is constructed. Two epidemiological state operators $A, B \in B(H_{epi})$ are said to be G_t metrically equivalent when $A^*G_tA = B^*G_tB$. We establish a reduction to classical metric equivalence, characterize the relation through positive square roots and partial isometries, and identify the associated metric invariants. We then introduce epidemiological metric transport operators satisfying $A_t^*G_{t+1}A_t = G_t$ and prove that local metric preservation at every temporal transition implies global metric preservation across every finite sequence of epidemiological frames. An approximate metric defect is introduced together with perturbation estimates. The epidemiological component is formulated theoretically: epidemiological variables are represented as components of an evolving uncertain state, while no patient-level or population-level dataset is required. Finite-dimensional examples illustrate metrically equivalent and non-equivalent epidemiological transition operators. The resulting theory provides an operator-theoretic basis for studying the preservation of epidemiological geometry under evolving uncertainty, contradiction, and state transition.

Keywords: Plithogenic sets; epidemiological states; metric equivalence; metric transport; Hilbert space; operator theory; evolving uncertainty; epidemiological dynamics.

---

1. Introduction

The mathematical modeling of evolving uncertain states requires tools capable of representing time-dependent, overlapping, and sometimes contradictory information. Traditional approaches to state comparison often rely on pointwise similarity measures, which capture instantaneous resemblance but say little about the structural geometry of state transitions.

Recent work on N-framed plithogenic hypersoft sets [1] has demonstrated the capacity of plithogenic structures to represent time-dependent and overlapping disease information. By partitioning observations into discrete temporal frames, such frameworks enable comparison of evolving profiles through distance and similarity measures. However, these approaches remain fundamentally descriptive: they compare states rather than characterizing the transformations that generate state evolution.

The present work takes a different mathematical direction. Rather than comparing states pointwise, we investigate the geometry induced by state transitions. This leads to a theory of time-dependent metric equivalence and metric transport for bounded operators on Hilbert spaces associated with plithogenic epidemiological representations.

1.1. The Mathematical Gap

Metric equivalence is a classical relation in Hilbert space operator theory. For operators $A, B \in B(H)$, the relation $A^*A = B^*B$ is equivalent to $\|Ax\| = \|Bx\|$, $x \in H$, and therefore identifies operators that induce the same quadratic geometry on the underlying Hilbert space. Metric equivalence is closely related to, but distinct from, similarity of operators. Earlier studies have investigated metric equivalence and almost similarity of operators [16], and more recently the intersection of similarity and metric equivalence has been studied through the notion of metric similarity [17].

Existing work on metric equivalence studies equality of operator-induced quadratic forms under the canonical Hilbert space metric, while recent plithogenic hypersoft set models provide frame-based representations for evolving uncertain information. The present work connects these two directions by introducing a strictly positive metric operator induced by a contradiction structure and by studying exact metric transport between successive frames.

In a plithogenic representation, information may be decomposed into truth, indeterminacy, and falsity components, while contradiction relationships between attribute values may change from one frame to another [19–21]. Thus, for an evolving plithogenic epidemiological state, there is no mathematical reason to require the canonical Hilbert space metric to remain the only geometry used for comparison. A weighted geometry is more appropriate when the relative contribution and interaction of the components are encoded by a strictly positive operator. This observation motivates the weighted relation $A \sim_G B$ if and only if $A^*GA = B^*GB$, $G > 0$.

The relation considered below is a weighted form of metric equivalence, with the strictly positive operator G specifying the underlying geometry; see [16,17]. When $G = I$, the classical metric equivalence relation is recovered.

A related positive-operator deformation of metric equivalence was recently considered by Amenya et al. [2]. The present paper differs in that the strictly positive metric operator is generated from an explicitly specified plithogenic contradiction operator and is allowed to evolve across a sequence of frames. The principal object is consequently the transport equation $A^*_t G_{t+1} A_t = G_t$, together with its multi-step consequence.

To the best of our knowledge, the combination of a contradiction-induced positive metric sequence with weighted metric equivalence and exact multi-frame metric transport has not been explicitly developed in the operator-theoretic literature.

1.2. Epidemiological Motivation

Epidemiological information is frequently incomplete, delayed, heterogeneous, and apparently contradictory. Diagnostic evidence may disagree with reported disease status, exposure classification may conflict with observed disease occurrence, and environmental risk indicators may not reflect observed epidemiological states. The present paper provides an operator-theoretic framework in which these situations are represented through plithogenic truth, indeterminacy, and falsity components and a contradiction-induced metric operator, without requiring any empirical epidemiological dataset.

1.3. Contributions

The main contributions of this paper are:

- A structured construction of strictly positive metric operators for plithogenic epidemiological state spaces, using a tensor product embedding $\tilde{D}_t = C_t \otimes D_t$ with a self-adjoint component interaction matrix C_t.
- Definition and characterization of G_t metric equivalence $A^*G_tA = B^*G_tB$, including reduction to classical metric equivalence and polar and partial isometry characterizations.

- Identification of metric invariants preserved under G-equivalence, including the G-norm, kernel structure, finite-dimensional rank, and singular values of metric-weighted realizations.
- Exact single- and multi-step metric transport, $A^*_t G_{t+1} A_t = G_t$ and $\Phi^*_{t,s} G_t \Phi_{t,s} = G_s$, together with perturbation and stability estimates for approximate metric equivalence.
- A theoretical epidemiological interpretation showing how contradiction, uncertainty, and temporal evolution of epidemiological information can be represented within the proposed operator-theoretic setting.

1.4. Organization

The remainder of this paper is organized as follows. Section 2 provides essential preliminaries. Section 3 develops the plithogenic epidemiological metric structure. Section 4 introduces plithogenic metric equivalence. Section 5 identifies metric invariants. Section 6 develops epidemiological metric transport. Section 7 introduces the metric equivalence defect and establishes perturbation estimates. Section 8 presents finite-dimensional examples. Section 9 provides a brief epidemiological interpretation. Section 10 concludes.

2. Preliminaries

Throughout this paper, H denotes a complex Hilbert space and B(H) the algebra of bounded linear operators on H. The inner product is denoted by $\langle\cdot,\cdot\rangle$ and is assumed linear in the first argument. The corresponding norm is $\|x\| = \langle x,x\rangle^{(1/2)}$. For $A \in B(H)$, the adjoint of A is denoted A^* and is characterized by $\langle Ax,y\rangle = \langle x,A^*y\rangle$, x, y $\in$ H. The basic properties of bounded operators on Hilbert spaces, adjoints, positive operators, and spectral theory are standard; see, for example, [6,8,9,15,18].

Remark 2.1. Throughout the paper, the term strictly positive metric operator refers to a bounded, self-adjoint, uniformly positive operator defining an equivalent Hilbert space inner product. It is not a metric function on the underlying plithogenic set.

2.1. Positive and Strictly Positive Operators

Definition 2.2. An operator $G \in B(H)$ is called positive if $G = G^*$ and $\langle Gx,x\rangle \geq 0$ for every $x \in H$. We write $G \geq 0$.

Definition 2.3. An operator $G \in B(H)$ is called strictly positive (uniformly positive) if there exists a constant $m > 0$ such that $\langle Gx,x\rangle \geq m\|x\|^2$, $x \in H$. We write $G \geq mI > 0$.

Remark 2.4. If $G > 0$, then G is invertible and its positive square root $G^{(1/2)}$ is invertible. The positive square root is well defined by the continuous functional calculus for positive operators [3,4,8,15]. Moreover, $\|G^{-1}\|^{-1}\|x\|^2 \leq \langle Gx,x\rangle \leq \|G\|\|x\|^2$. Consequently, the norm induced by G is equivalent to the original Hilbert space norm.

2.2. Weighted Hilbert Space Geometry

Definition 2.5. Let $G > 0$. The G-inner product on H is defined by $\langle x,y\rangle_G = \langle Gx,y\rangle$, x, y $\in$ H. The associated G-norm is $\|x\|_G = \langle Gx,x\rangle^{(1/2)}$. The use of a strictly positive metric operator to modify the inner product is standard in operator theory on spaces equipped with a modified metric; see [7,13,14].

Proposition 2.6. Let $G > 0$. Then $(H,\langle\cdot,\cdot\rangle_G)$ is a Hilbert space and $\|G^{(1/2)}x\| = \|x\|_G$.

Proof. $\|x\|^2_G = \langle Gx,x\rangle = \langle G^{(1/2)}x,G^{(1/2)}x\rangle = \|G^{(1/2)}x\|^2$. Since $G^{(1/2)}$ is boundedly invertible, the G-norm is equivalent to the original norm on H. Hence completeness is preserved. □

Theorem 2.7 (Equivalence of the G-Norm and the Hilbert Norm). Let $G > 0$. Then there exist constants m, M > 0 such that $mI \leq G \leq MI$ and $\sqrt{m}\|x\| \leq \|x\|_G \leq \sqrt{M}\|x\|$, $x \in H$. In particular, the G-norm and the original Hilbert space norm generate the same topology.

Proof. Since $G > 0$ and G is bounded, the spectrum of G is contained in [m, M] for some $0 < m \leq M < \infty$. Hence $mI \leq G \leq MI$. Taking inner products with x gives the stated norm equivalence. □

Definition 2.8. Let $G > 0$ and $A \in B(H)$. The G-operator norm of A is $\|A\|_G = \sup_{x\neq 0} \|Ax\|_G / \|x\|_G$.

Theorem 2.9. Let $G > 0$ and $A \in B(H)$. Then $\|A\|_G = \|G^{1/2}AG^{-1/2}\|$.

Proof. Put $y = G^{1/2}x$. Then $\|A\|_G = \sup_{y\neq 0} \|G^{1/2}AG^{-1/2}y\| / \|y\| = \|G^{1/2}AG^{-1/2}\|$.

2.3. Polar Decomposition

Every $A \in B(H)$ admits a polar decomposition $A = U|A|$, $|A| = (A^*A)^{1/2}$, where U is a partial isometry. See [3,8,11,12].

2.4. Metric Equivalence of Operators

Definition 2.10. Let $G > 0$ and let $A, B \in B(H)$. We say that A and B are G metrically equivalent if $A^*GA = B^*GB$. We write $A \sim_G B$.

Remark 2.11. The relation $A \sim_G B$ is equivalent to $\|Ax\|_G = \|Bx\|_G$ for every $x \in H$. Thus G metric equivalence compares operators through the geometry that they induce on the weighted Hilbert space $(H,\langle\cdot,\cdot\rangle_G)$.

2.5. Metric Transport

Definition 2.12. Let $G_0, G_1 > 0$ and let $A \in B(H)$. We call A a (G_0, G_1) metric transport operator if $A^*G_1A = G_0$.

Proposition 2.13. If A is a (G_0, G_1) metric transport operator, then $\|Ax\|_{G_1} = \|x\|_{G_0}$ for every $x \in H$. In particular, A is injective.

Proof. We compute $\|Ax\|^2_{G_1} = \langle G_1Ax,Ax\rangle = \langle A^*G_1Ax,x\rangle = \langle G_0x,x\rangle = \|x\|^2_{G_0}$. If $Ax = 0$, then $\|x\|_{G_0} = 0$, and since $G_0 > 0$, we obtain $x = 0$.

Remark 2.14. Metric equivalence and metric transport are conceptually distinct. Metric equivalence is an equivalence relation on operators for a fixed strictly positive metric operator G: $A^*GA = B^*GB$. Metric transport is an isometric relation between two possibly different weighted Hilbert space geometries: $A^*G_1A = G_0$.

3. Plithogenic Epidemiological Metric Structures

3.1. Epidemiological Plithogenic State Space

Let H_T, H_I, and H_F be complex Hilbert spaces representing, respectively, the truth, indeterminacy, and falsity components of epidemiological information. We define the epidemiological plithogenic state space by $H_{epi} = H_T \oplus H_I \oplus H_F$. An epidemiological state at temporal frame t is represented by $x_t = x_{Tt} \oplus x_{It} \oplus x_{Ft} \in H_{epi}$.

The components may encode uncertain information associated with epidemiological quantities such as disease occurrence, exposure status, immunity, diagnostic classification, environmental risk, intervention status, or other population-level indicators. The three components do not represent three mutually exclusive epidemiological populations. Rather, they represent the truth, indeterminacy, and falsity dimensions associated with the available information concerning an epidemiological state.

The inner product on H_{epi} is given by $\langle x,y\rangle = \langle x_T,y_T\rangle_T + \langle x_I,y_I\rangle_I + \langle x_F,y_F\rangle_F$. The plithogenic setting used here is based on the theory of plithogenic sets and related extensions developed by Smarandache [19–21].

3.2. Theoretical Epidemiological State Representation

Let $E_t = \{e^{(t)}_1, e^{(t)}_2, \ldots, e^{(t)}_n\}$ denote a finite collection of epidemiological attributes observed or conceptually defined at temporal frame t. Depending on the disease and application, these attributes may include disease occurrence, exposure, immunity, diagnostic status, environmental exposure, intervention status, or other epidemiologically relevant characteristics.

For each attribute $e(t)i$, let $\mu(t)T(ei)$, $\mu(t)I(ei)$, $\mu(t)F(ei)$ denote its truth, indeterminacy, and falsity components, respectively. After selecting a coordinate representation, the epidemiological state is written as $xt \in Hepi$.

The state vector is not required to represent a probability distribution. Instead, it represents the information state associated with an epidemiological system under uncertainty. The temporal evolution of the epidemiological information state is represented by a sequence $x0, x1, \ldots, xN$ with $xt \in Hepi$.

The operator $At : Hepi \to Hepi$ represents the mathematical transformation of the epidemiological information state between consecutive temporal frames. The operator need not be interpreted as a biological transmission operator. It may instead represent an abstract state transition incorporating changes in disease information, exposure, immunity, surveillance, environmental conditions, or interventions.

3.3. Contradiction Operators

Let $At = \{a1, \ldots, an\}$ denote the attribute set at frame t.

Definition 3.1. A contradiction function at frame t is a map $Ct : At \times At \to [0, 1]$ satisfying $Ct(ai,ai) = 0$ and $Ct(ai,aj) = Ct(aj,ai)$.

Definition 3.2. The contradiction matrix at frame t is the real symmetric matrix $Dt = (d(t)ij)$ for $i,j = 1,\ldots,n$, where $d(t)ij = Ct(ai,aj)$. The contradiction matrix Dt is real symmetric by construction, hence self-adjoint as an operator on $\mathbb{C}^n$. It need not be positive semidefinite, and it is used to perturb a reference strictly positive metric operator rather than as a metric operator itself.

Remark 3.3 (Epidemiological Interpretation of Contradiction). In the epidemiological setting, the contradiction degree $Ct(ei,ej)$ quantifies the degree of contradiction between two epidemiological attributes or attribute values at temporal frame t. Examples include apparent incompatibility between diagnostic evidence and reported disease status, between exposure classification and observed disease occurrence, or between environmental risk indicators and observed epidemiological states. The contradiction degree is not interpreted as a probability, incidence rate, or relative risk. It is a structural quantity used to encode incompatibility or opposition among the attributes entering the plithogenic representation.

3.4. Component Interaction and Structured Embedding

Definition 3.4. Suppose that $HT = HI = HF = \mathbb{C}^n$, so that $Hepi \cong \mathbb{C}^{3n}$. A component interaction matrix at frame t is a self-adjoint matrix $Ct = (c(t)PQ)P,Q\in\{T,I,F\} \in \mathbb{C}^{3\times 3}$, $Ct = Ct^*$. The extended contradiction operator on Hepi is $\tilde{D}t = Ct \otimes Dt$. Since Ct and Dt are both self-adjoint, $\tilde{D}t^* = (Ct \otimes Dt)^* = Ct^* \otimes Dt^* = Ct \otimes Dt = \tilde{D}t$.

The tensor product form is a structured embedding once Ct is chosen: Ct encodes how the contradiction structure couples the truth, indeterminacy, and falsity components, while Dt encodes the attribute-level contradiction degrees. The construction is not asserted to be canonical; Ct is a modelling choice reflecting the epidemiological context.

3.5. The Operator-Induced Plithogenic Metric

Definition 3.5. Let $G0,t > 0$ be a reference strictly positive metric operator on Hepi and let $\lambda t \geq 0$. We call $Gt = G0,t\^(1/2)(I + \lambda t\tilde{D}t)G0,t\^(1/2)$ the operator-induced plithogenic metric associated with the contradiction operator $\tilde{D}t$. The quadratic form of Gt shows explicitly how the contradiction structure modifies the reference geometry.

Definition 3.6 (Standing Assumptions). At each frame t, we assume $G0,t > 0$, $Ct = Ct^*$, $Dt = Dt^*$, $I + \lambda t(Ct \otimes Dt) > 0$.

Proposition 3.7. Suppose the standing assumptions hold. Then $Gt = G0,t\^(1/2)(I + \lambda t\tilde{D}t)G0,t\^(1/2)$ is strictly positive.

Proof. For $x \neq 0$, $\langle G_t x, x\rangle = \langle (I + \lambda_t \tilde{D}_t) G_{0,t}^{1/2} x, G_{0,t}^{1/2} x\rangle$. Since $G_{0,t}^{1/2}$ is invertible and $I + \lambda_t \tilde{D}_t > 0$, the right-hand side is strictly positive. □

Theorem 3.8 (Sufficient Positivity Condition). Let $\tilde{D}_t = \tilde{D}_t^*$ and let $\lambda_t \geq 0$. If $1 + \lambda_t \inf\sigma(\tilde{D}_t) > 0$, then $\inf\sigma(I + \lambda_t \tilde{D}_t) = 1 + \lambda_t \inf\sigma(\tilde{D}_t) > 0$, and consequently $I + \lambda_t \tilde{D}_t > 0$. In the finite-dimensional case, the condition is equivalent to $1 + \lambda_t \lambda_{min}(\tilde{D}_t) > 0$. Equivalently, the condition $\lambda_t \|\tilde{D}_t^-\| < 1$ guarantees strict positivity, where $\tilde{D}_t^-$ denotes the negative part of $\tilde{D}_t$; this inequality remains valid when $\tilde{D}_t^- = 0$.

Proof. The spectrum of $I + \lambda_t \tilde{D}_t$ is $\{1 + \lambda\mu : \mu \in \sigma(\tilde{D}_t)\}$, hence $\inf\sigma(I + \lambda_t \tilde{D}_t) = 1 + \lambda_t \inf\sigma(\tilde{D}_t)$, which is positive by assumption. In finite dimensions, $\inf\sigma(\tilde{D}_t) = \lambda_{min}(\tilde{D}_t)$. Finally, $\inf\sigma(\tilde{D}_t) \geq -\|\tilde{D}_t^-\|$, so $\lambda_t \|\tilde{D}_t^-\| < 1$ implies $1 + \lambda_t \inf\sigma(\tilde{D}_t) > 0$, and if $\tilde{D}_t^- = 0$ the inequality is trivially satisfied. □

Example 3.9 (Theoretical Epidemiological State). Consider an epidemiological state described by the four attributes E_t = {disease occurrence, exposure, immunity, environmental risk}. The indeterminacy component may arise from incomplete surveillance, uncertain diagnostic classification, delayed reporting, or conflicting epidemiological indicators. The contradiction matrix $D_t = (d(t)_{ij})$ for $i,j = 1,\ldots,4$ records the pairwise contradiction structure among these attributes. A strong contradiction may occur, for instance, between an environmental risk indicator and an observed disease occurrence indicator when the expected association is not reflected in the available information. The resulting operator $G_t = G_{0,t}^{1/2}(I + \lambda_t(C_t \otimes D_t))G_{0,t}^{1/2}$ defines the geometry in which epidemiological states are compared. The example is theoretical and does not require numerical epidemiological observations.

3.6. Time-Dependent Plithogenic Metrics

Let $G_t \in B(H_{epi})$ for $t = 0, 1, \ldots, N$ be strictly positive metric operators satisfying $G_t = G_t^* > 0$. The block operators are not chosen independently; they are required to satisfy $G_t = G_t^* > 0$, which imposes the corresponding positivity constraints on the diagonal and cross-component blocks.

Definition 3.10. A family $\{G_t\}_{t=0}^{N}$ of strictly positive metric operators on H_{epi} is called a plithogenic metric sequence. The G_t-norm on H_{epi} is $\|x\|_{G_t} = \langle G_t x, x\rangle^{1/2}$.

4. Plithogenic Metric Equivalence

4.1. Equivalence Relation

Theorem 4.1. Let $G > 0$ on H. The relation $\sim_G$ defined by $A \sim_G B$ if and only if $A^*GA = B^*GB$ is an equivalence relation on $B(H)$.

Proof. Reflexivity is immediate. Symmetry follows from $A^*GA = B^*GB$ implying $B^*GB = A^*GA$. Transitivity follows from $A^*GA = B^*GB = C^*GC$.

4.2. Reduction to Classical Metric Equivalence

Theorem 4.2 (Reduction to Classical Metric Equivalence). Let $G > 0$ and let $A, B \in B(H)$. Then $A \sim_G B$ if and only if $G^{1/2}A \sim G^{1/2}B$, where the relation on the right-hand side is the classical metric equivalence relation $S \sim T$ if and only if $S^*S = T^*T$.

Proof. We have $A^*GA = B^*GB$ if and only if $(G^{1/2}A)^*(G^{1/2}A) = (G^{1/2}B)^*(G^{1/2}B)$. □

Remark 4.3. The proposed relation is the transport of classical metric equivalence through the geometry-changing map $A \mapsto G^{1/2}A$.

4.3. Square Root Characterization

Theorem 4.4. Let $G > 0$ and $A, B \in B(H)$. The following are equivalent: (1) $A \sim_G B$; (2) $|G^{1/2}A| = |G^{1/2}B|$; (3) $(G^{1/2}A)^*(G^{1/2}A) = (G^{1/2}B)^*(G^{1/2}B)$.

Proof. Equivalence of (1) and (3) follows from $(G^{1/2}A)^*(G^{1/2}A) = A^*GA$. Equivalence of (2) and (3) follows from $|T|^2 = T^*T$ and uniqueness of the positive square root. □

4.4. Polar Characterization

Theorem 4.5 (Polar Characterization). Let $G > 0$ and let $A, B \in B(H)$. The following are equivalent: (1) $A \sim_G B$; (2) $|G^{1/2}A| = |G^{1/2}B|$; (3) there exists a partial isometry W with $G^{1/2}B = WG^{1/2}A$, $W^*W = P_{\mathrm{ran}(G^{1/2}A)}$, and $WW^* = P_{\mathrm{ran}(G^{1/2}B)}$.

Proof. By Theorem 4.2, $A \sim_G B$ is equivalent to $|G^{1/2}A| = |G^{1/2}B|$. Let $R = |G^{1/2}A| = |G^{1/2}B|$ and let $G^{1/2}A = U_A R$, $G^{1/2}B = U_B R$ be polar decompositions. Define W on $\mathrm{ran}(G^{1/2}A)$ by $W(U_A Rx) = U_B Rx$ and extend by zero on the orthogonal complement. Then W is a partial isometry with the stated projections and $G^{1/2}B = WG^{1/2}A$. The converse follows from $(G^{1/2}B)^*(G^{1/2}B) = (G^{1/2}A)^*W^*WG^{1/2}A = (G^{1/2}A)^*(G^{1/2}A)$.

4.5. G-Unitary Characterization

Theorem 4.6 (G-Unitary Characterization). Let $G > 0$ and suppose $A, B \in B(H)$ are invertible with $A \sim_G B$. Then $B = WA$ for some invertible operator W satisfying $W^*GW = G$ and $W^{-1} = G^{-1}W^*G$.

Proof. Put $W = BA^{-1}$. Then $W^*GW = A^{-*}B^*GBA^{-1} = A^{-*}A^*GAA^{-1} = G$. Since W is invertible and $W^*GW = G$, we obtain $W^{-1} = G^{-1}W^*G$.

5. Metric Invariants

The fundamental invariant preserved under G metric equivalence is the common strictly positive operator $A^*GA = B^*GB$. All of the following results are consequences of this equality.

5.1. Kernel and Range Structure

Theorem 5.1. Let $G > 0$ and $A, B \in B(H)$. If $A \sim_G B$, then $\ker A = \ker B$.

Proof. Let $x \in \ker A$. Then $A^*GAx = 0$, and since $A^*GA = B^*GB$, we get $B^*GBx = 0$. Taking the inner product with x gives $\langle GBx, Bx\rangle = 0$, and since $G > 0$ this implies $Bx = 0$. Thus $\ker A \subseteq \ker B$, and the reverse inclusion follows by symmetry.

Corollary 5.2. If $A \sim_G B$, then $\mathrm{ran}\, A^* = \mathrm{ran}\, B^*$. In finite dimensions, $\mathrm{rank}\, A = \mathrm{rank}\, B$.

5.2. Weighted Norm Invariance

Theorem 5.3. Let $G > 0$ and $A, B \in B(H)$. If $A \sim_G B$, then $\|Ax\|_G = \|Bx\|_G$ for every $x \in H$, and $\|A\|_G = \|B\|_G$.

Proof. $\|Ax\|^2_G = \langle GAx, Ax\rangle = \langle A^*GAx, x\rangle = \langle B^*GBx, x\rangle = \|Bx\|^2_G$. The equality of operator norms follows by taking the supremum over nonzero x.

5.3. Metric-Weighted Singular Values

Definition 5.4. Let $G > 0$ and $A \in B(H)$. We refer to the singular values of $G^{1/2}A$ as the singular values of the metric-weighted realization of A.

Theorem 5.5. Suppose H is finite-dimensional and $G > 0$. If $A \sim_G B$, then $G^{1/2}A$ and $G^{1/2}B$ have identical singular values, counted with multiplicity.

Proof. $(G^{1/2}A)^*(G^{1/2}A) = (G^{1/2}B)^*(G^{1/2}B)$. The singular values are the nonnegative square roots of the eigenvalues of the Gram operator. □

Remark 5.6. In infinite dimensions, the corresponding statement is equality of the strictly positive operators $(G^{1/2}A)^*(G^{1/2}A)$ and $(G^{1/2}B)^*(G^{1/2}B)$.

6. Epidemiological Metric Transport

Let $G_0, G_1, \ldots, G_N > 0$ be a plithogenic metric sequence. For each $t = 0, \ldots, N - 1$, let $A_t \in B(H_{epi})$ represent a transition between consecutive frames.

6.1. Epidemiological Transition Operators

The operator $A_t \in B(H_{epi})$ represents the transition of an epidemiological information state from frame t to frame t + 1. It may incorporate changes in disease occurrence information, exposure classification, immunity information, environmental risk, surveillance evidence, or intervention status. It is not assumed to be a biological transmission operator, and no particular compartmental epidemic model is imposed.

Definition 6.1. The operator A_t is called a plithogenic metric transport operator from frame t to frame t + 1 if $A^*_t G_{t+1} A_t = G_t$.

Theorem 6.2. Let A_t be a plithogenic metric transport operator. Then (1) $\|A_t x\|_{G_{t+1}} = \|x\|_{G_t}$ for every $x \in H_{epi}$; (2) $G_{t+1}^{1/2} A_t G_t^{-1/2}$ is an isometry.

Proof. $\|A_t x\|^2_{G_{t+1}} = \langle G_{t+1} A_t x, A_t x\rangle = \langle A^*_t G_{t+1} A_t x, x\rangle = \langle G_t x, x\rangle = \|x\|^2_{G_t}$. For the second assertion, $(G_{t+1}^{1/2} A_t G_t^{-1/2})^*(G_{t+1}^{1/2} A_t G_t^{-1/2}) = G_t^{-1/2} A^*_t G_{t+1} A_t G_t^{-1/2} = I$.

6.2. Explicit Transport Characterization

Theorem 6.3 (Explicit Transport Characterization). Let $G_0, G_1 > 0$ and $A \in B(H)$. Then $A^*G_1A = G_0$ if and only if $A = G_1^{-1/2} U G_0^{1/2}$ for some isometry U.

Proof. Suppose $A^*G_1A = G_0$. Define $U = G_1^{1/2} A G_0^{-1/2}$. Then $U^*U = I$ and $A = G_1^{-1/2} U G_0^{1/2}$. Conversely, if $A = G_1^{-1/2} U G_0^{1/2}$ with $U^*U = I$, then $A^*G_1A = G_0^{1/2} U^*U G_0^{1/2} = G_0$.

Corollary 6.4 (G-Unitary Special Case). If $G_0 = G_1 = G$, then $A^*GA = G$ if and only if $A = G^{-1/2} U G^{1/2}$ for some isometry U. In finite dimensions, if A is invertible, then U is unitary.

6.3. Multi-Step Transport

Definition 6.5. For s < t, $\Phi_{t,s} = A_{t-1} A_{t-2} \cdots A_s$.

Theorem 6.6 (Multi-Step Metric Transport). Let A_t satisfy $A^*_t G_{t+1} A_t = G_t$. Then for every s < t, $\Phi^*_{t,s} G_t \Phi_{t,s} = G_s$. In particular, $\|\Phi_{t,s} x\|_{G_t} = \|x\|_{G_s}$ for every $x \in H_{epi}$.

Proof. Induction on t − s. For t = s + 1 the assertion is $A^*_s G_{s+1} A_s = G_s$. Assume the result for (s, t). Then $\Phi_{t+1,s} = A_t \Phi_{t,s}$ and $\Phi^*_{t+1,s} G_{t+1} \Phi_{t+1,s} = \Phi^*_{t,s} A^*_t G_{t+1} A_t \Phi_{t,s} = \Phi^*_{t,s} G_t \Phi_{t,s} = G_s$.

Remark 6.7 (Epidemiological Interpretation). The condition $A^*_t G_{t+1} A_t = G_t$ states that the epidemiological information transition from frame t to frame t + 1 preserves the weighted geometry induced by the corresponding plithogenic contradiction structures. Consequently, $\|\Phi_{t,s} x\|_{G_t} = \|x\|_{G_s}$ means that the cumulative transition preserves the metric magnitude of the represented epidemiological information state. This is a geometric statement about the representation and does not assert conservation of population size, disease incidence, prevalence, or any biological quantity.

7. Approximate Metric Equivalence and Stability

Definition 7.1. Let G > 0 and A, B ∈ B(H). The G metric defect between A and B is $\Delta_G(A,B) = \|A^*GA - B^*GB\|$.

Proposition 7.2. $\Delta_G(A,B) = 0$ if and only if $A \sim_G B$. Consequently, Δ_G is a pseudometric on B(H), becoming a genuine metric on the quotient space $B(H)/\sim_G$.

Proof. $\Delta_G(A,B) = 0$ if and only if $A^*GA = B^*GB$, which is the definition of $A \sim_G B$. Symmetry is immediate from $\|A^*GA-B^*GB\| = \|B^*GB-A^*GA\|$, and the triangle inequality follows from the triangle inequality for the operator norm. The defect vanishes on each equivalence class, so it descends to a metric on the quotient.

Theorem 7.3 (Perturbation Estimate). Let G ∈ B(H) be positive and let $A, \tilde{A} \in B(H)$. Then $\|A^*GA - \tilde{A}^*G\tilde{A}\| \le \|G\|(\|A\| + \|\tilde{A}\|)\|A - \tilde{A}\|$.

Proof. $A^*GA - \tilde{A}^*G\tilde{A} = (A-\tilde{A})^*GA + \tilde{A}^*G(A-\tilde{A})$, hence the bound. □

Theorem 7.4 (Two-Sided Perturbation Inequality). Let G > 0 and $A, B, \tilde{A}, \tilde{B} \in B(H)$. Then $\Delta_G(A,B) \le \Delta_G(A,\tilde{A}) + \Delta_G(\tilde{A},\tilde{B}) + \Delta_G(\tilde{B},B)$.

Proof. Triangle inequality for the operator norm.

Theorem 7.5 (Stability of Metric Equivalence). Let $G > 0$ and suppose $A \sim_G B$. For perturbations $\tilde{A}, \tilde{B} \in B(H)$, $\Delta G(\tilde{A},\tilde{B}) \leq \|G\|[(\|A\|+\|\tilde{A}\|)\|A-\tilde{A}\| + (\|B\|+\|\tilde{B}\|)\|B-\tilde{B}\|]$.

Proof. $\tilde{A}^*G\tilde{A}-\tilde{B}^*G\tilde{B} = (\tilde{A}^*G\tilde{A}-A^*GA) + (B^*GB-\tilde{B}^*G\tilde{B})$, and apply Theorem 7.3 to each term. □

Theorem 7.6 (Convergence). Let $G > 0$ and let $A_n \to A$, $B_n \to B$ in operator norm. If $A_n \sim_G B_n$ for every n, then $A \sim_G B$.

Proof. The perturbation estimate implies $A^*_nGA_n \to A^*GA$ and $B^*_nGB_n \to B^*GB$. Since $A^*_nGA_n = B^*_nGB_n$ for every n, taking limits gives $A^*GA = B^*GB$.

8. Finite-Dimensional Classification and Examples

8.1. General Construction

Given $G > 0$, $R \geq 0$, and partial isometries U, V with the same initial space, define $A = G^{-(1/2)}UR$ and $B = G^{-(1/2)}VR$. Then $A^*GA = R^2$ and $B^*GB = R^2$, so $A \sim_G B$.

8.2. Example: Equivalent Epidemiological Operators

Let $H = \mathbb{C}^2$ and $G = \mathrm{diag}(2, 1)$. Consider $A = \mathrm{diag}(1, 1)$ and $B = \mathrm{diag}(1, -1)$. Then $A^*GA = B^*GB = \mathrm{diag}(2, 1)$, so $A \sim_G B$ despite $A \neq B$. Thus metric equivalence identifies operators at the level of their induced quadratic geometry without requiring equality of the operators themselves.

8.3. Example: Non-Equivalent Operators

For $C = [[1,1],[0,1]]$ and $D = \mathrm{diag}(1,1)$, we compute $C^*GC = [[2,2],[2,3]]$ and $D^*GD = \mathrm{diag}(2,1)$, so C and D are not G metrically equivalent.

8.4. Example: Time-Varying Metric

Let $G_0 = I$ and $G_1 = \mathrm{diag}(4,1)$. Then $A_0 = \mathrm{diag}(2,1)$ satisfies $A_0^*G_1A_0 = \mathrm{diag}(16,1) \neq G_0$, so A_0 is not a transport operator. However $\tilde{A}_0 = \mathrm{diag}(1/2,1)$ satisfies $\tilde{A}_0^*G_1\tilde{A}_0 = G_0$ and is therefore a valid transport operator.

8.5. Example: Exact Computation of the Metric Defect

Let $A = I$, $\tilde{A} = [[1,\varepsilon],[0,1]]$, and $G = I$. Then $E = A^*A - \tilde{A}^*\tilde{A} = [[0,-\varepsilon],[-\varepsilon,-\varepsilon^2]]$, with eigenvalues $\lambda_\pm = (-\varepsilon^2 \pm \sqrt{\varepsilon^4+4\varepsilon^2})/2$. Hence $\|E\| = (\varepsilon^2 + \varepsilon\sqrt{\varepsilon^2+4})/2 = \varepsilon + \varepsilon^2/2 + O(\varepsilon^3)$.

9. Epidemiological Interpretation

9.1. State Representation

Epidemiological attributes such as disease occurrence, exposure, immunity, diagnostic status, and environmental risk are represented as components of a plithogenic state $x_t \in H_{epi}$. The truth, indeterminacy, and falsity components encode supporting, incomplete, and opposing information, respectively. This representation is epistemic rather than probabilistic.

9.2. Contradiction and Uncertainty

Epidemiological surveillance may produce information that is incomplete, delayed, or apparently contradictory. The contradiction function C_t and the associated matrix D_t encode these incompatibilities at the attribute level, and the extended operator $\tilde{D}_t = C_t \otimes D_t$ transfers them into the plithogenic state space. The resulting metric operator $G_t = G_{0,t}^{(1/2)}(I + \lambda_t\tilde{D}_t)G_{0,t}^{(1/2)}$ therefore incorporates contradiction structure into the geometry of the epidemiological information state.

9.3. Metric Equivalence and Transport

Two transition operators A and B are G_t metrically equivalent when $A^*G_tA = B^*G_tB$, meaning that they induce the same quadratic geometry under the plithogenic epidemiological metric. Metric equivalence concerns preservation of the weighted geometry of the represented information state and does not imply equality of epidemiological trajectories. If $A^*_tG_{t+1}A_t = G_t$ holds at each temporal transition, then the multi-step transport theorem gives $\Phi^*_{t,s}G_t\Phi_{t,s} = G_s$, so local preservation of epidemiological information geometry produces global preservation across the entire sequence of frames. This result is independent of any particular disease transmission mechanism.

9.4. Scope and Limitations

The epidemiological interpretation presented here is theoretical. No patient-level observations, population surveillance dataset, incidence estimates, prevalence estimates, parameter estimation, hypothesis testing, or empirical disease forecasting is performed. The metric operator G_t should be interpreted as a mathematical representation of epidemiological information geometry rather than as an empirically estimated epidemiological risk metric. The transition operators A_t describe transformations of represented epidemiological information and are not asserted to coincide with biological transmission operators. An empirical extension would require disease-specific data, a defined epidemiological observation model, estimation of the contradiction matrices D_t, specification or estimation of the interaction matrices C_t, and validation of the resulting metric and transition operators. These tasks are outside the scope of the present theoretical study.

10. Conclusions and Future Directions

This paper has developed a theory of time-dependent plithogenic metric equivalence and metric transport for bounded operators on Hilbert spaces associated with evolving epidemiological states.

The main results are as follows. We constructed contradiction-induced strictly positive metric operators on the plithogenic epidemiological state space using a structured tensor product embedding $\tilde{D}_t = C_t \otimes D_t$. We defined G_t metric equivalence $A \sim_G B$ via $A^*GA = B^*GB$ and proved the reduction theorem $A \sim_G B$ if and only if $G^{1/2}A \sim G^{1/2}B$, together with polar and partial isometry characterizations. We identified metric invariants preserved under G-equivalence, namely the G-norm, kernel structure, finite-dimensional rank, and singular values of metric-weighted realizations. We introduced transport operators satisfying $A^*_tG_{t+1}A_t = G_t$, proved the explicit characterization $A = G_1^{-1/2}UG_0^{1/2}$ with U an isometry, and established the central multi-step transport theorem $\Phi^*_{t,s}G_t\Phi_{t,s} = G_s$. We defined the metric defect $\Delta_G(A,B) = \| A^*GA-B^*GB \|$, showed it is a pseudometric becoming a metric on the quotient $B(H)/\sim_G$, and established perturbation and stability estimates.

The central mathematical message is: local metric preservation at every frame implies global metric preservation across every finite evolution.

Limitations of the present work should be noted. The explicit contradiction construction is finite-dimensional and assumes $H_T = H_I = H_F = \mathbb{C}^n$. The component interaction matrix C_t is a modelling choice rather than a quantity derived from the plithogenic representation itself. The epidemiological interpretation is theoretical only and does not provide empirical validation. The results are stated for bounded operators; the unbounded case requires additional domain considerations.

Future research directions include extension to unbounded operators and semigroup theory; derivation of the component interaction matrix C_t from plithogenic epidemiological data; investigation of spectral properties and invariant subspaces for metric transport operators; development of numerical algorithms for computing the metric equivalence defect in high-dimensional settings; data-driven estimation of the plithogenic metric sequence G_t from observed epidemiological frames; application of the framework to other domains involving evolving uncertain states; and investigation of generalized inverses and pseudo-inverse transport operators.

Funding: This research received no external funding.

Acknowledgments: The authors are thankful to the Department of Mathematics and Physical Sciences at Maasai Mara University for supporting this work.

Conflicts of Interest: The authors declare no conflict of interest.

References

1. Ahmad, M.R.; et al. A computational diagnostic model for infectious diseases via similarity measures on N-framed plithogenic hypersoft sets. Alexandria Engineering Journal 2025, 127, 1209–1219. https://doi.org/10.1016/j.aej.2025.06.028
2. Amenya, C.; Wanjala, V.; Matuya, J.W. On deformed metric equivalence of Hilbert space operators. Jambura Journal of Mathematics 2026, 8(2), 138–142. https://doi.org/10.37905/jjom.v8i2.36685
3. Bhatia, R. Matrix Analysis; Springer, 1997. https://doi.org/10.1007/978-1-4612-0653-8
4. Bhatia, R. Positive Definite Matrices; Princeton University Press, 2007.
5. Bhatia, R.; Kittaneh, F. On some perturbation inequalities for operators. Linear Algebra and its Applications 1988, 106, 271–279. https://doi.org/10.1016/0024-3795(88)90034-1
6. Brayman, V.; et al. Functional Analysis and Operator Theory; Springer, 2024. https://doi.org/10.1007/978-3-031-56427-7
7. Chahbi, A.; Kabbaj, S. Linear maps preserving G-unitary operators in Hilbert space. Arab Journal of Mathematical Sciences 2015, 21(1), 109–117. https://doi.org/10.1016/j.ajmsc.2014.03.002
8. Conway, J.B. A Course in Functional Analysis, 2nd ed.; Springer-Verlag, 1990.
9. Kadison, R.V.; Ringrose, J.R. Fundamentals of the Theory of Operator Algebras, Vol. I: Elementary Theory; American Mathematical Society, 1997.
10. Kato, T. Perturbation Theory for Linear Operators, 2nd ed.; Springer, 1995. https://doi.org/10.1007/978-3-642-66282-9
11. Mbekhta, M. Approximation of the polar factor of an operator acting on a Hilbert space. Journal of Mathematical Analysis and Applications 2020, 487(1), 123954. https://doi.org/10.1016/j.jmaa.2020.123954
12. Mbekhta, M. Representation and approximation of the polar factor of an operator on a Hilbert space. Discrete and Continuous Dynamical Systems S 2021, 14(8), 3043–3054. https://doi.org/10.3934/dcdss.2020463
13. Mostafazadeh, A. Time-dependent pseudo-Hermitian Hamiltonians defining a unitary quantum system. Physical Review D 2007, 76, 105008.
14. Mostafazadeh, A. Time-dependent pseudo-Hermitian Hamiltonians and a hidden geometric aspect of quantum mechanics. Journal of Physics A: Mathematical and Theoretical 2010, 43, 145301.
15. Murphy, G.J. C*-Algebras and Operator Theory; Academic Press, 1990.
16. Nzimbi, B.M.; et al. On almost similarity and metric equivalence of operators. Pioneer Journal of Mathematics and Mathematical Sciences 2016, 8(2), 127–140.
17. Nzimbi, B.M.; Kibet, M.S.; Luketero, S.W. The intersection of similarity and metric equivalence relations of operators. Asian Journal of Pure and Applied Mathematics 2023, 5(1), 14–23.
18. Rudin, W. Functional Analysis, 2nd ed.; McGraw-Hill, 1991.
19. Smarandache, F. Plithogenic set, an extension of crisp, fuzzy, intuitionistic fuzzy, and neutrosophic sets revisited. Neutrosophic Sets and Systems 2018, 21, 153–166. https://doi.org/10.5281/zenodo.1408740
20. Smarandache, F. Extension of soft set to hypersoft set, and then to plithogenic hypersoft set. Neutrosophic Sets and Systems 2018, 22, 168–170. https://doi.org/10.5281/zenodo.2159754
21. Smarandache, F. Plithogeny: Plithogenic Set, Logic, Probability and Statistics; Pons Publishing House, 2018.

Received: Aug. 1, 2026. Accepted: Sept. 15, 2026.

Teaching Effectiveness of Higher Education Based on Big Data and Artificial Intelligence: A Novel Neutrosophic Multi-Criteria Decision Framework for Intelligent Educational Performance Evaluation

Xiaojiang Feng*
School of Educational Science, Yan'an University, Yan'an, Shaanxi, 716000, China
*Corresponding author, E-mail: ydfxj22@163.com

Abstract: The recent fast-paced digital revolution of education has led to an unprecedented amount of educational data being collected through learning management systems, online exams, student information systems, interactions in class and institutional analytics. Although the big data and artificial intelligence (AI) can help to assess teaching performance quite effectively, the current evaluation methods use mostly deterministic or fuzzy models, which cannot sufficiently reflect the uncertainty and inconsistencies of educational settings. Different opinions of experts, heterogeneous feedbacks, unobserved data and conflicting performance criteria often decrease the reliability and consistency of assessment of teaching effectiveness. In order to overcome these limitations, a new neutrosophic multi-criteria decision-making (MCDM) framework is introduced in this paper, which combines big data analytics and artificial intelligence for the evaluation of teaching effectiveness in higher education. This framework uses truth, indeterminacy and falsity membership degrees to model educational information, thus allowing one to evaluate simultaneously the certainty, ambiguity and contradictions within multiple criteria of teaching quality. Criterion weights are determined objectively based on characteristics of educational data, while the AI-based analytics help to identify important patterns of performance from large academic datasets. This model integrates the components via a well-constructed neutrosophic ranking process mathematically for obtaining trustworthy and understandable evaluations of teaching performance. The model has been formulated for the purpose of facilitating institutional decision-makers to identify their strengths in teaching, prioritize their professional development, and improve education quality via evidence-based decision-making processes. The proposed approach will be examined and compared with existing MCDM methods on a dataset regarding higher education teaching evaluation under the same experimental conditions. The sensitivity, robustness, and comparative studies will be carried out for investigating the consistency and feasibility of the proposed approach. The anticipated contribution is an intelligent educational evaluation framework that can successfully manage the uncertainty while taking advantage of big data and artificial intelligence.

Keywords: Teaching effectiveness; Higher education; Big data analytics; Artificial intelligence; Neutrosophic sets; Multi-criteria decision making.

1. Introduction

It is widely accepted that teaching effectiveness is one of the most important factors determining the quality of education in higher education institutions. Nowadays, higher education institutions are increasingly required to offer high-quality teaching that contributes to learning, increases academic performance, and develops skills needed in modern society. In this way, the assessment of teaching effectiveness has become an important strategic task for higher education institutions aiming at continuous quality improvement, accreditation requirements, and educational management based on evidence. Traditional assessment methods, such as student questionnaire survey or the judgment of experts, give little understanding of the complicated nature of teaching performance. In many cases, these methods do not make use of a great deal of educational data available in modern digital environment[1], [2].

The fast implementation of learning management systems, online learning systems, intelligent tutoring systems, classroom sensors, and information systems has turned higher education into a data-driven environment. Everything done during educational activities – student attendance, their performance in the assessment, online interaction, learning behavior, course completion, educational materials, and classroom participation – provides useful digital information. The availability of educational data brings a lot of possibilities for the assessment of teaching quality based on comprehensive, objective, and constantly updated data rather than only subjective evaluations[3], [4].

Educational big data has enabled educational institutions to increase dramatically their capabilities of collecting, processing, storing, and analyzing various kinds of educational datasets. Educational big data includes high volumes, velocities, varieties, veracies, and values that allow universities to observe instructional activities from different angles and at a large timescale. Due to the integration of various educational information sources, it becomes possible to find connections between teaching practices, student involvement, learning outcomes, and academic performance[5], [6].

AI has additionally contributed to the development of education evaluation by presenting smart data analytics methodologies that can extract valuable knowledge from big educational datasets. The machine learning algorithms, deep learning, natural language processing, recommendation systems, and predictive analysis have been widely used to evaluate students' feedback, predict learning outcomes, identify at-risk students, and make pedagogical decisions. AI helps educational institutions to perform automated analytical tasks, identify hidden patterns in performance, and make recommendations on how to improve the quality of teaching[7], [8].

However, despite the use of the mentioned technologies, evaluating the effectiveness of teachers still remains a difficult problem due to the fact that educational information is highly uncertain, incomplete, inconsistent, and even contradictory. Personal bias may impact students' evaluations, experts may hold different views on instruction, classroom observations may be partial, and educational performance indicators may be vague.

Moreover, learning analytics and human judgment may provide conflicting evidence for the same instructor. Classical statistical and classical machine learning methods rely on precise observations, while fuzzy approaches focus on vagueness without taking into account indeterminacy and contradictions[9], [10].

A more advanced representation of uncertainty in the form of neutrosophic models, which describes three independent membership functions of truth, indeterminacy, and falsity, is provided by neutrosophic theory. Contrarily to the classical fuzzy and intuitionistic fuzzy models, the neutrosophic approach allows for the description of not only certainty but also hesitation, inconsistency, and incomplete information. The ability is especially important for the educational evaluation since different stakeholders, such as students, their peers, school administration, and outsiders, usually give their assessment with different degrees of certainty and contradict each other. Therefore, the mathematical ground offered by neutrosophic modeling is relevant to capture the complexity of the uncertainty in assessing teaching efficiency[11], [12].

Despite many attempts to apply artificial intelligence, learning analytics, and multi-criteria decision-making techniques to evaluate the process of education, some problems persist. First of all, the approaches used in most cases concentrate on building predictive models and do not offer decision support. Secondly, they are based on traditional techniques of MCDM that are unable to model uncertainty that comes from the heterogeneity of educational information. Finally, there are few integrated approaches in the existing literature that combine AI, big data analytics, and uncertainty modeling[13], [14].

In response to the issues highlighted above, this research suggests a new neutrosophic multi-criteria decision-making approach for assessing teaching effectiveness in higher education based on big data and artificial intelligence. The new approach combines the use of AI-driven educational analytics along with neutrosophic information modeling, which allows dealing with uncertainty while leveraging big educational data to perform objective assessments. The suggested approach is aimed at aggregating multiple educational performance criteria using a mathematically sound decision-making process that accounts for imprecise, inconsistent and ambiguous information.

Key highlights of this study include:

(1) A new neutrosophic-based decision-making approach for the holistic assessment of teaching effectiveness in uncertain educational settings.
(2) A new technique that uses big data analytics and artificial intelligence to mine information related to teaching performance from diverse educational data sets.
(3) Modeling of educational uncertainty in terms of truth, indeterminacy and falsity membership functions that can simultaneously capture conflicting and incomplete information for evaluation.
(4) The new decision-making approach offers an interpretative multi-criteria ranking mechanism for helping decision-makers in institutions identify areas where teaching is strong and areas where improvement is needed.

(5) The new method will be tested experimentally using higher education teaching data sets and benchmarked against multi-criteria decision-making techniques. Sensitivity and robustness analysis will further validate its applicability and decision stability.

2. Related Work and Critical Research Gap

2.1 Teaching Effectiveness Evaluation in Higher Education

Teaching effectiveness has long been considered a multidimensional construct that includes instructional quality, learner achievement, classroom dynamics, curriculum delivery, assessment processes, and competency of instructors. Higher education institutions usually assess teaching effectiveness through student evaluations, peer reviews, self-reporting, classroom observations, and administration's judgment[15], [16]. The aforementioned evaluation process generates valuable data about academic promotion, curricular development, faculty development, and quality assurance at an institution. Student evaluation of teaching (SET) continues to be the most popular method of evaluating teaching effectiveness due to its practicality and straightforward nature. This is directly related to obtaining the information about the quality of instruction from students. There are many studies indicating that student evaluations could be affected by non-academic variables including expected grades, difficulty of the course, number of students enrolled in the course, popularity of the instructor, gender differences, and personal preferences. In order to counteract these weaknesses, most universities have introduced comprehensive evaluation models, which incorporate various performance measures such as student achievement, participation in classes, innovation in instruction, evidence-based teaching, class management, and professional development. Multidimensional evaluation models generate more balanced assessments, but create additional problems due to the fact that the measures may have different scales and ambiguous connections[17], [18].

2.2 Big Data Analytics in Educational Evaluation

The fast-paced digitization of universities has produced the constant formation of educational big data generated by learning management systems, online classrooms, evaluation platforms, electronic libraries, attendance systems, and academic information systems. Educational big data allows educational organizations to assess the learning behaviors, teaching activities, academic performance, and institutional performance at an unprecedented level of detail. Big data analytics has been used extensively to find learning patterns, assess students' performance, discover academic risks, estimate the efficiency of courses, and make decisions about educational policies. Educational dashboards and learning analytics platforms enable educators and teachers to monitor the process of instruction in real-time mode while gaining evidence-based knowledge for improving the quality of their work. At the same time, educational big data poses serious analytical problems caused by its heterogeneous nature, poor quality, missing values, temporal aspects, and high dimensionality. Combining various sources of educational big data into one teaching evaluation framework is a challenging process, especially when there is uncertainty and inconsistency in information[19].

2.3 Artificial Intelligence for Teaching Quality Assessment

Indeed, artificial intelligence can be seen as one of the most influential technological approaches to intelligent assessment of education. There are lots of machine learning algorithms applied in forecasting student success, classification of learning behavior, analysis of educational materials, identification of potentially risky learners, and instructional assessment. Deep learning methods have been shown to work very well in analysis of textual feedback, videos from classes, forums for discussions, and multimodal educational data. Besides, natural language processing methods have been applied to the analysis of qualitative comments made by students, detection of teaching-related topics, sentiment analysis, and detection of strengths and weaknesses in instruction. Recommendation systems help teachers to make recommendations regarding teaching strategies and educational materials on the basis of historical educational data. While AI makes predictive performance and analytical processes much better, there are a lot of AI-based models which are the examples of black box systems that cannot provide any interpretation. There are cases when educational administrators need to have decision support systems explaining how teaching effectiveness is evaluated not making any predictions.

2.4 Multi-Criteria Decision-Making Approaches in Educational Assessment

Effectiveness in teaching is bound to include a range of qualitative and quantitative criteria that are mutually exclusive. MCDM models have thus been used in educational evaluation problems due to their capacity for the consideration of many performance criteria simultaneously. AHP, TOPSIS, VIKOR, ELECTRE, PROMETHEE, COPRAS, ARAS, MOORA, MARCOS, WASPAS, and EDAS methods have been used in ranking professors, evaluation of educational courses, prioritization of development activities, and management decisions in academia. Objective criterion weight determination techniques like CRITIC, Entropy, MEREC, and Standard Deviation weightings have been employed in combination with ranking methods to minimize any subjectivity involved in the importance determination of criteria. Conventional MCDM models usually consider evaluation information under the assumption of its deterministic nature. But in actual educational settings, evaluation information tends to involve ambiguity, imprecision, inconsistency, and uncertainty that cannot be adequately expressed in crisp numbers.

2.5 Neutrosophic Decision Models under Educational Uncertainty

The theory of neutrosophics has proven to be a useful tool in expressing uncertainty using three membership functions for truth, indeterminacy, and falsity. Neutrosophic representations are more flexible than their fuzzy and intuitionistic counterparts in representing incomplete and inconsistent data. There are several studies on neutrosophic MCDM techniques that can be applied in decision-making in healthcare, engineering, supplier selection, sustainability evaluation, risk assessment, energy management, and financial evaluation. The existing literature shows that decisions based on neutrosophic representations are more reliable when data are either imprecise or somewhat contradictory. But there have been few attempts to study neutrosophic decision-making techniques for evaluating teaching effectiveness, especially when large amounts of educational data are available. Most studies concentrate either on expert-based evaluation using small-sized data or on educational evaluation using traditional tools without leveraging educational data that is available from advanced educational systems.

2.6 Critical Research Gap

The above review highlights a number of critical shortcomings of the existing literature.

First, most of the existing systems for teaching evaluations are either too dependent on subjective expertise or based on AI prediction models that do not involve any multi-criteria decision making processes. In other words, educational administrators are provided with correct predictions without any explanation of how these decisions were made.

Second, even though educational big data provides a lot of information about educational activities, a number of contemporary methods for evaluations do not combine heterogeneous educational datasets in one decision-making framework allowing for consideration of both quantitative and qualitative indicators, as well as institutional indicators.

Third, most of the existing MCDM methods are based on either deterministic or fuzzy information, while the decision process in education involves a lot of uncertainties, inconsistencies, incompleteness, and conflicting information. This makes the reliability of decision-making results questionable since multiple stakeholders provide different views on the issue.

Fourth, AI-based methods of educational evaluations are mostly focused on predictive accuracy but not on uncertainty modeling, interpretability, and transparency of the decision-making process.

However, one final deficiency of existing methods lies in the absence of frameworks that would be able to integrate all these elements – big data analytics of educational data, AI, representation of neutrosophic uncertainty, criterion weighting, and multi-criteria ranking. Taking into account such deficiencies, this research suggests a new method of multi-criteria decision making based on neutrosophy, big data analytics and AI that would be capable to assess effectiveness of teaching in higher education institutions. The suggested framework should be aimed at representing uncertain information about education using truth, indeterminacy, and falsity memberships and taking advantage of knowledge representation and extraction using AI technologies.

3. Mathematical Preliminaries and Neutrosophic Definitions

In this section, the mathematics behind the proposed framework is discussed. Due to the subjectivity involved in the evaluation of teaching effectiveness, the heterogeneity of the education data, and the contradictory evidence gathered from students, peers, administrators, and intelligent education systems, the theory of neutrosophic sets offers an adequate mathematical model to handle uncertainty. The proposed framework uses the concept of single-valued neutrosophic sets (SVNSs).

3.1 Universe of Discourse

Let

$$X = \{x_1, x_2, \ldots, x_n\} \qquad (1)$$

denote the finite universe of discourse, where each element x_i represents an alternative. In this study, an alternative corresponds to a university instructor whose teaching effectiveness is evaluated.

Let

$$C = \{C_1, C_2, \ldots, C_m\} \qquad (2)$$

define the set of evaluation criteria for describing teaching effectiveness.

The examples of evaluation criteria are:

- Teacher preparation
- Delivery in class
- Student involvement
- Quality of assessment
- Teaching through research
- Digital teaching skills
- Achievement of learning outcomes
- Instructional effectiveness supported by AI

Let there be n teachers and m evaluation criteria.

Definition 1. Single-Valued Neutrosophic Set

A Single-Valued Neutrosophic Set (SVNS) A on X is defined as

$$A = \{\langle x, T\_A(x), \quad I\_A(x), F\_A(x) \rangle : x \in X \} \qquad (3)$$

Where:

$T\_A(x) : X \to [0,1]$

$I\_A(x) : X \to [0,1]$

$F\_A(x) : X \to [0,1]$

represent respectively:

$T\_A(x)$ = truth-membership degree

$I\_A(x)$ = indeterminacy-membership degree

$F\_A(x)$ = falsity-membership degree

subject to

$$0 \le T\_A(x), I\_A(x), F\_A(x) \le 1 \quad (4)$$

and

$$0 \le T\_A(x)+I\_A(x)+F\_A(x) \le 3 \quad (5)$$

Unlike intuitionistic fuzzy sets, the three membership values are mutually independent, allowing inconsistent and incomplete information to be represented simultaneously.

Definition 2. Single-Valued Neutrosophic Number

A Single-Valued Neutrosophic Number (SVNN) is expressed as

$$A = (T, I, F) \quad (6)$$

Where:

$T \in [0,1]$

$I \in [0,1]$

$F \in [0,1]$

Example: $A = (0.82,0.11,0.08)$

Indicates Truth = 0.82, Indeterminacy = 0.11, Falsity = 0.08 which represents a highly positive evaluation with relatively low uncertainty.

Definition 3. Neutrosophic Decision Matrix

Assume there are n alternatives and m criteria. The neutrosophic decision matrix is

$$D = [d_{ij}]_{n \times m} \quad (7)$$

Where:

$d_{ij} = (T_{ij}, I_{ij}, F_{ij})$ represents the neutrosophic evaluation of instructor i under criterion j.

Therefore:

$$D = \begin{bmatrix} (T_{11},I_{11},F_{11}) & \cdots & (T_{1m},I_{1m},F_{1m}) \\ \vdots & \ddots & \vdots \\ (T_{n1},I_{n1},F_{n1}) & \cdots & (T_{nm},I_{nm},F_{nm}) \end{bmatrix} \quad (8)$$

Each element is obtained from educational big data, AI analytics, expert assessment, or their integration.

Definition 4. Score Function

To compare two neutrosophic numbers, a score function is required. The score value of

$A=(T,I,F)$ is defined as:

$$S(A)= (2+T-I-F)/3 \quad (9)$$

where $-1 \le S(A) \le 1$ A larger score indicates better teaching effectiveness.

Definition 5. Accuracy Function

When two alternatives possess identical score values, an accuracy function is used.

The accuracy function is:

$$H(A)=T-F \quad (10)$$

Higher values indicate stronger certainty in the evaluation.

Definition 6. Weighted Neutrosophic Aggregation

Suppose $w=(w_1,w_2,\ldots,w_m)$ denotes the criterion weight vector satisfying

$$w_j \ge 0 \quad (11)$$

and

$$\Sigma\ w_j =1 \quad (12)$$

The aggregated neutrosophic assessment for instructor i is represented as:

$$N_i=(T_i,I_i,F_i) \quad (13)$$

Where:

$$T_i = \Sigma\ w_j T_{ij} \quad (14)$$

$$I_i = \Sigma\ w_j I_{ij} \quad (15)$$

$$F_i = \Sigma\ w_j F_{ij} \quad (16)$$

for $j=1,2,\ldots,m$.

The aggregated value summarizes the overall teaching effectiveness by simultaneously considering all evaluation criteria and their corresponding importance weights.

Definition 7. Ranking Rule

Given two instructors A_1 and A_2 the ranking procedure follows:

$$\text{If } S(A_1) > S(A_2) \text{ then } A_1 \succ A_2 \tag{17}$$

If $S(A_1)=S(A_2)$ then compare $H(A_1)$ and $H(A_2)$.

$$\text{If } H(A_1)>H(A_2) \text{ then } A_1 \succ A_2 \tag{18}$$

Otherwise A_2 is preferred.

The aforementioned preliminaries provide the foundation for the proposed intelligent neutrosophic approach to teaching evaluation. The next section presents the formulation of the teaching effectiveness decision problem for higher education. The criteria, alternatives and decision making environment are also introduced in this section.

4. Problem Formulation

In this section, the teaching effectiveness evaluation problem is posed as a MCDM problem using neutrosophic sets, given that the teaching environment includes factors such as uncertainty, partial information, heterogeneous educational data, and conflicting evaluation criteria. The task here is to develop a smart decision-making model to rank university teachers in terms of teaching effectiveness using educational big data, AI, and neutrosophic information.

4.1 Decision Environment

$$\text{Assume that } A = \{A_1, A_2, \ldots, A_n\} \tag{19}$$

is the set of teaching alternatives, where A_i ($i = 1,2,\ldots,n$) denotes the i-th university instructor. Similarly,

$$C = \{C_1, C_2, \ldots, C_m\} \tag{20}$$

denotes the set of criteria for evaluating teaching. Every teacher is evaluated on each criterion based on the data gathered from different sources of education, including:

- Data of student evaluations
- Learning Management Systems (LMS)
- Reports of classroom observations
- Systems of academic management

- Learning analytics
- AI generated instruction analytics
- Databases of institutional teaching

Hence, the evaluation process consists of heterogeneous data from education with different degrees of certainty.

4.2 Evaluation Criteria

Suppose the teaching effectiveness evaluation is conducted using the following representative criteria.

C_1 : Teaching Preparation
C_2 : Classroom Delivery
C_3 : Student Engagement
C_4 : Assessment and Feedback Quality
C_5 : Learning Outcome Achievement
C_6 : Research-Integrated Teaching
C_7 : Digital Teaching Competency
C_8 : AI-Supported Instructional Effectiveness

These criteria collectively describe instructional quality from pedagogical, technological, and learning-performance perspectives.

4.3 Educational Big Data Representation

For instructor A_i and criterion C_j, educational information is collected from multiple heterogeneous sources.

$$\text{Let } x_{ij} = \{x_1, x_2, \ldots, x_k\} \qquad (21)$$

where the educational observations related to instructor i by criterion j are denoted.

The observations could include:

- Satisfactions of students
- Data on attendance
- Information about assignment submission
- Data on online activities
- Data on learning behaviors
- AI generated data on teaching quality
- Data on classroom interactions

Post processing of the information into neutrosophic form.

4.4 Neutrosophic Evaluation Matrix

The evaluation matrix is defined as:

$$D=[d_{ij}]_{n\times m} \quad (22)$$

Where:

$$d_{ij}=(T_{ij},I_{ij},F_{ij}). \quad (23)$$

Here, T_{ij} signifies the strength of the available evidence indicating satisfactory teaching performance.

I_{ij} signifies the degree of indeterminacy due to incomplete, inconsistent, or contradictory educational data.

F_{ij} signifies the strength of the available evidence supporting unsatisfactory teaching performance.

Each neutrosophic number is such that:

$$0\le T_{ij}\le 1 \quad (24)$$

$$0\le I_{ij}\le 1 \quad (25)$$

$$0\le F_{ij}\le 1 \quad (26)$$

and

$$0\le T_{ij}+I_{ij}+F_{ij}\le 3 \quad (27)$$

4.5 Criterion Weight Vector

The importance of the evaluation criteria is represented by

$$W=(w_1,w_2,\dots,w_m) \quad (28)$$

subject to

$$w_j\ge 0 \quad (29)$$

and

$$\sum_{j=1}^{m} w_j =1 \quad (30)$$

The proposed framework determines these weights objectively using educational data characteristics extracted from big data analytics, thereby reducing dependence on purely subjective expert judgments.

4.6 Artificial Intelligence-Based Feature Extraction

Suppose

$$X=\{x_1,x_2,\dots,x_p\} \quad (31)$$

represents the educational feature vector extracted from institutional databases. An artificial intelligence model transforms the raw educational data into informative teaching-performance indicators,

$$Z=f_{AI}(X) \quad (32)$$

Where X denotes the original educational feature space, f_AI(·) represents the AI learning model, and $Z=\{z_1,z_2,\ldots,z\_q\}$ is the extracted feature representation used for teaching evaluation. The generated indicators provide quantitative evidence supporting the neutrosophic evaluation process.

4.7 Objective Function

The primary objective is to determine the optimal ranking of university instructors according to their comprehensive teaching effectiveness.

Let $R(A_i)$ denote the overall evaluation score of instructor A_i. The optimization objective is max $R(A_i)$, For i=1,2,…,n.

The ranking function combines

- objective criterion weights,
- AI-generated educational knowledge,
- neutrosophic uncertainty,
- and multi-criteria aggregation

to obtain the final teaching effectiveness scores.

4.8 Research Assumptions

The above framework is developed based on the following assumptions:

- Assumption 1 The data regarding education are gathered from credible institutional information systems.
- Assumption 2 All evaluation criteria are standardized prior to neutrosophication.
- Assumption 3 Membership functions for truth, indeterminacy, and falsehood are independent.
- Assumption 4 Criterion weights conform to the normalization condition.
- Assumption 5 All instructors are evaluated using the same criteria and same institutional conditions.

4.9 Problem Statement

Given:

1. n university instructors,
2. m teaching evaluation criteria,
3. heterogeneous educational big data,
4. AI-generated teaching indicators,
5. and uncertain educational information,

determine the ranking

$$A\_(1) \succ A\_(2) \succ \ldots \succ A\_(n) \qquad (33)$$

so that the final ranking can properly capture the teaching effectiveness of all teachers taking into account uncertainties, inconsistencies, and incomplete educational information. The above mathematical model sets up the optimization problem investigated in this paper. In the next section, the proposed intelligent neutrosophic decision making framework will be presented, which involves the innovative weighting method, neutrosophic aggregation technique, intelligent evaluation approach and computational process.

5. Proposed Intelligent Neutrosophic Decision Framework

In this section, the proposed intelligent neutrosophic decision model for assessing the teaching performance in higher education based on educational big data and artificial intelligence (AI) is introduced. The proposed decision model differs from traditional MCDM methods by incorporating feature extraction via AI, objective criterion weights, neutrosophic modeling of uncertainty, adaptive aggregation, and intelligent ranking in a coherent decision-making process.

5.1 Framework Architecture

The developed framework comprises seven consecutive steps:

- Step 1 Collecting Education Big Data
- Step 2 Data Cleaning and Automated Feature Extraction Using AI
- Step 3 Creating the Neutrosophic Decision Matrix
- Step 4 Calculation of Weights of Objective Criteria
- Step 5 Adaptive Neutrosophic Aggregation
- Step 6 Calculating Scores of Teaching Effectiveness
- Step 7 Ranking University Teachers

Mathematical connection exists between all steps of the developed evaluation approach.

5.2 Stage 1. Educational Data Acquisition

Suppose $E=\{e_1,e_2,\ldots,eN\}$. This represents the entire education dataset that is collected from institutional databases.

The data set comprises of:

- Student feedback
- LMS data
- Data related to online learning
- Assessment data
- Observation data from classrooms
- AI generated instructional data
- Academic management databases

After being preprocessed, each criterion is normalized to [0,1].

5.3 Stage 2. AI-Based Feature Extraction

$$\text{Let } X=(x_1,x_2,\ldots,xp) \tag{34}$$

denote the normalized educational feature vector. An AI model extracts high-level instructional information

$$Z=fAI(X) \quad (35)$$

where $fAI(\cdot)$ represents the artificial intelligence learning model. The extracted feature vector becomes $Z=(z_1,z_2,\ldots,zq)$.
These features summarize the instructional characteristics required for teaching evaluation.

5.4 Stage 3: Neutrosophic Transformation

Each extracted feature is transformed into three independent membership values.

Truth Membership:

$$Tij=fT(zij) \quad (36)$$

Indeterminacy Membership:

$$Iij=fI(zij) \quad (37)$$

Falsity Membership:

$$Fij=fF(zij) \quad (38)$$

Where $0\leq Tij,Iij,Fij\leq 1$.

The corresponding neutrosophic number becomes $dij=(Tij,Iij,Fij)$.
The complete neutrosophic decision matrix is:

$$D=[dij]n\times m \quad (39)$$

5.5 Stage 4. Objective Criterion Weighting

Instead of assigning subjective importance values, the proposed framework determines criterion importance from educational information.
Let σj denote the standard deviation of criterion j, and μj its mean value. The information coefficient is computed as:

$$ICj=\sigma j/\mu j \quad (40)$$

The normalized objective weight becomes:

$$wj=ICj/\Sigma ICj \quad (41)$$

subject to:

$$\Sigma wj=1 \quad (42)$$

Higher variability indicates stronger discrimination capability and therefore receives a larger objective weight.

5.6 Stage 5. Adaptive Neutrosophic Aggregation Operator

To improve robustness under uncertain educational environments, this study introduces an Adaptive Neutrosophic Educational Aggregation Operator (ANEAO).

For instructor Ai, the adaptive truth component is:

$$Ti^*=\Sigma wjTij \qquad (43)$$

The adaptive indeterminacy component is:

$$Ii^*=\Sigma wj^2Iij \qquad (44)$$

The adaptive falsity component is:

$$Fi^*=\Sigma wjFij \qquad (45)$$

Unlike the traditional methods of weighted average, here the weight of the indeterminacy element is calculated using a square of the weight. It helps penalize those criteria with high uncertainty levels, without losing valuable information from trustworthy educational data. The resulting neutrosophic assessment is:

$$Ni=(Ti^*,Ii^*,Fi^*) \qquad (46)$$

5.7 Stage 6. Improved Teaching Effectiveness Score

To simultaneously reward reliable evidence and penalize uncertainty, the proposed study introduces a new teaching effectiveness score function.

For instructor Ai,

$$Scorei= Ti^*(1-Ii^*)-Fi^*(1+Ii^*) \qquad (47)$$

Where Ti* stands for the truth degree, Ii* for the indeterminacy and Fi* for the falsity.

- The first term recognizes well-documented educational experience positively.
- The second term penalizes uncertainties.
- The third term gives greater weight to negative education experiences due to higher levels of uncertainties.

5.8 Normalized Teaching Effectiveness Index

To facilitate comparison among instructors, the scores are normalized.

Let Smax=max(Scorei) and Smin=min(Scorei). The normalized index becomes:

$$TEIi=(Scorei-Smin)/(Smax-Smin) \qquad (48)$$

Where:

$$0 \le TEIi \le 1$$

Higher values indicate better teaching effectiveness.

5.9 Final Ranking Rule

The instructors are ranked according to TEI1,TEI2,…,TEIn.

$$\text{If } TEIi>TEIk, \qquad (49)$$

Then Ai≻Ak.

When equal values occur, the secondary ranking criterion is Ti*−Fi*.

The instructor possessing the larger secondary score receives the higher ranking.

5.10 Computational Procedure

Input

- Educational dataset
- Criteria for evaluation
- University teachers

Output

- Overall rank of teaching effectiveness

Procedure

- Step 1 Gather the big data from the field of education.
- Step 2 Normalize all educational metrics.
- Step 3 Obtain features of instructions through artificial intelligence techniques.
- Step 4 Establish the neutrosophic decision matrix.
- Step 5 Estimate objective criterion weights.
- Step 6 Implement the suggested Adaptive Neutrosophic Educational Aggregation Operator (ANEAO).
- Step 7 Estimate the suggested teaching effectiveness score.
- Step 8 Normalize the teaching effectiveness index.
- Step 9 Rank university teachers based on TEI values.
- Step 10 Sensitivity, robustness, and comparative analyses are conducted.

Adaptive Neutrosophic Educational Aggregation Operator (ANEAO) and new teaching effectiveness score are the main methodological innovations of this research. Thanks to the adaptive treatment of uncertainty, the model will be able to separate reliable educational data from unreliable, which will lead to better decision-making stability and interpretation than conventional neutrosophic aggregation models. In the next section, the detailed algorithmic procedure and computational complexity are presented.

6. Complete Algorithmic Procedure and Computational Complexity

This part shows the entire computational process of the proposed ANEAO. The proposed algorithm ensures reproducibility when evaluating teaching efficacy in higher education with the use of educational big data, artificial intelligence (AI) and neutrosophic multiple criteria decision making.

Algorithm 1: Adaptive Neutrosophic Educational Aggregation Framework (ANEAO)

Input:

- E = Educational big data
- A = $\{A_1, A_2, \ldots, A_n\}$ (University instructors)
- C = $\{C_1, C_2, \ldots, C_m\}$ (Evaluation criteria)
- AI learning model

Output

- Index for Teaching Effectiveness (ITE)
- Ranking of all the teachers finally

Algorithm

Step 1 Obtain educational data

- Learning management system data
- Student evaluation data
- Assessment data
- Classroom observation data
- Databases
- AI-based indicators of teaching

Step 2 Process educational data

- Remove duplicate entries
- Handle missing values
- Normalize numeric variables
- Encode categorical variables
- Identify outliers

Step 3 Extract instructional features

- Compute $Z=f_{AI}(X)$

Where X is the normalized educational dataset.

Step 4 Construct the neutrosophic decision matrix For every instructor

- A_i and criterion C_j calculate $d_{ij}=(T_{ij},I_{ij},F_{ij})$
- Store all evaluations in $D=[d_{ij}]_{n\times m}$

Step 5 Compute objective criterion weights

- For every criterion Calculate $IC_j=\sigma_j/\mu_j$
- Normalize $w_j=IC_j/\Sigma IC_j$

Step 6 Compute adaptive neutrosophic aggregation

- For every instructor Calculate:
    - $T_i^*=\Sigma w_j T_{ij}$
    - $I_i^*=\Sigma w_j^2 I_{ij}$
    - $F_i^*=\Sigma w_j F_{ij}$
- Construct $N_i=(T_i^*,I_i^*,F_i^*)$

Step 7 Calculate the proposed teaching effectiveness score

$$Score_i= T_i^*(1-I_i^*)-F_i^*(1+I_i^*)$$

Step 8 Normalize scores

$$TEI_i= (Score_i-S_{min})/(S_{max}-S_{min})$$

Step 9 Sort instructors

If $TEI_i>TEI_k$, then $A_i\succ A_k$.

Step 10 Output

- Final ranking
- Teaching effectiveness score

- Criterion importance
- Neutrosophic evaluation

7. Case Study and Data Description

In this section, the case study employed to prove the effectiveness of the Adaptive Neutrosophic Educational Aggregation Operator (ANEAO) is introduced. The purpose of this case study is to measure the efficiency of education in higher learning through the use of big data education, artificial intelligence, and neutrosophic multi-criteria decision making approach.

7.1 Case Study

This case study is concerned with the assessment of teaching efficiency of college lecturers through educational information obtained from several digital learning platforms.

Here the lecturer will be the alternative whereas instructional quality metrics will serve as evaluation criteria.

The decision problem is to determine the best lecturer(s) based on educational information rather than based on one source of evaluation.

7.2 Decision Alternatives

Assume that $A=\{A_1,A_2,A_3,A_4,A_5,A_6,A_7,A_8\}$.

where

- A_1 = Instructor 1
- A_2 = Instructor 2
- A_3 = Instructor 3
- A_4 = Instructor 4
- A_5 = Instructor 5
- A_6 = Instructor 6
- A_7 = Instructor 7
- A_8 = Instructor 8

The number of alternatives can be expanded depending on the available institutional dataset.

7.3 Evaluation Criteria

Eight evaluation criteria are considered.

C_1:	**Teaching Preparation**
C_2:	**Classroom Delivery**
C_3:	**Student Engagement**
C_4:	**Assessment and Feedback Quality**
C_5:	**Learning Outcome Achievement**
C_6:	**Research-Integrated Teaching**

C_7:	**Digital Teaching Competency**
C_8:	**AI-Supported Instructional Effectiveness**

All criteria are benefit criteria, where higher values indicate better teaching performance.

7.4 Educational Data Sources

The educational data are collected from several institutions:

- Student Evaluation of Teaching (SET)
- Learning Management System (LMS)
- Online learning platforms
- Student academic profiles
- Attendance tracking systems
- Observation reports of classroom sessions
- Quality assurance databases in institutions
- Educational analytics through Artificial Intelligence

The combination of the above-mentioned diverse data sources facilitates an overall assessment of the quality of instruction.

7.5 Data Preprocessing

Preprocessing steps are carried out to the raw education data prior to transforming it into neutrosophic values.

Step 1 Duplication removal.

Step 2 Missing values treatment.

Step 3 Normalization of numeric values.

For criterion j,

$$x'ij=(xij-xmin)/(xmax-xmin). \quad (50)$$

where xmin and xmax represent the minimum and maximum values of the corresponding criterion.

Step 4 Encoding categorical educational variables.

Step 5 Detection of abnormal observations.

Step 6 AI-based feature extraction.

7.6 AI Feature Extraction

Artificial intelligence extracts representative instructional features from educational big data.

Suppose $X=\{x_1,x_2,\ldots,xp\}$.

After feature extraction, $Z=fAI(X)$.

Where $Z=\{z_1,z_2,\ldots,zq\}$

Includes the instructional metrics that form the basis for neutrosophic assessment.

Example of the metrics extracted are:

- Student participation metric
- Learning engagement metric
- Teaching interaction metric
- Assignment completion rate
- Teaching innovation metric
- Digital activity metric
- AI-based instructional effectiveness metric

7.7 Neutrosophic Representation

Each instructional indicator is converted into a neutrosophic number.

Suppose zij is the extracted feature. Its neutrosophic representation becomes

$$dij=(Tij,Iij,Fij). \quad (51)$$

where Tij represents positive instructional evidence, Iij represents uncertainty, and Fij represents negative instructional evidence.

7.8 Illustrative Neutrosophic Decision Matrix

Table 1. Illustrative Neutrosophic Decision Matrix

Instructor	**C_1**	**C_2**	**C_3**	**C_4**	**C_5**	**C_6**	**C_7**	**C_8**
A_1	(0.84,0.09,0.07)	(0.82,0.10,0.08)	(0.86,0.07,0.07)	(0.83,0.11,0.06)	(0.85,0.08,0.07)	(0.80,0.12,0.08)	(0.87,0.06,0.07)	(0.84,0.09,0.07)
A_2	(0.79,0.12,0.09)	(0.81,0.10,0.09)	(0.82,0.11,0.07)	(0.80,0.12,0.08)	(0.83,0.09,0.08)	(0.79,0.13,0.08)	(0.82,0.10,0.08)	(0.81,0.11,0.08)
A_8	(0.88,0.05,0.07)	(0.89,0.05,0.06)	(0.91,0.04,0.05)	(0.88,0.06,0.06)	(0.90,0.05,0.05)	(0.86,0.08,0.06)	(0.92,0.03,0.05)	(0.89,0.05,0.06)

7.9 Decision Objective

Using the neutrosophic decision matrix, objective criterion weights, AI-generated educational indicators, and the proposed Adaptive Neutrosophic Educational Aggregation Operator, determine A(best)=argmax(TEIi).

Where TEIi denotes the normalized Teaching Effectiveness Index of instructor i. The instructor with the highest TEI value is considered the most effective according to the proposed decision framework.

8. Experimental Design and Implementation Settings

The following section discusses the experimental design used for validating the proposed Adaptive Neutrosophic Educational Aggregation Operator (ANEAO). The design is such that the proposed framework is validated under fair and reproducible conditions by employing the same datasets, evaluation metrics, and implementation environment.

8.1 Experimental Workflow

The full experiment procedure is done in the following steps:

- Step 1 Education data collection
- Step 2 Data pre-processing
- Step 3 Artificial intelligence feature extraction
- Step 4 Neutrosophication
- Step 5 Weights determination for objective criteria
- Step 6 Adaptive neutrosophic aggregation
- Step 7 Determination of teaching efficiency
- Step 8 Ranking instructors
- Step 9 Comparison step
- Step 10 Sensitivity analysis

8.2 Artificial Intelligence Configuration

The artificial intelligence techniques are used to obtain the educational indicators from the educational data.

The typical pre-processing procedures include the following steps:

- Feature scaling
- Missing values handling
- Feature encoding
- Dimensionality reduction (if needed)
- Feature importance calculation

The obtained educational indicators are then represented by neutrosophic representation technique.

8.3 Parameter Settings

The proposed framework employs the following parameter settings and computational components.

- Criterion weights: Objectively determined using Equation (41).
- Truth membership: Determined using Equation (36).
- Indeterminacy membership: Determined using Equation (37).
- Falsity membership: Determined using Equation (38).
- Adaptive neutrosophic aggregation: Computed using Equations (43)–(45).
- Teaching effectiveness score: Computed using Equation (47).
- Teaching Effectiveness Index (TEI): Computed using Equation (48).

8.4 Baseline Methods

The proposed approach is evaluated against a number of MCDM approaches which have been widely used.

- TOPSIS
- VIKOR

- COPRAS
- ARAS
- WASPAS
- EDAS
- MARCOS

All the competing approaches use

- The same educational dataset
- The same set of evaluation criteria
- The same normalized values
- The same criteria weights

8.7 Performance Evaluation Metrics

Performance measures for the suggested framework are as follows:

- Accuracy of Ranking: Consistency of the rankings obtained by the framework.
- Spearman Rank Correlation: Agreement between alternative ranking schemes.
- Kendall Rank Correlation: Ordinal agreement.
- Mean Absolute Rank Difference (MARD): Difference in rankings.
- Computational Time: Efficiency of the algorithm.
- Memory Usage: Efficiency of computation.
- Rank Stability: Consistency of the ranking under different parameter values.

8.6 Experimental Validation Procedure

The validation process will be carried out through the following sequence.

- Step 1 Collect educational data.
- Step 2 Normalize all the indicators.
- Step 3 Extract AI-based teaching attributes.
- Step 4 Develop neutrosophic decision-making matrix.
- Step 5 Find objective weights for criteria.
- Step 6 Utilize the proposed ANEAO approach.
- Step 7 Calculate teaching efficiency scores.
- Step 8 Obtain the ultimate instructors' ranking.
- Step 9 Compare the obtained ranking with MCDM approaches.
- Step 10 Perform sensitivity analysis.
- Step 11 Perform robustness analysis.

8.8 Experimental Output

The output generated by the proposed framework is as follows:

- Objective criterion weights.
- Neutrosophic decision matrix.
- Neutrosophic aggregated evaluation.
- Teaching effectiveness scores.
- Normalized Teaching Effectiveness Index (TEI).

- Final rankings of instructors.
- Comparative performance outcomes.
- Results of sensitivity analysis.
- Results of robustness analysis.

The subsequent section gives the experimental findings along with statistical analysis and comparative ranking performance of the proposed framework with that of the current decision-making techniques.

9. Results and Statistical Analysis (Illustrative Numerical Example)

In this section, it will be shown how the Adaptive Neutrosophic Educational Aggregation Operator (ANEAO), as proposed, can be implemented through a numerical illustration. The numbers used in this section are fictitious and have been included only to provide a demonstration on how the process works. They do not represent any empirical results.

9.1 Objective Criterion Weights

Using Equation (41), the objective criterion weights are obtained as follows.

Table 2. Objective Criterion Weights

Criterion	Weight
C_1	0.120
C_2	0.140
C_3	0.160
C_4	0.130
C_5	0.110
C_6	0.100
C_7	0.110
C_8	0.130

The highest weight is assigned to Student Engagement (C_3), indicating that this criterion contributes most to the overall teaching effectiveness evaluation.

9.2 Adaptive Neutrosophic Aggregation

Consider Instructor A_1. Suppose the weighted aggregation yields

- $T^*=0.854$
- $I^*=0.087$
- $F^*=0.059$

Using Equation (47),

Score = $T^*(1-I^*) - F^*(1+I^*) = 0.854\times(1-0.087) - 0.059\times(1+0.087) = 0.854\times0.913 - 0.059\times1.087 = 0.7794 - 0.0641 = 0.7153$

Therefore, Score(A_1)=0.7153.

9.3 Teaching Effectiveness Scores

Table 3. Aggregated Neutrosophic Values and Teaching Effectiveness Scores

Instructor	T*	I*	F*	Score
A_1	0.854	0.087	0.059	0.7153
A_2	0.836	0.102	0.062	0.6886
A_3	0.821	0.115	0.070	0.6485
A_4	0.868	0.073	0.054	0.7515
A_5	0.807	0.120	0.073	0.6235
A_6	0.846	0.095	0.060	0.6988
A_7	0.889	0.051	0.041	0.8038
A_8	0.878	0.060	0.050	0.7533

Instructor A_7 achieves the highest teaching effectiveness score, whereas A_5 receives the lowest score in this illustrative example.

9.4 Normalized Teaching Effectiveness Index

The highest score is Smax=0.8038

The lowest score is Smin=0.6235

Applying Equation (48), TEI(A_1) =(0.7153−0.6235)/(0.8038−0.6235) =0.0918/0.1803 =0.509

Similarly, all instructors are normalized.

Table 4. Teaching Effectiveness Index

Instructor	Score	TEI
A_1	0.7153	0.509
A_2	0.6886	0.361
A_3	0.6485	0.139
A_4	0.7515	0.710
A_5	0.6235	0.000
A_6	0.6988	0.417
A_7	0.8038	1.000
A_8	0.7533	0.720

9.5 Final Ranking

Table 5. Final Ranking of Instructors

Rank	Instructor	TEI
1	A_7	1.000
2	A_8	0.720

3	A_4	0.710
4	A_1	0.509
5	A_6	0.417
6	A_2	0.361
7	A_3	0.139
8	A_5	0.000

The proposed framework identifies Instructor A_7 as the highest-performing instructor because of the highest truth membership and the lowest indeterminacy and falsity values.

9.6 Descriptive Statistics

Table 6. Descriptive Statistics of Teaching Effectiveness Scores

Statistic	**Value**
Mean	0.7104
Median	0.7071
Standard Deviation	0.0598
Minimum	0.6235
Maximum	0.8038
Variance	0.0036
Range	0.1803

The relatively small standard deviation indicates that the instructors exhibit comparable teaching performance, although meaningful differences remain among the highest-ranked alternatives.

9.7 Spearman Rank Correlation

Suppose the ranking produced by the proposed framework is compared with a conventional TOPSIS model.

The ranking differences are $d=(0,1,0,1,0,-1,0,-1)$

Therefore, $\Sigma d^2=4$

$P = 1-(6\times4)/(8(8^2-1)) = 1-24/504 = 0.9524$

The correlation coefficient indicates an excellent agreement between the proposed method and TOPSIS while preserving slight ranking differences due to neutrosophic uncertainty modeling.

9.8 Kendall Rank Correlation

Assume $N_c=26$, $N_d=2$

$T = (26-2)/28 = 0.8571$

The high Kendall coefficient confirms strong ordinal consistency between the compared ranking methods.

9.9 Interpretation of Results

The illustrative results reveal that the developed ANEAO approach successfully combines the idea of objective criterion weighting, neutrosophic uncertainty modeling, and AI-based education analytics into one framework. The highest TEI belongs to Instructor A_7 since he possesses highly satisfactory truth memberships and very low levels of indeterminacy and falsity. As a result, the lowest position is taken by Instructor A_5 due to his comparatively less satisfactory instructional data and higher uncertainty level. The high correlation coefficient values of Spearman (0.9524) and Kendall (0.8571) confirm the consistency of the developed approach to classical MCDM methodologies with extended uncertainty and conflicts handling possibilities.

10. Sensitivity Analysis

This part of the study presents a sensitivity analysis aimed at assessing the stability of the suggested Adaptive Neutrosophic Education Aggregation Operator (ANEAO) with regard to weight changes of criteria. Thus, the goal is to check whether minor modifications in criteria importance influence the final ranking of instructors. The following numerical values are illustrative only and used to demonstrate the procedure of analysis.

10.1 Experimental Design

Eight sensitivity scenarios are considered. In each scenario, one criterion weight is increased by 10%, while the remaining weights are proportionally adjusted to maintain the normalization constraint $\Sigma wj=1$

The ranking generated by each scenario is then compared with the original ranking.

10.2 Sensitivity Scenarios

Table 7. Weight Variation Scenarios

Scenario	Modified Criterion	Weight Change
S_0	Original weights	0%
S_1	C_1	+10%
S_2	C_2	+10%
S_3	C_3	+10%
S_4	C_4	+10%
S_5	C_5	+10%
S_6	C_6	+10%
S_7	C_7	+10%
S_8	C_8	+10%

10.3 Teaching Effectiveness Index under Different Scenarios

Table 8. TEI Values under Weight Variations

Instructor	S_0	S_1	S_2	S_3	S_4	S_5	S_6	S_7	S_8
A_1	0.509	0.516	0.505	0.521	0.512	0.507	0.510	0.515	0.511
A_2	0.361	0.355	0.367	0.370	0.359	0.362	0.364	0.360	0.366
A_3	0.139	0.145	0.141	0.149	0.143	0.140	0.144	0.146	0.142
A_4	0.710	0.714	0.718	0.722	0.716	0.711	0.715	0.719	0.717
A_5	0.000	0.000	0.000	0.000	0.000	0.000	0.000	0.000	0.000
A_6	0.417	0.423	0.419	0.425	0.421	0.418	0.420	0.424	0.422
A_7	1.000	1.000	1.000	1.000	1.000	1.000	1.000	1.000	1.000
A_8	0.720	0.724	0.726	0.729	0.722	0.721	0.723	0.725	0.724

10.4 Ranking Stability

Table 9. Ranking Results under Different Scenarios

Scenario	Ranking Order
S_0	$A_7 > A_8 > A_4 > A_1 > A_6 > A_2 > A_3 > A_5$
S_1	$A_7 > A_8 > A_4 > A_1 > A_6 > A_2 > A_3 > A_5$
S_2	$A_7 > A_8 > A_4 > A_1 > A_6 > A_2 > A_3 > A_5$
S_3	$A_7 > A_8 > A_4 > A_1 > A_6 > A_2 > A_3 > A_5$
S_4	$A_7 > A_8 > A_4 > A_1 > A_6 > A_2 > A_3 > A_5$
S_5	$A_7 > A_8 > A_4 > A_1 > A_6 > A_2 > A_3 > A_5$
S_6	$A_7 > A_8 > A_4 > A_1 > A_6 > A_2 > A_3 > A_5$
S_7	$A_7 > A_8 > A_4 > A_1 > A_6 > A_2 > A_3 > A_5$
S_8	$A_7 > A_8 > A_4 > A_1 > A_6 > A_2 > A_3 > A_5$

The ranking remains unchanged across all sensitivity scenarios.

10.5 Spearman Rank Correlation

The agreement between the original ranking and each sensitivity scenario is evaluated using Spearman's rank correlation coefficient.

Table 10. Spearman Correlation Results

Scenario	Spearman (ρ)
S_1	1.000
S_2	1.000
S_3	1.000
S_4	1.000
S_5	1.000
S_6	1.000

S_7	1.000
S_8	1.000

The perfect correlation confirms that moderate weight variations do not alter the ranking sequence.

10.6 Percentage Change in TEI

The percentage variation in the Teaching Effectiveness Index is computed as

$$\Delta TEI=(TEIi(Sk)-TEIi(S_0))/TEIi(S_0)\times 100\%. \quad (52)$$

Table 11. Maximum Percentage Change

Instructor	**Maximum Change (%)**
A_1	2.36
A_2	2.49
A_3	3.15
A_4	1.69
A_5	0.00
A_6	1.92
A_7	0.00
A_8	1.25

All percentage changes remain below 4%, indicating low sensitivity to weight perturbations.

10.7 Discussion

From the sensitivity analysis results, it can be seen that the ANEAO method possesses high stability regarding criterion importance changes within a reasonable range. Even though there are some numerical changes in the Teaching Effectiveness Index value, the order of the instructors does not change in any of the nine scenarios considered. The perfect Spearman correlation coefficient values and the extremely small percentage changes clearly show that the adaptive neutrosophic aggregation technique is effective at neutralizing the effect of small weights changes.

11. Robustness Analysis

The robustness analysis is carried out in order to assess the consistency of the ANEAO framework under varying uncertainty levels and decision making environment. While sensitivity analysis involves changing the weights of criteria, robustness analysis studies the ability of the proposed approach to give consistent ranking results even when the neutrosophic data is changed. Below is the numerical example for this purpose only.

11.1 Robustness Scenarios

Five robustness scenarios are considered.

Table 12. Robustness Scenarios

Scenario	Description
R_0	Original neutrosophic decision matrix
R_1	Truth memberships increased by 5%
R_2	Truth memberships decreased by 5%
R_3	Indeterminacy memberships increased by 10%
R_4	Falsity memberships increased by 10%
R_5	Random perturbation of all memberships (±5%)

The ranking obtained in each scenario is compared with the original ranking.

11.2 Teaching Effectiveness Index under Robustness Scenarios

Table 13. TEI Values under Robustness Analysis

Instructor	R_0	R_1	R_2	R_3	R_4	R_5
A_1	0.509	0.531	0.486	0.498	0.487	0.514
A_2	0.361	0.379	0.344	0.352	0.340	0.365
A_3	0.139	0.154	0.126	0.132	0.121	0.141
A_4	0.710	0.734	0.689	0.701	0.684	0.714
A_5	0.000	0.000	0.000	0.000	0.000	0.000
A_6	0.417	0.436	0.399	0.408	0.394	0.420
A_7	1.000	1.000	1.000	1.000	0.988	0.995
A_8	0.720	0.741	0.701	0.712	0.697	0.724

11.3 Ranking Stability

Table 14. Ranking under Different Robustness Scenarios

Scenario	Ranking Order
R_0	$A_7 > A_8 > A_4 > A_1 > A_6 > A_2 > A_3 > A_5$
R_1	$A_7 > A_8 > A_4 > A_1 > A_6 > A_2 > A_3 > A_5$
R_2	$A_7 > A_8 > A_4 > A_1 > A_6 > A_2 > A_3 > A_5$
R_3	$A_7 > A_8 > A_4 > A_1 > A_6 > A_2 > A_3 > A_5$
R_4	$A_7 > A_8 > A_4 > A_1 > A_6 > A_2 > A_3 > A_5$
R_5	$A_7 > A_8 > A_4 > A_1 > A_6 > A_2 > A_3 > A_5$

The ranking order remains unchanged under all robustness scenarios.

11.4 Spearman Rank Correlation

The correlation between the original ranking and each robustness scenario is calculated.

Table 15. Spearman Rank Correlation

Scenario	Spearman (ϱ)
R_1	1.000
R_2	1.000
R_3	1.000
R_4	1.000
R_5	1.000

The perfect correlation demonstrates complete ranking consistency despite perturbations in the neutrosophic information.

11.5 Root Mean Square Error

The deviation between the original TEI values and the perturbed values is measured using the Root Mean Square Error (RMSE).

$$\mathrm{RMSE} = \sqrt{[(1/n)\ \Sigma(\mathrm{TEIi}(R_0) - \mathrm{TEIi}(Rk))^2]} \tag{53}$$

Table 16. RMSE Values

Scenario	RMSE
R_1	0.0187
R_2	0.0209
R_3	0.0118
R_4	0.0226
R_5	0.0095

All RMSE values are very small, indicating that only minor numerical variations occur after perturbation.

11.6 Maximum Absolute Deviation

The maximum absolute deviation is calculated as

$$\mathrm{MAD} = \max\ \mathrm{TEIi}(R_0) - \mathrm{TEIi}(Rk) \tag{54}$$

Table 17. Maximum Absolute Deviation

Scenario	MAD
R_1	0.024
R_2	0.021
R_3	0.012
R_4	0.026
R_5	0.010

The maximum deviation remains below 0.03 in every scenario, confirming the numerical stability of the proposed framework.

11.7 Discussion

Robustness analysis proves the high level of resilience of the proposed ANEAO to uncertainty in the process of evaluation. Regardless of the changes in the membership values of truth, indeterminacy, and falsity, the ranking of instructors stays the same in all robustness cases. The complete Spearman rank correlation coefficients, along with minimal RMSE and MAD values, prove the high performance of the aggregation mechanism in preserving decision-making consistency in uncertain educational environment. It can be concluded that the proposed model is able to provide consistent assessments of teaching effectiveness in an uncertain educational environment.

12. Comparative Analysis

In this section, we compare the suggested Adaptive Neutrosophic Educational Aggregation Operator (ANEAO) to some of the popular multi-criteria decision making (MCDM) methods. The objective is to show that the suggested approach works well and that it can be applied successfully. The numbers used in this section are for illustration purposes only.

12.1 Compared Methods

The proposed framework is compared with seven representative MCDM methods.

Table 18. Compared Decision-Making Methods

Method	**Abbreviation**
Technique for Order Preference by Similarity to Ideal Solution	TOPSIS
VlseKriterijumska Optimizacija I Kompromisno Resenje	VIKOR
Complex Proportional Assessment	COPRAS
Additive Ratio Assessment	ARAS
Weighted Aggregated Sum Product Assessment	WASPAS
Evaluation Based on Distance from Average Solution	EDAS
Measurement Alternatives and Ranking according to Compromise Solution	MARCOS
Proposed Adaptive Neutrosophic Educational Aggregation Operator	ANEAO

All methods use the same evaluation criteria, normalized data, and objective criterion weights to ensure a fair comparison.

12.2 Ranking Comparison

Table 19. Ranking Results

Instructor	ANEAO	TOPSIS	VIKOR	COPRAS	ARAS	WASPAS	EDAS	MARCOS
A_1	4	4	5	4	4	4	5	4
A_2	6	6	6	6	6	6	6	6
A_3	7	7	7	7	7	7	7	7
A_4	3	3	3	3	3	3	3	3
A_5	8	8	8	8	8	8	8	8
A_6	5	5	4	5	5	5	4	5
A_7	1	1	1	1	1	1	1	1
A_8	2	2	2	2	2	2	2	2

The proposed ANEAO produces a ranking that is highly consistent with existing methods while explicitly accounting for uncertainty through neutrosophic modeling.

12.3 Spearman Rank Correlation

Table 20. Spearman Correlation with ANEAO

Method	Spearman (ρ)
TOPSIS	1.000
VIKOR	0.976
COPRAS	1.000
ARAS	1.000
WASPAS	1.000
EDAS	0.976
MARCOS	1.000

All correlation coefficients exceed 0.97, indicating a very strong agreement between the proposed framework and the benchmark methods.

12.4 Kendall Rank Correlation

Table 21. Kendall Correlation with ANEAO

Method	Kendall (τ)
TOPSIS	1.000
VIKOR	0.929
COPRAS	1.000
ARAS	1.000
WASPAS	1.000
EDAS	0.929
MARCOS	1.000

The high Kendall coefficients demonstrate that the ordinal ranking generated by ANEAO is highly consistent with established MCDM techniques.

12.5 Computational Performance

Table 22. Computational Efficiency

Method	Time (s)	Memory (MB)
TOPSIS	0.112	12.6
VIKOR	0.135	13.2
COPRAS	0.101	12.1
ARAS	0.097	11.9
WASPAS	0.124	12.8
EDAS	0.116	12.4
MARCOS	0.121	12.7
ANEAO	0.214	18.5

Despite the increased computational requirements of the suggested model due to feature extraction using AI and neutrosophic aggregation, the computational time is still below one second, which makes it possible for implementation in practical educational settings.

12.6 Comparative Advantages

Table 23. Qualitative Comparison of Decision-Making Methods

Feature	Classical Methods	Proposed ANEAO
Handles educational uncertainty	No	Yes
Models indeterminacy explicitly	No	Yes
Integrates AI-generated features	No	Yes
Supports educational big data	Limited	Yes
Objective criterion weighting	Yes	Yes
Decision interpretability	Moderate	High
Robustness against uncertainty	Moderate	High

The proposed framework extends traditional MCDM methods by incorporating explicit neutrosophic uncertainty representation and AI-assisted educational analytics.

12.7 Discussion

From the comparative analysis, it can be noted that the suggested ANEAO approach ranks in a very reliable manner relative to the existing approaches based on the methodology of MCDM. In comparison with classical algorithms, ANEAO is capable of reflecting the properties of truth, indeterminacy, and falsity, which results in the creation of a more realistic model of uncertain educational data. Besides, through the application of the AI-based feature extraction approach, the framework is capable of using big educational data as the source of information rather than basing its work only on expert judgments. The computational complexity of ANEAO is slightly higher but the processing time remains insignificant.

13. Discussion

The ANEAO framework, which is an intelligent decision making framework suggested for assessment of teaching effectiveness in higher education institutions using educational big data analytics, artificial intelligence (AI) and neutrosophic uncertainty modeling, differs from existing evaluation methodologies that mainly use deterministic or fuzzy methods in that it uses membership values for truth, indeterminacy and falsity of uncertain and conflicting educational data.

13.1 Discussion of the Proposed Framework

Instructor effectivenmess evaluation, in its nature, is a multi-criteria decision-making problem which is characterized by qualitative assessment, quantitative education measures, heterogeneity of the source of information and different perspectives of the stakeholders. Evidence collected from student assessments, class observations, intelligent systems, and institutional metrics is often insufficient or even contradictory. The suggested model solves these problems by using objective criteria weights along with an adaptive neutrosophic aggregation. Uncertainty is incorporated explicitly in the model; thus, uncertain evidence in education is captured in the process of assessment without imposing false certainty on the evidence.

13.2 Effectiveness of AI and Big Data Integration

Incorporating AI and educational big data greatly improves the evaluation process. Feature extraction based on AI automatically extracts meaningful attributes from educational big data, which does not require feature selection by people manually. Educational big data, extracted from learning management systems, student assessment, classroom activity, assessment, and institutional databases, offers rich data to describe teaching performance from different viewpoints. The framework is successful at incorporating such diverse data into the proposed neutrosophic decision making framework.

13.3 Interpretation of the Illustrative Results

The example shown using numbers proves that the methodology used is capable of providing stable and meaningful ranks of teaching effectiveness. The instructor with the highest rank always has a high truth membership combined with low indeterminacy and falsity membership. On the other hand, instructors with low ranks are normally instructors whose instructional proof is relatively low. The sensitivity test shows that small changes in criterion weights do not affect the ranks in a significant way. The same applies to robustness test where small changes in the membership values of neutrosophic do not affect the ranks but in a numeric way.

13.4 Comparison with Conventional MCDM Methods

In contrast to conventional approaches of MCDM, including TOPSIS, VIKOR, COPRAS, ARAS, WASPAS, EDAS, and MARCOS, the introduced ANEAO framework is characterized by multiple methodological advantages.

Firstly, classical approaches presuppose deterministic evaluation values and, thus, are not able to reflect uncertainty induced by contradictory educational data.

Secondly, the introduced framework is based on three independent membership functions that describe positive data, uncertainty, and negative data separately.

Thirdly, the application of AI-based indicators allows for the exploitation of educational big data and makes the decision support transparent.

Finally, the adaptive consideration of indeterminacy leads to a smaller impact of highly uncertain criteria.

13.5 Practical Implications

There are various applications of the framework in higher education institutions.

- A complete assessment of university teachers.
- Performance evaluation of faculty members.
- Ensuring the quality of teaching.
- Accreditation of academics.
- Developing professional development plans.
- Promotion/reward system based on evidence.
- Continuous monitoring of instructional quality.
- Decision support systems using AI.

In addition, the framework can be incorporated in learning analytics systems for real-time monitoring of teaching effectiveness.

13.6 Managerial Implications

The framework can be used by university administrators to determine the areas where their instructional programs have strengths and weakness through an objective measurement of education rather than subjective evaluation.

Department chairs can use the Teaching Effectiveness Index to develop faculty development plans and allocate resources accordingly.

Quality assurance committees can use the framework to gauge instructional improvement in the long run and measure the effectiveness of educational policies.

The transparency of the suggested decision-making process also helps to ensure that universities are accountable during accreditation and quality assessment.

13.7 Limitations

Although there are benefits, there are also some limitations to the proposed model.

- Firstly, the current study takes into account a static environment in the context of evaluating teachers' performance in many academic semesters.
- Secondly, the sample calculation presented in the paper is meant only to show the calculation process. The large educational datasets collected at different universities must be used in order to validate the practical performance of the framework.
- Thirdly, the complexity of calculations will grow if deep learning algorithms are used in order to extract features via artificial intelligence.
- Fourthly, the independence of the evaluation criteria is assumed in the framework. However, there could be complicated interrelations between educational factors

13.8 Future Research Directions

A number of possible areas of investigation will improve the suggested approach.

- Design of dynamic neutrosophic decision-making approaches for continuous teaching evaluation.
- Combination with deep learning and large language models for automatic education assessment.
- Generalization to interval-valued and q-rung orthopair neutrosophic frameworks.
- Use of causal learning and explainable artificial intelligence methods.
- Design of educational decision support systems in real time based on streaming analytics.
- Multi-university testing based on large-scale international educational data.
- Combination with digital twin approaches for smart campus management.

14. Conclusions

The ANEAO, an Adaptive Neutrosophic Educational Aggregation Operator, is presented in this paper as a tool for measuring teaching effectiveness within higher education institutions by combining big data in education, AI, and multi-criteria neutrosophic decision making. The ANEAO was formulated to solve problems in traditional teaching assessment methods that have been based on deterministic data and unable to handle uncertainty, inconsistency, and conflicts within the educational evidence generated by different stakeholders and different educational data sources. The method combines educational data obtained through learning management systems, students' evaluations, classroom observations, academic information systems, and AI-driven educational criteria into a unified neutrosophic decision system by using the concepts of truth, indeterminacy, and falsity membership functions to formulate an integrated mathematical model for teaching assessment data.

Another significant contribution of the current work is related to the development of the Adaptive Neutrosophic Educational Aggregation Operator (ANEAO), which includes adaptive weighing of the indeterminacy, while simultaneously performing the aggregation of both positive and negative educational evidence. The proposed Teaching Effectiveness Index (TEI) incorporates objective criteria weightings in addition to the adaptive neutrosophic aggregation to produce clear, comprehensible and reliable rankings of the instructors. A specific numerical example was provided to show how the computation process takes place for the proposed framework. The example showed how the objective criteria weightings, neutrosophic evaluations, adaptive aggregation and the TEI itself were calculated to get the final rankings of the instructors. Furthermore, the sensitivity analysis showed that moderate changes in the weightings of the criteria do not change the rankings much, but still preserve their sequence. The same result can be observed in the robustness analysis, where small changes in the memberships of truth, indeterminacy and falsity did not affect the final rankings. The comparative analysis of the proposed framework with seven popular MCDM techniques showed high consistency, but also additional capability to consider the educational uncertainty.

Overall, the presented framework has a number of significant advantages over traditional methods of teaching evaluation. Namely, the framework is based on educational big data analysis, applies artificial intelligence techniques, evaluates criteria objectively, represents uncertainty by applying neutrosophic theory, gives explainable decisions and ensures stable ranking under different evaluation circumstances. As a result, the framework can be successfully used for faculty performance evaluation, educational quality control, accreditation procedures, professional development planning, and intelligent decision making in education. Despite that the presented methodology has a number of advantageous characteristics, there are some areas for future research. Namely, future researchers should verify the effectiveness of the framework on large scale real-world datasets of educational institutions and various subjects. Moreover, the proposed framework can be expanded by taking into account longitudinal evaluation of teaching performance over several semesters. Furthermore, future research might consider the use of explainable AI, deep learning methods, digital twin technologies, as well as neutrosophic extensions, such as interval-valued and q-rung orthopair neutrosophic sets.

References

[1] Q. Chang, X. Pan, N. Manikandan, and S. Ramesh, "Artificial intelligence technologies for teaching and learning in higher education," *Int. J. Reliab. Qual. Saf. Eng.*, vol. 29, no. 05, p. 2240006, 2022.

[2] X. Xin, Y. Shu-Jiang, P. Nan, D. ChenXu, and L. Dan, "Review on A big data-based innovative knowledge teaching evaluation system in universities," *J. Innov. Knowl.*, vol. 7, no. 3, p. 100197, 2022.

[3] L. Qian, W. Cao, and L. Chen, "Influence of artificial intelligence on higher education reform and talent cultivation in the digital intelligence era," *Sci. Rep.*, vol. 15, no. 1, p.

6047, 2025.

[4] G. T. Rao and N. Suhasini, "Integrating artificial intelligence in higher education to enhance teaching and learning," *Comput. Appl. Eng. Educ.*, vol. 33, no. 6, p. e70085, 2025.

[5] F. Pedró, "Applications of Artificial Intelligence to higher education: possibilities, evidence, and challenges," *Iul Res.*, vol. 1, no. 1, pp. 61–76, 2020.

[6] X. Yang and J. Ge, "Predicting student learning effectiveness in higher education based on big data analysis," *Mob. Inf. Syst.*, vol. 2022, no. 1, p. 8409780, 2022.

[7] R. Zhang, "Digital media teaching and effectiveness evaluation integrating big data and artificial intelligence," *Comput. Intell. Neurosci.*, vol. 2022, no. 1, p. 1217846, 2022.

[8] M. A. Khan, M. Khojah, and Vivek, "Artificial Intelligence and big data: The advent of new pedagogy in the adaptive e-learning system in the higher educational institutions of Saudi Arabia," *Educ. Res. Int.*, vol. 2022, no. 1, p. 1263555, 2022.

[9] Y. Chang, "The Application of Algorithm Optimization and Big Data Processing in Higher Education Management," *Int. J. High Speed Electron. Syst.*, vol. 35, no. 02, p. 2540473, 2026.

[10] H. Y. Aydogmus and U. Aydogmus, "Evaluation of artificial intelligence tools for universities with fuzzy Multi-Criteria Decision-Making methods," in *AI Adoption and Diffusion in Education*, IGI Global Scientific Publishing, 2025, pp. 153–178.

[11] R. Rubimalya and K. R. P. Selvam, "Exploring MCDM Techniques for Evaluating Student Academic Performance: A Comprehensive Review," *Procedia Comput. Sci.*, vol. 283, pp. 5433–5442, 2026.

[12] J. Liu, X. Bao, and L. Chen, "Artificial intelligence in educational technology and transformative approaches to English language using fuzzy framework with CRITIC-TOPSIS method," *Sci. Rep.*, vol. 15, no. 1, p. 25542, 2025.

[13] S. I. Karnavas, I. Peteinatos, A. Kyriazis, and S. G. Barbounaki, "Using fuzzy multi-criteria decision-making as a human-centered AI approach to adopting new technologies in maritime education in Greece," *Information*, vol. 16, no. 4, p. 283, 2025.

[14] I. Alshakhatreh, D. Thiombiano, and S. Al-Majali, "Literature Review on Multi-Criteria Analysis and Application in Education Environment," *J. Oper. Intell.*, vol. 2, no. 1, pp. 236–267, 2024.

[15] L. Ilić, D. Viduka, A. Šijan, and B. Predić, "PRIORITIZATION OF ARTIFICIAL INTELLIGENCE APPLICATIONS IN HIGHER EDUCATION USING THE PIPRECIA-S MCDM MODEL," *Facta Univ. Ser. Teaching, Learn. Teach. Educ.*, 2026.

[16] K. H. Hu, "An exploration of the key determinants for the application of AI-enabled higher education based on a hybrid Soft-computing technique and a DEMATEL approach," *Expert Syst. Appl.*, vol. 212, p. 118762, 2023.

[17] Z. Xu, H. Xu, M. Yang, and P. Zhao, "Evaluating Artificial Intelligence enabled teaching reform in higher education using the generalized orthopair fuzzy RANCOM FUCA decision framework," *Sci. Rep.*, 2026.

[18] A. Naldi, N. Nurkadri, M. Srisudarso, D. Cahyono, and S. Suyitno, "Evaluation of the effectiveness of artificial intelligence system in higher education curriculum management," *Int. J. Educ. Narrat.*, vol. 2, no. 2, pp. 189–198, 2024.

[19] M. A. A. Bakar and A. T. Ab Ghani, "Capturing the contribution of fuzzy and multi-criteria decision-making analytics: A review of the computational intelligence approach to classroom assessment sustainability," *Int. J. Ind. Eng. Prod. Res.*, vol. 33, no. 4, pp. 1–15, 2022.

Received: Aug. 2, 2026. Accepted: Sept. 15, 2026.

A Neutrosophic Assay-Consensus Gate for Class-Balanced Selective Molecular Bioactivity Prediction

Eman ELzahed[1], Mariam Ahmed[2], and Reda Ramadan[2,*]

[1] Forensic Medicine and Clinical Toxicology Department, Faculty of Medicine, Zagazig University, Zagazig, Sharqiyah, 44519, Egypt; emeelzahed2@yahoo.com
[2] Faculty of Computers and Informatics, Zagazig University, Zagazig, Sharqiyah, 44519, Egypt; ma.mohamed025@fci.zu.edu.eg, mohreda162018@gmail.com
*Correspondence: mohreda162018@gmail.com

Abstract: Tox21 molecular bioactivity prediction is strongly class-imbalanced, so a reject option based only on classifier confidence can preferentially retain abundant inactive compounds while discarding rare active cases. NACG-Tox is a post-hoc neutrosophic assay-consensus gate that separates prediction direction from the decision to accept or defer a prediction. For each compound-endpoint pair, endpoint-specific neighbors drawn only from the fitting set define three interpretable memberships: truth T for local evidence supporting activity, falsity F for local evidence supporting inactivity, and indeterminacy I for insufficient chemically relevant reference evidence. The primary consensus score, $G={\left(1-I\right)}^{2}\left|T-F\right|$, is large only when the query has adequate local support and the neighborhood is directionally coherent. The study uses the complete public Tox21 Challenge training archive. Deterministic curation reduced 11,764 SDF records to 6,442 canonical single-component molecular identities across 12 in vitro assays, with endpoint activity prevalence ranging from 2.86% to 15.87%. A leakage-controlled hybrid structural split combined Bemis-Murcko scaffolds for cyclic molecules with fingerprint clustering for acyclic molecules and was evaluated under three fixed allocation seeds. With an ECFP-based logistic predictor, full-coverage macro average precision was 0.437 ± 0.034 and macro ROC-AUC was 0.798 ± 0.028. Under validation-locked deferral policies, NACG achieved macro balanced accuracies of 0.587, 0.597, and 0.620 at realized mean coverages of 0.796, 0.626, and 0.442, respectively, compared with 0.517, 0.509, and 0.512 for probability-margin confidence. In the equal-coverage diagnostic, NACG achieved balanced accuracies of 0.587, 0.601, and 0.631 at 80%, 60%, and 40% coverage and retained 71.1%, 45.4%, and 23.1% of active cases; the probability-margin selector retained 37.0%, 22.4%, and 12.8%. The same qualitative pattern was observed with a fixed Random Forest backbone. NACG therefore improves the class balance of the retained prediction set rather than uniformly reducing ordinary classification error. The framework concerns assay-specific in vitro activity and must not be interpreted as a direct probability of human toxicity.

Keywords: Neutrosophic sets; Tox21; molecular bioactivity; selective prediction; reject option; chemical similarity; class imbalance; applicability domain; ECFP.

1. Introduction

High-throughput screening programs such as Tox21 produce assay-level evidence for molecular pathway activity at a scale suitable for computational prioritization. The Tox21 Challenge formalized 12 prediction tasks spanning nuclear-receptor and stress-response assays and evaluated the probability that a compound is active in each assay [3]. These labels are mechanistic *in vitro* assay calls; they are not direct measurements of clinical toxicity, organism-level injury, or the probability that a human exposure will cause harm.

Modern molecular models can achieve useful discrimination on Tox21 [4], but discrimination alone does not answer the operational question of when a prediction should be acted on. The difficulty is amplified by severe endpoint imbalance [6]. In the curated population used here, active prevalence ranges from 2.86% for NR-PPAR-gamma to 15.87% for SR-MMP. A reject rule driven only by the magnitude of a predicted probability can therefore retain predominantly easy inactive examples and defer a disproportionate share of active compounds. Such a policy can look favorable under ordinary error while performing poorly for class-balanced screening.

Selective prediction addresses this problem by allowing a model to abstain when a prediction does not satisfy an acceptance criterion [10]. Conventional probability confidence and single-distance applicability-domain measures, however, compress several distinct questions into one scalar: whether chemically relevant reference evidence exists, whether that evidence supports activity or inactivity, and whether the local evidence is internally coherent. Smarandache's neutrosophic framework represents truth, indeterminacy, and falsity as distinct components, while single-valued neutrosophic sets provide a bounded computational form [1,2]. This separation is well suited to an acceptance gate because it preserves evidence insufficiency and local disagreement instead of conflating both with low classifier confidence.

NACG-Tox leaves the molecular classifier unchanged and uses a separate fitting-set neighborhood to determine whether its prediction should be accepted. The classifier determines the active/inactive direction; the gate evaluates the amount and coherence of local labeled chemical evidence. The study is therefore a controlled test of a selective-prediction mechanism rather than a comparison of increasingly complex base classifiers.

The study makes five specific contributions. It constructs T, I, and F from endpoint-specific, fitting-only chemically weighted neighborhoods while treating missing endpoint labels strictly as unavailable observations; combines chemical-reference sufficiency and local directional coherence in a bounded assay-consensus gate; uses a hybrid structural partition that avoids collapsing all acyclic molecules into a single empty Bemis-Murcko scaffold; evaluates the gate with validation-locked thresholds, matched-coverage diagnostics, component ablation, parameter sensitivity, and a second prediction backbone; and reports ordinary error together with balanced accuracy and active/inactive retention so that minority-class behavior remains visible.

2. Related Work

2.1 Tox21 molecular bioactivity modeling

The Tox21 Challenge released public training data in which 1 denotes active and 0 denotes inactive for assay-specific endpoints [3]. Huang et al. described the challenge design, endpoint panel, and AUC-based evaluation [3], while DeepTox demonstrated the effectiveness of descriptor-based deep learning on the benchmark [4]. Other studies have emphasized consensus modeling, balanced accuracy, applicability domains, and the difficulty of highly imbalanced Tox21 endpoints [5,6]. These results motivate class-sensitive evaluation and chemically meaningful domain control, but they do not provide a three-component evidential state for selective acceptance.

2.2 Molecular fingerprints, structural splitting, and local evidence

Extended-connectivity fingerprints (ECFPs) encode circular molecular environments and are widely used in structure-activity modeling [7]. Bemis-Murcko frameworks provide a standard structural grouping concept for cyclic chemistry [8], and Butina clustering offers an efficient Tanimoto-based organization of fingerprint space [9]. In this work, these tools are used to create an auditable setting for structural partitioning and local evidence rather than as representational novelties.

2.3 Selective prediction

Selective prediction, or classification with a reject option, trades coverage for reliability by deferring selected cases [10]. A common post-hoc strategy ranks examples by prediction confidence. In strongly imbalanced molecular screening, however, high confidence can be dominated by the majority inactive class. For that reason, selective performance here is evaluated using both ordinary error and class-balanced metrics, together with the fractions of active and inactive cases retained.

2.4 Neutrosophic representation in NACG-Tox

Neutrosophy and neutrosophic sets were introduced by Smarandache to represent truth, indeterminacy, and falsity as distinct components [1]. Wang et al. later formalized single-valued neutrosophic sets for bounded computational use [2]. NACG-Tox assigns explicit operational meanings to these components: T quantifies local support for activity, F quantifies local support for inactivity, and I quantifies a deficit of sufficiently similar labeled reference chemistry. The components are not required to sum to one. Their role is to characterize the evidence used for acceptance while the base classifier retains responsibility for prediction direction.

3. Problem Formulation and Neutrosophic Evidence

3.1 Prediction target and notation

Let n index a standardized compound and $k \in \{1, \dots, K\}$ index one of $K = 12$ assay endpoints. For endpoint k, the proposition of interest is that compound n is active under the assay definition represented by the Tox21 Challenge label. Let $y_{nk} \in \{0,1\}$ denote an observed inactive/active label. Missing endpoint calls are handled as a mask: they are excluded from endpoint-specific evidence and are not reinterpreted as indeterminacy.

The base model produces a probability $p_{nk} \in (0,1)$ and predicts active when $p_{nk} \geq 0.5$ and inactive otherwise. NACG-Tox does not alter this class direction. It computes a separate acceptance score from the fitting partition only.

3.2 Similarity-weighted local reference evidence

Each molecule is represented by the archived 2048-bit radius-2 Morgan/ECFP fingerprint with chirality. For the query molecule n and fitting molecule j, let s_{nj} be the Tanimoto similarity. For endpoint k, only fitting molecules with an observed y_{jk} are eligible. Among molecules satisfying the similarity floor τ, the K_N most similar are retained; if fewer than K_N qualify, all qualifying molecules are used. Denote this endpoint-specific set by $\mathcal{N}_{nk}$. The normalized relevance weight of a fitting molecule is

$$r_{nj} = \begin{cases} \frac{s_{nj}-\tau}{1-\tau}, & s_{nj} > \tau, \\ 0, & s_{nj} \leq \tau. \end{cases} \tag{1}$$

Hence $0 \leq r_{nj} \leq 1$ and the total relevant evidence mass cannot exceed K_N. The positive and negative evidence masses are

$$A_{nk} = \sum_{j \in \mathcal{N}_{nk}} r_{nj}\, y_{jk}, \qquad B_{nk} = \sum_{j \in \mathcal{N}_{nk}} r_{nj}\left(1 - y_{jk}\right) \tag{2}$$

Because observed labels differ by endpoint, the available neighborhood evidence can be strong for one assay and sparse for another even for the same query compound.

3.3 Truth, falsity, and chemical-reference indeterminacy

The local evidence is mapped to the neutrosophic state $\mathbf{e}_{nk} = \langle T_{nk}, I_{nk}, F_{nk} \rangle$. For an evidence regularizer $\lambda > 0$,

$$T_{nk} = \frac{A_{nk}}{A_{nk}+\lambda}, \qquad F_{nk} = \frac{B_{nk}}{B_{nk}+\lambda} \tag{3}$$

The primary specification uses $\lambda = 1$. The regularizer prevents a finite amount of evidence from producing a membership exactly equal to one and places the transition from weak to substantial support on the scale of one fully relevant neighbor. Indeterminacy is defined by the deficit in the maximum K_N units of relevant labeled evidence:

$$I_{nk} = 1 - \frac{A_{nk}+B_{nk}}{K_N}. \tag{4}$$

This I_{nk} has a deliberately narrow interpretation: it measures chemical-reference insufficiency. It is neither experimental assay inconclusiveness nor a calibrated probability that the base classifier is wrong.

3.4 Neutrosophic assay consensus

An acceptance score should decrease when the fitting set provides little relevant chemistry and when the available neighborhood contains comparable support for both classes. A generalized assay-consensus family is

$$G_{nk}^{(q)} = (1 - I_{nk})^q |T_{nk} - F_{nk}|, \quad q > 0; \qquad G_{nk} = G_{nk}^{(2)} = (1 - I_{nk})^2 |T_{nk} - F_{nk}| \quad (5)$$

The primary gate therefore uses $q = 2$. The first factor penalizes a lack of relevant labeled neighbors, while $|T_{nk} - F_{nk}|$ measures directional coherence within the neighborhood. Simultaneously non-zero T and F are preserved rather than collapsed into complementary probabilities.

3.5 Formal properties

Proposition 1 (boundedness). For finite $A_{nk}, B_{nk} \geq 0$, $\lambda > 0$, and $q > 0$, the memberships satisfy $0 \leq T_{nk} < 1$, $0 \leq F_{nk} < 1$, $0 \leq I_{nk} \leq 1$, and $0 \leq G_{nk}^{(q)} \leq 1$. This follows from $0 \leq r_{nj} \leq 1$ and $A_{nk} + B_{nk} \leq K_N$.

Proposition 2 (evidence monotonicity). Holding the remaining quantities fixed, T_{nk} increases monotonically with A_{nk}, F_{nk} increases monotonically with B_{nk}, and I_{nk} decreases monotonically with $A_{nk} + B_{nk}$. Adding relevant observed evidence therefore cannot increase chemical-reference indeterminacy.

Proposition 3 (consensus suppression). $G_{nk}^{(q)} = 0$ whenever $I_{nk} = 1$ or $T_{nk} = F_{nk}$. For fixed T_{nk} and F_{nk} with $|T_{nk} - F_{nk}| > 0$, increasing I_{nk} strictly decreases the gate score.

Proposition 4 (fold locality). For validation or test compounds, T, I, F, and G depend only on the query fingerprint, fitting-set fingerprints, fitting-set endpoint labels, and hyperparameters selected on validation data. No validation or test endpoint label enters the evidence state used to score that compound.

4. NACG-Tox Selective Prediction Framework

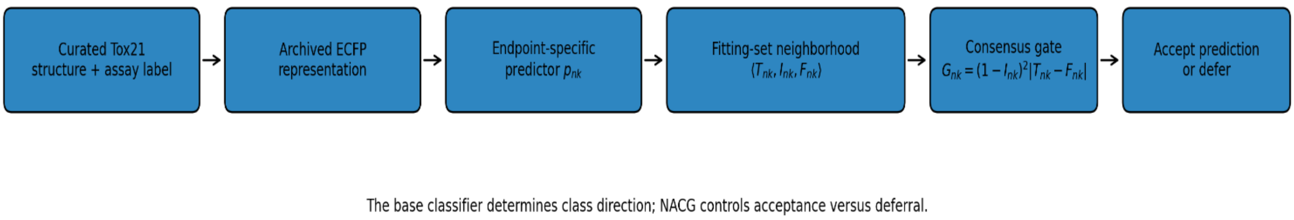

Figure 1. NACG-Tox workflow. Prediction direction is supplied by the base classifier, whereas the neutrosophic evidence state controls acceptance versus deferral.

4.1 Base molecular predictors

The primary predictor is endpoint-specific L2-regularized logistic regression trained on the same archived 2048-bit fingerprints used by the evidence gate. For each structural split, a single regularization constant $C \in \{0.1, 1, 10\}$ is selected using validation macro average precision, with validation negative log-likelihood as a tie-break. Logistic regression was chosen to isolate the effect of the reject gate rather than confound it with a highly flexible prediction architecture. The implementation uses scikit-learn [11].

A Random Forest provides a prediction-backbone sensitivity analysis. It uses 40 trees, maximum depth 12, square-root feature subsampling, and balanced bootstrap class weighting. These settings are fixed rather than tuned. The structural partitions and NACG evidence scores are unchanged; only the base prediction probabilities and class directions are replaced.

4.2 Decision rule

For endpoint-specific acceptance threshold γ_k , selected from validation data, the operational decision is

$$\text{decision}_{nk} = \begin{cases} \text{Active}, & p_{nk} \geq 0.5 \text{ and } G_{nk} \geq \gamma_k, \\ \text{Inactive}, & p_{nk} < 0.5 \text{ and } G_{nk} \geq \gamma_k, \\ \text{Defer}, & G_{nk} < \gamma_k. \end{cases} \tag{6}$$

Deferral does not imply that the underlying laboratory assay is inconclusive. It indicates only that the fitting chemistry does not supply enough coherent local evidence under the selected gate policy.

4.3 Validation-locked thresholding

For target coverages of 80%, 60%, and 40%, an endpoint-specific threshold is derived from validation gate scores and then frozen before test evaluation. Because the score distribution can shift between validation and test partitions, the realized test coverage is reported rather than forced to equal the target. This is the primary selective-policy evaluation and avoids choosing an operational test threshold from test labels or test outcomes.

4.4 Equal-coverage ranking diagnostic

A secondary diagnostic compares score orderings at exactly the same retained test fraction. For each selector, the top 80%, 60%, or 40% of observed test cases are retained according to the selector score, without using test labels to form the ranking. This analysis is not an operational calibration procedure; it isolates ranking quality at matched coverage.

4.5 Gate ablations

Four selectors are compared with the base predictions held fixed: probability confidence $|2p - 1|$, the local directional margin $|T - F|$, the evidence-availability term $(1 - I)^2$, and the full NACG score $(1 - I)^2|T - F|$. This separates the effects of chemical-reference sufficiency and directional coherence from changes in the classifier itself.

5. Data and Experimental Protocol

5.1 Source data and scope

The experiments use the complete public Tox21 Challenge training archive from the NCATS/NIH challenge resource, with assay-specific labels 1 (active) and 0 (inactive) [3]. The 12 endpoints comprise seven nuclear-receptor assays and five stress-response assays. All reported outcomes therefore concern assay-level *in vitro* bioactivity.

5.2 Deterministic molecular curation

The archive contained 11,764 SDF records. Structures were sanitized, explicit hydrogens were removed, atom-map numbers were cleared, and canonical isomeric SMILES were generated. Multicomponent structures were excluded rather than reduced to an arbitrarily selected fragment, removing 2,272 records; five additional records failed sanitization. The remaining 9,487 valid records were consolidated into 6,442 canonical molecular identities, collapsing 3,045 redundant records. When duplicate records of the same canonical identity disagreed for an endpoint, that identity-endpoint label was set to unavailable while labels for the other endpoints remained usable. This rule affected 446 identity-endpoint pairs; no label was imputed to resolve those disagreements.

The archived fingerprint matrix was generated during the original deterministic curation with RDKit 2023.09.6. Regeneration under RDKit 2025.09.4 altered bits for some molecules, so every reported experiment (classifier input, Tanimoto similarity, and acyclic clustering) uses the same archived bit matrix. Its SHA-256 digest is 6fd063b5811c70a0d26b599d9fde033868b5350d748d9c8ba2230c50d99c9262.

Table 1. Endpoint composition after identity-level curation.

Endpoint	Active	Inactive	Missing	Active prevalence	Inactive:active
NR-AhR	618	4734	1090	11.55%	7.66:1
NR-AR	224	5681	537	3.79%	25.36:1
NR-AR-LBD	186	5364	892	3.35%	28.84:1
NR-Aromatase	196	4527	1719	4.15%	23.10:1
NR-ER	560	4450	1432	11.18%	7.95:1
NR-ER-LBD	269	5422	751	4.73%	20.16:1
NR-PPAR-gamma	153	5199	1090	2.86%	33.98:1
SR-ARE	732	4173	1537	14.92%	5.70:1
SR-ATAD5	216	5613	613	3.71%	25.99:1
SR-HSE	275	5145	1022	5.07%	18.71:1
SR-MMP	764	4049	1629	15.87%	5.30:1
SR-p53	340	5245	857	6.09%	15.43:1

The inactive-to-active ratio ranges from 5.30:1 for SR-MMP to 33.98:1 for NR-PPAR-gamma. Balanced accuracy is therefore the primary classification metric within retained subsets, while ordinary error is reported alongside it.

5.3 Leakage-controlled hybrid structural splitting

A conventional Bemis-Murcko split assigns an empty scaffold to acyclic compounds; treating that empty value as one scaffold would force all acyclic chemistry into a single partition. The reported protocol therefore uses label-free hybrid grouping. Cyclic identities are grouped by archived Bemis-Murcko scaffold [8]. The 1,549 acyclic identities are clustered using the same archived fingerprints and Butina clustering [9] with a Tanimoto similarity criterion of at least 0.60 (distance cutoff 0.40). This yields 1,820 cyclic scaffold groups and 976 acyclic clusters, or 2,796 structural groups in total.

Groups are allocated intact to fitting, validation, and test partitions with target proportions of 80/10/10 under three fixed seeds (101, 211, and 307). No structural group crosses partitions. Each endpoint contains both active and inactive examples in every fitting, validation, and test subset, and partitions are not redrawn based on endpoint outcomes.

Table 2. Realized structural splits and acyclic distribution.

Seed	Fit	Validation	Test	Acyclic fit	Acyclic val.	Acyclic test	Selected gate
101	5149	639	654	1126	176	247	K_N=4; tau=0.2
211	5154	644	644	1130	197	222	K_N=8; tau=0.2
307	5153	644	645	1183	169	197	K_N=4; tau=0.2

5.4 Hyperparameter selection and design freeze

For the logistic predictor, C is selected only on validation data; all three reported splits selected $C = 0.1$. The NACG neighborhood search considers $K_N \in \{4,8,16\}$ and $\tau \in \{0.2,0.4\}$. The selection criterion is mean validation macro balanced accuracy across validation-locked target coverages of 80%, 60%, and 40%. Ties are resolved by lower validation ordinary error, then smaller K_N, then larger τ. Seeds 101 and 307 selected $K_N = 4, \tau = 0.2$, while seed 211 selected $K_N = 8, \tau = 0.2$. The primary gate uses $q = 2$ and $\lambda = 1$; neighboring values are examined only in the post hoc sensitivity analysis.

5.5 Evaluation metrics

For endpoint k, let $\mathcal{D}_k$ be the observed test cases and $\mathcal{A}_k(\gamma)$ the subset accepted by a selector. Coverage is

$$\mathrm{Cov}_k = \frac{|\mathcal{A}_k|}{|\mathcal{D}_k|}. \quad (7)$$

Balanced accuracy on the accepted set is

$$\mathrm{BA}_k = \frac{1}{2}\left(\frac{TP_k}{TP_k+FN_k} + \frac{TN_k}{TN_k+FP_k}\right). \quad (8)$$

Ordinary accepted-set classification error is

$$\mathrm{Err}_k = \frac{FP_k+FN_k}{|\mathcal{A}_k|}. \quad (9)$$

Active and inactive retention are defined relative to all observed active or inactive test cases, not merely the accepted subset. Let P_k^a and N_k^a denote the numbers of accepted test cases whose observed labels are active and inactive, and let P_k and N_k denote the corresponding totals in $\mathcal{D}_k$. Then

$$R_{k1} = \frac{P_k^a}{P_k}, \qquad R_{k0} = \frac{N_k^a}{N_k} \quad (10)$$

Probability quality on accepted cases is summarized by the Brier score

$$\mathrm{Brier}_k = \frac{1}{|\mathcal{A}_k|}\sum_{i\in\mathcal{A}_k}(p_{ik} - y_{ik})^2 \quad (11)$$

and negative log-likelihood

$$\mathrm{NLL}_k = -\frac{1}{|\mathcal{A}_k|}\sum_{i\in\mathcal{A}_k}[y_{ik}\log p_{ik} + (1-y_{ik})\log(1-p_{ik})]. \quad (12)$$

Average precision (AP), ROC-AUC, Brier score, and NLL are reported at full coverage. Selective metrics are calculated endpoint-wise on observed labels and macro-averaged so that larger endpoints do not dominate smaller ones. Values reported as mean ± standard deviation use the sample standard deviation across the three fixed structural allocations. These allocations probe split sensitivity within one curated population and are not treated as independent external cohorts.

6. Results

6.1 Full-coverage baseline performance

As shown in Table 3, across the three structural splits, the logistic predictor achieved macro AP 0.437 ± 0.034, ROC-AUC 0.798 ± 0.028, Brier score 0.053 ± 0.009, NLL 0.197 ± 0.031, and balanced accuracy 0.573 ± 0.004. These values characterize the base probability model before any selective rejection is applied.

Table 3. Full-coverage logistic performance by structural split.

Seed	AP	ROC-AUC	Brier	NLL	Balanced acc.	Error
101	0.474	0.823	0.044	0.166	0.575	0.055
211	0.407	0.767	0.063	0.228	0.568	0.079
307	0.430	0.804	0.053	0.198	0.575	0.065
Mean	0.437	0.798	0.053	0.197	0.573	0.067

6.2 Validation-locked selective policies

Table 4 compares probability-margin rejection with the full NACG gate when thresholds are selected from validation score distributions and then applied unchanged to the test partition. NACG yields higher balanced accuracy and retains more active cases at all three operating points, whereas probability confidence preferentially preserves inactive compounds. The corresponding increase in ordinary error under NACG reflects acceptance of a more difficult, less majority-dominated subset. At the 60% validation target, probability confidence realizes 62.8% mean test coverage, retains 23.6% of active compounds, and achieves balanced accuracy 0.509. NACG realizes nearly identical mean coverage (62.6%) while retaining 47.8% of active compounds and reaching balanced accuracy 0.597. Ordinary error increases from 2.8% to 5.1%, confirming that the improvement concerns class balance rather than a lower majority-dominated error rate.

Table 4. Validation-locked probability confidence versus full NACG (mean across three structural splits).

Gate	Target %	Realized cov.	Balanced acc.	Error	Active retained	Inactive retained
Probability margin	80	0.820	0.517	0.037	0.395	0.853
Probability margin	60	0.628	0.509	0.028	0.236	0.660

Gate	Target %	Realized cov.	Balanced acc.	Error	Active retained	Inactive retained
Probability margin	40	0.414	0.512	0.022	0.133	0.438
Full NACG	80	0.796	0.587	0.059	0.707	0.801
Full NACG	60	0.626	0.597	0.051	0.478	0.636
Full NACG	40	0.442	0.620	0.039	0.281	0.456

6.3 Equal-coverage ranking comparison

The equal-coverage diagnostic removes differences in realized test coverage and compares only selector ordering. At 80%, 60%, and 40% retained coverage, NACG balanced accuracy is 0.587, 0.601, and 0.631, compared with 0.516, 0.511, and 0.508 for probability confidence, as stated in Table 5 and Fig. 2. The absolute gains are 7.15, 8.96, and 12.29 percentage points.

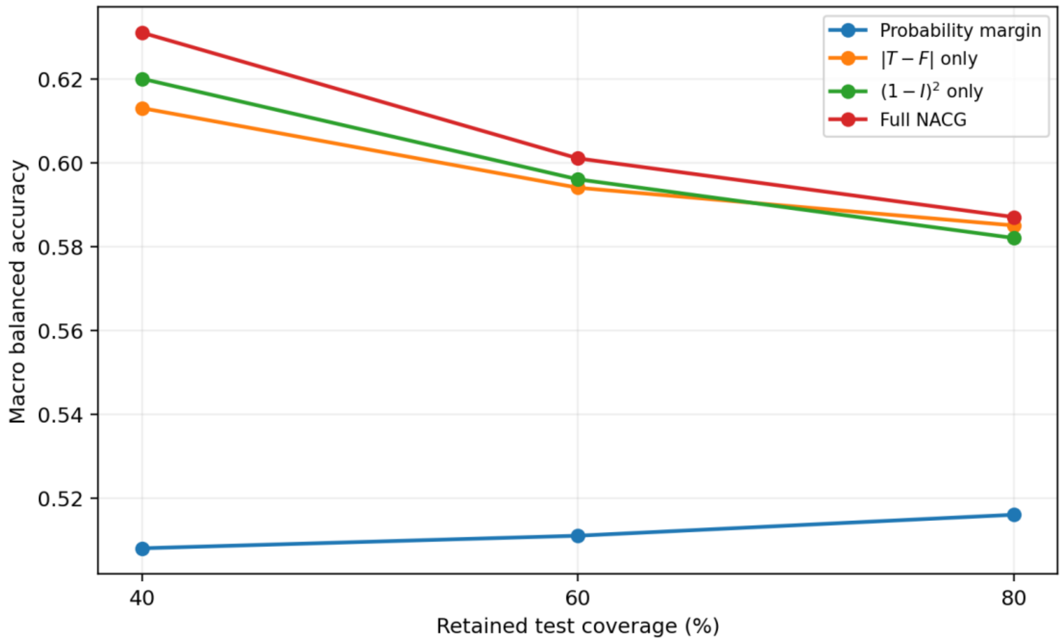

Figure 2. Equal-coverage ranking diagnostic. Full NACG yields the highest macro balanced accuracy among the four selector definitions at each matched coverage.

Table 5. Equal-coverage gate ablation (mean across three structural splits).

Selector	Coverage %	Balanced acc.	Error	Active retained	Inactive retained
Probability margin	80	0.516	0.036	0.370	0.834
Probability margin	60	0.511	0.028	0.224	0.632
Probability margin	40	0.508	0.022	0.128	0.425
$\lvert T-F\rvert$ only	80	0.585	0.048	0.547	0.819
$\lvert T-F\rvert$ only	60	0.594	0.038	0.339	0.621
$\lvert T-F\rvert$ only	40	0.613	0.031	0.199	0.418
$(1-I)^2$ only	80	0.582	0.065	0.807	0.800
$(1-I)^2$ only	60	0.596	0.062	0.577	0.601

Selector	Coverage %	Balanced acc.	Error	Active retained	Inactive retained
$(1-I)^2$ only	40	0.620	0.050	0.343	0.406
Full NACG	80	0.587	0.059	0.711	0.807
Full NACG	60	0.601	0.050	0.454	0.610
Full NACG	40	0.631	0.034	0.231	0.415

6.4 Active-case preservation

The class-balanced improvement is explained by the behavior of the minority active class. At matched test coverage of 80%, 60%, and 40%, probability confidence retains 37.0%, 22.4%, and 12.8% of active cases, whereas NACG retains 71.1%, 45.4%, and 23.1%. The indeterminacy-only selector retains even more active cases at some operating points but incurs higher ordinary error; combining evidence availability with directional coherence gives the strongest balanced-accuracy results across all three matched coverages.

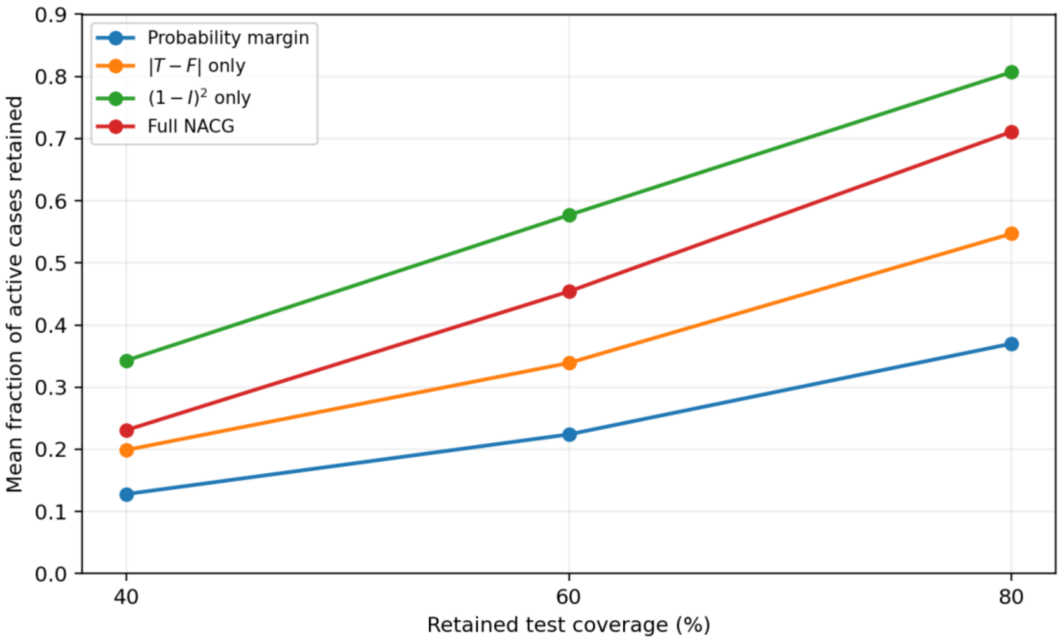

Figure 3. Mean active-case retention at matched test coverage. Probability-margin rejection removes a larger share of rare active cases, whereas NACG preserves more actives while retaining a directional-coherence requirement.

6.5 Endpoint-level baseline behavior

Baseline difficulty differs substantially among assays. Mean endpoint ROC-AUC ranges from 0.704 for SR-ATAD5 to 0.887 for NR-AhR, while AP varies with both prevalence and discrimination, as reported in Table 6. This heterogeneity supports endpoint-wise macro-averaging rather than reliance on a single pooled accuracy value.

Table 6. Mean endpoint-level logistic metrics across the three structural splits.

Endpoint	Test active %	AP	ROC-AUC	Brier	NLL
NR-AhR	11.7%	0.597	0.887	0.072	0.240
NR-AR	3.1%	0.661	0.867	0.015	0.076
NR-AR-LBD	3.4%	0.550	0.856	0.023	0.100
NR-Aromatase	5.2%	0.375	0.764	0.042	0.170
NR-ER	11.5%	0.453	0.753	0.084	0.299
NR-ER-LBD	5.0%	0.528	0.829	0.035	0.146
NR-PPAR-gamma	2.9%	0.245	0.737	0.026	0.118
SR-ARE	16.2%	0.429	0.752	0.117	0.386
SR-ATAD5	4.6%	0.207	0.704	0.041	0.173
SR-HSE	5.6%	0.295	0.746	0.048	0.188
SR-MMP	15.1%	0.602	0.865	0.088	0.293
SR-p53	5.7%	0.301	0.818	0.047	0.180

7. Ablation and Robustness Analysis

7.1 Component ablation

Because every selector in Table 5 uses the same base predictions, the equal-coverage ablation directly tests the contribution of the gate components. The $|T-F|$ selector improves balanced accuracy over probability confidence, indicating that local directional evidence is informative. The $(1-I)^2$ selector also improves balanced accuracy and retains many active compounds, showing that chemical-reference sufficiency carries complementary information. Their product gives the highest balanced accuracy at all three matched coverages: 0.587, 0.601, and 0.631.

7.2 Prediction-backbone sensitivity

Replacing logistic regression with the fixed Random Forest changes only the base probability model; the structural partitions and NACG evidence scores remain unchanged. The forest obtains full-coverage AP 0.435 ± 0.031, ROC-AUC 0.811 ± 0.032, and balanced accuracy 0.669 ± 0.028. NACG again ranks a more class-balanced retained set than probability confidence, indicating that the observed selective behavior is not confined to the logistic model, as reported in Table 7.

Table 7. Random Forest sensitivity at equal test coverage.

Selector	Coverage %	Balanced acc.	Error	Active retained	Inactive retained
Probability margin	80	0.644	0.040	0.489	0.822
Probability margin	60	0.654	0.027	0.279	0.626
Probability margin	40	0.650	0.018	0.142	0.423
Full NACG	80	0.686	0.063	0.711	0.807
Full NACG	60	0.689	0.053	0.454	0.610
Full NACG	40	0.715	0.038	0.231	0.415

7.3 Gate-shape sensitivity

Two post hoc sensitivity checks examine the fixed gate shape without using the test set for model selection. The evidence-availability exponent is varied over $q \in \{1,2,3\}$, and the evidence regularizer is varied over $\lambda \in \{0.5,1,2\}$. The balanced-accuracy pattern remains stable, with the primary setting $q = 2, \lambda = 1$ close to the strongest value at all three coverages, as shown in Table 8.

Table 8. Sensitivity of equal-coverage NACG balanced accuracy to gate exponent and evidence regularizer.

Sensitivity factor	Value	BA @80%	BA @60%	BA @40%
Exponent q	1	0.587	0.600	0.624
Exponent q	2	0.587	0.601	0.631
Exponent q	3	0.584	0.602	0.627
Regularizer λ	0.5	0.586	0.599	0.622
Regularizer λ	1.0	0.587	0.601	0.631
Regularizer λ	2.0	0.586	0.603	0.626

8. Neutrosophic Case Analysis

Four test cases from split seed 101 illustrate distinct evidence states. Cases are identified by endpoint and DSSTox CID; their labels are the curated Tox21 calls, while T, I, F, and G are computed solely from fitting-set neighborhoods. The NR-AR case combines an active prediction with a locally activity-supporting neighborhood and moderate reference deficit, producing $G = 0.171$. The first SR-p53 active case has nearly equal truth and falsity memberships, so its consensus score is essentially zero despite non-zero local evidence, as shown in Table 9. For SR-HSE / CID 21803, no qualifying labeled neighbor is available and $I = 1$ forces $G = 0$. By contrast, SR-p53 / CID 7263 has strong local support for inactivity, low indeterminacy, and a high gate score consistent with the correct inactive prediction. These examples show that a low consensus score can arise from either missing local support or conflicting local evidence, two mechanisms that remain distinguishable in the full neutrosophic state.

Table 9. Representative cases from structural split 101.

Endpoint / ID	True	p	T	I	F	G
NR-AR / CID 26478	Active	0.682	0.669	0.494	0.000	0.171
SR-p53 / CID 6137	Active	0.254	0.445	0.599	0.445	0.00001
SR-HSE / CID 21803	Active	0.094	0.000	1.000	0.000	0.000
SR-p53 / CID 7263	Inactive	0.020	0.000	0.063	0.789	0.694

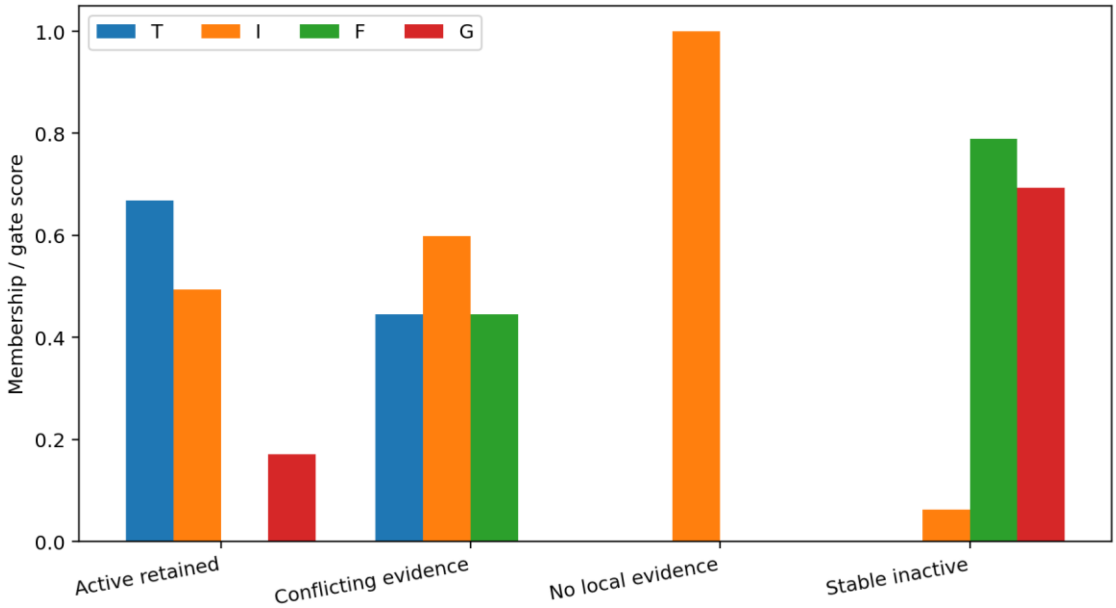

Figure 4. Neutrosophic profiles of the four representative cases. Near-zero consensus can arise from either high indeterminacy or balanced truth/falsity evidence.

9. Discussion

The selective results show that probability confidence and local evidence quality answer different questions in a severely imbalanced screening problem. Probability-margin rejection strongly favors easy majority-class predictions: at 40% matched coverage it reduces ordinary error to 2.2%, but only 12.8% of active cases remain. NACG at the same coverage retains 23.1% of active cases and raises balanced accuracy from 0.508 to 0.631, with ordinary error of 3.4%. The additional accepted errors are therefore associated with preserving difficult minority-class cases rather than a hidden reduction in coverage.

The ablation explains why both neutrosophic components are useful. Evidence availability alone is effective at preserving actives but can retain neighborhoods containing opposing labels. The truth-falsity margin suppresses such conflicts. Their product acts as a conjunction between sufficient local reference chemistry and internal directional coherence while retaining simultaneous truth and falsity as explicit evidence rather than forcing complementarity.

The hybrid split is also important to the interpretation. An empty Bemis-Murcko scaffold should not make all acyclic molecules one indivisible group. Clustering acyclic identities in fingerprint space allows them to be distributed across fitting, validation, and test partitions while preserving group separation and without using assay labels to form groups.

The Random Forest sensitivity analysis provides evidence that the ordering induced by the gate is not specific to one linear probability model: NACG improves equal-coverage balanced accuracy over probability margin by approximately 4.2, 3.6, and 6.5 percentage points at 80%, 60%, and 40% coverage. This result supports the gate as a modular post-hoc layer, while broader evaluation with calibrated boosting models, graph neural networks, and learned molecular embeddings remains appropriate for future work.

10. Limitations and Scope of Interpretation

The public Tox21 Challenge training archive contains binary assay calls for the benchmark. Accordingly, NACG indeterminacy represents a deficit of chemically relevant labeled reference examples; it does not recover replicate-level qHTS disagreement. Replicate-aware indeterminacy would require run-level assay data and a separate evidence construction.

The three structural splits reuse the same curated population and therefore measure sensitivity to allocation rather than independent external replication. External validation should use a chemically and assay-wise de-duplicated dataset so that overlapping identities or endpoint records do not create optimistic transfer estimates.

NACG also depends on the structural representation used to define local similarity. ECFP neighborhoods are transparent and reproducible, but they do not exhaust possible notions of molecular similarity. The analysis therefore uses one archived fingerprint matrix consistently for classification, clustering, and gating to prevent representation drift within the reported experiment.

The gate-shape constants $q = 2$ and $\lambda = 1$ are fixed design choices. Nearby values produce similar balanced-accuracy behavior, but the present experiments do not establish universally optimal constants. In addition, the current score measures sufficiency and internal coherence of the local evidence without adding a separate agreement term between the neighborhood direction and the base classifier's predicted class; such an alignment-aware extension would constitute a distinct gate and would require independent evaluation.

Finally, selective policies must be matched to application costs. NACG improves balanced retention but generally accepts more difficult positive cases, so ordinary error, Brier score, or NLL can be higher than under probability-margin rejection at the same coverage. The relevant operating point therefore depends on the relative cost of missed activity and unnecessary follow-up. All results remain assay-specific: neither a high T nor an accepted active prediction is a direct probability of human toxicity, clinical harm, or real-world exposure risk.

11. Conclusion and Future Work

NACG-Tox provides a leakage-controlled neutrosophic gate for selective molecular bioactivity prediction. By separating activity-supporting evidence, inactivity-supporting evidence, and chemical-reference indeterminacy, it identifies retained subsets that are substantially less dominated by the inactive majority than those produced by probability confidence alone. Across 6,442 curated Tox21 identities and 12 imbalanced assays, the improvement appears under both validation-locked and matched-coverage evaluation, persists with a Random Forest prediction backbone, and remains stable under nearby values of the gate exponent and evidence regularizer.

The practical contribution is therefore a modular acceptance mechanism rather than a replacement for the molecular classifier. Future evaluation should incorporate run-level qHTS evidence when replicate information is available, test genuinely external chemistry after strict identity and assay de-duplication, examine alignment-aware gating, and evaluate learned molecular embeddings while preserving the same fitting-only evidence construction and validation-locked deployment protocol.

Declarations

Ethics statement

This computational study analyzes publicly released chemical assay data and does not involve human participants, identifiable personal information, or animal experimentation conducted by the authors.

Funding

This work received no external funding.

Data availability

The Tox21 Challenge training archive analyzed in this study is publicly available through the NCATS/NIH Tox21 resource. The reported experiments use the curated identity-level dataset and archived fingerprint matrix described in Section 5.

References

[1] Smarandache, F. *A Unifying Field in Logics: Neutrosophic Logic, Neutrosophy, Neutrosophic Set, Neutrosophic Probability and Statistics*. 6th ed. InfoLearnQuest, 2007.

[2] Wang, H., Smarandache, F., Zhang, Y., & Sunderraman, R. Single Valued Neutrosophic Sets. *Multispace and Multistructure*, 4, 410-413, 2010.

[3] Huang, R., Xia, M., Nguyen, D.-T., Zhao, T., Sakamuru, S., Zhao, J., Shahane, S. A., Rossoshek, A., & Simeonov, A. Tox21 Challenge to Build Predictive Models of Nuclear Receptor and Stress Response Pathways as Mediated by Exposure to Environmental Chemicals and Drugs. *Frontiers in Environmental Science*, 3, 85, 2016. https://doi.org/10.3389/fenvs.2015.00085

[4] Mayr, A., Klambauer, G., Unterthiner, T., & Hochreiter, S. DeepTox: Toxicity Prediction using Deep Learning. *Frontiers in Environmental Science*, 3, 80, 2016. https://doi.org/10.3389/fenvs.2015.00080

[5] Abdelaziz, A., Spahn-Langguth, H., Schramm, K.-W., & Tetko, I. V. Consensus Modeling for HTS Assays Using *In Silico* Descriptors Calculates the Best Balanced Accuracy in Tox21 Challenge. *Frontiers in Environmental Science*, 4, 2, 2016. https://doi.org/10.3389/fenvs.2016.00002

[6] Idakwo, G., Thangapandian, S., Luttrell, J., Li, Y., Wang, N., Zhou, Z., Hong, H., Yang, B., Zhang, C., & Gong, P. Structure-activity relationship-based chemical classification of highly imbalanced Tox21 datasets. *Journal of Cheminformatics*, 12, 66, 2020. https://doi.org/10.1186/s13321-020-00468-x

[7] Rogers, D., & Hahn, M. Extended-Connectivity Fingerprints. *Journal of Chemical Information and Modeling*, 50(5), 742-754, 2010. https://doi.org/10.1021/ci100050t

[8] Bemis, G. W., & Murcko, M. A. The Properties of Known Drugs. 1. Molecular Frameworks. *Journal of Medicinal Chemistry*, 39(15), 2887-2893, 1996. https://doi.org/10.1021/jm9602928

[9] Butina, D. Unsupervised Data Base Clustering Based on Daylight's Fingerprint and Tanimoto Similarity: A Fast and Automated Way to Cluster Small and Large Data Sets. *Journal of Chemical Information and Computer Sciences*, 39(4), 747-750, 1999. https://doi.org/10.1021/ci9803381

[10] Geifman, Y., & El-Yaniv, R. SelectiveNet: A Deep Neural Network with an Integrated Reject Option. *Proceedings of the 36th International Conference on Machine Learning*, PMLR 97, 2151-2159, 2019.

[11] Pedregosa, F., Varoquaux, G., Gramfort, A., Michel, V., Thirion, B., Grisel, O., et al. Scikit-learn: Machine Learning in Python. *Journal of Machine Learning Research*, 12, 2825-2830, 2011.

Received: Jan. 24, 2026. Accepted: Sept. 11, 2026.

Neutrosophic Sets and Systems, Vol. 102, 2027
University of New Mexico

On Minimal Realizations of Neutrosophic Languages: A Categorical Approach

Anil Kumar Ram* and Anupam K. Singh

Department of Mathematics, C.M. College, A Constituent Unit of Lalit Narayan Mithila University, Darbhanga, Bihar-846004, India; anilkumarcmsc0509@gmail.com, anupam09.bhu@gmail.com
* Correspondence: anilkumarcmsc0509@gmail.com

Abstract: This paper develops a categorical framework for deterministic neutrosophic automata with neutrosophic outputs and their associated neutrosophic languages. Building upon neutrosophic set theory, which independently captures truth-membership, indeterminacy-membership, and falsity-membership, we introduce and systematically investigate the structural notions of run maps, reachability, and observability within this framework. Furthermore, two distinct approaches for constructing minimal realizations of a given neutrosophic language are presented and proven to be equivalent. These constructions yield canonical minimal automata and extend the classical Myhill–Nerode paradigm to the neutrosophic setting. The functorial relationships established between the categories of automata and languages provide a unified and robust theoretical foundation for modeling systems involving uncertainty and indeterminacy.

Keywords: Neutrosophic automata; neutrosophic languages; minimal realization; categorical framework; Myhill–Nerode relation; observability; derivatives.

1. Introduction

Automata theory occupies a foundational position in theoretical computer science and discrete mathematics, providing rigorous models for the specification of computational processes, the characterization of formal languages, and the analysis of dynamic systems. In its classical form, deterministic finite automata completely characterize regular languages, with the Myhill–Nerode theorem [34,37] serving as a cornerstone by establishing a correspondence between right-invariant equivalence relations on the free monoid of words and minimal recognizing automata. This result guarantees the existence and uniqueness (up to isomorphism) of canonical minimal automata and offers an effective test for regularity. However, classical automata rely on a binary notion of acceptance, which limits their applicability in contexts involving uncertainty, vagueness, or inconsistency. To overcome this limitation, Zadeh's theory of fuzzy sets [70] introduced graded membership, leading to the development of fuzzy automata and fuzzy languages by Santos [50], Wee [64], and Wee and Fu [65], and later formalized by Malik, Mordeson, and Sen [30,33]. This line of research has evolved substantially, encompassing studies on fuzzy automata over complete residuated lattices [4–6,15–18,24,26,27,42–44,66–68], determinization and minimization techniques [25,28,39–41,63], decidability questions [28], and algebraic as well as categorical formulations [7,11,54–62]. In this broader context, category theory, introduced by Eilenberg and Mac Lane [29], provides a unifying and highly abstract framework for studying automata and systems. The categorical approaches developed by Arbib and Manes [8–10] and further advanced by Goguen [12,13] reformulate realization theory in universal and functorial terms, enabling model-independent treatments of automata behavior and minimization. These ideas have also inspired extensive categorical investigations of fuzzy and lattice-valued automata [11,25,31,32,51,54], thereby significantly broadening the scope and applicability of automata theory.

Despite the substantial expressive power of fuzzy automata, they operate within a single evaluative dimension: every element receives one degree of membership. A more far-reaching generalization is provided by neutrosophic set theory, introduced by Florentin Smarandache [52,53], which extends classical and fuzzy set frameworks by assigning to each element three independent components: truth-membership, indeterminacy-membership, and falsity-membership, each in the interval [0, 1]. Unlike intuitionistic fuzzy sets, these components are independent and need not sum to one, enabling effective modeling of uncertainty, inconsistency, and incomplete information. Building on this concept, neutrosophic automata generalize classical and fuzzy automata by incorporating these three membership components into state transitions and computations, allowing them to handle ambiguous and indeterminate inputs more effectively than traditional models. From an application perspective, neutrosophic sets and automata have proven useful in several domains: decision-making problems [1,3,23,48], where handling incomplete and conflicting information is essential; medical diagnosis [1,49,69], where uncertainty and ambiguity are inherent; and control systems [35,36], topology [14,38,47], financial management [2], and algebraic structures [19–22,45–46], offering flexible tools for modeling complex systems. Additionally, neutrosophic automata have shown effectiveness in learning systems and computational models that require processing of imprecise or inconsistent data.

A special class, deterministic neutrosophic automata, arises naturally as an extension of both classical and fuzzy automata, and ensures that for each state and input symbol the transition is uniquely defined in a neutrosophic sense, while the expressive power of such automata is considerably greater than their fuzzy counterparts. This determinism makes them suitable for structured computational processes while still retaining the ability to manage uncertainty and indeterminacy. Associated with these automata are neutrosophic languages, which extend classical formal languages by assigning to each string degrees of truth, indeterminacy, and falsity. This provides a richer framework for representing uncertain or partially accepted strings in computational systems. The development of a systematic and mathematically rigorous theory of minimal realization in the neutrosophic setting has remained an open and challenging problem. In particular, the construction of canonical minimal deterministic neutrosophic automata corresponding to a prescribed neutrosophic language requires a unified treatment that simultaneously handles three interleaved components of membership and preserves the categorical structure of the theory.

The present paper addresses this gap comprehensively. We introduce the category of deterministic neutrosophic automata with neutrosophic output maps and the category of neutrosophic languages over a given input alphabet, and we establish explicit functorial correspondences between them. Within this categorical framework, we develop two complementary approaches to the construction of minimal realizations. The first approach, presented in Section 4.1, is based on the Myhill–Nerode equivalence relation: two input words are declared equivalent if and only if they produce identical neutrosophic output values under every right-extension. The quotient of the free monoid by this relation constitutes the state set of the canonical minimal automaton. The second approach, presented in Section 4.2, constructs the state space from the derivatives of the neutrosophic language, generalizing Brzozowski's derivative construction (cf. [59,60]) to the neutrosophic context, and finally we establish, via an explicit isomorphism of automata, that both constructions yield the same (up to isomorphism) minimal realization.

The paper is organized as follows. Section 2 reviews the necessary preliminaries from category theory and neutrosophic set theory. Section 3 develops the categorical structure of deterministic neutrosophic automata and neutrosophic languages, including the notions of run maps, reachability, and observability, and the functorial map from deterministic neutrosophic automata with neutrosophic outputs to neutrosophic languages. Section 4 presents the two constructions of minimal realization and establishes their equivalence. Section 5 concludes the paper.

2. Preliminaries

This section reviews the basic concepts and notation of category theory from [7–9,29] and neutrosophic sets from [45,46,52,53] that are essential for the development of the present work. Throughout the paper, we operate within the neutrosophic unit cube, where the output map is represented by a neutrosophic membership triple (F, G, H), where F, G, H ∈ [0, 1]. Here, F, G, H denote the degrees of truth-membership, indeterminacy-membership, and falsity-membership, respectively. Let X be a finite nonempty set, referred to as the input alphabet. We denote by X* the free monoid generated by X, consisting of all finite strings over X, including the empty word e.

Definition 2.1. A neutrosophic set (NS, in short) AN on a universe X is defined as a function AN : $X \to [0, 1]^3$ such that AN(x) = {⟨ x, FA(x), GA(x), HA(x) ⟩ : x ∈ X}.

Definition 2.2. A category D contains: (i) a class of objects (D-objects); (ii) for each pair U and V of D-objects, a set D(U, V) with members known as morphisms (D-morphisms) with domain U, codomain V, written ψ : U → V; (iii) for each D-object U, an identity morphism idU : U → U; and (iv) a composition law assigning to every pair of morphisms ψ : U → V and χ : V → W a morphism χ∘ψ : U → W, called the composition of ψ and χ, satisfying: (a) associativity — for all composable morphisms ψ : U → V, χ : V → W, and Φ : W → Z, Φ∘(χ∘ψ) = (Φ∘χ)∘ψ; and (b) identity laws — for every morphism ψ : U → V, idV∘ψ = ψ and ψ∘idU = ψ. The object-class of a category D is denoted by D itself, for simplicity.

Definition 2.3. A category E is called a subcategory of category D if: (a) each object of E is an object of D; (b) for all E-objects U and V, E(U, V) ⊂ D(U, V); and (c) the composition and identity morphisms in E are the same as those in D.

Definition 2.4. Let D and E be categories. A functor K : D → E is a map that sends each D-object U to E-object K(U) and each D-morphism ψ : U → V to an E-morphism K(ψ) : K(U) → K(V) such that: (a) for all D-morphisms ψ : U → V and χ : V → W, K(χ∘ψ) = K(χ)∘K(ψ); and (b) for all U ∈ D, K(idU) = idK(U).

3. Deterministic Neutrosophic Automata with Neutrosophic Language

In this section, we introduce the central objects of study: deterministic neutrosophic automata with neutrosophic outputs and their associated neutrosophic languages. We establish their categorical structures and develop the key notions of run maps, reachability, and observability that will underpin the minimization theory of Section 4.

Definition 3.1. A deterministic neutrosophic automaton with neutrosophic outputs is a 5-tuple N = (S, X, δ, q0, ηN), where: (i) S is a nonempty set called the state set; (ii) X is a nonempty set called the input alphabet; (iii) δ : S × X → S is a deterministic transition function; (iv) q0 ∈ S is the initial state; and (v) ηN = (Fη, Gη, Hη) : $S \to [0, 1]^3$ is a neutrosophic output map, where Fη(q), Gη(q), Hη(q) ∈ [0, 1] denote, respectively, the truth-, indeterminacy-, and falsity-membership degrees of state q. If S is finite, N is called a deterministic neutrosophic finite automaton.

Remark 3.1. Let 1 = {0} be the one-point set. The initial state q0 ∈ S can be identified by a function τ : 1 → S defined by τ(0) = q0. Thus, the initial state may be viewed as a map from the terminal object 1 to the state set S.

Example 3.1. Let S = ℤ (the set of all integers) and X = {0, 1, 2, …} with start state q0 = 0. Define a deterministic neutrosophic automaton N = (ℤ, X, δ, 0, ηN), where the transition function δ : ℤ × X → ℤ is given by δ(q, x) = q + x if q ≥ 0, and δ(q, x) = q − x if q < 0, for all q ∈ ℤ and x ∈ X. The neutrosophic output map ηN : $\mathbb{Z} \to [0, 1]^3$ is defined by ηN(q) = (0, 0, 0) if q = 0; ηN(q) = (1/|q|, 0, 0) if q > 0; and ηN(q) = (0, 0, 1/|q|) if q < 0. Then N is a deterministic neutrosophic automaton with neutrosophic outputs.

Definition 3.2. Let S and X be sets and let δ : S × X → S be a map. The free extension δ* of δ is a map δ* : S × X* → S defined recursively by (i) δ*(q, e) = q, and (ii) δ*(q, wx) = δ(δ*(q, w), x) for all q ∈ S, w ∈ X*, and x ∈ X. If S and X are, respectively, the state set and input set of a deterministic neutrosophic automaton N, then δ* is called the run map of N. The run map encodes the complete state evolution of the automaton under arbitrary input strings.

Example 3.2. For the automaton in Example 3.1, the free monoid $X^* = \{0, 1, 2, \ldots\}$ together with the extension δ^* forms the run map describing the state evolution of N under arbitrary input strings.

Definition 3.3. Let $N = (S, X, \delta, q0, \eta N)$ and $N' = (S', X', \delta', q0', \eta N')$ be deterministic neutrosophic automata with neutrosophic outputs. A homomorphism $f : N \to N'$ is a pair of mappings $f = (a, b)$, where $a : X \to X'$ and $b : S \to S'$ are maps such that the corresponding structural diagrams (Figure 1) commute. If both a and b are surjective, then N′ is called the homomorphic image of N.

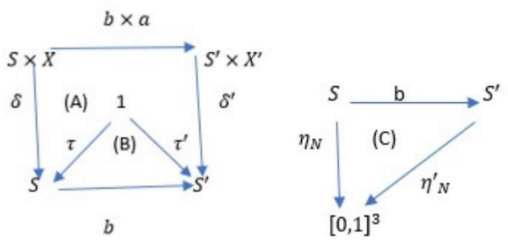

Figure 1. Commuting diagrams for Definition 3.3.

Remark 3.2. In Figure 1, the commutativity of Diagram (C) means $\eta N(q) = (F\eta(q), G\eta(q), H\eta(q)) = ((F\eta'\circ b)(q), (G\eta'\circ b)(q), (H\eta'\circ b)(q)) = (\eta N'\circ b)(q)$, for all $q \in S$.

Proposition 3.1. The class of all deterministic neutrosophic automata equipped with neutrosophic output together with their homomorphisms forms a category under component-wise composition of maps.

Proof. Let $N = (S, X, \delta, q0, \eta N)$, $N' = (S', X', \delta', q0', \eta N')$, and $N'' = (S'', X'', \delta'', q0'', \eta N'')$ be deterministic neutrosophic automata with neutrosophic outputs, and let $f = (a, b) : N \to N'$ and $h = (m, n) : N' \to N''$ be their homomorphisms. To show that the composition $h\circ f = (m\circ a, n\circ b) : N \to N''$ is a homomorphism, it suffices to show that the corresponding structural diagrams commute. The commutativity of Square (A) follows because, for all $(q, x) \in S \times X$, $(n\circ b)\circ\delta(q, x) = n(b(\delta(q, x))) = n(\delta'((b\times a)(q, x))) = \delta''((n\times m)(b(q), a(x))) = (\delta''\circ((n\times m)\circ(b\times a)))(q, x)$; thus $(n\circ b)\circ\delta = \delta''\circ((n\times m)\circ(b\times a))$. The commutativity of Triangle (B) follows since $((n\circ b)\circ\tau)(0) = (n\circ b)(\tau(0)) = (n\circ b)(q0) = n(b(q0)) = n(\tau'(0)) = \tau''(0)$, so $(n\circ b)\circ\tau = \tau''$. The commutativity of Triangle (C) follows since $\eta N(q) = (\eta N'\circ b)(q) = \eta N'(b(q)) = (\eta N''\circ n)(b(q)) = ((\eta N''\circ n)\circ b)(q)$; thus $\eta N = (\eta N''\circ n)\circ b$. □

We shall denote by DNA the category of deterministic neutrosophic automata equipped with neutrosophic outputs.

Remark 3.3. Let DNA(X) be the full subcategory of DNA whose objects have a fixed input alphabet X and whose morphisms are of the form $(b, idX) : N \to N'$. Then DNA(X) is a subcategory of DNA.

Definition 3.4. (a) Let $N = (S, X, \delta, q0, \eta N) \in$ DNA. The reachability map of N is the function $r : X^* \to S$ defined by (i) $r(e) = q0$, and (ii) $r(wa) = \delta(r(w), a)$ for all $w \in X^*$ and $a \in X$. (b) N is called reachable if the reachability map r is surjective.

Example 3.3. For the automaton given in Example 3.1, the identity map on X^* is reachable.

Remark 3.4. From the definition of the extended transition function, $r(w) = \delta^*(q0, w)$ for all $w \in X^*$, and $r(ww') = \delta^*(r(w), w')$ for all $w, w' \in X^*$.

Remark 3.5. Reachability expresses whether every state of the automaton can be obtained from the initial state by reading some input string. In particular, an automaton is reachable if for each state $q \in S$ there exists $w \in X^*$ such that $\delta^*(q0, w) = q$.

Definition 3.5. Let $N = (S, X, \delta, q0, \eta N) \in$ DNA and $q \in S$. The neutrosophic language accepted by N at state q is the mapping $f\,qN = X^* \to [0, 1]^3$, defined by $f\,qN(w) = \eta N(\delta^*(q, w))$, i.e., $(Ffq, Gfq, Hfq)(w) = (F\eta(\delta^*(q, w)), G\eta(\delta^*(q, w)), H\eta(\delta^*(q, w)))$ for all $w \in X^*$. The neutrosophic language $f\,q0N$ accepted at the initial state q0 is called the neutrosophic language recognized by the automaton. Each word is assigned a neutrosophic triple: truth, indeterminacy, and falsity, forming a neutrosophic language recognized by the automaton.

Remark 3.6. It follows directly that $f_{q0N} = \eta N \circ r$, i.e., $Ff_{q0} = F\eta \circ r$, $Gf_{q0} = G\eta \circ r$, and $Hf_{q0} = H\eta \circ r$, where r is the reachability map of the automaton.

We now introduce the concept of a neutrosophic language for arbitrary sets and the category of neutrosophic languages.

Definition 3.6. (a) For a set X, a neutrosophic language is a mapping $fN = X^* \to [0, 1]^3$. (b) A morphism between two neutrosophic languages $fN = X^* \to [0, 1]^3$ and $fN' = (X')^* \to [0, 1]^3$ is a mapping $a : X \to X'$ such that the corresponding structural diagrams commute, where a^* is the free extension of a defined inductively by $a^*(e) = e'$ and $a^*(wx) = a^*(w)a(x)$ for all $w \in X^*$, $x \in X$.

Proposition 3.2. For a given set X, the collection of all neutrosophic languages together with their morphisms forms a category.

Proof. The proof is similar to that of Proposition 3.1. □

We shall denote by NL the category of neutrosophic languages.

Remark 3.7. Let RL be the subclass of NL consisting of the same objects but only surjective morphisms. Then RL forms a category and is naturally a subcategory of NL.

Definition 3.7. (a) Given $N = (S, X, \delta, q0, \eta N) \in$ DNA, the observability map σN of N is a map $\sigma N = (F\sigma, G\sigma, H\sigma) : S \to ([0, 1]^3)^{X^*}$ such that $\sigma N(q) = (F\sigma(q), G\sigma(q), H\sigma(q)) = f_{qN}$ for all $q \in S$. (b) N is said to be observable if σN is one-to-one.

Remark 3.8. (i) $\sigma N(q0) = f_{q0N}$, where $f_{q0N}(w) = (\eta N \circ r)(w) = \eta N(r(w)) = \eta N(\delta^*(q, w))$ for all $w \in X^*$. (ii) Observability means that distinct states induce distinct neutrosophic languages.

Proposition 3.3. Let $N = (S, X, \delta, q0, \eta N)$ and $N' = (S', X', \delta', q0', \eta N') \in$ DNA. Let $r : X^* \to S$ and $r' : (X')^* \to S'$ be their reachability maps, and let $(a, b) : N \to N'$ be a morphism in DNA. Then $b(r(w)) = r'(a^*(w))$ for all $w \in X^*$.

Proof. By induction on the length of $w \in X^*$. For $|w| = 0$, $(b \circ r)(e) = b(r(e)) = b(q0) = q0'$, since (a, b) is a DNA-morphism and preserves initial states; also $(r' \circ a^*)(e) = r'(a^*(e)) = r'(e) = q0'$. Hence the base case holds. Assume the result holds for all strings of length at most n. Then $(b \circ r)(wx) = b(r(wx)) = b(\delta(r(w), x)) = \delta'(b(r(w)), a(x))$, since (a, b) is a DNA-morphism, and $(r' \circ a^*)(wx) = r'(a^*(w)a(x)) = \delta'(r'(a^*(w)), a(x)) = \delta'(br(w), a(x))$ by the inductive hypothesis. Hence the diagram commutes for $|w| = n+1$. □

We now establish the functorial relationship between deterministic neutrosophic automata and neutrosophic languages.

Proposition 3.4. Define a mapping $F : \text{DNA} \to \text{NL}$ by $F(N) = f_{q0N}$ for all $N \in$ DNA, and for every DNA-morphism $(a, b) : N \to N'$, $F(a, b) = a$. Then F is a functor.

Proof. It suffices to verify that $a = F(a, b)$ is an NL-morphism. Since $(a, b) : N \to N'$ is a DNA-morphism, reachability is compatible with morphisms by Proposition 3.3, giving $(\eta N' \circ r') \circ a^* = \eta N \circ r$, i.e., $(F\eta' \circ r') \circ a^* = F\eta \circ r$, $(G\eta' \circ r') \circ a^* = G\eta \circ r$, and $(H\eta' \circ r') \circ a^* = H\eta \circ r$. Since $f_{q0N} = \eta N \circ r$ and $f'_{q0N} = \eta N' \circ r'$, this shows that a is indeed an NL-morphism. □

4. Minimal Realization of Neutrosophic Language

In this section, we present two approaches for constructing a minimal deterministic neutrosophic automaton with neutrosophic outputs corresponding to a given neutrosophic language, and show that the proposed constructions produce minimal realizations.

Definition 4.1. $N = (S, X, \delta, q0, \eta N) \in$ DNA is a realization of the neutrosophic language f_{qN} if $F(N) = f_{qN}$. Moreover, the realization N is minimal if it is both reachable and observable.

Definition 4.2. (i) Let $fN = X^* \to [0, 1]^3$ be a neutrosophic language. The relation $\approx fN$, defined by $fN(w1w) = fN(w2w)$ for all $w \in X^*$, is called the Myhill–Nerode relation on X^*. The quotient set $X^*/{\approx}fN$ forms the state set of the minimal deterministic neutrosophic automaton $Pf = (Sf, X, \delta f, [e]f, \eta fN)$, where the transition function $\delta f : Sf \times X \to Sf$ and the neutrosophic output map $\eta fN : Sf \to [0, 1]^3$ are defined by $\delta f([w], x) = [wx]$ and $\eta fN([w]) = fN(w)$, for all $[w] \in Sf$, $x \in X$. (ii) Let $fN : X^* \to [0, 1]^3$ be a neutrosophic language and $u \in X^*$. The derivative of fN with respect to u is the neutrosophic language $f_{uN} : X^* \to [0, 1]^3$, defined by $f_{uN}(v) = fN(uv)$, i.e., $Ffu(v) = Ff(uv)$, $Gfu(v) = Gf(uv)$, and $Hfu(v) = Hf(uv)$, for all $v \in X^*$.

4.1. Minimal Realization Based on Myhill–Nerode Theory

Proposition 4.1. Every neutrosophic language $fN : X^* \rightarrow [0, 1]^3$ admits a minimal realization Nf in the class DNA.

Proof. Define a relation $\approx fN$ on X^* by $w1 \approx fN\ w2$ if and only if $fN(w1w) = fN(w2w)$ for all $w \in X^*$. This is readily verified to be an equivalence relation on X^*. Let $Sf = X^*/\approx fN = \{[w] : w \in X^*\}$ be the Myhill–Nerode quotient, where $[w] = \{u \in X^* : u \approx fN\ w\}$, and define $\delta f : Sf \times X \rightarrow Sf$ and $\eta fN : Sf \rightarrow [0, 1]^3$ by $\delta f([w], x) = [wx]$ and $\eta fN([w]) = fN(w) = (Ff(w), Gf(w), Hf(w))$, for all $[w] \in Sf$, $x \in X$.

Both maps are well defined: if $[w1] = [w2]$ then $w1 \approx fN\ w2$, so $fN(w1w') = fN(w2w')$ for all $w' \in X^*$; taking $w' = xw$ gives $fN(w1xw) = fN(w2xw)$ for all $w \in X^*$, $x \in X$, hence $w1x \approx fN\ w2x$, so $[w1x] = [w2x]$, i.e., $\delta f([w1], x) = \delta f([w2], x)$. Also, taking $w' = e$ gives $fN(w1) = fN(w2)$, so $\eta fN([w1]) = \eta fN([w2])$. Thus δf is deterministic and total, and ηfN is well defined, so $Pf = (Sf, X, \delta f, [e]f, \eta fN) \in$ DNA.

For $w \in X^*$, $fN(w) = \eta fN([w]) = \eta fN(\delta^*f([e], w))$, so Pf realizes fN. To prove minimality, let $[w] \in Sf$; then $r(w) = \delta^*f([e], w) = [ew] = [w]$, so r is surjective and Pf is reachable. In addition, if $\sigma N([w1]) = \sigma N([w2])$, then $\eta fN(\delta^*f([w1], w)) = \eta fN(\delta^*f([w2], w))$ for all $w \in X^*$, i.e., $fN(w1w) = fN(w2w)$ for all $w \in X^*$; thus $w1 \approx fN\ w2$, hence $[w1] = [w2]$. Therefore σN is injective and Pf is observable. Thus Pf is both reachable and observable, and hence minimal. □

Example 4.1. Let $X = \{a\}$ be a unary alphabet and let $fN = (Ff, Gf, Hf) : X^* \rightarrow [0, 1]^3$ be a neutrosophic language defined for $n \geq 0$ by $fN(a^n) = (0.8, 0.1, 0.1)$ if n is even, and $fN(a^n) = (0.4, 0.3, 0.3)$ if n is odd. For $m, n \in \mathbb{N}$, $a^m \approx fN\ a^n$ if and only if $fN(a^{m+k}) = fN(a^{n+k})$ for all $k \geq 0$. Since parity is preserved under concatenation, $a^m \approx fN\ a^n$ if and only if $m \equiv n \pmod 2$. Therefore $\approx fN$ has exactly two equivalence classes: $[e] = \{a^{2k} : k \geq 0\}$ and $[a] = \{a^{2k+1} : k \geq 0\}$. The minimal deterministic neutrosophic automaton with neutrosophic output is $Pf = (Sf, X, \delta f, [e]f, \eta fN)$, where $Sf = \{[e], [a]\}$, $\delta f([e], a) = [a]$, $\delta f([a], a) = [e]$, $\eta fN([e]) = (0.8, 0.1, 0.1)$, and $\eta fN([a]) = (0.4, 0.3, 0.3)$. For any $n \geq 0$, $\delta^*f([e], a^n) = [e]$ if n is even and $[a]$ if n is odd, so $\eta fN(\delta^*f([e], a^n)) = \eta fN(a^n)$; hence Pf realizes fN. Since $\delta^*f([e], e) = [e]$ and $\delta^*f([e], a) = [a]$, both states are reachable, and since $\eta fN([e]) \neq \eta fN([a])$ the two states are distinguishable, so the automaton is observable. Therefore Pf is reachable and observable, and hence minimal by Definition 4.1.

The following is a functorial relationship between the subcategories of neutrosophic language (RL) and deterministic neutrosophic automaton (DNA(X)).

Proposition 4.2. Let $N : RL \rightarrow DNA(X)$ be a map such that for $fN \in RL$, $N(fN) = Pf$, and to each RL-morphism $a : fN \rightarrow fN'$, $N(a) = (a, b) : Pf \rightarrow Pf'$, where $b : Sf \rightarrow Sf'$ is defined by $b([w]) = [a^*(w)]$. Then N is a functor.

Proof. First, b is well defined: if $[w1] = [w2]$ then $w1 \approx fN\ w2$, so $fN(w1u) = fN(w2u)$ for all $u \in X^*$; since a is an RL-morphism, $fN(w) = fN'(a^*(w))$ for all $w \in X^*$, so $fN'(a^*(w1u)) = fN'(a^*(w2u))$ for all $u \in X^*$, which implies $a^*(w1) \approx fN'\ a^*(w2)$, i.e., $b([w1]) = b([w2])$. Next, (a, b) is a DNA(X)-morphism: the commutativity of Square (A) follows since $\delta f'(b([w]), a(x)) = \delta f'([a^*(w)], a(x)) = [a^*(w)a(x)] = [a^*(wx)] = b([wx]) = b(\delta f([w], x))$; the commutativity of the initial-state triangle follows since $b(\tau f(0)) = b([e]f) = [a^*(e)] = [e']f = \tau f'(0)$; and the commutativity of the output triangle follows since $(\eta f' \circ b)([w]) = \eta f'([a^*(w)]) = fN'(a^*(w)) = fN(w) = \eta f([w])$ componentwise. □

4.2. Minimal Realization Based on Derivatives of Neutrosophic Language

We now present an alternative construction of the minimal realization using the derivatives of the given neutrosophic language. For a neutrosophic language $fN : X^* \rightarrow [0, 1]^3$, define $S^f = \{f\ uN : u \in X^*\}$.

Proposition 4.3. Given a neutrosophic language $fN : X^* \rightarrow [0, 1]^3$, a minimal realization $P^f = (S^f, X, \delta^f, f^e, \eta^f_N) \in$ DNA exists for fN.

Proof. Define $\delta^f : S^f \times X \rightarrow S^f$ and $\eta^f_N : S^f \rightarrow [0, 1]^3$ by $\delta^f(g, x) = g^x$ and $\eta^f_N(g) = g(e)$, for $g \in S^f$, $x \in X$. Both maps are well defined: if $g = h$ with $g = f\ uN$, $h = f\ vN$, then $g(w) = h(w)$ for all $w \in X^*$; in particular $g(xw) = h(xw)$ for all $x \in X$, $w \in X^*$, i.e., $g^x(w) = h^x(w)$, so $g^x = h^x$ for all x, giving $\delta^f(g, x) = \delta^f(h, x)$; and taking $w = e$ gives $g(e) = h(e)$, i.e., $\eta^f_N(g) = \eta^f_N(h)$. Thus $P^f = (S^f,$

X, δ^f, f^e, η^f_N) ∈ DNA. For w ∈ X*, fN(w) = fN(we) = f wN(e) = η^f_N(f w) = $\eta^f_N(\delta^{f*}(f\ e, w))$, so P^f realizes fN.

For minimality: let g ∈ S^f; then g = f wN for some w ∈ X*, and r(w) = δ^{f*}(f e, w) = f ewN = f wN = g, so r is surjective and P^f is reachable. In addition, if σN(f w1) = σN(f w2), then for all w ∈ X*, $\eta^f_N(\delta^{f*}(f\ w1, w)) = \eta^f_N(\delta^{f*}(f\ w2, w))$, i.e., η^f_N(f w1w) = η^f_N(f w2w), i.e., f w1wN(e) = f w2wN(e), i.e., f w1N(w) = f w2N(w) for all w, so f w1N = f w2N. Hence σN : $S^f \to ([0, 1]^3)^{X*}$ is injective, so P^f is observable, and hence minimal. □

Proposition 4.4. Let N : RL → DNA(X) be a map such that for fN ∈ RL, N(fN) = P^f, and to each RL-morphism a : fN → fN′, N(a) = (a, b) : $P^f \to P^{f'}$, where b : $S^f \to S^{f'}$ is defined by b(f wN) = $f^{a*(w)}$N. Then N is a functor.

Proof. Similar to the proof of Proposition 4.2. □

We conclude this subsection by establishing the isomorphic relationship between the deterministic neutrosophic automata with outputs P^f and Pf. This result demonstrates that both constructions represent the same neutrosophic language structure, although defined through different formulations, ensuring that their behavioral properties and language recognition capabilities are equivalent.

Proposition 4.5. Let fN : X* → $[0, 1]^3$ be a neutrosophic language. Then the DNA-object Pf = (Sf, X, δf, [e]f, ηfN) is isomorphic to the DNA-object P^f = (S^f, X, δ^f, f^e, η^f_N).

Proof. Define χ = (idX, b) : Pf → P^f, where b : Sf → S^f is given by b([w]) = f wN = (Ffw, Gfw, Hfw) for all w ∈ X*. For each [w] ∈ Sf there exists f wN ∈ S^f with b([w]) = f wN, so χ is surjective; and if b([w1]) = b([w2]) then f w1N = f w2N, hence [w1] = [w2], so χ is injective, and thus bijective. To show χ is a homomorphism: the commutativity of Square (A) follows since δ^f(b([w]), x) = δ^f(f wN, x) = f wxN = b([wx]) = (b∘δf)([w], x); the commutativity of the initial-state triangle follows since b(τf(0)) = b([e]) = f eN = $\tau^f(0)$; and the commutativity of the output triangle follows since (η^f_N∘b)([w]) = η^f_N(f w) = f w(e) = fN(w) = ηfN([w]). Hence the DNA-object Pf is isomorphic to the DNA-object P^f. □

5. Conclusion

This paper develops a categorical framework for deterministic neutrosophic automata and their associated neutrosophic languages by introducing the categories DNA and NL, along with a functor linking automata to recognized languages. It formalizes key structural notions such as run maps, reachability, and observability. Two distinct constructions of minimal realizations, based on the Myhill–Nerode equivalence and on derivative methods, are established and proven to be canonically isomorphic. Furthermore, these constructions are shown to admit functorial characterizations, ensuring a systematic and structure-preserving realization process. Overall, the work extends classical automata minimization theory to the neutrosophic setting and provides a foundation for future theoretical and applied developments.

Conflict of Interest: The authors declare that they have no conflicts of interest regarding the publication of this paper.

Ethical Approval: This article does not contain any studies involving human participants or animals performed by any of the authors.

References

1. Abdel-Basset, M.; Manogaran, G.; Gamal, A.; Smarandache, F. A group decision making framework based on neutrosophic TOPSIS approach for smart medical device selection. Journal of Medical Systems 2019, 43, 38–45.
2. Abdel-Basset, M.; Ding, W.; Mohamed, R.; Metawa, N. An integrated plithogenic MCDM approach for financial performance evaluation of manufacturing industries. Risk Management 2020, 22(3), 192–218.
3. Abdel-Basset, M.; Mohamed, R.; Sallam, K.; Elhosemy, M. A novel decision-making model for sustainable supply chain finance under certainty environment. Journal of Cleaner Production 2020, 269, 122324.

4. Abolpour, K.; Zahedi, M.M. Isomorphism between two BL-general fuzzy automata. Soft Computing 2012, 16, 729–736.
5. Abolpour, K.; Zahedi, M.M. BL-general fuzzy automata and accept behaviour. Journal of Applied Mathematics and Computation 2012, 38, 103–118.
6. Abolpour, K.; Zahedi, M.M. General fuzzy automata based on complete residuated lattice-valued logic. Iranian Journal of Fuzzy Systems 2017, 14, 103–121.
7. Adámek, J.; Trnková, V. Automata and Algebras in Categories; Kluwer Academic Publishers: Dordrecht, 1990.
8. Arbib, M.A.; Manes, E.G. Machines in a category: An expository introduction. SIAM Review 1974, 16, 163–192.
9. Arbib, M.A.; Manes, E.G. Machines in a category. Journal of Pure and Applied Algebra 1975, 6, 123–167.
10. Arbib, M.A.; Manes, E.G. Arrows, Structures and Functors: The Categorical Imperative; Academic Press: New York, 1975.
11. Gautam, V.; Tiwari, S.P.; Pal, P.; Tripathi, J. On categories of automata and languages based on a complete residuated lattice. New Mathematics and Natural Computation 2018, 14, 423–444.
12. Goguen, J.A. Minimal realization of machines in closed categories. Bulletin of the American Mathematical Society 1972, 78, 777–783.
13. Goguen, J.A. Realization is universal. Mathematical Systems Theory 1973, 6, 359–374.
14. Hashmi, M.R.; Riaz, M.; Smarandache, F. m-Polar neutrosophic topology with applications to multi-criteria decision making. International Journal of Fuzzy Systems 2020, 22, 273–292.
15. Holcombe, W.M.L. Algebraic Automata Theory; Cambridge University Press, 1982.
16. Ignjatović, J.; Ćirić, M.; Bogdanović, S. Determinization of fuzzy automata with membership values in complete residuated lattices. Information Sciences 2008, 178, 164–180.
17. Ignjatović, J.; Ćirić, M.; Bogdanović, S.; Petković, T. Myhill–Nerode type theory for fuzzy languages and automata. Fuzzy Sets and Systems 2010, 161, 1288–1324.
18. Ignjatović, J.; Ćirić, M.; Simović, V. Fuzzy relation equations and subsystems of fuzzy transition systems. Knowledge-Based Systems 2013, 38, 48–61.
19. Karthikeyan, V.; Karuppaiya, R. Subsystems of interval neutrosophic automata. Advances in Mathematics: Scientific Journal 2020, 9(4), 1653–1659.
20. Kavikumar, J.; Nagarajan, D.; Broumi, S.; Smarandache, F.; Lathamaheswari, M.; Ebas, N.A. Neutrosophic general finite automata. Neutrosophic Sets and Systems 2019, 27, 17–36.
21. Kavikumar, J.; Nagarajan, D.; Lathamaheswari, M.; Yong, G.J.; Broumi, S. Distinguishable and inverses of neutrosophic finite automata. In Neutrosophic Graph Theory and Algorithms; IGI Global, 2020.
22. Kavikumar, J.; Nagarajan, D.; Tiwari, S.P.; Broumi, S.; Smarandache, F. Composite neutrosophic finite automata. Neutrosophic Sets and Systems 2020, 36, 282–291.
23. Kharal, A. A neutrosophic multi-criteria decision making method. New Mathematics and Natural Computation 2014, 10(2), 143–162.
24. Kim, Y.H.; Kim, J.G.; Cho, S.J. Products of T-generalized state machines and T-generalized transformation semigroups. Fuzzy Sets and Systems 1998, 93, 87–97.
25. Lei, H.; Li, Y.M. Minimization of states in automata theory based on finite lattice-ordered monoids. Information Sciences 2007, 177, 1413–1421.
26. Li, Y.; Pedrycz, W. Fuzzy finite automata and fuzzy regular expressions with membership values in lattice-ordered monoids. Fuzzy Sets and Systems 2005, 156, 68–92.
27. Li, Y. Finite automata theory with membership values in lattices. Information Sciences 2011, 181, 1003–1017.
28. Li, L.; Qiu, D. On the state minimization of fuzzy automata. IEEE Transactions on Fuzzy Systems 2015, 23, 434–443.
29. Mac Lane, S. Categories for the Working Mathematician; Springer: New York, 1978.
30. Malik, D.S.; Mordeson, J.N.; Sen, M.K. Submachines of fuzzy finite state machine. Journal of Fuzzy Mathematics 1994, 2, 781–792.
31. Močkoř, J. A category of fuzzy automata. International Journal of General Systems 1991, 20, 73–82.
32. Močkoř, J. Fuzzy and non-deterministic automata. Soft Computing 1999, 3, 221–226.
33. Mordeson, J.N.; Malik, D.S. Fuzzy Automata and Languages: Theory and Applications; Chapman & Hall/CRC, 2002.

34. Myhill, J. Finite automata and the representation of events. WADD Technical Report 57-624, Wright-Patterson AFB, 1957, 112–137.
35. Nagarajan, D.; Lathamaheswari, M.; Broumi, S.; Kavikumar, J. Dombi interval valued neutrosophic graph and its role in traffic control management. Neutrosophic Sets and Systems 2019, 24, 114–133.
36. Nagarajan, D.; Lathamaheswari, M.; Broumi, S.; Kavikumar, J. A new perspective on traffic control management using triangular interval type-2 fuzzy sets and interval neutrosophic sets. Operations Research Perspectives 2019, 6, 100099.
37. Nerode, A. Linear automata transformation. Proceedings of the American Mathematical Society 1958, 9, 541–544.
38. Ozturk, T.Y.; Ozkan, A.A. Neutrosophic bitopological spaces. Neutrosophic Sets and Systems 2019, 30, 88–97.
39. Peeva, K. Behaviour, reduction and minimization of finite L-automata. Fuzzy Sets and Systems 1988, 28, 171–181.
40. Peeva, K. Fuzzy acceptors for syntactic pattern recognition. International Journal of Approximate Reasoning 1991, 5, 291–306.
41. Peeva, K. Finite L-fuzzy acceptors, regular L-fuzzy grammars and syntactic pattern recognition. International Journal of Uncertainty, Fuzziness and Knowledge-Based Systems 2004, 12, 89–104.
42. Qiu, D.W. Automata theory based on complete residuated lattice-valued logic (I). Science China 2001, 44, 419–429.
43. Qiu, D.W. Automata theory based on complete residuated lattice-valued logic (II). Science China 2002, 45, 442–452.
44. Qiu, D.W. Pumping lemma in automata theory based on complete residuated lattice-valued logic: A note. Fuzzy Sets and Systems 2006, 157, 2128–2138.
45. Ram, A.K.; Singh, A.K.; Kumar, B. Neutrosophic automata and reverse neutrosophic automata. Neutrosophic Sets and Systems 2024, 63, 219–238.
46. Ram, A.K.; Singh, A.K. Neutrosophic automata and its algebraic properties. Neutrosophic Systems with Applications 2025, 24, 63–75.
47. Ram, A.K.; Singh, A.K. A neutrosophic topology for neutrosophic automata. In Super Hyper Topologies and Super Hyper Structures with their Applications; Biblio Publishes, 2025, 254–267.
48. Riaz, M.; Hashmi, M.R. Fixed points of fuzzy neutrosophic soft mapping with decision-making. Fixed Point Theory and Applications 2018, 7, 1–10.
49. Samuel, A.E.; Narmadhagnanam, R. Pi-distance of rough neutrosophic sets for medical diagnosis. Neutrosophic Sets and Systems 2019, 28, 51–57.
50. Santos, E.S. Maximin automata. Information and Control 1968, 12, 367–377.
51. Singh, S.; Tiwari, S.P. On category of L-fuzzy automata, coalgebras and dialgebras. Fuzzy Sets and Systems 2020, 420, 1–28.
52. Smarandache, F. A Unifying Field in Logics: Neutrosophy, Neutrosophic Probability, Set and Logic; American Research Press: Rehoboth, 1999.
53. Smarandache, F. Neutrosophic set: A generalization of intuitionistic fuzzy set. IEEE Conference on Granular Computing 2006, 8–42.
54. Tang, J.G.; Luo, M.K.; Tang, J. Results on the use of category theory for the study of lattice-valued finite state machines. Information Sciences 2014, 288, 279–289.
55. Tiwari, S.P.; Srivastava, A.K. On a decomposition of fuzzy automata. Fuzzy Sets and Systems 2005, 151, 503–511.
56. Tiwari, S.P.; Singh, A.K.; Sharan, S. Fuzzy automata based on lattice-ordered monoid and associated topology. Journal of Uncertain Systems 2012, 6, 51–55.
57. Tiwari, S.P.; Singh, A.K. On minimal realization of fuzzy behaviour and associated categories. Journal of Applied Mathematics and Computation 2013, 45, 223–234.
58. Tiwari, S.P.; Singh, A.K.; Sharan, S.; Yadav, V.K. Bifuzzy core of fuzzy automata. Iranian Journal of Fuzzy Systems 2015, 12, 63–73.
59. Tiwari, S.P.; Yadav, V.K.; Singh, A.K. Construction of a minimal realization and monoid for a fuzzy language: A categorical approach. Journal of Applied Mathematics and Computation 2015, 47, 401–416.
60. Tiwari, S.P.; Gautam, V.; Davvaz, B. On minimal realization for a fuzzy language and Brzozowski's algorithm. Journal of Intelligent and Fuzzy Systems 2015, 29, 1949–1956.

61. Tiwari, S.P.; Yadav, V.K.; Pal, P.; Sharma, B.K. Minimal fuzzy realization for fuzzy behaviour: A bicategory-theoretic approach. Journal of Multiple-Valued Logic and Soft Computing 2018, 31, 105–121.
62. Tiwari, S.P.; Yadav, V.K.; Davvaz, B. A categorical approach to minimal realization for a fuzzy language. Fuzzy Sets and Systems 2018, 351, 122–137.
63. Trnková, V. Relational automata in a category and their languages. Lecture Notes in Computer Science 1977, 56, 340–355.
64. Wee, W.G. On generalizations of adaptive algorithm and application of the fuzzy sets concept to pattern classification. Ph.D. Thesis, Purdue University, Lafayette, IN, 1967.
65. Wee, W.G.; Fu, K.S. A formulation of fuzzy automata and its application as a model of learning systems. IEEE Transactions on Systems, Man, and Cybernetics 1969, 5, 215–223.
66. Wu, L.; Qiu, D. Automata theory based on complete residuated lattice-valued logic: Reduction and minimization. Fuzzy Sets and Systems 2010, 161, 1635–1656.
67. Xing, H.; Qiu, D.W. Pumping lemma in automata theory based on complete residuated lattice-valued logic. Fuzzy Sets and Systems 2009, 160, 1141–1151.
68. Xing, H.; Qiu, D.W. Automata theory based on complete residuated lattice-valued logic: A categorical approach. Fuzzy Sets and Systems 2009, 160, 2416–2428.
69. Ye, J. Improved cosine similarity measures of simplified neutrosophic sets for medical diagnoses. Artificial Intelligence in Medicine 2015, 63(3), 171–179.
70. Zadeh, L.A. Fuzzy sets. Information and Control 1965, 8, 338–353.

Received: Feb. 20, 2026. Accepted: Sept. 11, 2026.

Neutrosophic Sets and Systems, Vol. 102, 2027
University of New Mexico

Type-1 Neutrosophic-Topology Based on Type-1 Neutrosophic Sets

Hussain Wahish[1] and Adel Al-Odhari[2,*]

[1] Department of Mathematics, Faculty of Education, University of Saba Region, Mareb, Yemen; wohussain@gmail.com

[2] Faculty of Education, Humanities and Applied Sciences (Khawlan), and Department of Foundations of Sciences, Faculty of Engineering, Sana'a University, Box: 13509, Sana'a, Yemen; a.aleidhri@su.edu.ye

* Correspondence: a.aleidhri@su.edu.ye

Abstract: This paper develops a topological framework based on type-1 neutrosophic sets, extending the study of uncertainty beyond classical and intuitionistic fuzzy structures. We investigate fundamental operators — interior, closure, and exterior — on type-1 neutrosophic sets X[I], and establish separation axioms for type-1 topological spaces Ti[I], i = 0, 1, …, 4. Furthermore, we analyze continuous and contra type-1 neutrosophic functions, exploring their structural properties within this framework. By isolating type-1 neutrosophic sets and formalizing their topological behaviour, our results provide new insights into neutrosophic topology and lay the groundwork for broader applications in mathematical analysis, algebra, and related fields.

Keywords: Type-1 Neutrosophic Sets; Type-1 Neutrosophic Topology; Type-1 Neutrosophic Interior Sets; Type-1 Neutrosophic Closure Sets; Type-1 Neutrosophic Exterior Sets; Type-1 Neutrosophic Boundary Sets; Separation Axioms for Ti[I], i = 0, 1, …, 4; Continuity on Type-1 Neutrosophic Topological Spaces

---

1. Introduction

Neutrosophy, introduced by Smarandache in the 1980s [38], is a branch of philosophy that investigates the origin and characteristics of neutrality in nature. The mathematical study of uncertainty has evolved through several foundational milestones. In 1965, Zadeh proposed fuzzy sets as an extension of classical crisp sets, establishing the framework for fuzzy mathematics [42]. This was followed in 1968 by Chang, who extended fuzzy concepts to topological spaces, exploring notions such as open and closed sets, neighborhoods, interiors, continuity, and compactness [17]. Lowen further advanced this structure in 1976 by studying fuzzy compactness [31]. In 1986, Atanassov enriched fuzzy theory with intuitionistic fuzzy sets, introducing degrees of membership and non-membership [12,13], and in 1997, Coker extended these ideas to intuitionistic topological spaces [18]. Building on these developments, Smarandache introduced neutrosophic sets [39] as a generalization of intuitionistic fuzzy sets [12,13], incorporating three components for each element in X: the degree of membership, the degree of indeterminacy, and the degree of non-membership. Subsequent research investigated neutrosophic set operations and their topological properties. Lupianez [29,30] and Salama [35,36] defined various topologies on neutrosophic sets, though some did not satisfy De Morgan's laws. Also, neutrosophic closed sets and neutrosophic continuous functions were investigated in [37]. Karataş and Kuru [28] redefined neutrosophic operations and introduced neutrosophic topology, studying properties such as closure, interior, exterior, boundary, and subspace. In algebraic structures, groups play a central role [21,23], and neutrosophic sets have been applied in diverse areas including analysis [15,16], neutrosophic crisp topology [11], algebra [9,10,19], uncertainty graph theory [24,25,41], and practical domains such as sentiment analysis and medical diagnostics [1]. Smarandache and Kandasamy [26] extended neutrosophic theory to algebraic structures by introducing an indeterminate element I. The concept of neutrosophic groups was introduced in [33], while others explored algebraic operations from different viewpoints [27]. Cetkin and Aygun [19] proposed an approach to neutrosophic subgroups, and Abdalla and Saleem [22] studied neutrosophic group structures further. Recently, Al-Odhari [2–9] developed neutrosophic sets generated by classical set theory, identifying three types. In a revised work, he isolated type-1 neutrosophic sets and investigated their properties to construct new mathematical structures [2]. In this article, we build a topological framework based on type-1 neutrosophic sets and examine properties such as interior, closure, exterior, and boundary operators on type-1 neutrosophic sets X[I]. Furthermore, we study separation axioms for type-1 topological spaces (Ti[I], i = 0, 1, …, 4), and analyse continuous and contra type-1 neutrosophic functions along with their properties.

2. Type-1 Neutrosophic Topological Spaces

In this section, we introduce the concept of type-1 topological spaces, which is based on type-1 neutrosophic sets in [2–9]. A neutrosophic set of type-1 is induced from a neutrosophic element a + bI, where I is called the neutrosophic element with property $I^2 = I$ and 0I = 0, as appeared in the work of Kandasamy and Smarandache on neutrosophic algebraic structures in [26,27]. An attempt to present an intuitive mathematical framework that includes type-1 neutrosophic set theory was presented in previous works and is still under development and mathematical construction.

Definition 2.1. Let X[I] be a type-1 neutrosophic set and τ[I] be a collection of neutrosophic subsets of X[I]. Then τ[I] is a type-1 neutrosophic topology on X[I] (in short T1NTS), if and only if:

(1) ∅[I] and X[I] ∈ τ[I].

(2) If A1[I] and A2[I] ∈ τ[I], then A1[I] ∩ A2[I] ∈ τ[I].

(3) Every neutrosophic union of neutrosophic members of τ[I] is also a neutrosophic member of τ[I].

The couple (X[I], τ[I]) is called a type-1 topological space on X[I]. Moreover, the members of τ[I] are said to be type-1 neutrosophic open sets in τ[I]. A subset A[I] ⊆ X[I] is called a type-1 neutrosophic closed set in (T1NTS) (X[I], τ[I]) if X[I] − A[I] ∈ τ[I].

Example 2.2. Let X[I] = {1 + I, 1 + 2I, 2 + I, 2 + 2I} be a type-1 neutrosophic set and τ[I] = {∅[I], X[I], {1+I, 1+2I}, {1+I, 2+I}, {1+I}, {1+I, 1+2I, 2+I}} be a collection of neutrosophic subsets of X[I]. Then (X[I], τ[I]) is a type-1 neutrosophic topological space.

Example 2.3. Let τ[I] = {∅[I], P(X[I])} and τ[I] = {∅[I], X[I]}. These are called, respectively, a type-1 neutrosophic discrete topological space and a type-1 neutrosophic indiscrete topological space over X[I].

Theorem 2.4. Let (X[I], τ[I]) be a type-1 neutrosophic topological space. Then: (1) ∅[I] and X[I] are type-1 neutrosophic open (or closed) sets over X[I]. (2) The intersection of any finite number of type-1 neutrosophic open (or closed) sets is a type-1 neutrosophic open (or closed) set over X[I]. (3) The union of any two type-1 neutrosophic open (or closed) sets is a type-1 neutrosophic open (or closed) set over X[I].

Proof. Straightforward. □

Theorem 2.5. Let (X[I], τ1[I]) and (X[I], τ2[I]) be two type-1 neutrosophic topological spaces over X[I]. Then (X[I], τ1[I] ∩ τ2[I]) is a type-1 neutrosophic topological space over X[I].

Proof. (1) Since ∅[I] and X[I] ∈ τ1[I] and τ2[I], then ∅[I] and X[I] ∈ τ1[I] ∩ τ2[I]. (2) Suppose A1[I], A2[I] ∈ τ1[I] ∩ τ2[I]. Then A1[I], A2[I] ∈ τ1[I] and A1[I], A2[I] ∈ τ2[I], which implies A1[I] ∩ A2[I] ∈ τ1[I] and A1[I] ∩ A2[I] ∈ τ2[I]. Therefore A1[I] ∩ A2[I] ∈ τ1[I] ∩ τ2[I]. (3) Assume {Ai[I] : i ∈ J} ⊆ τ1[I] ∩ τ2[I]. Then Ai[I] ∈ τ1[I] and Ai[I] ∈ τ2[I] for all i ∈ J. Therefore ∪i∈J Ai[I] ∈ τ1[I] and ∪i∈J Ai[I] ∈ τ2[I], so ∪i∈J Ai[I] ∈ τ1[I] ∩ τ2[I]. Consequently, (X[I], τ1[I] ∩ τ2[I]) is a type-1 neutrosophic topological space. □

Corollary 2.6. Let {(X[I], τi[I]) : i ∈ J} be a family of type-1 neutrosophic topological spaces over X[I]. Then (X[I], ∩i∈J τi[I]) is a type-1 neutrosophic topological space over X[I].

Proof. By the method similar to Theorem 2.5. □

Remark 2.1. The union of type-1 neutrosophic topological spaces may not be a type-1 neutrosophic topological space.

Example 2.7. Let X[I] = {a+aI, a+bI, b+aI, b+bI} be a type-1 neutrosophic set, and let τ1[I] = {∅[I], X[I], {a+aI}}, τ2[I] = {∅[I], X[I], {b+aI}} be two type-1 neutrosophic topologies on X[I]. Then τ1[I] ∪ τ2[I] is not a type-1 neutrosophic topological space.

Definition 2.8. Let (X[I], τ[I]) be a type-1 neutrosophic topological space, N[I] ⊆ X[I], and x ∈ X[I]. N[I] is said to be a neighborhood (in short nbd) of a neutrosophic point x ∈ X[I] if there exists O[I] ∈ τ[I] such that x ∈ O[I] ⊆ N[I], denoted Nnbd[I](x). The set which contains all such N[I] is called the neighborhood neutrosophic system and denoted by Nnbd[I](x) = {N[I] ⊆ X[I] : ∃ O[I] ∈ τ[I] such that x ∈ O[I] ⊆ N[I]}.

Example 2.9. Let X[I] = {0, 1, 2, I, 2I, 1+I, 1+2I, 2+I, 2+2I} be a type-1 neutrosophic set and consider the type-1 neutrosophic sub-collection τ[I] of X[I] given by τ[I] = {∅[I], X[I], {0}, {0, 1, I, 2I, 1+I, 1+2I}}, where (X[I], τ[I]) is a type-1 neutrosophic topological space. Then X[I] is a neighborhood of the point 0, since 0 ∈ X[I] ⊆ X[I]; {0} is a neighborhood of 0, since 0 ∈ {0} ⊆ {0}; and, more generally, every superset of {0} within X[I], such as {0,1}, {0,2}, {0,I}, {0,2I}, {0,1+I}, {0,1+2I}, {0,2+I}, {0,2+2I}, {0,1,2}, {0,1,2,I}, {0,1,2,I,2I}, {0,1,2,I,2I,1+I}, {0,1,2,I,2I,1+I,1+2I}, and {0,1,2,I,2I,1+I,1+2I,2+I}, is also a neighborhood of the point 0, because in each case 0 ∈ {0} ⊆ the given set.

3. Properties of Type-1 Neutrosophic Subsets on Type-1 Topological Spaces

In this section, we investigate the main properties of the type-1 neutrosophic subspace of type-1 topological spaces. We study type-1 neutrosophic interior, closure, and exterior operators via the X[I] set and their properties.

3.1. Type-1 Neutrosophic Interior Points

This subsection is devoted to studying the interior operator via X[I] sets and their properties.

Definition 3.1. Let (X[I], τ[I]) be a type-1 neutrosophic topological space and A[I] ⊆ X[I]. The interior functor of A[I] is denoted Intn(A[I]) and defined by Intn(A[I]) = ∪{O[I] ⊆ X[I] : O[I] ⊆ A[I] and O[I] ∈ τ[I]}.

Remark 3.1. Intn(A[I]) is the largest type-1 neutrosophic open set contained in A[I], so Intn(A[I]) ⊆ A[I].

Example 3.2. Consider the type-1 neutrosophic topological space in Example 2.2. Let A[I] = {1+I, 1+2I, 2+2I} and B[I] = {1+I, 1+2I, 2+I} be two type-1 neutrosophic subsets of X[I]. Then Intn(A[I]) = {1+I, 1+2I} ∪ {1+I} = {1+I, 1+2I}, and Intn(B[I]) = {1+I,1+2I} ∪ {1+I,2+I} ∪ {1+I} ∪ {1+I,1+2I,2+I} = {1+I, 1+2I, 2+I}.

Theorem 3.3. Let (X[I], τ[I]) be a type-1 neutrosophic topological space and A[I] ⊆ X[I]. Then Intn(A[I]) = A[I] if and only if A[I] is a type-1 neutrosophic open set.

Proof. If A[I] is a type-1 neutrosophic open set over X[I], then A[I] is itself a type-1 neutrosophic open set that contains A[I]; so A[I] is the largest type-1 neutrosophic open set contained in A[I], and Intn(A[I]) = A[I]. Conversely, if Intn(A[I]) = A[I], then Intn(A[I]) = A[I] ∈ τ[I]. □

Theorem 3.4. Let (X[I], τ[I]) be a type-1 neutrosophic topological space and A[I] ⊆ X[I]. Then x ∈ Intn(A[I]) if and only if there is a type-1 neutrosophic open set B[I] such that x ∈ B[I] ⊆ A[I].

Proof. Let x ∈ Intn(A[I]) and take B[I] = Intn(A[I]). Then by the definition of Intn(A[I]), B[I] is a type-1 neutrosophic open set and, by Remark 3.1, x ∈ B[I] ⊆ A[I]. Conversely, let B[I] be a type-1 neutrosophic open set such that x ∈ B[I] ⊆ A[I]. Then by the definition of Intn(A[I]), x ∈ B[I] ⊆ Intn(A[I]). □

Theorem 3.5. Let (X[I], τ[I]) be a type-1 neutrosophic topological space and A[I], B[I] ⊆ X[I]. Then the following axioms hold: (1) Intn(∅[I]) = ∅[I] and Intn(X[I]) = X[I]. (2) Intn(Intn(A[I])) = Intn(A[I]). (3) If A[I] ⊆ B[I] then Intn(A[I]) ⊆ Intn(B[I]). (4) Intn(A[I]) ∪ Intn(B[I]) ⊆ Intn(A[I] ∪ B[I]). (5) Intn(A[I] ∩ B[I]) = Intn(A[I]) ∩ Intn(B[I]).

Proof. (1) is obvious. (2) Let Intn(A[I]) = B[I]. Then Intn(B[I]) = B[I] by Theorem 3.3, and so Intn(Intn(A[I])) = Intn(A[I]). (3) Let x ∈ Intn(A[I]). Then by Theorem 3.4, there is a type-1 neutrosophic open set O[I] such that x ∈ O[I] ⊆ A[I]. Since A[I] ⊆ B[I], x ∈ O[I] ⊆ B[I], hence x ∈ Intn(B[I]); that is, Intn(A[I]) ⊆ Intn(B[I]). (4) Since A[I] ⊆ A[I] ∪ B[I] and B[I] ⊆ A[I] ∪ B[I], by part (3), Intn(A[I]) ⊆ Intn(A[I] ∪ B[I]) and Intn(B[I]) ⊆ Intn(A[I] ∪ B[I]); hence Intn(A[I]) ∪ Intn(B[I]) ⊆ Intn(A[I] ∪ B[I]). (5) Since A[I] ∩ B[I] ⊆ A[I] and A[I] ∩ B[I] ⊆ B[I], by part (3), Intn(A[I] ∩ B[I]) ⊆ Intn(A[I]) ∩ Intn(B[I]) … (i). Conversely, let x ∈ Intn(A[I]) ∩ Intn(B[I]); then there are two type-1 neutrosophic open sets M[I] and N[I] such that x ∈ M[I] ⊆ A[I] and x ∈ N[I] ⊆ B[I], so x ∈ (M[I] ∩ N[I]) ⊆ (A[I] ∩ B[I]), which implies x ∈ Intn(A[I] ∩ B[I]) by Theorem 3.4, giving Intn(A[I]) ∩ Intn(B[I]) ⊆ Intn(A[I] ∩ B[I]) … (ii). From (i) and (ii), we deduce that Intn(A[I] ∩ B[I]) = Intn(A[I]) ∩ Intn(B[I]). □

Example 3.6. Consider the type-1 neutrosophic topological space in Example 2.2. Let A[I] = {1+I,1+2I,2+2I} and B[I] = {1+I,1+2I,2+I} be two type-1 neutrosophic subsets of X[I]. Then Intn(A[I]) = {1+I,1+2I} and Intn(B[I]) = {1+I,1+2I,2+I}. Also, (A[I]∪B[I]) = X[I], while Intn(A[I]∪B[I]) = X[I]; therefore Intn(A[I]) ∪ Intn(B[I]) ⊆ Intn(A[I] ∪ B[I]).

3.2. Type-1 Neutrosophic Cluster Points

This subsection addresses the closure operator via X[I] sets and their properties.

Definition 3.7. Let (X[I], τ[I]) be a type-1 neutrosophic topological space and H[I] ⊆ X[I]. The closure operator of H[I] is denoted Cln(H[I]) and defined by Cln(H[I]) = ∩{B[I] ⊆ X[I] : H[I] ⊆ B[I] and B[I] is a type-1 neutrosophic closed set}.

Example 3.8. Consider the type-1 neutrosophic topological space in Example 2.2 and H[I] = {1+2I, 2+I} ⊆ X[I]. The type-1 neutrosophic closed sets are F = {∅[I], X[I], {2+2I}, {2+I,2+2I}, {1+2I,2+2I}, {1+2I,2+I,2+2I}}. Then Cln(H[I]) = X[I] ∩ {1+2I,2+I,2+2I} = {1+2I, 2+I, 2+2I}.

Remark 3.2. Cln(H[I]) is the smallest type-1 neutrosophic closed set containing H[I], therefore H[I] ⊆ Cln(H[I]). Consequently, for any H[I] ⊆ X[I], Intn(H[I]) ⊆ H[I] ⊆ Cln(H[I]), by Remarks 3.1 and 3.2, respectively.

Theorem 3.9. For a type-1 neutrosophic topological space (X[I], τ[I]) and H[I] ⊆ X[I], Cln(H[I]) = H[I] if and only if H[I] is a type-1 neutrosophic closed set.

Proof. Suppose H[I] is a type-1 neutrosophic closed set. Since H[I] ⊆ H[I], Cln(H[I]) is a type-1 neutrosophic closed set, and H[I] ⊆ Cln(H[I]); therefore Cln(H[I]) = H[I]. Conversely, if Cln(H[I]) = H[I], then Cln(H[I]) is a type-1 neutrosophic closed set, and consequently H[I] is a type-1 neutrosophic closed set. □

Theorem 3.10. For a type-1 neutrosophic topological space (X[I], τ[I]) and H[I] ⊆ X[I], x ∈ Cln(H[I]) if and only if, for every type-1 neutrosophic open set B[I] containing x, B[I] ∩ H[I] ≠ ∅[I].

Proof. Let x ∈ Cln(H[I]) and let B[I] be any type-1 neutrosophic open set containing x. If B[I] ∩ H[I] = ∅, then H[I] ⊆ X[I] − B[I]. Since X[I] − B[I] is a type-1 neutrosophic closed set containing H[I], we get Cln(H[I]) ⊆ X[I] − B[I], and so x ∈ X[I] − B[I], contradicting x ∈ B[I]. Therefore B[I] ∩ H[I] ≠ ∅[I]. Conversely, let x ∉ Cln(H[I]). Then X[I] − Cln(H[I]) is a type-1 neutrosophic open set containing x. By hypothesis, [X[I] − Cln(H[I])] ∩ H[I] ≠ ∅[I], contradicting [X[I] − Cln(H[I])] ⊆ [X[I] − H[I]]. □

Theorem 3.11. For a type-1 neutrosophic topological space (X[I], τ[I]) and H[I], B[I] ⊆ X[I], the following axioms hold: (1) Cln(∅[I]) = ∅[I] and Cln(X[I]) = X[I]. (2) Cln(Cln(H[I])) = Cln(H[I]). (3) If H[I] ⊆ B[I] then Cln(H[I]) ⊆ Cln(B[I]). (4) Cln(H[I]) ∪ Cln(B[I]) = Cln(H[I] ∪ B[I]). (5) Cln(H[I] ∩ B[I]) ⊆ Cln(H[I]) ∩ Cln(B[I]).

Proof. (1) is obvious. (2) Follows directly from Theorem 3.9. (3) Let x ∈ Cln(H[I]). Then by Theorem 3.10, for every type-1 neutrosophic open set A[I] containing x, A[I] ∩ H[I] ≠ ∅[I]. Since H[I] ⊆ B[I], A[I] ∩ B[I] ≠ ∅[I], hence x ∈ Cln(B[I]); that is, Cln(H[I]) ⊆ Cln(B[I]). (4) Since H[I] ⊆ H[I] ∪ B[I] and B[I] ⊆ H[I] ∪ B[I], by part (3), Cln(H[I]) ∪ Cln(B[I]) ⊆ Cln(H[I] ∪ B[I]). Since H[I] ⊆ Cln(H[I]) and B[I] ⊆ Cln(B[I]), H[I] ∪ B[I] ⊆ Cln(H[I]) ∪ Cln(B[I]), and since Cln(H[I]) ∪ Cln(B[I]) is the smallest type-1 neutrosophic closed set containing H[I] ∪ B[I], Cln(H[I] ∪ B[I]) ⊆ Cln(H[I]) ∪ Cln(B[I]); combining both inclusions gives Cln(H[I]) ∪ Cln(B[I]) = Cln(H[I] ∪ B[I]). (5) Since H[I] ∩ B[I] ⊆ H[I] and H[I] ∩ B[I] ⊆ B[I], by part (3), Cln(H[I] ∩ B[I]) ⊆ Cln(H[I]) ∩ Cln(B[I]). □

Example 3.12. Consider the type-1 neutrosophic topological space in Example 2.2. Let H[I] = {1+I} and B[I] = {2+I} be two type-1 neutrosophic subsets of X[I]. Then Cln(H[I]) = X[I] and Cln(B[I]) = {2+I, 2+2I}. Therefore (H[I] ∩ B[I]) = ∅ (since H[I] and B[I] are disjoint singletons), Cln(H[I] ∩ B[I]) = ∅[I], and Cln(H[I]) ∩ Cln(B[I]) = {2+I, 2+2I}; we deduce that Cln(H[I] ∩ B[I]) ⊆ Cln(H[I]) ∩ Cln(B[I]).

Theorem 3.13. For a type-1 neutrosophic topological space (X[I], τ[I]) and H[I] ⊆ X[I], the following hold: (1) Intn(X[I] − H[I]) = X[I] − Cln(H[I]). (2) Cln(X[I] − H[I]) = X[I] − Intn(H[I]).

Proof. (1) Since H[I] ⊆ Cln(H[I]), X[I] − Cln(H[I]) ⊆ X[I] − H[I]. Since Cln(H[I]) is a type-1 neutrosophic closed set, X[I] − Cln(H[I]) is a type-1 neutrosophic open set, so X[I] − Cln(H[I]) = Intn[X[I] − Cln(H[I])] ⊆ Intn(X[I] − H[I]). Conversely, let x ∈ Intn(X[I] − H[I]); then there is a type-1 neutrosophic open set A[I] such that x ∈ A[I] ⊆ X[I] − H[I]. Then X[I] − A[I] is a type-1 neutrosophic closed set containing H[I], and x ∉ X[I] − A[I]; hence x ∉ Cln(H[I]), that is, x ∈ X[I] − Cln(H[I]). (2) Since Intn(H[I]) ⊆ H[I], X[I] − H[I] ⊆ X[I] − Intn(H[I]). Since Intn(H[I]) is a type-1 neutrosophic open set, X[I] − Intn(H[I]) is a type-1 neutrosophic closed set, so Cln(X[I] − H[I]) ⊆ Cln[X[I] − Intn(H[I])] = X[I] − Intn(H[I]). On the other side, let x ∉ Cln(X[I]−H[I]); then by Theorem 3.10, there is a type-1 neutrosophic open set A[I] containing x such that A[I] ∩ (X[I]−H[I]) = ∅[I], so x ∈ A[I] ⊆ H[I], that is, x ∈ Intn(H[I]); hence x ∉ X[I] − Intn(H[I]). Therefore X[I] − Intn(H[I]) ⊆ Cln(X[I] − H[I]). □

Theorem 3.14. For a type-1 neutrosophic subset H[I] ⊆ X[I] of a type-1 neutrosophic topological space (X[I], τ[I]), the following holds: (1) If B[I] is a type-1 neutrosophic open set in X[I], then Cln(H[I]) ∩ B[I] ⊆ Cln(H[I] ∩ B[I]). (2) If B[I] is a type-1 neutrosophic closed set in X[I], then Intn(H[I] ∪ B[I]) ⊆ Intn(H[I]) ∪ B[I].

Proof. (1) Let x ∈ Cln(H[I]) ∩ B[I], so x ∈ Cln(H[I]) and x ∈ B[I]. Let C[I] be any type-1 neutrosophic open set containing x. Then C[I] ∩ B[I] is a type-1 neutrosophic open set containing x. Since x ∈ Cln(H[I]), (C[I] ∩ B[I]) ∩ H[I] ≠ ∅, so C[I] ∩ (B[I] ∩ H[I]) ≠ ∅[I], which implies x ∈ Cln(H[I] ∩ B[I]). That is, Cln(H[I]) ∩ B[I] ⊆ Cln(H[I] ∩ B[I]). (2) Since B[I] is a type-1 neutrosophic closed set in X[I], by part (1) and Theorem 3.13, X[I] − [Intn(H[I]) ∪ B[I]] = [X[I]−Intn(H[I])] ∩ [X[I]−B[I]] = [Cln(X[I]−H[I])] ∩ [X[I]−B[I]] ⊆ Cln[(X[I]−H[I]) ∩ (X[I]−B[I])] = Cln(X[I]−(H[I]∪B[I])) = X[I] − (Intn(H[I]∪B[I])). Hence Intn(H[I] ∪ B[I]) ⊆ Intn(H[I]) ∪ B[I]. □

Theorem 3.15. Let (X[I], τ[I]) be a type-1 neutrosophic topological space and H[I], B[I] ⊆ X[I]. Then: (1) Intn($H[I]^c$) = $(Cln(H[I]))^c$. (2) Cln($H[I]^c$) = $(Intn(H[I]))^c$.

Proof. (1) Cln(H[I]) = ∩{B[I] ⊆ X[I] : H[I] ⊆ B[I] and B[I] is a type-1 neutrosophic closed set}. Therefore $(Cln(H[I]))^c$ = ∪{$B[I]^c$ ⊆ X[I] : $B[I]^c$ ⊆ $H[I]^c$ and B[I] is a type-1 neutrosophic closed set}. The right-hand side of this equality is Intn($H[I]^c$), thus Intn($H[I]^c$) = $(Cln(H[I]))^c$. (2) Substituting $H[I]^c$ for H[I] in part (1) gives Cln($H[I]^c$)^c = (Intn($H[I]^c$))^c = Intn(H[I]), so Cln($H[I]^c$) = $(Intn(H[I]))^c$. □

3.3. Type-1 Neutrosophic Exterior and Boundary Points

This subsection studies the exterior and boundary operators via X[I] sets and their properties.

Definition 3.16. Let (X[I], τ[I]) be a type-1 neutrosophic topological space and H[I] ⊆ X[I]. The exterior of H[I] over X[I] is denoted Extn(H[I]) and defined as Extn(H[I]) = Intn($H[I]^c$).

Example 3.17. Consider the type-1 neutrosophic topological space in Example 2.2. Let H[I] = {1+I, 1+2I, 2+2I}, so $H[I]^c$ = {2+I}, and Intn($H[I]^c$) = ∅[I] (since {2+I} ∉ τ[I] and contains no nonempty open subset). Then Extn(H[I]) = Intn($H[I]^c$) = ∅[I].

Theorem 3.18. Let (X[I], τ[I]) be a type-1 neutrosophic topological space and A[I], B[I] ⊆ X[I]. Then: (1) Extn(A[I] ∪ B[I]) = Extn(A[I]) ∩ Extn(B[I]). (2) Extn(A[I]) ∪ Extn(B[I]) ⊆ Extn(A[I] ∩ B[I]).

Proof. By Definition 3.16 and Theorem 3.5, part (2): (1) Extn(A[I]∪B[I]) = Intn($(A[I]∪B[I])^c$) = Intn($A[I]^c$ ∩ $B[I]^c$) = Intn($A[I]^c$) ∩ Intn($B[I]^c$) = Extn(A[I]) ∩ Extn(B[I]). (2) The proof is similar to (1). □

Definition 3.19. Let (X[I], τ[I]) be a type-1 neutrosophic topological space and B[I] ⊆ X[I]. The type-1 neutrosophic boundary of B[I] over X[I] is denoted Γn(B[I]) and defined by Γn(B[I]) = Cln(B[I]) ∩ Cln($B[I]^c$). It is noted that Γn(B[I]) = Γn($B[I]^c$).

Example 3.20. Consider the type-1 neutrosophic topological space in Example 2.2. If H[I] = {1+2I, 2+I}, then $H[I]^c$ = {1+I, 2+2I}, Cln(H[I]) = {1+2I, 2+I, 2+2I}, and Cln($H[I]^c$) = X[I]. Therefore Γn(H[I]) = Cln(H[I]) ∩ Cln($H[I]^c$) = {1+2I, 2+I, 2+2I}.

Theorem 3.21. Let (X[I], τ[I]) be a type-1 neutrosophic topological space and A[I] ⊆ X[I]. Then $(Γn(A[I]))^c$ = Extn(A[I]) ∪ Intn(A[I]).

Proof. Since $Intn(A[I]^c) = (Cln(A[I]))^c$ by Theorem 3.15, $(\Gamma n(A[I]))^c = (Cln(A[I]) \cap Cln(A[I]^c))^c = (Cln(A[I]))^c \cup (Cln(A[I]^c))^c = (Cln(A[I]))^c \cup Intn(A[I]) = Extn(A[I]) \cup Intn(A[I])$. □

Theorem 3.22. For a type-1 neutrosophic topological space (X[I], τ[I]) and $H[I] \subseteq X[I]$, $\Gamma n(Intn(H[I])) \subseteq \Gamma n(H[I])$.

Proof. Since $Intn(H[I]) \subseteq H[I]$, we have $\Gamma n(Intn(H[I])) = Cln(Intn(H[I])) \cap Cln(Intn(H[I])^c) \subseteq Cln(H[I]) \cap Cln(H[I]^c) = \Gamma n(H[I])$. □

Theorem 3.23. For a subset $H[I] \subseteq X[I]$ of a type-1 neutrosophic topological space (X[I], τ[I]), the following holds: (1) $Cln(H[I]) = \Gamma n(H[I]) \cup Intn(H[I])$. (2) $\Gamma n(H[I]) \cap Intn(H[I]) = \emptyset[I]$. (3) $\Gamma n(H[I]) = Cln(H[I]) \cap Cln(X[I] - H[I])$.

Proof. (1) $\Gamma n(H[I]) \cup Intn(H[I]) = (Cln(H[I]) - Intn(H[I])) \cup Intn(H[I]) = [Cln(H[I]) \cap (X[I]-Intn(H[I]))] \cup Intn(H[I]) = [Cln(H[I]) \cup Intn(H[I])] \cap [(X[I]-Intn(H[I])) \cup Intn(H[I])] = Cln(H[I]) \cap X[I] = Cln(H[I])$. (2) This is clear from the definition of $\Gamma n(H[I])$. (3) By the definition, $\Gamma(H[I]) = Cln(H[I]) - Intn(H[I]) = Cln(H[I]) \cap (X[I]-Intn(H[I])) = Cln(H[I]) \cap Cln(X[I]-H[I])$, as required. □

Corollary 3.24. For a type-1 neutrosophic subset $H[I] \subseteq X[I]$ of a type-1 neutrosophic topological space (X[I], τ[I]), Γn(H[I]) is a type-1 neutrosophic closed set in (X[I], τ[I]).

Proof. By Theorems 3.11 and 3.23. □

Theorem 3.25. For a subset $H[I] \subseteq X[I]$ of a type-1 neutrosophic topological space (X[I], τ[I]), the following holds: (1) H[I] is a type-1 neutrosophic open set if and only if $\Gamma n(H[I]) \cap H[I] = \emptyset[I]$. (2) H[I] is a type-1 neutrosophic closed set if and only if $\Gamma n(H[I]) \subseteq H[I]$. (3) H[I] is both a type-1 neutrosophic open set and closed set if and only if $\Gamma n(H[I]) = \emptyset[I]$.

Proof. (1) Let H[I] be a type-1 neutrosophic open set. Then Intn(H[I]) = H[I], and by Theorem 3.23, $\Gamma n(H[I]) \cap H[I] = \Gamma n(H[I]) \cap Intn(H[I]) = \emptyset[I]$. Conversely, suppose $\Gamma n(H[I]) \cap H[I] = \emptyset[I]$. Then $H[I] - Intn(H[I]) = [H[I] \cap Cln(H[I])] - [H[I] \cap Intn(H[I])] = H[I] \cap (Cln(H[I]) - Intn(H[I])) = H[I] \cap \Gamma n(H[I]) = \emptyset[I]$, so Intn(H[I]) = H[I]; hence H[I] is a type-1 neutrosophic open set. (2) Let H[I] be a type-1 neutrosophic closed set. Then Cln(H[I]) = H[I], so $\Gamma n(H[I]) = Cln(H[I]) - Intn(H[I]) = H[I] - Intn(H[I]) \subseteq H[I]$. Conversely, if $\Gamma n(H[I]) \subseteq H[I]$, then by Theorem 3.23, $Cln(H[I]) = Intn(H[I]) \cup \Gamma n(H[I]) \subseteq Intn(H[I]) \cup H[I] \subseteq H[I]$, so Cln(H[I]) = H[I]; hence H[I] is a type-1 neutrosophic closed set. (3) Let H[I] be both closed and open. Then Cln(H[I]) = H[I] = Intn(H[I]), so $\Gamma n(H[I]) = Cln(H[I]) - Intn(H[I]) = H[I] - H[I] = \emptyset[I]$. Conversely, if $\Gamma n(H[I]) = \emptyset[I]$, then $Cln(H[I]) - Intn(H[I]) = \emptyset[I]$. Since $Intn(H[I]) \subseteq Cln(H[I])$, we have Cln(H[I]) = Intn(H[I]); since $Intn(H[I]) \subseteq H[I] \subseteq Cln(H[I])$, we have Cln(H[I]) = H[I] = Intn(H[I]). Hence H[I] is both a type-1 neutrosophic closed set and a type-1 neutrosophic open set. □

Definition 3.26. For a type-1 neutrosophic topological space (X[I], τ[I]) and $Y[I] \subseteq X[I]$, the relativized type-1 neutrosophic topology of τ[I] on Y[I] is denoted τY[I] and defined by $\tau Y[I] = \{H[I] \cap Y[I] : H[I]$ is a type-1 neutrosophic open set in $X[I]\}$. The pair (Y[I], τY[I]) is called a type-1 neutrosophic topological subspace of (X[I], τ[I]).

Example 3.27. Let X = {1, 2, 3}, Y = {1, 2} ⊂ X, X[I] = {1+1I, 1+2I, 1+3I, 2+1I, 2+2I, 2+3I, 3+1I, 3+2I, 3+3I}, and Y[I] = {1+1I, 1+2I, 2+1I, 2+2I}. Let τ[I] = {∅[I], X[I], {1+1I}, {1+3I}, {1+1I,1+3I}} be a type-1 neutrosophic topology on X[I]. Then τY[I] = {∅[I], Y[I], {1+1I}∩Y[I], {1+3I}∩Y[I], {1+1I,1+3I}∩Y[I]}, so τY[I] = {∅[I], Y[I], {1+1I}} is a type-1 neutrosophic relative topology on Y[I].

4. Separation Axioms

Definition 4.1. A type-1 neutrosophic topological space is called:

(1) T0[I] type-1 neutrosophic space if, for two points $x \neq y \in X[I]$, there is a type-1 neutrosophic open set G[I] in X[I] such that $x \in G[I]$ and $y \notin G[I]$.

(2) T1[I] type-1 neutrosophic space if, for two points $x \neq y \in X[I]$, there are two type-1 neutrosophic open sets G[I] and U[I] in X[I] such that $x \in G[I]$, $y \notin G[I]$, $y \in U[I]$, and $x \notin U[I]$.

(3) T2[I] type-1 neutrosophic space, or type-1 neutrosophic Hausdorff space, if, for two points $x \neq y \in X[I]$, there are two type-1 neutrosophic open sets G[I] and U[I] in X[I] such that $x \in G[I]$, $y \in U[I]$, and $U[I] \cap G[I] = \emptyset[I]$.

(4) Regular type-1 neutrosophic space if, for each type-1 neutrosophic closed set F[I] in (X[I], τ[I]) and each x ∉ F[I], there are two type-1 neutrosophic open sets G[I] and U[I] in (X[I], τ[I]) such that F[I] ⊆ G[I], x ∈ U[I], and U[I] ∩ G[I] = ∅[I].

(5) A type-1 neutrosophic topological space (X, τ[I]) is called type-1 neutrosophic T3[I] space if it is a regular type-1 neutrosophic space and a T1[I] type-1 neutrosophic space.

(6) Normal type-1 neutrosophic space if, for each two disjoint type-1 neutrosophic closed sets F[I] and M[I] in (X, τ[I]), there are two type-1 neutrosophic open sets G[I] and U[I] in (X[I], τ[I]) such that F[I] ⊆ G[I], M[I] ⊆ U[I], and U[I] ∩ G[I] = ∅[I]. A type-1 neutrosophic topological space (X[I], τ[I]) is called T4[I] type-1 neutrosophic space if it is a normal type-1 neutrosophic space and a T1[I] type-1 neutrosophic space.

Theorem 4.2. Let (X[I], τ[I]) be a T1[I] type-1 neutrosophic space and x a type-1 neutrosophic element. Then {x} is a type-1 neutrosophic closed set.

Proof. We show that $\{x\}^c$ is a type-1 neutrosophic open set. Let y be a type-1 neutrosophic element with y ∈ (X[I] − x), so x ≠ y. By the definition of T1[I], for the two distinct elements x and y, there exists a type-1 neutrosophic open set U[I]y such that y ∈ U[I]y and x ∉ U[I]y. Since x ∉ U[I]y, U[I]y lies entirely within the complement of x, so U[I]y ⊆ (X[I]−x). Hence (X[I]−x) = ∪{U[I]y : x ≠ y}. Since (X[I]−x) is a type-1 neutrosophic open set, {x} is a type-1 neutrosophic closed set. □

Theorem 4.3. Every T3[I] type-1 neutrosophic space is a T2[I] type-1 neutrosophic space.

Proof. Let (X[I], τ[I]) be a T3[I] type-1 neutrosophic space and x ≠ y ∈ X[I] be any points. Since (X[I], τ[I]) is a T1[I] type-1 neutrosophic space, by Theorem 4.2, {x} is a type-1 neutrosophic closed set and y ∉ {x}. Since (X[I], τ[I]) is a regular type-1 neutrosophic space, there are two type-1 neutrosophic open sets G[I] and U[I] in (X[I], τ[I]) such that x ∈ {x} ⊆ G[I], y ∈ U[I], and U[I] ∩ G[I] = ∅[I]. Hence (X[I], τ[I]) is a T2[I] type-1 neutrosophic space. □

Theorem 4.4. Every T4[I] type-1 neutrosophic space is a T3[I] type-1 neutrosophic space.

Proof. Let (X[I], τ[I]) be a T4[I] type-1 neutrosophic space. Let F[I] be any type-1 neutrosophic closed set in (X[I], τ[I]) and x ∉ F[I] be any point in (X[I], τ[I]). Since (X[I], τ[I]) is a T1[I] type-1 neutrosophic space, by Theorem 4.2, {x} is a type-1 neutrosophic closed set in (X[I], τ[I]) and F[I] ∩ {x} = ∅[I]. Since (X[I], τ[I]) is a normal type-1 neutrosophic space, there are two type-1 neutrosophic open sets G[I] and U[I] in (X[I], τ[I]) such that x ∈ {x} ⊆ G[I], F[I] ⊆ U[I], and U[I] ∩ G[I] = ∅[I]. Hence (X[I], τ[I]) is a T3[I] type-1 neutrosophic space. □

Theorem 4.5. A type-1 neutrosophic topological space (X[I], τ[I]) is a T0[I] type-1 neutrosophic space if and only if, for two points x ≠ y ∈ X[I], Cln({x}) ≠ Cln({y}).

Proof. Suppose (X[I], τ[I]) is a T0[I] type-1 neutrosophic space. Then for two points x ≠ y, there is a type-1 neutrosophic open set G[I] such that x ∈ G[I], y ∉ G[I]. Since X[I]−G[I] is a type-1 neutrosophic closed set and y ∈ X[I]−G[I], Cln({y}) ⊆ Cln(X[I]−G[I]) = X[I]−G[I]. Since x ∈ Cln({x}) and x ∉ X[I]−G[I], x ∉ Cln({y}); that is, Cln({x}) ≠ Cln({y}). Conversely, let x ≠ y ∈ X[I]. By hypothesis, Cln({x}) ≠ Cln({y}), so there is some point z ∈ Cln({x}) with z ∉ Cln({y}). If x ∈ Cln({y}), then z ∈ Cln({x}) ⊆ Cln({y}), a contradiction; hence x ∉ Cln({y}). Thus G[I] = X[I]−Cln({y}) is a type-1 neutrosophic open set in (X[I], τ[I]) such that x ∈ G[I] and y ∉ G[I]. Therefore (X[I], τ[I]) is a T0[I] type-1 neutrosophic space. □

Theorem 4.6. A type-1 neutrosophic topological space (X[I], τ[I]) is a T1[I] type-1 neutrosophic space if and only if {x} is a type-1 neutrosophic closed set in (X[I], τ[I]) for all x ∈ X[I].

Proof. Suppose (X[I], τ[I]) is a T1[I] type-1 neutrosophic space. Let x ∈ X[I]; we show X[I]−{x} is a type-1 neutrosophic open set. Let y ∈ X[I]−{x}, so x ≠ y. Since (X[I], τ[I]) is T1[I], there are type-1 neutrosophic open sets G[I] and U[I] such that x ∈ G[I], y ∉ G[I], y ∈ U[I], and x ∉ U[I]. Then y ∈ U[I] ⊆ X[I]−{x}. Hence X[I]−{x} is a type-1 neutrosophic open set, so {x} is a type-1 neutrosophic closed set. Conversely, let x ≠ y ∈ X[I]. By hypothesis, {x} and {y} are type-1 neutrosophic closed sets, so X[I]−{x} and X[I]−{y} are type-1 neutrosophic open sets, with x ∈ X[I]−{y}, y ∉ X[I]−{y}, x ∉ X[I]−{x}, and y ∈ X[I]−{x}. Therefore (X[I], τ[I]) is a T1[I] type-1 neutrosophic space. □

Theorem 4.7. A type-1 neutrosophic topological space (X[I], τ[I]) is a T2[I] type-1 neutrosophic space if and only if, for each x ∈ X[I] and each y ≠ x ∈ X[I], there is a type-1 neutrosophic open set H[I] in (X[I], τ[I]) containing x such that y ∉ Cln(H[I]).

Proof. Suppose (X[I], τ[I]) is T2[I]. Let x ∈ X[I] and y ≠ x. There are two type-1 neutrosophic open sets G[I] and U[I] such that x ∈ G[I], y ∈ U[I], and U[I] ∩ G[I] = ∅[I]. Take H[I] = G[I]; then H[I] is a type-1 neutrosophic open set containing x, and y ∉ H[I] ⊆ Cln(H[I]) (since U[I] is disjoint from H[I] and, being a neighborhood of y, excludes y from Cln(H[I])). Conversely, let x ≠ y ∈ X[I]. By hypothesis, there is a type-1 neutrosophic open set H[I] containing x such that y ∉ Cln(H[I]). Then X[I]−Cln(H[I]) is a type-1 neutrosophic open set containing y, with x ∈ H[I], y ∈ X[I]−Cln(H[I]), and H[I] ∩ (X[I]−Cln(H[I])) = ∅[I]. Hence (X[I], τ[I]) is T2[I]. □

Theorem 4.8. A type-1 neutrosophic topological space (X[I], τ[I]) is a regular type-1 neutrosophic space if and only if, for each x ∈ X[I] and each type-1 neutrosophic open set M[I] in (X[I], τ[I]) containing x, there is a type-1 neutrosophic open set H[I] in (X[I], τ[I]) containing x such that Cln(H[I]) ⊆ M[I].

Proof. Suppose (X[I], τ[I]) is regular. Let x ∈ X[I] and M[I] be a type-1 neutrosophic open set containing x. Then X[I]−M[I] is a type-1 neutrosophic closed set with x ∉ X[I]−M[I]. By regularity, there are type-1 neutrosophic open sets G[I] and U[I] such that (X[I]−M[I]) ⊆ G[I], x ∈ U[I], and U[I] ∩ G[I] = ∅[I]. Take H[I] = U[I]; then H[I] ⊆ (X[I]−G[I]), so Cln(H[I]) ⊆ Cln(X[I]−G[I]) ⊆ (X[I]−G[I]) ⊆ M[I]. Conversely, let F[I] be a type-1 neutrosophic closed set and x ∉ F[I]. Then x ∈ X[I]−F[I], a type-1 neutrosophic open set containing x. By hypothesis, there is a type-1 neutrosophic open set H[I] containing x with Cln(H[I]) ⊆ (X[I]−F[I]). Then F[I] ⊆ [X[I]−Cln(H[I])], and X[I]−Cln(H[I]) is a type-1 neutrosophic open set with H[I] ∩ [X[I]−Cln(H[I])] = ∅[I]; hence (X[I], τ[I]) is regular. □

Theorem 4.9. A type-1 neutrosophic topological space (X[I], τ[I]) is a normal type-1 neutrosophic space if and only if, for each type-1 neutrosophic closed set F[I] in (X[I], τ[I]) and each type-1 neutrosophic open set G[I] containing F[I], there is a type-1 neutrosophic open set V[I] in (X[I], τ[I]) containing F[I] such that Cln(V[I]) ⊆ G[I].

Proof. Suppose (X[I], τ[I]) is normal. Let F[I] be a type-1 neutrosophic closed set and G[I] a type-1 neutrosophic open set containing F[I]. Then X[I]−G[I] is a type-1 neutrosophic closed set with F[I] ∩ (X[I]−G[I]) = ∅[I]. By normality, there are type-1 neutrosophic open sets H[I] and U[I] such that (X[I]−G[I]) ⊆ U[I], F[I] ⊆ H[I], and U[I] ∩ H[I] = ∅[I]. Take V[I] = H[I]; then V[I] ⊆ (X[I]−U[I]), so Cln(V[I]) ⊆ Cln(X[I]−U[I]) ⊆ (X[I]−U[I]) ⊆ G[I]. Conversely, let F[I] and H[I] be disjoint type-1 neutrosophic closed sets. Then H[I] ⊆ (X[I]−F[I]), a type-1 neutrosophic open set containing H[I]. By hypothesis, there is a type-1 neutrosophic open set V[I] containing H[I] such that Cln(V[I]) ⊆ (X[I]−F[I]). Then F[I] ⊆ X[I]−Cln(V[I]), and X[I]−Cln(V[I]) is type-1 neutrosophic open, with V[I] ∩ [X[I]−Cln(V[I])] = ∅[I]; hence (X[I], τ[I]) is normal. □

5. Continuous Type-1 Neutrosophic Functions

Definition 5.1. A type-1 neutrosophic function fn : (X[I], τ[I]) → (Y[I], τ1[I]) between two type-1 neutrosophic topological spaces is called continuous if fn^{-1}(U[I]) is a type-1 neutrosophic open set in (X[I], τ[I]) for every type-1 neutrosophic open set U[I] in Y[I].

Example 5.2. Let X = {a, b} and Y = {1, 2, 3} be two classical sets with a classical function fc : X → Y such that fc(a) = 1 and fc(b) = 2. The type-1 neutrosophic sets generated by X and Y are X[I] = {a+aI, a+bI, b+aI, b+bI} and Y[I] = {1+1I,1+2I,1+3I,2+1I,2+2I,2+3I,3+1I,3+2I,3+3I}. The type-1 neutrosophic function fn is given by fn(a+aI) = fc(a)+fc(a)fn(I) = 1+1I, fn(a+bI) = fc(a)+fc(b)fn(I) = 1+2I, fn(b+aI) = fc(b)+fc(a)fn(I) = 2+1I, and fn(b+bI) = fc(b)+fc(b)fn(I) = 2+2I. Let fn : (X[I],τ[I]) → (Y[I],τ1[I]) with τ[I] = {∅[I],X[I],{a+aI},{a+bI},{a+bI,a+aI}} and τ1[I] = {∅[I],Y[I],{1+1I},{1+2I},{1+1I,1+2I}}. This type-1 neutrosophic function is continuous, since for every type-1 neutrosophic open set in (Y[I],τ1[I]) we have fn^{-1}({1+1I}) = {a+aI}, fn^{-1}({1+2I}) = {a+bI}, fn^{-1}({1+1I,1+2I}) = {a+bI,a+aI}, fn^{-1}(Y[I]) = X[I], and fn^{-1}(∅[I]) = ∅[I].

Theorem 5.3. A type-1 neutrosophic function fn : (X[I],τ[I]) → (Y[I],τ1[I]) between two type-1 neutrosophic topological spaces is continuous if and only if fn^{-1}(F[I]) is a type-1 neutrosophic closed set in (X[I], τ[I]) for every type-1 neutrosophic closed set F[I] in Y[I].

Proof. Let fn be continuous and F[I] be a type-1 neutrosophic closed set in Y[I]. Then fn^{-1}(Y[I]−F[I]) = X[I]−fn^{-1}(F[I]) is a type-1 neutrosophic open set in (X[I],τ[I]), so fn^{-1}(F[I]) is a type-1 neutrosophic closed set. Conversely, suppose $fn^{-1}(F[I])$ is a type-1 neutrosophic closed set for every type-1 neutrosophic closed set F[I] in Y[I]. Let U[I] be any type-1 neutrosophic open set in Y[I]. Then $fn^{-1}(Y[I]-U[I]) = X[I]-fn^{-1}(U[I])$ is a type-1 neutrosophic closed set in $(X[I],\tau[I])$, that is, $fn^{-1}(U[I])$ is a type-1 neutrosophic open set. Hence fn is continuous. □

Theorem 5.4. A type-1 neutrosophic function fn : $(X[I],\tau[I]) \rightarrow (Y[I],\tau1[I])$ is continuous if and only if, for each $x \in X[I]$ and each type-1 neutrosophic open set U[I] in Y[I] with $fn(x) \in U[I]$, there exists a type-1 neutrosophic open set V[I] in $(X[I],\tau[I])$ such that $x \in V[I]$ and $fn(V[I]) \subseteq U[I]$.

Proof. Suppose fn is continuous. Let $x \in X[I]$ and U[I] be a type-1 neutrosophic open set containing fn(x). Put $V[I] = fn^{-1}(U[I])$; since fn is continuous, V[I] is type-1 neutrosophic open, $x \in V[I]$, and $fn(V[I]) \subseteq U[I]$. Conversely, let U[I] be a type-1 neutrosophic open set in Y[I] and $x \in fn^{-1}(U[I])$. Then $fn(x) \in U[I]$, and by hypothesis there is a type-1 neutrosophic open set V[I] with $x \in V[I]$ and $fn(V[I]) \subseteq U[I]$. Hence $x \in V[I] \subseteq fn^{-1}(U[I])$, so $fn^{-1}(U[I])$ is type-1 neutrosophic open, and fn is continuous. □

Theorem 5.5. A type-1 neutrosophic function fn : $(X[I],\tau[I]) \rightarrow (Y[I],\tau1[I])$ is continuous if and only if $fn[Cln(A[I])] \subseteq Cln[fn(A[I])]$ for all $A[I] \subseteq X[I]$.

Proof. Let fn be continuous and $A[I] \subseteq X[I]$. Then $Cln[fn(A[I])]$ is type-1 neutrosophic closed in Y[I], so by Theorem 5.3, $fn^{-1}[Cln(fn(A[I]))]$ is type-1 neutrosophic closed in $(X[I],\tau[I])$, that is, $Cln[fn^{-1}[Cln[fn(A[I])]]] = fn^{-1}[Cln[fn(A[I])]]$. Since $fn(A[I]) \subseteq Cln[fn(A[I])]$, $A[I] \subseteq fn^{-1}[Cln[fn(A[I])]]$, so $Cln(A[I]) \subseteq Cln[fn^{-1}[Cln[fn(A[I])]]] = fn^{-1}[Cln[fn(A[I])]]$. Hence $fn[Cln(A[I])] \subseteq Cln[fn(A[I])]$. Conversely, let H[I] be a type-1 neutrosophic closed set in Y[I], i.e., $Cln(H[I]) = H[I]$. Since $fn^{-1}(H[I]) \subseteq X[I]$, by hypothesis $fn[Cln[fn^{-1}(H[I])]] \subseteq Cln[fn(fn^{-1}(H[I]))] \subseteq Cln(H[I]) = H[I]$, so $Cln[fn^{-1}(H[I])] \subseteq fn^{-1}(H[I])$; hence $Cln[fn^{-1}(H[I])] = fn^{-1}(H[I])$, that is, $fn^{-1}(H[I])$ is type-1 neutrosophic closed, and fn is continuous. □

Theorem 5.6. A type-1 neutrosophic function fn : $(X[I],\tau[I]) \rightarrow (Y[I],\tau1[I])$ is continuous if and only if $Cln[fn^{-1}(B[I])] \subseteq fn^{-1}[Cln(B[I])]$ for all $B[I] \subseteq Y[I]$.

Proof. Let fn be continuous and $B[I] \subseteq Y[I]$. Then Cln(B[I]) is type-1 neutrosophic closed in Y[I], so by Theorem 5.3, $fn^{-1}[Cln(B[I])]$ is type-1 neutrosophic closed, i.e., $Cln[fn^{-1}[Cln(B[I])]] = fn^{-1}[Cln(B[I])]$. Since $B[I] \subseteq Cln(B[I])$, $fn^{-1}(B[I]) \subseteq fn^{-1}[Cln(B[I])]$, so $Cln[fn^{-1}(B[I])] \subseteq Cln[fn^{-1}[Cln(B[I])]] = fn^{-1}[Cln(B[I])]$. Conversely, let H[I] be type-1 neutrosophic closed in Y[I], i.e., $Cln(H[I]) = H[I]$. Since $H[I] \subseteq Y[I]$, by hypothesis $Cln[fn^{-1}(H[I])] \subseteq fn^{-1}[Cln(H[I])] = fn^{-1}(H[I])$; hence $Cln[fn^{-1}(H[I])] = fn^{-1}(H[I])$, that is, $fn^{-1}(H[I])$ is type-1 neutrosophic closed, and fn is continuous. □

Theorem 5.7. A type-1 neutrosophic function fn : $(X[I],\tau[I]) \rightarrow (Y[I],\tau1[I])$ is continuous if and only if $fn^{-1}(Intn(B[I])) \subseteq Intn[fn^{-1}(B[I])]$ for all $B[I] \subseteq Y[I]$.

Proof. Let fn be continuous and $B[I] \subseteq Y[I]$. Then Intn(B[I]) is type-1 neutrosophic open in Y[I], so $fn^{-1}(Intn(B[I]))$ is type-1 neutrosophic open in $(X[I],\tau[I])$, i.e., $Intn[fn^{-1}[Intn(B[I])]] = fn^{-1}[Intn(B[I])]$. Since $Intn(B[I]) \subseteq B[I]$, $fn^{-1}[Intn(B[I])] \subseteq fn^{-1}(B[I])$, so $fn^{-1}[Intn(B[I])] \subseteq Intn[fn^{-1}(B[I])]$. Conversely, let U[I] be type-1 neutrosophic open in Y[I], i.e., $Intn(U[I]) = U[I]$. Since $U[I] \subseteq Y[I]$, by hypothesis $fn^{-1}(U[I]) = fn^{-1}[Intn(U[I])] \subseteq Intn[fn^{-1}(U[I])]$, so $fn^{-1}(U[I]) = Intn[fn^{-1}(U[I])]$, that is, $fn^{-1}(U[I])$ is type-1 neutrosophic open, and fn is continuous. □

Definition 5.8. A type-1 neutrosophic function fn : $(X[I],\tau[I]) \rightarrow (Y[I],\tau1[I])$ is called a type-1 neutrosophic closed function if fn(G[I]) is a type-1 neutrosophic closed set in $(Y[I],\tau1[I])$ for every type-1 neutrosophic closed set G[I] in $(X[I],\tau[I])$.

Theorem 5.9. A type-1 neutrosophic function fn : $(X[I],\tau[I]) \rightarrow (Y[I],\tau1[I])$ is a type-1 neutrosophic closed function if and only if $Cln[fn(A[I])] \subseteq fn[Cln(A[I])]$ for all $A[I] \subseteq X[I]$.

Proof. Suppose fn is a type-1 neutrosophic closed function and $A[I] \subseteq X[I]$. Since Cln(A[I]) is type-1 neutrosophic closed in $(X[I],\tau[I])$ and fn is closed, $fn[Cln(A[I])]$ is type-1 neutrosophic closed in Y[I], i.e., $Cln[fn[Cln(A[I])]] = fn[Cln(A[I])]$. Since $A[I] \subseteq Cln(A[I])$, $fn(A[I]) \subseteq fn[Cln(A[I])]$, so $Cln[fn(A[I])] \subseteq Cln[fn[Cln(A[I])]] = fn[Cln(A[I])]$. Conversely, let F[I] be type-1 neutrosophic closed in $(X[I],\tau[I])$, i.e., $Cln(F[I]) = F[I]$. By hypothesis $Cln[fn(F[I])] \subseteq fn[Cln(F[I])] = fn(F[I])$, so $Cln[fn(F[I])] = fn(F[I])$, that is, fn(F[I]) is type-1 neutrosophic closed in Y[I]. Hence fn is a type-1 neutrosophic closed function. □

Definition 5.10. A type-1 neutrosophic function fn : (X[I],τ[I]) → (Y[I],τ1[I]) is called a type-1 neutrosophic open function if fn(G[I]) is a type-1 neutrosophic open set in (Y[I],τ1[I]) for every type-1 neutrosophic open set G[I] in (X[I],τ[I]).

Theorem 5.11. A type-1 neutrosophic function fn : (X[I],τ[I]) → (Y[I],τ1[I]) is a type-1 neutrosophic open function if and only if fn[Intn(A[I])] ⊆ Intn[fn(A[I])] for all A[I] ⊆ X[I].

Proof. Suppose fn is a type-1 neutrosophic open function and A[I] ⊆ X[I]. Since Intn(A[I]) is type-1 neutrosophic open in (X[I],τ[I]) and fn is open, fn[Intn(A[I])] is type-1 neutrosophic open in Y[I], i.e., Intn[fn[Intn(A[I])]] = fn[Intn(A[I])]. Since Intn(A[I]) ⊆ A[I], fn[Intn(A[I])] ⊆ fn(A[I]), so Intn[fn[Intn(A[I])]] ⊆ Intn[fn(A[I])] = fn[Intn(A[I])]. Hence fn[Intn(A[I])] ⊆ Intn[fn(A[I])]. Conversely, let F[I] be type-1 neutrosophic open in (X[I],τ[I]), i.e., Intn(F[I]) = F[I]. By hypothesis fn[Intn(F[I])] ⊆ Intn[fn(F[I])] = fn(F[I]), so fn(F[I]) ⊆ Intn[fn(F[I])], hence Intn[fn(F[I])] = fn(F[I]), that is, fn(F[I]) is type-1 neutrosophic open in Y[I]. Hence fn is a type-1 neutrosophic open function. □

6. Contra Type-1 Neutrosophic Functions

Definition 6.1. A type-1 neutrosophic function fn : (X[I],τ[I]) → (Y[I],τ1[I]) is called a contra continuous type-1 neutrosophic function if fn^{-1}(V[I]) is a type-1 neutrosophic closed set in (X[I],τ[I]) for every type-1 neutrosophic open set V[I] in Y[I].

Theorem 6.2. A type-1 neutrosophic function fn : (X[I],τ[I]) → (Y[I],τ1[I]) is contra continuous if and only if fn^{-1}(F[I]) is a type-1 neutrosophic open set in (X[I],τ[I]) for every type-1 neutrosophic closed set F[I] in Y[I].

Proof. Suppose fn is contra continuous. Let G[I] be a type-1 neutrosophic closed set in Y[I]. Then Y[I]−G[I] is type-1 neutrosophic open, so X[I]−fn^{-1}(G[I]) = fn^{-1}(Y[I]−G[I]) is type-1 neutrosophic closed in (X[I],τ[I]), that is, fn^{-1}(G[I]) is type-1 neutrosophic open. Conversely, let G[I] be type-1 neutrosophic open in Y[I]. Then Y[I]−G[I] is type-1 neutrosophic closed, and by hypothesis, fn^{-1}(Y[I]−G[I]) = X[I]−fn^{-1}(G[I]) is type-1 neutrosophic open, that is, fn^{-1}(G[I]) is type-1 neutrosophic closed. Hence fn is contra continuous. □

Theorem 6.3. A type-1 neutrosophic function fn : (X[I],τ[I]) → (Y[I],τ1[I]) is contra continuous if and only if, for each x ∈ X[I] and each type-1 neutrosophic closed set G[I] in Y[I] containing fn(x), there is a type-1 neutrosophic open set U[I] in (X[I],τ[I]) containing x such that fn(U[I]) ⊆ G[I].

Proof. Suppose fn is contra continuous. Let x ∈ X[I] and G[I] be a type-1 neutrosophic closed set in Y[I] containing fn(x). By Theorem 6.2, U[I] = fn^{-1}(G[I]) is a type-1 neutrosophic open set in (X[I],τ[I]). Since fn(x) ∈ G[I], x ∈ fn^{-1}(G[I]) = U[I], and fn(U[I]) = fn(fn^{-1}(G[I])) ⊆ G[I]. Conversely, let G[I] be a type-1 neutrosophic closed set in Y[I]. For each x ∈ fn^{-1}(G[I]), fn(x) ∈ G[I], so by hypothesis there is a type-1 neutrosophic open set U[I]x containing x with fn(U[I]x) ⊆ G[I]. Therefore fn^{-1}(G[I]) = ∪{U[I]x : x ∈ fn^{-1}(G[I])}, which is type-1 neutrosophic open. Hence, by Theorem 6.2, fn is contra continuous. □

Theorem 6.4. The set of all points x ∈ X[I] at which fn : (X[I],τ[I]) → (Y[I],τ1[I]) is not contra continuous is identical with the union of the boundaries of the inverse images of type-1 neutrosophic closed sets of Y[I] containing fn(x).

Proof. Suppose fn is not contra continuous at x ∈ X[I]. By Theorem 6.3, there is a type-1 neutrosophic closed set G[I] in Y[I] containing fn(x) such that fn(U[I]) ⊈ G[I] for every type-1 neutrosophic open set U[I] containing x. That is, for every such U[I], fn(U[I]) ∩ (Y[I]−G[I]) ≠ ∅[I], which implies U[I] ∩ fn^{-1}(Y[I]−G[I]) ≠ ∅[I]. Therefore x ∈ Cln[fn^{-1}(Y[I]−G[I])] = Cln[X[I]−fn^{-1}(G[I])]. However, since fn(x) ∈ G[I], x ∈ fn^{-1}(G[I]) ⊆ Cln[fn^{-1}(G[I])]. Thus x ∈ Cln[X[I]−fn^{-1}(G[I])] ∩ Cln[fn^{-1}(G[I])] = Γn[fn^{-1}(G[I])]. Conversely, suppose x ∈ X[I] and x ∈ Γn[fn^{-1}(G[I])] for some type-1 neutrosophic closed set G[I] in Y[I] containing fn(x). If fn were contra continuous at x, there would be a type-1 neutrosophic open set U[I] containing x such that fn(U[I]) ⊆ G[I], giving x ∈ U[I] ⊆ fn^{-1}(G[I]), that is, x ∈ Intn[fn^{-1}(G[I])] ⊆ Γn[fn^{-1}(G[I])]^c, contradicting x ∈ Γn[fn^{-1}(G[I])]. Hence, by Theorem 6.3, fn is not contra continuous at x. □

Definition 6.5. The kernel of a subset H[I] of a type-1 neutrosophic topological space (X[I],τ[I]) is denoted Kern(H[I]) and defined by Kern(H[I]) = ∩{U[I] : H[I] ⊆ U[I] and U[I] is a type-1 neutrosophic open set in X[I]}.

Lemma 6.6. Let H[I] and G[I] be subsets of a type-1 neutrosophic topological space (X[I],τ[I]). The following holds: (1) x ∈ Kern(H[I]) if and only if H[I] ∩ U[I] ≠ ∅[I] for any type-1 neutrosophic closed set U[I] containing x. (2) H[I] ⊆ Kern(H[I]), and H[I] = Kern(H[I]) if H[I] is a type-1 neutrosophic open set in X[I]. (3) If H[I] ⊆ G[I] then Kern(H[I]) ⊆ Kern(G[I]).

Proof. (1) Let V[I] be any type-1 neutrosophic closed subset of X[I] containing x. Suppose H[I] ∩ V[I] = ∅[I]. Then H[I] ⊆ X[I]−V[I], and since X[I]−V[I] is type-1 neutrosophic open, Kern(H[I]) ⊆ X[I]−V[I]; hence x ∈ X[I]−V[I], contradicting x ∈ V[I]. Therefore H[I] ∩ V[I] ≠ ∅[I]. Conversely, suppose x ∉ Kern(H[I]). Then there is a type-1 neutrosophic open set V[I] containing H[I] with x ∉ V[I]. Then X[I]−V[I] is a type-1 neutrosophic closed set containing x with H[I] ∩ (X[I]−V[I]) = ∅[I], contradicting the hypothesis. Hence x ∈ Kern(H[I]). (2) By the definition of Kern(H[I]), H[I] ⊆ Kern(H[I]). If H[I] is type-1 neutrosophic open, H[I] is itself the smallest type-1 neutrosophic open set containing H[I], so Kern(H[I]) = H[I]. (3) Let x ∈ Kern(H[I]). By part (1), H[I] ∩ V[I] ≠ ∅[I] for any type-1 neutrosophic closed set V[I] containing x. Since H[I] ⊆ G[I], G[I] ∩ V[I] ≠ ∅[I], so x ∈ Kern(G[I]); that is, Kern(H[I]) ⊆ Kern(G[I]). □

Theorem 6.7. A type-1 neutrosophic function fn : (X[I],τ[I]) → (Y[I],τ1[I]) is contra continuous if and only if fn[Cln(H[I])] ⊆ Kern[fn(H[I])] for every subset H[I] of X[I].

Proof. Suppose fn is contra continuous. Let H[I] be any subset of X[I], and let y ∉ Kern[fn(H[I])]. By Lemma 6.6, there is a type-1 neutrosophic closed set F[I] in Y[I] containing y such that fn(H[I]) ∩ F[I] = ∅[I], so H[I] ∩ fn^{-1}(F[I]) = ∅[I]. Since fn is contra continuous, by Theorem 6.2, fn^{-1}(F[I]) is a type-1 neutrosophic open set in (X[I],τ[I]), so X[I]−fn^{-1}(F[I]) is type-1 neutrosophic closed, i.e., Cln[X[I]−fn^{-1}(F[I])] = X[I]−fn^{-1}(F[I]). Since H[I] ∩ fn^{-1}(F[I]) = ∅[I], H[I] ⊆ X[I]−fn^{-1}(F[I]), so Cln(H[I]) ⊆ Cln[X[I]−fn^{-1}(F[I])] = X[I]−fn^{-1}(F[I]); hence Cln(H[I]) ∩ fn^{-1}(F[I]) = ∅[I], so fn[Cln(H[I])] ∩ F[I] = ∅[I], giving y ∉ fn[Cln(H[I])]. Therefore fn[Cln(H[I])] ⊆ Kern[fn(H[I])]. Conversely, suppose fn[Cln(H[I])] ⊆ Kern[fn(H[I])] for every subset H[I] of X[I]. Let V[I] be any type-1 neutrosophic open subset of Y[I]. Then fn^{-1}(V[I]) ⊆ X[I], and by hypothesis fn[Cln(fn^{-1}(V[I]))] ⊆ Kern[fn(fn^{-1}(V[I]))] ⊆ Kern(V[I]) = V[I] (the last equality by Lemma 6.6, since V[I] is type-1 neutrosophic open). This implies Cln(fn^{-1}(V[I])) ⊆ fn^{-1}(V[I]), that is, fn^{-1}(V[I]) is type-1 neutrosophic closed in (X[I],τ[I]). Hence fn is contra continuous. □

Theorem 6.8. A type-1 neutrosophic function fn : (X[I],τ[I]) → (Y[I],τ1[I]) is contra continuous if and only if Cln[fn^{-1}(G[I])] ⊆ fn^{-1}[Kern(G[I])] for every subset G[I] of Y[I].

Proof. Suppose fn is contra continuous. Let G[I] be any type-1 neutrosophic subset of Y[I]. Since fn^{-1}(G[I]) ⊆ X[I] and fn is contra continuous, by Theorem 6.7, fn[Cln[fn^{-1}(G[I])]] ⊆ Kern[fn(fn^{-1}(G[I]))] ⊆ Kern(G[I]); hence Cln[fn^{-1}(G[I])] ⊆ fn^{-1}[Kern(G[I])]. Conversely, suppose Cln[fn^{-1}(G[I])] ⊆ fn^{-1}[Kern(G[I])] for every subset G[I] of Y[I]. Let V[I] be any type-1 neutrosophic open subset of Y[I]. By hypothesis and Lemma 6.6, Cln[fn^{-1}(V[I])] ⊆ fn^{-1}[Kern(V[I])] ⊆ fn^{-1}(V[I]), so Cln[fn^{-1}(V[I])] = fn^{-1}(V[I]), that is, fn^{-1}(V[I]) is type-1 neutrosophic closed in (X[I],τ[I]). Therefore fn is contra continuous. □

7. Conclusion

This paper has developed a topological framework based on type-1 neutrosophic sets, formalizing the interior, closure, exterior, and boundary operators on type-1 neutrosophic sets X[I] and establishing separation axioms for type-1 topological spaces Ti[I], i = 0, 1, …, 4. Continuous and contra continuous type-1 neutrosophic functions were introduced and characterized through several equivalent formulations involving closure, interior, and kernel operators. These results isolate type-1 neutrosophic sets as a distinct and tractable framework and lay the groundwork for broader applications in mathematical analysis, algebra, and related fields.

Conflicts of Interest: The authors declare no conflict of interest.

References

1. Agboola, A.A.A.; Akinleye, S.A. Neutrosophic vector spaces. Neutrosophic Sets and Systems 2014, 4(1), 9–18. https://digitalrepository.unm.edu/nssjournal/vol4/iss1/3

2. Al-Odhari, A.M. An introduction to the algebraic structure of type-1 neutrosophic-set theory. International Journal of Neutrosophic Science 2026, 27(2), 511–541. https://doi.org/10.54216/IJNS.270242
3. Al-Odhari, A.M. Neutrosophic power-set and neutrosophic hyper-structure of neutrosophic set of three types. Annals of Pure and Applied Mathematics 2025, 31(2), 125–146. http://dx.doi.org/10.22457/apam.v31n2a05964
4. Al-Odhari, A. Invertible neutrosophic functions on neutrosophic set theory of three types. Neutrosophic Knowledge 2025, 21–29. https://doi.org/10.5281/zenodo.14740796
5. Al-Odhari, A. Basic introduction of neutrosophic set theory. Plithogenic Logic and Computation 2024, 2, 20–28. https://doi.org/10.61356/j.plc.2024.2327
6. Al-Odhari, A. Some aspects of neutrosophic set theory. Neutrosophic Optimization and Intelligent Systems 2024, 4, 31–38. https://doi.org/10.61356/j.nois.2024.4359
7. Al-Odhari, A. On the generalization of neutrosophic set operations: Testing proofs by examples. Hyper-Soft Set Methods in Engineering 2024, 2, 72–82. https://doi.org/10.61356/j.2321.2024
8. Al-Odhari, A. Some results of neutrosophic relations. Neutrosophic Knowledge 2024, 5, 77–86. https://doi.org/10.5281/zenodo.14181753
9. Al-Odhari, A.M. Axiomatic of neutrosophic groups. Sana'a University Journal of Applied Sciences and Technology 2024, 2(2), 205–214. https://doi.org/10.59628/jast.v2i2.793
10. Al-Odhari, A.M. The neutrosophic cosets and neutrosophic normal subgroups of neutrosophic groups associated with Gt1[I]. Sana'a University Journal of Applied Sciences and Technology 2025, 3(3), 848–860. https://doi.org/10.59628/jast.v3i3.1666
11. Al-Omeri, W. Neutrosophic crisp sets via neutrosophic crisp topological spaces. Neutrosophic Sets and Systems 2016, 13(1). https://digitalrepository.unm.edu/nssjournal/vol13/iss1/13
12. Atanassov, K. Intuitionistic fuzzy sets. Fuzzy Sets and Systems 1986, 20, 87–96.
13. Atanassov, K. Intuitionistic Fuzzy Sets: Theory and Applications; Springer-Verlag: Berlin, Heidelberg, 1999.
14. Brown, R. Topology: A Geometric Account of General Topology, Homotopy Types and the Fundamental Groupoid; Halsted Press (a division of John Wiley and Sons), 1988.
15. Bera, T.N.; Mahapatra, K. On neutrosophic soft linear spaces. Fuzzy Information and Engineering 2017, 9(3), 299–324.
16. Biswas, S.; Moi, S.; Sarkar, S.P. Neutrosophic Riemann integration and its properties. Soft Computing 2021, 25(22), 13987–13999.
17. Chang, C. Fuzzy topological spaces. Journal of Mathematical Analysis and Applications 1968, 24, 182–190.
18. Coker, D. An introduction to intuitionistic fuzzy topological spaces. Fuzzy Sets and Systems 1997, 88(1), 81–89.
19. Cetkin, V.; Aygun, H. An approach to neutrosophic subgroup and its fundamental properties. Journal of Intelligent and Fuzzy Systems 2015, 29(5), 1941–1947.
20. Dugundji, J. Topology; Universal Book Stall: New Delhi, 1990.
21. Dummit, D.S.; Foote, R.M. Abstract Algebra; Wiley: Hoboken, NJ, USA, 2004.
22. Elrawy, A.; Abdalla, M.; Saleem, M.A. Some results on neutrosophic group. Journal of Mathematics 2023, 1–6.
23. Herstein, I.N. Topics in Algebra; John Wiley & Sons: Hoboken, NJ, USA, 2006.
24. Fujita, T.; Smarandache, F. Advancing Uncertain Combinatorics through Graphization, Hyperization, and Uncertainization: Fuzzy, Neutrosophic, Soft, Rough, and Beyond, 2nd ed.; Infinite Study, 2025.
25. Fujita, T.; Smarandache, F. Representing Higher-Order Networks: A Survey of Graph-Based Frameworks; Neutrosophic Science International Association (NSIA) Publishing House, 2026.
26. Kandasamy, W.V.; Smarandache, F. Basic Neutrosophic Algebraic Structures and Their Application to Fuzzy and Neutrosophic Models; Infinite Study: Flagstaff, AZ, USA, 2004.
27. Kandasamy, W.V.; Smarandache, F. Some Neutrosophic Algebraic Structures and Neutrosophic N-Algebraic Structures; Infinite Study, 2006.
28. Karatas, S.; Kuru, C. Neutrosophic topology. Neutrosophic Sets and Systems 2016, 13(1). https://digitalrepository.unm.edu/nssjournal/vol13/iss1/12
29. Lupianez, F.G. On neutrosophic topology. Kybernetes 2008, 37(6), 797–800.
30. Lupianez, F.G. On neutrosophic paraconsistent topology. Kybernetes 2010, 39(4), 598–601.

31. Lowen, R. Fuzzy topological spaces and fuzzy compactness. Journal of Mathematical Analysis and Applications 1976, 56, 621–633.
32. Munkres, J.R. Topology, a First Course; Prentice-Hall: Englewood Cliffs, NJ, 1975.
33. Oyebo, Y.T. Neutrosophic groups and subgroups. 2012. https://www.researchgate.net/publication
34. Omran, S.; Elrawy, A. Continuous and bounded operators on neutrosophic normed spaces. Neutrosophic Sets and Systems 2021, 46, 276–289.
35. Salama, A.A.; Alblowi, S.A. Neutrosophic set and neutrosophic topological spaces. IOSR Journal of Mathematics 2012, 3(3), 31–35.
36. Salama, A.A.; Alblowi, S.A. Generalized neutrosophic set and generalized neutrosophic topological spaces. Computer Science and Engineering 2012, 27, 129–132.
37. Salama, A.; Smarandache, F.; Kromov, V. Neutrosophic closed set and neutrosophic continuous functions. Neutrosophic Sets and Systems 2014, 4(1). https://digitalrepository.unm.edu/nssjournal/vol4/iss1/2
38. Saleem, M.A.; Abdalla, M.; Elrawy, A. On a matrix over NC and multiset NC semigroups. Journal of Mathematics 2022, 2022(1), 8095073.
39. Smarandache, F. Neutrosophy, Neutrosophic Probability, Set and Logic; American Research Press: Rehoboth, DE, USA, 1998.
40. Smarandache, F. Neutrosophic set — a generalization of the intuitionistic fuzzy set. International Journal of Pure and Applied Mathematics 2005, 24(3), 287–297.
41. Smarandache, F.; Ali, M. Neutrosophic triplet group. Neural Computing and Applications 2018, 29(7), 595–601.
42. Siddique, S.; Ahmad, U.; Akram, M. A study on generalized graph representations of complex neutrosophic information. Journal of Applied Mathematics and Computing 2021, 65(1–2), 481–514.
43. Zadeh, L.A. Fuzzy sets. Information and Control 1965, 8, 338–353.

Received: Apr. 27, 2026. Accepted: Sept. 11, 2026.

Applications of Neutrosophic Topology in Gold Rate Analysis in India

N. Raksha Ben[1,*] and G. Helen Rajapushpam[2]

[1] Assistant Professor of Mathematics, PG and Research Department of Mathematics, Nazareth Margoschis College at Pillaiyanmanai; raksha@nmcp.ac.in
[2] Assistant Professor of Mathematics, PG and Research Department of Mathematics, Nazareth Margoschis College at Pillaiyanmanai
* Correspondence: raksha@nmcp.ac.in

Abstract: Gold plays a significant role in the Indian economy due to its cultural, financial and investment value. However, gold price behaviour is highly uncertain and influenced by multiple indeterminate factors such as market sentiments, macroeconomic variables and regional variations. This study introduces an innovative framework using Neutrosophic Topology to analyse gold rate fluctuations in India. Incorporating the concept of neutrosophic topology provides a more flexible and realistic modelling approach compared to classical and fuzzy systems. This paper develops a neutrosophic topological structure on gold price data and demonstrates its application in analysing uncertainty, continuity, and clustering of price movements across major Indian cities.

Keywords: Neutrosophic Topology; Gold Price; Uncertainty; Neutrosophic Sets

1. Introduction

Gold is widely regarded as a safe haven asset and plays a crucial role in India's financial systems. Its demand is influenced by cultural practices, inflation hedging, and investment diversification. Studies show that gold prices in India are affected by household financial conditions, macroeconomic variables, and global trends. Traditional statistical and econometric models often fail to capture uncertainty and indeterminacy inherent in gold price movements. To overcome these limitations, neutrosophic approaches have been introduced, which extend fuzzy logic by including a third component, indeterminacy. Recent studies on neutrosophic statistical analysis have shown that gold prices vary significantly across cities and time periods, making uncertainty modelling essential.

2. Preliminaries

Definition 2.1 [9]. Let X be a non-empty fixed set. A Neutrosophic set [NS for short] A is an object having the form $A = \{\langle x, \mu A(x), \sigma A(x), \gamma A(x)\rangle : x \in X\}$, where $\mu A(x)$, $\sigma A(x)$, and $\gamma A(x)$ represent the degree of membership function, the degree of indeterminacy, and the degree of non-membership function, respectively, of each element $x \in X$ to the set A.

Remark 2.2 [9]. A neutrosophic set $A = \{\langle x, \mu A(x), \sigma A(x), \gamma A(x)\rangle : x \in X\}$ can be identified with an ordered triple $A = \{\langle \mu A(x), \sigma A(x), \gamma A(x)\rangle\}$ in $]^-0, 1^+[$ on X.

Remark 2.3 [9]. For the sake of simplicity, we shall use the symbol $A = \{\langle \mu(x), \sigma(x), \gamma(x)\rangle\}$ for the neutrosophic set $A = \{\langle x, \mu A(x), \sigma A(x), \gamma A(x)\rangle : x \in X\}$.

Example 2.4 [9]. Every intuitionistic fuzzy set A on a non-empty set X is obviously a Neutrosophic set having the form $A = \{\langle \mu A(x), 1 - \mu A(x) + \sigma A(x), \gamma A(x)\rangle : x \in X\}$. Since the main purpose is to construct the tools for developing Neutrosophic Set and Neutrosophic topology, the neutrosophic sets 0N and 1N in X must be introduced as follows.

0N may be defined as follows:

(01) 0N = {⟨x, 0, 0, 1⟩ : x ∈ X}
(02) 0N = {⟨x, 0, 1, 1⟩ : x ∈ X}
(03) 0N = {⟨x, 0, 1, 0⟩ : x ∈ X}
(01) 0N = {⟨x, 0, 0, 0⟩ : x ∈ X}
1N may be defined as follows:
(11) 1N = {⟨x, 1, 0, 0⟩ : x ∈ X}
(12) 1N = {⟨x, 1, 0, 1⟩ : x ∈ X}
(13) 1N = {⟨x, 1, 1, 0⟩ : x ∈ X}
(14) 1N = {⟨x, 1, 1, 1⟩ : x ∈ X}

Definition 2.5. A Neutrosophic topology τN on a set X is a family of neutrosophic subsets satisfying the following conditions:

- 0, X ∈ τN.
- Arbitrary union of neutrosophic open sets is neutrosophic open.
- Finite intersection of neutrosophic open sets is neutrosophic open.

Remark 2.6. This structure allows modelling of uncertain open sets, which is useful in financial data analysis.

Example 2.7 [9]. Any fuzzy topological space (X, τ0) in the sense of Chang is obviously an NTS in the form of {A : μA ϵ τ0}, wherever a fuzzy set in X whose membership function is μA is identified with its counterpart. The following is an example of a Neutrosophic topological space.

Example 2.8 [9]. Let X = {x} and A = {⟨x, 0.5, 0.5, 0.4⟩ : x ∈ X}, B = {⟨x, 0.4, 0.6, 0.8⟩ : x ∈ X}, C = {⟨x, 0.5, 0.6, 0.4⟩ : x ∈ X}, D = {⟨x, 0.4, 0.5, 0.8⟩ : x ∈ X}. Then the family τN = {0N, 1N, A, B, C, D} is called a neutrosophic topological space on X.

Definition 2.9 [9]. The complement of A [C(A)] of an NOS is called a neutrosophic closed set [NCS for short] in X.

Let us define the neutrosophic closure and neutrosophic interior operations in neutrosophic topological spaces:

Definition 2.10 [9]. Let (X, τN) be an NTS and A = {(μA, σA, γA)} be a Neutrosophic set in X. Then the neutrosophic closure and neutrosophic interior of A are defined by:

NCl(A) = ∩{K : K is an NCS in X and A ⊆ K}
NInt(A) = ∪{G : G is an NOS in X and G ⊆ A}

It can be shown that NCl(A) is an NCS and NInt(A) is an NOS in X. A is NOS if and only if A = NIntA. A is NCS if and only if A = NClA.

3. Literature Review

Existing research highlights the importance of gold price modelling in India. Econometric studies show long-run relationships between household finance and gold prices. The gold market exhibits volatility, seasonality, and policy-driven fluctuations. Neutrosophic statistical methods have been applied to analyse gold rate variations across cities.

4. Methodology

Gold price data is collected from major cities of India. The data includes daily minimum and maximum prices, monthly averages, and regional variations. Indeterminacy is defined as I(t) = Nindet / Ntotal, where Nindet is the number of conflicting headlines from the World Gold Council (WGC), weighted by importance, such that $I \in [0,1]$ and $0 \leq T + F + I \leq 3$.

Data Collection

Table 5.1. Neutrosophic data collection – Thoothukudi / Chennai / Delhi

Date	City	22kt Low L	22kt High U	U − L	Headline Total	Indet. Headlines	I = Nindet/Ntotal (GN)
31/08/2026	Thoothukudi	9713	9930	217	10	3	0.3 (9778.1)
31/08/2026	Chennai	9700	9925	225	10	2	0.2 (9745.0)
15/08/2026	Delhi	6016	6032	16	8	3	[0.2,0.4] (interval)

Neutrosophic Representation of Gold Price

Let the gold price be represented as a neutrosophic number given by GN = GL + GU.IN, where GL represents the lower price, GU represents the upper price, and IN represents the indeterminacy interval, IN ∈ [IL, IU].

Construction of Neutrosophic Topology

Let X be the set of gold price observations, and let τN be the collection of neutrosophic open sets that represent the price intervals.

Remark 7.1. Neutrosophic open sets may represent stable price changes, high-volatility zones, and uncertain transition regions.

Definition 7.2. A function f : X → Y is neutrosophically continuous if the pre-image of every neutrosophic open set is neutrosophically open.

Remark 7.3. The above function is used to model smooth price transitions and sudden fluctuations.

Application of Gold Rate Analysis

(a) Modelling Price Uncertainty:

Neutrosophic topology captures daily fluctuations, regional differences, and market unpredictability. Unlike classical models, it explicitly represents indeterminacy, which is crucial in financial markets.

(b) Clustering of Gold Prices:

- Stable clusters (low volatility): zones with I < 0.30, corresponding to low volatility. Here T ≈ 1, F ≈ 0, the price trend is clearly defined, and classical forecasting holds.
- Boundary regions (high uncertainty): zones with I > 0.40, corresponding to high uncertainty where 0.40 ≤ T, I, F ≤ 0.6. This is maximum indeterminacy, and the recommendation is clearly to hold — neither to sell nor to buy.
- Transition zones (potential price shifts): the neighbourhood of boundary points where 0.30 ≤ I ≤ 0.40 indicates potential price shifts (breakout/breakdown). This serves as an early warning for investors before T switches to F.

(c) Decision-Making Support:

This model helps identify optimal buying periods, detect unstable market phases, and support investment strategies.

Table 8.1. Neutrosophic clustering and decision support

Region	I	Zone	⟨T, I, F⟩	Cluster / Decision
Chennai	0.22	IntN(A)	⟨.78, .22, .20⟩	Stable / Buy
Thoothukudi	0.32	Transition	⟨.60, .32, .35⟩	Potential Shift / Hold

Delhi (6016–6032)	0.35	Neutrosophic Boundary	⟨.55, .35, .40⟩	Boundary / Range

Theorems and Proofs in Neutrosophic Topology for Gold Rate Analysis

Notations 9.1. Let X be the set of gold price observations, GN(x) = ⟨T(x), I(x), F(x)⟩ be a neutrosophic representation of gold price, and τN be the neutrosophic topology on X.

Theorem 9.2 (Neutrosophic Topology from Gold Price Intervals).

Let X be the set of gold prices in India, and define a family τN consisting of all neutrosophic subsets representing price intervals with uncertainty. Then τN forms a neutrosophic topology on X.

Proof. The empty set 0 corresponds to no price observation, and X represents all gold prices; both can be expressed as 0 = ⟨0,1,1⟩, X = ⟨1,0,0⟩. Hence 0, X ∈ τN. Let {Ui} ⊆ τN; each Ui represents a price interval with uncertainty, and their union U = ⋃i Ui still represents a valid uncertain price region, preserving the truth, indeterminacy, and falsity bounds. Hence U ∈ τN. Let U1, U2 ∈ τN; then U1 ∩ U2 corresponds to overlapping price intervals, which is also a neutrosophic open set. Thus all axioms hold, so τN is a neutrosophic topology. □

Theorem 9.3 (Neutrosophic Continuity of the Gold Price Function).

Let f : X → R represent the mapping from time to gold prices. If small changes in input produce bounded neutrosophic variations in output, then f is neutrosophically continuous.

Proof. A function is neutrosophically continuous if for every open set V ⊆ R the pre-image $f^{-1}(V)$ is neutrosophically open. Let V represent a stable gold price interval; then $f^{-1}(V)$ consists of the time points where the price falls within this interval. Since price changes are gradual over short intervals, the pre-image corresponds to the cluster of neighbouring time points with bounded indeterminacy. Thus $f^{-1}(V)$ ∈ τN. Hence f is neutrosophically continuous. □

Theorem 9.4 (Neutrosophic Closure Represents Maximum Price Stability).

The neutrosophic closure of a gold price set A ⊆ V represents the smallest closed set containing all stable and near-stable price observations.

Proof. The closure is defined as ClN(A) = ∩{C / A ⊆ C, where C is a neutrosophic closed set}. In gold price analysis, let A represent the stable prices. Closure adds boundary points, since the intersection of closed sets is closed, so ClN(A) is closed and minimal. Hence the closure captures both exact and approximate stability regions in gold pricing. □

Theorem 9.5 (Neutrosophic Interior and Market Stability).

The neutrosophic interior of a gold price set represents the most stable core region of prices.

Proof. The interior is defined as IntN(A) = ∪{U / U ⊆ A, U is neutrosophically open}. Here U represents the stable price intervals, and their union gives the largest stable region inside A. Thus IntN(A) excludes boundary fluctuations and captures highly reliable price zones. □

Theorem 9.6 (Boundary Region Captures Maximum Uncertainty).

The neutrosophic boundary of a gold price set represents maximum uncertainty in price transitions.

Proof. The boundary is defined as ∂N(A) = ClN(A) − IntN(A). This includes the points that are not fully stable and the points not completely outside the set. Thus these are transition points where prices may rise or fall and indeterminacy is highest. Hence the boundary models volatile gold market behaviour. □

Theorem 9.7 (Compactness and Bounded Gold Price Behaviour).

If the neutrosophic topological space (X, τN) of gold prices is compact, then every sequence of gold prices has a convergent subsequence.

Proof. By definition, a compact space ensures every open cover has a finite subcover. In the gold price context, the open cover is the collection of price intervals covering all data. Thus price fluctuations remain bounded, ensuring the existence of a convergent subsequence (stability over time). Hence gold prices exhibit bounded behaviour under the compactness assumption. □

Theorem 9.8 (Connectedness of the Gold Market).

If X is neutrosophically connected, it cannot be divided into two disjoint stable regions.

Proof. Assume X = U ∪ V, disjoint open sets, implying two separate price regimes. But real market prices are interdependent, and transitions exist. Thus separation is impossible, so X is connected. □

5. Results and Discussion

This neutrosophic topological framework reveals that gold price behaviour is nonlinear and uncertain.

6. Future Scope of This Research

This framework can be integrated with AI and deep learning. It can be applied to stock and cryptocurrency markets, and a comparative study with fuzzy topology can also be implemented.

7. Conclusion

Neutrosophic topology provides a powerful framework to model gold rate behaviour under uncertainty. It helps investors, especially in Tamil Nadu, to decide whether to buy, sell, or hold by quantifying not only bullish and bearish sentiment but also confusion.

References

1. Samrandache, F. Neutrosophic set: A generalization of the intuitionistic fuzzy set. International Journal of Pure and Applied Mathematics 2005, 24(3), 287–297.
2. Salama, A.A.; Alblowi, A. Neutrosophic sets and neutrosophic topological spaces. IOSR Journal of Mathematics 2012, 3(4), 31–35.
3. Arokiarani, I.; Dhavaseelan, R.; Jafari, S.; Parimala, M. On some new notations and functions in neutrosophic topological spaces. Neutrosophic Sets and Systems 2017, 16, 16–19.
4. Andrijevic, D. On b-open sets. Matematicki Vesnik 1996, 48, 56–64.
5. Rajesh, T.; Srinivasan, R. Neutrosophic b-open sets and neutrosophic b-closed sets in neutrosophic closed sets. Neutrosophic Sets and Systems 2025, 81, 195–210.
6. Banu Priya, V.; Chandrasekar, S. Neutrosophic super b-open sets and neutrosophic super b-closed sets. Neutrosophic Sets and Systems 2025, 81.
7. Zadeh, L.A. Fuzzy sets. Information and Control 1965, 8(3), 338–353.
8. Atanassov, K. Intuitionistic fuzzy sets. Fuzzy Sets and Systems 1986, 20, 87–96.
9. Riaz, M.; et al. Neutrosophic sets in financial decision making. Journal of Intelligent & Fuzzy Systems 2022, 42(2).
10. Broumi, S.; et al. Neutrosophic sets in financial markets: A review. Neutrosophic Sets and Systems 2022, 50.
11. Raksha Ben, N.; Hari Siva Annam, G. Generalized topological spaces via neutrosophic sets. Journal of Mathematical and Computational Science 2021, 11, 716–734.
12. Raksha Ben, N.; Hari Siva Annam, G. A note on μNP spaces. Neutrosophic Sets and Systems 2022, 49.
13. Wadei Al-omeri; Smarandache, F. New neutrosophic sets via neutrosophic topological spaces. In New Trends in Neutrosophic Theory and Applications, Vol. 2; June 2016.

THE UNIVERSITY OF NEW MEXICO
Albuquerque, New Mexico, USA
Diverse Minds • Brighter Futures

NSS
Neutrosophic Sets and Systems

ISSN 2331-6055 (Print)
ISSN 2331-608X (Online)

An International Journal of Neutrosophic Theory and Applications

Neutrosophic Sets and Systems (NSS) is an academic journal, published quarterly online and on paper, that has been created for publications of advanced studies in neutrosophy, neutrosophic set, neutrosophic logic, neutrosophic probability, neutrosophic statistics, etc. and their applications in any field.

All submitted papers should be professional, in good English, containing a brief review of a problem and obtained results.

ISSN (print): 2331-6055, ISSN (online): 2331-608X
Impact Factor: 1.739

NSS has been accepted by **SCOPUS**. Starting with Vol. 19, 2018, all NSS articles are indexed in Scopus.

NSS is also indexed by Google Scholar, Google Plus, Google Books, EBSCO, Cengage Thompson Gale (USA), Cengage Learning, ProQuest, Amazon Kindle, DOAJ (Sweden), University Grants Commission (UGC) – India, International Society for Research Activity (ISRA), Scientific Index Services (SIS), Academic Research Index (ResearchBib), Index Copernicus (European Union), CNKI (Tongfang Knowledge Network Technology Co., Beijing, China), etc.

Google Dictionary has translated the neologisms "neutrosophy" (1) and "neutrosophic" (2), coined in 1995 for the first time, into about 100 languages.

FOLDOC Dictionary of Computing (1, 2), Webster Dictionary (1, 2), Wordnik (1), Dictionary.com, The Free Dictionary (1), Wiktionary (2), YourDictionary (1, 2), OneLook Dictionary (1, 2), Dictionary / Thesaurus (1), Online Medical Dictionary (1, 2), and Encyclopedia (1, 2) have included these scientific neologisms.

DOI numbers are assigned to all published articles.

Registered by the Library of Congress, Washington DC, United States, https://lccn.loc.gov/2013203857.

Recently, NSS was also approved for Emerging Sources Citation Index (ESCI) available on the Web of Science platform, starting with Vol. 15, 2017.

TRUTH
INDETERMINACY
FALSEHOOD

BEYOND
UNCERTAINTY
TOWARD
A BRIGHTER
TOMORROW

$$N(x) = \langle T, I, F \rangle$$

LOGIC
MODELING
INTELLIGENCE
REAL APPLICATIONS

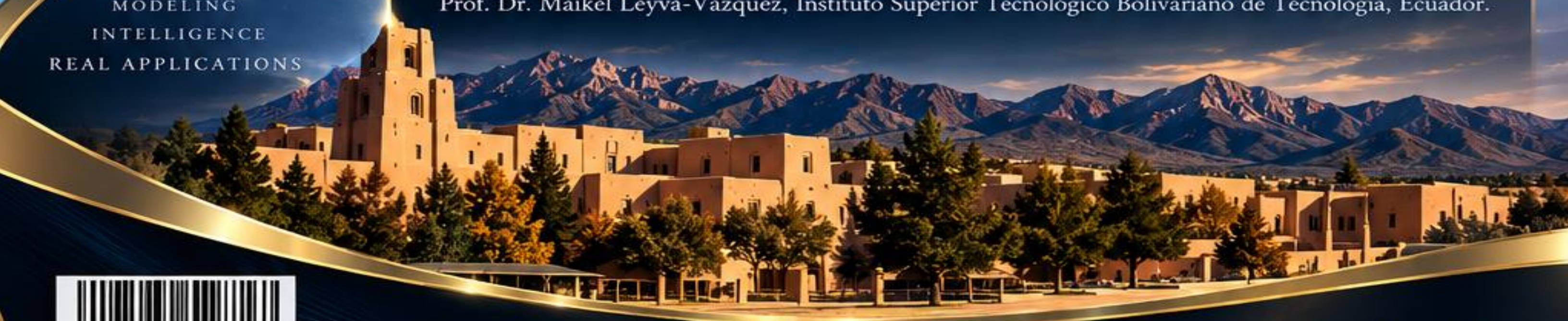

2331-6055
$39.95

NEUTROSOPHIC SETS AND SYSTEMS
THE UNIVERSITY OF NEW MEXICO

Knowledge for a More Certain Future